# SYNTHESIS AND CHARACTERISATION OF IMPRINTED POLYMERIC RECEPTOR MIMICS

Aisha Ali

Doctor of Philosophy

ASTON UNIVERSITY

August 2005

# ACKNOWLEDGEMENTS

*Dedicated to my parents*

# ABSTRACT

Molecularly imprinted polymers (MIPs) are crosslinked polymers containing bespoke functionalised cavities arising from the inclusion of template molecules in the polymerisation mixture and their later extraction. When the polymers are prepared functional polymerisable monomers are included which become part of the polymer matrix and serve to decorate the cavities with functionality appropriate to the template molecules. Overall, binding sites are created which have a memory for the templates both in terms of shape and matching functionality. Fluorescent molecularly imprinted polymers have the benefit of a fluorophore in their cavities that may respond to the presence of bound test compound by a change in their fluorescence output. The work presented falls into three main areas.

A series of fluorescent MIPs was prepared with a view to generating material capable of mimicking the binding characteristics of the metabolically important cytochrome isoform CYP2D6. The MIPs re-bound their templates and various cross-reactivities were encountered for test compound/drug recognition. One MIP in particular exhibited a rational discrimination amongst the related synthetic templates and was reasonably successful in recognising CYP2D6 substrates from the drug set tested.

In order to give some insights into binding modes in MIPs, attempts were made to produce functional monomers containing two or more fluorophores that could be interrogated independently. A model compound was prepared which fitted the dual-fluorophore criteria and which will be the basis for future incorporation into MIPs.

A further strand to this thesis is the deliberate incorporation of hydrophobic moieties into fluorescent functional monomers so that the resulting imprinted cavities might be biomimetic in their impersonation of enzyme active sites. Thus the imprinted cavities had specific hydrophobic regions as well as the usual polar functionality with which to interact with binding test compounds.

Keywords: Molecular imprinting, fluorescence, cytochrome P450, binding mimic, hydrophobic interactions

## Abbreviations

| | |
|---|---|
| AIBN | 2,2`-Azobis(2-methyl-propionitrile) |
| Asp | Aspartate |
| BM3 | *Bacillus megaterium* |
| Cam | Camphor |
| cAMP | Adenosine3`:5`-cyclic monophosphate |
| CSP | Chiral stationary phases |
| CYP2D6 | Cytochrome P450 2D6 (isoenzyme) |
| DCM | Dichloromethane |
| DMAP | 4-(Dimethylamino)pyridine |
| DMF | Dimethylformamide |
| DNA | Deoxyribonucleic acid |
| EGDMA | Ethyleneglycol dimethacrylate |
| ELISA | Enzyme-linked immunosorbent assay |
| EM | Extensive metaboliser |
| FAD | Flavin adenine dinucleotide |
| FFM | Fluorescent Functional Monomer |
| FMN | Flavin mononucleotide |
| Glu | Glutamic acid |
| HPLC | High performance liquid chromatography |
| Hünig's base | N,N-diisopropylethylamine |
| Ig | Immunoglobulins |
| IM | Intermediate metaboliser |
| MIA | Molecular imprinted absorbent assay |
| MIP | Molecularly imprinted polymers |
| NADPH | Nicotinamide adenine dinucleotide phosphate |
| NAT1 & NAT2N | Acetyltransferases 1&2 |
| PEG | Poly (ethylene glycol) methyl ether |
| PM | Poor metaboliser |
| PMMA | Poly (methyl methacrylate) |
| QCM | Quartz-crystal microbalance |
| RNA | Ribonucleic acid |
| SNP | Single nucleotide polymorphism |
| TEGDMA | Triethyleneglycol dimethacrylate |
| Terp | Terpredoxin |
| THF | Tetrahydrofuran |
| TLC | Thin layer chromatography |
| TMPTA | Trimethylolpropane triacrylate |
| UM | Ultraextensive metaboliser |
| VBIDA | N-(4-vinylbenzyl)-iminodiacetic acid |

5

# CONTENTS

List of Figures, Schemes and Tables

## Overview of aims

### The use of fluorescent MIPs as active-site binding mimics for CYP2D6.

It is proposed that a receptor mimic for CYP2D6 could be prepared by synthesising a series of fluorescent molecularly imprinted polymers templated to represent the interior shape, volume and functionality of that the enzyme. The polymers proposed would have the possibility to form the sensing element in a high-throughput assay to predict CYP2D6 affinity. In general such polymers can act as a starting point for screening protocols for cytochrome P450 metabolism and can be applicable to any other poorly characterised receptor where a set of known substrates exists.

### The preparation of MIPs using dual-fluorophore functional monomers.

Molecular imprinting has been successful in generating highly selective materials, though characterisation of the cavities present in the MIPs has not been fully explored. In addition, inferences are drawn from binding studies and there is nothing to measure directly. Therefore designing suitably multifunctional fluorescent imprinted polymers would be very useful in gaining more information concerning the interactions between the polymer cavity and test compounds. The aim would therefore be to create MIPs containing dual fluorescence-labelled cavities.

### The preparation of fluorescent MIPs containing cavities with both hydrogen-bonding regions and hydrophobic regions.

The objective of this study is to incorporate this hydrophobicity within the imprinted polymer by employing a fluorescent functional monomer that contains within its structure the hydrophobic and hydrogen-bonding components. Such specific components within the imprinted cavities would then interact with binding test compounds.

The aims shall be discussed in detail in a chapter 2.

# Chapter 1: Introduction

## 1.1 Molecular recognition

The interaction and recognition of diverse molecules is necessary to the activity of biological species. The formation of complexes between complementary molecules is caused by intra and inter molecular interactions. These interactions play a key role in biochemical molecular recognition and are essential to the action of enzymes, receptors and antibodies. Synthesising mimics for the recognition elements mentioned above is of major interest to the research community. Additionally, recognition processes are important in catalysis, selective separations, chemical sensors and many chemical assays.

## 1.1.1 Biological molecular recognition

### 1.1.1.1 Enzymes

Enzymes are biological catalysts that display an example of natural molecular recognition that is very specific. They are high molecular weight compounds made up principally of chains of amino acids linked together by peptide bonds. Enzymes like any catalyst, work by lowering the activation energy of a reaction, thus allowing the reaction to proceed to its steady state or completion much faster than it otherwise would; the enzyme (again, as with any catalyst) remains unaltered by the completed reaction and can therefore continue catalysis. In addition they regulate biocatalytic, synthetic and breakdown processes in organisms. The active sites of enzymes exhibit functionality dependent on the amino acid sequence and are highly substrate specific i.e. form a enzyme-substrate complex. These complexes are formed through non-covalent interactions between specifically positioned functional groups of the polypeptide chain and those of the substrate molecule. Many enzymes require the presence of an additional, non-protein, cofactor. If the cofactor is organic, then it is called a coenzyme. Coenzymes are relatively small molecules compared to the protein part of the enzyme. Many of the coenzymes are derived from vitamins i.e. the B vitamins: thiamine (B1), riboflavin (B2) and nicotinamide. The coenzymes make up a part of the active site, since without the coenzyme the enzyme will not function. Note, that some of these cofactors are metal ions such as $Zn^{2+}$ (the cofactor for carbonic anhydrase), $Cu^{2+}$, $Mn^{2+}$, $K^+$, and $Na^+$. The specific action of an enzyme with a single substrate can be explained using a `Lock and Key `analogy first postulated in 1894 by Emil Fischer. In this analogy, the lock is the enzyme and the key is the substrate. Only the correctly sized key (substrate) fits into the keyhole (active site) of the lock (enzyme). The induced-fit theory proposed by Koshland (1968) however, is accepted more widely. The induced-fit theory assumes that the substrate plays a role in determining the final shape of the enzyme and that the enzyme is partially flexible. This explains why certain compounds can bind to the enzyme but do not react because the enzyme has been distorted too much. Other molecules may be too small to induce the proper alignment and therefore cannot react. Only the proper substrate is capable of inducing the proper alignment of the active site (Ritter 1996; Patrick 1995).

## 1.1.1.2 Receptors

Receptors, similar to enzymes exhibit a specific recognition within biological systems. In cellular signalling the receptors located on the cells surface, are known as transmembrane proteins or glycoproteins. These are embedded or otherwise attached to the cells plasma membrane and have a binding site for specific ligands (cytokines, hormones, growth factors, neurotransmitters, adhesion molecules, etc) exposed to the extracellular environment. Ligand binding to a cell surface receptor leads to its activation, caused by changes in its conformation and this generates a cascade of intracellular signals that predictably changes the behaviour of the cell. The three types of cell surface receptors are: ion-channel linked receptors, G-protein linked receptors and enzyme-linked receptors. The ion-channel linked receptors, are fast acting receptors, often used in synaptic signaling between electrically excitable cells. The protein acts as both the receptor and effector. Both the G-protein linked receptors and enzyme-linked receptors usually have high affinity for their ligands since the ligands are present in very low quantities due to the fact that they are dilute in the blood stream. The G-protein linked receptors indirectly regulate the activity of a separate plasma membrane-bound target protein e.g. an enzyme. The enzyme-linked receptors are usually single-pass transmembrane proteins upon activation they function as an enzyme or are linked with enzymes (Alberts *et al* 1994).

## 1.1.1.3 Antibodies

Antibodies are proteins that bind very tightly to their targets (antigens) and are produced in vertebrates as a defence against infection. These are found in the blood and tissue fluids, as well as many secretions. They are part of the of the humoral immune response and act as recognition elements. Each antibody molecule is a Y-shaped protein consisting of four polypeptide chains, two identical light chains and two identical heavy chains connected by disulfide bonds. The two identical binding sites on the antibody bind to the surface of the antigen. They are soluble proteins called immunoglobulins, that are synthesised and secreted by B cells of the immune system (B cells are lymphocytes that play a large role in the humoral immune response). According to differences in their heavy chain constant domains, immunoglobulins are grouped into five classes or isotypes: IgG, IgA, IgM, IgD, and IgE. Each class is characterised by its specific heavy chain amino acid sequence and this specificity gives each class its own unique functional properties. The antibody consists of two specific identical binding sites that bind to the surface of the antigen. The binding or the recognition of the antibody to the antigen surface involves only a small site known as the epitope. The formation of the antibody-antigen complex activates further immune responses such as the complement cascade, complement is a group of serum proteins which work with (complement) antibody activity to eliminate pathogens i.e. foreign bodies. The interactions in the antigen-antibody reaction are mainly based on non-covalent interactions between ionic and polar groups of the amino acid groups, but van der Waals and hydrophobic interactions also play a role (Patrick 1995).

To explain the mechanism of antibody formation, Linus Pauling (1940) was one of first to establish this by his 'instructional theory'. He proposed that the body formation took place in the presence of an antigen

25

that acts as a template around which the antibody is formed. Subsequently, this theory was proven wrong, the perception however inspired other researchers to adapt the theory to make synthetic receptors, such as molecularly imprinted polymers.

## 1.1.2 Synthetic molecular recognition

Molecular recognition is inherent to the function of biological systems, more specifically for biological activity, where the recognition processes demonstrated by naturally occurring macromolecules such as antibodies, enzymes and receptors rely upon the highly specific complementary interactions between the binding site and binding moiety. The recognition system that provides the basis for these to take place is based on the protein. This has been further developed in laboratories with techniques such as protein-based assays, immuno-affinity chromatography columns, protein-based high-performance liquid chromatography (HPLC) columns and enzyme catalysed reactions. Then again, these techniques were extremely sensitive to changes in conditions, intolerant to misuse and expensive. Due to this a lot of attention on synthesising biomimetic systems that possess innate durability, relability and cost-effectiveness for such recognition elements is being invested on by the scientific research world (Allender et al 1999).

One such example of this was guest-host chemistry that led to some elegant approaches to synthetic molecular recognition. Intermolecular forces allow its complementary arrangement to hold the guest-host complex together. The guest is defined as being either an organic molecule or ion whose binding site diverges n the complex. Whereas the host is defined as being either an organic molecule or ion whose binding site converge in the complex (Kyba et al 1997). This guest-host approach has been utilised by the groups of Pedersen, Lehn and Cram to perform pioneering work that in 1987 enabled them to achieve the Nobel Prize in Chemistry. The pioneering work was performed on compounds such as the crown ethers, cryptands and spherands. The first crown ether, dibenzo-18-crown-6 was synthesised by Pedersen (1967; 1967a). From this study it was established that the crown ether had an ability to carry inorganic ions and primary ammonium ions through organic media. Crown ethers are macrocyclic compounds containing several oxygen atoms, usually in a regular pattern. Cryptands are similar to the crown ether but also contain nitrogen and were first synthesised by Lehn et al (1969; 1969a). The study performed on these compounds showed similar properties to that established by the crown ethers. Spherands synthesised by Cram (Cram and Cram 1978; Cram et al 1979) possess a single conformation ideally arranged for binding cations. Despite this, this approach has major negative aspects in that it is far from generic with each recognition problem necessitating a novel solution. Once more this involves expensive, time-consuming and complex chemistry (Allender et al 1999).

This approach has been the use of naturally-produced macromolecular recognition systems such as cyclodextrins. Cyclodextrins are cyclic (α-1,4)-linked oligosaccharides of a-D-gluco-pyranose containing a relatively hydrophobic central cavity and hydrophilic outer surface and form a cone shape. The natural cyclodextrins are produced from starch by the action of cyclodextrin glycosyltransferase (CGTase), an

enzyme produced by several organisms and act generally as recognition sites. These molecules have the ability to remove hydrophobic organic molecules from aqueous media. The group led by Breslow (1982) combined the hydrophobic binding pocket of cyclodextrins with other functionalities to attain derivatives, which possess catalytic activities. In addition, to this other examples of synthetic molecular recognition include molecular clefts as recognition elements with different structures developed by Rebek (1990). These compounds were not only able to recognise certain molecules (such as guanine) but also had catalytic abilities. Artificial receptors have been synthesised for a variety of molecules such as caffeine (Ballester *et al* 2000), amino acids (Lustenberger *et al* 1998) and proteins (Park *et al* 1999).

### 1.1.3 Molecular imprinting

This thesis belongs within the area that has, within the past few years shown a stimulation of interest of molecular Imprinting, especially during the nineteen-nineties. It mainly involves systems related to that developed by the group of Mosbach, which generally demonstrated the versatility of the non-covalent approach, as well as the use of molecular imprinting in various applications.

Molecular Imprinting involves the functional monomer (small multi-functional molecule) undergoing a regiospecific and complementary association (usually *via* hydrogen bonding) about the template and the spatial orientation of the monomer being fixed by copolymerisation with a cross-linking agent. The functional monomer becomes part of the polymer backbone whereas the template is held only by non-covalent interactions hence, resulting in the synthesis of a molecularly imprinted polymer (MIP). Subsequent removal of the template leads to the formation of cavities within the polymeric structure that function as specific recognition sites (**Figure 1**) (Castro *et al* 2001). These mimic the binding sites of antibodies and other biological receptor molecules.
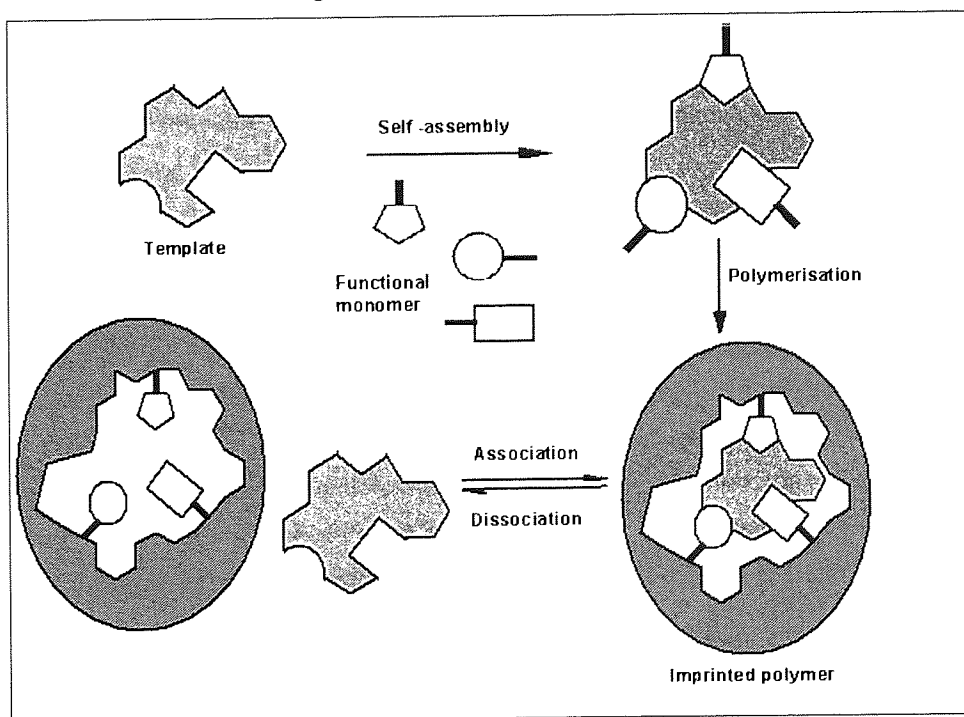


**Figure 1:** The Molecular imprinting process.

## 1.1.4 An historical overview on the development of molecular imprinting

Although the widespread interest in molecular imprinting is new, the concept itself has a long history. In 1972, the concept of molecular imprinting, was reported independently by, Wulff and Sarhan (1972), and Klotz and Takagishi (1972) involving the preparation of organic polymers with predetermined ligand selectivities. This innovative concept was further developed by laboratories of Wulff, Mosbach and Shea. Even as early as the 1930s, forty papers describing a similar concept appeared. This work involved the preparation of ligand-selective recognition sites in inorganic matrix silica.

### M.V.Polyakov

Around the thirties a soviet chemist M.V.Polyakov demonstrated molecular imprinting, when investigating the use of silica in chromatography. He prepared silica by acidifying sodium silicate solutions and allowed these to dry, resulting in a rigid matrix. In his 1931 paper, he investigated silica pore structure with the presence of additives like benzene, toluene and xylene. These different additives or templates were added at the drying stage for a period of about 20-30 days at room temperature then washing off the additives. After that two polymerisation initiators were used one being sulphuric acid and the other ammonium carbonate. The former initiator rendered a positive correlation between surface areas and molecular weight of the additives. The latter gave a different result in that the extent of adsorption of different additives depended upon the structure of the additives.

Polyakov came to the conclusion that the differences observed for silica polymer formation rate and extent were directly linked to the ammonium carbonate that caused the evident selectivity. This selectivity was related to the variations in the silica structure caused by the presence of the additive that was expected to replace the water on the silica surface. More detailed work was published in 1933 and 1937 concerning this selective molecular recognition. From these studies it was gathered that additives (templates) directly affected the resultant silica surface. In spite of that, Polyakov's studies went unnoticed (Sellergren 2003).

### Pauling

After this work more focus was being put on biochemical processes and structures of biomolecules. Linus Pauling carried out the most vital studies to establish this area. His work involved practical implications of the nature of the chemical bond (in protein structure and function), α-helix and β-sheet structures, the molecular-level explanation to sickle-cell anaemia and early transition-state theory of catalysis.

Another important contribution made by Pauling concerned the study of the mechanism of antibody formation in an immune defence system. For this many diverse concepts had developed this included 'selective theory' and 'instructional theory'. The former theory postulated that white blood cells had diverse antibodies on its surface and when an antigen linked chemically to it, this in turn provoked production of copies of that particular selective antibody. The latter theory was suggested by a number of scientist including Pauling (see section 1.1.1.3).

Pauling's fellow student, Frank Dickey whose experiments were similar to that of Polyakov, did more work. The key difference in Dickey's method was that instead of adding the additives (template) at the drying stage, he added these prior to polymerisation (Dickey, 1949; 1955). Dickey used a collection of alkyl orange dyes as templates that were extracted and evaluated molecular recognition properties of the resulting silica polymers.

The work carried out by Dickey, however, laid the basis for molecular imprinting, but the actual term came into existence in the 1960s after seminal investigations carried out by Mosbach and Mosbach (1966). Following on from that it was in the 1970s that the science population due to Wulff's studies accepted the imprinting process. In the 1970s Wulff, formed reversible covalent bonds between a monomer and the template molecule, followed by polymerisation in the presence of a cross-linking monomer and porogen. This was followed by template cleavage to yield a specific binding site. Then again the limitations with this method is that chemical cleavage of the template molecule from the polymer needs to take place (Wulff and Sarhan 1973). In contrast Mosbach's approach of constructing a pre-polymerisation complex between monomer-template was done non-covalently in solution and this advancement enabled molecular imprinting to be used in a variety of applications.

## 1.1.5 Different approaches to molecular imprinting

The fundamental part of molecular imprinting is to create a stable pre-polymerisation complex between a template and monomer. Covalent bonding, non-covalent interactions or a combination of both can establish this complex. The monomer is incorporated into the polymer matrix during polymerisation by using cross-linking agents and forms the recognition site in the cross-linked polymer matrix. In the imprinting process the polymeric matrix structure is very important as this governs the fixed arrangement of the binding sites, therefore the optimisation of the polymer structure is very important. The polymer matrix should therefore be rigid enough to maintain its shape, size and functionality within the binding sites, as without this rigidity, the specificity is greatly decreased. Then again the binding sites should be accessible to allow the ligand to rebind to the site in the rebinding process. Thus a compromise between accessibility and flexibility has to be made. Another aspect of the polymer matrix is mechanical and thermal stability that should be enough to withstand the treatment in the preparation, process and application of the molecularly imprinted polymers. The traits that will be discussed later in the section that affect the characteristics of the polymer matrix are such as functional monomer, cross-linker, porogen/solvent, template, temperature of polymerisation and finally initiator.

At present the use of the molecular imprint methodology can be applied to various fields and shall be discussed in the applications section.

## 1.1.5.1 Covalent imprinting approach

In the covalent approach the monomer and template interact by forming covalent bonds between them to form the pre-polymerisation complex. This complex has to have the ability to endure polymerisation conditions such as high temperature. Co-polymerising the complex with cross-linking agents follows this and hence this incorporates the template within the polymer matrix. The most vital prerequisite is that the bond between the template and polymer has to be readily reversible to allow ease of template removal and the covalent bonds between template and polymer are cleaved. The cleavage of a template has to be performed under conditions that do not modify the functionality and spatial arrangement of the imprinted site. This process then renders vacant imprinted sites. Rebinding of the template to its binding site within the polymer matrix can be achieved by restoring the original bonds or by non-covalent interactions formed for the functional groups originally within the imprinted site.

Wulff, as a basis of his covalent approach, used the rapid and reversible nature of the boronic acid/diol reaction (Wulff 1995). One such example that utilised this nature is for the imprinting of phenyl-α-D-mannopyranoside (PMP) to which two molecules of 4-vinylphenylboronic acid (VPBA) are bound by esterification with two hydroxyl groups of the sugar to form the boronate diester of PMP. The resultant boronate sugar was then cross-linked by employing acrylic cross-linker monomer to give a macroporous polymeric product. The removal of the template PMP was performed under mild hydrolytic conditions (**Figure 2**). Note that this approach has been used considerably in the imprinting of fructose derivatives in which the resultant polymers have been used to resolve free-sugar racemates (Wulff *et al* 1977; Wulff and Schauhoff 1991).
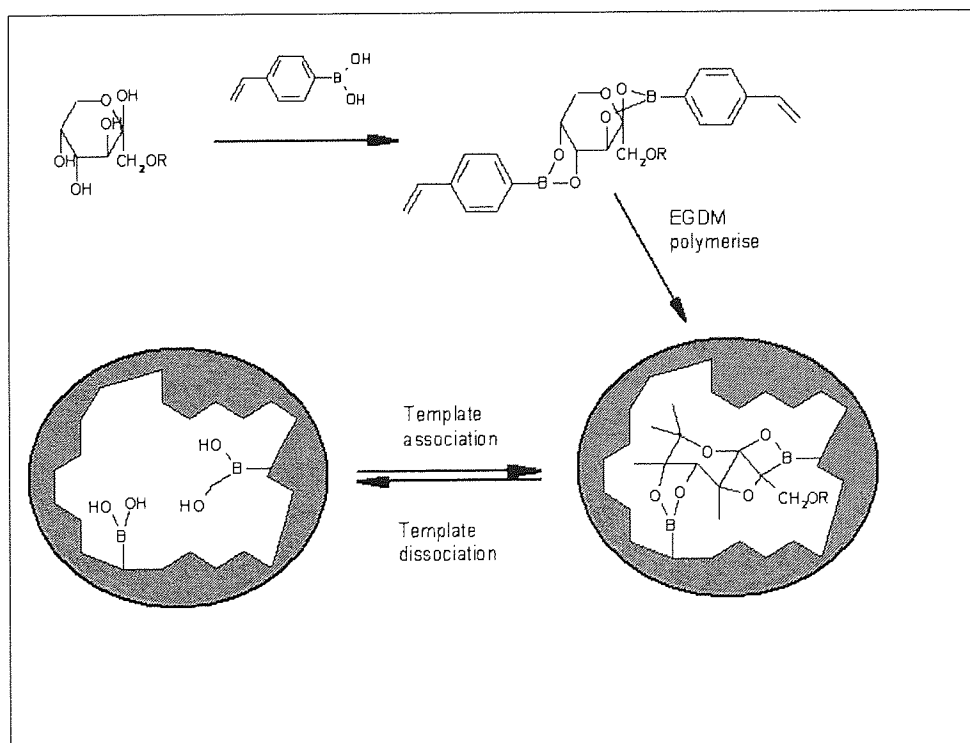


**Figure 2**: Covalent molecular imprinting utilising boronic ester approach for PMP using VPBA.

Wulff's first covalent system used a boronic ester in combination with an amide bond during polymerisation to yield binding sites where the rebinding involved the reformation of a boronic ester linkage, and where the primary amine resulting from cleavage of the preorganised complex bound the analyte through non-covalent interactions (Wulff and Sarhan 1972). There are other examples of other types of covalent bonds that have been applied for molecular imprinting (**Table 1**).
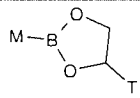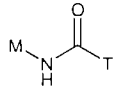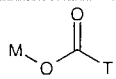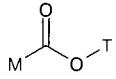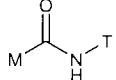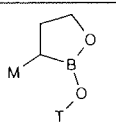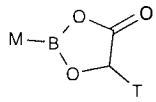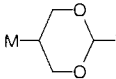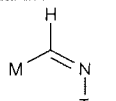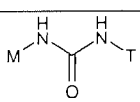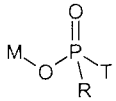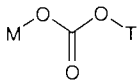
| Bond Type | | Monomer Functionality | Template Functionality | Reference |
|---|---|---|---|---|
| Boronic ester | | Boronic acid | Vic-diols | Wulff and Sarhan 1972 |
| Carboxylic amide | | Amine | Carboxylic acid | Wulff and Sarhan 1972 |
| Carboxylic ester | | Alcohol | Carboxylic acid | Shea and Thompson 1978 |
| Carboxylic ester | | Carboxylic acid | Alcohol | Sellergen and Andersson 1990 |
| Carboxylic amide | | Carboxylic acid | Amine | Sellergen and Andersson 1990 |
| Boronaphtalide ester | | Boronaphtalide | Alcohol | Smith et al 1994 |
| Dioxaboronanone | | Boronic acid α-hydroxy | Carboxylic acid | Sarhan 1982 |
| Ketal | | Diol | Ketene | Shea and Dougherty 1986 |
| Imine | | Aldehyde | Amine | Wulff et al 1984 |
| Dialkyl urea | | Isocyanate | Amine | Lübke et al, 1998 |
| Phosphonic ester | | Alcohol | Phosphonic acid | Sellergen and Shea, 1994 |
| Carbonic ester | | Carbonic acid | Alcohol | Whitcombe et al 1995 |

**Table 1**: Covalent bonds used in molecular imprinting, where M denotes monomer residue and T template residue.

Shea *et al* used an alternative approach based on ketone/ketal. In this approach the ketone templates were reversibly bound to the functional monomers creating the ketals. Similar to the covalent approach the ketal templates were employed to pre-situate the functional groups within the polymer cavity. The reversibility of the reaction allowed the removal of the ketone template as well as allowing the rebinding to accurately positioned 2-(p-vinylphenyl)-1,3-propanediol (VPD) groups under specific conditions (**Figure 3**) (Shea and Dougherty 1986; Shea and Sasaki 1989; Shea and Sasaki 1991).
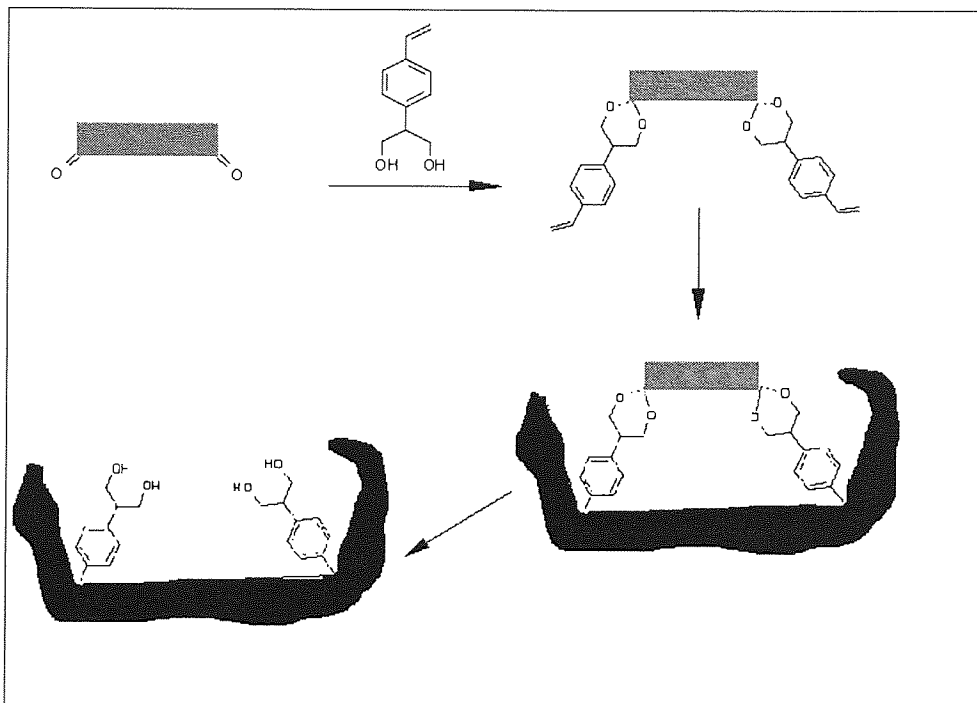


**Figure 3**: Ketone/Ketal approach to covalent imprinting using VPD.

To establish the rebinding specificity of diketones a variety of ketones with differing inter-carbonyl distances were employed and rebinded to a single template imprinted polymer. The study found that small changes in the carbonyl distances compared to the original distance changed the rebinding selectivity.

Another approach to covalent imprinting was by utilising Schiff bases as monomers to generate highly specific polymers. In this particular study it was determined that the equilibrium position was favourable but the rate of formation and breaking of the imino bond was slow. Hence this rate was too slow to be applicable for chromatographic application, which is a means of assessing the selectivity of the imprint (Wulff *et al* 1984).

## 1.1.5.2 Non-covalent imprinting approach

Mosbach *et al* first established the non-covalent approach in 1981 (Arshady and Mosbach 1981) and it is in the early eighties that increased interest in this method was given due to it generating comparable results to the covalent approach. In this approach and in any approach to form MIPs the stabilisation of the pre-polymerisation complex is vital and in this approach the interaction between the monomer and template is non-covalent. Non-covalent interactions include ionic interactions, hydrogen bonding, van der

waals and charge transfer. Note that hydrophobic, dipole-dipole and π – π coulombic forces also have a role in template polymerisation (Arshady and Mosbach 1981; Nicholls *et al* 1995a). The integrity of the pre-polymerisation complex that is held by non-covalent interactions determines the binding properties of the polymer (Nicholls 1995). The next important part of imprinting is polymerisation of the pre-polymerisation complex that takes place in the presence of a cross-linking monomer, porogen and thermal initiation, UV or γ-irradiation. The porogen employed for such studies are non-polar solvents such as chloroform, toluene, dichloromethane and benzene that favour polar interactions between the template and monomer, however acetonitrile has also been widely utilised for these studies (Allender *et al* 1999). The polymer monolith obtained is normally ground to gain a particle size that is appropriate for the study in question followed by sieving and sedimenting.

One such example of non-covalent imprinting is for theophylline, where methacrylic acid (MAA) was used as a functional monomer to form hydrogen bond interaction with the print molecule (**Figure 4**). In this study the pre-polymerisation complex was co-polymerised with a cross-linker, trimethylolpropane trimethacrylate (TMPTA) that provides a binding site specific to the template molecule, e.g. the polymer was able to recognise minor differences between theophylline and the closely related caffeine (Vlatakis *et al* 1993; Ye *et al* 1999).
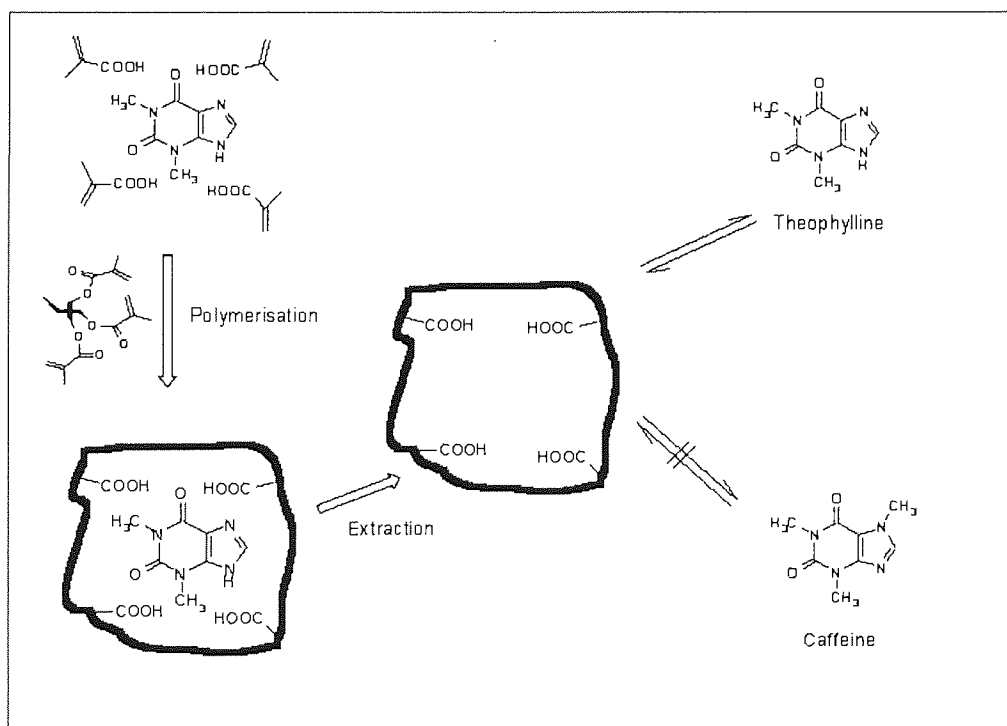


**Figure 4**: An example of non-covalent molecular imprinting of theophylline.

The drawback however, in gaining a particle in the manner mentioned before, is that the starting material is removed in large quantities (Mayes and Mosbach 1997). Thus an approach was developed that circumvented this problem, by developing MIPs as beads (Ye *et al* 1999a), membranes (Piletsky *et al* 1999) and coated particles (Vidyasankar *et al* 1997). After completion the template was easily removed by solvent extraction leaving a vacant complementary imprinted site in the polymer. The rebinding specificity

relied upon re-establishing non-covalent interactions that were present initially when forming the stabilised pre-polymerisation complex.

Wizeman and Kofinas (2001) performed a study by employing MIPs as hydrogels to isomerically resolve glucose rebinding. This involved non-covalently molecular imprinting of poly(allylamine hydrochloride) with glucose phosphate mono-sodium salt to produce a MIP hydrogel when cross-linked. The hydrogels demonstrated higher binding capacities of glucose than fructose in the same polymer. In addition MIP hydrogels have also been employed for studying protein imprinting by Hawkins *et al* (2005).

### 1.1.5.3 Metal coordination

The very first reported metal-ion imprinted resins that absorb guest metal ion selectively from weak acid solution was demonstrated by Nishide *et al* (1976). The metal-ion imprinted polymers are classified on the basis of the polymerisation procedures established by Tsukagoshi *et al* (1993) into three groups. The first is the linear chain polymers that carry metal-ion binding groups that are cross-linked with bifunctional monomers in the presence of metal ions (Nishide *et al* 1976). The second is the polymerisation of a mixture of monomers containing complexing groups (Kato *et al* 1981). The third is surface imprinting, where the guest ion interacts with the carboxylate polymeric spheres in the water suspension to form a complex. These spheres are then cross-linked *via* γ-radiation to generate a rigid structure. Removal of the metal-ions leaves the carboxylate groups in a fixed position on the surface that is required for complexing with their corresponding cations (Yu *et al* 1992).

Metal complexes have also been employed for imprinting, as metal-ion coordination, used for binding purposes. They used specific coordination site for chiral amino acids, where a Schiff base-$Co^{3+}$ complex was co-polymerised with styrene and divenylbenzene. The amino acid bound to metal complex was removed. A very high selectivity in optical resolution of the ligand (α-682) was obtained, but mass transfer rate was to slow for chromatographic separation applications (Fujii *et al* 1984; Fujii *et al* 1985). More recently Yamazaki *et al* (2001) have used $Co^{2+}$-imidazole complexes to prepare hydrolytically active MIP phosphotriesterase mimics.

A further example of this approach is the $Cu^{2+}$ chelation employed for imprinting organic molecules developed by Dhal and Arnold (1991). This approach is similar to the non-covalent approach in the choice of cross-linker, initiator and method of polymerisation. The template models are based on a series of bis-imidazoles (protein analogues) that are used for the recognition of proteins (**Figure 5**). The preparation of the MIPs was performed in methanol successfully, as allowed by the relatively high stabilities of the ternary coordination complexes (Dhal and Arnold 1992). The commonly used chelator for such systems was N-(4-vinylbenzyl)-iminodiacetic acid, VBIDA (pentadentate ligand). This complex was co-polymerised with ethylene glycol dimethacrylate, yielding a selective polymer that after the reintroduction of copper ions, revealed a preference for the template when the rebinding was analysed.
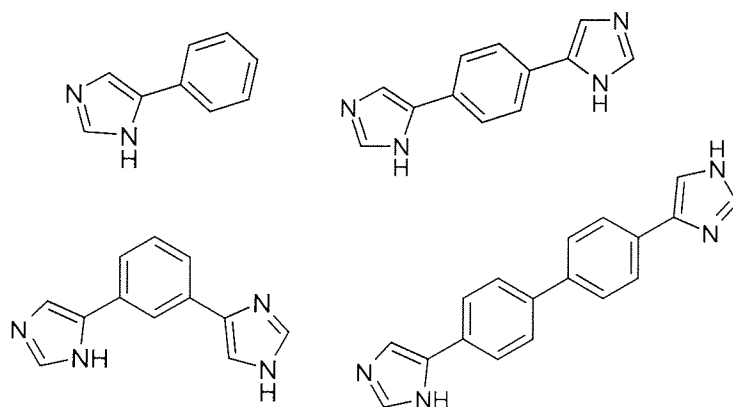
**Figure 5**: A selection of templates used by Dhal and Arnold (1991) for the development of $Cu^{2+}$ chelation based MIP systems.

$Cu^{2+}$ complexes were used to imprint ribonuclease A on the surface of silica particles as reported by the work of Kempe *et al* (1995). During pre-arrangement, two ribonuclease A surfaced the histadine residues to coordinate with polymerisable $Cu^{2+}$ chelating monomers. The complex become immobilised on the surface of the activated silica particles during polymerisation. Enzyme removal left specific recognition sites (**Figure 6**).
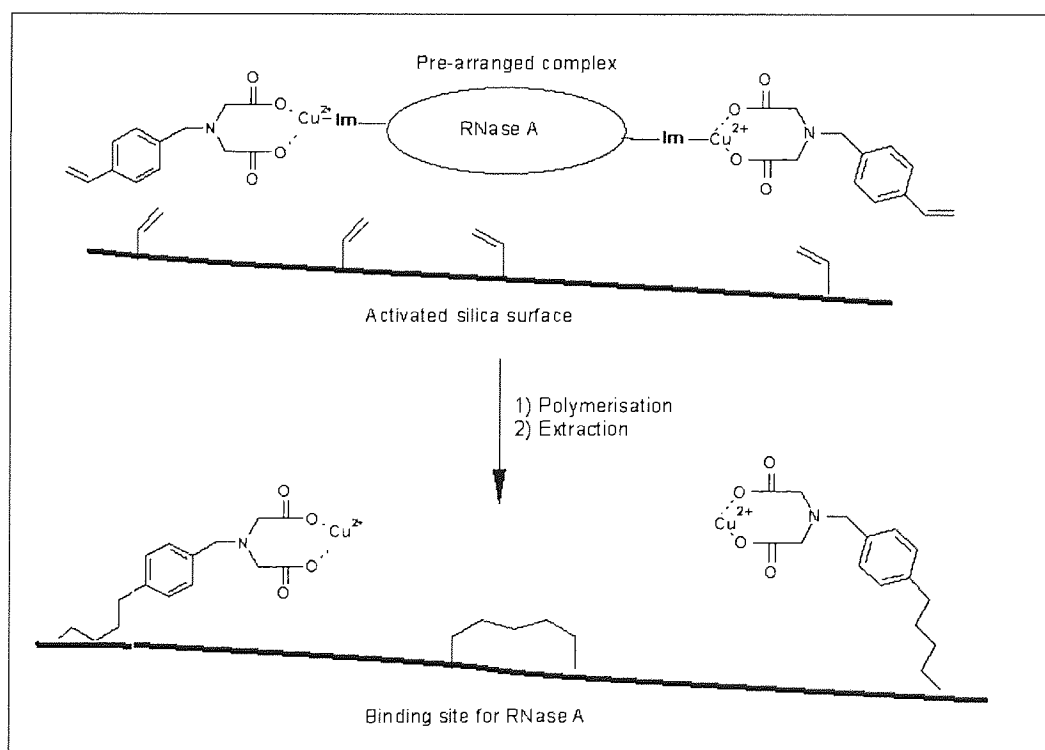


**Figure 6**: Schematic representation of protein imprinting on silica surfaces derivatised with methylacylate groups. Imidazole (Im) of surface-exposed histidines on the protein and the monomer N-(4-vinylbenzyl)-iminodiacetic acid (VBIDA) coordinate metal ions. The derivatised silica particles were added and the polymerisation was initiated. The protein was subsequently removed by treatment with EDTA. The metal-binding ligands were positioned on the surface so as to selectively recognise and rebind, in the presence of metal ions, the protein present during the imprinting.

Beads have also been employed as ion-imprinted polymers for the selective removal of ions. Such as in the case for the work reported by Yavuz et al (2005) for the removal of iron (III) from iron (III)-overdosed human plasma. The iron (III) was complexed with N-methacryloly-(l)-glutamic acid (MAGA) and the iron (III)-imprinted poly(HEMA–MAGA) beads were synthesised by suspension polymerisation. The study found that the selective coefficient of imprinted beads for the ion was greater than that for the non-imprinted matrix.

## 1.1.5.4 Combination of covalent and non-covalent imprinting

This approach is a combination of non-covalent and covalent approaches. The strategy for this method involves using the covalent bonds for imprinting that allows the functional groups to be fixed within the MIP and the non-covalent bonds to be used for the rebinding step. The approach of combining both has improved binding site homogeneity, reduced non-specific binding and improved kinetics (Sellergren and Andersson 1990).

This approach was initially demonstrated by Sellergren and Andersson (1990) for the imprinting of structural analogues such as the one in question in this particular study for L-p-aminophenylalanine ethyl ester. An analogue a diacrylol ester of $N^2$-propionyl-L-2- amino-3-(4-hydroxyphenyl)-1-propanol was used and covalently bound to a polymer group *via* ester linkage that would appropriately position carboxylic acid residues in the polymer. This function was done after polymerisation and basic hydrolysis, the two carboxyl groups were left in the polymer matrix that were capable of forming hydrogen bonding and ionic interactions with the amine group of the amino acid. The drawback of this study was that resultant polymer had binding preference for the D-form instead of the practically used L-form. A study performed by Byström et al (1993) used this approach to synthesis MIPs for the selective reduction of ketones.

Sarhan and Wulff (1982) covalently imprinted D-glyceric acid *via* boronic and amino acid groups. The amine group in the binding site was capable of establishing electrostatic interactions with the template molecule. Practically only a reasonable separation of D and L-form of glyceric acid was attained. Joshi *et al* (1999) demonstrated MIP recognition sites for phenol by employing phenyl methacrylate as a template monomer. After ester hydrolysis the carboxylic acid residue was hydrogen bond to phenolic hydroxy group and the resultant polymers had the capability to distinguish between phenol and biphenol A.

This approach was further developed by Whitcombe *et al* (1995) to imprint cholesterol a poorly functionalised molecule. The method employed a 'sacrificial spacer', the carbonate group. The cholesterol molecule was transformed into the template cholesteryl (4-vinyl)phenyl carbonate and was covalently imprinted to the polymer. The carbonyl group ('sacrificial spacer') after basic hydrolysis and loss of $CO_2$, cleaved the group, which rendered a recognition site that has a phenolic residue that is capable of interacting with cholesterol *via* hydrogen bonding (**Figure 7**).
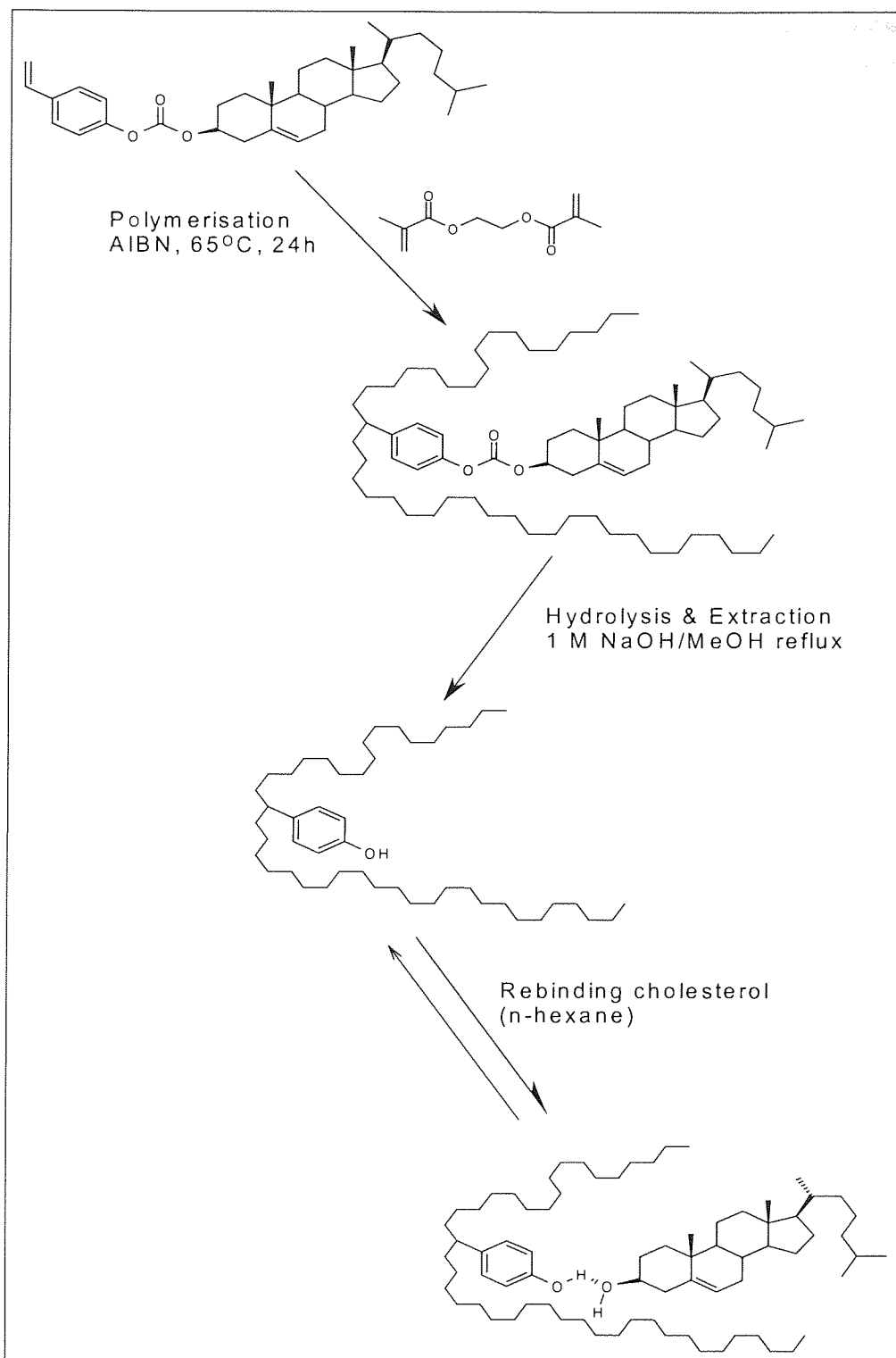
**Figure 7:** Scheme illustrating the imprinting of cholesterol by the sacrificial spacer method.


## 1.1.5.5 Non-covalent vs. covalent approach

The advantage of the covalent approach is that the functional binding groups are placed only in the binding sites rather than throughout the polymer matrix and this results in polymers with low-specific binding in comparison to the non-covalent approach (Wulff and Biffis 2001). Then again the limitations for

this method is that a suitable system in which the covalent bonds can be easily cleaved and re-formed is not possible in every case. In addition, the template requires chemical modification that results in the preparation to become complex and time-consuming. Besides this, the kinetics of formation and disruption of these reversible covalent interactions are limiting for many applications. It is only in the case of boronic esters that the rebinding reactions were sufficiently fast to be applied in chromatography (Wulff and Poll 1986; Wulff and Vesper 1978). Another limitation is the removal of a template. In cases where boronates and Schiff bases are used, washing in methanol to remove them can hydrolyse these. For chemical bonds like ketals, amides and carboxylic esters more harsh reaction conditions are required for template removal.

The non-covalent approach has accounted for the rapid rise in the number of publication and MIP research groups. This is due to the simplicity of polymer preparation and the wide range of compounds, which can be applied. This approach in comparison to the covalent approach is more versatile, practically more straightforward and rebinding kinetics are greater.

Nevertheless this method does have some drawbacks. For instance, the association constant between the template and monomer in solution is low and thus more monomer is required to shift the equilibrium towards the pre-polymerisation complex state. The excess number of functional monomers results in random binding with the polymer matrix, causing an increase in the formation of unfavourable non-selective binding sites i.e. heterogeneity (Sellergren 2001). Then again polymerisations at low temperature can also be utilised, as these conditions also favour association. In contrast the monomer and template ratio is stoichiometric in the covalent approach and this leads to the reduction in non-specific binding. Another associated problem in particular with this approach, is template leaching, which is as a result of incomplete template removal. This is a major issue when MIPs are being considered for quantification purposes especially at low concentrations of analytes (Ellwanger et al 2001).

## 1.1.5.6 Template

A template in simple terms can be your foot leaving its footprint in the mud or as suggested by Steinke et al 1995: "A template induces the self-assembly of molecular components to allow reaction or transformation to take place in forming a novel molecular structure; thereafter the template is separated from the novel structure".

The template that is utilised in the imprinting process must contain a certain level of functionality that can be paired with reciprocating moieties on the functional monomer. Template molecules that are small and multi-functional give rise to more specific polymers, however other factors like solubility and rigidity also contribute towards this specificity. Then again if a template has multiplicity of functional groups that are able to interact with the monomer, this can cause heterogeneity of the binding site (Takeuchi and Matsui, 1996). As for large and mono-functional templates these give rise to less specific imprints.

By employing the non-covalent approach a diverse number of templates have been successfully imprinted. For instance steroids (Cheong et al 1997), proteins (Shi et al 1999), peptides (Rachkov and

Minoura 2001), amino acids (Sellergren *et al* 1985; Andersson *et al* 1984; Andersson and Mosbach 1990; Kempe and Mosbach, 1995a), drugs (Suedee *et al*, 2000), dyes (Arshady and Mosbach, 1981), nucleosides (Spivak and Shea 2001), metal ions (Rosatzin *et al* 1991) and more recently polycyclic aromatic hydrocarbons (Dickert *et al* 1999). In contrast the covalent approach entails more specific requirements that leads to the limited number of templates utilised (**Table 2**).

| Template molecules | Pre-polymerisation bond type | Refeference |
|---|---|---|
| Androst-5-enols | Dioxaboronanone | Smith *et al*, 1994 |
| Castasterone | Boronic ester | Kugimiya *et al*, 1998 |
| Testosterone | Carboxylic ester | Cheong *et al*, 1997a |
| L-DOPA | Boronic ester | Glad *et al*, 1985 |
| L-Glutamic acid | Carboxylic ester & imine | Wulff *et al*, 1985 |
| L-Phenylalanine | Imine | Wulff *et al*, 1984 |
| Fructose | Boronic ester | Wulff and Schauhoff, 1991 |
| Galactose | Boronic ester | Wulff and Schauhoff, 1991 |
| D-glyceric acid | Amide & boronic ester | Wulff *et al*, 1973 |
| D-mannitol | Boronic esters | Wulff *et al*, 1973 |
| Sialic acid | Boronic ester | Kugimiya *et al*, 1995 |
| Nicotinamide adenine dinucleotide | Boronic ester | Norrlöw *et al*, 1987 |

**Table 2:** Templates utilising the covalent approach for molecular imprinting.


### 1.1.5.7 Functional monomer


The two main roles played by the functional monomer are firstly that it undergoes a regiospecific, weak and complementary interaction with the template. This enables the template-monomer complex to be incorporated into the polymer matrix by means of a polymerisable unit. Secondly the ability of MIP to recognise a template is directly linked to the functional monomer. To fulfil such roles the choice of monomers is dependent on the template, which has an impact on the molecular recognition process and properties of the end polymer. Note, that the recognition is also improved when the template is attached to more than one functional group, found on the functional monomer. In addition, the choice of monomer can also be influenced by factors such as solubility, stability, the ability of polymerisation and even the cross-interactions with other monomers. As well these factors the conformation also has to be taken into consideration such that conformational rigidity gives higher affinities and conformational flexibility improves kinetics.

In addition to this, the amount of functional monomer influences the number of binding sites found in the MIP. Thus if too little monomer is used this can limit the capacity of the MIP, by producing insufficient MIP–template interaction possibilities. In contrast, more monomer can result in a MIP consisting of highly unspecific binding sites, with interacting groups present in undefined and random areas of polymer rather than the well-defined binding sites (Davies *et al* 2004).

An example of such a monomer that fulfils the criteria is the commonly used methacrylic acid (MAA), which is small, rigid, is both a hydrogen acceptor and donor, and it is able to form ionic bonds with basic functional groups (Andersson and Mosbach 1990; Sellergren and Shea 1993).

This monomer along with other commonly used functional monomers in the non-covalent imprinting is based on acidic, basic and neutral monomers (**Figure 8**). The acidic monomers **2-4** (**Figure 8**) demonstrate analogous characteristics like MAA. The more acidic monomers such as **5-6** (**Figure 8**) in certain studies have improved selectivities (Dunkin *et al* 1993; Matsui *et al* 1997). The most commonly employed basic monomers are based on the vinylpyridines and the vinylimidazoles illustrated in **Figure 8** as monomers **7-10** (Kempe *et al* 1993; Ramström *et al* 1993). Besides these styrylamidines like monomer **14** (**Figure 8**) are able to form very stable complexes with carboxylic acids (Wulff and Schönfeld 1998). The neutral monomers such as **17-20** demonstrates the MIP recognition ability, in addition to this the monomers **20-24** are also able to give hydophilicity, porosity or MIP rigidity.

As for the covalent approach this has utilised a limited number of functional monomers (**Table 1**-previously shown in section 1.1.5.1, gives examples of these monomers).
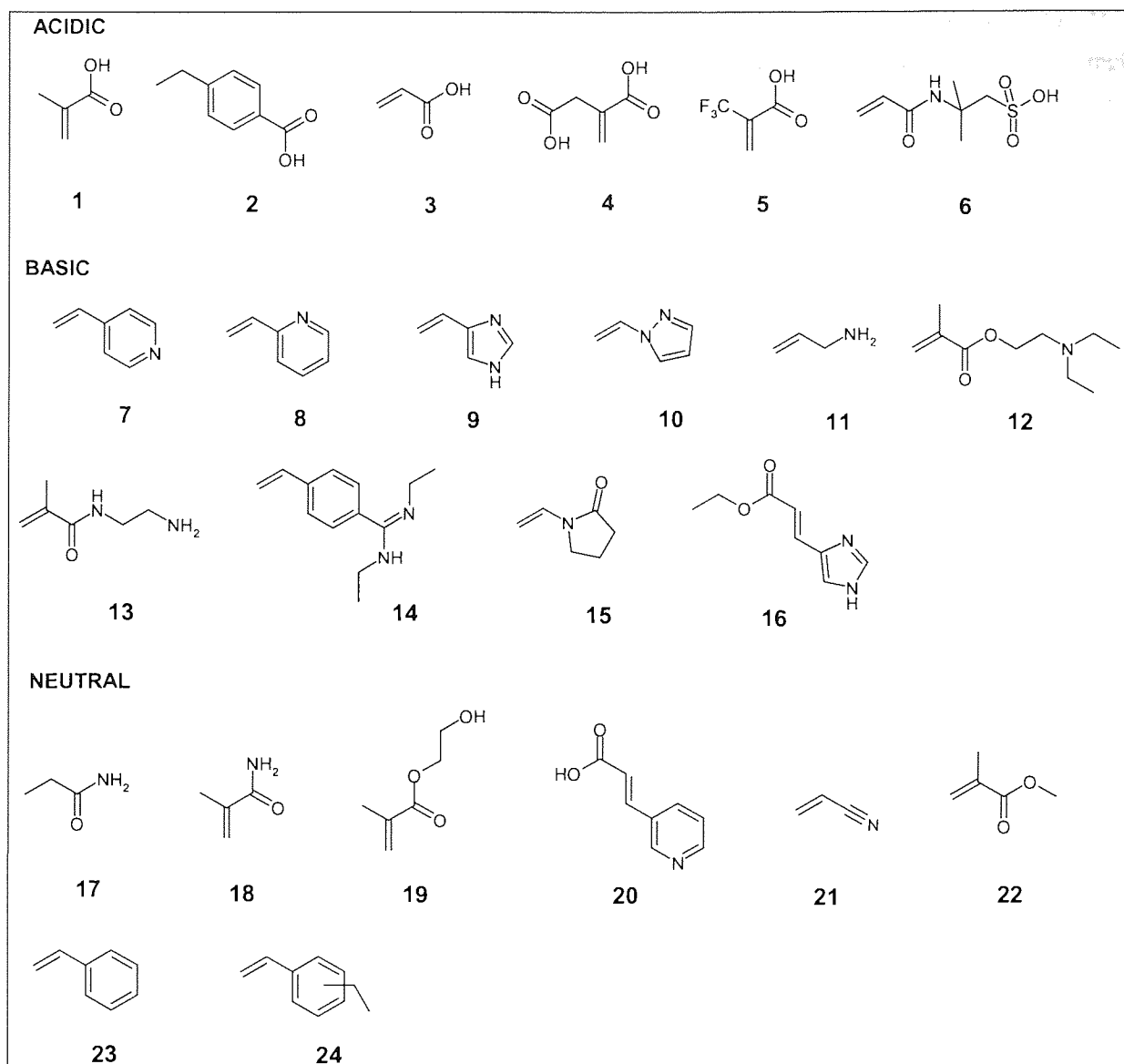
Figure 8: A selection of monomers used in the non-covalent approach.

**Acidic**; **1**: methacrylic acid (MAA), **2**: p-vinylbenzoic acid, **3**: acrylic acid (AA), **4**: itaconic acid, **5**: 2-(trifluoromethyl)-acrylic acid (TFMAA), **6**: acrylamide-(2-methyl)-2-propane sulfonic acid (AMPSA).

**Basic**; **7**: 4-vinylpyridine (4-VP), **8**: 2-vinylpyridine (2- VP), **9**: 4-(5)-vinylimidazole, **10**: 1-vinylimidazole, **11**: allylamine, **12**: N-N'-diethyl aminoethylmethacrylamide (DEAEM), **13**: N-(2-aminoethyl)-mathacrylamide, **14**: N-N'-diethyl-4-styrylamidine, **15**: N-vinylpyrrolidone (NVP), **16**: urocanic ethyl ester.

**Neutral**; **17**: acrylamide, **18**: methacrylamide, **19**: 2-hydroxyethyl methacrylate (2-HEMA), **20**: trans-3-(3-pyridyl)-acrylic acid, **21**: acrylonitrile (AN), **22**: methyl methacrylate (MMA), **23**: styrene, **24**: ethylstyrene.


## 1.1.5.8 Cross-linkers

The cross-linkers ethylene glycol dimethacrylate (EGDMA) (Wulff 1995; Kempe and Mosbach 1995a) and divinylbenzene (DVB) (Villamena and De La Cruz 2001) are most commonly used in the MIP systems, since they are cheap and easy to purify. Other cross-linkers however are available (**Figure 9**).

The cross-linker is a major component in most MIPs as the cross-linking agent makes 80 to 95% by weight. The polymers generated can be rigid that gives ligand accessibility and maintains template definition or flexible that provides good kinetics (free movement of the template molecule), adequate porousity and rapid equilibration of the template in the rebinding step. Thus the choice of cross-linker has to be a compromise between both (Wulff 1986). Note, that besides the type and proportion of the cross-linker, the solvent (porogen) and the method of polymerisation also affect the porosity and internal surface area (Allender et al 1999). Furthermore the choice of cross-linker is also influenced by solubility. Thus the cross-linker should be miscible with the functional monomer, the template and the solvent/porogen to give sufficient flexibility, surface area and framework in the molecularly imprinted polymers.

In a study by Wulff et al (1982) the importance of proportion of cross-linker to selectivity was demonstrated by employing three different cross-linkers EGDMA (27), DVB (25) and tetramethylene dimethacrylate (TDMA, 28). In this study it was established that 0-10% of cross-linker exhibited no selectivity. Increasing the percentage of cross-linker towards 50 rendered a steady rise in selectivity. By further increasing this to 50-70% a rapid improvement in selectivity was observed. From this study EGDMA in comparison to the other structurally variant cross-linkers was considered to be the best, as this cross-linker is suitable for many other imprinting processes. In addition, EGDMA gave better selectivity and resolution in comparison to other new optically active cross-linkers. Overall this study established that a higher proportion of cross-linker gave greater selectivity (Wulff et al 1982; Sellergren 1989). A study reported by Shea (Shea and Sasaki 1989; Shea and Sasaki 1991) on the cross-linkers DVB (25) and diisopropenylbenzene (DIP, 26) found that the latter cross-linking agent was better than DVB. Besides influencing the rigidity and stability of the resultant polymer the cross-linker also plays a role in porosity and hydrophobicity of the polymer.

A comparison study between cross-linkers 27, 32 and 36, 38 (Figure 9) was reported by Sellergren and Shea (1993) to examine their ability to effect enantioselective recognition by employing these to molecular imprint L-phenylalanine anilide. The study revealed that cross-linkers with less free internal rotation such as 27, 32 and 36 in comparison to 38, with a longer and a more flexible spacer, were able to give high enantioselectivities i.e. high separation factor. The EGDMA based MIP (27) showed the highest selectivity.

Kempe (Kempe and Mosbach 1995b; Kempe 1996) investigated the use of tri and tetra functional monomers as cross-linkers i.e. 42-44 (Figure 9). MIPs prepared with trimethylolpropane trimethacrylate (TRIM-42) and pentaerythritol (PETRA-43) as cross-linkers showed a higher loading capacity and selectivity than those prepared with EGDMA.
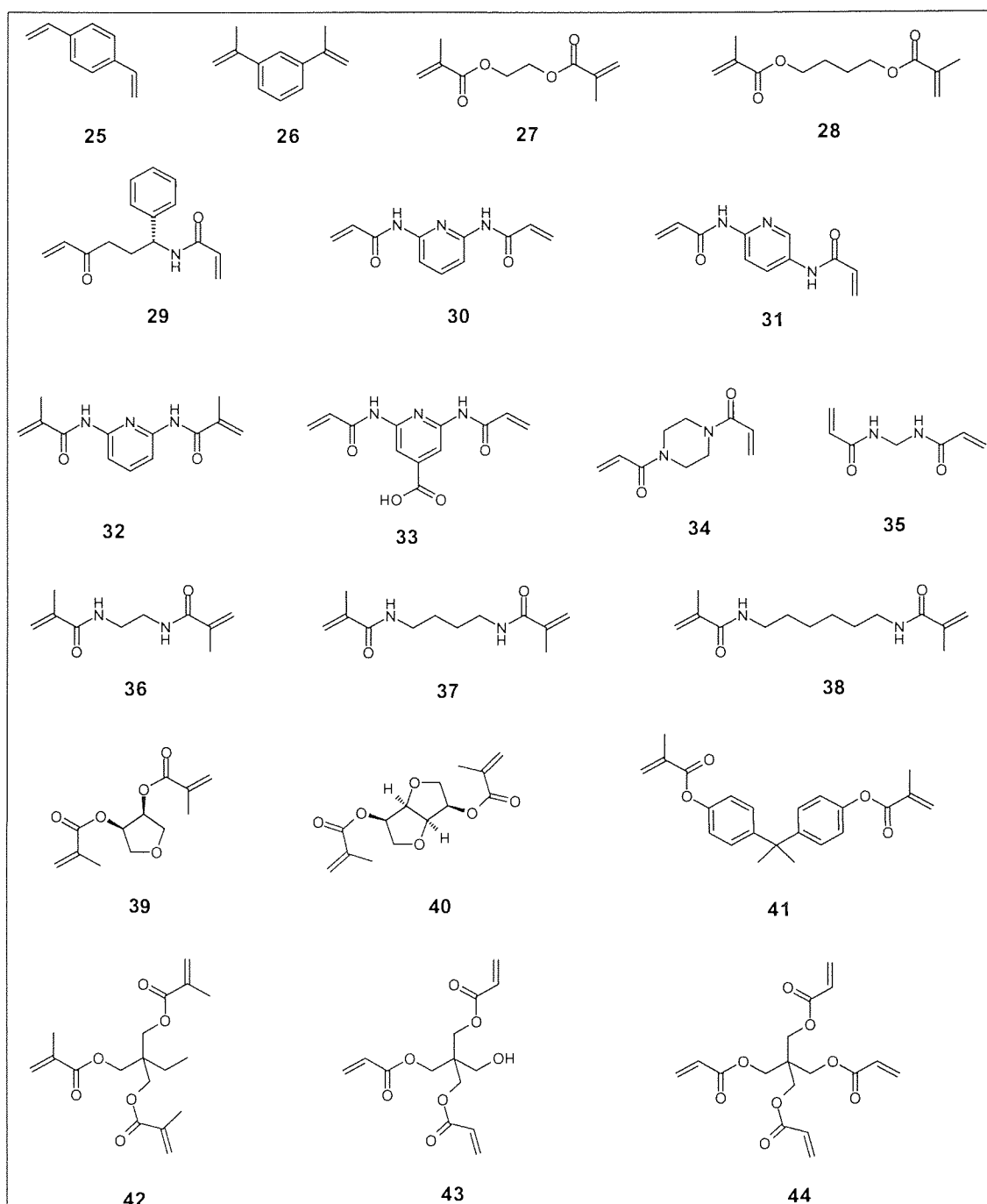
**Figure 9:** A selection of cross-linkers used for molecular imprinting.

**25:** p-divinylbenzene (DVB), **26:** 1,3- diisopropenyl benzene (DIP), **27:** ethylene glycol dimethacrylate (EGDMA), **28:** tetramethylene dimethacrylate (TDMA), **29:** N,O-bisacryloyl-L-phenylalaninol, **30:** 2,6-bisacryloylamidopyridine, **31:** 1,4-phenylene diacrylamide, **32:** N,N'-1,3-phenylenebis(2-methyl-2-propenamide) (PDBMP), **33:** 3,5-bisacrylamido benzoic acid, **34:** 1,4-diacryloyl piperazine (DAP), **35:** N,N'-methylene bisacrylamide (MDAA), **36:** N,N'-ethylene bismethacrylamide, **37:** N,N'-tetramethylene bismethacylamide, **38:** N,N'-hexamethylene bismethacrylamide, **39:** anhydroerythritol dimethacrylate, **40:** 1,4;3,6-dianhydro-D-sorbitol-2,5-dimethacrylate, **41:** isopropylenebis (1,4-phenylene) dimethacrylate, **42:** trimethylolpropane trimethacrylate (TRIM), **43:** pentaerythritol triacrylate (PETRA), **44:** pentaerythritol tetraacrylate (PETEA).

## 1.1.5.9 Solvent/porogen

To gain a highly macroporous polymer a high proportion of cross-linker with solvent in the polymerisation process is required. The reason to synthesise such a material is to allow the free diffusion of molecules inside the polymer matrix. The presence of solvent is necessary as the polymer forms around solvent molecules and hence the solvent is referred to most appropriately as a porogen.

To make the choice of the porogen three significant features have to be taken into consideration: First is that the porogen has the ability to solubilise all polymer constituents; secondly, the porogen effect on the complex forming between the template and monomer i.e. pre-polymerisation complex; thirdly the effect on the resultant polymers morphology i.e. porosity and surface area. For instance in a poor solvent the polymer formed would have random formation of large pores (up to ~10000 Å) and low surface area (~10-50 $m^2g^{-1}$). Whereas in a good solvent the polymer formed would render small pores (~30 Å) and high surface area (up to ~1000 $m^2g^{-1}$). Thus it is the porosity that increases the surface area of the resulting polymer allowing the accessibility of the binding sites during the removal of the template and the rebinding of the ligand. (Sellegren and Shea 1993; Ramström and Ansell 1998)

A study by Sellegren and Shea (1993) and Wulff and Poll (1987) established that porogen influenced polymer morphology, but further established that morphology had no link with MIP selectivity i.e. no structure–selectivity relationship. Moreover, it was recognised that the hydrogen bonding capacity of the porogen influenced MIP selectivity.

In the non-covalent imprinting process, apolar solvents such as dichloromethane, chloroform and toluene are employed, as the polar non-covalent interactions are maximised in this environment. That leads to a stabilised pre-polymerisation complex (Mosbach and Ramström 1996). This occurs because the solutes are not drawn to interact with the solvent and are therefore available in greater quantity to complex. Useful MIPs however, have been synthesised in acetonitrile, where the increased polarity of solvent has been dealt with the increased porosity and internal surface area (Sellegren and Shea 1993). If the interaction is ion-ion, more hydrophilic solvents such as DMF or alcohols may be used. The stability level of the polymer can be directly measured by the recognition capability of the resultant polymer (Nicholls 1995). In addition a study performed by Spivak et al (1997) revealed that MIP selectivity is maximised if the polymer is evaluated in the solvent that it was originally made in (i.e. porogen).

For apolar complexation of more hydrophobic templates, polar solvents have been employed such as water and alcohols (Kirsch et al 2001). Although apolar interactions are maximised in polar solvents these interaction alone are not solely responsible for a stable pre-polymerisation complex, that results in a high performing molecular imprint. Then again these interactions probably play an important role in the recognition process (Dunkin et al 1993; Nicholls et al 1995). Progress in making MIPs in water using the non-covalent approach as yet requires development, even though the basic approach itself has been successful (Andersson 1996).

## 1.1.5.10 Initiator and temperature of polymerisation

Majority of the MIPs are prepared by free-radical polymerisation. Usually the polymerisation process is performed with reaction times between 10 and 24 hours. The polymerisation process is initiated either photochemically or thermally. The commonly employed initiators are azobis-(isobutyronitrile) (AIBN- **45**), azobis-(cyclohexanecarbonitrile) (ACHCN- **46**) and 2,2.-azobis-(2,4-dimethylvaleronitrile) (ABDV- **47**) (**Figure 10**). In addition hydroperoxides, redox initiators and persulfate have also been employed (Ozawa and Klibanov 2000; Haginaka *et al* 1998; Norrlöw *et al* 1984). Examples of these are such as tert-butyl hydroperoxide that is one of the general cationic emulsion and suspension polymerisation initiators for ethylene, vinylacetate and acrylates. Also redox initiators like ammonium persulfate and N,N'-tetramethyl ethylenediamine (TEMED) (Schacht 2004).
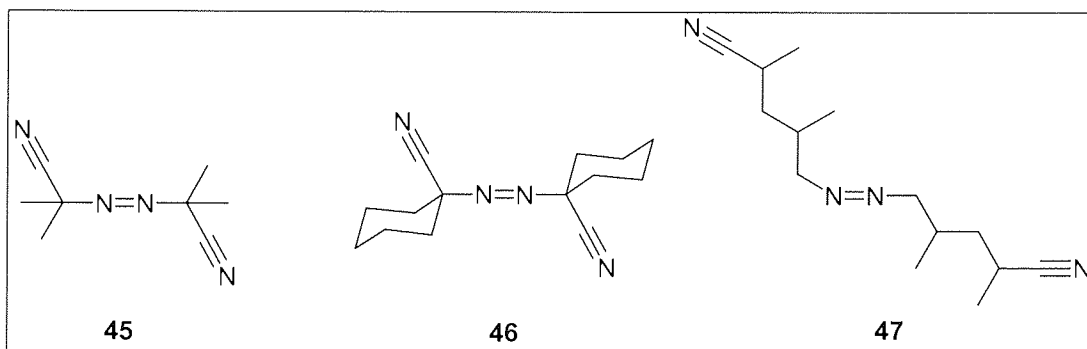


**Figure 10:** The commonly employed initiators.
**45**: azobis-(isobutyronitrile) (AIBN), **46**: azobis-(cyclohexanecarbonitrile) (ACHCN) and **47**: 2,2.-azobis-(2,4-dimethylvaleronitrile) (ABDV).

The azobisnitriles like ABDV and AIBN are decomposed by heat at 40 °C and 60 °C respectively or by ultraviolet light for AIBN that is 366 nm. The polymerisation process involves three main stages: initiation, propagation and termination that will be discussed later on. In the polymerisation process degassing and purging the monomer mixture prior to polymerisation with inert gases such as nitrogen, argon or helium can exclude the problem of premature chain termination. Or applying high vacuum combined with cycles of freezing and warming can also be performed This problem is caused by the presence of atmospheric oxygen that has the ability to accept an additional electron from the radical and results in this event. On the whole most polymerisations to prepare MIPs employ photochemical cleavage of AIBN or ABDV, given that at high temperatures the pre-polymerisation complex has revealed to be unstable by studies performed by O'shannessey *et al* (1989; 1989a).

Studies performed by Milojkovic *et al* (1997) and Sreenivasan (1997) described a polymerisation method that used γ-radiation ($^{60}$ Co) as the source of free radicals and excluded the need of using an initiator in the polymerisation mixture. This method was applied to the imprinting of (+/-) –menthol and testosterone. The polymerisation temperature employed for a thermal polymerisation needs to be low enough to allow the template molecules to arrange the functional monomer to generate a stable pre-polymerisation complex. At the same time allow the formation of radicals throughout the polymerisation process, for a

growing polymer. As the pre-polymerisation complex is formed in solution, entropic factors are decreased. This is obtained by using lower temperatures for polymerisation that reduce the kinetic energy and allow more stability to take place between a template and monomer. Its success in turn generates a stronger recognition site with homogeneity. Studies performed by O'shannessey *et al* (1989; 1989a) have revealed that MIPs prepared photochemically at low temperatures displayed better selectivity than thermally prepared MIPs. In addition polymers prepared at lower temperatures have shown to exhibit higher capacity and resolution factors (Sellergren 1989)

## 1.1.6 The polymerisation process

In general the polymerisation process involves chemically combining relatively small molecules, called monomers to create very large chain-like or network molecules, called polymers. These small units of monomers can be either alike or they can be 2 or more different compounds.

The polymerisation process can be broken down into stages: initiation, propagation, chain transfer and termination (**Figure 11**). The one in consideration for this study is free-radical polymerisation.
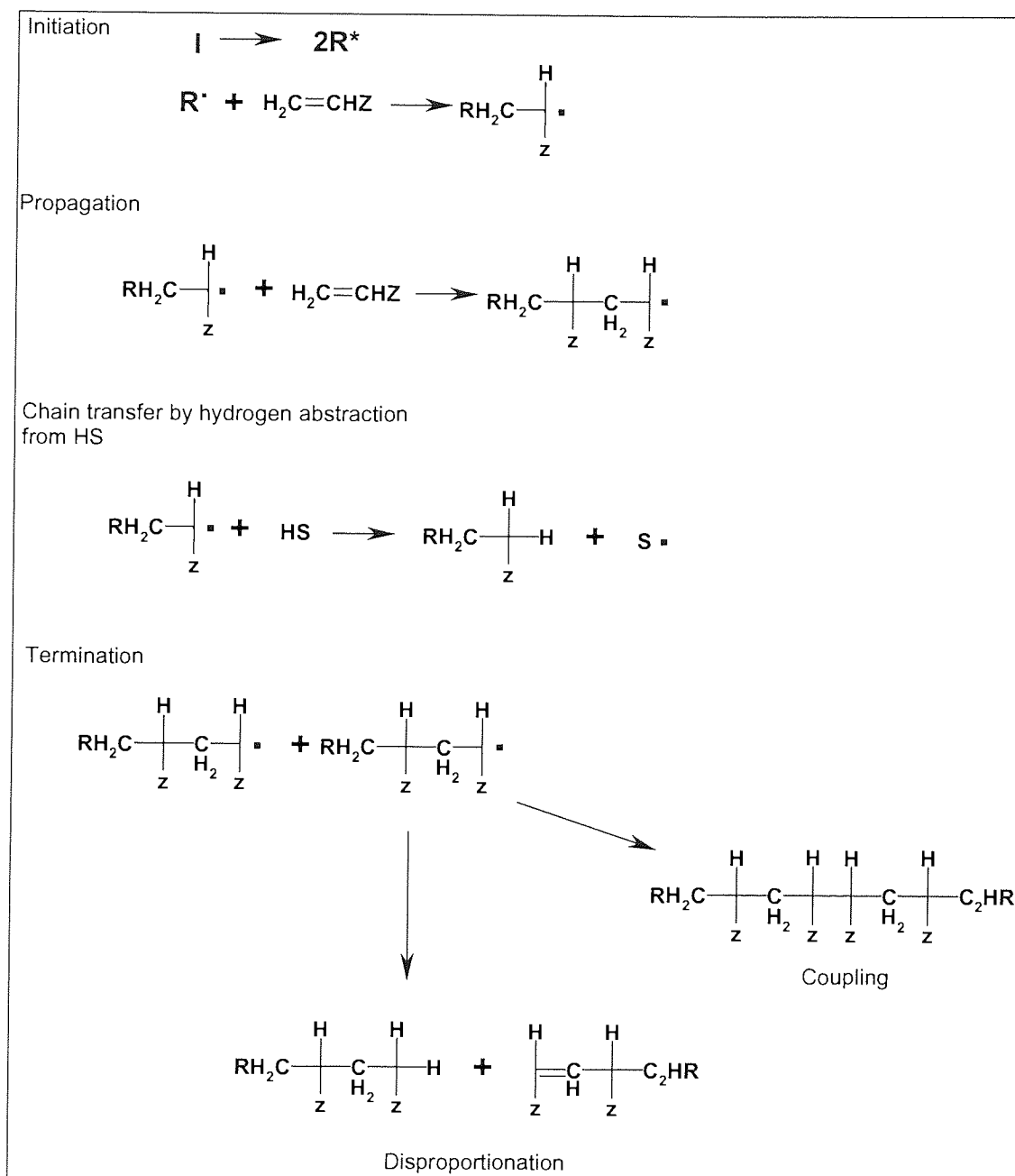
**Figure 11:** The polymerisation process.

I= initiator, **R**= radical, **Z**= side group, **HS**= hydrogen abstracted from solvent, monomer, chain transfer agent, initiator or the polymer.

Free-radical reactions are less affected by the presence of acids, bases and changes in polarity of solvents. In terms of molecular imprinting more flexibility in the choice of conditions to perform imprinting can be possible (Sellergren 2003a).

In the initiation step free radicals are produced from the process known as homolytic fission that can be initiated either by thermal processes, microwave or ultraviolet (UV) radiation processes and electron transfer (redox) processes. Examples of Initiators that form radicals are such as AIBN and benzoyl peroxide (**Figure 12**).

47
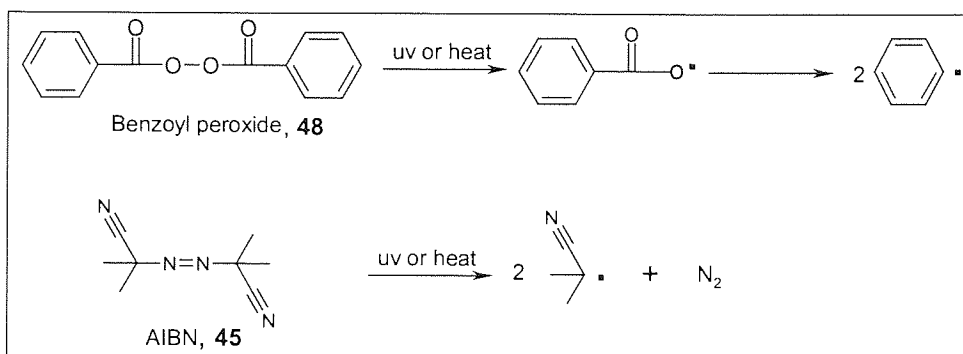
**Figure 12:** The formation of radical species from the decomposition of benzoyl peroxide and AIBN.

Note, that if azo-initiators are initiated by UV radiation at a wavelength for maximum absorption this may result in a rate of production (free-radicals) that maybe either too high or too low. In the former case a large concentration of reactive centres generated lead to early termination and low molecular weight polymers. As for the latter case polymerisation would not be completed at a practical time-scale (Sellergren 2003a). In addition, if photochemical initiation is chosen to generate free-radicals then intensity of UV light, distance from the light source and penetration depth have to be taken into consideration. This is due to the fact that these factors determine rate of production of the free-radicals.

Once formed, however, these radicals attack the double bonds of vinyl monomers. This is due to the instability of carbon-carbon double bonds in the monomer making them susceptible to reaction with the unpaired electrons in the radical. The initiated monomer radical then goes on to attacking other monomers. The competence of an initiator can be measured by comparing the amount of initiator decomposed to that of the number of polymer chains formed.

The next step is propagation and in a free radical polymerisation process, this reaction usually takes place within a fraction of a second. The propagation reaction involves the successive attachment of monomers to the growing chain which prolates i.e. elongates at each terminus. Chain transfer involves the abstraction of hydrogen from the solvent, monomer, chain transfer agent, initiator or the polymer and this is carried out by the radical end of a growing chain-polymer. This leads to the growth of the polymer chain to be terminated i.e. the original radical stablised, and at the same time a new radical, capable of chain propagation and polymerisation is created.

The final step is termination in which the free radicals pair up to form covalent bonds. Termination typically occurs in two ways by symmetrical coupling also known as combination or hydrogen transfer that results in disproportionation. Combination termination involves a free radical joining with an active growing polymer to form a stable chain and end the growth of the polymer. In disproportionation this involves a free radical stripping a hydrogen atom from another free radical, so that one chain stabilises with the hydrogen, and the other with a double bond.

## 1.1.6.1 Polymer preparation methods

In this research and the most commonly used method to produce polymers is free radical polymerisation. This type of polymerisation can be performed in a number of ways with each giving a different characteristic and property to the resultant polymer. These various methods shall be discussed in this section.

## 1.1.6.1.1 Bulk polymerisation

This type of polymerisation takes place in the absence of any medium other than an initiator. The monomers employed are usually liquids, however this can also be applied to gases and solids in the absence of solvents. In most cases the monomer mixture is degassed of atmospheric oxygen and purged with inert gases such as argon or nitrogen. This process employs free–radical polymerisation that is initiated by applying heat, ultraviolet light or high-energy radiation. MIPs are usually prepared by this method and are produced as bulk monoliths (O'shannessey et al 1989). These are typically then ground either by hand or by a mechanical mortar and subsequently passed through a sieve. Then the sieved fraction is sedimented to obtain the desired particle size (μm).

The advantage of such a polymerisation is that there is no problem with getting solvent out of the finished product, since no solvent is used. Furthermore, with the absence of the solvent, excludes it from becoming involved as the chain transfer agent and so does not encourage the production of low molecular weight polymers.

The disadvantage associated with such a process is that a yield around 30-50% of the original bulk imprinted polymers is obtained, and more than 50% of the starting material is lost during this step. This process is also time-consuming and produces irregular shaped particles that are not suited for chromatographic purposes. In addition this process has poor reproducibility (Andersson 2000). The main associated problem with this method however is the dissipation of the heat of polymerisation that increases as the polymerisation reaction advances. When the reaction advances the reaction becomes very viscous and so the dissipation of heat becomes uncontrollable. Owing to this problem the polymer takes a variable structure due to local temperature variation. This also limits the desired polymers molecular weight.

## 1.1.6.1.2 Suspension polymerisation

Hoffman and Delbruch first developed suspension polymerisation in 1909. In suspension polymerisation the organic imprinting phase has soluble in it the template, monomers and initiator, and a highly polar organic or aqueous solvent, with which the organic imprinting phase is immiscible. Suspension polymerisation usually requires the addition of small amounts of a stabiliser to hinder coalescence and break-up of droplets during polymerisation. This is due to the fact that polymerisation proceeds in the

droplet phase i.e. monomer droplets suspended in aqueous phase, and in most cases occurs by a free radical mechanism. The free radical polymerisation is initiated thermally and affords polymer beads.

The size distribution of the initial emulsion droplets and consequently also of the polymer beads that are formed, depends upon the number of droplets breaking-up and coalescence that have to be equal. The bead size is then also controlled by the speed of at which the two phases are stirred, the volume fraction of the monomer phase, and the type and concentration of stabiliser used. The advantages of this polymerisation method are that better heat control of the reaction is possible. Following polymerisation, ease in retrieving beads from the aqueous phase and being able to determine polymer morphology. The morphology of the final particles is related to the degree by which the polymer dissolves, swells or precipitates in the monomer phase. If they are soluble or swellable, the resultant beads would be smooth and non-porous in texture, but if insoluble or non-swelling then they would be rough and porous in texture. For example, polystyrene and poly(methyl methacrylate) dissolve and swell in their own monomers and thus produce smooth and translucent microbeads. In contrast, polyacrylonitrile and poly(vinyl chloride) are insoluble in their own monomers and thus produce porous particles (Xu *et al* 1998)

Polymer beads have been applied to molding plastics, but largely in chromatographic separation media (as ion exchange resin and as supports for enzyme immobilisation). Such applications frequently require large particle surface areas, which necessitates the formation of pores (of the required dimensions) in the bead structure. This type of polymerisation has also been applied to covalent (Damen and Neckers 1980) and non-covalent studies, even though the aqueous phase interferes with the monomer and template interaction (Lai *et al* 2001; Flores *et al* 2000). As result other alternatives to the aqueous phase have been sought such as the fluorocarbons (Mayes and Mosbach 1996). These do not affect the monomer and template interactions, are chemically inert and immiscible with organic solvents. To prevent the problem of droplet coalescence an innovative polymeric surfactant was employed in this process and afforded a well-defined particle size distribution (Ansell and Mosbach 1997).

## 1.1.6.1.3 Dispersion/precipitation polymerisation

In precipitation polymerisation the polymer being formed is insoluble in its own monomer or in a particular monomer-solvent combination and thus precipitates out as it is formed. As a comparison both use an excess of solvents in which the monomer, initiator and template are dissolved. Note that the polymer is not soluble in this medium. The polymerisation processes are free radical based and are initiated thermally. The resultant polymer particles can be retrieved by sedimentation, centrifugation or filtration. In the precipitation polymerisation process the resultant polymer particles that precipitate are, however, coagulated and thus afford an irregular shape. In dispersion polymerisation this problem is dealt by having a stabiliser included in the system such as polyacrylic acid. This addition allows the particles to grow uniformly as monodispersed spherical material.

In molecular imprinting a stabiliser is not required due to the rigid cross-linked surfaces that make them stabilised. This in turn eliminates non-specific binding caused by the stabiliser. This technique has been employed by number of research groups. The precipitation approach was used to make polymer aggregates *in situ* in the chromatography columns without having to post-polymerise the column packing (Sellergren 1994). This approach was also used by Ye *et al* (2000; 1999a) to synthesise sub-micron polymer lattices that recognise 17-β estradiol and theophylline in acetonitrile. Bruggemann *et al* (1997) also employed this for capillaries for electro-chromatography and Ye and Mosbach (2001) for antibody binding mimics.

### 1.1.6.1.4 Emulsion polymerisation

In the emulsion polymerisation process the monomer is insoluble (slightly soluble) in the polymerisation medium. With help of a surfactant, however or an emulsifier the monomer is emulsified. The initiator is also soluble in the polymerisation medium but not in the monomer. Emulsion polymerisation can be differentiated into three different steps. In the first step the polymer particles are being formed. In the second step the polymerisation process develops with a constant supply of new monomer, which results in growth of the polymer particles. In the final third step all the monomer is consumed and so a gradual decrease in rate of polymerisation takes place.

The initiator generating free radicals by thermal decomposition in the aqueous phase starts the polymerisation. The free radicals react with monomers present in the aqueous phase to form oligomer chains. These oligomers (oligoradicals) can either be absorbed into the micelles or be surrounded by the dissolved monomer and emulsifier molecules.

The oligoradical that diffuses into the swollen micelle that contains a monomer, reacts with the monomer and starts the polymerisation process. As the polymerisation precedes forming polymer particles, more monomer is absorbed from the aqueous solution into the micelle. Note, as monomer parts from the aqueous solution, more monomer from monomer droplets leave and therefore maintains a steady concentration of monomer in the aqueous solution, until all the monomer is consumed. This polymerisation has no problems with heat dissipation. The developing polymer particles are stabilised by the emulsifier. It should be noted however, that the exact details of particle formation are strongly dependent on the nature of the polymerisation mixture.

There are two types of emulsion polymerisation, the oil-in-water (O/W) and the water-in-oil (W/O). In the O/W the initiator is water-soluble and the monomer is insoluble. The monomer is emulsified in oil in the presence of oil-water emulsifier. In the W/O the initiator is oil-soluble, the monomer is water-soluble and the emulsifier is water-oil based.

The O/W emulsion technique has been used in molecular imprinting to synthesis highly specific metal ion surface-imprinted divinylbenzene / styrene resin particles. This technique involved the pre-organisation of

51

the functional surfactants (amphiphilic host monomers) on the oil-water surface by interacting with the target molecule (template guest i.e. metal ion) in the aqueous phase. The organised structure that consists of template and functional surfactants was then immoblised by polymerisation in the oil phase from the vinyl monomers. Subsequent removal of the template (metal ion) resulted in polymeric resins that carried the functional groups spatially arranged on their surfaces (i.e. recognition sites) that gave preference to the rebinding of the template molecule (i.e. the metal ion) (**Figure 13**). Kido *et al* (1992) used potassium oleate and Maeda *et al* (1994) used dioleyl phosphoric acid as their amphiphilic monomers to surface template resin for $Cu^{2+}$. Murata *et al* (1996) used oleyl phenyl hydrogenphophate as the amphiphilic monomer to surface template resins for metal ions such as $Cu^{2+}$, $Zn^{2+}$ and $Cd^{2+}$.
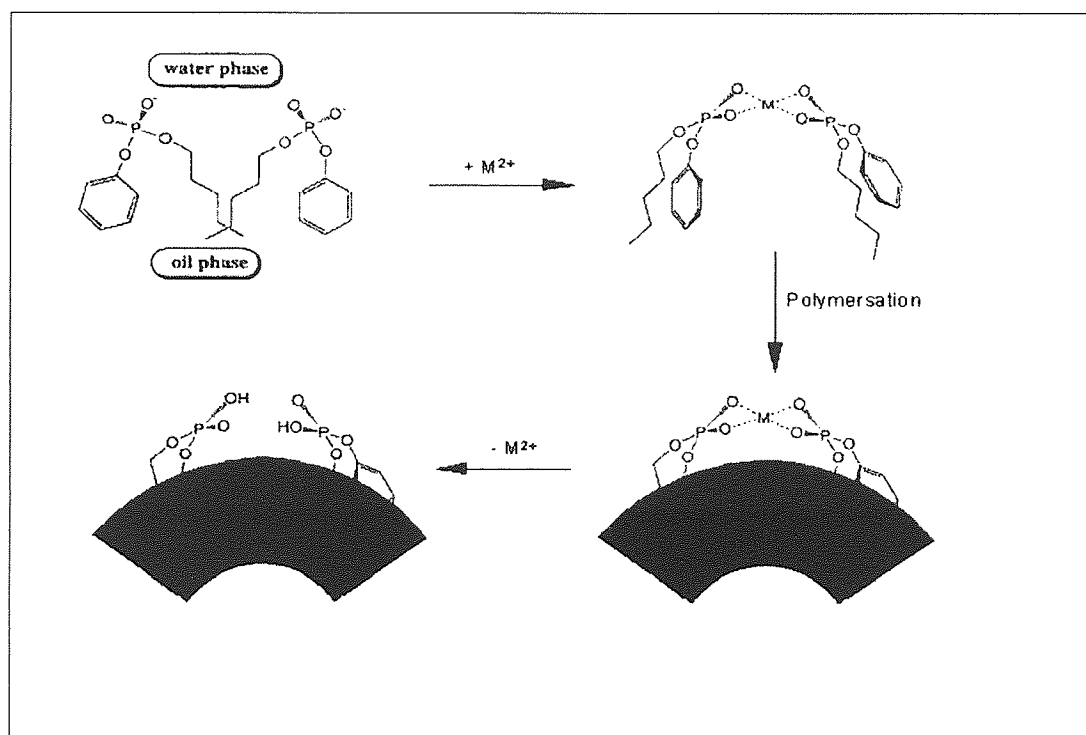


**Figure 13**: Schematic illustration of surface template polymerisation using oleyl phenyl hydrogenphosphate as an amphiphilic host monomer, divinylbenzene as a resin-forming monomer (oil phase) and divalent metal ion as a target (Adapted from Murata *et al* 1996).

W/O emulsion polymerisation has also been employed for a novel surface template polymerisation to produce bulk metal ion imprinted resins. In this method the functional monomer, emulsion stabiliser, polymer matrix forming monomer (divinylbenzene) and template molecule are self-assembled at the water-oil interface to form a recognition site. The functional monomer (amphiphilic) complexes with the template molecule during emulsion and therefore the complex formed remains at the reaction surface. After polymerisation, the coordination structure is imprinted on the polymer surface, and not in the polymer matrix (**Figure 14**). Uezu *et al* (1999) prepared a resin for $Zn^{2+}$ by employing dioleyl phosphoric acid. Yoshida *et el* (1998; 1999) separated $Zn^{2+}$ and $Cu^{2+}$ ions by synthesising the novel bi-functional monomer 1,12-dodecanediol-O,O'-diphenyl phosphoric acid (DDDPA).
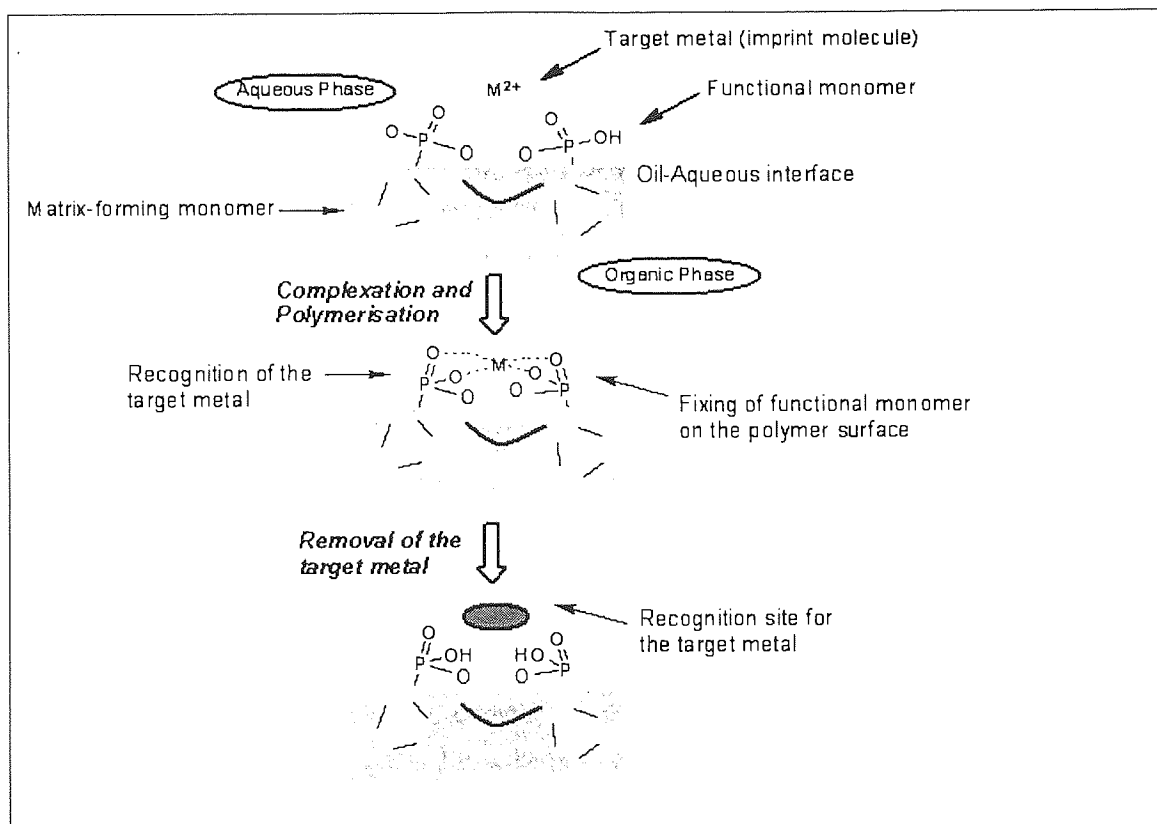
**Figure 14:** Schematic illustration of surface template polymerisation technique (Adapted from Yoshida *et al* 1999).

### 1.1.6.1.5 Multi-step swelling procedure

Multi-step swelling procedure has been employed to generate uniform macroporous molecular imprinting beads that have been employed for chromatography purposes. This was first applied by Hosoya *et al* (1994). This technique involves a polystyrene seed (latex) particle the size of ~ 1µm (diameter) that is aqueous dispersed and is allowed to swell in a micro-emulsion of activating solvent (e.g. dibutyl phtalate) and dispersion stabiliser (e.g. sodium dodecyl sulphate). The seed particles are stirred vigorously for number of hours until the emulsion droplets are absorbed into the particles. These swollen particles are then added to a second micro-emulsion of initiator, porogen and dispersion stabiliser and allowed to swell for the second time. In the final step the particle is again allowed to swell, after adding a dispersion of cross-linking monomer, template and stabiliser. The dispersion is then purged with inert gas to remove dissolved oxygen and raised to polymerisation temperature. For HPLC purposes particle size 5-6µm are required and are obtained after sedimentation in excess water, methanol and THF, then followed by filtration and drying.

As mentioned earlier these particles are employed for HPLC purposes such as the analysis of MIPs imprinted with a number of templates. For instance for β-estradiol (Haginaka and Sanbe 1998), (S)-ibuprofen (Haginaka *et al* 1999), (S)-naproxen (Haginaka *et al* 1998; Haginaka and Sanbe 2001), propranolol (Haginaka and Sakai 2000) and biphenol A (Haginaka and Sanbe 1999).

## 1.1.6.1.6 Membranes and films

Molecular imprinted polymers have been prepared as membranes and films for applications such as affinity separation, membrane chromatography and membrane sensors (Piletsky *et al*, 1999). Yoshikawa *et al* (1996) employed this for amino acid optical resolution. Piletsky *et al* (1995) used this for atrazine (herbicide) monitoring purposes. As monitoring of herbicides in drink water, food and the environment is based on gas chromatography that requires large and expensive instruments. Wang *et al* (1996) employed membranes for theophylline and Sallacan *et al* (2002) for nucleotides (adenosine 5'-monophosphate, guanosine 5'-monophosphate, cytosine 5'-monophosphate and uridine 5'-monophosphate).

Molecularly imprinted polymers of such form have been applied to enzyme-linked immunosorbent assay (ELISA), where a new technique for coating of microtitre plates with MIPs, specific for low molecular weight analytes i.e. epinephrine and atrazine, and protein was presented by Piletsky *et al* (2001). Another application is in the area of chemical sensors e.g. for atrazine, was performed by Sergeyeva *et al* (1999; 1999a). Solid phase extraction is another application for these membranes. For instance work by Sergeyeva *et al* (2001) used this for triazine herbicides to provide a straightforward and inexpensive method for separation purposes.

A number of approaches has been developed that include methods such as *in situ* bulk polymerisation, dry phase inversion, wet phase inversion and surface imprinting/grafting. The *in situ* bulk polymerisation involves preparing films with a template and polymerisable complementary functional monomers. The 'free standing' films of imprinted polymers are obtained by simultaneously polymerising and film formation. This method was employed by Krotz and Shea (1996) for preparing imprinted polymer membranes for selective transport of targeted neutral molecules. In addition, membranes have also been prepared with a photo-isomerisable functional monomer (merocyanine acrylate), in zwitter-ionic state imprinted with tryptophan by Piletsky *et al* (1999a). Polymerisation between glass plates has also been performed by Guo *et al* (2000) to study binding characteristics and transportation properties of a 4-aminopyridine imprinted polymer membrane. Sergeyeva *et al* (1999) used quartz slides to prepare a MIP membrane designed for atrazine-sensitive conductimetric sensors. Kimaro *et al* (2001) used Teflon moulds to prepare a membrane ionically permeable for uranyl ion.

Dry phase inversion was employed by Yoshikawa *et al* (1995; 1996a; 1997; 2001) to prepare membranes by using casting/solvent evaporation process. Kobayashi *et al* (1998; 1998a) employed wet phase inversion, this involves casting/ immersion precipitation inversion and was used for imprinting theophylline. Finally grafting of polymer layers onto the surface has been demonstrated by Piletsky *et al* (1998) on glass plates and on silicon wafers by Hedborg *et al* (1993). In addition, grafting onto micro-filtration/titre plates by Piletsky *et al* (2001) and electrodes by Yoshimi *et al* (2001).

Araki *et al* (2005) reported a new method of preparing an ion-selective polymer membrane by surface molecular imprinting for zinc (II) (**Figure 15**). The surface imprinting employed the water-in-oil emulsion polymerisation method to prepare the membrane. This emulsion polymerisation was performed with the functional monomer, 1,12-dodecanediol-O,O'-diphenylphosphonic acid, L-glutamic acid dioleylester ribitol as the emulsion stabiliser and divinylbenzene as the polymer matrix-forming monomer. To attain flexible and mechanically stable membranes the polymerisation was conducted in the presence of acrylonitrile-butadiene rubber (NBR) and hydrophilised poly(tetrafluoroethylene) (PTFE) membrane. The zinc (II) imprinted membrane gave high adsorption affinity and permeation selectivity towards the zinc ion in comparison to the non-imprinted membrane.
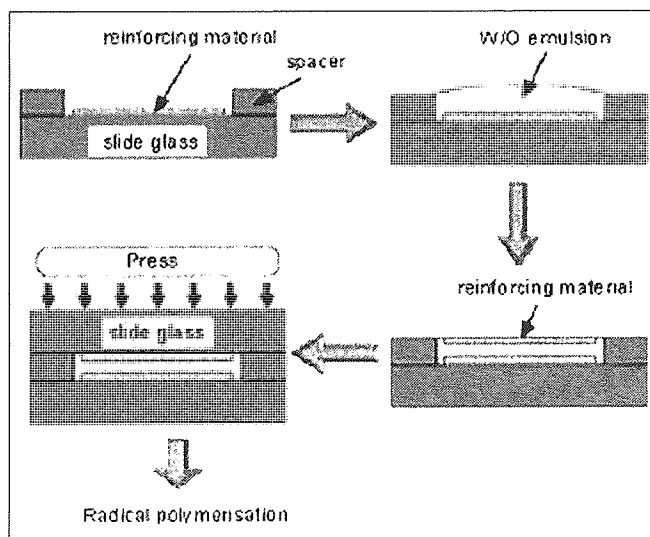


**Figure 15:** Schematic illustration of preparation of metal-ion imprinted membrane (Adapted from Araki *et al* 2005).

## 1.1.7 Towards rational design for molecular imprinted polymers

To initiate towards the rational design for MIPs a number of optimisation studies have been performed. These involve using various monomer-template ratios and degree of cross-linking (Yilmaz *et al* 1999). Andersson *et al* (1999) used a range of monomer–template ratios to prepare a series of (-) nicotine molecularly imprinted acrylic polymers. Similarly, Mayes *et al* (1998) performed optimisation studies for radio-ligand binding assays in drug-development assay approaches. Such studies established the effect that these factors i.e. monomer-template ratios and degree of cross-linking, had on the recognition properties of the polymer and could thus be used for optimising polymer design. Optimisation studies of this type, however, do not cover the scope of the MIP protocol that consists of a vast number of variable factors. These are such as type and quantity of monomer, cross-linker, porogen, initiator and initiation process i.e. thermal or photochemical, and temperature, as well as the polymerisation process and the reaction time. Optimisation methods of the type mentioned earlier that involves changing one factor at a time can be time-consuming.

Other approaches that help towards the rational designing of polymers have used thermodynamics and computational analysis of template monomer complex formation (Whitcombe *et al* 1998; Nicholls 1998). Besides this a combinatorial approach has also been used. This approach uses libraries of MIPs that are screened for high affinity and selectivity towards the selected template using semi-automatic approaches. The use of automated procedures for MIP synthesis enables high-throughput preparation and screening of MIPs at a small scale, allowing for testing of the compatibility between a variety of functional monomers and a given template in a library approach. Takeuchi *et al* (1999) employed this approach, where MIPs with varying monomer-template ratios were prepared in situ on the base of glass vials. These were initially screened for template release from the MIPs and analysed by HPLC. Then followed by another screening for template uptake. In 2001 Takeuchi *et al* further developed this study, which allowed the analysis to become throughput and faster. This improvement was demonstrated by using a 96-well plate in which a fluorescent template was used in the synthesis of the MIPs and performed a similar study of release and rebinding using a fluorescence plate reader. ]

Lanza and Sellergren (1999) used a similar approach to the one described by Takeuchi *et al* (1999) for the combinatorial synthesis of molecularly imprinted polymers. This study however prepared MIPs on the bottom surface of chromatographic vials instead of glass vials and likewise studied the release/rebinding of the template. The MIPs that retained the template strongly were studied further. In 2001 Lanza *et al* further optimised the automation system i.e. the HPLC apparatus.

Besides the approaches described so far, the optimisation of MIP synthesis has also been demonstrated by using a computational approach. This approach involves stimulating interactions between functional monomer-template *via* hydrogen bonding, van der Waals, ionic, and dipole-dipole interactions. These interactions are then assigned with binding energy scores. Thus monomers that give rise to high binding energy scores would then be selected and be used in the MIP synthesis or further stimulated to determine the number of interactions that take place with a template (Subrahmanyam *et al* 2001; Piletsky *et al* 2001a; Chianella *et al* 2002). Such studies improved the selectivity of the MIPs in comparison to the polymer synthesised with commonly used monomers.

To rationally design MIPs Davies *et al* (2004) have employed chemometrics. Chemometrics is basically "the science of relating measurements made on a chemical system or process to the state of the system *via* application of mathematical or statistical methods". Such methods can be used for designing or selecting the optimal experimental parameters or procedures (design of experiments), and extracting the maximum relevant information from data analysis. The study combined multi-analyte competition rebind assay and chemometrics to rationally synthesis MIPs. At first a multi-analyte competition assay was efficient at screening which combination of sulfonamides was preferable for use as the template and rebind analyte. This assay involved preparing rebinding solutions consisting of the various sulfonamides and MIP or non-imprinted polymer that were shaken, centrifuged and the supernatant analysed by a gradient HPLC. This procedure allowed the total sulfonamide bound to MIP or non-imprinted polymer to be calculated. Then chemometrics was used to predict an optimum template:monomer:cross-linker ratio

for the production of an sulfonamide MIP, capable of rebinding the highest capacity to close structural analogues of sulfonamide. This study demonstrated that chemometrics could be used as a rational approach to MIP optimisation.

## 1.1.8 Template extraction

In molecular imprinting the most frequent problem associated is that small amounts of template remain entrapped in the polymer after extraction. It is estimated that the amount of template recovered has usually been more than 95% (Allender et al 1999). The remaining portion, however, tends to leach out of the polymer upon solvent changes whilst in use (Martin et al 1997; Martin et al 1998; Venn and Goody 1999). For most applications for instance preparative separations and catalysis, template leaching causes no problems. The problem of template leaching, however, has been associated with solid phase extraction and has been reported by Venn and Goody (1998) and Rashid et al (1997). Where due to analysis involving trace levels or ultratrace levels of analyte, template leaching has been accountable for the observed variability in results. To minimise the problem associated with template leaching, Andersson et al (1997) imprinted a template analogue of sameridine, such studies however reduced the imprinted polymers specificity (Stevenson 1999). Besides this approach, other approaches have optimised the washing procedure and used post polymerisation heat treatment (Zander et al 1998). Ellwanger et al (2001) imprinted polymers with clenbuterol and used these to study the influence of various post-polymerisation treatments such as thermal annealing, microwave assisted extraction (MAE), Soxhlet extraction and supercritical fluid template desorption on template leaching. Of the four treatments the optimised MAE was the most efficient at template extraction. Another important observation form this study was that efficient removal of the template takes place when the same porogen i.e. in the preparation is employed for washing purposes. This is due to the fact that similar swelling properties are established and thus results in the efficient diffusion of the template out of the polymer. On the whole the study, however, failed to recognise the fact that polymers consist of various template, monomer, porogen and cross-linker types and quantities, as well as, varying polymerisation conditions. Thus such variations directly affect the binding character, porosities and swelling properties of the polymer and so the extraction approach employed is specific for each polymer.

## 1.1.9 Applications of molecular imprinting

The ability of a MIP to be able to distinguish between structural and spatial aspects has caused this to be greatly recognised within the scientific body. Moreover, ease of preparation, cost effectiveness and being able to prepare MIPs by using commercially available monomers adds to their attraction. In addition, stability against mechanical stress, high temperatures or pressures. Areas such as the chemical industry, research bodies, health care and the environmental control areas have benefited from this and have led the applications of this technology to amplify, some of these are summarised below.

## 1.1.9.1 Liquid chromatography

Enantiomer separation by chromatographic means is an area that has received research. Such research has increased the number of available chiral stationary phases (CSP) that are able to resolve a large amount of the racemic mixtures. Despite this fact still no method has been developed to identify a suitable candidate and conditions for undocumented separation, this itself can be a costly task to perform. Then again to aid this process of identification of a CSP, introducing into the chiral phase a `tailor-made` MIP that is designed for specific separation by employing a pure single enantiomer as a template is able to address this problem (Allender et al 1999). Work reported by Sellergren et al (1985), O`Shannessey et al (1989b) and Kempe and Mosbach (1995) used enantiomeric template molecules to prepare enantio-selective MIP CSPs. Ching-Chiang Hwang and Wen-Chien Lee (2001) chromatographically resolved the enantiomers of phenylpropanolamine by using MIP as the stationary phase. MIP CSPs were processed by employing a pure single enantiomer to prepare a imprinted polymer that would be packed into a HPLC column to resolve racemic mixtures. Comparing the retention times of the template enantiomer with that of the non-template enantiomer would assess the resultant MIP. Enantioseparation of a wide variety of templates by using MIPs has been demonstrated on amino acid derivatives, peptides and proteins (Ramström et al 1994; Kempe and Mosbach 1995; Sellergren et al 1998; Dobashi et al 2002). Drugs such as β-blockers (Haginaka and Sanbe 1998; Haginaka and Sakai 2000) and anti-inflammatories (Kempe and Mosbach 1994). MIP CSPs have also been prepared for compounds that contain several chiral centres such as for carbohydrates and peptides (Mayes et al 1994).

Watabe et al (2004) used a MIP as an on-line pretreatment device and employed HPLC method for the micro-analysis of bisphenol A, that is contained in environmental water. Blomgren et al (2002) extracted clenbuterol by using MIPs and assessed this by HPLC with UV detection. Kempe et al in 1993 reported a novel MIP created by functional monomers 4-vinylpyridine and 1-vinylimidazole. This MIP was developed for enantioselective recognition of carboxylic and N-protected amino acids. The recognition sites within the polymer were as a result of non-covalent (hydrogen and ionic bonding) interactions between the functional monomer and template molecules. The molecular recognition of the MIP was studied by using the polymers as stationary phases in HPLC. From this study it was established that polymers generated by 4-vinylpyridine were more efficient in racemic resolution in comparison to 1-vinylimidazole.

Matsui et al (1995) used the monomer 2-(trifluoromethyl) acrylic acid (TFMAA) to create complementary binding sites within polymers for the herbicide prometryn, 49 (**Figure 16**). The molecular recognition of the imprinted polymers was chromatographically studied. It was found that TFMAA based polymers gave high affinity and selectivity for the template prometryn, in contrast to the methacrylic acid (MAA) based polymers. The reason for observing this result is that TFMAA has a higher acidity compared to MAA due to the strong electron withdrawing effect of the trifluoromethyl group. Thus as a result of this strong electron withdrawing group effect, the TFMAA monomer interacts strongly with the basic template.
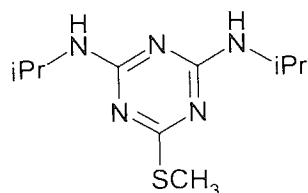
**Figure 16:** Structure of prometryn, **49** (Matsui *et al* 1995).

Practically, however, using MIPs in HPLC at times could be limited by the broadening and tailing of the peaks caused by the heterogeneity of the sites that causes variations in the site affinities and binding kinetics (Sellergren and Shea 1995). Besides this, the irregular particle size distribution obtained after grinding and sieving of the MIPs produced by bulk polymerisation can also be a limiting factor. A further problem lies in the low capacity for binding (generally less than 500 µg/g.pol). To improve the chromatographic performance and to overcome these problems a number of approaches have been adopted: for instance optimising the separation procedure such as the mobile phase composition, separation temperature and gradient elution can help improve peak shapes (Sellergren and Shea 1995; Kempe 1996; Yu and Mosbach 2000; Lu *et al* 2002). Another solution is using alternative polymerisation methods that give a uniform sized particle distribution and improve mass transfer. Work by Glad *et al* (1995) reported forming spherical MIP particles, by preparing beads from TMPTA and then imprinting the pores through *in situ* formation. This method gave a more homogenous particle size distribution that caused the elution from the column to generate narrow peak shapes. Hosoya *et al* (1996) reported preparing by a two-step swelling method, porous beaded MIPs with a diameter of 5.6 µm. In this method a microemulsion of polystyrene particles was swollen and then cross-linked in a two-phase system, consisting of toluene/cyclohexane and water, and polyvinyl alcohol as the dispersion stabiliser. Another alternative is the production of agglomerates of globular micron sized MIP particles *via* non-stabilising dispersion polymerisation, reported by Sellergren (1994). Matsui *et al* (1995a; 1998) similarly prepared *in situ* polymer rods inside columns. Note, that such *in situ* methods eliminated the working-up and packing procedure that is associated with MIP being prepared for chromatographic purposes. In addition, molecularly imprinted monodisperse microspheres have also been prepared *via* precipitation polymerisation by Ye *et al* (1999). In a study reported by Haginaka and Kagawa (2002) they formed a selective uniform sized MIP for D-chlorpheniramine by using a multi-step swelling and polymerisation method, using methacrylic acid as a functional monomer and ethylene glycol dimethacrylate as a cross-linker. The enantioselectivity was assessed of chlorpheniramine and its structurally related compounds on the MIP, by using aqueous mobile phase. In this media the retention and enantioseparation relied upon electrostatic and hydrophobic interactions. In the 2004 study by Haginaka and Kagawa (2004) in addition to the methacrylic acid functional monomer, 2-(trifluoromethyl)acrylic acid was employed as a functional monomer to synthesise uniform MIPs for D-chlorpheniramine and d-brompheniramine. The enantioselectivity and retention of the compounds and their related compounds on the MIP were evaluated in a hydro-organic mobile phases. In this study both polymers gave high enantioselectivity for their respective template molecules. Another approach to produce more homogenous binding sites has been to use stoichiometric template to monomer ratios (Spivak and Shea 1999).

## 1.1.9.2 Molecularly imprinted Solid phase extraction (MISPE)

A particularly promising and the first commercial application of MIPs has been as selective phases in solid phase extraction of analytes present in low concentrations or in complex matrices (Sellergren 1999). This being possible due to the MIP having high affinity for its ligand, permitting it to extract small quantities from biological solutions for subsequent assays. Moreover, this also allows selective enrichments and an efficient means of sample clean-up commonly used in food, environmental analysis and in medical analysis. The other benefits of MISPE is that its stationary phases can be tailor- made for specific analytes, that are low in cost to make, compatible and adaptable in organic solvent, and have better robustness (Haupt 2001). The disadvantage of MISPE is the leakage of template molecule, which is not removed after MIP preparation interferes with the analysis as expected. This interference in a solution of low concentration may be significant. Though to counteract this Andersson *et al* (1997) reported imprinting a template analogue of sameridine (**51**) (**Figure 17**). The analogue was N,N-dimethylsameridine (**50**) (**Figure 17**) that yielded a MIP exhibiting strong affinity for sameridine.

Studies that demonstrated the use of MISPE include work by Martin *et al* (1997) for the selective extraction of `propranolol` (**52**) (**Figure 17**) from urine and plasma samples. Rashid *et al* (1997) extracted tamoxifen (**53**) (**Figure 17**) from biological samples, using a tamoxifen based imprinted polymer, for HPLC and UV detection. Theophylline (**54**) (**Figure 17**) was extracted from serum samples (Vlatakis *et al*, 1993; Mullet and Lai, 1998). Sellergren (1994a) extracted pentamidine (**55**) (**Figure 17**), Walshe *et al* (1997) extracted coumarine (**56**) (**Figure 17**) and Berggren *et al* (2000) extracted clenbuterol (**57**) (**Figure 17**) from urine samples. Muldoon and Stanker (1997) extracted atrazine (**58**) (**Figure 17**) from liver, nicotine (**59**) (**Figure 17**) from chewing gum (Zander *et al* 1998) and tobacco (Mullet *et al* 1999). MISPE has also been used for environmental water samples (Matsui *et al* 1997a; 2000; Ferrer *et al* 2000; Mena *et al* 2002). Additionally, SPE have also been used within the area of desulphurising fuels such as diesel, where the content of sulphur in crude oil act as a parameter of its quality, since combustion of organosulphur compounds results in the emission of sulphur oxides (i.e. acid rain) (Castro *et al* 2001). MISPE has also been used to determine Sudan I from food matrices and has allowed the compound to be concentrated enough for HPLC detection (Puoci *et al* 2005). Zurutuza *et al* (2005) reported using MISPE to determine cocaine metabolites from aqueous samples. Wang *et al* (2005) used MISPE to determine (−)-ephedrine from Chinese Ephedra and Caro *et al* (2004) used it to determine naphthalene sulfonates from water.
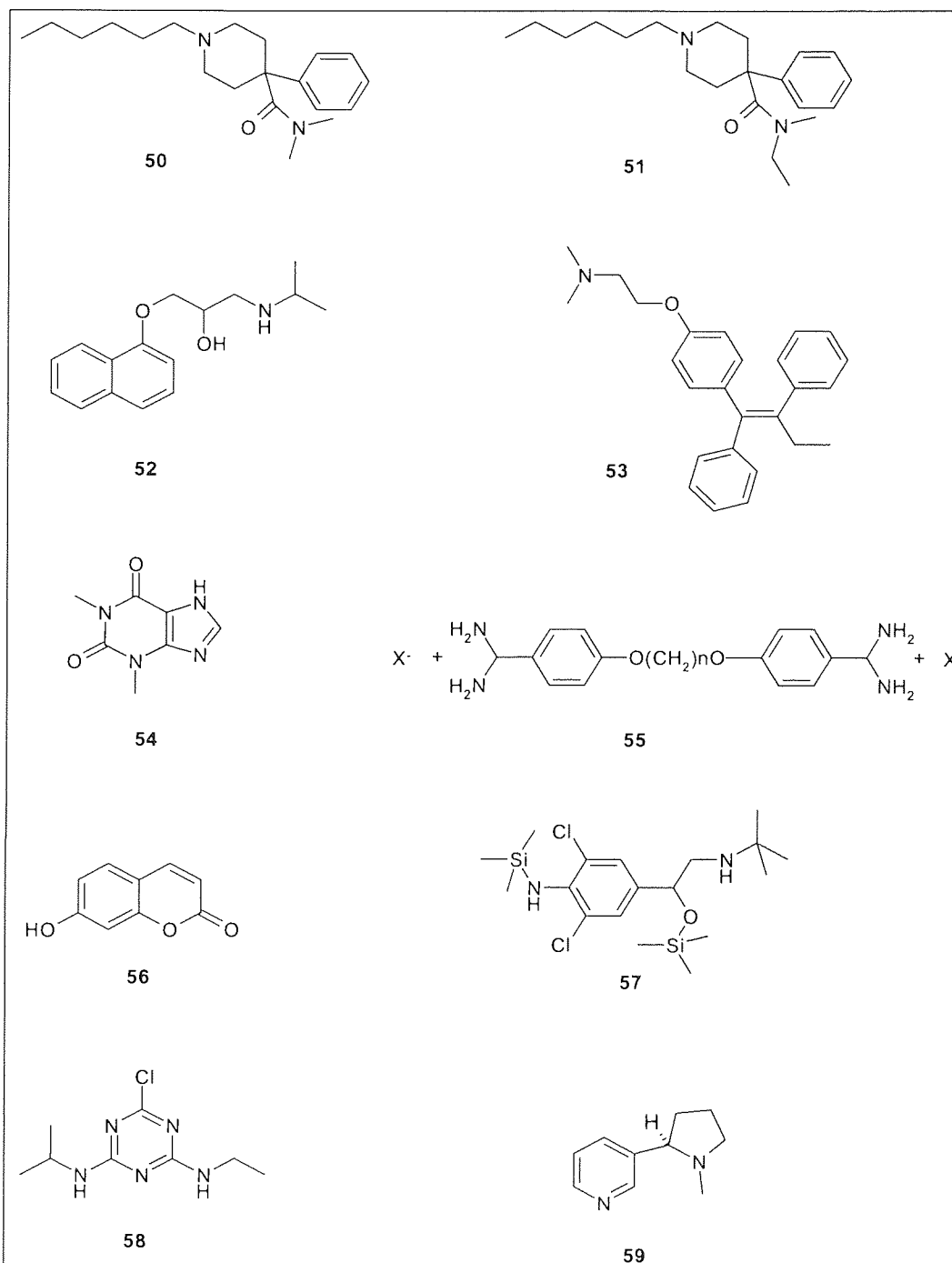
**Figure 17:** Structures of the analytes extracted by MISPE.

**50:** N,Ń-dimethylsameridine, **51:** sameridine, **52:** propranolol **53:** tamoxifen, **54:** theophylline, **55:** pentamidine, **56:** coumarine, **57:** clenbuterol, **58:** atrazine, **59:** nicotine.

## 1.1.9.3 Thin-layer chromatography (TLC)

The use of MIPs as the stationary phase for TLC plates for enantiomeric separation has been reported by Kriz *et al* (1994) and involved using a L-phenylalanine MIP enabled them to separate L- and D-enantiomers. The successful separations of racemates using (-)-pseudoephedrine or (-)-norephedrine molecularly imprinted TLC for compounds such as adrenergis drugs, norephedrine, pseudoephedrine,

61

ephedrine and epinephrine have been reported by Suedee *et al* (1999). The same group led by Suedee performed resolution studies using (+)-pseudoephedrine, (+)-ephedrine and (+)-norephedrine (Suedee *et al* 1999a).

## 1.1.9.4 Capillary electrophoresis (CE) / capillary electrochromatography (CEC)

A number of research groups took the challenge to combine the idea of MIP and capillary electrophoresis (CE)/ capillary electrochromatography (CEC) to widen the scope of new separation systems. These systems reduced the peak tailing and broadening, a problem associated with HPLC based on MIPs. As a result separation and resolution of the peaks also increased. Nilsson *et al* (1997) were the first to report this technique by *in situ* dispersion polymerisation of the MIP, imprinted against the antiparasitic drug L-pentamidine in fused silica capillaries, which were used in an electrophoresis system. The separation of enantiomers of amino acids in a MIP-CE system was acquired by Lin *et al* (Lin *et al* 1997; 1997a; 1997b; 1997c) they used the method of post-bulk polymerisation to pack the sieved MIP by incorporating with acrylamide gel into the capillary i.e. an *in situ* polymerisation method. Schweitz *et al* (1997) used imprinted polymer monoliths to resolve racemic samples of ropivacaine, mepivacaine and bupivacaine. Bruggemann *et al* (1997) used an *in situ* film coating technique to fill the capillary and showed resolution of racemic 2-phenylpropionic acid. Similarly, Tan and Remcho (1998) used this approach to resolve the enantiomer D- and L-dansyl phenylalanine. Using MIP-CEC with imprinted polymer monolith that were *in situ* prepared, Schweitz *et al* demonstrated enantiomeric separation of propranolol, metroprolol and β-blockers (Schweitz *et al* 1997a, 2001). The research group further developed the study by using precipitation polymerisation to prepare microparticles, for the same purpose (Schweitz *et al* 2000). In 2002 Schweitz prepared molecularly imprinted polymer coatings in fused-silica capillary columns by using a surface-coupled radical initiator.

## 1.1.9.5 Binding assays

The use of MIPs as alternatives to antibodies has its benefits. Such that the MIPs not only mimic the characteristics of the antibodies but are also faster, easier and cost effective to prepare. The polymers obtained can also be used in harsh environments such as high temperature, pressure, pH, and organic solvents. Furthermore, the polymers can be prepared against molecules that are difficult or expensive to make antibodies for, for example immunosuppressive agents like cyclosporin.

MIPs are being employed in competitive radioligand-binding assays and are prepared in the same manner. For instance the imprinted polymers are cast around the template molecule, subsequent removal of the template allows a radio-labelled substrate to bind into the cavity, which is then displaced by a non-labelled analogue (Takeuchi and Matsui 1996; Kempe 1996; Ansell *et al* 1996; Sellergren 1997; 1997a). In the initial MIP assays the studies have demonstrated high specificity, selectivity and cross-reactivity profiles that are comparable to their respective antibodies. Vlatakis *et al* (1993) were the first authors who developed molecular imprinted absorbent assay (MIA) for the bronchodilator theophylline and the tranquilliser diazepam. These polymers were assessed in competitive radioligand binding assays. The

MIA for theophylline and diazepam exhibited good correlation with commercially available antibody assay systems, as well as giving a highly specific cross-reactivity profile that was comparable to the antibodies. This format was further used in other studies such as the work reported by Andersson (1996). In this study a MIA for the β-blocker (S)- propranolol was synthesised and the obtained MIA displayed high enantioselectivity. Haupt *et al* (1998) prepared a MIA for the herbicide, 2,4-dichlorophenoxyacetic acid. MIA systems have also been developed for atrazine (Muldoon and Stanker 1995; Siemann *et al* 1996), morphine (Andersson *et al* 1995), (S)- propranolol (Bengtsson *et al* 1997) cortisol (Ramström *et al* 1996) and for immunosuppressive drugs, like cyclosporin A (Senholdt *et al* 1997).

Further development of the assays involved using fluorescence (Piletsky *et al* 1997; Haupt *et al* 1998; 1998a) and electrochemical probes (Haupt 1999; Kröger *et al* 1999) for detection. Such developments avoided the use of radiolabels that are harmful to handle and cause radioactive waste.

MIPs have also been used in ELISA-type assays where the analyte was labeled with an enzyme i.e. peroxidase, colorimetry (Piletsky *et al* 2000) and chemiluminescence (Surugiu *et al* 2000) was used for detection. Piletsky *et al* (2001b) reported a new technique that involved coating microtitre plates with MIPs. These MIPs would substitute antibodies and receptors in enzyme-linked and fluorescent assays. The MIPs synthesised were specific for low molecular weight analytes such as epinephrine, atrazine and proteins. The MIPs were prepared by oxidation polymerisation in the presence of template molecules: 3-aminophenylboronic acid, 3-thiopheneboronic acid and aniline, polymerised in water. Then the MIPs were finally grafted onto the polystyrene surface of the microplates. MIPs synthesised in this manner generated antibody-like binding properties, gave high stability and good reproducible measurements that made MIP-coating an alternative to conventional antibodies or receptors, that are employed in ELISA.

In the ELISA type assays the use of enzyme-labelled template is less practical in MIP assays for two reasons: firstly due to the enzyme functioning only in aqueous buffer, whereas most of the MIPs function in organic solvents: secondly, given that the enzyme labels are large in size as compared to the template, the accessibility of the template to the binding sites can thus be affected. The MIPs functioning well in aqueous solvent and dealing with the binding site accessibility has been demonstrated by studies preformed by Andersson *et al* (1995; 1996), Haupt *et al* (1998), Bengtsson *et al* (1997) and Ansell and Mosbach (1998). Piletsky *et al* (2000) reported an approach that synthesised an imprinted polymer *in situ* in the wells of a polystyrene microtitre plate. Aminophenylboronic acid was polymerised in the presence of epinephrine (target analyte) using oxidation of the monomer by ammonium persulfate and resulted in the grafting of a thin polymer layer on the surface of the wells. Here, a competitive enzyme linked assay with a conjugate of horseradish peroxidase and norepinephrine was developed.

Due to the increasing demand for automated, high-throughput assaying and screening of natural products, biological and chemical combinatorial libraries, MIPs have been employed as alternatives to biological receptors. This is especially useful in cases where the natural receptor does not exist or is difficult to obtain in large quantities (Haupt 2003). Surugiu *et al* (2000) reported developing a chemiluminescence

high-performance MIP-based assay. Microtitre plates were coated with MIP microspheres using polyvinyl alcohol as an adhesive. The same polymer and detection mode was used by Surugiu *et al* (2001) to design a flow-injection ELISA-type MIP assay. A glass capillary coated with the imprinted polymer was mounted in a flow system and the photomultiplier tube (PMT) was employed for detection.

Ye and Mosbach (2001a) and Ye *et al* (2002) coupled proximity scintillation with molecular imprinting, to develop an assay for (S)-propranolol (**Figure 18**). The scintillation fluorophore was incorporated into the polymer by copolymerisation. When the scintillation fluorophore was irradiated with β–rays, it emitted fluorescence light that was easily quantifiable by a PMT. As the scintillation fluorophore are located closely to the binding sites, binding of a radio-labelled template (analyte) caused excitation and then emission of the fluorescent light. The decease in fluorescence, however, was observed for unlabelled template binding to the site.
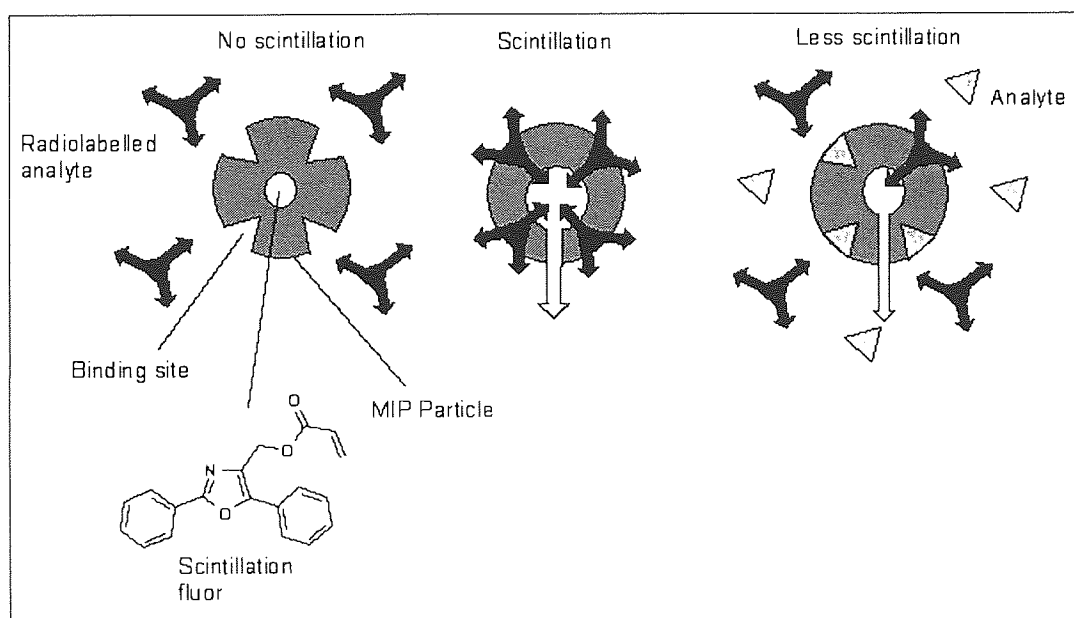


**Figure 18:** Schematic representation of a competitive binding assay format based on proximity scintillation (Adapted from Haupt 2003).

## 1.1.9.6 Sensors

The binding of an analyte to a biological recognition element such as, an antibody, a receptor or an enzyme generates a signal of either a chemical or a physical nature (i.e. termed as a biosensor). This binding is then converted into a quantifiable output signal by the transducer. The over sensitivity of the biological element however limits its commercial success. Instead, replacing the recognition element with a MIP helps overcome this problem. In addition, MIPs are: robust; chemically inert; stable; reusable, and they can be used in harsh environments, and so replacing the biological recognition elements with MIPs, attracts substantial commercial interest.

The binding of an analyte can be depicted by a simple change in mass i.e. mass accumulation, pH, fluorescence, electrical resistance or capacitance and luminescence. This chemical signal is then

transduced into an electrical signal that is amplified and monitored (**Figure 19**). The specific property like fluorescence or electrochemical activity could be possessed by the analyte itself, on the other hand a reporter group could be integrated within the polymer to either generate or enhance the sensor response.
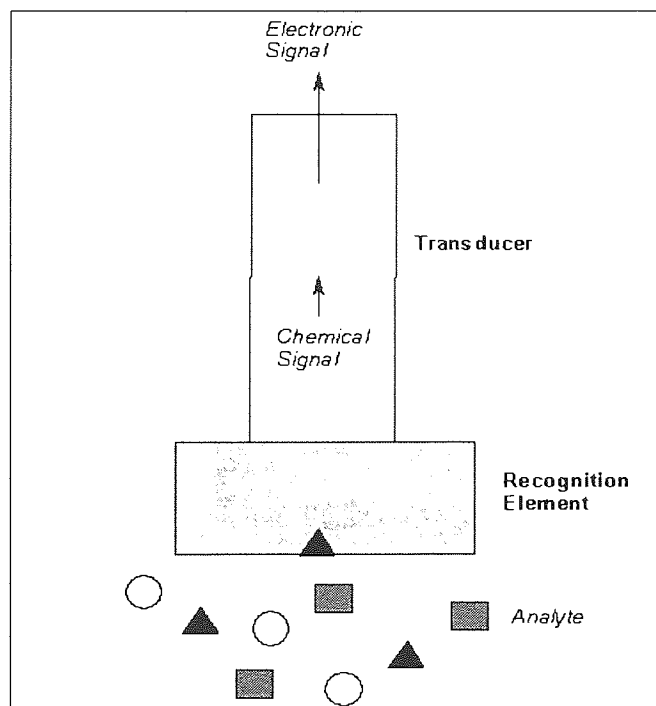


**Figure 19:** Schematic representation of a biosensor.

A recognition element, selective for a certain analyte, is connected to a transducer, which converts the recognition signal to an electrical signal (Adapted from Ramström and Ansell 1998).

The first to report on a MIP-sensor based on capacitance was Hedborg *et al* (1993) this sensor consisted of a field-effect capacitor covered with a thin phenylalanine anilide-imprinted polymer membrane. In this study enantioselectivity was not evident though regioselectivity was observed. Panasyuk *et al* (1999) reported the detection of polycyclic aromatic hydrocarbons (PAHs) in liquid media they used capacitive detection in combination with imprinted electropolymerised polyphenol layers on gold electrodes. Sensors based on capacitance have also been generated for glucose (Cheng *et al* 2001) and creatinine (Panasyuk *et al* 2002).

Recently, the success of integrating MIPs with sensors based on mass sensitive transducers especially the quartz-crystal microbalance (QCM - MIP) for recognition purposes have been applied for both biomimetic and chemical fields (**Figure 20**). QCMs are piezoelectric devices fabricated of a thin plate of quartz with electrodes affixed to each side of the plate. A thin imprinted layer is deposited on one side of the disk. Mass change occurs by the analyte accumulating in the MIP and causes a reduction in oscillation frequency that is quantified by frequency counting. Robust and low costing sensors based on this format have allowed sensors to be developed for (S)-propranolol (a beta-blocker) (Haupt 1999) that demonstrated enantioselectivity. QCM - MIP sensors have also been prepared for glucose (Malitesta *et al* 1999), caffeine (Liang *et al* 1999; Kobayashi *et al* 2001), plant hormones like indole-3-acetic acid

(Kugimiya and Takeuchi, 1999) and 2-methylisoborneol (Ji *et al,* 1999; 2000). Combining QCM with imprinted polymer was reported by a number of research groups for instance Kriz *et al* (1997), Kanekiyo *et al* (1999) and Ersöz *et al* (2005). Dickert and Hayden (2002) have reported using the stamping method where whole yeast cells have been imprinted onto polyurethane and sol-gel layers on the surface of the QCM crystal. This method allowed quantifiable measurements of the cells within suspensions of various concentrations to be made.
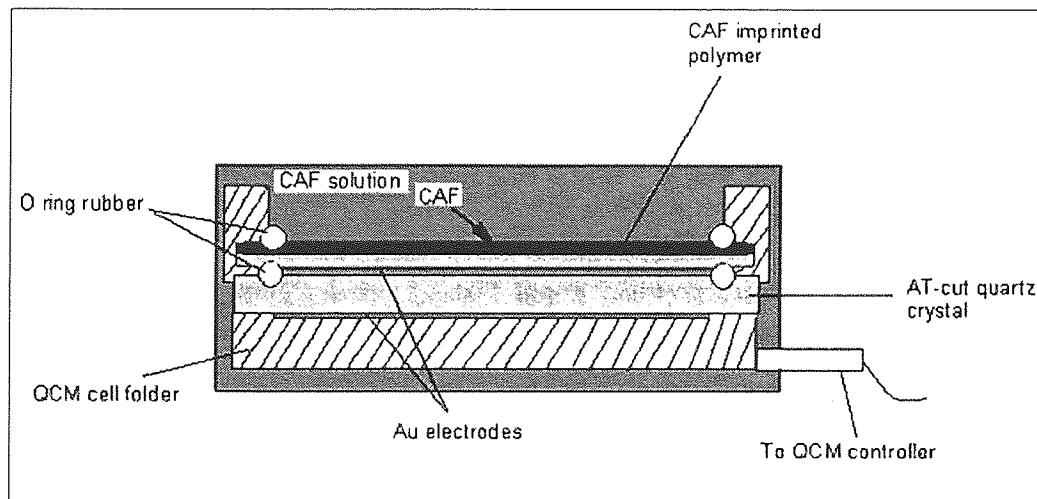


**Figure 20:** Schematic representation of an experimental set-up for QCM attached with imprinted polymer (Adapted from Kobayashi *et al* 2001).

MIP sensors have also been based on conductometric transducers. In this method an imprinted polymer membrane disconnects the two electrodes. Thus binding of an analyte to the polymer changes its conductivity and this can be translated into an electric signal. Studies that have used this method is work by Kriz *et al* (1996) they constructed a chemical sensor specific for benzyltriphenylphosphonium ions, and demonstrated that the polymer synthesised exhibited strong binding to the imprint species, benzyltriphenylphosphonium ions. Chemical senors have also been developed for L-phenylalanine (Piletsky *et al* 1998b) and atrazine (Piletsky *et al* 1995; Sergeyeva *et al* 1999). The sensor for atrazine was based on a free-standing atrazine-imprinted acrylic polymer membrane and conductometric measurements were taken.

MIP sensors have also been designed on the basis that the analyte itself carries a specific property such as fluorescence or electrochemical activity. For fluorescent analytes a study by Kriz *et al* (1995) reported using a fiber-optic sensing device based MIPs, for the determination of an amino acid derivatised with a fluorescent labelling group, dansyl-L-phenylalanine. Dickert *et al* (1999) imprinted sensor layers for detecting PAHs in water. For electrochemical active analytes, Kriz and Mosbach (1995) prepared a competitive amperometric morphine sensor- based on an agarose immobilised MIP.

If the analyte however, does not possess fluorescence or electrochemical activity then a sensor is based on competitive or displacement method. The work reported by Kröger *et al* (1999) demonstrates this method. In this study MIP particles were coated as a thin layer onto a screen-printed carbon electrode and used for the electrochemical sensing of 2,4-dichlorophenoxyacetic acid (2,4-D). A non-related

electroactive compound was used, which was able to bind to some extent to the 2,4-D binding sites. In the presence of the print molecule only part of the probe bound and the analyte concentration could be electrochemically quantified by the unbound fraction of the probe. Sensors have also been prepared on the basis of competitive displacement where fluorescence and HPLC were used as detecting systems. For instance work reported by Levi *et al* (1997) prepared a sensor for the determination of chloramphenicol using MIPs and HPLC. Here a competitive displacement of a chloramphenicol-methyl red (CAP-MR) dye conjugate from specific binding cavities in an imprinted polymer by the analyte was performed and the HPLC with a mobile phase containing CAP-MR was used as the detection system. Similarly, Liao *et al* (1999) synthesised a fluorescent sensor for L-tryptophan by using a FFM. The sensor's diansyl moiety however had low sensitivity to the binding event. This led researchers to use an external quencher (p-nitrobenzaldehyde) to study binding of the fluorescent polymer. Displacement of the quencher from the binding cavities by L-tryptophan caused a concentration dependent change in fluorescence and therefore counteracted the problem successfully. In the same manner, Piletsky *et al* (1999b) displaced non-specific dyes from MIP chromatographic stationary phases as a means of detecting and quantifying of ligand-polymer binding events.

Sensors have also been developed where the signalling system is incorporated into polymer structure and the work reported by Matsui *et al* (2000a) uses this format. In this study they used a metalloporphyrin based monomer as the recognition element for 9-ethylamine (9-EA). The resultant MIP showed fluorescence quenching if the template was rebound and the degree of the quenching depended on the concentration of 9-EA. The structurally related adenine and 4-aminopyridine mimicking a partial structure of 9-EA however showed higher rebinding than the template.

## 1.1.9.7 Catalysis and artificial enzymes

MIPs have also been used as catalysts and enzyme mimics, and for this application five different methods have been used. The first is the imprinting of transition state analogues by using metal ion co-ordination. This method has been employed for instance to develop catalyst for the hydrolysis of p-nitrophenyl acetate (Robinson and Mosbach 1989; Ohkubo *et al* 1994; 1994a). Subsequently from these preliminary studies catalytic MIPs were developed for the hydrolysis of amino acid esters (Ohkubo *et al* 1995; 1995a). The second method involves using coenzyme analogues as print molecules to provide a useful predetermined catalytic mechanism i.e. in the study by Andersson and Mosbach (1989) imprinted for the enzymatic transformation of amino acids. The third approach used the metal ion co-ordination compounds to mediate catalytic reactions. Work reported by Matsui *et al* (1996) used this method to imprint transition state analogue for synthetic preparation of `class II aldolase` mimics that act as catalysts for the aldol condensation reaction. Their approach was to form a pre-polymerisation complex with the transition state analogue $Co^{2+}$ co-ordinated dibenzoylmethane and the monomers vinylpyridine, styrene and divinylbenzene. Similarly, Kim *et al* (2001) used this method for imprinting transition state analogues for the hydrolysis of diphenyl carbonate and cholesteryl 4-nitrophenyl carbonate (Kim *et al* 2001a). The fourth method is to imprint a substrate analogue to specifically arrange the configuration of these groups in the

formed polymer. This approach was used for the dehydrofluorination of 4-fluoro-4-p-nitrophenyl-butan-2-one (Muller *et al* 1993; Beach and Shea 1994) and used for the hydrolysis of amino acid esters by Leonhardt and Mosbach (1987). The last method involves removing product to achieve equilibrium shifting in favour of a particular reaction. Ye *et al* (1998) demonstrated this for a thermodynamically unfavourable reaction by removing the reaction product *via* a MIA.

## 1.1.9.8 Molecular imprinted polymers as receptor mimics

In outlining the functions of imprinted polymers so far their role depends upon the ability to recognise and rebind either their original template or its structural analogues. This ability can be compared between MIPs and natural receptors.

## 1.1.9.8.1 Steroid receptor mimics

Mimics for steroids have been made. For instance work by Cheong *et al* (1997b) reported a testosterone receptor-binding mimic. This mimic was formed by preparing a series of MIPs templated with testosterone with ethylene glycol dimethacrylate as the crosslinker and methacrylic acid (MAA) as the functional monomer. The MIPs in general recognised their template although some exhibited cross-reactivity towards four other related steroids in particular β-estradiol but also progesterone, testosterone propionate and estrone. The key feature needed to determine dominant affinity of the substrates for the receptor was the 17-hydroxyl which was present in testosterone and β-estradiol but not in the others. MIPs were also synthesised with the crosslinker propylene glycol dimethacrylate as an alternative to the original cross-linker. The MIPs generated exhibited significant characteristic changes. This includes the MIP binding to β-estradiol more strongly than the template testosterone and change in the elution order of the steroids.

A similar study by Piscopo *et al* (2002) generated MIPs for 17β-estradiol using ethylene glycol dimethacrylate as the crosslinker and 4-vinylpyridine instead of MAA as the functional monomer. The MIPs were challenged chromatographically with four other related estrogens e.g. 17α-estradiol, estrone, estriol and 17α-ethynylestradiol. The study revealed some selectivity towards template along with considerable cross-reactivity towards the other estrogens.

## 1.1.9.8.2 Folate receptor mimics

Detailed research by the Quaglia *et al* (2001) was performed on MIP receptors for folic acid. Such receptors would be used to screen compound libraries for new inhibitor of enzyme dihydrofolate reductase (DHFR). The structures of the compounds used in this study are given in **Figure 21**. Methotrexate (MTX), with its close resemblance to folic acid and being a very potent strong-binding inhibitor of DHFR, was initially investigated as a template for creating the folic acid receptor. Consequently from this study the problem of imprinting with relatively large multifunctional biologically important compounds was highlighted. Due to MTX having two carboxyl functions and two primary amino groups, it holds an

amphoteric character and is highly polar. In the traditional imprinting approach a preference would be to have the template interacting with the functional monomer through hydrogen bonding interaction in a non-polar aprotic solvent. This however is difficult for MTX, as the pteridine and tertiary aliphatic amine substrucutres could be best targeted with acidic functional monomers whereas the glutamic acid substructure maybe better with basic functional monomers. A folate receptor with a range of functional monomers was attained but its chromatographical usefulness was limited. From the study it was determined that rather than addressing the template MTX as a whole only a part of it would be probed i.e. the pteridine moiety. A number of lipophilic inhibitors had been developed that exhibited selectivity for microbial DHFR; trimethoprim (TMP), 2,4-diamino-6,7-diisopropylpteridine (DIP) and trimetrexate (TRX). Owing to their high solubility in organic solvents these were imprinted in DCM using MAA as the functional monomer. The three MIPs displayed imprinting effect for their templates and for the folic acid analogues. The DIP based MIP demonstrated poor selectivity. In the aqueous mobile phase however the MIP exhibited enhanced retention of folic acid and its analogues Leu and MTX. The study established that in the aqueous chromatography "the recognition was driven by a combination of specific hydrophobic and ionic forces". On the whole, this study successfully illustrated the utility of engaging a substructure of a complex target molecule where the target itself proves to be uncooperative in the imprinting process.

Figure 21: Templates and test compounds by Quaglia *et al* 2001.


## 1.1.9.8.3 Adrenergic receptor binding mimics

Molecularly imprinted polymers mimicking the binding characteristics of β-adrenergic receptors were prepared by Ramstrom *et al* (1996a). The structures of the agonists and antagonists to the receptor used in their study are given in **Figure 22**.
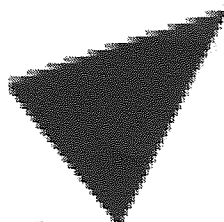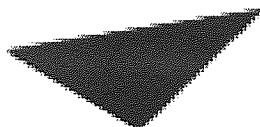
**Figure 22:** β-Adrenergic receptor agonists and antagonists used by Ramstrom *et al* 1996a.

In this study closely related compounds (1*S*,2*R*)-(+)-ephedrine and (1*S*,2*S*)-(+)-pseudoephedrine were employed as the templates. This is due to the fact that the endogenous ligand epinephrine had low solubility in the imprinting solvents. A functional monomer to template ratio of 4:1 was employed to encourage saturation of the ligand in the pre-polymerisation mixture. The polymerisation was photolytically initiated in the presence of trimethylolpropane trimethacrylate forming functionalised cavities as illustrated in **Figure 23**. It was anticipated that the particular ionic attraction between the carboxyl derived from the methacrylic acid and the templates' amino function, together with the remainder of the template resting in an otherwise hydrophobic cavity, would simulate the known binding features of the target adrenergic receptors. The resulting imprinted polymers were probed chromatographically.
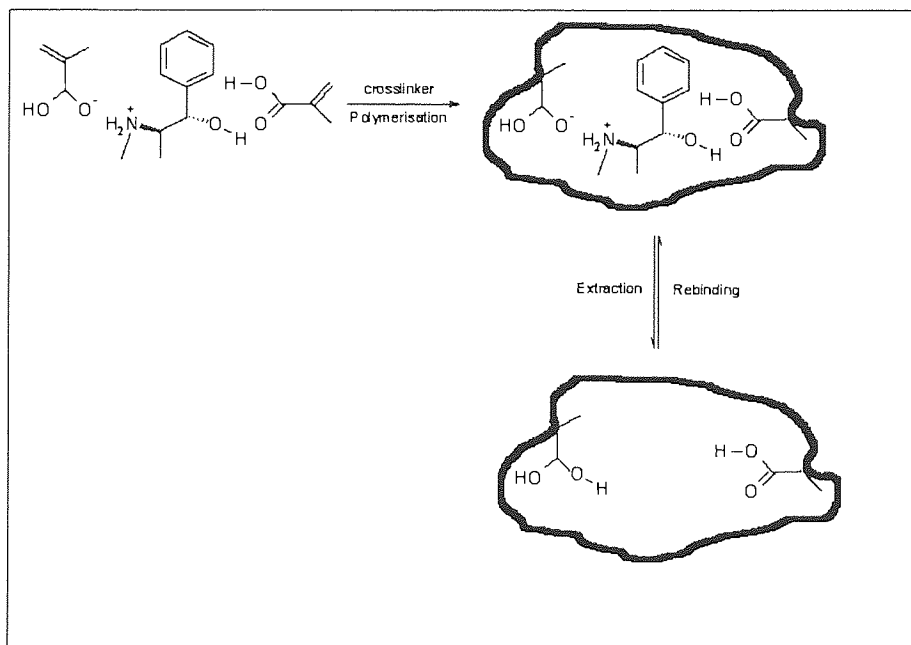
**Figure 23:** Formation of imprinted sites mimicking adrenergic receptors (Adapted from Ramstrom *et al* 1996a).

From this study the individual imprinted polymers demonstrated the ability to recognise the original template and were able to discriminate against the enantiomers of their own templates. However poor enantiodiscrimination was exhibited between diastereoisomers of the template.

It was also discovered that of the two chiral centres for determining the chiral recognition, β-carbon of ephedrine was the most important given that the 1-*S* compounds were more strongly retained than the 1-*R* isomers. In addition it was observed that higher capacity factors for the isomers of epinephrine were as a result of the presence of the catechol moiety that gave rise to an increase in non-specific binding to the polymers. As for the β-adrenergic receptor antagonists their MIPs exhibited lower enantiodiscrimination owing to the increased distance between the amino function and the aromatic portion. With respect to timolol, no enantiodiscrimination was revealed. This is due to the fact that the aromatic portion is a polar five-membered ring heterocycle, which has little likeness to the aryl portions of the templates in both shape and polarity (Rathbone 2005).

### 1.1.9.8.3.4 Cinchona alkaloid receptor mimics

Receptor mimics have also been made for cinchona alkaloid. For example work by Matsui *et al* (1996a) imprinted two antimalarial alkaloids (-)-cinchonidine and (+)-cinchonine. The structures of these templates along with the other compounds used in this study are illustrated in **Figure 24**.
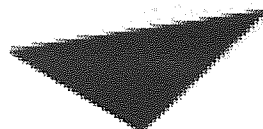
**Figure 24**: Alkaloid structures used by Matsui *et al* (1996a).

A distinctive selectivity with high stereoseparation factors was exhibited by the two MIPs. It was suggested that the rigidity of the templates was responsible for the resulting imprinted sites. To evaluate the MIPs molecular similarity between the templates and the other test compounds, **Table 3** illustrates this by showing the normalised retention indices (RI). The other two compounds quinine and quinidine have two structural variations: a methoxy substituent and the inversion of two chiral centres. Having one structural variation resulted in the RI dropping to 0.14 or 0.34 and when both variations were applied these values halved. Overall the results suggested that the closer the structure of the test compound to that of the template the more strongly it would interact with the MIP. In addition, the study also established that it was possible to separate partially the enantiomers of the β-adrenergic antagonist, propranolol. Closely assessing the structure of propranolol revealed some molecular similarities to the templates, namely, a bicyclic aromatic part connected to a β-hydroxy ethylamine thus further signifying the possibilities for using MIPs for detection of molecular similarity or pharmacophore patterns.

**Table 3**: Chromatographic capacity factors, calculated imprinting factors and retention indices from Matsui *et al* (1996a).

## 1.1.9.9 Other applications of MIP

The other applications of MIPs that have also been investigated are:

- Combinatorial libraries (Berglund *et al* 1996; Bowman *et al* 1998; Ramström *et al* 1998; Takeuchi *et al* 1999; Ye *et al* 2001; Cederfur *et al* 2003).

- Controlled drug release (Allender *et al* 1997; Allender *et al* 1997a; Sreenivasan *et al* 1997a; Karmalkar *et al* 1997; Norell *et al* 1998; Vlatakis *et al* 1993; Suedee *et al* 2000; Suedee *et al* 2002; Allender *et al* 2000)

The applications outlined in this section, however, only refer to some of its many potential applications.

## 1.1.10. Cytochrome P450

## 1.1.10.1 CYP2D6 receptor mimics

Cytochrome P450 (CYP450) is a family of enzymes that are involved in the metabolism of many drugs and dietary substances. Where the problem begins is that some P450s are subject to polymorphisms and a significant percentage of any given population either poorly express or do not express the enzyme at all. As a result, if the main route of metabolism for a group of compounds is through CYP2D6 isoenzyme for example, a proportion of future patients that do not express this enzyme would be subject to toxicity (i.e. drug accumulation) (Foye *et al* 1995).

At present identification of potential substrates of the main P450 isoenzymes is by either using known specific chemical inhibitors or inhibiting antibodies in either human microsomal incubations or human heterologously expressed isoenzyme systems. These systems, however, are expensive and time-consuming to use. In addition to this they are unsuitable for mixtures of agents and generate data over long periods. These systems are only compatible with small groups of compounds and incompatible with large groups of compounds (mass-screening) that are combinatorially synthesised. Therefore, developing a robust and chemically stable receptor that mimics the binding character of CYP2D6 would then make it possible to provisionally identify both its inhibitors and substrates. This would then narrow the scope of compounds to be put through detailed studies such as human heterologously expressed or microsomal human P450s (Foye *et al* 1995).

## 1.1.10.2 Overview on Cytochrome P450

Cytochrome P450 (CYP450) is the generic name given to a large family of enzymes that play an significant role in metabolising most drugs and xenobiotics in humans. In particular, the catalyses of phase I drug metabolism (Wilkinson 2001).

These enzymes metabolise over 90% of currently available pharmaceutical agents. CYP450 plays its role by converting drugs to more polar compounds (i.e. water soluble) and thus get directly excreted from the

body after their desired effects have been exerted. Besides this they can also convert some prodrugs into their corresponding therapeutically active compounds. In spite of this, it can also result in the formation of more toxic compounds that carry cancerogenic properties (Parkinson 1996; Guengerich and Shimada 1998).

Drugs can be metabolised either in the phase I (reactions involve oxidation, reduction and hydrolysis) or phase II (reactions involve: acetylation, glucuronidation, sulfation and methylation). As well as its role in metabolism, many CYP450 enzymes play a pivotal role in diverse physiological processes including steroid and cholesterol biosynthesis, fatty acid metabolism and the maintenance of calcium homeostasis (Ritter 1996a).

P450 refers to a superfamily of heme-thiolate enzymes whose $Fe^{2+}$ carbon monoxide complex shows an unusual absorption spectrum at maximum at 450 nm. Which is caused by the binding of carbon monoxide to a reduced form of the heme; this led to the initial P450 designation. Denaturing of this ferrous-CO complex has an associated shift of 420nm, i.e. similar to myoglobin (Woolf 1999).

Cytochrome P450 (CYP450) was discovered in 1958 (Klingenberg 1958; Garfinkel 1958) and since then a great deal of diversity within the P450 has been found. The P450 enzymes can be found in virtually all organisms including bacteria, fungi, yeast, plants, insects, fish and mammals. More specifically in mammals are places such as the liver, tissues of the kidney, intestine and lungs. All CYP450 genes are derived from a single ancestral gene, which existed more than 2 billion years ago (Nelson *et al* 1996).

The enzymes in question are located in the endoplasmic reticulum (ER) a winding membrane system that runs throughout a eukaryotic cell. These are involved in the transport and synthesis of certain proteins and lipids. There also found in the inner membrane of the mitochondria (oxidation of fuel; energy production) that has in place several P450s, which metabolise steroid hormones, vitamin D and bile acids (Ritter 1996).

As all the mammalian P450 enzymes are membrane-bound proteins and are lipophilic, this causes challenges when trying to carry out solubilisation and purification techniques. Bacterial P450 enzymes, in contrast, are water-soluble and this facilitates their purification and crystallisation. Examples of bacterial P450 enzymes include P450cam (CYP 101 - pseudomonas putida) (Gibson and Skett 2001), P450 bm-3 (CYP 102 – bacillus megaterium) (Gibson and Skett 2001), P450 terp (CYP 108) (Hasemann and Ravichandran 1994) and P450 eryF (CYP 107A1) (Cupp-Vickery and Poulos 1995)

The structural characterisation of mammalian cytochrome P450 was made through comparison with the available bacterial P450cam enzymes. This allowed some structural assumptions to be made, such that it is a triangular prism and has 12 helical segments (45% accounted by amino acid residues). Likewise, the heme prosthetic compound is bound in P450cam by at least three interactions. The first interaction entails

the co-ordination of cysteine thiolate ligand to the iron, second is pincer action of the 2 helices on the heme, and third is the hydrogen bonding to the heme propionic acid groups (Woolf 1999a).

Recently crystallisation on mammalian cytochrome P450 has taken place with CYP2C5 protein (rabbit). This crystallisation was made possible by modifications carried out on the membrane-binding portion of the enzyme. Such modifications included the removal of the N-terminal anchor peptide and replacement of an internal hydrophobic sequence with a more water-soluble sequence from a related enzyme. The X-ray structure (Williams *et al* 2000) of this enzyme showed significant differences from the bacterial enzymes (Williams *et al* 2000; Cosme and Johnson .2000).

The validity of such structures, however, are questionable. This is due to the drastic modification process which undoubtedly would not only affect its chemistry but also give rise to question on whether the crystal structure is a true representative of the actual structure of the enzyme.

More recently the crystal structures of CYP2C9 (Williams *et al* 2003), CYP2B4 (Scott *et al* 2004) and CYP2C8 (Schoch *et al* 2004) have been published.

The crystal structure of the human cytochrome P450, CYP2C9, was determined both in the presence and in the absence of its substrate, the anti-coagulant drug warfarin. The interaction of warfarin and CYP2C9 revealed a new binding pocket. The new warfarin binding pocket and the crystal structure of CYP2C9 suggested that CYP2C9 was capable of accommodating multiple ligands/substrates during its biological function. This is in accordance with the studies that implied a 'two-site model' for CYP2C9. The new warfarin binding site could possibly be one of these sites that when occupied activate the CYP2C9 to go through an allosteric mechanism, this being evident by the adequate space for other substrate molecules to bind at the same time at the haem, such as fluconazole.

The molecular structure of microsomal cytochrome P450 2B4 was complexed with 4-(4-chlorophenyl) imidazole and determined by X-ray crystallography at 1.9-Å resolution. This structure was determined by means of a closed conformation of CYP2B4, which was more similar to the mammalian 2C enzymes than was the previous open structure of CYP2B4. The open and closed conformation structures of 2B4, besides showing variations in their structures, also gave an insight into the control of substrate access and the structural changes involved in tight inhibitor binding, in addition to the coordination of substrate and redox partner binding.

CYP2C8 is a hepatic drug-metabolising enzyme, which oxidises therapeutic drugs like taxol, cerivastatin and endobiotics like retinoic acid and arachidionic acid. The structure of CYP2C8 was determined by X-ray crystallography at 2.7-Å resolution after modifying the membrane protein for crystallisation. This modification involved replacing the hydrophobic N-terminal transmembrane domain by a short hydrophilic sequence. The structure determination for of CYP2C8 was carried out without using multiple internal

mutations to the catalytic domain which is the first time its been reported. This study identified a peripheral binding site in P450s that could possibly contribute to drug-drug interactions in P450 metabolism.

### 1.1.10.3 Cytochrome P450 (CYP450s) reactions

Oxidative metabolism by cytochrome P450 enzymes is a primary method of drug and xenobiotic metabolism. These are often known as the mixed-function oxidases or monooxygenases. This is due to there being an oxygen atom incorporated within the substrate, as well as the production of water. Other reactions besides the most important method mentioned above include isomerisations, deaminations, dealkylations and dehydrogenations (Foye *et al* 1995).

Nicotinamide adenine dinucleotide phosphate (NADPH) is a coenzyme derived from niacin (which is vitamin B, whose amide form is known as nicotinamide) and is anchored to the membrane by an $NH_2$-terminal hydrophobic peptide. NADPH acts as a reducing agent for many anabolic enzymes. These enzymes are involved in synthesising fatty acids and steroids (Woolf 1999a).

NADPH-cytochrome P450 reductase is a flavoprotein that contains flavin adenine dinucleotide (FAD) and flavin mononucleotide (FMN) are involved in the sequential electron transfer process (**Figure 25**).



**NADPH** ⟶ **FAD** ⟶ **FMN** ⟶ **Cyctochrome P450**

⟹ *electron flow* ⟹
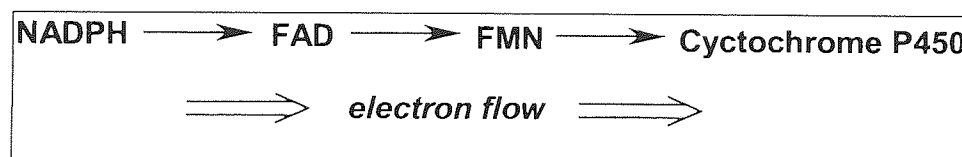
**Figure 25**: NADPH involved in the sequential electron transfer process.

This initial transfer of an electron is carried out on the complex generated by the binding of a substrate to a ferric form of the enzyme i.e. the heme the active centre of the cytochrome. This results in a reduction of the complex, followed by the binding of the molecular oxygen to the complex. To this oxygen-complex the NADPH transfers a second electron, followed by the addition of a proton. The final addition of another proton generates a homolytic cleavage of oxygen and hence liberating water. The other oxygen atom is incorporated into the substrate to give rise to an oxidised product and is released. Besides this, the ferric form of the enzyme is also regenerated (Gibson and Skett 2001; Ritter 1996a).

### 1.1.10.4 Multiplicity in CYP450 and nomenclature

P450 enzymes are found to be variable in many identified mammal cells. In the human genome alone there are 55 different P450 genes. These are divided into 17 families. Families like CYP1-3 are mainly expressed in the liver these are involved in drug and endogenous compound metabolism. These families of enzymes exhibit a broad and overlapping substrate specificity. The physiologically important CYP4-17 families, however, exhibit a stricter substrate specificity and tissue distribution. In contrast, mammalian CYP2-4 families, have a large spread difference in their substrate specificity, expression distribution and the number of enzymes in their subfamilies.

The prime cause of variations found within the same species, in its expression and metabolic rate are due to gene polymorphism, although other contributing factors can be related to this such as physiological, environmental and pathological factors. P450 gene mutation also causes the differences in protein substrate specificity and catalytic activity.

The large influx in enzymes discovered particularly from bacterial, insect and plant origins, as well as the multiplicity found within CYP450, were first exposed by enzyme purification and recognised by recombinant DNA technology. This has led to the development of a nomenclature system (Woolf 1999). A standard nomenclature system was developed in 1987. Initially, the system was based upon electrophoretic mobility, absorption spectrum and substrate specificity. The system, however, evolved on the basis of identities in protein sequence more specifically on structural and functional similarities. The enzymes are named CYP i.e. the root symbol, representing cytochrome P450, followed by a number denoting the family, a letter designating the subfamily and a second numeral representing the individual enzyme, e.g. CYP450 2D6. Enzymes that have >40% amino acid sequence identity are considered to belong to the same family, whereas enzymes with >55% sequence identity are in the same subfamily (Nelson *et al* 1996).

In addition to this naming system, it is also indicated that some alleles have the same type of mutations but differ with respect to other base changes, these are therefore given the same number (allele group) and made distinguishable by capital letters, such as CYP2D6*4A and CYP2D6*4B which have the same mutation but differ by a single base substitution (Daly *et al* 1996).

## 1.1.10.5 Polymorphisms in CYP450s

A gene variation in the human DNA is commonly termed single nucleotide polymorphism (SNP) or gene polymorphism collectively. This is found at 1% or higher in a population. If SNP causes changes in amino acid sequences these changes can influence gene expression, as well as their functional character.
Variations in enzymes are known as the 'phenotype' of the enzyme. This is usually characterised as being poor metaboliser (PM), intermediate metaboliser (IM), extensive metaboliser (EM) and ultraextensive metaboliser (UM). Although, as mentioned earlier other factors do also contribute such as: physiological, environmental and pathological (Gibson and Skett 2001).

Polymorphic genes show an array of effects from complete loss of protein function to increased enzyme activity. The actions of such proteins cause adverse reactions to many marketed drugs and drug-combination therapies. These have also contributed to many failures in drug development, such that drugs may either be rapidly metabolised before any effectiveness has taken place, or broken down into smaller molecules which causes toxicity, or even interfere with the activity of CYP450s so that other drugs given at the same time cause side effects or become dangerous (Vermeulen 2003).

Particularly noteworthy are the six isoforms that are polymorphic and account for almost half of all clinically used drugs metabolism, namely CYP1A2, CYP2C9, CYP2C19, CYP2D6, CYP3A3 and CYP3A4

(Wong *et al* 1991). These polymorphisms can create a problem in clinical pharmacology, especially in areas such as drug interactions and interindividual variability in drug metabolism (Wong *et al* 1991).

## 1.1.10.6 Polymorphism in CYP2D6

One such major contender in drug metabolism polymorphism is CYP2D6. This was originally discovered as a result of prominent differences in the pharmacokinetics and therapeutic effects of drugs metabolised by this enzyme, such as drugs like codeine, metoprolol, dextromethorphan, and nortriptyline, as well as others (Kroemer and Eichelbaum 1995).

At present 17 different allelic variants of CYP2D6 have been identified, where 95% of the European population show the presence of these allelic variants, such as the CYP2D6*3, CYP2D6*4, CYP2D6*5 and CYP2D6*7 alleles determined by using polymerase chain reaction methods (Woolf 1999c). In contrast, the other 5% are likely to be carrying homo/heterozygous alleles. These mutations are either deletions or point mutations due to splicing defects.

Asians are usually intermediate metabolisers as they maybe either heterozygous for one inactive mutation or homozygous for alleles that have impaired metabolism. For Chinese and Japanese the common CYP2D6*10 variant allele is linked to reducing the activity of CYP2D6 (Woolf 1999c). Africans also come under the category of intermediate metabolisers, partly due to the presence of CYP2D6*17 variant allele (Woolf 1999c). Variations in metabolism (i.e. poor or extensive) can be demonstrated by debrisoquine (a cardiac drug) and other modern drugs. These include anti-depressants, anti-psychiotics, anti-arrythmics and beta-adrenergic blockers.

Significant drug metabolism differences that occur between species and those that occur within species are linked towards 'gene polymorphism'. Studies that quantifiably (i.e. same metabolic route but different rates) and qualitatively (different metabolic rate) demonstrated these species differences were undertaken. One study that has shown species differences is in the case of caffeine (phase I metabolism), where its metabolite paraxanthine is at higher levels in a man compared to a monkey. In contrast the level of production for theophylline is higher in the monkey compared to a man (Gibson and Skett 2001).

In man, molecular biological techniques facilitated the study in variations in drug metabolism, as well as identifying sub-populations present in the human population. This is clearly shown in the study of 'isoniazid slow acetylators'. Acetylating of amino, hydroxyl and sulfydryl groups is catalysed in humans by 2 N-acetyltransferases termed NAT1 and NAT2, due to the existence of polymorphism, this results in the inability to acetylate a large number of drugs like hydralazine, procainamide and isoniazid. The study on the latter drug showed in subjects a bimodal distribution of plasma isoniazid concentrations. These subjects were grouped into slow or rapid acetylators, according to their capacity to acetylate isoniazid (Price *et al* 1960; Gibson and Skett 2001).

A more extensive study based on debrisoquine 4-hydroxylation illustrates the polymorphism found in CYP2D6, the result showed a bimodal distribution in the population. Notably, it was observed that poor metabolisers of debrisoquine also showed impaired ability in their metabolism of drugs like sparteine, amitriptyline, phenformin, haloperidol and phenacetin as well as others. Subjects with poor metabolism of drugs like the anti-arrhythmic and sparteine had lower urinary concentrations of metabolites and higher plasma concentrations of the parent drug, compared with extensive metabolism subjects (Gibson and Skett 2001; Eichelbaum *et al* 1979).

Further observations revealed that such subjects had amplified effects from drugs. In addition, studies involving twins, families and populations concluded that poor oxidation of debrisoquine and sparteine were linked to the inheritance of autosomal recessive characteristics, (Mahgoub *et al* 1977; Eichelbaum *et al* 1979) owing to the inheritance of two mutational CYP2D6 alleles that either allowed no activity or decreased activity of enzyme CYP2D6. In comparison to the extensive metabolisers that had at least one functional allele.

To classify subjects as either being poor or extensive metabolisers, debrisoquine and sparteine were administrated as 'probe drugs'. These would be metabolised by genetically polymorphic enzymes in pharmacogenetic studies. Nonetheless such an approach was not able to be easily adapted for routine clinical work. Therefore, molecular genetic techniques were applied to determine molecular mechanisms responsible for genetic polymorphism and aided the creation of high-throughput clinical tests. The latter test could be performed on DNA isolated from blood samples a method being used for routine diagnosis in clinical work.

Advances in molecular genetic techniques facilitated the development of cloning of complementary DNA and CYP2D6 gene encoding (Gonzalez *et al* 1988; Kimura *et al* 1989). Such advances assisted the characterisation of a series of genetic variants causing low levels of CYP2D6 activity or no activity. Studies took into account SNP that altered amino acid sequence of the encoded protein to SNP that altered RNA splicing or even deletions of the gene CYP2D6 (Ingelman-Sundberg and Evans 2001). Moreover, UM subjects also showed the possession of multiple copies of the gene and resulted in an insufficient therapeutic response to doses of drugs normally metabolised by CYP2D6. The presence of multiple copies is low in northern Europeans. In contrast, in East Africans this is as high as 29%.

## 1.1.10.7 Previous molecular modelling studies

The characterisation of the active site of mammalian cytochrome P450 enzymes like CYP2D6 is still an area that needs further studying. This is essential in the development of pharmacologically potent novel drug entities that the P450 enzymes that metabolise the groups of compounds of interest are identified. Note that some novel agents may also be inhibitors of this enzyme, therefore leading to interference with the metabolism of endogenous compounds as well as changing the pharmacokinetics of other agents. As yet the crystal coordinates for CYP2D6 are not known, though, as mentioned earlier studies on P450cam

(Gibson and Skett 2001) have allowed an understanding of the catalytic functions of cytochrome P450. As a result of this the preceding studies have revealed that minor structural details such as changes in single amino acid residues on CYP2D6 greatly effects its catalytic activity and stereoselectivity (Ellis *et al* 1996). The known substrates for CYP2D6 usually have at least one basic nitrogen; this interacts with the carboxylic acid present in the side chains of Asp301 or Glu216. The distances of the basic nitrogen and a particular site of metabolism lie approximately between 5-10 Å.

A large amount of work based on molecular modelling exists in which the known substrates of CYP2D6 have been superimposed in a rational manner and used to probe internal space of the active site (**Table 4**: list of substrates for CYP2D6). In conjunction with these studies, crystallisation information on P450 (cam, BM3, terp) and use of NMR spectroscopy on the enzyme have assisted the designing of various models of the active site of CYP2D6 and at the same time being able to use this to predict metabolites of molecules (Islam *et al* 1991; Venhorst *et al* 2003; Modi *et al* 1996).

The first substrate models for CYP2D6 were based on substrates containing a basic nitrogen atom at a distance of either 5 (Wolff *et al* 1985) or 7 Å (Meyer *et al* 1986) from the site of oxidation and aromatic rings that were coplanar. In the 5 Å model that used debrisoquine as its template, no substrates were actually fitting onto each other. The 7 Å model used dextromethorphan and bufuralol as its template to construct its model, however, one of the main problems of both of these initial models were that neither could explain the metabolism of the other group of substrates.

From these initial model observations Islam *et al* (1991) combined the distances 5 to 7 Å between a basic nitrogen atom and the site of oxidation to derive to their extended model. This model contained a heme moiety from the crystal structure of P450cam (CYP 101 - pseudomonas putida) (Poulos *et al* 1986) above which debrisoquine the template molecule was positioned, in a similar way to the positioning adopted by camphor in the CYP 101 or P450cam crystal structure (Poulos *et al* 1985). The heme moieties iron is bound to an oxygen atom, which is involved in the hydroxylation process. A set of 15 compounds was fitted onto debrisoquine. From this model it was found that known substrates like sparteine and amitriptyline of CYP2D6 did not fit. Further use of this model was its use in predicting that 4-(N-methyl-N-nitrosamino)-1-(3-pyridyl)-1-butanone (NNK) is not a substrate for CYP2D6. This was confirmed by experiments using human liver microsomes (Vermeulen 2003).

Another model for CYP2D6 was derived by (Koymans *et al* 1992). This model was based on the assumption that the carboxylate group within the protein was responsible for the well-defined distance of either 5 or 7 Å between the basic nitrogen atom and the site of oxidation within the substrate. This model used debrisoquine to represent the 5 Å compound and used dextromethorphan as the 7 Å compound. The oxidation sites of the two templates were superimposed and the areas next to the site of oxidation were fitted coplanar, and the basic nitrogen atom was placed at a distance of 2.5 Å so that it would interact with the assumed oxygen atoms of the carboxylate group within the protein. Predicting the metabolism of four compounds giving 14 possible CYP-dependent metabolites tested the model's reliability. The predictive

value of this model was confirmed by in vivo and in vitro metabolism studies on these substrates that indicated 13 out of the 14 predictions were correct (Koymans *et al* 1992). Further confirmation of this predictive value was carried out recently, by correctly predicting the two metabolites of 1-(2-(bis(4-fluorophenyl)methoxy)-ethyl)-4-(3-phenyl-propyl)-piperazine (GBR 12909) and shown to be formed by heterologous expressed CPY2D6 (de Groot *et al* 1995).

From the protein homology model of CPY2D6, the positions of the heme moiety and the I-helix containing the Asp301 were incorporated into the model (de Groot *et al* 1996). By doing this, steric restrictions and preferences in orientation were included into the model (de Groot *et al* 1997). In this refined model, the aspartic acid residue was coupled to the basic nitrogen atoms, and allowed a sense of direction of the hydrogen bond between the aspartic acid in the protein and the protonated basic nitrogen atoms (de Groot *et al* 1997). The variety of substrates used to fit into the original models for CYP2D6 (Koymans *et al* 1992; de Groot *et al* 1995; 1997) could be fitted into the refined model, indicating that this model accommodates the same variety of structures as the original models. This refined model was later used successfully to design a novel and selective high-throughput screening for substrates of CYP2D6 to provide an insight in explaining the hydroxylation of debrisoquine (Vermeulen 2003).

Recently, a combined model of pharmacophore and homology models has been made (de Groot *et al* 1999; 1999a). Advantages of such a model is that it takes the positive attributes of both of the models, for instance the pharmacophore model's reproducible starting points and atom-atom overlap, and the homology models steric interactions and the possibility to identify the amino acids involved in binding. This model was made of two pharmacophores, one was for O-dealkylation reactions and the second was for N-dealkylation reactions.

Another model for CYP2D6 has been derived to understand the specificity of this enzyme towards inhibitors (**Table 5**: list of inhibitors for CYP2D6). Using strong competitive inhibitors, like ajmalicine and quinidine, created this pharmacophore model. (Strobl *et al* 1993) Ajmalicine was used as a template for this model due to it being the strongest known inhibitor as well as its rigid structure. Performing inhibition studies with derivatives of ajmalicine and quinidine tested the models validity. The model's substrate was bufuralol and the amount of its metabolite 1'-hydroxybufuralol formed determined the potency of compounds to inhibit CYP2D6 –dependent reactions. The overall result from this pharmacophore model is very similar to the results found from substrate models of CYP2D6 (Islam *et al* 1991; Koymans *et al* 1992; de Groot *et al* 1997) The pharmacophore consists of tertiary nitrogen atom, a flat hydrophobic region, a region with additional functional groups with lone pairs that seemed to cause enhanced inhibitory potency, and a hydrophobic region that caused no enhanced inhibitory effect. (Strobl *et al* 1993) Due to the similarities in there findings these models could be combined.

The incentive of such models is that its made it permissible to predict metabolites of CYP2D6 without having to synthesise the molecules in question, such that virtual libraries maybe screened *in silico* and the selection process for synthesis be based upon favourable conclusions.

81

Despite having such models available there is still this ongoing problem in ensuring that the potential substrate within the active site has covered its full conformational ability. In contrast, fluorescent imprinted polymers that mimic the binding criteria of CYP2D6 will allow potential substrates to cover all the diversity of its conformations; this would be evident, as the actual physical interactions would take place.

**Table 4** and **5**: A list showing some of CYP2D6 Substrates and Inhibitors (Abraham and Adithan 2001)
**Table 4** Substrates for CYP2D6.
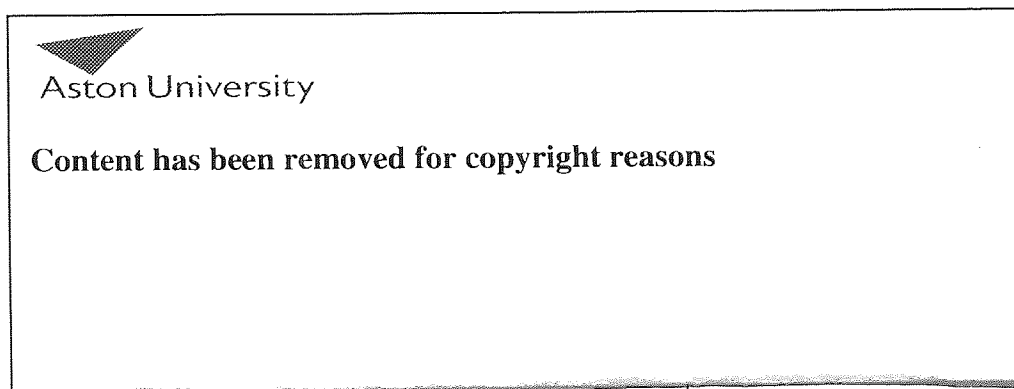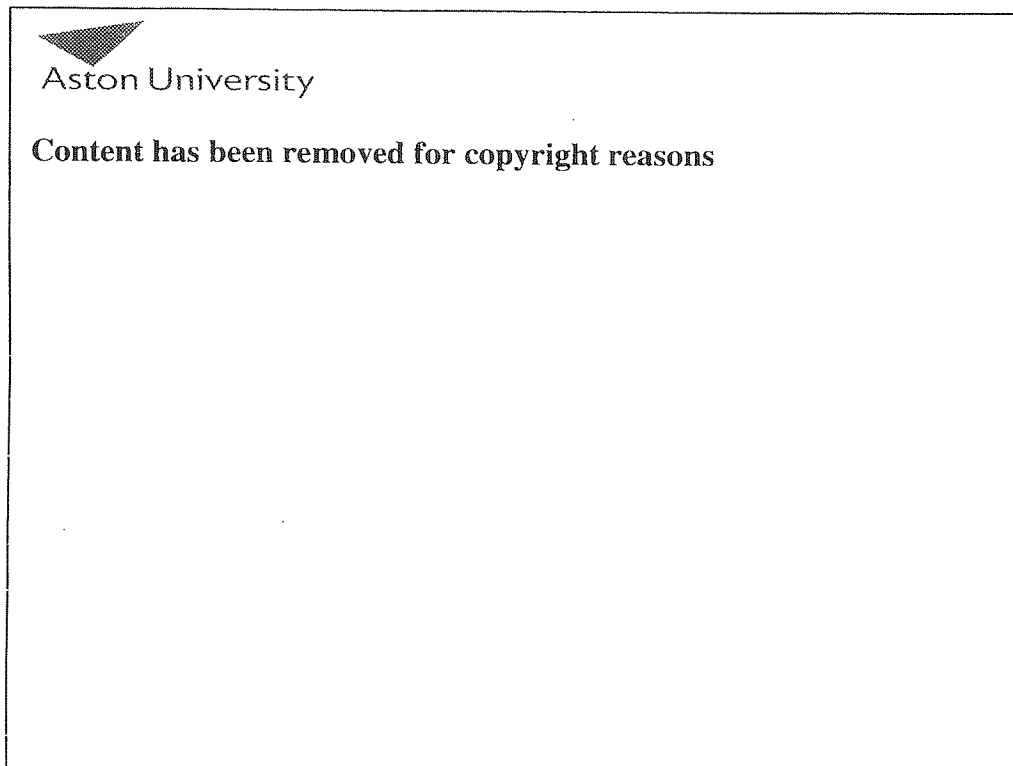
Aston University

**Content has been removed for copyright reasons**

Aston University

**Content has been removed for copyright reasons**

**Table 5** Inhibitors for CYP2D6.

## 1.1.11 Fluorescent imprinted receptors

### 1.1.11.1 Background on fluorescent molecularly imprinted polymers

The development in the design of MIPs has moved into an exciting area where the recognition element (template) together with the transducer element allows the polymer itself to generate information on the recognition of the template (binding). This transducer is based on fluorescence i.e. fluorescence sensor that has the advantage of being readily detectable, highly sensitive and a non-destructive method. This concept is described in **Figure 26** where the Fluorescent Functional Monomer (FFM) associates with the template to form the pre-polymerisation complex. Then to polymerise about the functional monomers a cross-linking agent is employed. This polymerised complex is then extracted of its template to leave a 'fluorescent' complementary binding site (i.e. complementary to the template molecule in shape, size and functional groups orientation).
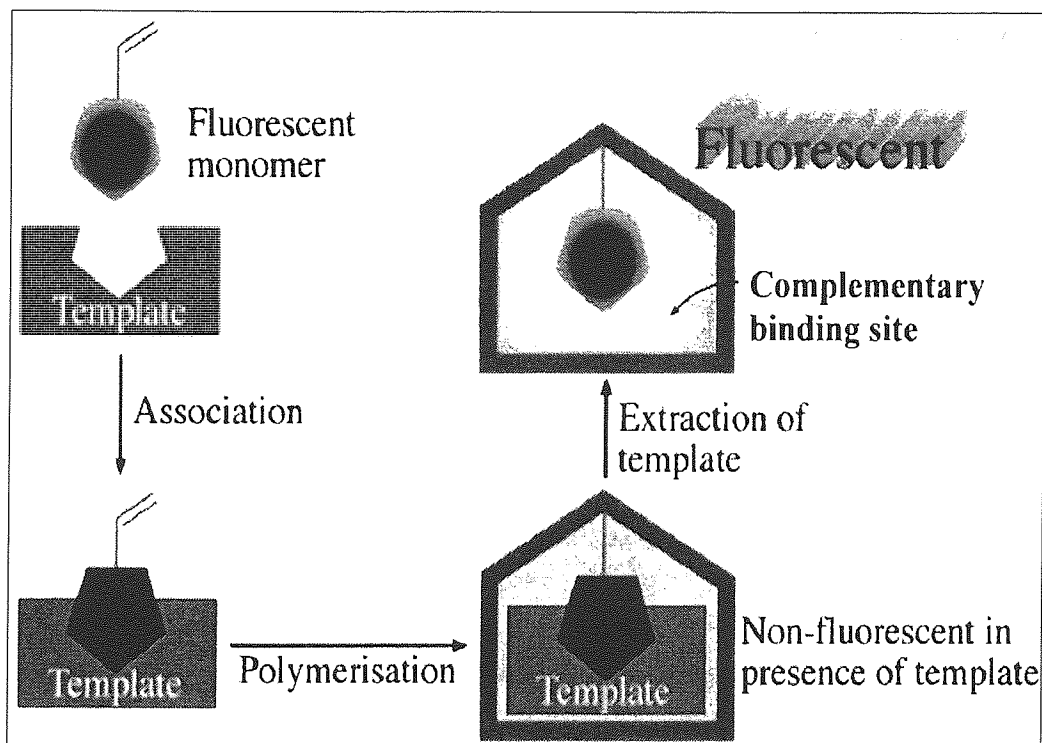
**Figure 26:** Fluorescent molecular imprinting process (Diagram adapted from Graham Smith at Aston University, further modified by Dr Dan Rathbone).

One of the advantages of using fluorescent imprinting polymers is that lower template loading is required. This can be very important when the template is expensive or has been prepared at small quantities. As mentioned earlier the sensor is also readily detectable and sensitive, this is beneficial when identifying small changes in the fluorescence that occur due to binding.

Different research groups that do not involve fluorescent MIPs however have used the fluorescence sensing system in various ways. For instance, Rachkov et al (2000) reported developing a fluorescence sensing system to determine β-estradiol (a intrinsically fluorescent template) by combining MIPs with HPLC. The MIPs were prepared by the methacrylic acid (functional monomer), β-estradiol (template), ethylene glycol dimethacrylate (cross-linking agent) and AIBN. This combined system was able to rapidly and effectively measure β-estradiol concentration in the range of 0.1-4μM with satisfactory reproducibility. In particular this system demonstrated excellent selectivity, owing to the fluorescence properties of the analyte. In addition, the MIP was high selectivity and short analysis time was required. Rodriguez-Suárez and Diaz-Garcia (2000) prepared a selective MIP for 3-hydroxyflavone (flavonol – a fluorescent template) by using the non-covalent imprinting approach. This MIP was utilised as a recognition element in a flow-through optosensing system with fluorescence detection that exhibited desirable sensitivity and selectivity characteristics, such that the MIP was able to distinguish flavonoids that differed slightly in the placement of the hydroxyl groups. Similarly, Rodriguez-Suárez and Diaz-Garcia in 2001 prepared MIPs for fluorescent competitive flow-through assay for chloramphenicol (CAP). This entailed synthesising different MIPs by employing various monomers and polymerisation conditions. The different MIPs were then tested

84

by HPLC as stationary phases, until an optimised MIP composition that was selective for CAP was attained. This optimised MIP was then utilised as a recognition phase in the fluorescent competitive flow-through assay to determine CAP.

In contrast, Chow et al (2002) synthesised a MIP for a non-fluorescing analyte, homocysteine. The analyte was derivatised with a fluoro-tagging agent before imprinting. This fluoro-tagging agent was a thiol-specific fluorogenic maleimide derivatised agent, N-(1-pyrenyl)maleimide. This gave the N-(1-pyrenyl)maleimide-DL-homocysteine (PM-H) as the template to generate a non-covalent MIP. The PM-H-MIP revealed a good specificity for PM-H.

In the early stages of using fluorescence as the detection method in MIP-guest binding studies, fluorescent MIP sensors required the fluorescent tag to be attached to the template. This adjustment often altered the binding properties of the template (Liao et al 1999). Incorporating the fluorescence property, however, to the functional monomers i.e. a FFM (as can be seen from **Figure 26**) produced successfully tailored MIP sensors for any template without any modification. This approach of using a FFM was used by Liao et al (1999) to make a fluorescent sensor for L-tryptophan. The sensor's diansyl moiety however had low sensitivity to changes in its enviroment resulting from the binding event. This led researchers to use an external quencher (p-nitrobenzaldehyde) to study binding of the fluorescent polymer. Displacement of the quencher from the binding cavitities by L-tryptophan caused a concentration dependent change in fluorescence and therefore counteracted the problem successfully.

Similar work on designing a FFM was carried out by Wang et al (1999) where the objective was to design and synthesise a fluorescent monomer that was intrinsically sensitive to the binding event, and its eventual use as a fluorescent sensor of cis diols using molecular imprinting methods. The use of an external fluorescence quencher was not required in this study. The FFM had both anthryl and phenyl boronic acid groups as well as a methacrylate moiety attached to allow it to become apart of the polymer backbone (**Figure 27**). The attached boronic acid moieties upon ester formation with cis diols from D-fructose resulted in significant changes to the fluorescence intensity (**Figure 27**- illustrates the formation of the ester linkage to give the D-fuctose-boronic acid complex). The FFM was used in the ongoing work of Gao et al (2001) and demonstrated that this can be used for the preparation of fluorescent imprinted polymers and the imprinted polymers created by atom transfer radical polymerisation (ATRP) and AIBN-initiated free radical polymerisation favoured the recognition of the template molecule, D-fructose.

**Figure 27:** Schematic representation of the D-fuctose-boronic acid complex (Wang *et al* 1999).

More recent work on fluorescent sensors was carried out by Rathbone *et al* (2000). In this study four fluorescent hydrogen-bonding monomers were synthesised to prepare imprinted polymers that exhibit binding dependent fluorescence. This synthesis involved using hydrogen-bond donor/acceptor scaffolds: 2-aminopyridine, 7-hydroxy-4-methylcoumarin and 3-aminorhodanine and gave the desired monomers: 2-acrylamidopyridine (**60**), two fluorescent 3-acrylamidorhodanines (**61, 62**) and 7-hydroxy-4-methylcoumarin acrylate (**63**), which have both the fluorescence and polymerisable moieties present to create a complete FFM (**Figure 28**). Of the four polymers, **60** and **61** gave the larger fluorescence output and **64** revealed the greatest fluorescence count ratios between the empty and re-exposed MIP i.e. 2 fold difference was observed for the entire wavelength range studied.
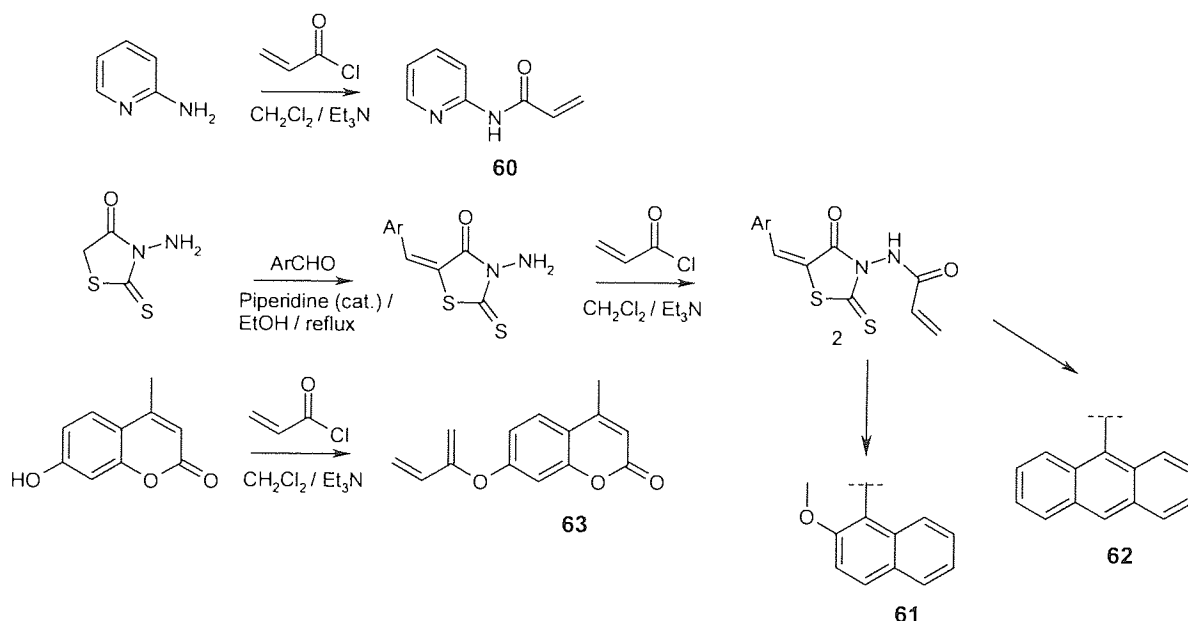
**Figure 28:** Preparation of fluorescent monomers.

The 3-acrylamidorhodanine FFM (**61**) (**Figure 29**) was used further for studies performed by Rathbone and Ge (2001). This involved preparing fluorescent polymers imprinted with various N`-benzylidene pyridine-2-carboxamidrazones which were evaluated for their recognition of the original template and cross-reactivity to similar molecules. In most cases a great deal of fluorescence quenching approaching background levels were observed when 'empty' MIPs were re-exposed to their templates. Molecules that were large in size compared with the cavity, could not enter the cavity and gave no reduction in fluorescence. A general trend that emerged with their study was that large and relatively inflexible molecules such as the polycyclic aromatics were more easily discriminated against those more flexible alkoxy-substituted benzylidene compounds. As well as this an approach was established that would make this more suitable for high-throughput screening, involving weighing of very dry polymer samples that can be a tedious task to do. Such tasks however, can be sidestepped by using the ratiometric approach. This approach requires the use of fluorescence measurements at two wavelengths, one wavelength for which the polymer exhibits a totally non-specific fluorescence and the other wavelength exhibits a specific fluorescence for the template binding. Finally, the non-specific and specific wavelengths are compared to the non-specific emission wavelengths i.e. the ratiometric approach.
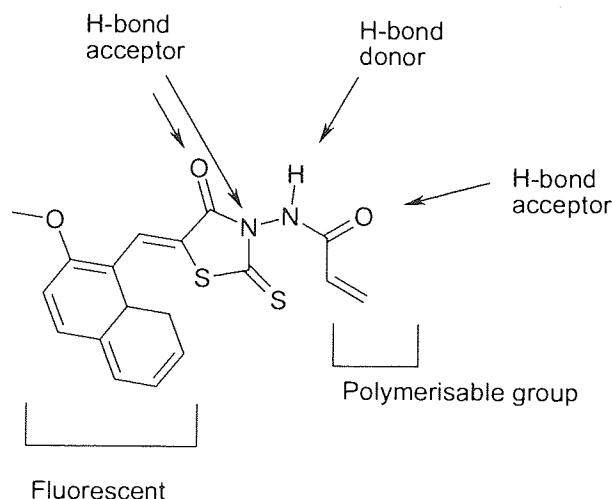
Figure 29: A FFM (61) capable of forming multi-point hydrogen-bonding interactions with matching substrates.

A multiple hydrogen bonding based fluorescent imprinted polymer for cyclobarbital was prepared with 2,6-bis(acrylamido)pyridine, a FFM (64) (Figure 30). The cyclobarbital-imprinted polymer exhibited selective binding for cyclobarbital and demonstrated fluorescence enhancement, indicating that this MIP could be used as a selective fluorescence probe. This was established by evaluating the polymer by chromatographically comparing the retention time of cyclobarbital (65) to structurally related compounds like allobarbital (66), primidon (67) and 3-ethyl-3-methylglutarimide (68) (Figure 30). The established results were further evaluated by fluorescence quenching studies performed on these compounds. Overall, the results suggested that the more points of connection between the monomer and template, the stronger the interaction and more stable the complex formed. Therefore the more selective and sensitive the polymer becomes during the imprinting process, as well as being selective towards it template molecule (Kubo *et al* 2003).



64: 2,6-bis(acrylamido)pyridine
65: cyclobarbital
66: allobarbital
67: primidon
68: 3-ethyl-3methylglutarimide
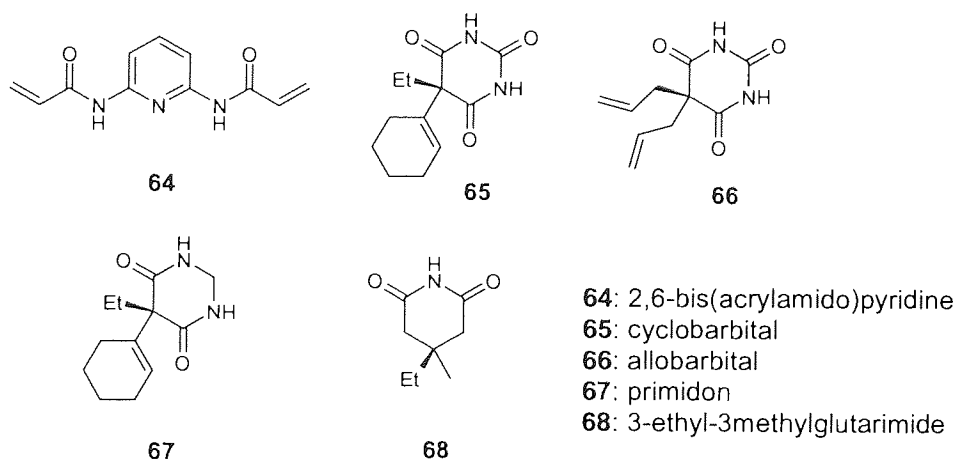
Figure 30: Structures of the test compounds (66-68), template (65) and FFM (64).

A further example of development is work by Lavignac *et al* (2004) they synthesised 4-(3-aminopropylene)-7-nitrobenzofurazan as a polymerisable fluorescent monomer (**Figure 31**) and prepared a fluorescent atrazine imprinted polymer. Preparing a homogeneous sorbent fluoroassay for atrazine further developed this. In addition work by Zhang *et al* (2001) deals with synthesising a suitable fluorescent monomer for MIPs by using 9-(guanidinomethyl)-10-vinylanthracene.
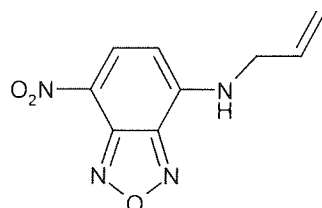


**Figure 31**: Structure of 4-(3-aminopropylene)-7-nitrobenzofurazan, FFM.

Takeuchi *et al* (2000; 2001a) synthesised a MIP with zinc(II)-porphyrin as a functional monomer for the selective recognition of 9-ethyladenine and cinchonidine. Following on from these particular studies Tong *et al* (2002) synthesised a molecular imprinted-based fluorescent chemosensor for histamine by using zinc(II)-protoporphyrin (ZnPP) as a functional monomer (**Figure 32**). In this study it was found that the ZnPP fluorescent functional monomer exhibited high binding affinity and created highly specific recognition sites for histamine in comparison to the methacrylic acid based polymer.
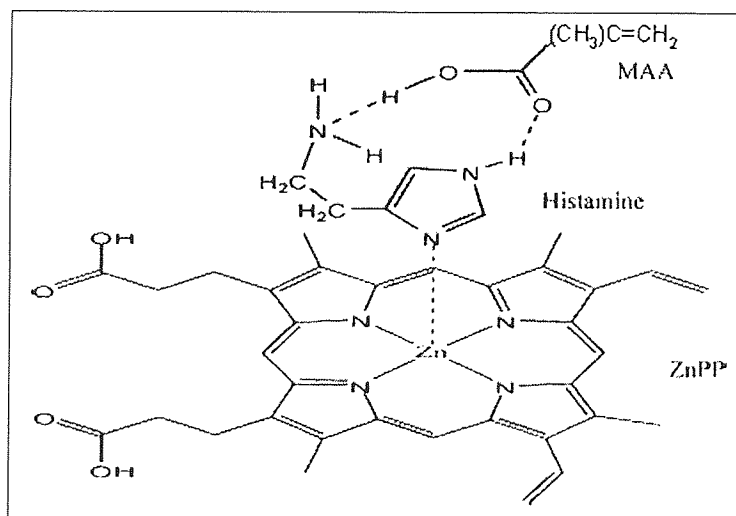


**Figure 32**: A presumed assembly of histamine with ZnPP and MAA.

Molecular imprints have also been prepared against adenosine-3`,5`-cyclic monophosphate (cAMP) (**71**) that contain a fluorescent dye (FFM); trans-4-[p-(N,N-dimethylamino)styryl]-N-vinylbenzylpyridinium chloride (DMASP) (**69**), as an integral part of the recognition cavity thus serving as both the recognition element and the measuring element for the fluorescence detection of cAMP (**71**) in aqueous media (**Figure 33**). This stilbene based functional monomer's fluorescence sensitivity is due to its intramolecular charge transfer with its positive charge on the nitrogen that associates with the negatively charged nucleotides (cAMP) (**71**), together with a vinyl group that is capable of covalently attaching itself to the polymer matrix. This innovative work of making a sensor that has the ability to function in aqueous media

is very important for biological systems, because binding of biological molecules occurs under these conditions, so such a sensor is an remarkable achievement by Turkewitsch *et al* (1998).

**Figure 33:** The fluorescent functional monomer **(69)** and the functional monomer, HEMA **(70)** are arranged around the template molecule, cAMP **(71)**, as a result of the non-covalent interactions between complementary chemical functionalities. Polymerisation captures the topographical relationship present in solution. Extraction of the template molecule exposes recognition sites of complementary shape and functional topography. Arrows represent additional potential hydrogen-bonding interactions between HEMA and cAMP (Turkewitsch *et al* 1998).

This MIP was further used by Wandelt *et al* (2002) to assess the specificity and affinity of the binding of the template molecule, cAMP **(71)** to the MIP by employing time-resolved fluorescence decay analysis. The cAMP-imprinted polymer exhibited high selectivity for the template molecule, cAMP **(71)**. The study however, also recognised a problem, that is associated with the imprinting method, is that after the extraction procedure only part of the imprinted sites were available for cAMP **(71)** molecules to bind too. In addition, these accessible binding sites located on the surface of the particles were damaged by the

mechanical grinding procedure. To overcome this problem, Wandelt *et al* (2004) copolymerised the polymer in thin-layer films. The thin-layer films were a new, more effective and applicable method to address the problem of mechanical grinding associated with the imprinting process. The polymer synthesised in this manner gave highly specific and selective binding sites towards the template molecule, cAMP (71). This was monitored by using steady-state and time-resolved fluorescence techniques, similar to the methods employed by Wandelt *et al* (2002; 2003) for previous studies.

Subrahmanyam *et al* (2001) reported a method for the selective detection of creatinine. This method was based on the reaction between polymerised hemithioacetal (consists of allyl mercaptan and o-phthalic aldehyde) and primary amine, forming the fluorescent isoindole complex (**Figure 34**). Note, that when creatinine covalently attaches itself to the MIP cavity it forms a fluorescent product. The traditional method of creating MIP failed to differentiate between creatine and creatinine. This report developed a new MIP selective for creatinine by using computer simulation to design the MIP with a 'Bite-and-Switch' approach to detect polymer-template interaction. The research group has previously used this approach in 2000 (Subrahmanyam *et al* 2000). The 'Bite-and-Switch' concept is defined in terms of polymers ability to bind to the template (bite) and generate the signal (switch). The computer simulation involved using molecular modelling software to screen a virtual library of functional monomers against the target molecule, creatinine. Monomers with high binding scores were then taken further in the testing cycle, until an optimised MIP composition was achieved. The study found that computer designed polymers exhibited greater selectivity compared to polymers prepared using traditional methods that used methacrylic acid.
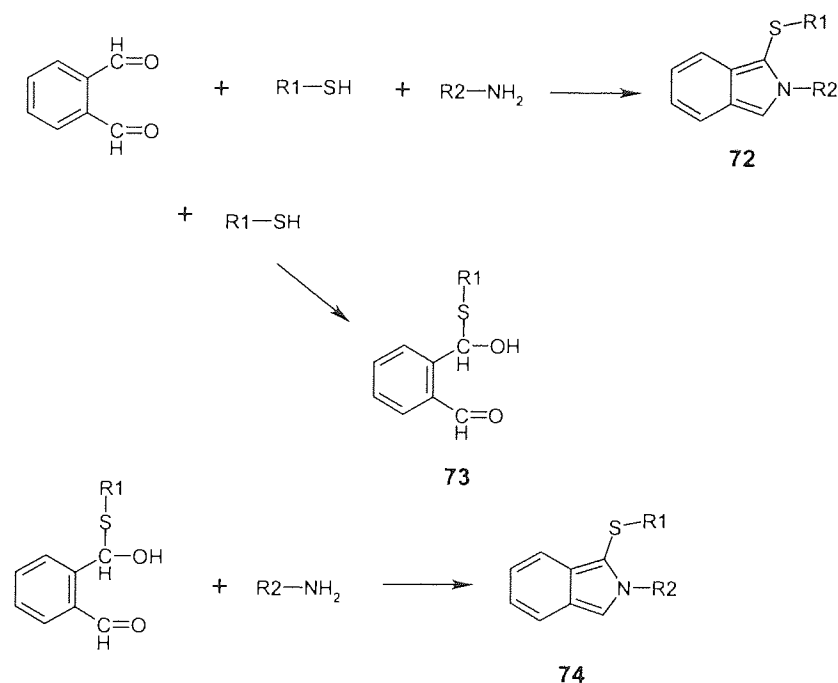


**Figure 34:** Interaction between phthalic dialdehyde, mercaptan group (OPA reagents) and primary amine (**72**); thioacetal formation (**73**); formation of fluorescent complex between hemithioacetal and primary amine (**74**) (Adapted from Subrahmanyam *et al* 2001).

## 1.1.12 Hydrophobic effect

### 1.1.12.1 Hydrophobic functional monomers

The method of monomer-ligand interaction that this thesis study is concerned with is based on the hydrophobic effect. This is studied by incorporating the hydrophobicity within the imprinted polymer by employing a functional monomer that contains within its structure the hydrophobic component. Examples of studies that have explicitly attempted in doing this are based on β-cyclodextrin. For instance Piletsky *et al* (1998a) used rationally the hydrophobic effect to produce template-assembled polymers. This MIP was synthesised with two functional monomers, β-cyclodextrin as the hydrophobic moiety-selective recognition element and 2-acryloylamido-2-methylpropane sulfonic acid, and cross-linked with N,N'-diacryloylpiperazine to create a MIP for D-phenylalanine. Similarly in 1999a Piletsky *et al* synthesised a MIP for D- and L-phenylalanine with 2-acryloylamido-2,2'-dimethylpropane sulfonic acid and bisacryloyl β-cyclodextrin as functional monomers, and cross-linked with N,N'-diacryloylpiperazine. Asanuma *et al* (1997; 1998) prepared polymeric receptors for cholesterol by cross-linking β-cyclodextrin with diisocyanates in dimethyl sulfoxide in the presence of cholesterol as template. The study found that a templated β-cyclodextrin polymer cross-linked with hexamethylene diisocyanate adsorbed cholesterol efficiently. In contrast a non-templated β-cyclodextrin polymer (no cholesterol) did not adsorb cholesterol to a measurable extent. The study further established that the polymer templated with toluene-2,4-diisocyanate exhibited an even greater adsorption of cholesterol. The reason for this observation was due to toluene-2,4-diisocyanate being a more rigid cross-linker than hexamethylene diisocyanate and thus was able to fix the β-cyclodextrin residue more effectively. In 1999 Asanuma *et al* further improved this study by making the method applicable to templates with carboxyl or amino groups that would have otherwise reacted with diisocyanates (cross-linker) in the previous studies (Asanuma *et al* 1997; 1998). In addition the study also improved the interaction between template and β-cyclodextrin in water that was weaker in the previously reported studies (Asanuma *et al* 1997; 1998). This study entailed using the vinyl monomer of cyclodextrin. The vinyl monomer of cyclodextrin was synthesised by ester-exchange reaction of *m*-nitrophenyl acrylate with 6-O-α-D-glucosyl-β-cyclodextrin (G1-β-cyclodextrin) in water. Here, G1-β-cyclodextrin replaced β-cyclodextrin in order to improve the solubility in water and assist in the column chromatography. The vinyl monomer of cyclodextrin formed highly selective dipeptide-receptors by radical polymerisation of cyclodextrin monomer in the presence of various templates in bulk water.

The limitation of employing β-cyclodextrin as a hydrophobic functional monomer, however is that the monomer gives a defined cavity size and so any large template can not be accommodated by this. In contrast the aim of my study is to create a hydrophobic functional monomer that has a general scope that allows even large templates to be accommodated. In addition some templates may have solubility problems when employed with β-cyclodextrin.

# 2. Detailed aims and objectives

## 2.1 The use of fluorescent MIPs as active-site binding mimics for CYP2D6.

### 2.1.1 Template Design for the preparation of imprinted polymers mimicking the binding profile of CYP2D6

Owing to the absence of a crystal structure for CYP2D6, a series of templates was designed (Rathbone *et al* 2005) based upon a set of superimposed substrate coordinates supplied by Islam *et al* (1991). These coordinates were determined by superimposing the substrates metabolites onto the attacked C5 atom of the camphor from the X-ray structure of P450cam. This resulted in the substrates having no steric clashes with the haem and also the basic (protonated) nitrogen would be able to interact with the proposed anion location, as well as all the aromatic rings being coplanar.

The conformationally more flexible substrates were removed and a set of relatively rigid compounds was retained (dextromethorphan, codeine, sparteine (2 orientations), debrisoquine, desipramine and amitriptyline). A set of compounds related to desipramine would be superimposed, these were template molecules **75**, **76** and **77** (Rathbone *et al* 2005). The proposed synthetic template molecules were then superimposed upon desipramine in the unmodified CYP2D6 substrates file (**75-77**) (Rathbone *et al* 2005), so that the basic nitrogen on each template was superimposed on either the ring nitrogen or the exocyclic nitrogen of desipramine. This superimposition of templates onto desipramine found that a significant portion of the volume was covered as well as possessing a range of basic nitrogens.

The modified superimposed substrates structure set is shown in **Figure 35** with desipramine and codeine highlighted and also compounds **75-77** superimposed on desipramine. Note that the known CYP2D6 substrate codeine (Gosham *et al* 1999) was chosen due to its large size and rigidity, as it is assumed that its rigidity would contribute towards a good imprinting effect.



Aston University

Illustration removed for copyright restrictions

(c)                          (d)                         (e)

**Figure 35:** Reduced set of superimposed CYP2D6 substrates with the haem unit shown for reference. (Rathbone *et al* 2005)

(a) Desipramine highlighted; (b) Codeine highlighted; (c) **75** superimposed on desipramine; (d) **76** superimposed on desipramine; (e) **77** superimposed on desipramine.

## 2.2 The preparation of MIPs using dual-fluorophore functional monomers.

The reason for designing dual fluorescence-labelled cavities is that two points of contact are available for a template/test compound to interact with, which is in contrast to mono-labelled cavities with one point contact. Thus the template/test compound may quench either of the two-fluorophore labels and indicate the orientation adopted within the MIP cavity.

Functionalised monomers containing two or more fluorophores in a relatively rigid scaffold at a distance such that the fluorophores do not quench each other's fluorescence (**Figure 36**) would be synthesised, with a view to gaining information about the orientation of a guest molecule within the MIP cavity.
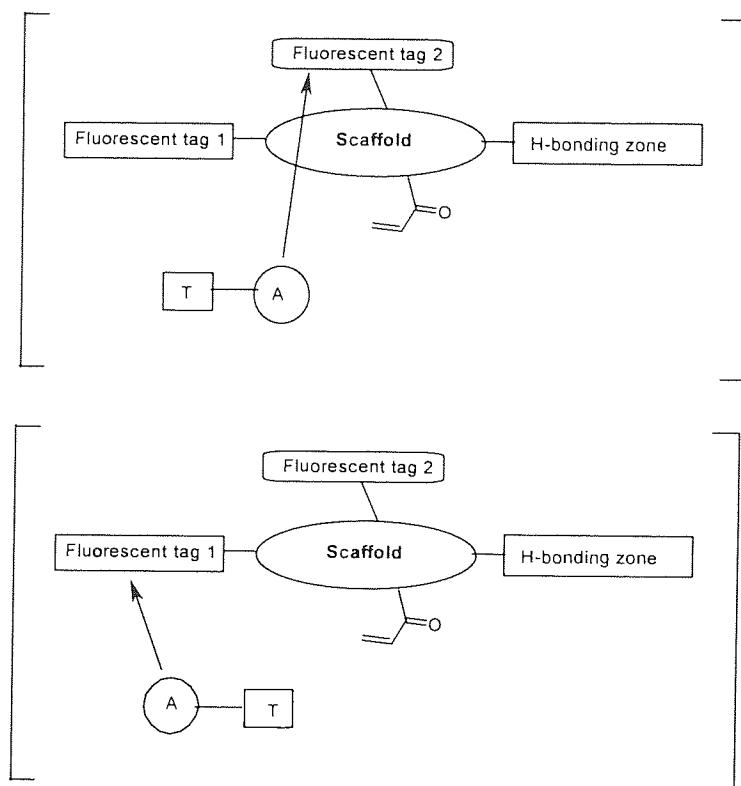
**Figure 36:** Deployment of fluorescent tags from a scaffold to give a poly-fluorescent monomer.

T is a template/test compound and **A** is any group that quenches the fluorescence of either fluorescent tag 1 or 2 depending on the orientation adopted within the MIP cavity.

The fluorescence spectra of the individual fluorophores will be determined by analysis of the corresponding mono-tagged scaffolds and imprinted polymers derived therefrom. MIPs will be prepared featuring the poly-functional monomers in association with N`-benzylidene heteroarylcarboxamidrazones as templates. Extraction of the templates from the cross-linked polymers will yield functionalised cavities matching the shape of the templates. The MIPs will be probed with a range of related N`-benzylidene heteroarylcarboxamidrazones and the fluorescence responses of the individual tags present in the cavities will be ascertained by measurements taken over a range of excitation energies. This will give an insight on the positioning of a test molecule within a cavity.

### 2.2.1 Quinine (rigid) based scaffold

The construction of the functionalised monomer capable of containing two fluorescent fluorophores will be based upon the quinine scaffold (**Figure 37**). Further studies in this area will be based upon quinine acrylate (**Figure 37**) as the fluorescent functional monomer (FFM), by preparing MIPs from this and testing the MIPs with N[1]-benzylidene pyridine-2-carboxamidrazone based test compounds.

Fluorophore 2
(long wavelength)



Polymerisable
function

Fluorophore tag 1,
intrinsic to quinine
(short wavelength)

Quinine scaffold

Quinine acrylate
FFM
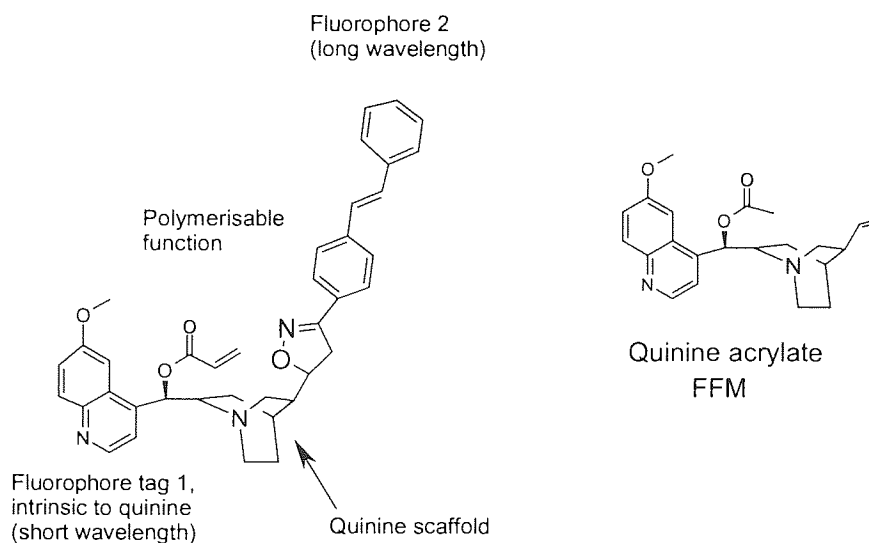
**Figure 37:** Quinine based dual fluorophore and quinine acrylate from which MIPs would be synthesised.

### 2.2.2 Piperazine based scaffold

Scaffold

Fluorophore 2
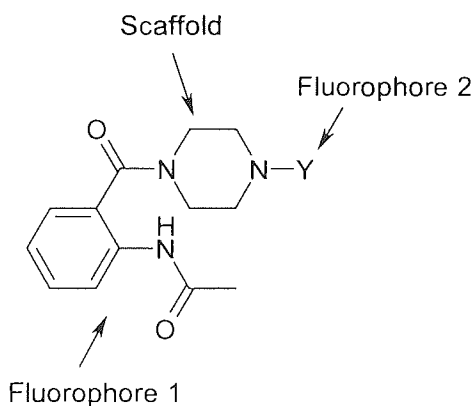


Fluorophore 1

**Figure 38:** Piperazine based scaffold with Y = COR or $SO_2R'$. R = Biphenyl, 1 Naphthyl and 2- Naphthyl R' = Dimethyl-naphthalen-1-yl-amine and Lissamine rhodamine.

This scaffold would be based on piperazine (**Figure 38**) which consists of two fluorophores with the N-(2-formyl-phenyl)-acetamide being one of them and the other depending on the initial material (Y) used. The anticipation is that the N-(2-formyl-phenyl)-acetamide functionality (fluorophore 1) would give a fluorescence output that is distinguishable from the other fluorophore (Y) at a set excitation wavelength. Once a FFM that is able to distinguish between its two fluorophores further studies would involve synthesising a series of MIPs to study cross-reactivity and selectivity of the MIP

## 2.2.3 Methyl hydrazine based scaffold
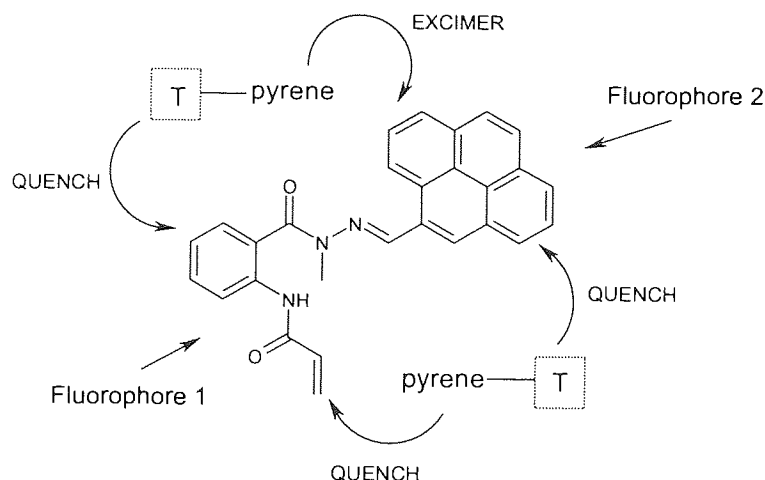


**Figure 39:** Structure of dual fluorophore based on a methyl hydrazine scaffold (T) template/test compound.

This dual fluorophore would be based on a methyl hydrazine scaffold with N-(2-formyl-phenyl)-acetamide functionality being one of the fluorophores and the other a pyrene **Figure 39**. The N-methyl moiety would 'insulate' the two fluorophores from each other i.e. prevent enolisation of the carbonyl group attached to the N-methyl moiety and thus prevent the two fluorophores joining together to form a single fluorophore. By doing this, the FFM N-(2-formyl-phenyl)-acetamide moiety fluorescence could either be quenched by the template/test compound or with the alignment of two pyrenes in a MIP (one coming from the test compounds that contain a pyrene unit) may produce an excimer (**Figure 39**) and hence act as a dual fluorophore functional monomer. This dual fluorophore functional monomer would thus act as a probe to investigate the positioning of a template/test compound within the MIP cavity.

## 2.2.4 A single fluorophore based on pyrene carboxaldehyde (no N-(2-formyl-phenyl)-acetamide moiety)
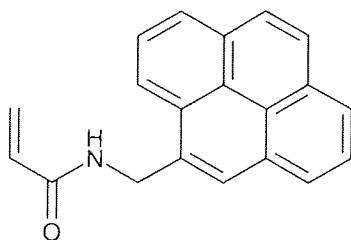


**Figure 40:** Structure of single fluorophore based on pyrene carboxaldehyde.

As an extension to the study based on a methyl hydrazine scaffold (**Figure 39**) a single fluorophore i.e. a subunit of the dual fluorophore would also be investigated (**Figure 40**). It is proposed with the absence of the conjugated N-(2-formyl-phenyl)-acetamide moiety would allow further assessment of the pyrene moiety to form an excimer (with the alignment of two pyrene units in a MIP).

## 2.3 The preparation of fluorescent MIPs containing cavities with both hydrogen-bonding regions and hydrophobic regions.

In this study it was proposed that various functional monomers would be synthesised that either create the hydrophobic pocket or create a hydrophobic environment to which the test compounds may dock into and are outlined in this section.

### 2.3.1 Anthranilamide containing hydrophobic pockets
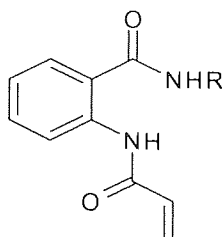


R = Cyclododecyl
R = Cyclopentyl
R = Cyclohexyl

**Figure 41:** Anthranilamide containing hydrophobic pockets.

The FFM would be based on anthraniloyl acrylamide and the hydrophobic pocket would be created by a cyclododecyl moiety (**Figure 41**), from which a series of MIPs would be synthesised. These MIPs would be probed with a range of related N`-benzylidene heteroarylcarboxamidrazones. Before synthesising the MIPs, however, a stable model version (non-polymerisable) of the FFM would be generated as a acetate to study the fluorescence behaviour.

The size of the hydrophobic pocket would be varied to discern the effect that this has on the binding characteristics of the MIPs derived there from. To vary the size of the pocket cyclo-pentyl and hexyl will be employed (**Figure 41**).

### 2.3.2 2-(Acryloyl-anthracen-9-ylmethyl-amino)-benzamide based hydrophobic pocket

Another angle to address the hydrophobic pocket area would be based on the functional monomer, 2-(acryloyl-anthracen-9-ylmethyl-amino)-benzamide (**Figure 42**). The proposed idea here is to have two polycyclic aromatic groups to form a hydrophobic groove, terminated by the hydrogen bond donors and acceptors of the anthanilanido portion, into which a test compound may dock (illustrated in **Figure 42**). If the test compound aromatic part is able to lodge between the two polycyclic aromatic groups coming from the functional monomer, then it is hoped that such an interaction may result in a significant change in the fluorescence output from any related MIP.

Note, that prior to synthesising the MIPs a stable model version (non-polymerisable) of the FFM would be generated i.e. an acetate to study the functional monomer fluorescence behaviour.
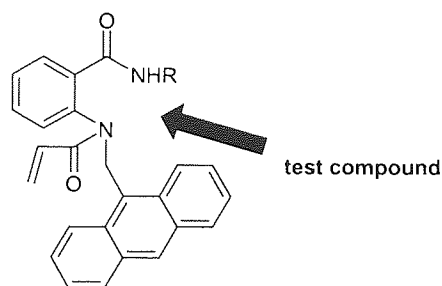


R = 1-(Aminomethyl)-napthalene
R = 1-Aminopyrene

**Figure 42:** 2-(Acryloyl-anthracen-9-ylmethyl-amino)-benzamide containing hydrophobic portions illustrates the manner in which the test compound could slot into this hydrophobic groove and is indicated by the thick black arrow.

## 2.3.3 N,N'-Bis-pyren-1-ylmethyl-benzene-1,3-diamine based hydrophobic pocket

Similar to the FFM, 2-(acryloyl-anthracen-9-ylmethyl-amino)-benzamide, outlined in **Figure 42**. This FFM is based on N,N'-Bis-pyren-1-ylmethyl-benzene-1,3-diamine and employs the same methodology in creating a hydrophobic groove i.e. formed by the two polycyclic aromatic groups coming from the FFM, in which the test compound would dock in between (**Figure 43**).

Again here it is assumed that the docking of the aromatic part of the test compounds between the two polycyclic aromatic groups from the functional monomer would present large changes in the fluorescence from any corresponding MIP.

Once more prior to synthesising the MIPs a stable model version (non-polymerisable) of the FFM would be generated as an acetate to study the fluorescence behaviour.
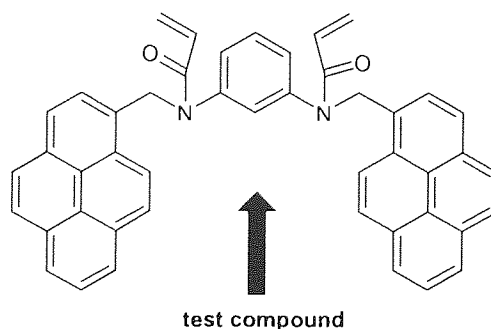


**Figure 43:** N,N'-Bis-pyren-1-ylmethyl-benzene-1,3-diamine containing hydrophobic portions. Note, that the thick black arrow indicates the manner in which the test compound would slot into this hydrophobic groove.

# 3. Results and discussion

*Note, that these brackets in this chapter { } give the section number of the experimental section the brackets with (Procedure number) outline the procedure taken to obtain the results and these brackets i.e. (Figure ) gives the section number of the Figure, for instance for a compound structure or study.*

## 3.1 Cyctochrome P450

### 3.1.1 Preparation of templates, test compounds and fluorescent monomer

The napthylmethylene group containing template **75** {5.3.1}, was prepared by alkylating iminostilbene under biphasic conditions and assisted by a phase transfer catalysis (tetrabutyl ammonium). The method employed to benzylate iminostilbene is different to the previously published method by Gozlan *et al* (1982). Templates **76** {5.3.2} and **77** {5.3.3} and test compound **78** {5.3.4} underwent a Schiff-base formation between N,N-dihphenylhydrazine and their corresponding aldehydes in their preparation. The fluorescent monomer, 2-acrylamidobenzamide (**79**) {5.3.5} was prepared by acrylating 2-aminobenzamide with acrylol chloride (**Figure 44**).

### 3.1.2 Preparation of imprinted polymers and exposure to templates and test compounds
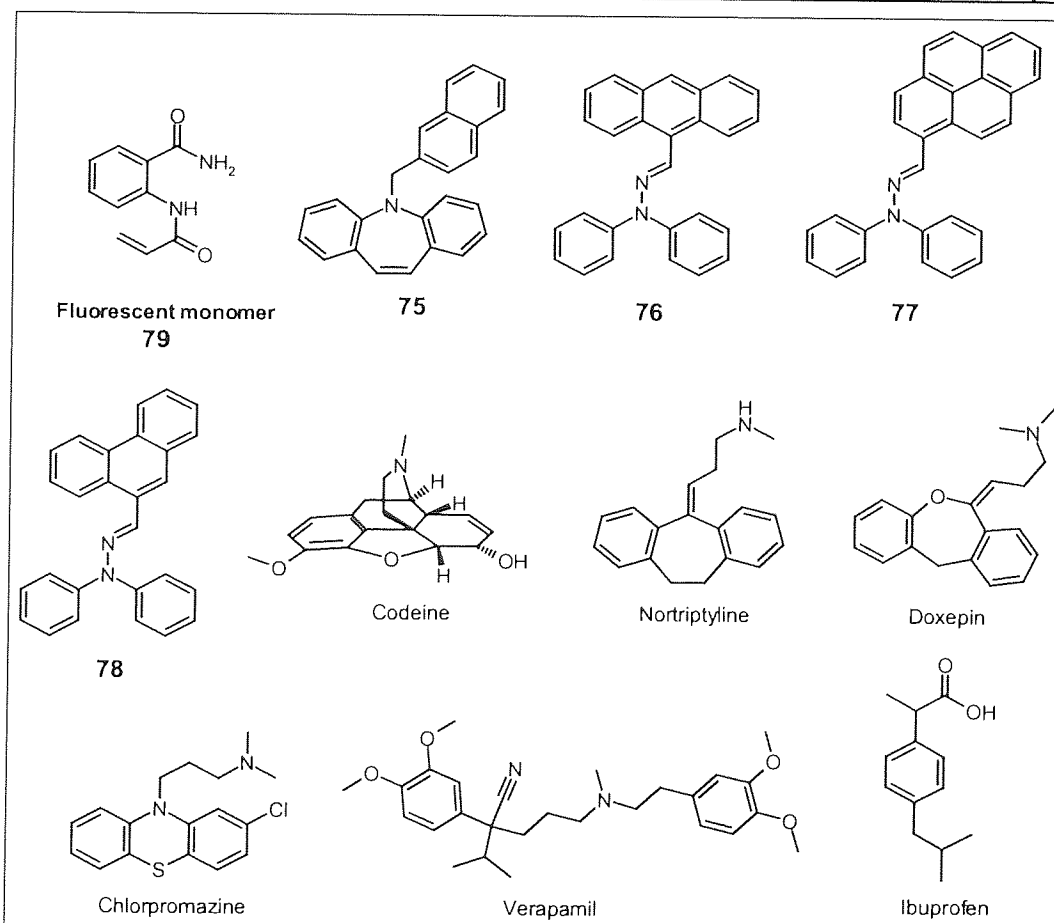


**Figure 44:** Structures of the template (**75-77**, **78** and codeine), test compounds, and 2-acrylamidobenzamide (FFM) (**79**).

100

Selections of MIPs were constructed with 2-acrylamidobenzamide (**79**) (**Figure 44**) acting as both the functional monomer and a fluorophore. This FFM was chosen due to it being small in size, and possessing functionalities such as a polymerisable acrylamide group that would become apart of the polymer backbone, along with three hydrogen donors capable of interacting with the acceptor nitrogen present on each of the templates.

Compounds **75-77** and codeine (**Figure 44**) were used as templates along with 2-acrylamidobenzamide as the FFM to construct the MIPs. As for the templates **75** and 76, an initial selection of 6 polymers was synthesised with varying ratios of its monomer: template (M:T) i.e. 1:2, 1:1, 2:1 and the cross-linkers were ethyleneglycol dimethacrylate (EGDMA) or trimethylolpropane triacrylate (TMPTA) (Rathbone *et al* 2005). The six MIPs were subjected to grinding (pestle and mortar) followed by sieving to establish a known particle size range and finally the template was extracted using a soxhlet apparatus. This final step of this procedure resulted in empty MIPs being re-exposed to their templates at various concentrations (i.e. 0.1, 1.0, 5.0 mg/mL) collected by filtration and analysed by fluorescence. The parameters used to analyse the various concentrations were determined by using the empty polymers and found that 309 nm was the optimum excitation wavelength and 460 nm was the wavelength of the fluorescence emission maximum. From this study it was observed that each of the MIPs after being re-exposed to their original templates had shown dose-dependant fluorescence quenching. An example is shown in **Figure 45**.
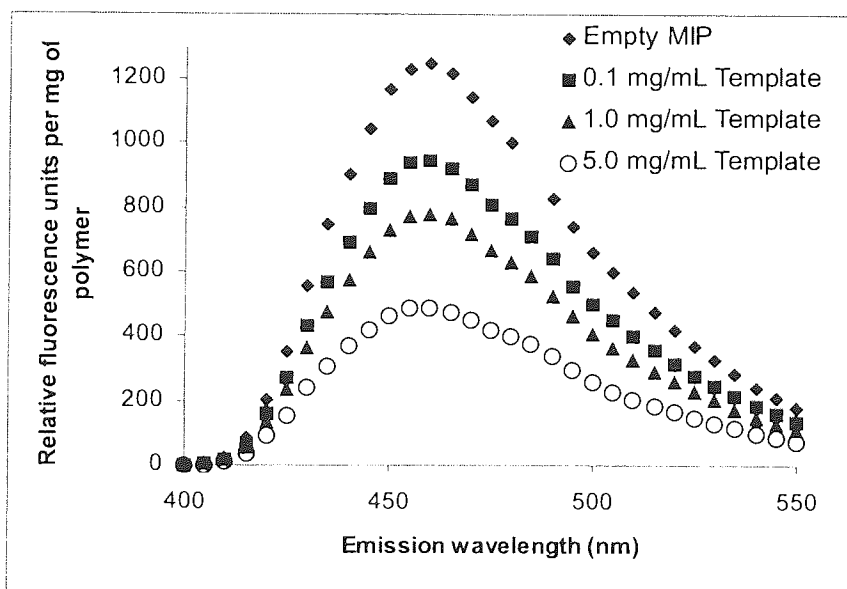


**Figure 45:** Dose-dependent fluorescence spectra for **MIP1** (template **75**, TMPTA, M:T = 2:1) re-exposed to solutions of its template ($\lambda_{ex}$ = 309 nm).

The results for 5 mg/mL re-exposure solutions are shown in **Table 6**. These show for template **75** the best fluorescence quenching was observed at M:T ratio of 2:1 with TMPTA as the cross-linker. For template 76 ratio of M:T of 1:1 with EGDMA as the cross-linker was found to be optimal. These experimentally determined ratios were then taken into consideration when synthesising the MIPs for the next study to establish the optimum cross-linker content.

The importance of such a study is that if a polymer is too rigid then the rebinding (thermodynamically controlled batch rebinding) would be too slow and in contrast if the polymer is not as rigid then specificity of the polymer suffers. Therefore when choosing cross-linkers for a polymer, choice and proportion of cross-linker are of equal importance.
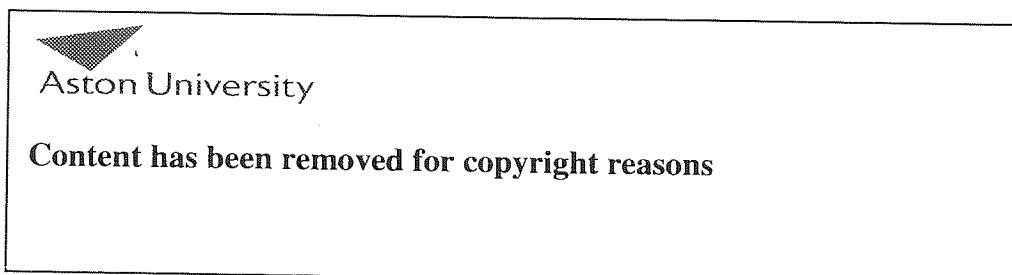
**Table 6:** Fluorescence relative to the empty MIPs after re-exposure to template at 5 mg/mL. $\lambda_{ex}$ = 309 nm, $\lambda_{em}$ = 460 nm . (Rathbone *et al* 2005)

From the results of the studies determining M:T ratios and cross-linkers choice, the corresponding new MIPs were prepared where the cross-linkers were diluted with styrene to give different cross-linker contents of 95%, 90%, 85% and 80% w/w. (Rathbone *et al* 2005) The MIPs were prepared and exposed to their templates in the same manner as mentioned before and the fluorescence results can be seen in **Table 7**. These results show that MIPs for template **75** upon dilution of the cross-linker do not improve the recognition of its template. The cross-linker content at 95% shows worse fluorescence quenching, however as the cross-linker content reduces a slight improvement can be seen. As for template **76** MIPs the same trend is observed as with MIPs for template **75** where 95% shows worse fluorescence quenching then again with 85% and 80% their level of quenching taking into consideration experimental error is similar to the quenching observed for 100% cross-linker content. Overall by diluting the content of the cross-linkers no improvement of template recognition was observed.

Fluorescence relative to the empty MIPs after exposure to template
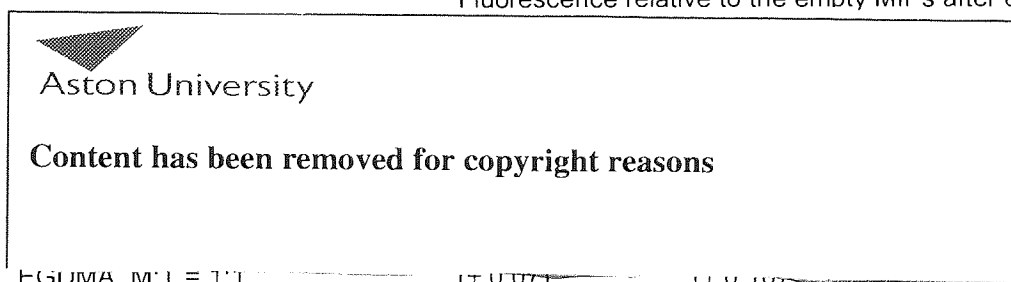
EGDMA, M:1 = 1:1 ($\pm$ 0.07) ($\pm$ 0.10) ($\pm$ 0.00)

*Standard deviations for triplicate results are given parentheses.

**Table 7:** Fluorescence relative to the empty MIPs with reduced crosslinker content after re-exposure to template. The 100% crosslinker result is included for comparison (Rathbone *et al* 2005).

As for the MIPs derived from templates, **77** and codeine, these were cross-linked with triethyleneglycol dimethacrylate (TEGDMA) to give the respective MIPs, **MIP3** {5.4.7} and **MIPcod** {5.4.6}. The reason for

the change from a rigid cross-linker TMPTA to a more flexible and longer cross-linker TEGDMA was justified by our observation that using 100% cross-linkers EGDMA or TMPTA made it difficult to extract from monolithic polymers of templates that contained rigid subjects the size of pyrene or greater such as codeine and **77**. Therefore such a change would allow adequate extraction of codeine and **77** from their corresponding MIPs to take place effectively.

All four MIPs were assessed with solutions of templates and test compounds in THF to concentrations of 0.1, 1.0, 5.0 mg/mL. The structures of the test compounds are shown in **Figure 44** and include the CYP2D6 substrates nortriptyline, doxepin, codeine, the CYP2D6 inhibitor chlorpromazine, the CYP3A4 substrate verapamil, and the CYP2C9 substrate ibuprofen.

From this study, as before, all MIPs showed dose-dependent fluorescence quenching. At a concentration of 5 mg/mL this effect is more noticeable and this result is shown in **Table 8**, normalised to the fluorescence output per unit mass of the empty MIPs.

Composition and fluorescence output of imprinted polymers after exposure to test compound solutions at a concentration of 5 mg/mL

|  | MIP1 | MIP2 | MIP3 | MIPcod |
|---|---|---|---|---|
| Crosslinker (content) | TMPTA (5.0 g) | EGDMA (5.0 g) | TEGDMA (5.0 g) | TEGDMA (5.0 g) |
| Functional monomer | 0.05 mmol | 0.025mmol | 0.025mmol | 0.025mmol |
| Template | **75** | **76** | **77** | **codeine** |
|  | 0.025mmol | 0.025mmol | 0.025mmol | 0.025mmol |

| Test compound | Fluorescence output of MIPs after exposure to test compound solutions at a concentration of 5 mg/mL | | | |
|---|---|---|---|---|
| **75** | 0.27 ($\pm$ 0.05) | 0.54 ($\pm$ 0.04) | 0.59 ($\pm$ 0.05) | 0.79 ($\pm$ 0.12) |
| **76** | 0.49 ($\pm$ 0.10) | 0.27 ($\pm$ 0.06) | 0.20 ($\pm$ 0.06) | 0.66 ($\pm$ 0.04) |
| **77** | 0.61 ($\pm$ 0.01) | 0.95 ($\pm$ 0.21) | 0.07 ($\pm$ 0.02) | 0.60 ($\pm$ 0.07) |
| **78** | 0.72 ($\pm$ 0.05) | 1.03 ($\pm$ 0.22) | 0.20 ($\pm$ 0.03) | 0.90 ($\pm$ 0.25) |
| Nortriptyline | 0.89 ($\pm$ 0.13) | 0.24 ($\pm$ 0.08) | 0.45 ($\pm$ 0.14) | 0.92 ($\pm$ 0.25) |
| Doxepin | 1.15 ($\pm$ 0.23) | 0.25 ($\pm$ 0.05) | 0.38 ($\pm$ 0.06) | 1.08 ($\pm$ 0.25) |
| Chlorpromazine | 1.08 ($\pm$ 0.22) | 0.54 ($\pm$ 0.08) | 0.38 ($\pm$ 0.06) | 0.55 ($\pm$ 0.13) |
| Verapamil | 1.30 ($\pm$ 0.19) | 0.95 ($\pm$ 0.51) | 0.67 ($\pm$ 0.13) | 0.83 ($\pm$ 0.23) |
| Ibuprofen | 1.34 ($\pm$ 0.15) | 0.35 ($\pm$ 0.08) | 0.65 ($\pm$ 0.12) | 0.99 ($\pm$ 0.10) |
| Codeine | 1.24 ($\pm$ 0.05) | 0.76 ($\pm$ 0.23) | 0.74 ($\pm$ 0.11) | 0.86 ($\pm$ 0.02) |

**Table 8:** The results are normalised to the fluorescence of the unquenched MIP and the quoted errors are the standard deviations of triplicate wells. $\lambda_{ex}$ = 309 nm, $\lambda_{em}$ = 460nm.

From the table above what can be gathered about the fluorescence quenching profiles of the four MIPs is that for **MIP1** it is able to recognise its own template and is able to distinguish between its closely related compounds 76-77 and **78** against the drug test compounds which it rejected. In contrast, **MIP3** {5.4.7} showed no selectivity as all compounds were able to quench its fluorescence. As for **MIPcod** {5.4.6} this was able to recognise all four synthesised templates (**75-77** and **78**) and chlorpromazine. **MIP2** was also able to recognise its own template and able to discriminate against the closely related compounds **77** and **78**, and verapamil, however, it also recognised template **75**, nortriptyline, doxepin, chlorpromazine, ibuprofen and codeine.

### 3.1.3 Preparation of a soluble co-octadecylacrylate-79 and fluorescence quenching in deposited thin films

The reason for preparing a soluble copolymer of octadecylacrylate and 2-acrylamidobenzamide (FFM) (**79**) (**Figure 44**, 3.1.2) as a polymer film, was to help in the interpretation of the fluorescence quenching MIP results. The issue that caused such a study to be initiated was that if fluorescence quenching does take place in a MIP then the test compound must have entered the cavity for it to do so. In contrast, if fluorescence quenching does not take place or very weak quenching is observed, then the issue of the result being ambiguous arises, as it is possible that the test compound may have entered the cavity but was unable to quench the fluorescence of the polymer-bound fluorophore. Thus by having the co-polymer film the quenching ability of each test compound towards the fluorophore would be addressed and so help towards a better understanding of the MIP results. (Procedure 2a refer to 4.2)

The polymer films were prepared by putting polymer solutions together with the templates and test compounds solutions into a flat bottomed microtitre plate wells and allowed the solution to evaporate followed by the careful application of the vacuum to afford smooth polymer films at the bottom of the wells. Practically this method has demonstrated more reliability in forming smooth films, than simply evaporating a solution containing the fluorophore and a test compound. The latter method usually results in an uneven deposition on the well floor and as a result highly variable fluorescence readings are produced.

The fluorescence of the polymer films was determined. This allowed the relative fluorescence quenching abilities of each template/test compound to be distinguished in a polymer environment, which in turn helped towards the interpretation of the fluorescence quenching MIP results. The fluorescence parameters were exactly the same as those applied for the MIPs i.e. that were optimum excitation wavelength of 309 nm and maximum emission wavelength of 460 nm and these results are presented in **Figure 46**, normalised to that of the polymer film without test compound.
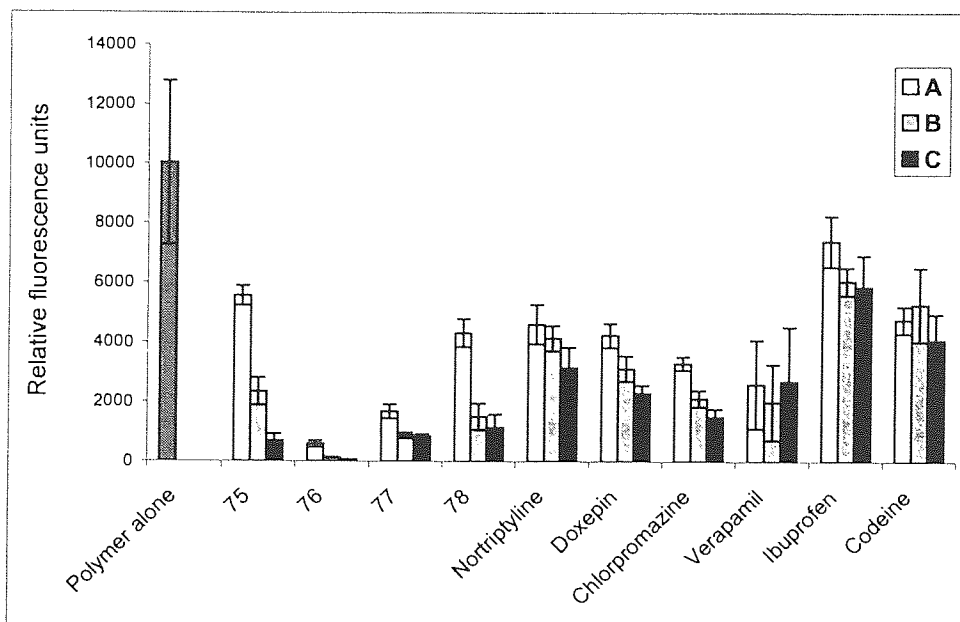
**Figure 46:** Fluorescence output of a co-octadecylacrylate-**79** film (4.6 mg per well) after co-evaporation of solutions of test compounds (**A**, 0.02; **B**, 0.05; **C**, 0.1 mg per well). The fluorescence of the unquenched polymer film is shown at the left hand side. The quoted errors are the standard deviations of triplicate wells. $\lambda_{ex}$ = 309 nm, $\lambda_{em}$ = 460 nm.

All the test compounds caused fluorescence quenching at various levels at the emission maximum of the polymer film, 460 nm. Polycyclic aromatic compounds (**75-77** and **78**) were the best fluorescence quenchers of the polymer film. They also gave rise to low level broad featureless emissions at longer wavelengths, which can be seen in **Figure 44**. Taking these results into consideration a level of quenching ability (good. moderate, poor) was given to each test compound (**Table 9**).
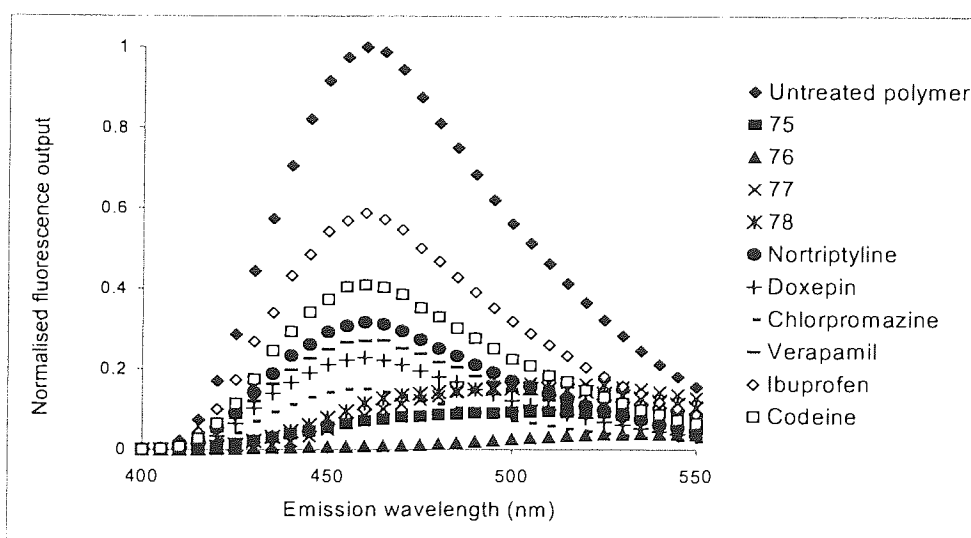


**Figure 47:** Fluorescence spectra ($\lambda_{ex}$ = 309 nm) of a co-octadecylacrylate-**79** film (4.6 mg per well) after co-evaporation of solutions of test compounds (0.1 mg per well). The emission curves are normalised to that of the untreated polymer and result from the average of three wells.

105

## 3.1.4 Interpretation of the MIP fluorescence quenching observations

The first most important observation is that all test compounds were able to quench in at least one of the MIPs. Taking this and the polymer films results together, allowed the reassessment of the MIP cross-reactivity profiles this is presented in Table 4.

Sometimes it was observed that if a test compound was rated as being a poor quencher by the polymer film, in the MIP it was observed as either being a moderate to good quencher. An example of such a case can be seen for ibuprofen that was rated as being a poor quencher but exhibited in **MIP2** as a good quencher. From this it can be assumed that the test compound and fluorophore may have opted for a different orientation in the MIP compared to non-imprinted polymer film.

| Test substance | | Fluorescence quenching ability | MIP1 | MIP2 | MIP3 | MIPcod |
|---|---|---|---|---|---|---|
| 75 | | Good | + | + | + | - |
| 76 | | Good | + | + | + | + |
| 77 | | Good | + | - | + | + |
| 78 | | Good | + | - | + | - |
| Nortriptyline | CYP2D6 substrate | Moderate | - | + | + | - |
| Doxepin | CYP2D6 substrate | Moderate | - | + | + | - |
| Chlorpromazine | CYP2D6 inhibitor | Moderate | - | + | + | + |
| Verapamil | CYP3A4 substrate | Moderate | - | - | + | + |
| Ibuprofen | CYP2C9 substrate | Poor | - | + | + | - |
| Codeine | CYP2D6 substrate | Poor | - | + | + | + |

**Table 9**: Interpretation of the MIP fluorescence quenching observations.

+  Test substance recognised by the MIP
-  Test substance not recognised by the MIP

For **MIP1** the interpretation of its cross-reactivity results together with the polymer film results remained the same. This MIP was able to recognise compounds **75-77**, **78** (**Figure 44**, 3.1.2) and reject the drug test compounds. **MIP2** recognised **75** along with its own template **76** and was able to distinguish against closely related compounds **77** and **78**. **MIP3** cross-reactivity results also remained the same and demonstrated the point of being a very non-selective MIP, which can be explained by its large template. **MIPcod** accepted **76** and **77** but rejected **75** and **78**. This is interesting as compound **78** is two ethylene smaller than **77** (a pyrene). As for compound **75** being rejected this could be explained by the observation that even though this compound slightly quenches (0.79 ± 0.12 fluorescence relative to the empty MIP), **75** had been shown to be a good quencher. In comparison, codeine was rated as being a poor quencher and was recognised (0.86 ± 0.02 fluorescence relative to the empty MIP). In general **MIPcod** recognised half of the test drugs but was unable to be specific towards CYP2D6 substrates.

On the whole **MIP2** is the best starting point to synthesis a binding mimic receptor for CYP2D6. Having exhibited an imprinting effect with compounds (**75-77, 78**), it also accepted CYP2D6 substrates / inhibitors nortriptyline, doxepine, chlorpromazine and codeine, and rejected the CYP3A4 substrate verapamil. Ibuprofen a CYP2C9 substrate, however, was accepted.

Overall from these studies based on different templates it suggests that **75** is too small, **76** is approximately the correct size, **77** is too large and codeine has the wrong profile.

### 3.1.5 Conclusion

A selection of MIPs was constructed with 2-acrylamidobenzamide **79** (**Figure 44**, 3.1.2) as the FMM and compounds **75-77** and codeine as templates to generate MIPs that would be able to mimic the binding characteristics of one of the most important drug metabolising enzymes, CYP2D6.

The MIPs were re-exposed to their original templates and various cross-reactivity profiles were created with synthesised test compounds / drug test compounds to test recognition abilities (selectivity). From these studies **MIP2** demonstrated an ability to distinguish between closely related synthetic templates and was relatively successful in recognising CYP2D6 substrates / inhibitors from the drug set.

**MIP2** and its template (**76**) are undergoing further investigations to broaden its results and make further progress towards a binding mimic for polymorphic isoenzyme CYP2D6.

### 3.2 Comparison of linear co-hexyl acrylate-quinine acrylate anchored to cellulose filtration membrane (used to aid the interpretation of the quinine based MIPs) and a soluble co-octadecylacrylate-2-acrylamidobenzamide deposited in thin films

The co-octadecylacrylate-**79** {5.4.1} (structure of **79**, **Figure 44**, 3.1.2) films were formed by putting the polymer solutions together with the templates and test compounds solutions into a flat bottomed microtitre plate wells. The solutions were allowed to evaporate, followed by the careful application of the vacuum to afford smooth polymer films at the bottom of the wells. In contrast, the linear co-hexylacrylate-(**80**) {5.3.6} was anchored to cellulose filtration membrane *via* an ester linkage.

## 3.2.1 Preparation of a quinine based MIP



Quinine acrylate (80)
(FFM)

Template
(81)

$\xrightarrow{\text{TMPTA}}{\text{AIBN}}$ MIP4
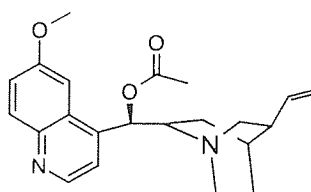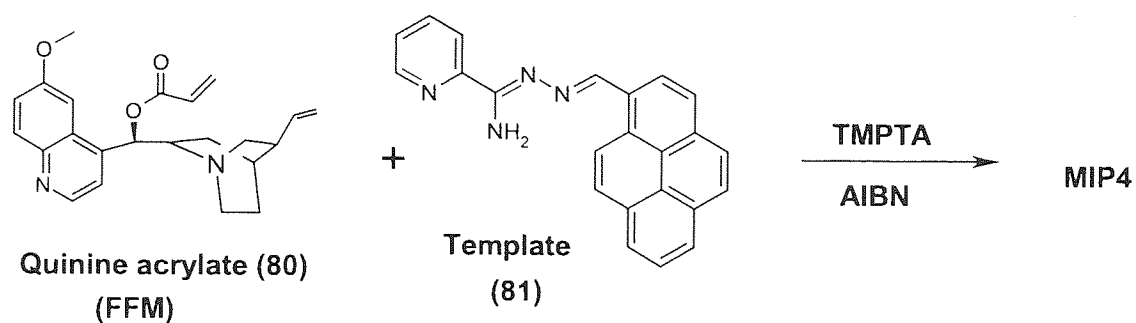
Quinine acetate (82)

83

84

85

86

87

88

C
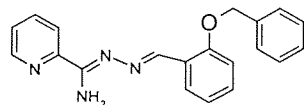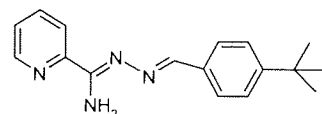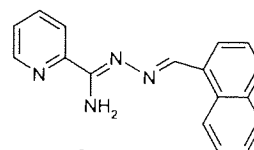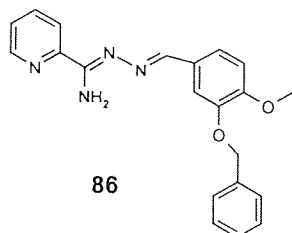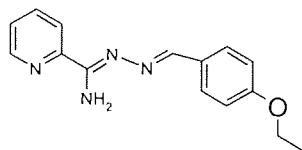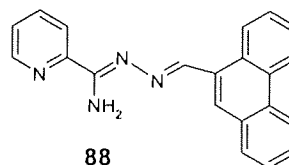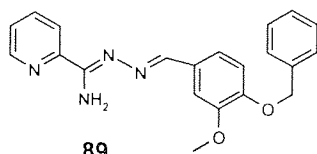
89
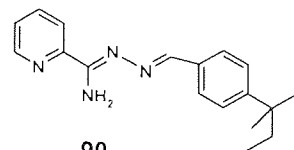
90
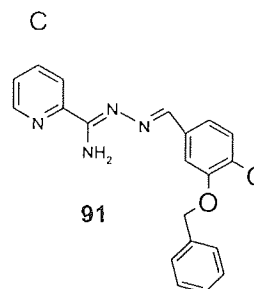
91
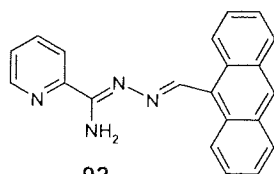
92

**Figure 48:** Quinine acrylate (**80**) and (**81**) based MIP (**MIP4**) tested with N[1]-benzylidene pyridine-2-carboxamidrazone based test compounds (**83-92**).

The linear copolymer anchored to the cellulose filtration membrane was employed (Rathbone and Bains 2005) to aid the interpretation of the MIP results generated by the FFM, quinine acrylate **80** templated with compound **81** and cross-linked with trimethylolpropane triacrylate (TMPTA) to create MIPs with cavitities containing quinine as the fluorophore.

**MIP4** {5.4.8} was subjected to grinding (pestle and mortar) followed by sieving to establish a known particle size range and finally the template was extracted using a soxhlet apparatus.

**MIP4** was re-exposed to its own template **81** and to series of related $N^1$-benzylidene pyridine-2-carboxamidrazone based test compounds (**83-92**) (structures shown in **Figure 48**), to investigate its cross reactivity profile. The test compounds used in this study provided a good system to test the MIP since they contained hydrogen bonding domains, lipophilic moieties and a span of relative flexibility

### 3.2.2 Ratiometric measurements

The accurate weighing out of very dry polymer samples can be a tedious task to do. Such tasks however, can be sidestepped by using a ratiometric approach. This approach requires the use of fluorescence measurements at two wavelengths, one wavelength for which the polymer exhibits a binding independent fluorescence, which is proportional to the mass of polymer present, and the other wavelength exhibits a binding sensitive fluorescence. Finally, the non-specific and specific wavelengths are compared to the non-specific emission wavelengths i.e. the ratiometric approach.

The fluorescence results for **MIP4** indicated that conventional accurate weighing followed by fluorimetry and the ratiometric approach gave similar results, that is besides quenching its own template (**81**) (**Figure 48**) it also quenches the test compounds which suggests that this MIP is non-selective. This however, is not entirely unexpected in that this MIP was imprinted using a comparatively large template molecule, producing a MIP with a large cavity. As a consequence, it could easily be possible for compounds that are smaller than the template, if not in terms of molecular weight, then certainly in terms of spatial occupancy, to enter the cavity and quench the MIP. This MIP, however, provides a further validation for the ratiometric approach as mentioned earlier. (**Figure 49**)
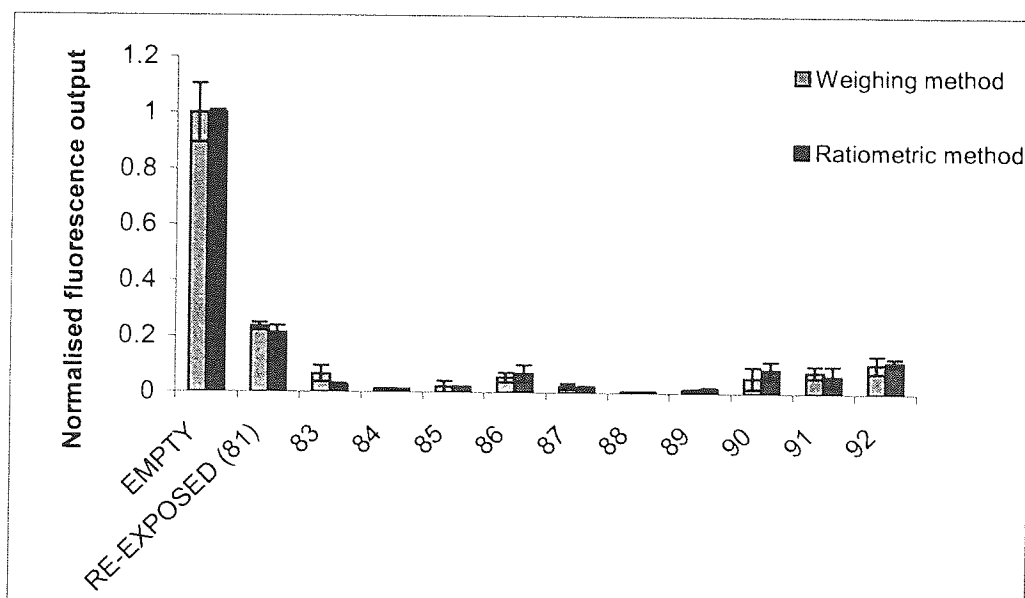
**Figure 49:** Fluorescence output normalised against empty MIP after exposure to template **81** and to a series of related compounds (**83-92**).

## 3.2.3 Three different approaches to interpret fluorescence quenching results of MIP4

The fluorescence quenching results for **MIP4** need to be interpreted due to the same reasons as mentioned previously with the ambiguity of fluorescence quenching taking place or not.

To aid the interpretation of the fluorescence results for **MIP4**, three different approaches were proposed. The first was to synthesis MIPs with every template, which would answer the questions mentioned above, but would be extremely time consuming. A second proposed route was to use linear polymers with an anchored fluorophore, being a half way between a cross-linked MIP and a simple solution phase fluorescence quenching experiment and has the added advantage of being re-useable. The third was solution phase quenching of a monomeric fluorophore. This simple option however does not necessarily represent what really goes on inside the MIP. In addition, if the fluorophore or test compounds were in limited supply, recovery of such materials would require chromatographic separation.

Note that the second and third proposed routes to address the ambiguity of fluorescence quenching MIP results was performed by Rathbone and Bains (2005) and the MIP used was provided from the **MIP4** study.

The linear co-hexylacrylate- (**80**) (quinine being the fluorophore) was prepared anchored to the cellulose filtration membrane *via* ester linkage were investigated and comparison studies involving solution phase quenching on quinine acetate **82** {5.3.7} were performed (Rathbone *et al* 2004). Quinine acetate **(82)** was used because it is a stable, non-polymerisable version of quinine acrylate (**80**) and most importantly resembles the fluorophore found in the MIP. Furthermore, it allowed the effect of the test compounds on

the quinine acetate (82) to be measured and helped create an image of their effects on the MIP, removed of all its polymer hindrance.

As a consequence any differences observed in the relative effects of the test compounds were ascribed to steric hindrance arising from the cavity size i.e. the specificity of the MIP.

The results as shown in **Figure 50** indicate that solution phase quenching of the monomeric fluorophore was virtually identical to that of the fluorophore present in the anchored linear polymer (non-imprinted). The MIP results are broadly similar as all compounds caused fluorescence quenching. In the case of re-exposure of the empty MIP to its template **81** (a bulky inflexible compound somewhat larger than the test compounds) in the MIP system the slightly lower quenching level was presumably due to the bulky template having difficulty in re-entering the polymer matrix within the timescale of the experiment.
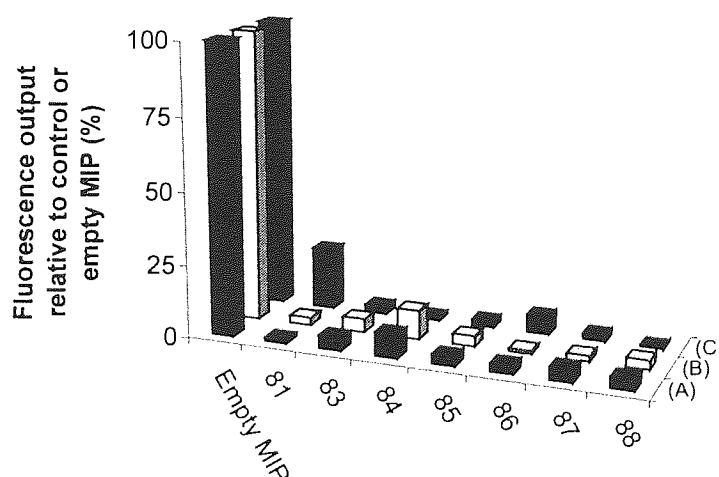


**Figure 50:** Normalised fluorescence results for (**A**) solution phase quenching of Quinine Acetate (**82**), (**B**) linear polymer derived from Quinine Acrylate (**80**), (**C**) MIP imprinted with compound **81** and using a fluorophore derived from Quinine Acrylate (**80**). Note (**A**) and (**B**) performed by Rathbone and Bains (2005).

Comparison of the linear copolymer anchored to cellulose filtration membrane and a soluble copolymer deposited in thin films was made; both techniques provided a convenient technique as fluorescence quenching control experiments for validating fluorescence studies for MIPs. The preparation of co-octadecylacrylate-**79** film was, however, simple in that it just required the mixing of two components. In contrast, the preparation of the linear copolymer anchored to cellulose membrane is more tedious and time consuming as the cellulose discs punched from the filter paper, which is derivatised with acryloyl chloride, from these covalent anchoring points linear polymers are grown. Nevertheless such a technique does have its advantages in that it is easily re-usable for screening multiple substrates and recovery. This is quite the opposite with the preparation of co-octadecylacrylate-**79** film that is not re-usable and would require a chromatography separation to recover its individual materials. In addition this non-imprinted

polymer film technique have a limited use in comparison to the imprinted linear copolymer anchored to cellulose membrane, as fluorescence MIPs attached to the cellulose filter membrane could provide a system to conduct binding studies.

## 3.3 Dual fluorophore molcularly imprinted polymers

### 3.3.1 Quinine (rigid) based scaffold

Quinine itself is fluorescent. It was hoped that a second fluorophore, styryl in the example shown in **Scheme 1**, could be incorporated into this relatively rigid scaffold by means of a 1,3-dipolar cycloaddition. Conversion of the remaining hydroxyl group to the corresponding acrylate ester would enable this proposed dual-fluorophore rigid entity to be incorporated into an imprinted polymer (**Scheme 1**).
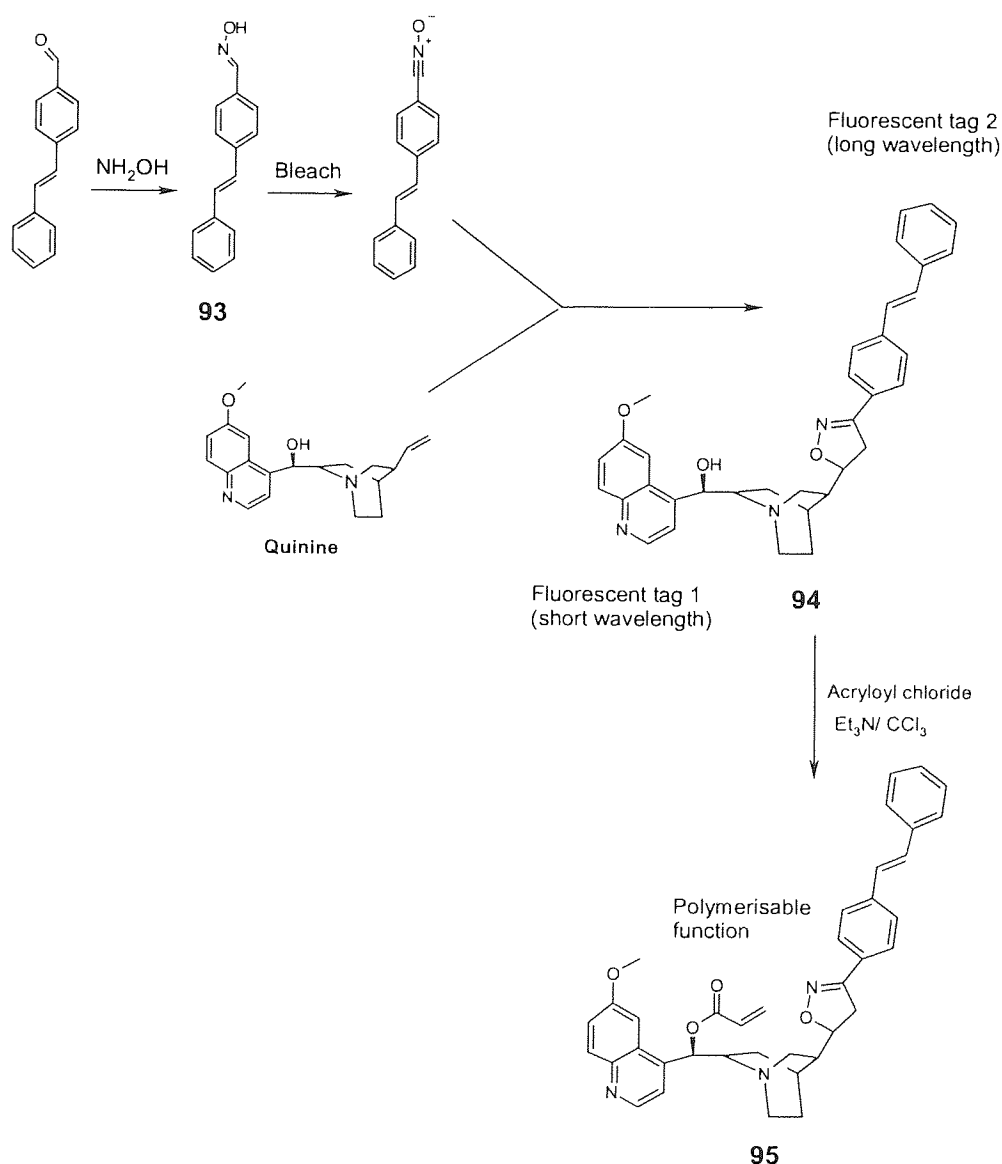


**Scheme 1**: A proposed synthesise of quinine-based dual fluorophore monomer.

The 4-styryl-benzaldehyde was reacted with hydroxylamine hydrochloride to afford an oxime **93**. The 1,3-dipolar-cycloaddition reaction between the nitrile oxide derived from the oxime **93** and the exocyclic alkene of quinine, performed in a solution of sodium hypochlorite was unsuccessful. Even though it was observed that the starting material quinine was consumed in this reaction, a complex mixture of products was formed from which it was impossible to isolate any of the desired product, compound **94**.

The sodium hypochlorite might have also reacted with the nitrogens present on the quinine, and hence led to N-oxide products. The N-oxide products could be formed on the nitrogen present on the 6-methoxy–quinoline or the 1-aza-bicyclo[2,2,2]octane moieties or even both. These reasons led to the oxime **93** not being able to be incorporated into the quinine based scaffold and hindered its use as a probe to investigate the positioning of a template within a MIP cavity.

## 3.3.2 Piperazine based scaffold



R= 4-Biphenyl
R= 1, Naphthyl
R= 2, Naphthyl

R'= N,N-Dimethyl-naphthalenyl
R'= Lissamine rhodamine

**96** R= 4-Biphenyl
**97** R= 1, Naphthyl
**98** R= 2, Naphthyl

**99** R'= N,N-Dimethyl-naphthalenyl
**100** R'= Lissamine rhodamine

**101** R= 4-Biphenyl

**102** R'= N,N-Dimethyl-naphthalenyl

**103** R= 4-Biphenyl

**104** R'= N,N-Dimethyl-naphthalenyl

**105** R'= N,N-Dimethyl-naphthalenyl
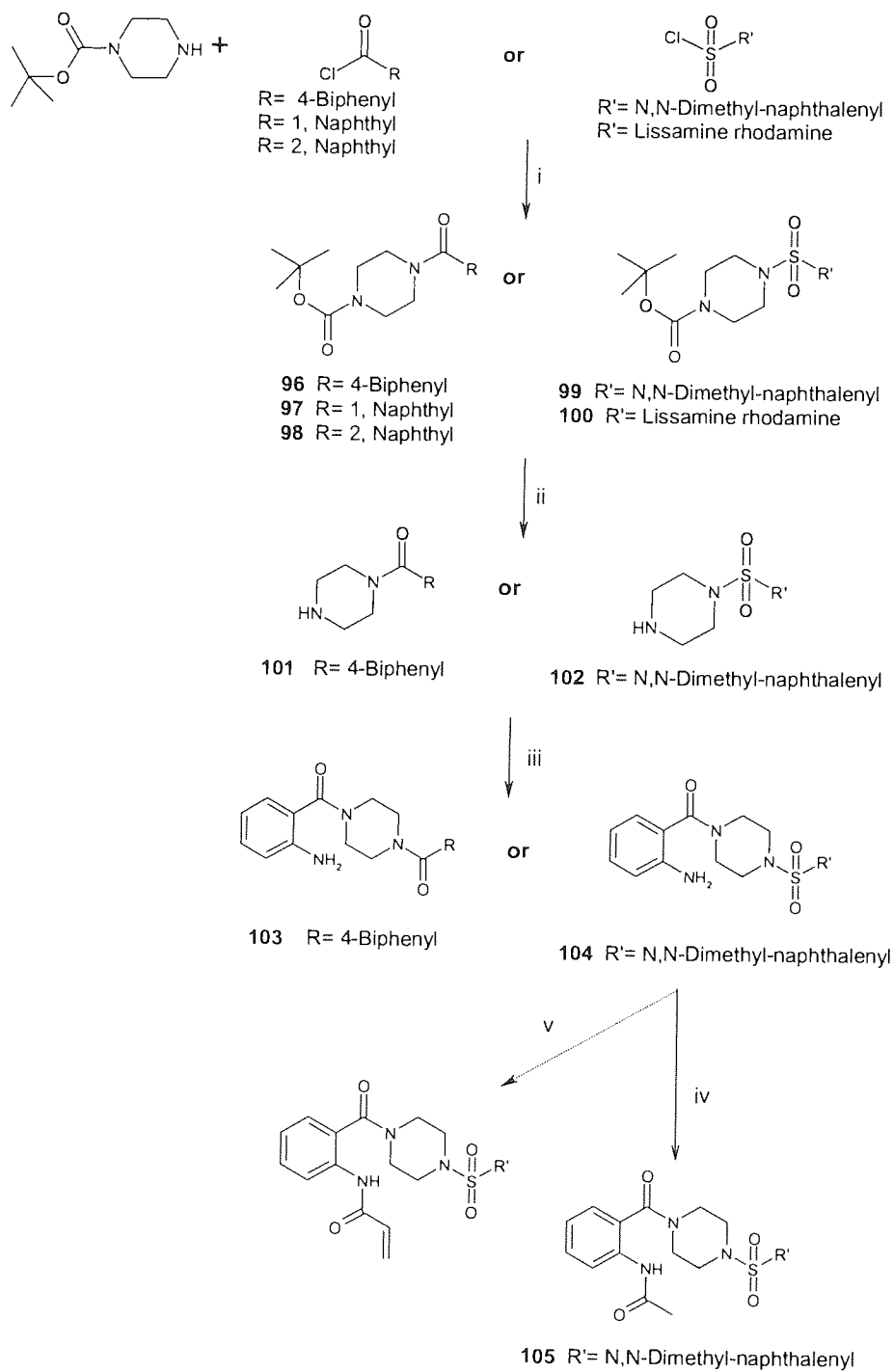
i Hünig base/THF, ii trifluoroacetic acid (TFA)/DCM, iii Isatoic anhydride/ethanol (reflux) iv triethylamine/THF/acetyl chloride, v triethylamine/THF/acrylol chloride

**Scheme 2:** Synthesis of piperazine scaffold compounds containing two fluorophores.

To develop the concept of a dual fluorophore functional monomer, an alternative scaffold based on piperazine was proposed (**Scheme 2**). The proposed piperazine scaffold as can be seen in **Figure 51** consists of two fluorophores with the N-(2-formyl-phenyl)-acetamide being one of them and the other

114

depending on the starting material (Y) used. It was anticipated that the N-(2-formyl-phenyl)-acetamide functionality (fluorophore 1) would render a fluorescence output that is distinguishable from the other fluorophore (Y) at a set excitation wavelength. This synthesis involved the reaction between piperazine-1-carboxylic acid *tert*-butyl ester with either a sulphonyl chloride or an acyl chloride to add the first fluorophore. This product would then be treated with trifluoroacetic acid (TFA) in dichloromethane to remove the tert-butyl ester functionality so that further chemistry on its amino functionality could be done. The next step for this product would involve reacting the amino functionality present on the piperazine scaffold with isatoic anhydride to afford compound **104** (**Scheme 2**). Compound **104** {5.3.16} would then be acetylated to form non-polymerisable fluorescence monomer to perform solution phase fluorescence studies. This would establish the maximum excitation/emission wavelengths and also reveal the capability of the functional monomer to distinguish apart its fluorophore moieties. Compound **104** would also undergo acrylation from which an imprinted polymer could then be formed. The imprinted polymer would be employed as a probe to investigate the positioning of the template/test compounds within the MIP cavity *via* the two-fluorophore tags. Hence the template/test compounds may quench either of the tags to reveal their positioning.
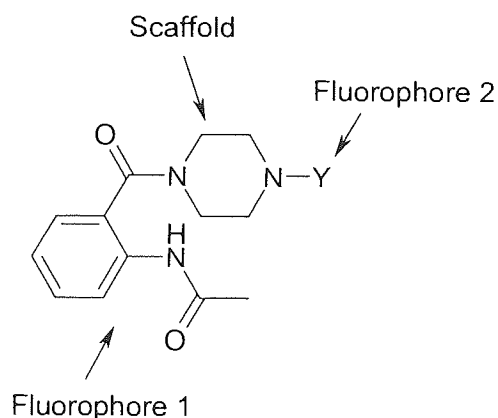


**Figure 51**: Piperazine based scaffold with Y= COR or SO$_2$R'.

To establish the excitation wavelengths that could make it possible to distinguish the two fluorophores, compound **106** {5.3.18} was employed (**Figure 52**). This is due to the presence of N-(2-formyl-phenyl)-acetamide functionality in this compound, which is one of the fluorophores present in the compounds being assessed e.g. compound **105** {5.3.17} from **Scheme 2**. The emission of **106** at excitation wavelengths of 305 nm and 345 nm are at 455 nm and 415 nm respectively (**Figure 53** and **54**) (Procedure 3a refer to 4.3).
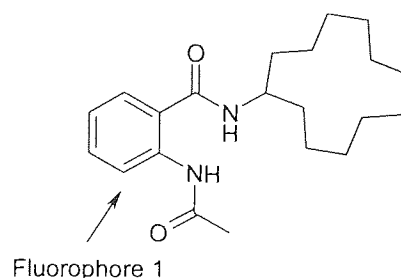


**Figure 52**: Compound **106** (2-Acetylamino-*N*-cyclododecyl-benzamide).
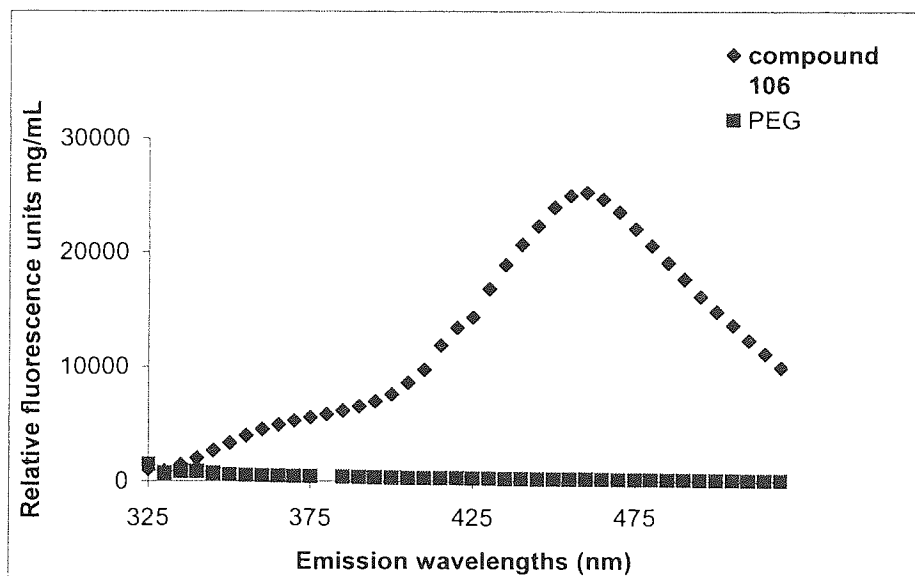
**Figure 53**: Fluorescence spectra for compound **106** (0.016 mg in 200 μL of PEG 62.5 : 1 ethyl acetate) against the control PEG. ($\lambda_{ex}$ = 305 nm).
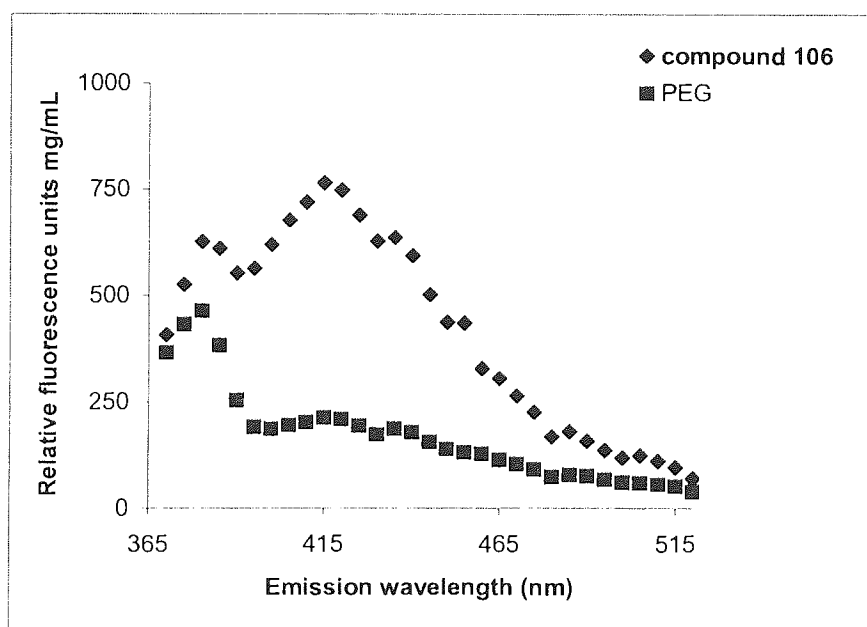


**Figure 54**: Fluorescence spectra for compound **106** (0.016 mg in 200 μL of PEG 62.5 : 1 ethyl acetate) against the control PEG. ($\lambda_{ex}$ = 345 nm).

Following the reaction sequence in **Scheme 2** (3.3.2), the reaction between piperazine-1-carboxylic acid *tert*-butyl ester and 4-biphenylcarbonyl chloride resulted in compound **96** {5.3.8}. This was then treated with 10% trifluoroacetic acid (TFA) in dichloromethane to remove the tert-butyl ester functionality from its product so that further chemistry on its amino functionality could be done (**101**). The next step for **101** {5.3.13} was to react the amino functionality with isatoic anhydride to gain amide **103** {5.3.15}.

116

When assessing the fluorescence output of **96** (fluorophore 2) no fluorescence could be observed, even though it was anticipated that the biphenyl group would give rise to fluorescence ($\lambda_{max}$ =246 nm for biphenyl) (Procedure 3b refer to 4.3).

As an alternative to the proposed biphenyl-containing dual fluorophore, four other compounds (5-dimethylamino-naphtalene-1-sulphonyl chloride, 1-napthoyl chloride, 2-napthoyl chloride and lissamine rhodamine B-sulphonyl chloride) were reacted with the piperazine-1-carboxylic acid *tert*-butyl ester, which afforded the corresponding compounds **99** {5.3.11}, **97** {5.3.9}, **98** {5.3.10} and **100** {5.3.12} (**Scheme 2**) (3.3.2). The fluorescence of these four compounds was investigated at the same excitation wavelengths of 305 nm and 345 nm, as those determined by the compound **106** studies (N-(2-formyl-phenyl)-acetamide moiety present) (Procedure 3b refer to 4.3).

The fluorescence output of **99** at excitation wavelengths of 305 nm and 345 nm respectively gave emission maximum at 535 nm and 530 nm (as shown in **Figure 55** and **56**) in contrast to the **106** emissions of 455 nm and 415 nm at these excitations (**Figure 53** and **54**).
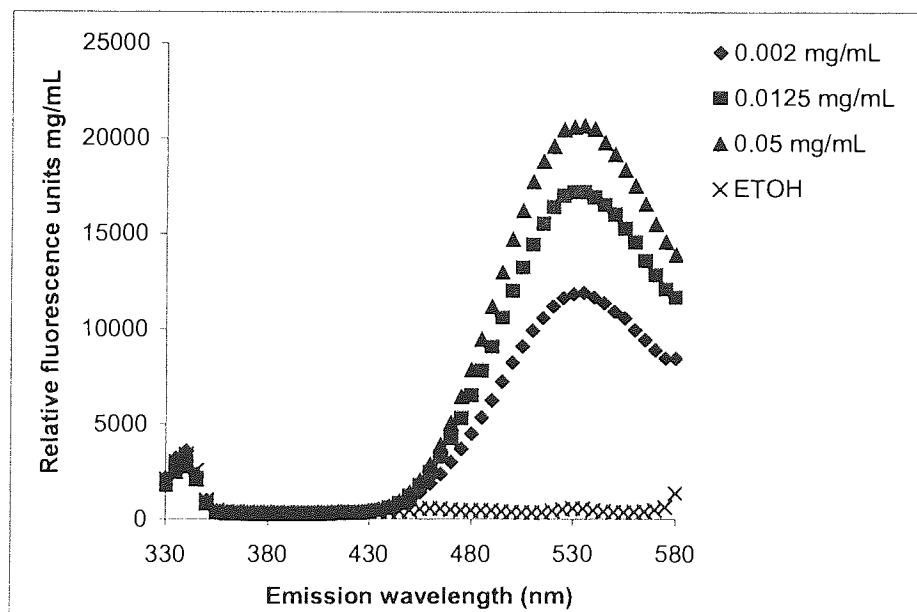


**Figure 55:** Fluorescence spectra for compound **99** at various concentrations ($\lambda_{ex}$ = 305 nm) in ethanol.
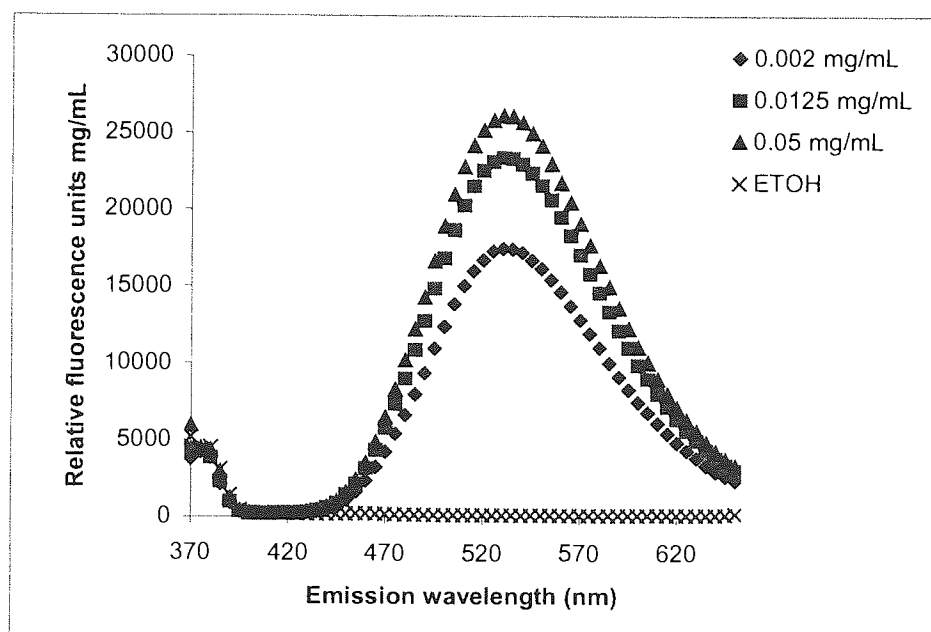
**Figure 56:** Fluorescence spectra for compound **99** at various concentrations ($\lambda_{ex}$ = 345 nm) in ethanol.

Compound **98** was investigated at excitation wavelengths ranging from 250 nm to 300 nm. The optimum excitation wavelength was found to be 280 nm. The maximum fluorescence emission was observed at 360 nm. At excitation wavelengths of 305 nm and 345 nm fluorescence was at background. It was proposed that by adding the second fluorophore, N-(2-formyl-phenyl)-acetamide, the two fluorophores could be interrogated independently.

For **97** no fluorescence could be observed at either excitation wavelengths of 305 or 345 nm and even at other wavelength ranges.

Finally compound **100**, at excitation wavelengths of 305 and 345nm, gave an emission maximum at 590nm. With this observation the emission was fixed at this particular wavelength and the excitation wavelength scanned. The optimum excitation wavelength was found to be 530nm. Again it is proposed that on addition of the second fluorophore, N-(2-formyl-phenyl)-acetamide, the two fluorophores could be interrogated independently.

From the fluorescence study it was determined that three of the four compounds **99, 98, 100** except for **97** gave fluorescence outputs that would be distinguishable from the N-(2-formyl-phenyl)-acetamide component (second fluorophore) of the proposed dual fluorophore.

Compound **99** was taken further and treated with 40% trifluoroacetic acid (TFA) in dichloromethane to remove the tert-butyl ester, so that further chemistry on its amino functionality could be performed to give secondary amine **102** {5.3.14}. The amino functionality of compound **102** was reacted with isatoic anhydride to gain an amide **104** {5.3.16}. This was followed by acetylation of **104** with acetyl chloride, forming a stable model compound **105** {5.3.17} for further fluorescence studies (**Scheme 2**) (3.3.2).

118

The fluorescence study on compounds **105** and **102**, the latter having no N-(2-formyl-phenyl)-acetamide functionality present, was to determine whether the dimethyl-naphthalen-1-yl-amine (fluorophore 2) present in **105** and N-(2-formyl-phenyl)-acetamide (fluorophore 1) could be distinguished (Procedures 3c & d). For the N-(2-formyl-phenyl)-acetamide as mentioned earlier the excitation wavelengths of 305 and 345 nm and emissions respectively at 455 and 415 nm, would be used from the compound **106** fluorescence studies (shown in **Figures 53** and **54**).

Compound **105** at excitation wavelengths of 305 and 345 nm gave maximum fluorescence emission at 530nm. (**Figures 57a** and **58a**) In addition to this observation an `extra` peak with an emission maximum at 395 nm can be seen in **Figures 57b** and **58b**, which could possibly be due to the N-(2-formyl-phenyl)-acetamide moiety.
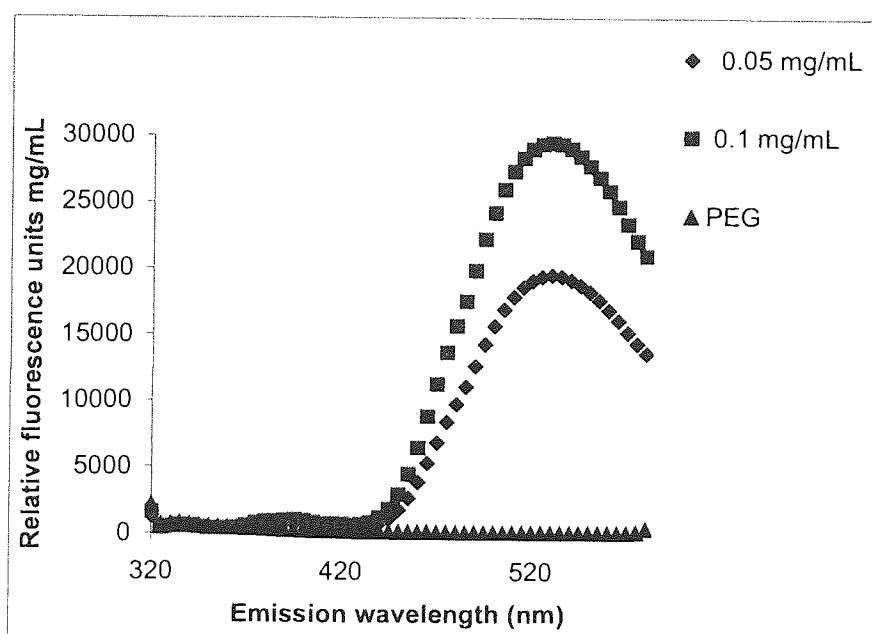


**Figure 57a:** Fluorescence spectra for compound **105** in PEG ($\lambda_{ex}$ = 305 nm).
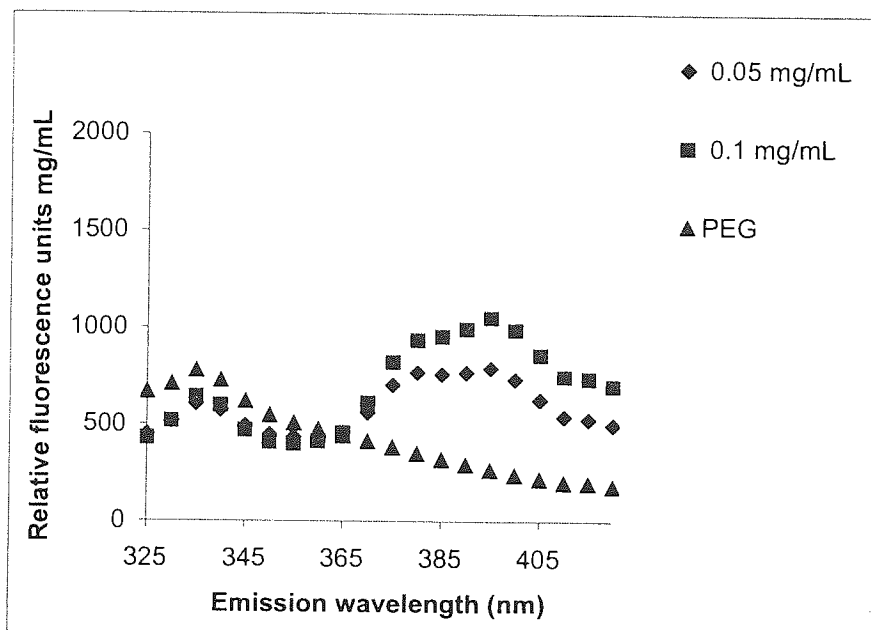
**Figure 57b:** Fluorescence spectra for compound **105** in PEG (an expansion of **57a** to show the `extra` peak) ($\lambda_{ex}$ = 305 nm).
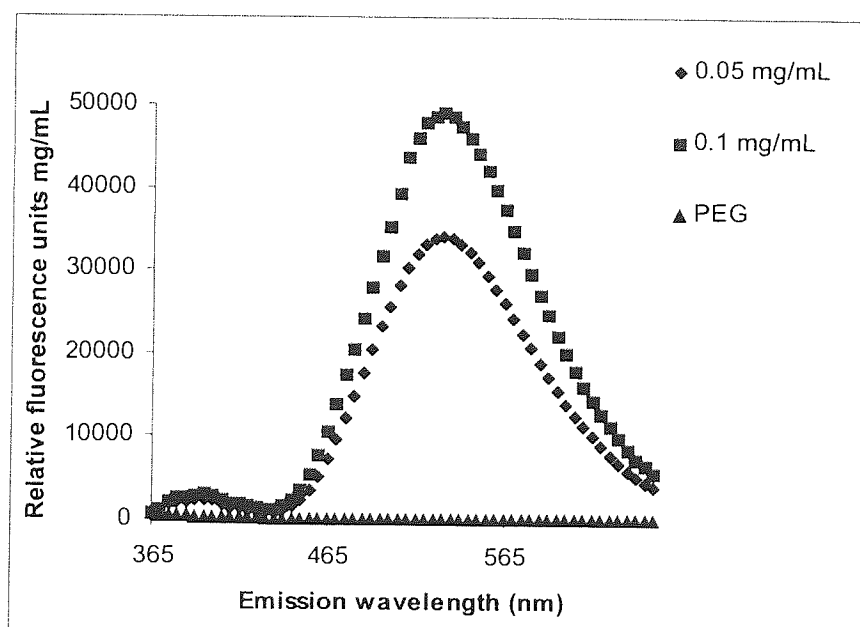


**Figure 58a:** Fluorescence spectra for compound **105** in 200 µL (PEG) ($\lambda_{ex}$ = 345 nm).
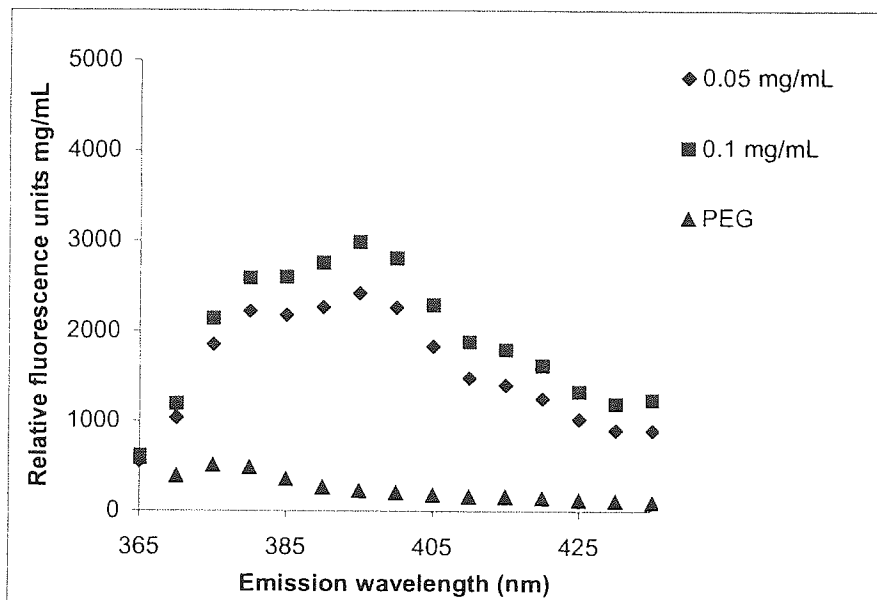
**Figure 58b:** Fluorescence spectra for compound **105** in PEG (an expansion of **58a** to show the `extra` peak) ($\lambda_{ex}$ = 345 nm).

Besides examining the fluorescence of compound **105** in PEG, the compound was also tested in ethanol. Excitation wavelengths of 305 and 345 nm gave emission at 530 nm, however no `extra` peak with emission maximum of 395 nm could be observed (Figure **59a-59b** and **60a-60b**).

Extra evidence that the `extra` peak for compound **105** could be due to the presence of the N-(2-formyl-phenyl)-acetamide moiety was obtained by looking at the earlier Figures **55** and **56** for compound **99** were no peak could be seen at emission maximum of 395nm.
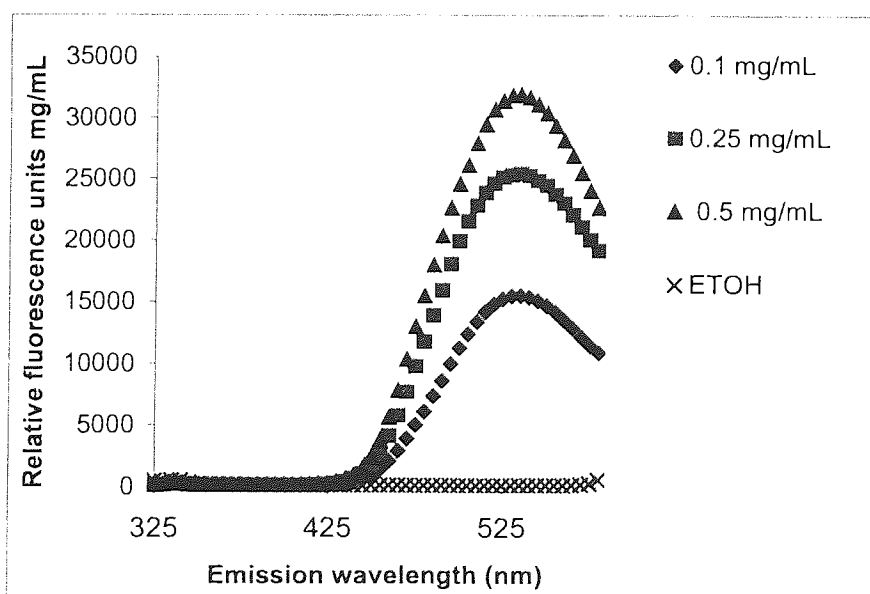


**Figure 59a:** Fluorescence spectra for compound **105** in ethanol ($\lambda_{ex}$ = 305 nm).
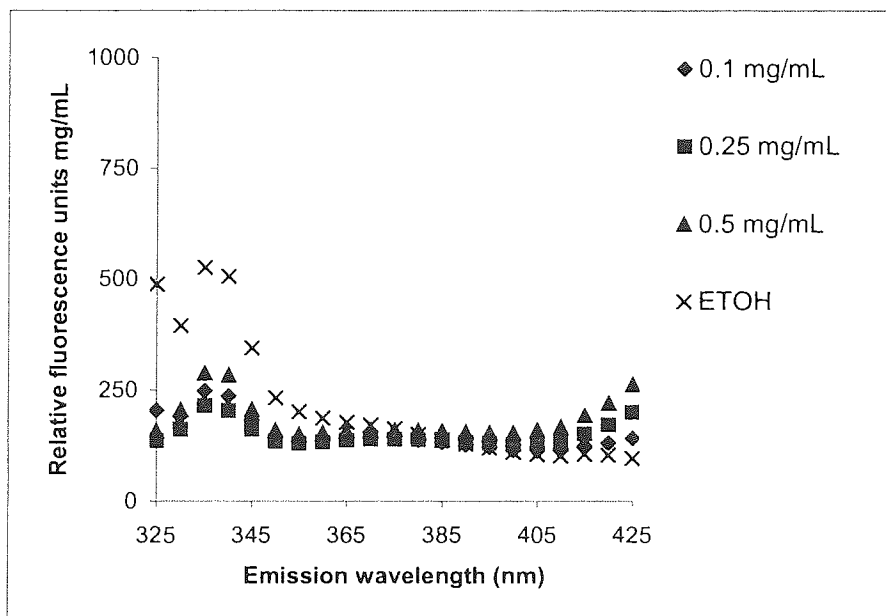
**Figure 59b:** Fluorescence spectra for compound **105** in ethanol (an expansion of **59a** to show the absence of the 'extra' peak) ($\lambda_{ex}$ = 305 nm).
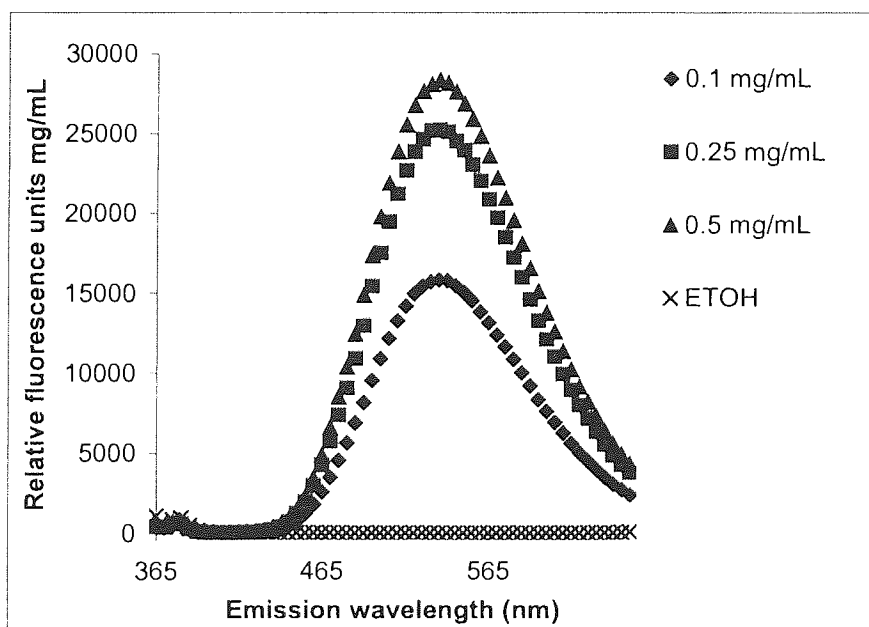


**Figure 60a:** Fluorescence spectra for compound **105** in 200 µL ethanol ($\lambda_{ex}$ = 345 nm).

**Figure 60b:** Fluorescence spectra for compound **105** in ethanol (an expansion of **60a** to show the absence of the `extra` peak) ($\lambda_{ex}$ = 345 nm).

The `extra` peak in the fluorescence emission spectra for compound **105** could only be seen in PEG and not in the ethanol or in compound **99**. This could possibly be due to the ethanol quenching the fluorescence at that particular emission maximum of 395nm.

Conclusions based on the data obtained so far could possibly be ambiguous in that the 'extra' peak is due to the N-(2-formyl-phenyl)-acetamide moiety. Therefore fluorescence studies were carried out on compound **102**, a compound related to **105**, that has no N-(2-formyl-phenyl)-acetamide moiety present (**Figure 61**). Thus if a peak with emission maximum of 395 nm does not appear then the possibly of this `extra` peak being due to N-(2-formyl-phenyl)-acetamide increases.



N-(2-formyl-phenyl)-acetamide not present

**102**

**105**

**Figure 61:** illustrates the absence of N-(2-formyl-phenyl)-acetamide moiety in compound **102** in comparison to compound **105**.

In addition to examining the fluorescence of compound **102** in PEG, the compound was also tested in ethanol. Excitation wavelength of 305 and 345 nm gave emission at 530 nm for both the PEG and ethanol method. No 'extra' fluoroscence could be observed at emission maximum of 395 nm (**Figures 62 - 65**).
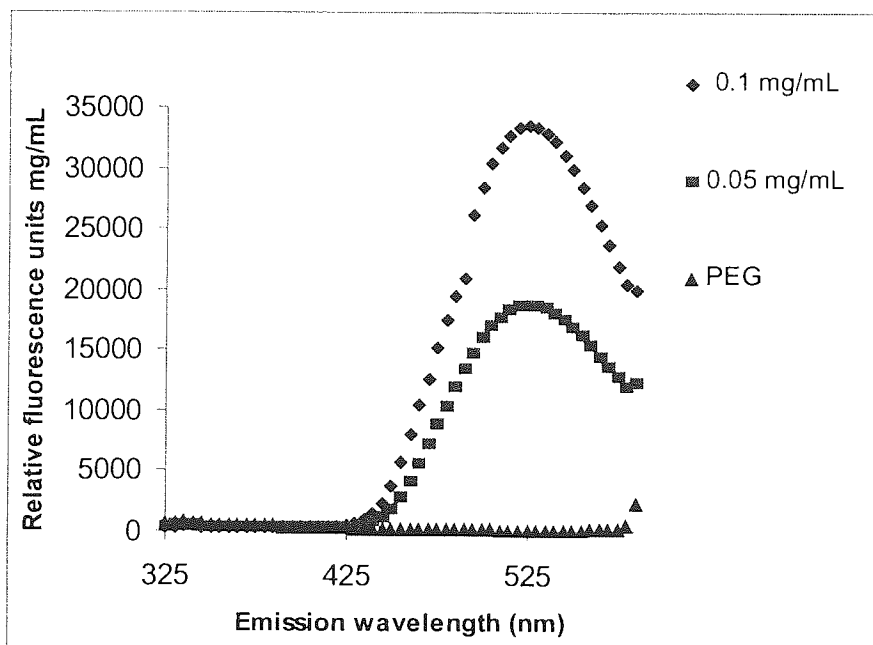


**Figure 62a**: Fluorescence spectra for compound **102** in PEG ($\lambda_{ex}$ = 305 nm).
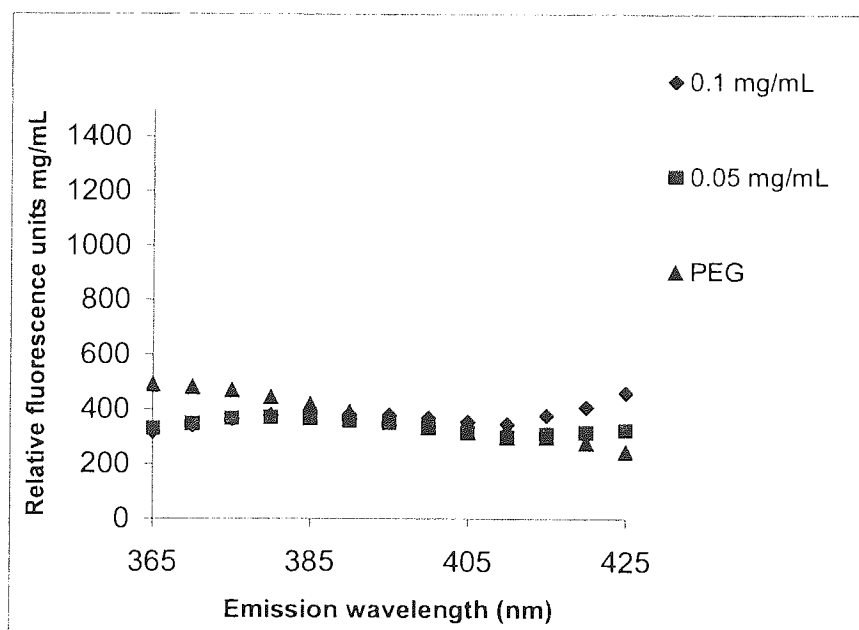


**Figure 62b:** Fluorescence spectra for compound **102** in PEG (an expansion of **62a** to show the absence of the 'extra' peak) ($\lambda_{ex}$ = 305 nm).
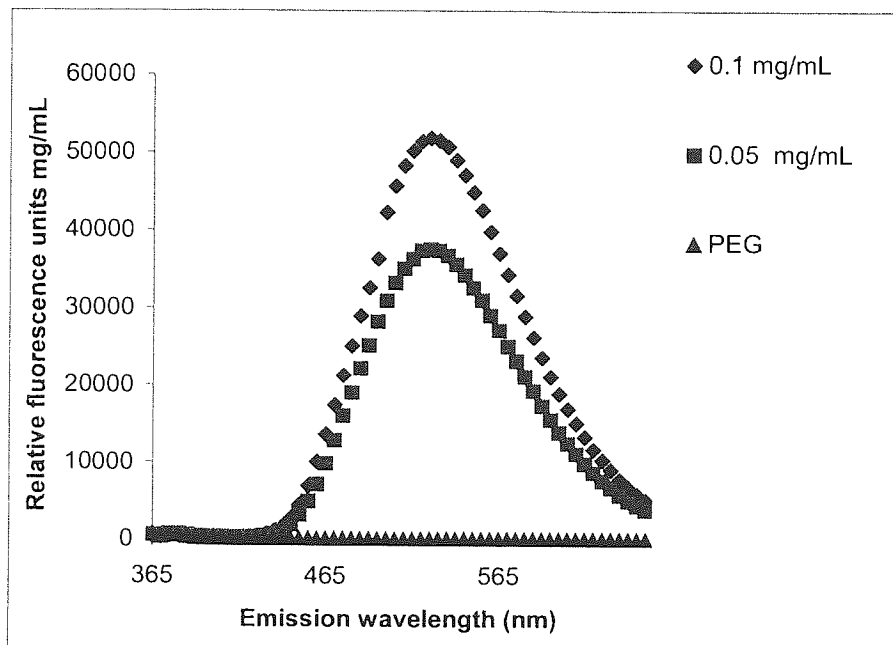
**Figure 63a**: Fluorescence spectra for compound **102** in PEG ($\lambda_{ex}$ = 345 nm).
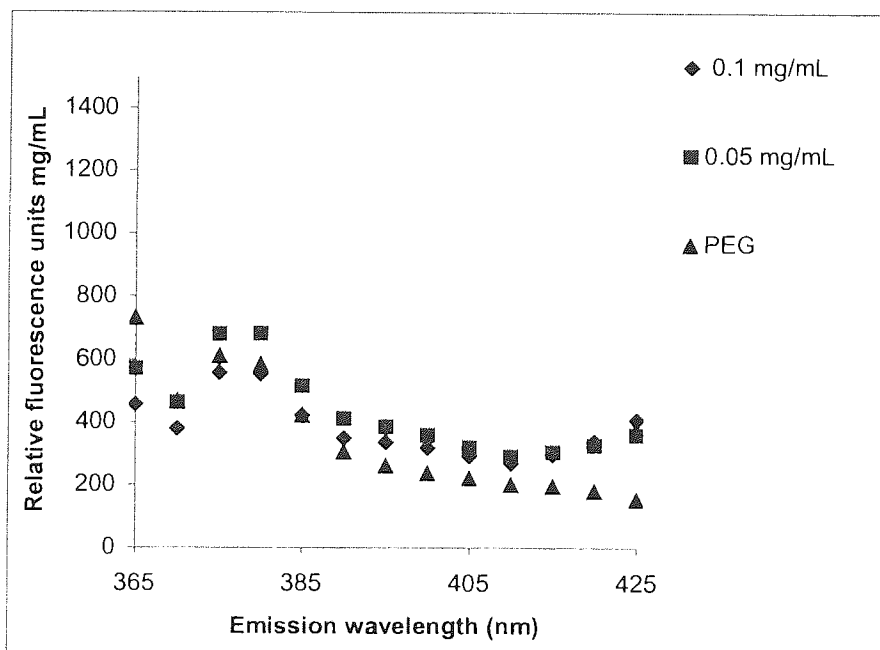


**Figure 63b**: Fluorescence spectra for compound **102** in PEG (an expansion of **63a** to show the absence of the 'extra' peak) ($\lambda_{ex}$ = 345 nm).
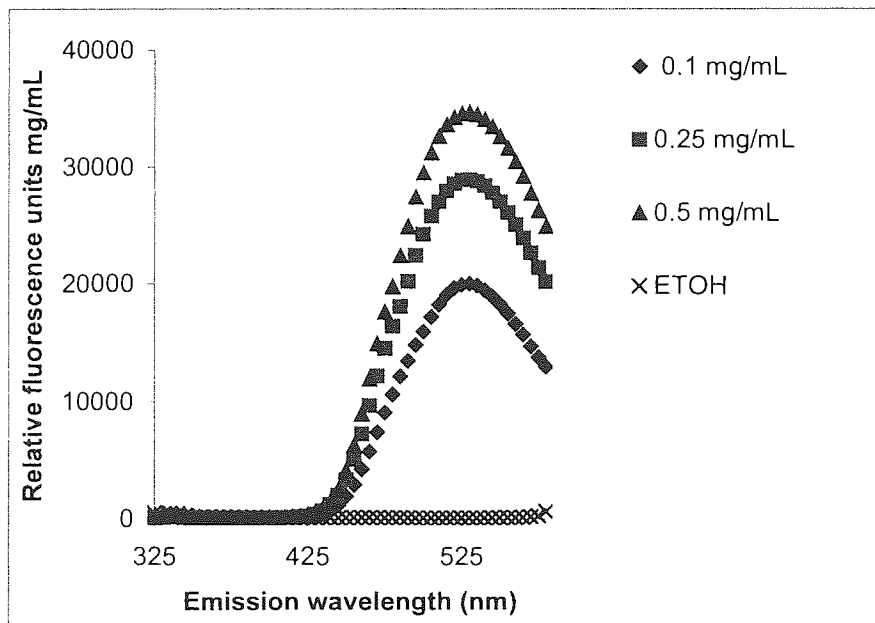
**Figure 64a**: Fluorescence spectra for compound **102** in ethanol ($\lambda_{ex}$ = 305 nm).
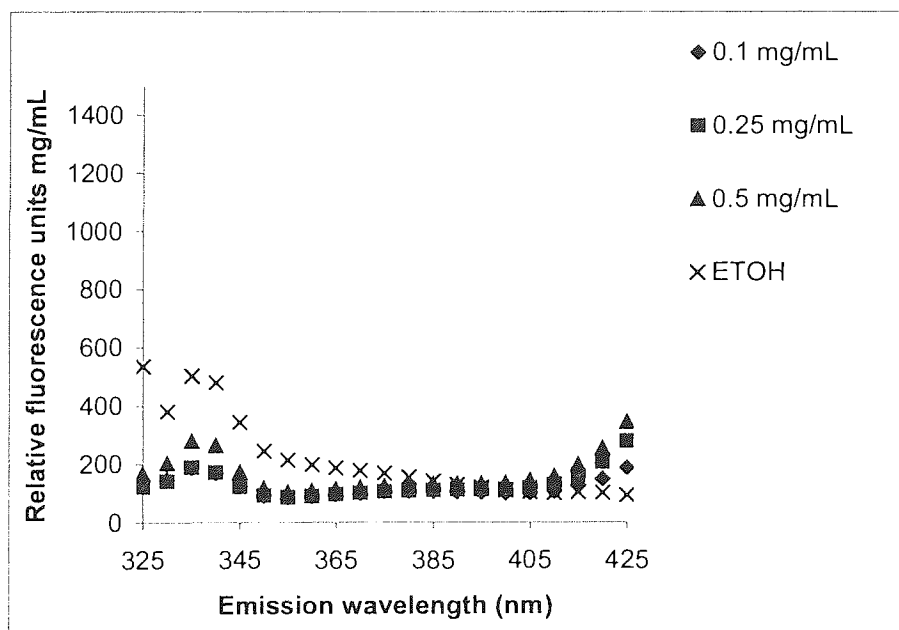


**Figure 64b**: Fluorescence spectra for compound **102** in ethanol (an expansion of **64a** to show the absence of the `extra` peak) ($\lambda_{ex}$ = 305 nm).
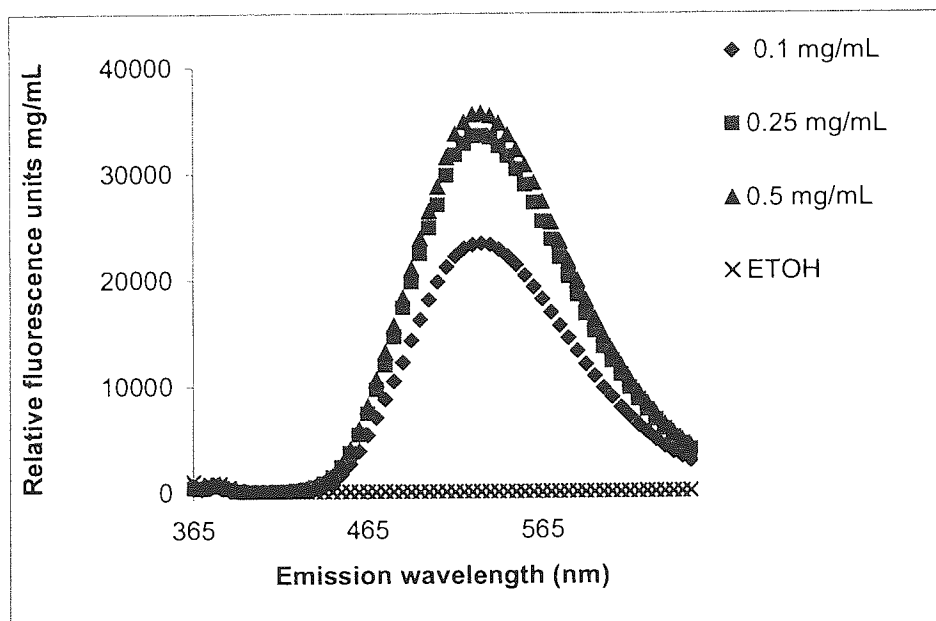
**Figure 65a**: Fluorescence spectra for compound **102** in ethanol ($\lambda_{ex}$ = 345 nm).
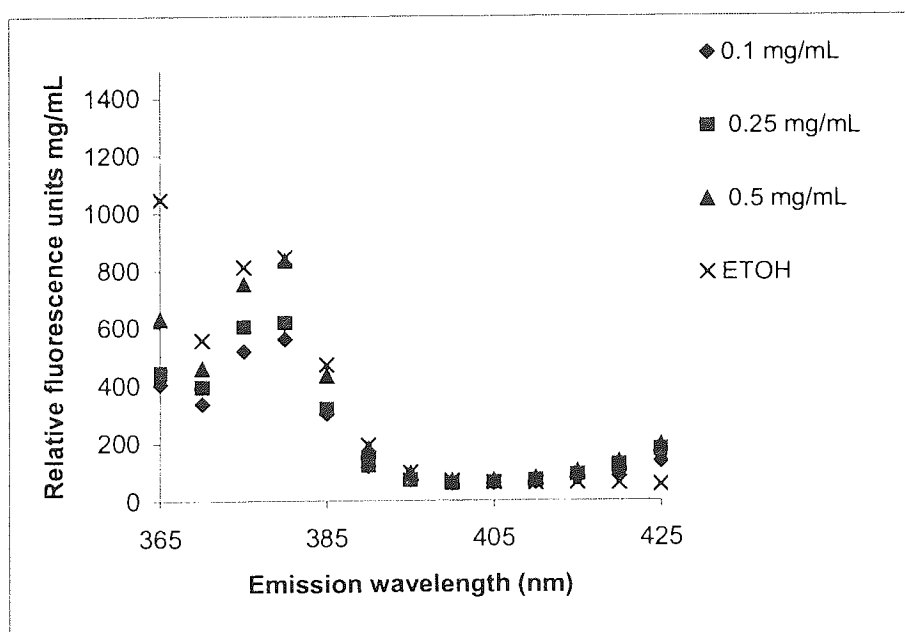


**Figure 65b**: Fluorescence spectra for compound **102** in ethanol (an expansion of **65a** to show the absence of the 'extra' peak) ($\lambda_{ex}$ = 345 nm).

From these results it can be concluded that the 'extra' peak observed at emission maximum of 395 nm for compound **105** is that of N-(2-formyl-phenyl)-acetamide as this peak does not appear in either compound **99** or compound **102** (neither have N-(2-formyl-phenyl)-acetamide moiety). This alternative dual fluorophore (**99**) based on dansyl chloride demonstrates the ability that at excitation wavelengths of 345 and 305 nm, the N-(2-formyl-phenyl)-acetamide moiety responds by emitting at emission maximum of 395 nm and the dimethyl-naphthalen-1-yl-amine moiety responds by given an emission maxima wavelength at 530 nm, hence both components can be distinguished.

### 3.3.2.1 Conclusion

The first attempt to synthesise a dual fluorophore functional monomer from **96** (biphenyl) based on a piperazine scaffold was unsuccessful in that no fluorescence output could be observed for this compound (**Scheme 2**) (3.3.2). Due to this, alternative compounds **99, 97, 98** and **100** were synthesised (**Scheme 2**) (3.3.2). Fluorescence studies revealed that three out of the four compounds gave fluorescence outputs that would be distinguishable from the N-(2-formyl-phenyl)-acetamide functionality (fluorophore 1) of the proposed dual fluorophore. The ability to interrogate the two fluorophores independently was however, only proved for compound **99** by performing further studies on dimethyl-naphthalen-1-yl-amine based compounds **99, 102** (N-(2-formyl-phenyl)-acetamide moiety not present) and **105**. The latter compound successfully demonstrated that the N-(2-formyl-phenyl)-acetamide (fluorophore 1) functionality responded at different emission wavelengths between 365-415 nm in comparison to the other fluorophore dimethyl-naphthalen-1-yl-amine at 530nm.

Compound **104** was not synthesised to a polymerisable functional monomer (reacting this with acrylol chloride), to form MIPs due to lack of time. Even though it was proposed that such MIPs would be used as probes to investigate the positioning of the template/test compounds within the MIP cavity.

### 3.3.3 Methyl hydrazine based scaffold
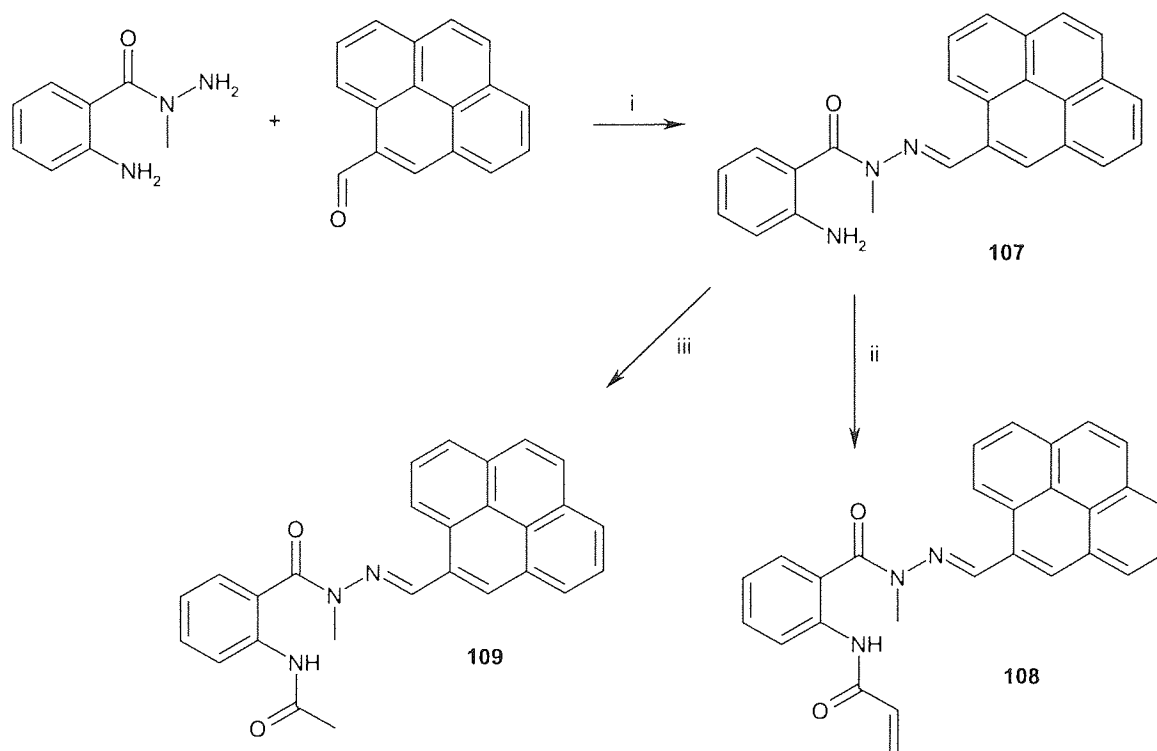


i Ethanol (reflux) ii triethylamine/THF/ acrylol chloride iii triethylamine/THF/ acetyl chloride

**Scheme 3:** A proposed scheme for a dual fluorophore based on methyl hydrazine scaffold.

Another branch to the area of dual fluorophore possibilities was based on a methyl hydrazine scaffold with N-(2-formyl-phenyl)-acetamide functionality being one of the fluorophores and the other a pyrene (illustrated in **Scheme 3** and **Figure 66**). Pyrene carboxaldehyde was reacted with 1-(2-aminobenzoyl)-1-methylhydrazine to give compound **107** {5.3.19} (**Scheme 3**). This compound was acylated with acrylol chloride to form compound **108** {5.3.20} (**Figure 66**).



Fluorophore 1
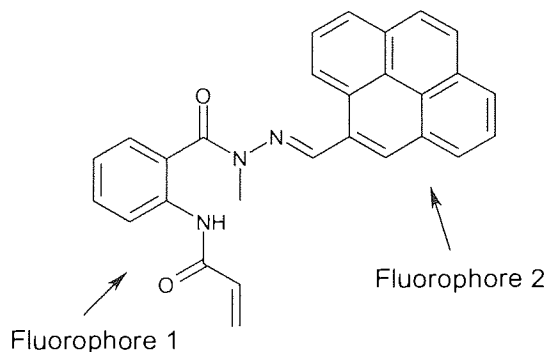
Fluorophore 2

**Figure 66:** Structure of dual fluorophore, *N*-(2-{*N*-Methyl-*N'*-[1-pyren-1-yl-meth-(E)-ylidene]-hydrazinocarbonyl}-phenyl)-acrylamide, compound **108**.

Compound **108** was used both as a functional monomer and a fluorophore such that the MIP cavities would exhibit binding-dependant fluorescence. It is also proposed that the two fluorophores present on the functional monomer, compound **108** would be 'insulated' from each other by the N-methyl moiety. This moiety would be able to prevent enolisation of the carbonyl group attached to the N-methyl moiety and thus prevent the two fluorophores becoming conjugated. By doing this, the N-(2-formyl-phenyl)-acetamide moiety could be quenched by the template/test compound and possibly with the alignment of two pyrenes in a MIP may produce an excimer. Note, that one of the pyrenes would be from the MIP-bound fluorophore and the other from the test/template compound (**Figure 67**), and hence act as a dual fluorophore functional monomer. Thus it was hoped that this dual fluorophore functional monomer would act as a probe to investigate the positioning of a template/test compound within the MIP cavity. This proposed FFM however, behaved as single fluorophore, but due to the presence of the pyrene moiety on the FFM this was used instead to investigate excimer formation i.e. the alignment of two pyrenes in a MIP, one coming from a test compound containing a pyrene, may produce an excimer and be detected readily by fluorescence (**Scheme 3**). (Fujimoto *et al* 2004; Wagner *et al* 2002; Jin Takashi and Monde Kenji 1998; Graceffa and Lehrer 1980; Kostenko *et al* 2001)
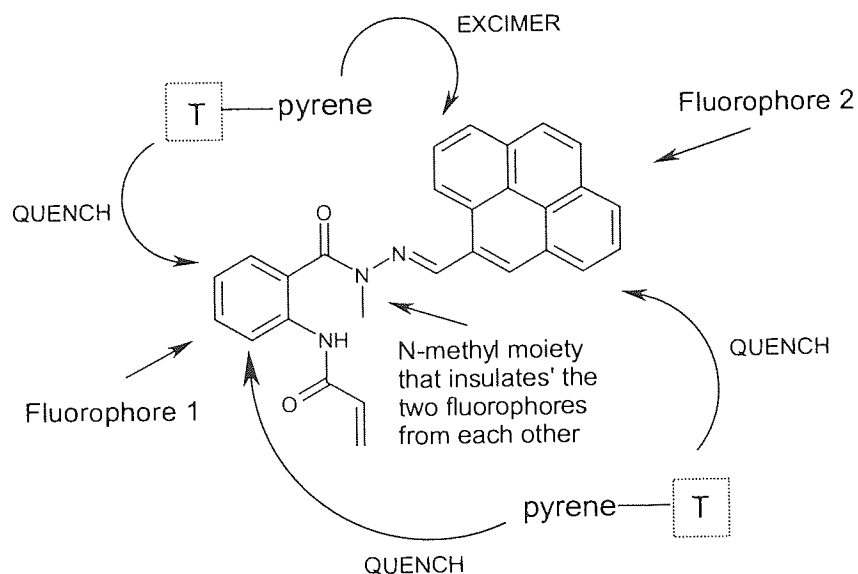
**Figure 67:** Shows compound **108** as a probe to investigate template/test compound (T) positioning.

A series of MIPs was constructed with **108** as the fluorescent functional monomer and compounds **76** {5.3.2}, **78** {5.3.4} and **77** {5.3.3} were used as templates and cross-linked with triethyleneglycol dimethacrylate (TEGDMA). These three MIPs were subjected to grinding (pestle and mortar) followed by sieving to establish a known particle size range and finally the templates were extracted using a soxhlet apparatus. The final step of the procedure resulted in empty MIPs being re-exposed to their templates and test compounds at various concentrations (i.e. 0.1, 1.0, 5.0 mg/mL) collected by filtration and analysed by fluorescence (**Figure 69**, illustrates the structures of the templates/test compounds employed). The optimum excitation wavelength of 340 nm and the fluorescence emission maximum at 430 nm were the parameters to be used to analyse the three MIPs. These parameters were determined by carrying out a study on the stable version (non-polymerisable) of compound **108**, formed by reacting **107** with acetyl chloride giving compound **109** (**Scheme 3**).

Compound **109** {5.3.21} established that at an excitation wavelength of 340nm, a fluorescence emission maximum was observed at an wavelength of 430nm, however no excimer peak could be observed between 470 and 500 nm (Fujimoto *et al*, 2004; Wagner *et al*, 2002; Jin Takashi and Monde Kenji, 1998; Graceffa and Lehrer, 1980; Kostenko *et al*, 2001)) even at a concentration as high as 0.125 mg/mL in PEG (**Figure 68**) (Procedure 3e refer to 4.3).

130
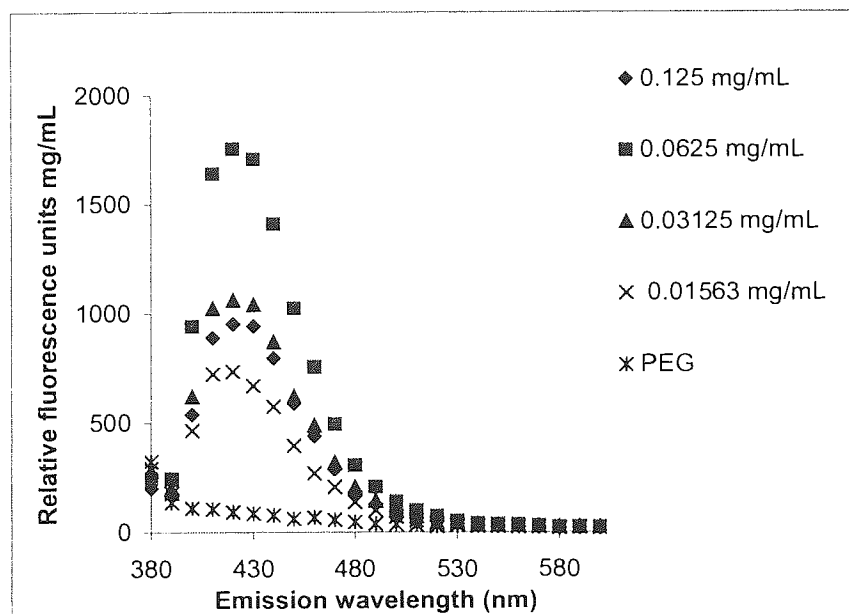
**Figure 68:** Fluorescence spectra for compound **109** in (PEG) ($\lambda_{ex}$ = 340 nm).

## Templates / test compounds employed for MIP

Templates and test compounds (**Figure 69**, illustrates the structures of the templates/test compounds employed) **76** {5.3.2}, **78** {5.3.4} and **77** {5.3.3} constituted a closely related set of relatively rigid polycyclic analogues. The hydroxylated compounds **110** {5.3.22}, **111** {5.3.23} and **112** {5.3.24} were to probe the effect presence of a varying number of polar groups on an otherwise fixed template. As for the pyrene-based compounds **113** (5.3.25}, **114** {5.3.26}, **115** {5.3.27} and **116** {5.3.28} these all have varying number, type and size i.e. sulphur, nitrogen and oxygen, as hydrogen-bond acceptors and donors. Thus these variations could possibly influence the fluorescence outcome when employed as test compounds. Also note that compounds such as **77**, **113**, **114**, **115** and **116** all contain pyrenes and so could possibly demonstrate excimer fluorescence when interacting with the polymer-bound fluorophore i.e. **108** (**Figure 66**).

Note that all of these compounds would serve the same purpose when employed later on for the FFM **118**.
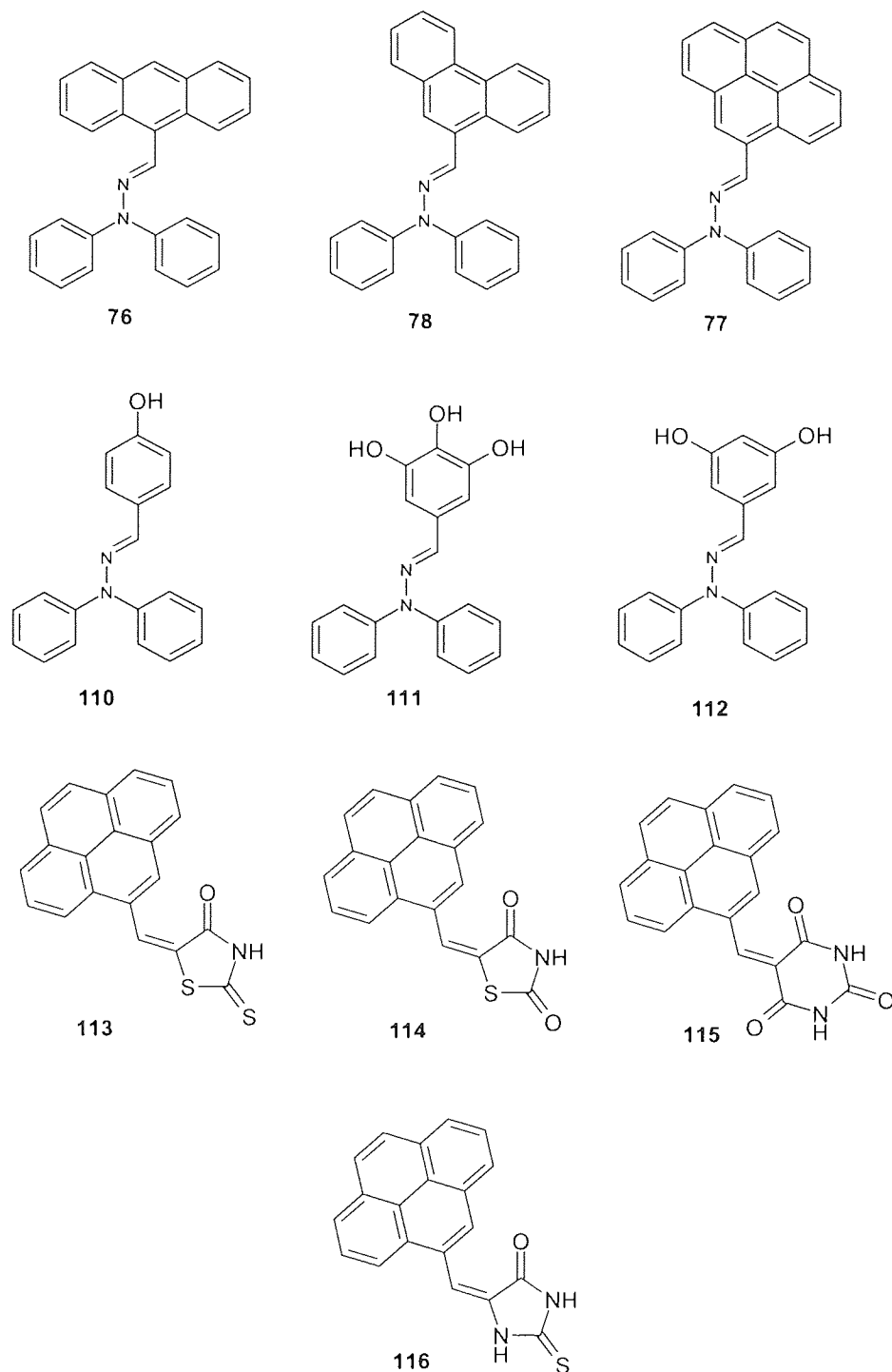
**Figure 69:** Structures of templates and test compounds.

### 3.3.3.1 A solution based study on the ability of each test compound and template to fluoresce

In this study each test/template compound's fluorescence ability, without the hindrance or contributing fluorescence of any other compound such as that found in a MIP environment was studied. To determine this, solution phase fluorescence quenching was performed on each compound (Procedure 3f refer to

132

4.3). This study would help reveal the characteristic fluorescence output and emission maxima for each compound, and help towards interpreting the results found for each compound in a MIP.

The characteristic fluorescence outputs for each test compound were obtained at 0.02 mg/mL in THF these are presented in **Figures 70**, **71** and **72**. The structures of each compound can be seen in **Figure 69**.
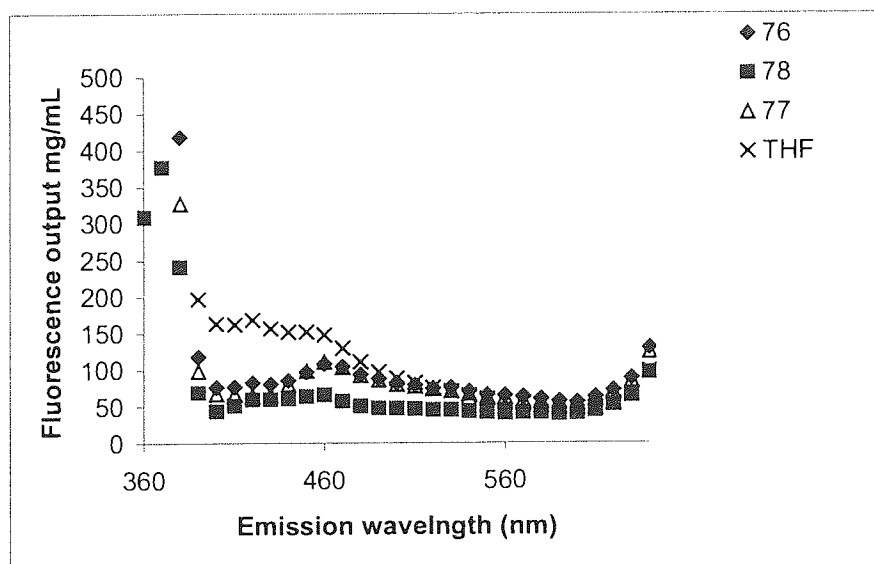


**Figure 70:** Fluorescence spectra for compounds (**76-77**) at 0.02 mg/mL in THF. ($\lambda_{ex}$ = 340 nm).
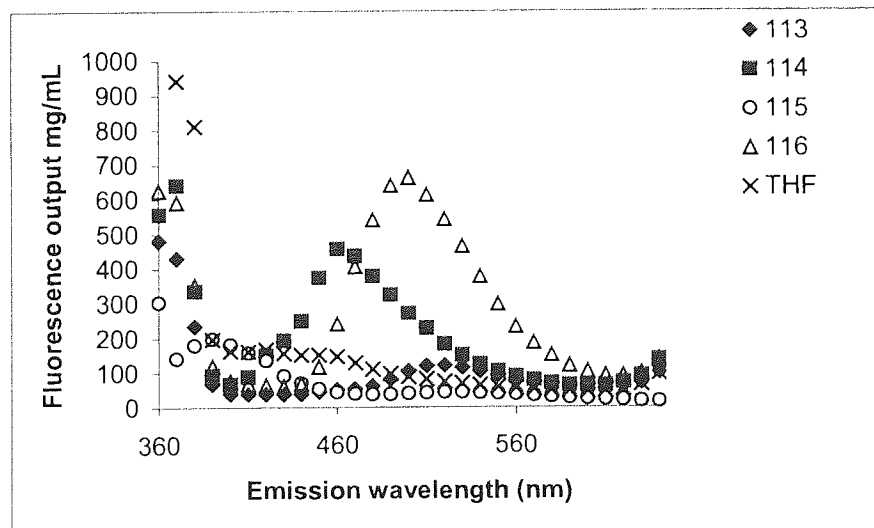


**Figure 71:** Fluorescence spectra for pyrene-based compounds (**113-116**) at 0.02 mg/mL in THF. ($\lambda_{ex}$ = 340 nm).
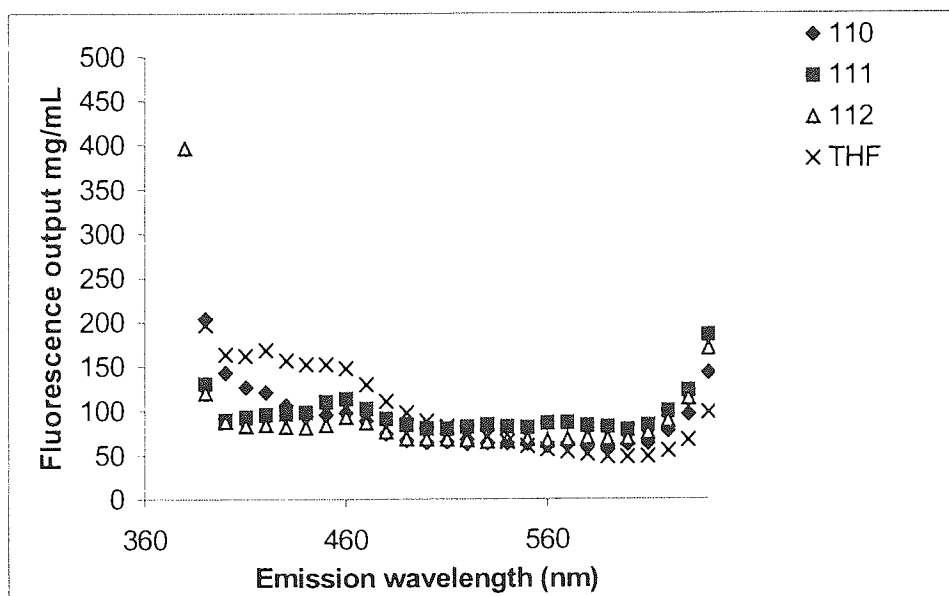
**Figure 72:** Fluorescence spectra for hydroxylated compounds (**110-112**) at 0.02 mg/mL in THF. ($\lambda_{ex}$ = 340 nm).

### 3.3.3.2 Preparation of soluble copolymers of N-(2-{N-Methyl-N'-[1-pyren-1-yl-meth-(E)-ylidene]-hydrazino-carbonyl}-phenyl)-acrylamide,compound 108

The reason for preparing soluble copolymers of co-styrene-**108** {5.4.3} and co-octadecylacrylate-**108** {5.4.2} (**Figure 67**) as polymer films was to help in the interpretation of the fluorescence quenching MIP results. In addition, having the co-polymer films, the quenching ability of each test compound towards the fluorophore could be addressed and in a polymeric environment but without the variable constraint of an imprinted cavity. This represents a halfway house between completely unhindered solution-phase molecular interactions and the restricted environment of a MIP (Procedure 2b & c refer to 4.2).

The fluorescence conditions were exactly the same as those applied for the MIPs, i.e. an excitation wavelength of 340nm. Note that the amount of co-polymer i.e. 5.0 mg per well was kept constant and the amount of test compound was varied for this study. The results for both co-polymer films are presented in **Figures 73** (co-styrene-**108**) and **Figures 74** (co-octadecylacrylate-**108**).

### 3.3.3.2.1 Co-styrene-108
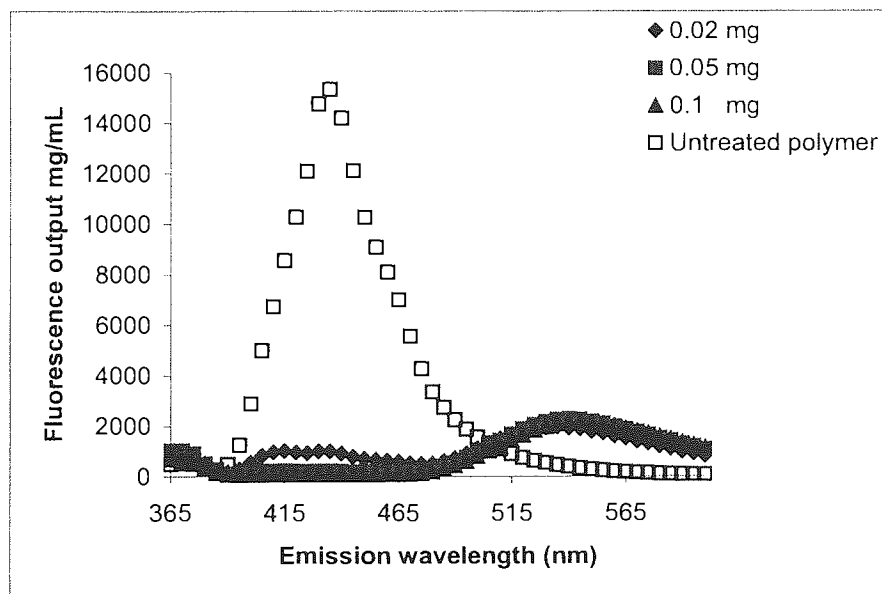


**Figure 73a:** Fluorescence spectra of co-styrene-**108** with compound **76**. ($\lambda_{ex}$ = 340 nm).
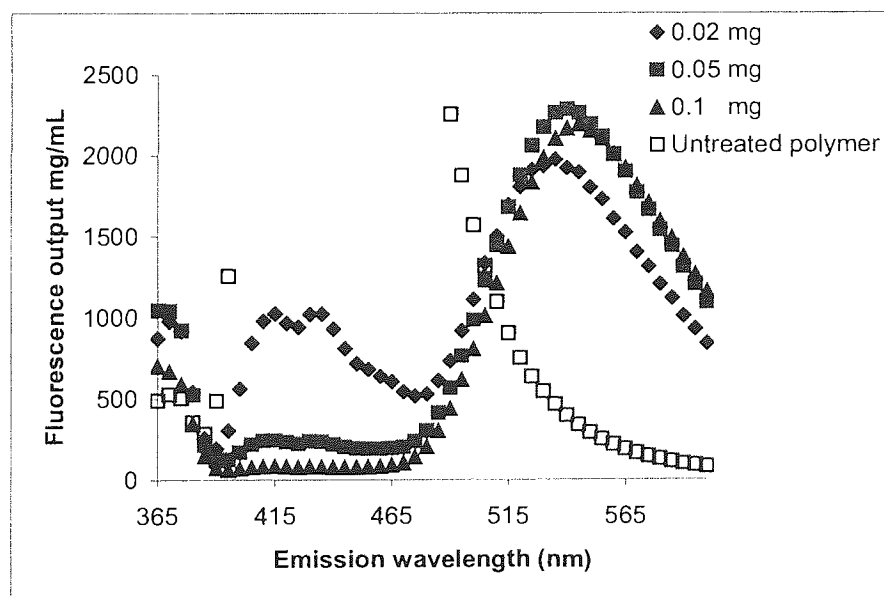


**Figure 73a1:** Fluorescence spectra of co-styrene-**108** with compound 76 (an expansion of **73a**) ($\lambda_{ex}$ = 340 nm).
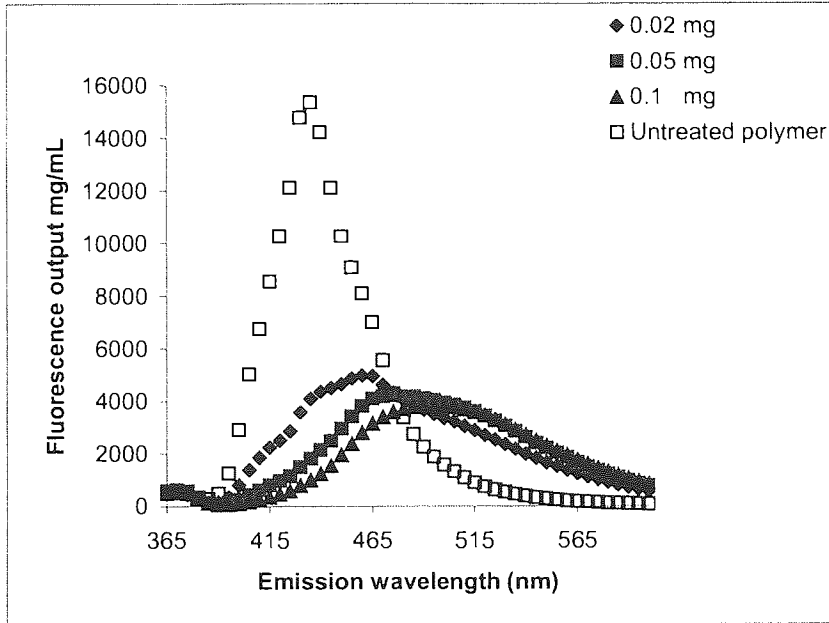
**Figure 73b:** Fluorescence spectra of co-styrene-**108** with compound **78** ($\lambda_{ex}$ = 340 nm).
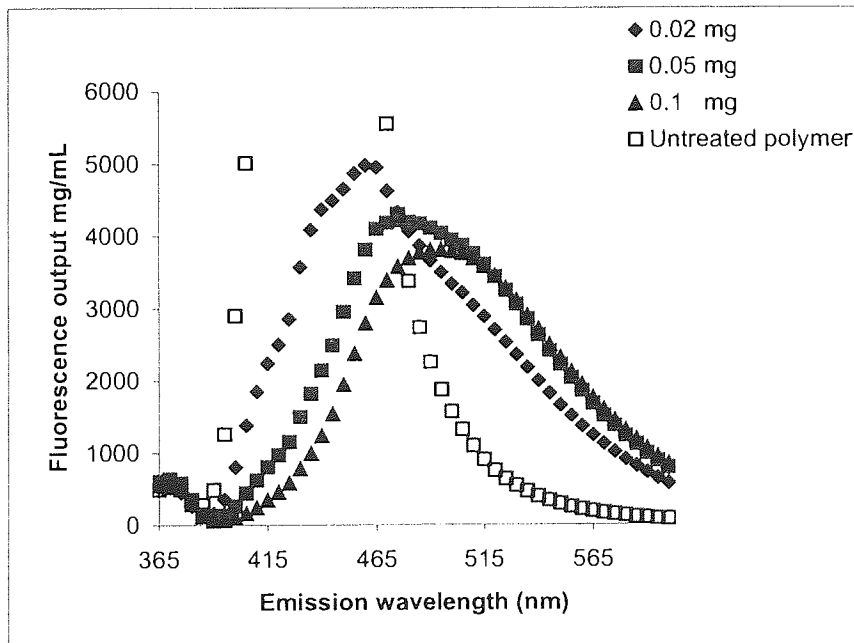


**Figure 73b1:** Fluorescence spectra of co-styrene-**108** with compound **78** (an expansion of **73b**) ($\lambda_{ex}$ = 340 nm).
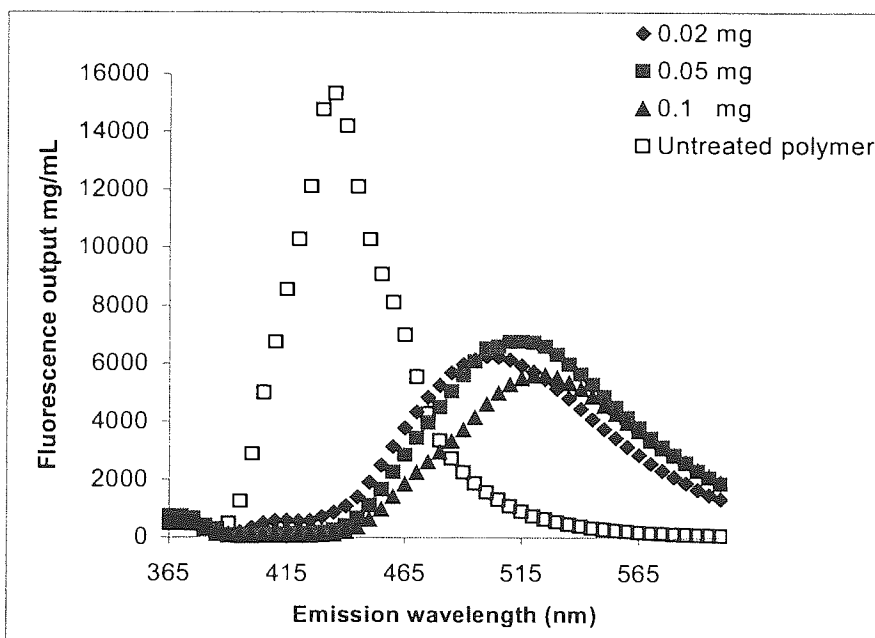
**Figure 73c:** Fluorescence spectra of co-styrene-**108** with compound **77** ($\lambda_{ex}$ = 340 nm).
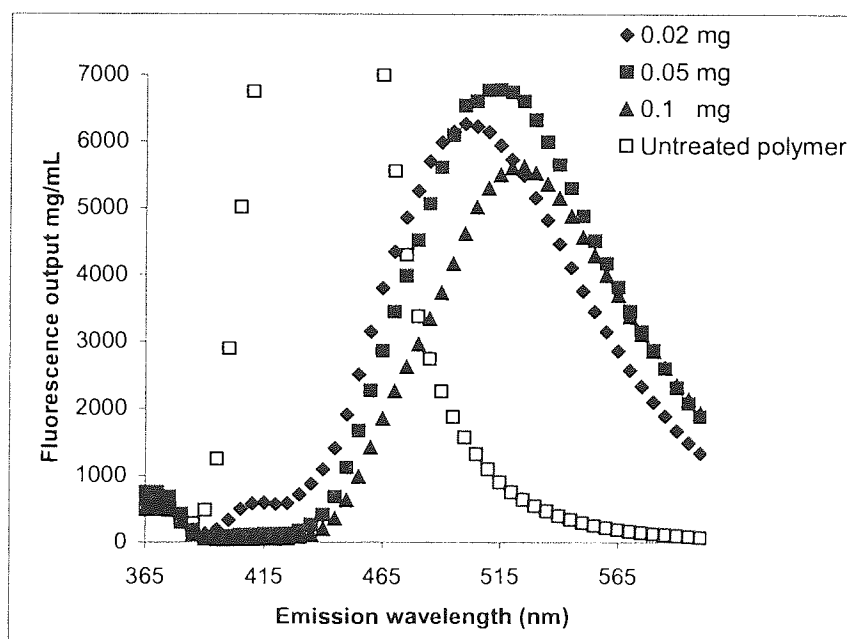


**Figure 73c1:** Fluorescence spectra of co-styrene-**108** with compound **77** (an expansion of **73c**) ($\lambda_{ex}$ = 340 nm).
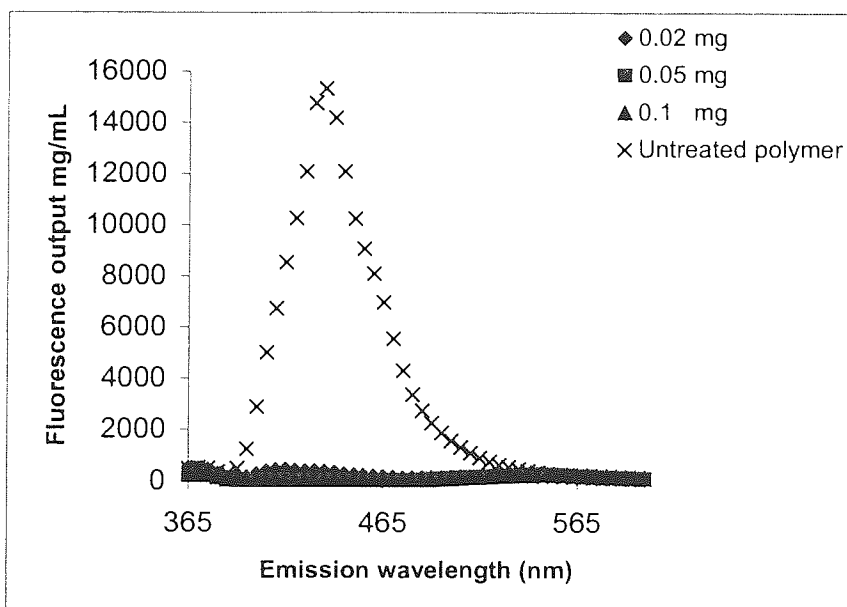
**Figure 73d**: Fluorescence spectra of co-styrene-**108** with compound **113** ($\lambda_{ex}$ = 340 nm).
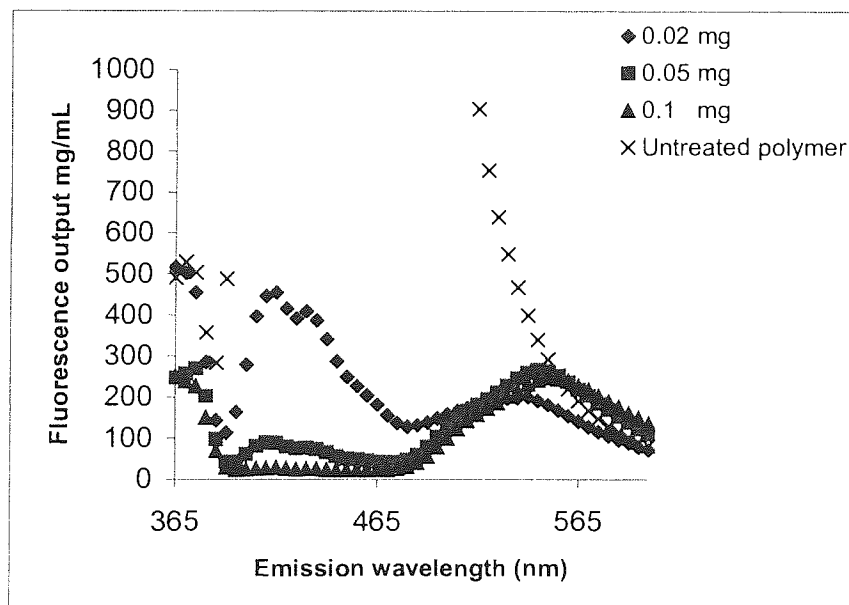


**Figure 73d1**: Fluorescence spectra of co-styrene-**108** with compound **113** (an expansion of **73d**) ($\lambda_{ex}$ = 340 nm).
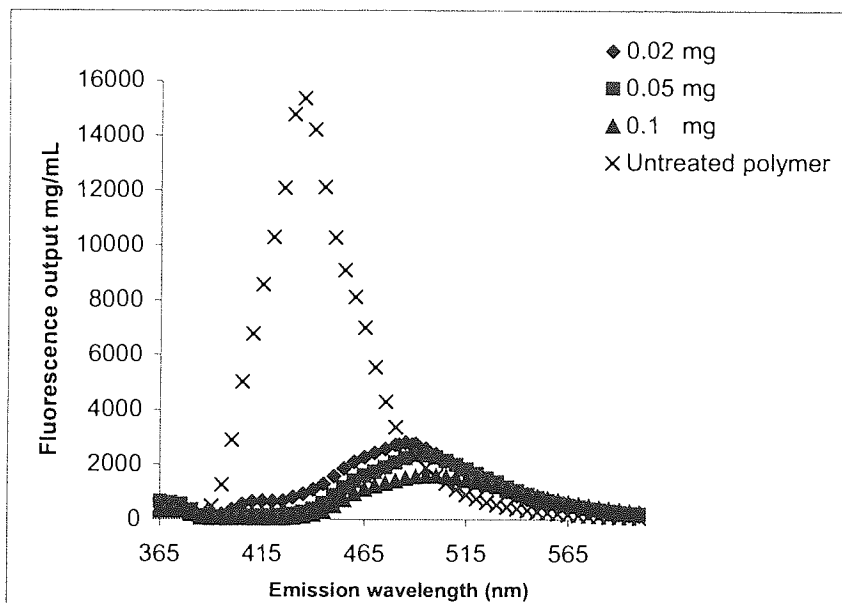
**Figure 73e**: Fluorescence spectra of co-styrene-**108** with compound **114** ($\lambda_{ex}$ = 340 nm).
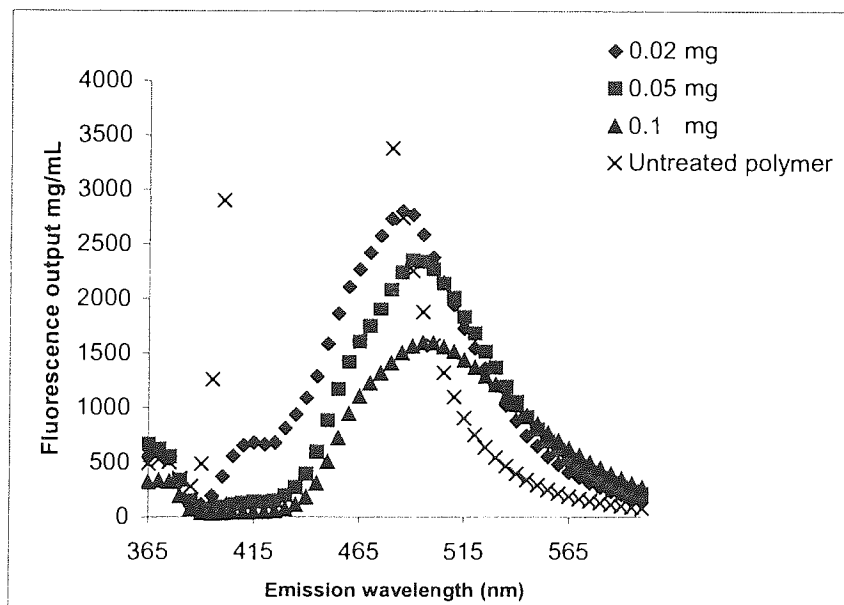


**Figure 73e1**: Fluorescence spectra of co-styrene-**108** with compound **114** (an expansion of **73e**) ($\lambda_{ex}$ = 340 nm).
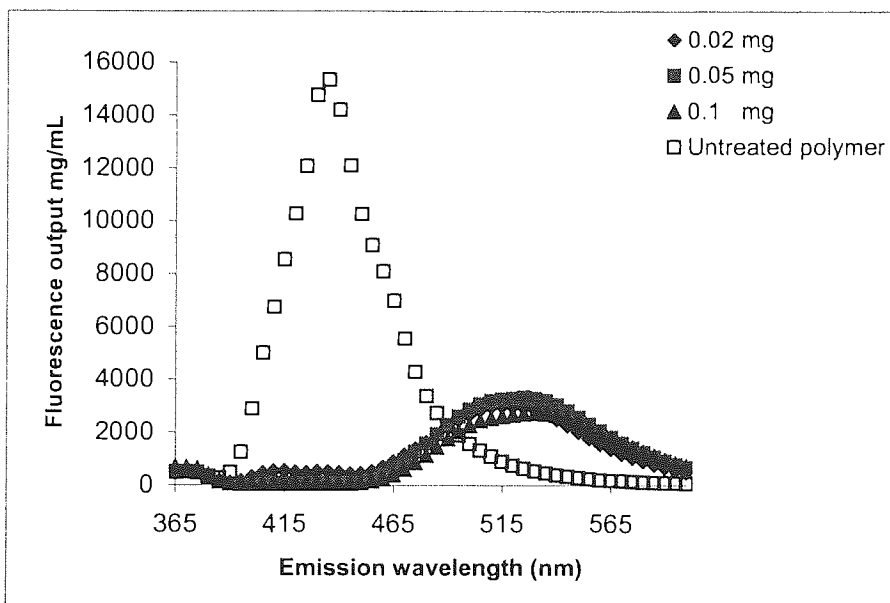
**Figure 73f**: Fluorescence spectra of co-styrene-**108** with compound **116** ($\lambda_{ex}$ = 340 nm).
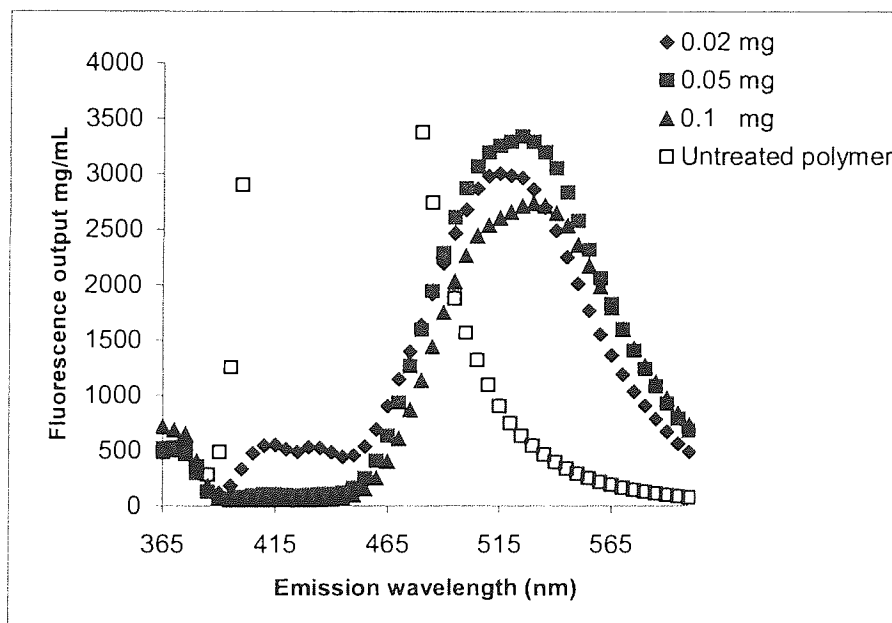


**Figure 73f1**: Fluorescence spectra of co-styrene-**108** with compound **116** (an expansion of **73f**) ($\lambda_{ex}$ = 340 nm).

## 3.3.3.2.2 Co-octadecylacrylate-108
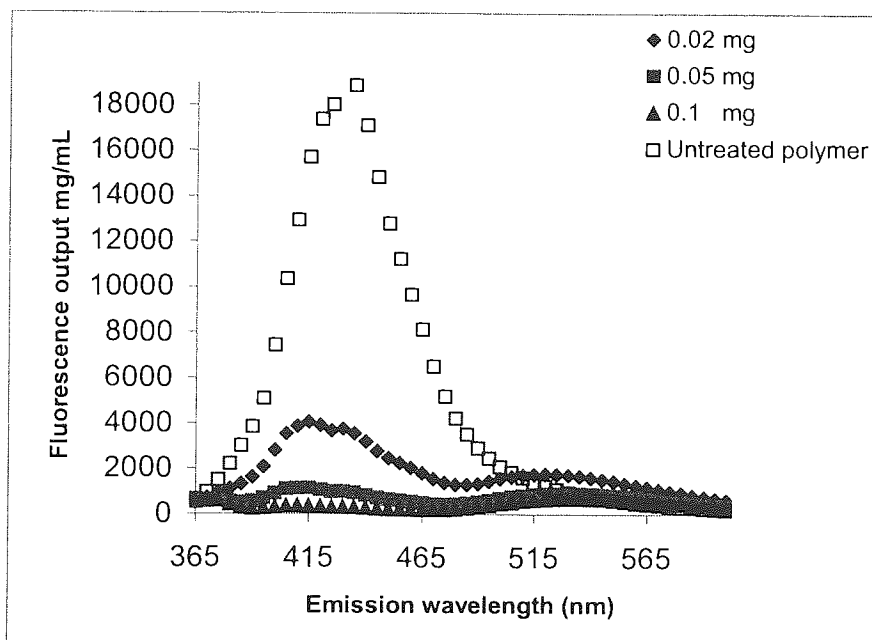


**Figure 74a**: Fluorescence spectra of co-octadecylacrylate-**108** with compound **76**. ($\lambda_{ex}$ = 340 nm).
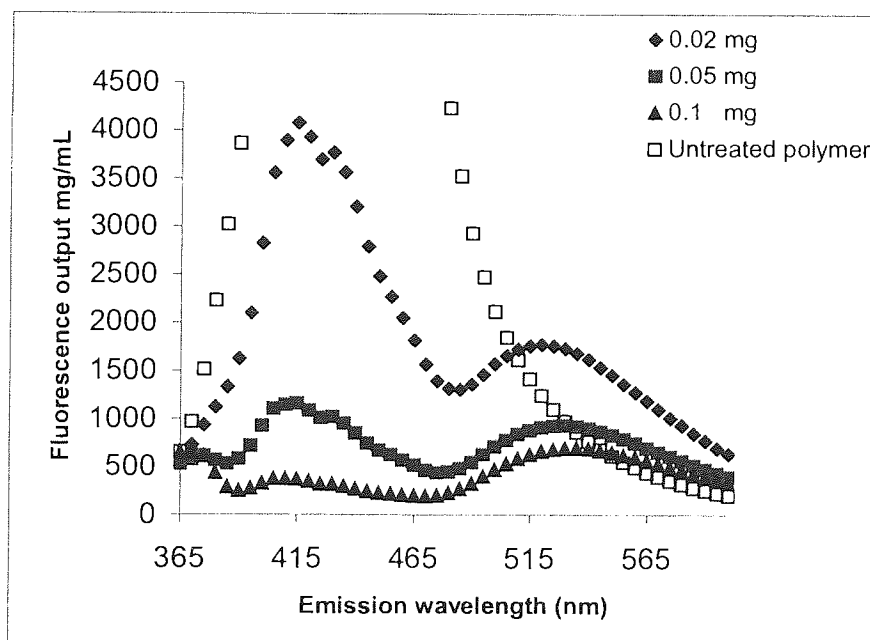


**Figure 74a1**: Fluorescence spectra of co-octadecylacrylate-**108** with compound **76** (an expansion of **74a**) ($\lambda_{ex}$ = 340 nm).
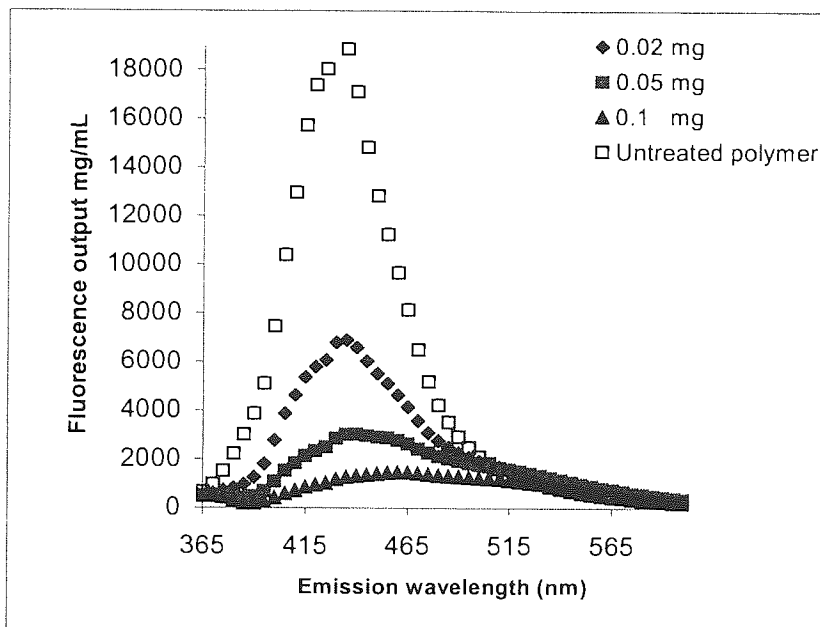
**Figure 74b**: Fluorescence spectra of co-octadecylacrylate-**108** with compound **78**. ($\lambda_{ex}$ = 340 nm).
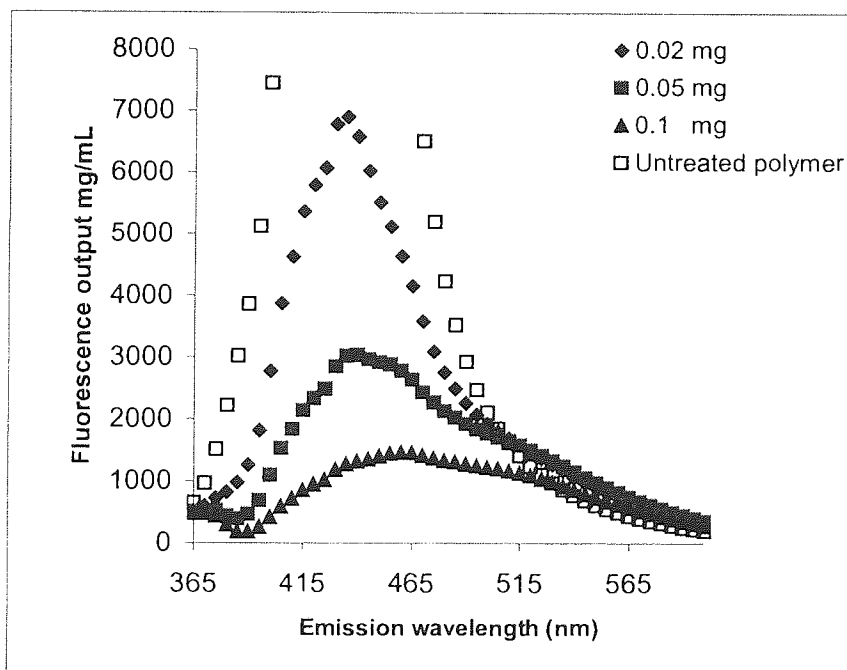


**Figure 74b1**: Fluorescence spectra of co-octadecylacrylate-**108** with compound **78** (an expansion of **74b**) ($\lambda_{ex}$ = 340 nm).
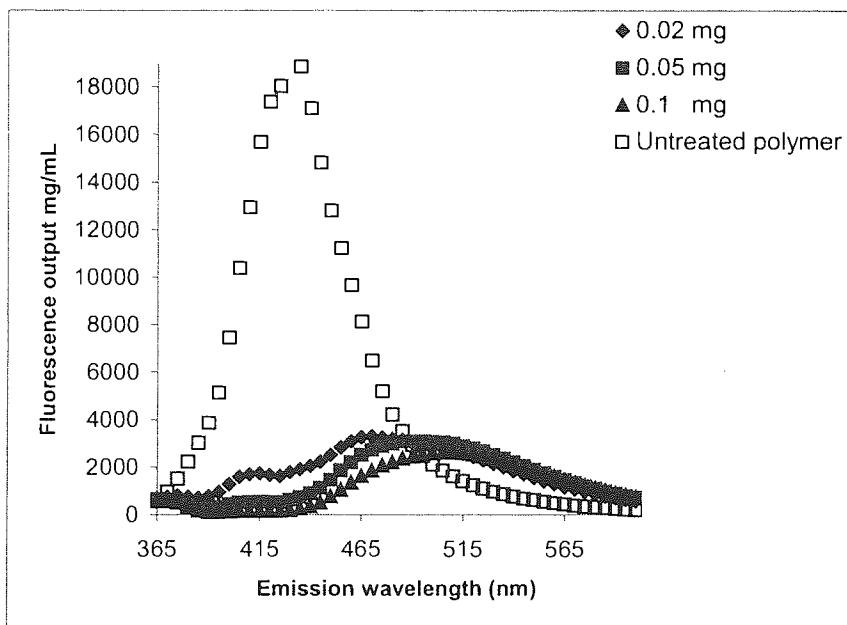
**Figure 74c**: Fluorescence spectra of co-octadecylacrylate-**108** with compound **77** ($\lambda_{ex}$ = 340 nm).
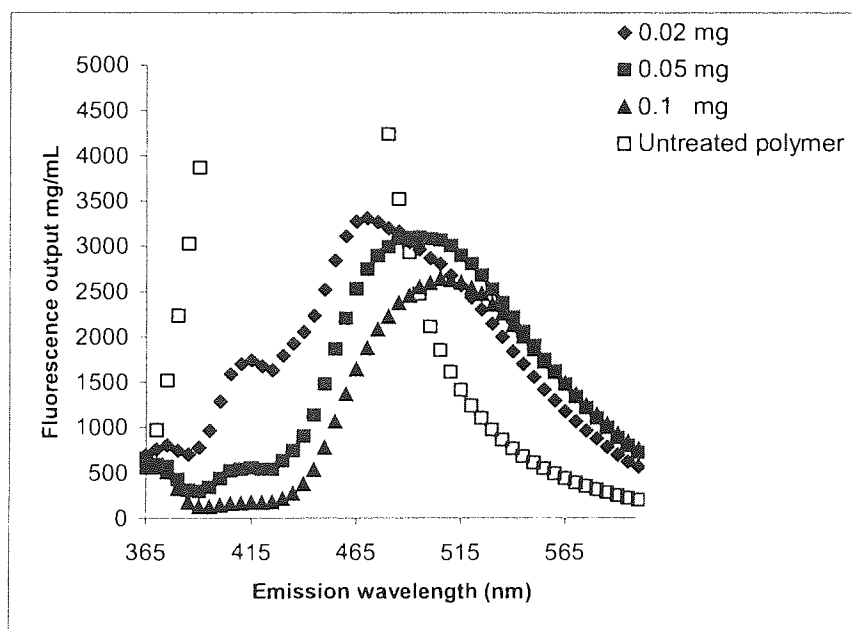


**Figure 74c1**: Fluorescence spectra of co-octadecylacrylate-**108** with compound **77** (an expansion of **74c**) ($\lambda_{ex}$ = 340 nm).
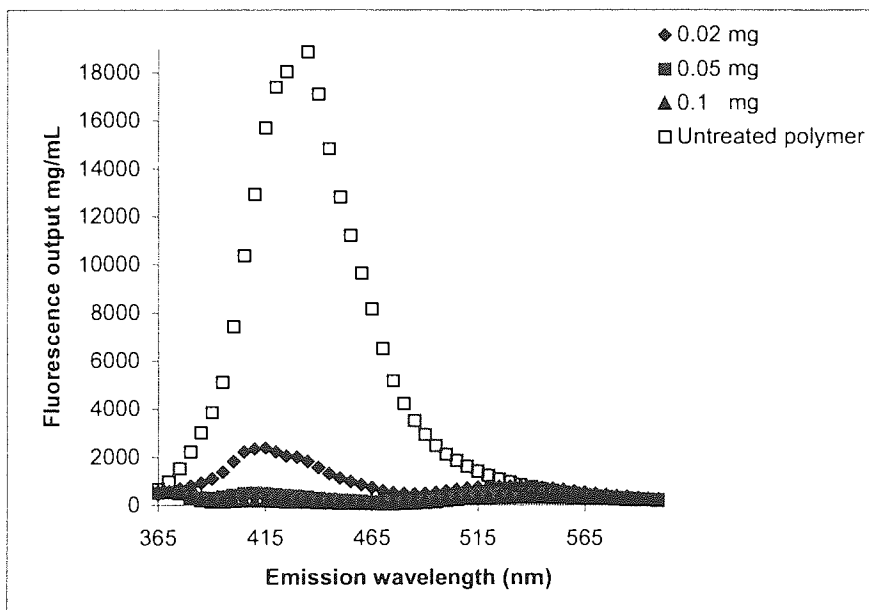
**Figure 74d**: Fluorescence spectra of co-octadecylacrylate-**108** with compound **113** ($\lambda_{ex}$ = 340 nm).
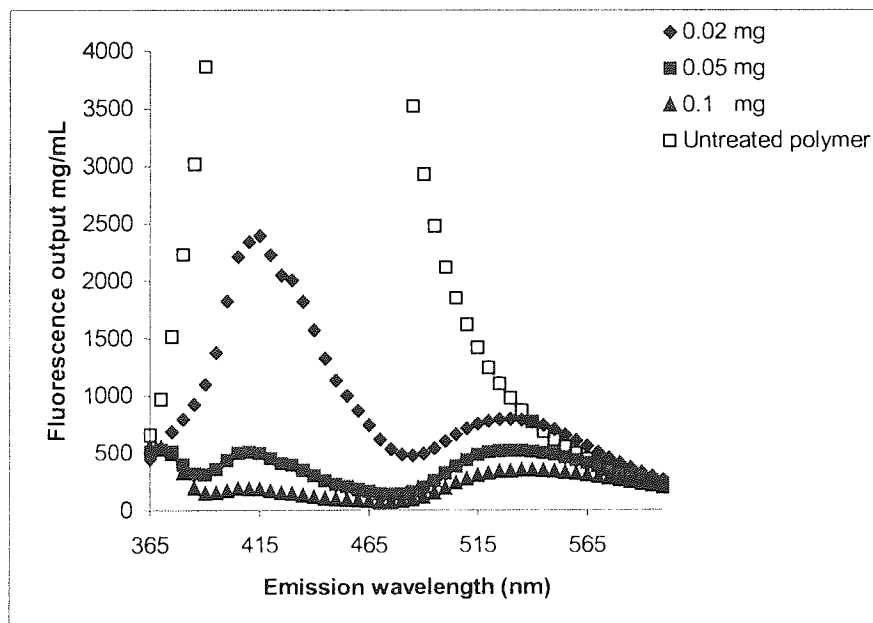


**Figure 74d1**: Fluorescence spectra of co-octadecylacrylate-**108** with compound **113** (an expansion of **74d**) ($\lambda_{ex}$ = 340 nm).
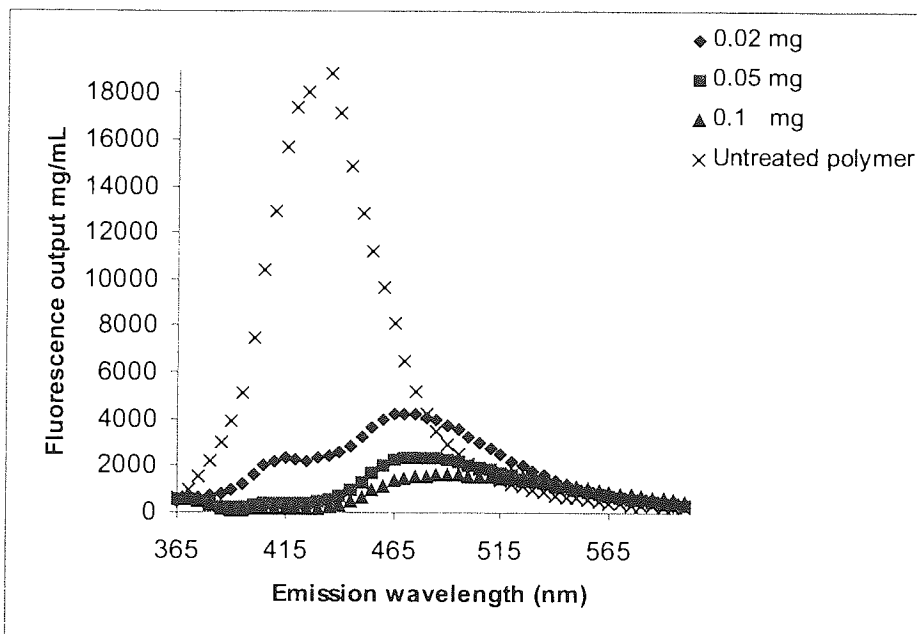
**Figure 74e**: Fluorescence spectra of co-octadecylacrylate-**108** with compound **114** ($\lambda_{ex}$ = 340 nm).
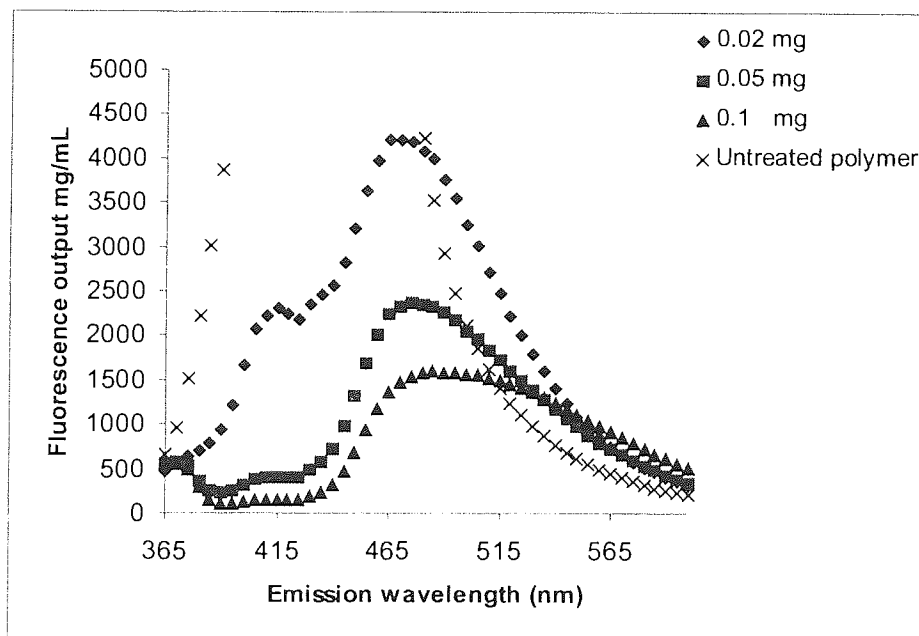


Figure **74e1**: Fluorescence spectra of co-octadecylacrylate-**108** with compound **114** (an expansion of **74e**) ($\lambda_{ex}$ = 340 nm).
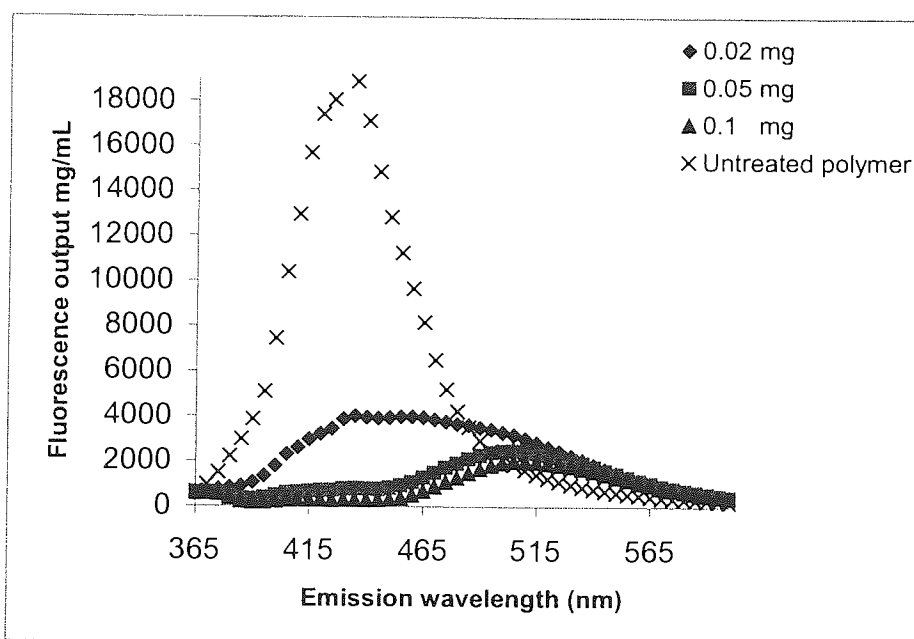
Figure **74f**: Fluorescence spectra of co-octadecylacrylate-**108** with compound **116** ($\lambda_{ex}$ = 340 nm).
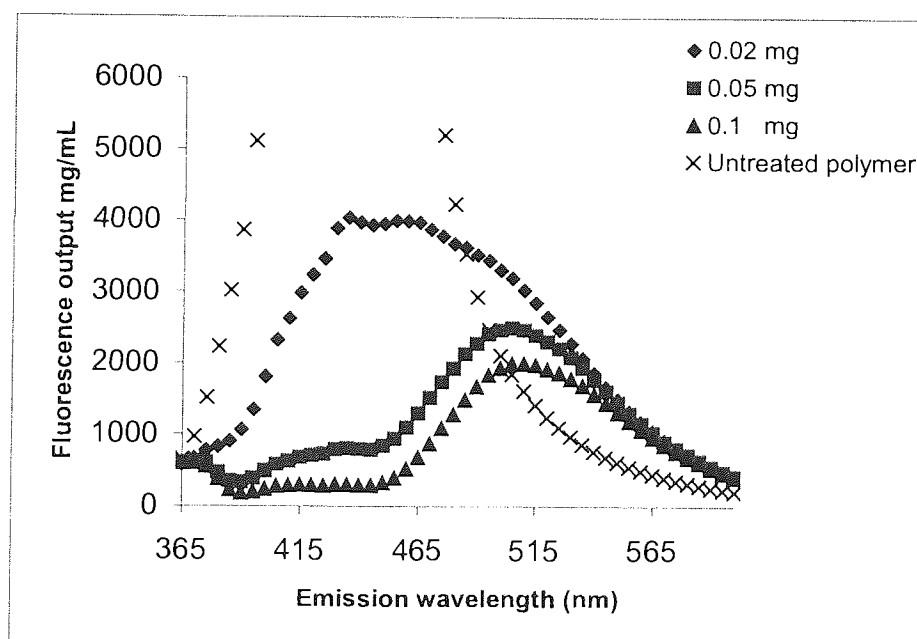


Figure **74f1**: Fluorescence spectra of co-octadecylacrylate-**108** with compound **116** (an expansion of **74f**) ($\lambda_{ex}$ = 340 nm).

From the data collected by using the two co-polymer films a **Table 10** has been devised that judges the test compounds either as a poor, moderate to good quenchers. Note that all the test compounds caused fluorescence quenching at various levels, but compound **113** (**Figure 69**) gave the best fluorescence quenching for both of the polymer films (**Figure 73d** and **74d**).

| Test substance | Fluorescence quenching ability | Fluorescence quenching ability order as derived from co-octadecylacrylate-**108** | Fluorescence quenching ability order as derived from co-styrene-**108** |
| --- | --- | --- | --- |
| **76** | Good | 2 | 3 |
| **78** | Good | 3 | 5 |
| **77** | Good | 6 | 6 |
| **113** | Good | 1 | 1 |
| **114** | Good | 4 | 2 |
| **116** | Good | 5 | 4 |

**Table 10:** Representing the fluorescence quenching ability order from 1 to 6, as collated by both of the co-polymers.

### 3.3.3.3 MIPs prepared using compound 108 as the fluorescent functional monomer

The 'empty' MIPs were re-exposed to their own templates and other test compounds at various concentrations of 0.1, 1.0, 5.0 mg/mL. Note that the concentration discussed for all MIPs created by compound **108** (**Figure 67**, 3.3.3) will be 5.0 mg/mL as the effects at this concentration are more pronounced. (Procedure 1-refer to 4.1)

### 3.3.3.3.1 MIP5 templated with compound 76
### 3.3.3.3.1.1 MIP5 tested with closely related set of relatively rigid polycyclic analogues

**MIP5** {5.4.9} exposed to its own template **76**, and its analogues **78** and **77** (**Figure 69**-structures, 3.3.3) all caused quenching of the MIP to various extents. The best fluorescence quenching however was demonstrated by **78**, which also exhibited a broad fluorescence emission spectrum (**Figure 75a**). The fluorescence quenching output at excitation/emission wavelength of 340/430 nm is presented in bar chart form in **Figure 75b**.

*Interpretation of* **MIP5** *results with the aid of solution based study* (Refer to section 3.3.3.1)
In the solution based study the test compounds **76**, **78** and **77** (**Figure 67**) exhibited background levels of fluorescence. Thus there is no contribution of fluorescence from these compounds towards the displayed fluorescence emission spectra presented in **Figure 75a**.

*Interpretation of* **MIP5** *results with the aid of co-polymer film based study* (Refer to section 3.3.3.2)
The peak that is observed at emission maximum of 530 nm in both co-polymer films for **76** (**Figure 73a** and **74a**) is not present in the MIP result (**Figure 75a**). The peak at emission maximum of 415 nm (**Figure**

**73a** and **74a**) for the films is however present in the MIP result, as expected since both the polymer film and the MIP contain the same fluorophore. As for compound **78** the fluorescence emission spectrum generated for the MIP (**Figure 75a**), has a similar spectrum shape as observed in the co-octadecylacrylate-**108** film spectrum for this particular test compound (**Figure 74b**). For compound **77** the fluorescence emission spectrum (**Figure 75a**) is not comparable to the observed spectra for the co-polymer films (**Figure 73c** and **74c**).

Overall from this co-polymer film study all the test compounds (**76**, **78** and **77**) exhibited good quenching ability. The MIP cavity however, accepted only compound **78** and rejected **76** and **77** (**Figure 75b**) that gave fluorescence outputs that were similar to the output of the untreated polymer.
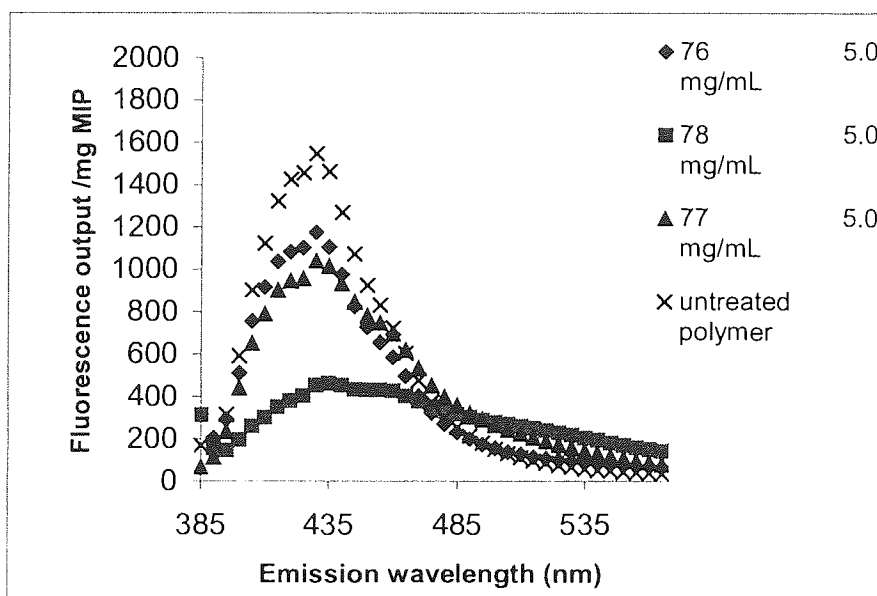


**Figure 75a**: Fluorescence spectra for **MIP5** in PEG. ($\lambda_{ex}$ = 340 nm).
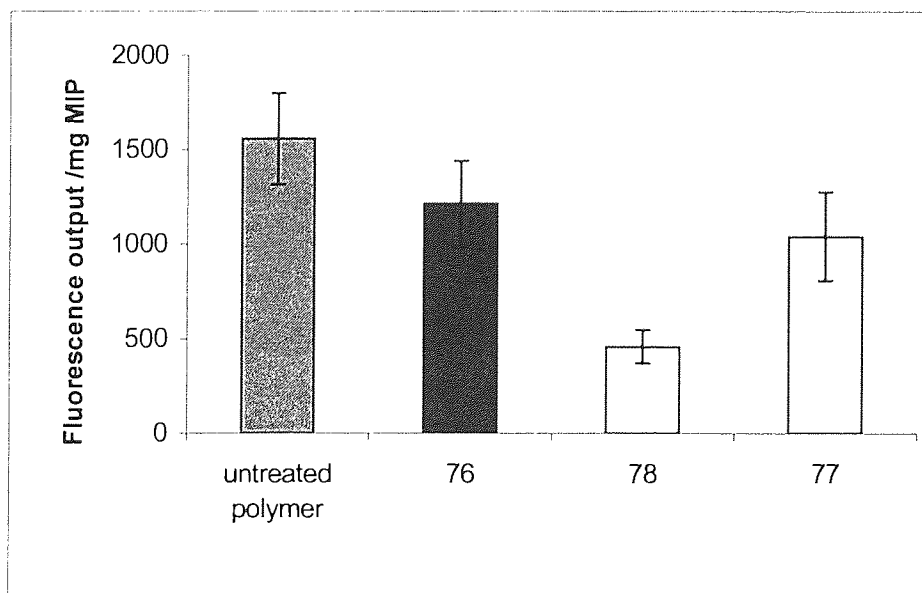


**Figure 75b**: Fluorescence output of **MIP5** in PEG. The error bars are the standard deviations of triplicate wells. $\lambda_{ex}$ = 340 nm, $\lambda_{em}$ = 430nm.

148

## 3.3.3.3.1.2 MIP5 tested with pyrene-based test compounds

The pyrene-based test compounds **113**, **114**, **115** and **116** exposed to the 'empty' **MIP5** all caused quenching (**Figure 69**-structures, 3.3.3). Compound **116** in contrast to the others quenched the fluorescence by a lesser amount (shown in **Figure 76**). No conclusive excimer fluorescence however was observed in this study. The fluorescence quenching output at excitation/emission wavelength of 340/430 nm is presented in bar chart form in **Figure 76b**.

*Interpretation of* **MIP5** *results with the aid of solution based study* (Refer to section 3.3.3.1)
In the study the pyrene-based test compound **113** displayed an emission maximum at 520 nm (**Figure 71**) and this feature is not present when exposing this to **MIP5** (**Figure 76a**). Compound **114** demonstrated an emission maximum at 460 nm (**Figure 71**) in its solution based study, and in **Figure 73a** for the **MIP5** this emission maximum is observed for this test compound. Thus no excimer has been formed for this test compound. Compound **115** in contrast does not contribute towards the observed fluorescence emission spectrum displayed in **MIP5**. As for compound **116** this gave an emission maximum at 500 nm and its fluorescence could possibly be a factor in what is observed for this in **MIP5**.

*Interpretation of* **MIP5** *results with the aid of co-polymer film based study* (Refer to section 3.3.3.2)
For compound **113** the peak observed in both the co-polymer film studies, at emission maximum of 540 nm (**Figure 73d** and **74d**), is not present in the MIP result (**Figure 73a**). For compound **114** that gave an emission maximum at 460 nm when exposed to the MIP (**Figure 73a**) resembles the emission maximum observed in the solution phase study and thus establishes that no excimer has formed (**Figure 71**). This can also be supported by the copolymer film studies that generated similar spectra for this compound (**Figure 73e** and **74e**). For compound **116** the emission spectra generated by the copolymer films (**Figure 73f** and **74f**) suggests fluorescence contribution at emission maximum of 500nm, as observed when exposing this test compound to the MIP (**Figure 76a**).

Overall from the co-polymer film study all the test compounds (**113**, **114** and **116**) exhibited good quenching ability. The MIP cavity accepted all the test compounds (**Figure 76b**).
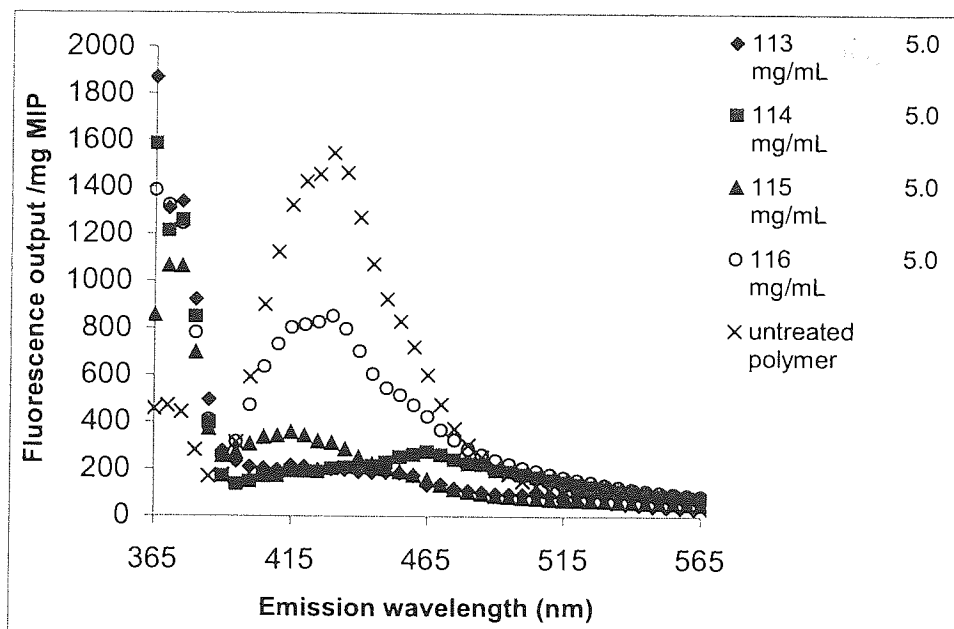
**Figure 76a**: Fluorescence spectra for **MIP5** in PEG. ($\lambda_{ex}$ = 340 nm).
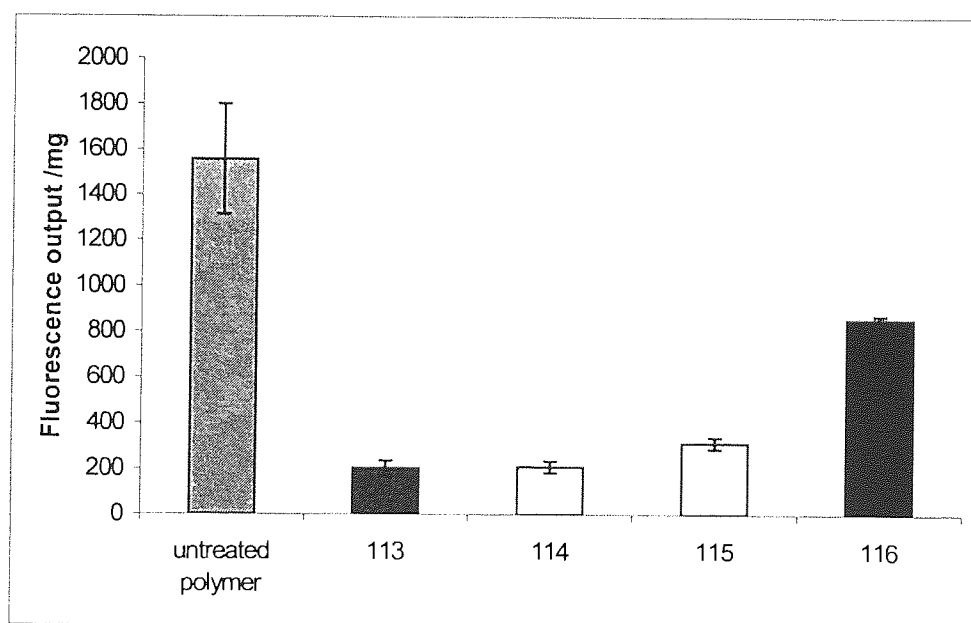


**Figure 76b**: Fluorescence output of **MIP5** in PEG. The error bars are the standard deviations of triplicate wells. $\lambda_{ex}$ = 340 nm, $\lambda_{em}$ = 430nm.

### 3.3.3.3.1.3 MIP5 tested with hydroxylated test compounds

The hydroxylated compounds **110**, **111** and **112** (**Figure 69**), similar to other test compounds caused fluorescence quenching of **MIP5** (**Figure 77a**). The fluorescence quenching output at excitation/emission wavelength of 340/430 nm is presented in bar chart form in **Figure 77b**.

*Interpretation of* **MIP5** *results with the aid of solution based study* (Refer to section 3.3.3.1)

The hydroxylated compounds **110**, **111** and **112** (**Figure 72**) in the solution based study exhibited background levels of fluorescence. Thus there is no contribution of fluorescence from these compounds towards the displayed emission spectra presented in **Figure 77a**.
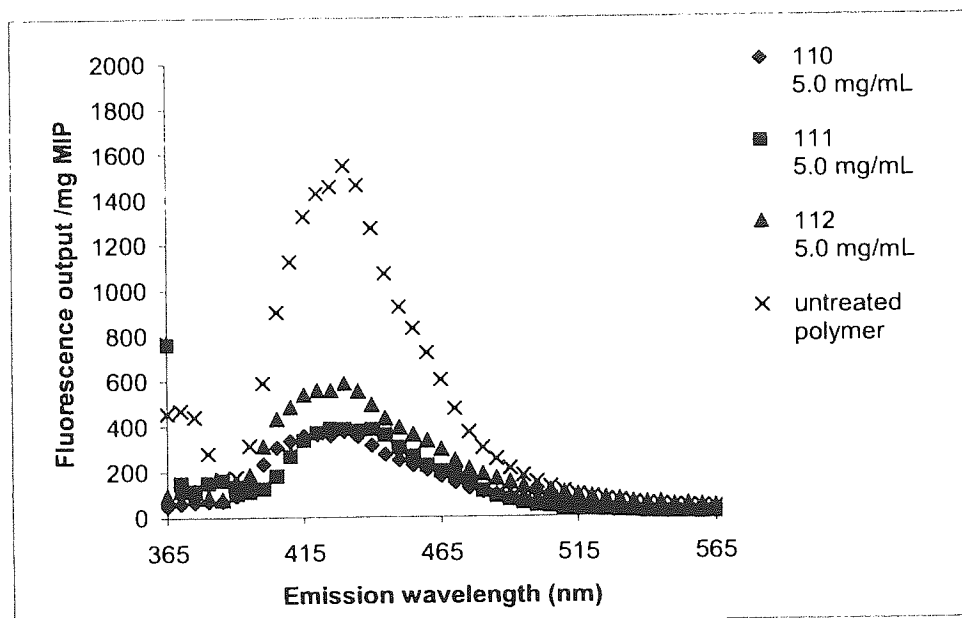


**Figure 77a**: Fluorescence spectra for **MIP5** in PEG. ($\lambda_{ex}$ = 340 nm).
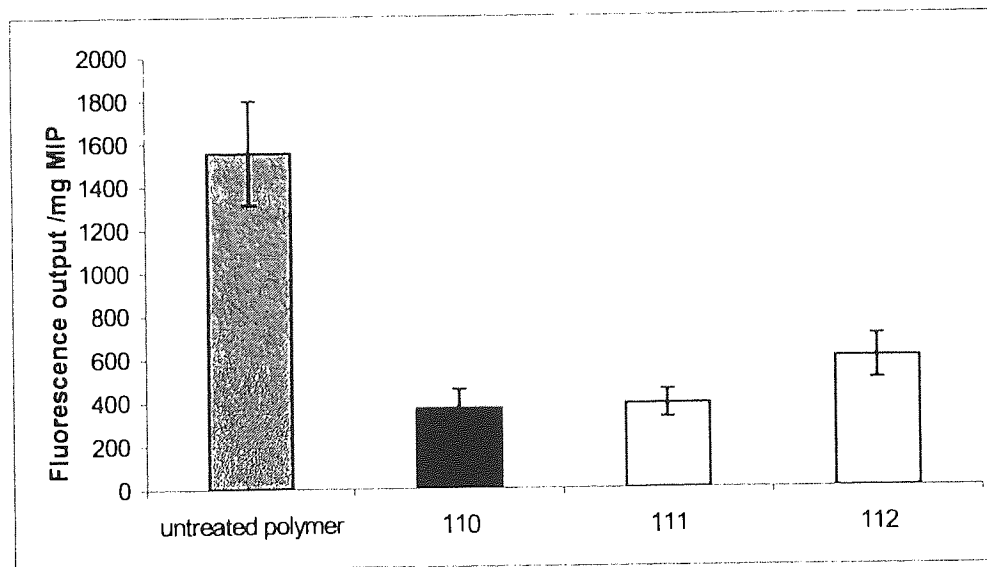


**Figure 77b**: Fluorescence output of **MIP5** in PEG. The error bars are the standard deviations of triplicate wells. $\lambda_{ex}$ = 340 nm, $\lambda_{em}$ = 430nm.

From the MIP results and the solution based study performed on these hydroxylated compounds suggests that the MIP cavity accepted these compounds.

### 3.3.3.3.2 MIP6 templated with compound 78

### 3.3.3.3.2.1 MIP6 tested with closely related set of relatively rigid polycyclic analogues

Similarly to **MIP5**, the 'empty' **MIP6** {5.4.10} was exposed to its own template **78** and its analogues **76** and **77** (**Figure 69**-structures, 3.3.3) at concentrations of 0.1, 1.0, 5.0 mg/mL. Although all the test compounds caused quenching, **MIP6** exposed to its own template, **78**, caused less quenching in comparison. In addition the other two test compounds exhibited broad fluorescence emission spectra (**Figure 78a**). The fluorescence quenching output at excitation/emission wavelength of 340/430 nm is presented in bar chart form in **Figure 78b**.

*Interpretation of* **MIP6** *results with the aid of solution based study* (Refer to section 3.3.3.1)
Due to the background levels of fluorescence exhibited by compounds **76**, **78** and **77** (**Figure 70**) the interpretation of the **MIP6** fluorescence emission results remains the same (**Figure 78a**). Therefore the broad fluorescence emission spectra presented by **76** and **77**, and the fluorescence emission spectrum revealed by **78** when exposed to the MIP, are characteristic of quenching of the polymer-bound fluorophore in the MIP by these compounds.

*Interpretation of* **MIP6** *results with the aid of co-polymer film based study* (Refer to section 3.3.3.2)
 The peak that is observed at emission maximum of 530 nm in both co-polymer films for **76** (**Figure 73a** and **74a**) is not present in the MIP result (**Figure 78a**). The peak at emission maximum of 415 nm (**Figure 73a** and **74a**) for the films is however present in the MIP result, as expected since both the polymer film and the MIP contain the same fluorophore. For compound **78** the spectrum generated when exposed to the MIP (**Figure 78a**) is similar to the spectrum observed for co-octadecylacrylate-108 (**Figure 77b**). For compound **77** the fluorescence emission spectrum generated when exposed to the MIP (**Figure 78a**) is not comparable to the observed spectra for the films (**Figure 73c** and **74c**).

Overall from the co-polymer films study all the test compounds (**76**, **78** and **77**) exhibited good quenching ability. The MIP cavity accepted all the compounds (**Figure 78b**).
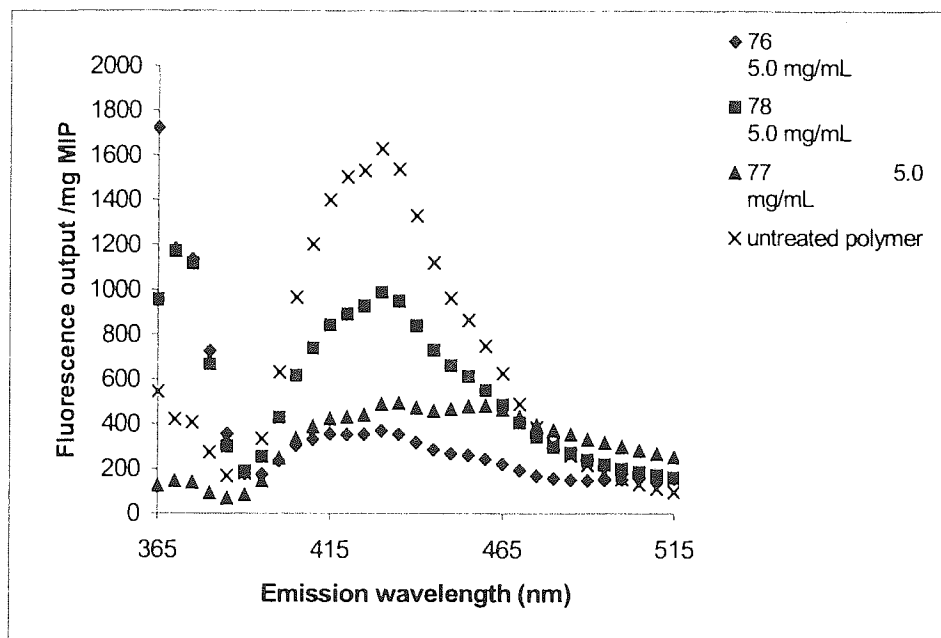
**Figure 78a**: Fluorescence spectra for **MIP6** in PEG. ($\lambda_{ex}$ = 340 nm).
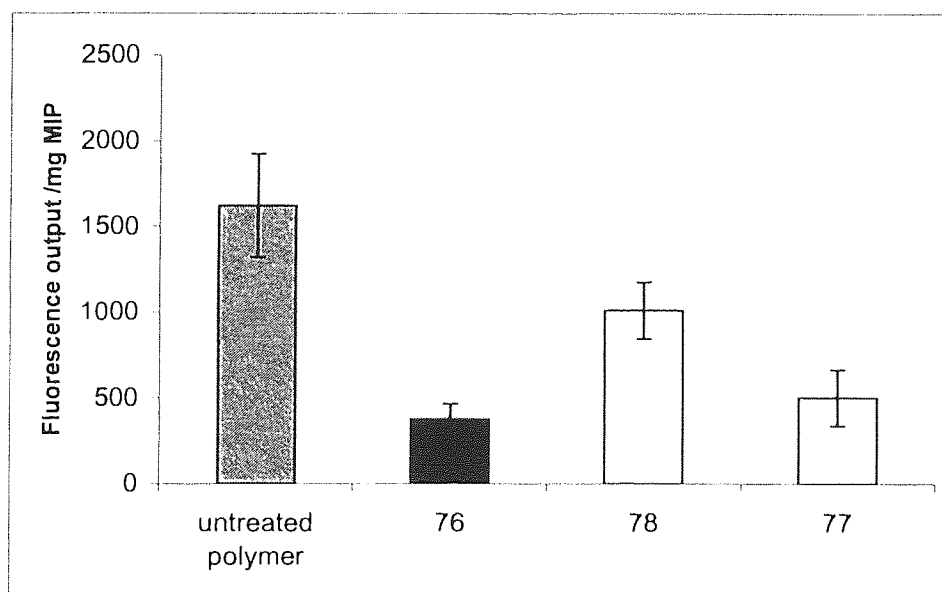


**Figure 78b**: Fluorescence output of **MIP6** in PEG. The error bars are the standard deviations of triplicate wells. $\lambda_{ex}$ = 340 nm, $\lambda_{em}$ = 430nm.

### 3.3.3.3.2.2 MIP6 tested with pyrene-based test compounds

The pyrene-based test compounds **113**, **114**, **115** and **116** (**Figure 69**- structures, 3.3.3) exposed to the 'empty' **MIP6** all caused fluorescence quenching. No conclusive excimer fluorescence however was observed in this study. The fluorescence quenching output at excitation/emission wavelength of 340/430 nm is presented in bar chart form in **Figure 79b**.

*Interpretation of* **MIP6** *results with the aid of solution based study* (Refer to section 3.3.3.1)

The pyrene-based test compound **113** displayed an optimum emission wavelength at 520 nm (**Figure 71**) and this fluorescence output is not present when exposed to the **MIP6** environment (**Figure 79a**). Therefore the emission spectrum presented by **113** shows quenching of the polymer-bound fluorophore in the MIP. Compound **114** demonstrated an emission maximum at 460 nm (**Figure 71**), which resembles the emission observed for this compound in the **MIP6**, of 465nm. As for compound **116** which exhibited a two-peak emission spectrum at 410 nm and 495 nm, the latter wavelength is due to test compound as from the solution phase fluorescence results the emission maximum is observed at 500 nm. Thus neither compounds **114** nor **116** have formed an excimer. Test compound **115** in the solution phase results gave an optimum emission wavelength at 395 nm and this is comparable to what is observed in the **MIP6** for this compound.

*Interpretation of* **MIP6** *results with the aid of co-polymer film based study* (Refer to section 3.3.3.2)

For compound **113** the peak observed at emission maximum of 540 nm (**Figure 73d** and **74d**) is not present in the MIP result (**Figure 79a**) for this test compound. As for compound **114** that gave an emission maximum at 460 nm in the MIP (**Figure 79a**) was not due to excimer formation as this was also observed in the solution phase study (**Figure 71**). In addition this can also be supported by the copolymer film studies that generated similar spectra for this compound (**Figure 73e** and **74e**). For compound **116** the emission spectra generated by the films (**Figure 73f** and **74f**) is similar to the spectrum observed when this compound is exposed to the MIP (**Figure 79a**).

Overall from the co-polymer film study all the test compounds (**113**, **114** and **116**) exhibited good quenching ability. The MIP cavity accepted all the test compounds (**Figure 79b**).
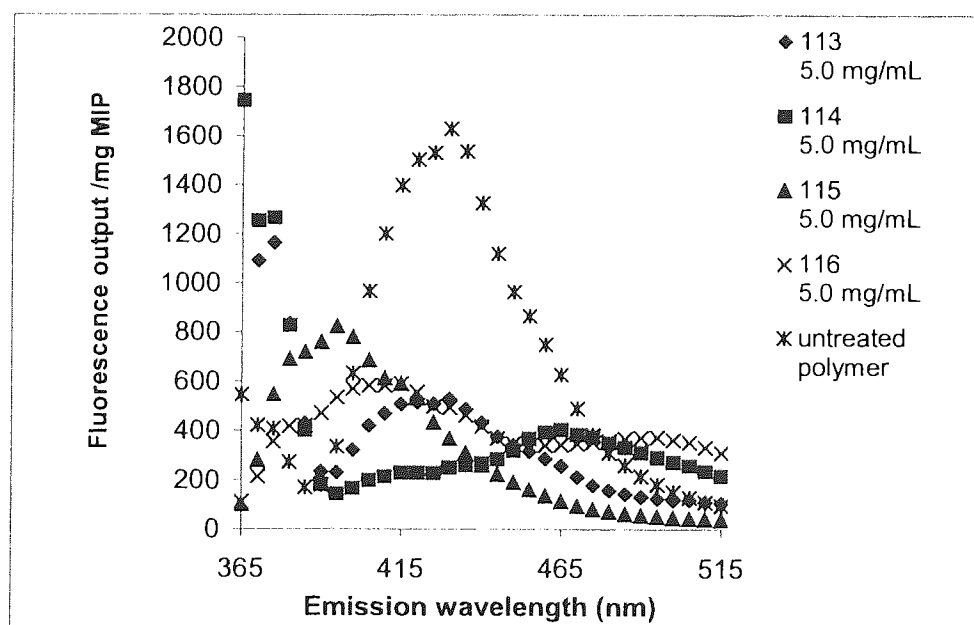


**Figure 79a**: Fluorescence spectra for **MIP6** in PEG. ($\lambda_{ex}$ = 340 nm).
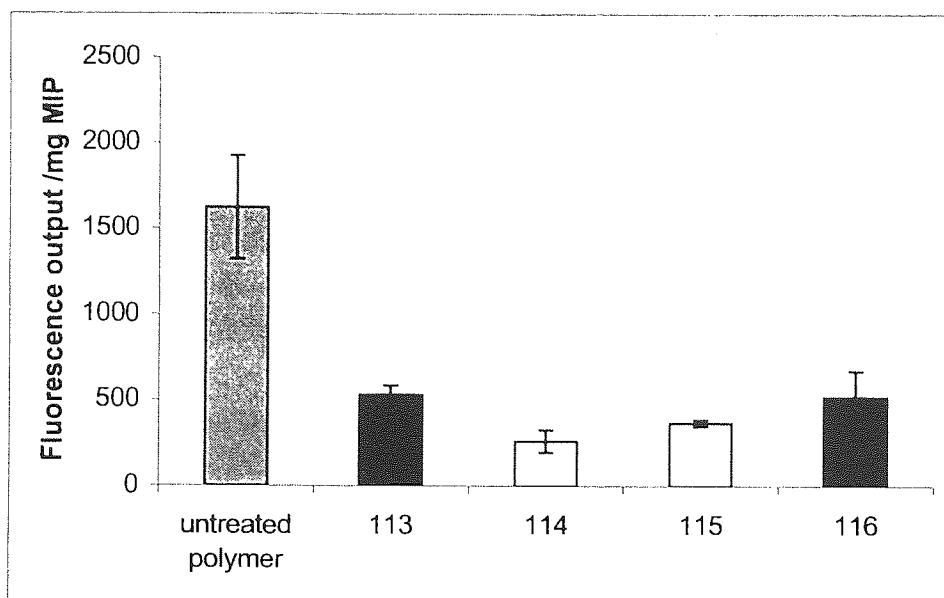
**Figure 79b**: Fluorescence output of the empty **MIP6** in PEG. The error bars are the standard deviations of triplicate wells. $\lambda_{ex}$ = 340 nm, $\lambda_{em}$ = 430nm..

### 3.3.3.3.2.3 MIP6 tested with hydroxylated test compounds

The hydroxylated compounds **110, 111** and **112** (**Figure 69**- structures, 3.3.3) similar to the other test compounds caused fluorescence quenching of **MIP6** (**Figure 80a**). The fluorescence quenching output at excitation/emission wavelength of 340/430 nm is presented in bar chart form in **Figure 80b**.

*Interpretation of* **MIP6** *results with the aid of solution based study* (Refer to section 3.3.3.1)
The solution phase fluorescence exhibited by the hydroxylated compounds **110, 111** and **112** was at background levels (**Figure 72**). Thus there is no contribution of fluorescence from these compounds towards the displayed fluorescence emission spectra presented in **Figure 80a**.

**Figure 80a**: Fluorescence spectra for **MIP6** in PEG. ($\lambda_{ex}$ = 340 nm).



**Figure 80b**: Fluorescence output of the empty **MIP6** in PEG. The error bars are the standard deviations of triplicate wells. $\lambda_{ex}$ = 340 nm, $\lambda_{em}$ = 430nm.

From the MIP results and the solution based study performed on these hydroxylated compounds suggests that the MIP cavity accepted these compounds.

### 3.3.3.3.3 MIP7 templated with compound 77

### 3.3.3.3.3.1 MIP7 tested with closely related set of relatively rigid polycyclic analogues

The 'empty' **MIP7** {5.4.11} was exposed to its own template **77** and its analogues **76** and **78** (**Figure 69**- structures, 3.3.3). All the test compounds caused fluorescence quenching. Most interestingly test compound **76** yielded an emission spectrum with shoulder at emission maximum of 455 nm and tailing off thereafter. This could possibly be due to excimer formation. Another interesting observation is that after exposure to its own template, **MIP7** afforded an emission peak that gave an emission maximum at 460 nm instead of 430 nm (the optimum emission wavelength of the 'empty' **MIP7**) and hence could be due to excimer formation (**Figure 81a**). The fluorescence quenching output at excitation/emission wavelength of 340/430 nm is presented in bar chart form in **Figure 81b** with the error bars.

*Interpretation of* **MIP7** *results with the aid of solution based study* (Refer to section 3.3.3.1)

Test compounds **76**, **78** and **77** (**Figure 70**) exhibited background levels of fluorescence in the solution based study. The interpretation of the MIP result observed for compound **77** remains the same, as the emission maximum at 460 nm is not present in the solution phase result for this compound. Therefore the spectrum presented by **77** could demonstrate an excimer formation (**Figure 81a**) and thus constitute evidence for the close proximity of the pyrene of the MIP fluorophore to that of the test compound **77**. The MIP result for compound **76** that revealed an emission spectrum with a shoulder at emission maximum of 455 nm could still possibly be due to excimer formation. Similarly to **77**, the close proximity of the anthracene moiety present on **76** with the pyrene on the polymer-bound fluorophore, **108**, may cause excimer formation.

*Interpretation of* **MIP7** *results with the aid of co-polymer film based study* (Refer to section 3.3.3.2)

The peak that is observed at emission maximum of 530 nm in both co-polymer films for **76** (**Figure 73a** and **74a**) could possibly have caused the shoulder that is observed at emission maximum of 455nm, in the MIP (**Figure 81a**). As for compound **78** the fluorescence emission spectrum generated when exposed to the MIP (**Figure 81a**) is similar to the spectrum observed in the co-octadecylacrylate-**108** film (**Figure 74b**). For compound **77** the emission spectrum observed after exposure to the MIP (**Figure 81a**) suggested excimer formation by giving an emission maximum at 460nm. The co-polymer films spectra for this test compound, however, revealed that no excimer has formed as at this particular emission wavelength fluorescence is observed (**Figure 73c** and **74c**).

Overall from the co-polymer films study all the test compounds (**76, 78** and **77**) exhibited good quenching ability. The MIP cavity accepted all the compounds but no excimer fluorescence was observed (**Figure 81b**).
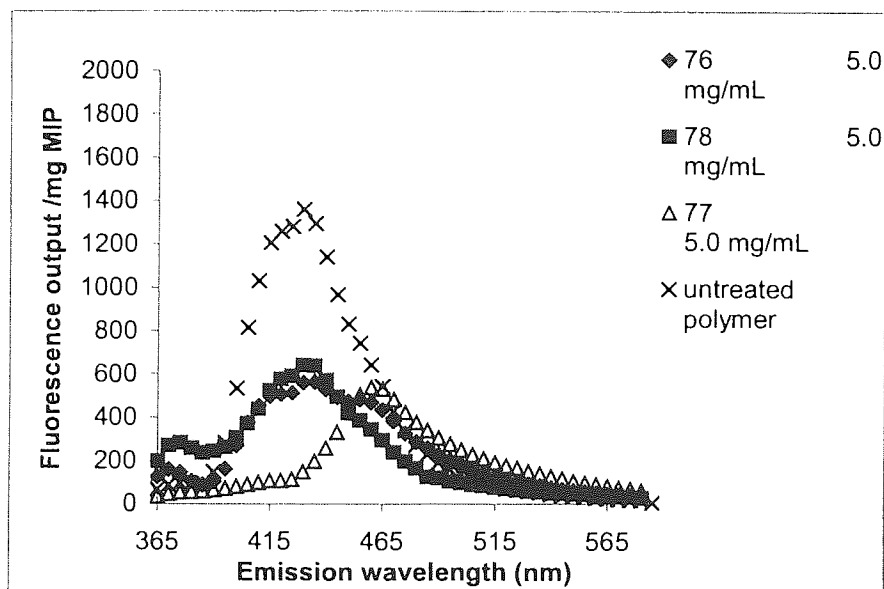
**Figure 81a**: Fluorescence spectra for **MIP7** in PEG. ($\lambda_{ex}$ = 340 nm).
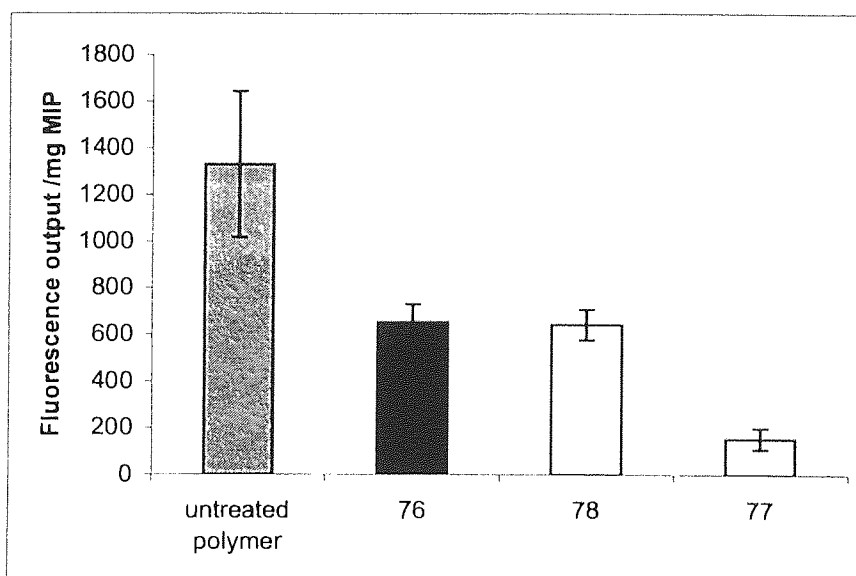


**Figure 81b**: Fluorescence output of the empty **MIP7** in PEG. The error bars are the standard deviations of triplicate wells. $\lambda_{ex}$ = 340 nm, $\lambda_{em}$ = 430nm.

### 3.3.3.3.3.2 MIP7 tested with pyrene-based test compounds

The pyrene-based test compounds **113**, **114**, **115** and **116** (**Figure 69**-structures, 3.3.3) exposed to the 'empty' **MIP7** all caused fluorescence quenching, except for test compound **115** that gave a similar fluorescence output as the untreated polymer i.e. 'empty' **MIP7**. The fluorescence quenching output at excitation/emission wavelength of 340/430 nm is presented in bar chart form in **Figure 82b** with the error bars.

*Interpretation of* **MIP7** *results with the aid of solution based study* (Refer to section 3.3.3.1)

The pyrene-based test compound **113** in **MIP7** demonstrated a two-peak emission spectrum with maxima at 415 nm and 485 nm. The latter wavelength is due to the fluorescence of the actual test compound (**Figure 71**) therefore no excimer has been formed. For compound **114** this afforded a broad emission spectrum with a maximum at 465 nm when exposed to the MIP. This is the same wavelength as that determined by solution phase study and thus the fluorescence output measured has the contribution of the test compound. For compound **115** in the solution phase study background levels of fluorescence was observed. This suggests that the compound is not contributing towards the MIP result that reveals no fluorescence change. Compound **116** in the MIP gave an optimum emission wavelength at 510 nm and this is similar to that determined by the solution phase study, and thus no excimer has formed (**Figure 82a**).

*Interpretation of* **MIP7** *results with the aid of co-polymer film based study* (Refer to section 3.3.3.2)

Compound **113** exhibited a two-peak emission spectrum with maxima at 415 nm and 485 nm in the MIP (**Figure 82a**), and this is similar to the spectra generated by the co-polymer films for this compound (**Figure 73d** and **74d**). Therefore this data supports the suggestion made by the solution phase study that this compound forms no excimer. For compound **114** that gave emission maximum at 465 nm in the MIP (**Figure 82a**), the same wavelength was determined by solution phase study and thus the fluorescence output measured had the contribution of the test compound. This can also be supported by the copolymer film studies that generated similar spectra for this compound (**Figure 73e** and **74e**) that revealed fluorescence contribution at this wavelength. For compound **116** the emission spectra generated by the films (**Figure 73f** and **74f**) is similar to the spectrum presented when exposed to the MIP (**Figure 82a**) and thus suggests no excimer formation, as was suggested by the MIP result.

Overall from the co-polymer film study all the test compounds (**113**, **114** and **116**) exhibited good quenching ability. The MIP cavity accepted test compounds **113**, **114** and **116** (**Figure 82b**). As for compound **115**, the MIP result together with the solution-based study performed on this compound suggests that the MIP cavity rejected this compound.
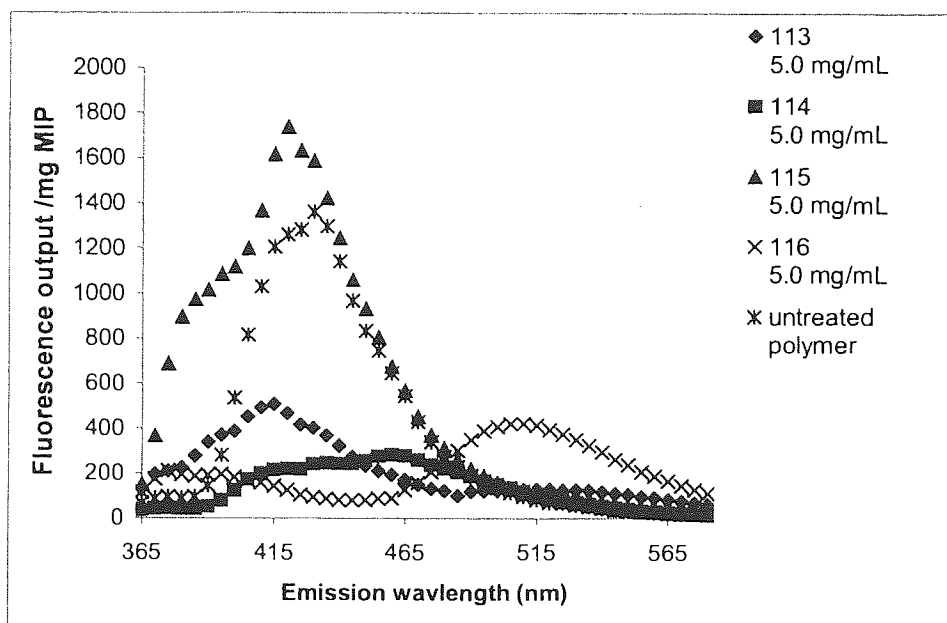
**Figure 82a**: Fluorescence spectra for **MIP7** in PEG. ($\lambda_{ex}$ = 340 nm).
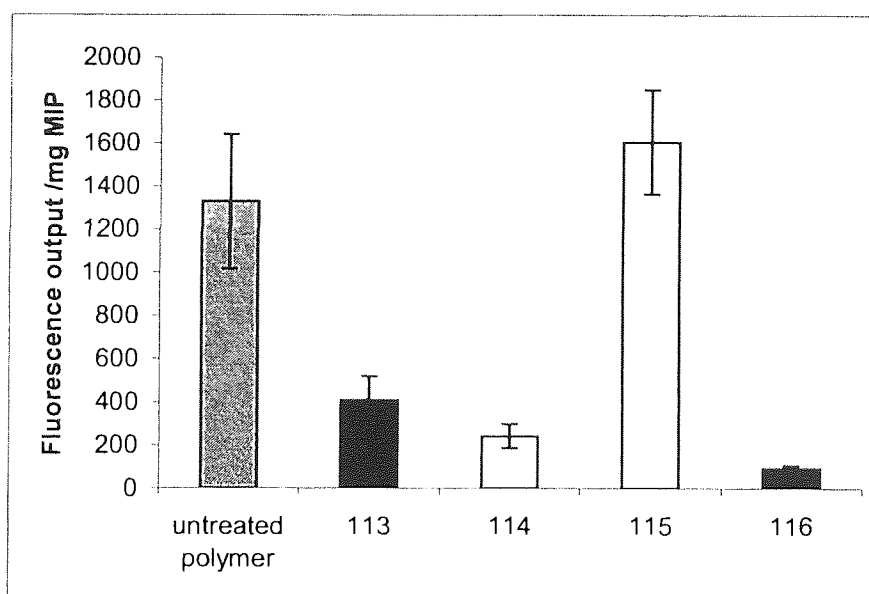


**Figure 82b**: Fluorescence output of the empty **MIP7** in PEG. The error bars are the standard deviations of triplicate wells. $\lambda_{ex}$ = 340 nm, $\lambda_{em}$ = 430nm.

### 3.3.3.3.3 MIP7 tested with hydroxylated test compounds

The hydroxylated compounds **110**, **111** and **112** (**Figure 69**-structures, 3.3.3) all caused fluorescence quenching of **MIP7**. Test compounds **110** and **111** gave optimum emission wavelength at 405nm. In contrast test compound **112** emitted at wavelength of 430 nm which is similar to the 'empty' **MIP7** (**Figure 83a**) emission wavelength. The fluorescence quenching output at excitation/emission wavelength of 340/430 nm is presented in bar chart form in **Figure 83b** with the error bars.

*Interpretation of* **MIP7** *results with the aid of solution based study* (Refer to section 3.3.3.1)

The hydroxylated compounds **110**, **111** and **112** (**Figure 72**) exhibited background levels of fluorescence. Thus there is no contribution of fluorescence from these compounds towards the displayed emission spectra presented in **Figure 83a**.
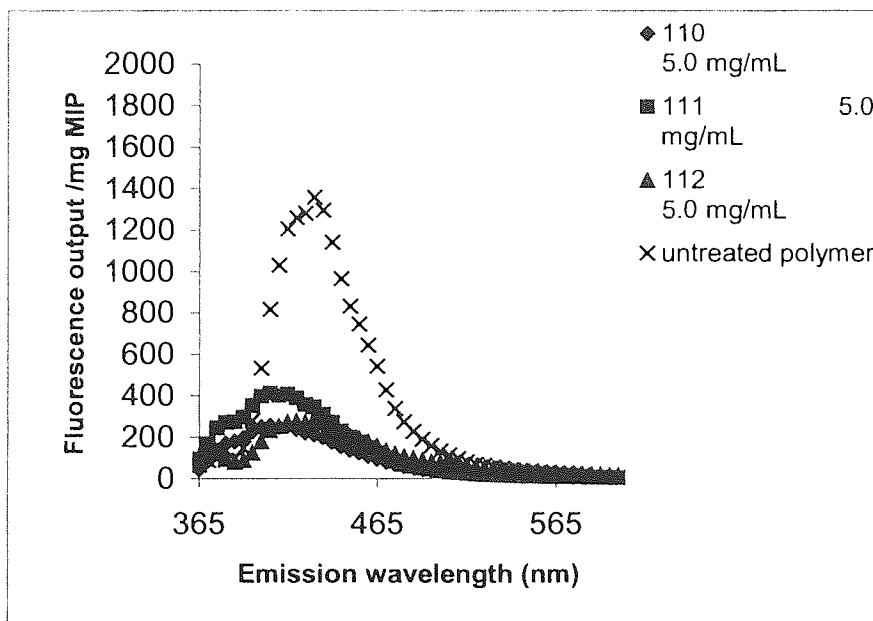


**Figure 83a**: Fluorescence spectra for **MIP7** in PEG. ($\lambda_{ex}$ = 340 nm).
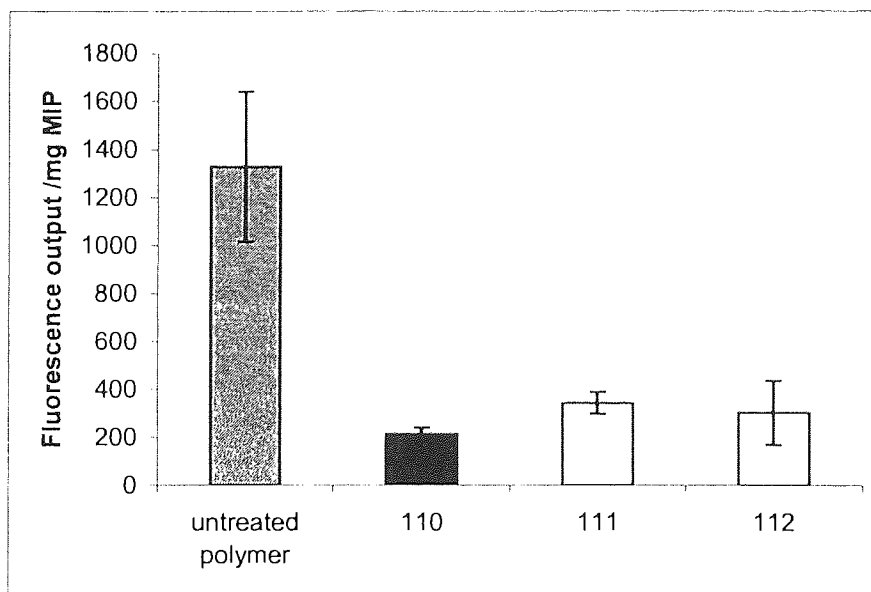


**Figure 83b**: Fluorescence output of the empty **MIP7** in PEG. The error bars are the standard deviations of triplicate wells. $\lambda_{ex}$ = 340 nm, $\lambda_{em}$ = 430nm.

From the MIP results and the solution based study performed on these hydroxylated compounds suggests that the MIP cavity accepted these compounds.

### 3.3.4 Imprinted polymers derived from a single-fluorophore functional monomer containing pyrenes
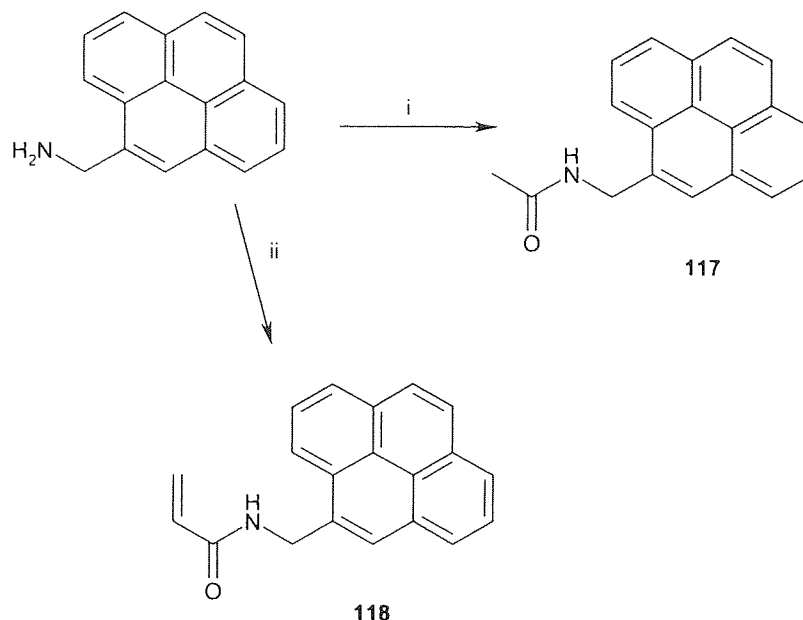


i triethylamine/THF/ acetyl chloride ii triethylamine/THF/ acryloyl chloride

**Scheme 4:** Preparation of pyrene-based single fluorophore functional monomer.

As an extension to work detailed on a methyl hydrazine based scaffold that employed compound **108** (**Figure 67**-structure of this compound, 3.3.3) to form a conjugated pyrene system, a non-conjugated pyrene system was investigated. Note that the conjugation is in the N-(2-formyl-phenyl)-acetamide moiety part. It is proposed that without the conjugation by employing compound **118** {5.3.30} as a FFM (**Scheme 4**), such a study would allow further assessment of the ability of the pyrene moiety in a MIP to form an excimer. Note that this non-conjugated pyrene system acts as a single fluorophore i.e. a subunit of the dual fluorophore and it is proposed that by studying this unit that a further fluorophore could be incorporated. This would be made possible by the fact that the pyrene moiety fluorescence behaviour would be assessed individually and then by incorporating another fluorophore further examination on how this alters the behaviour of this fluorophore could be made

As a prelude to this the fluorescence characteristics of the fluorophore were studied by recourse to solution phase observations of the non-polymerisable model compound **117** {5.3.29}.

The non-conjugated system was prepared by reacting 1-pyrenemethylamine with acetyl chloride to synthesise compound **117** (**Scheme 4**). To establish whether an excimer can be formed a study was performed on the non-polymerisable, acetate compound **117** in solution. This study would also determine the parameters to be used to analyse the MIPs synthesised using the polymerisable version of compound **117**, compound **118** (Procedure 4 refer to 4.4).

The study successfully demonstrated that at lower concentrations i.e. between the 0.003125 to 0.1563 mg/mL in PEG, the monomer optimum emission wavelength was observed at 390 nm and was seen as a gradual increase in fluorescence output. From the test compound content of 0.1563 mg/mL in PEG, a decline in the fluorescence count was observed, hence lower levels of monomer. At higher concentration levels an extra emission maximum at 470 nm began to appear with the fluorescence output increasing gradually, indicating excimer formation

**Figure 84** presents the monomer and excimer formation in a graphical manner with lowest, moderate and highest concentrations. **Figure 85** presents the result for both of the specific emission wavelengths of 390 nm (monomer emission) and 470 nm (excimer emission) as bar charts for the concentration range used to establish excimer formation.
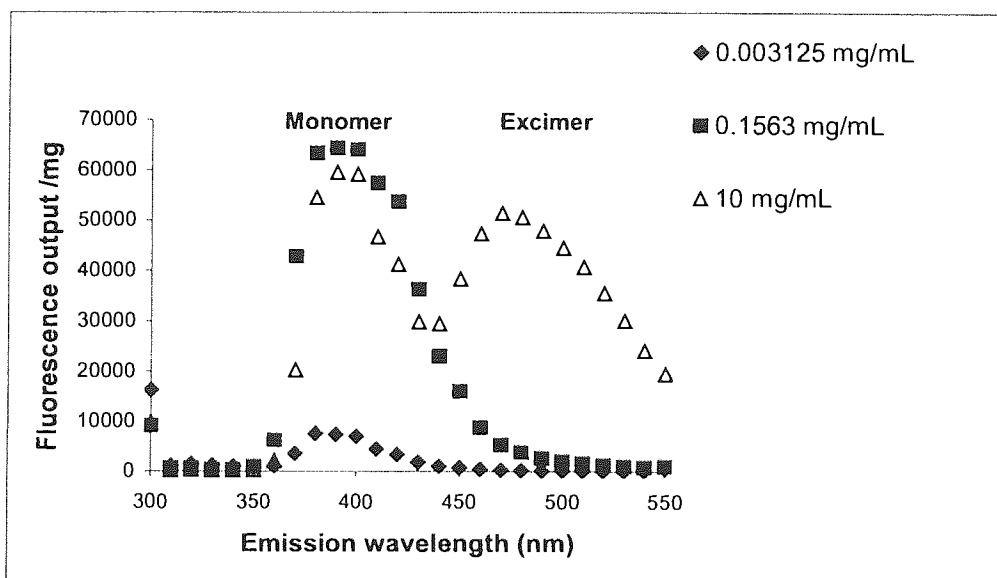


**Figure 84**: Fluorescence spectra for compound **117** in PEG. The emission wavelength of 390 nm (monomer) and 470 nm (excimer). ($\lambda_{ex}$ = 290 nm).
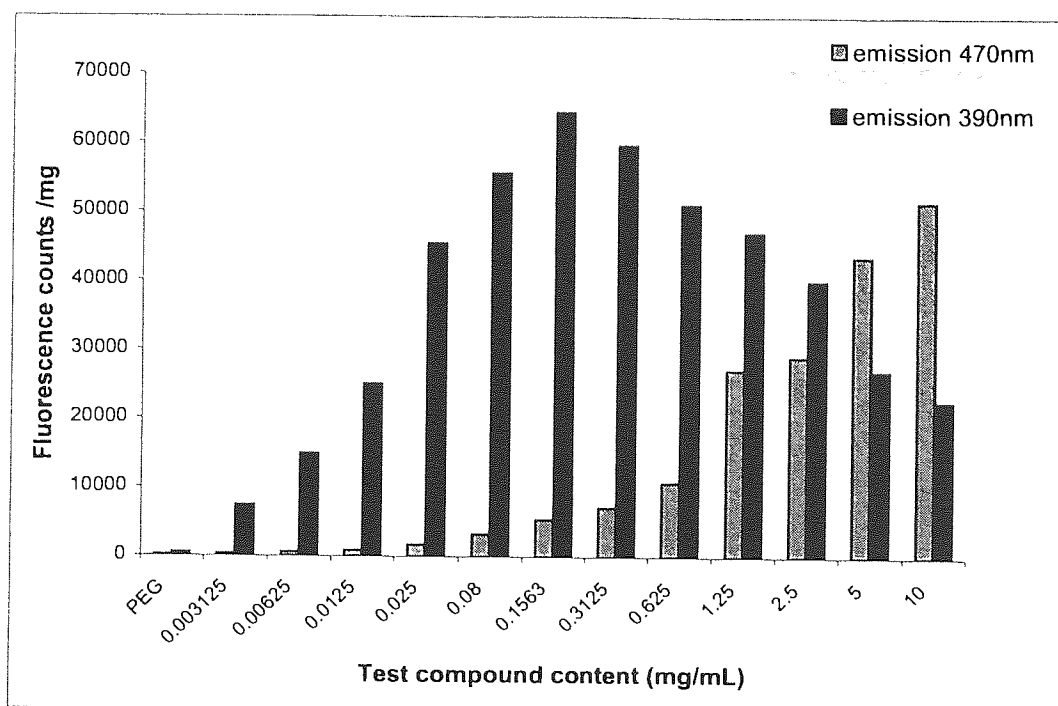
**Figure 85**: Fluorescence output of compound **117** In PEG. The error bars are the standard deviations of duplicate wells, at $\lambda_{ex}$ = 290 nm for both emissions at $\lambda_{em}$ = 390 nm (monomer) and $\lambda_{em}$ = 470 nm(excimer).

### 3.3.4.1 MIPs prepared using compound 118 as the fluorescent functional monomer

A series of MIPs was constructed with the fluorescent functional monomer **118** such that the MIP cavities would exhibit binding-dependant fluorescence and possibly with the alignment of two pyrenes in a MIP may produce an excimer as was proposed in the study based on compound **117**. Compounds **76** {5.3.2}, **78** {5.3.4} and **77** {5.3.3} (**Figure 69**-structures, 3.3.3) were used as templates and the polymer was cross-linked with triethyleneglycol dimethacrylate (TEGDMA). These three MIPs were subjected to the same procedures as mentioned earlier for MIP preparation to derive the imprinted polymers free of their templates. Then the empty MIPs were re-exposed to their templates and test compounds at concentrations of 0.1, 1.0, 5.0 mg/mL, collected by filtration and analysed by fluorescence. The optimum excitation wavelength of 290 nm and maximum fluorescence emission wavelength of 390 nm (monomer) and 470 nm (excimer) were the parameters used to analyse the three MIPs. These parameters were determined earlier by carrying out a study on the stable version (non-polymerisable) of compound **117**.

Note that the concentration discussed to demonstrate whether an excimer has been formed, for all the MIPs created by compound **118** will be at 5.0 mg/mL as the effects at this concentration are more pronounced. (Procedure 1 refer to 4.1)

164

### 3.3.4.1.1 MIP8 templated with compound 76

### 3.3.4.1.1.1 MIP8 tested with closely related set of relatively rigid polycyclic analogues

MIP8 {5.4.12} was exposed to its own template 76 and its analogues 78 and 77 (**Figure 69**-structures, 3.3.3). Some additional fluorescence output produced by 78 and 77 in comparison to the output of each compound in the solution based study indicates excimer formation (**Figure 86**). Compound 76 typically presented an emission spectrum that demonstrated the quenching of the polymer-bound fluorophore in the MIP.

*Interpretation of* **MIP8** *results with the aid of solution based study* (Refer to section 3.3.3.1)
In the solution based study the test compounds 76, 78 and 77 (**Figure 70**) exhibited background levels of fluorescence. Thus there is no contribution of fluorescence from these compounds towards the displayed fluorescence emission spectra presented in **Figure 86**.

The MIP cavity accepted all the test compounds (**Figure 86**) but no conclusive excimer fluorescence was observed.
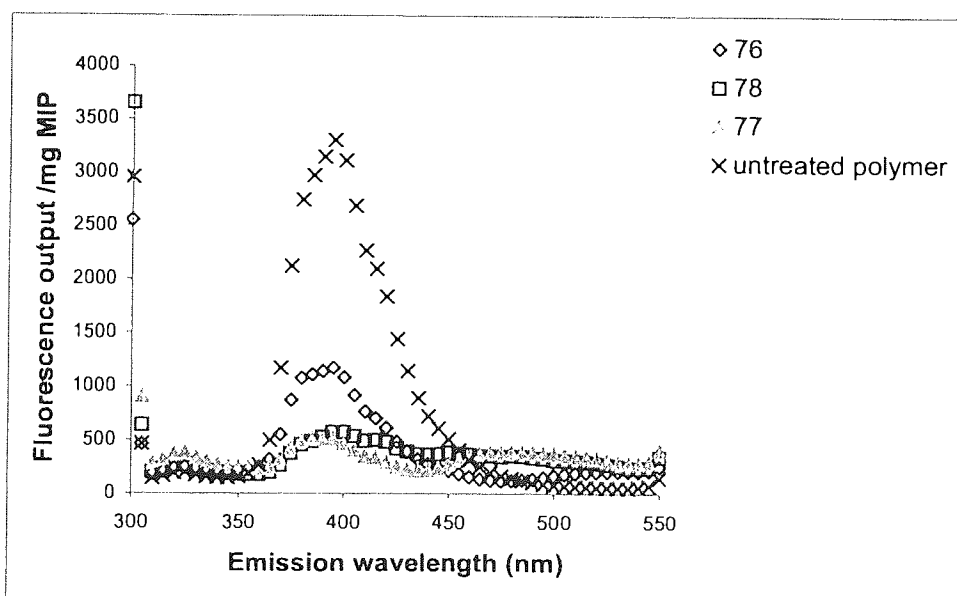


**Figure 86**: Fluorescence spectra for **MIP8** in PEG. ($\lambda_{ex}$ = 290 nm).

### 3.3.4.1.1.2 MIP8 tested with pyrene-based test compounds

The pyrene-based test compounds 113 {5.3.25}, 114 {5.3.26}, 115 {5.3.27} and 116 {5.3.28} (**Figure 69**-structures, 3.3.3) exposed to the 'empty' **MIP8** all caused quenching. No conclusive excimer fluorescence however was observed in this study.

*Interpretation of* **MIP8** *results with the aid of solution based study* (Refer to section 3.3.3.1)
Compound 113 displayed a fluorescence emission maximum at 520 nm in the solution phase study (**Figure 71**) and this feature is not present when exposing this to the MIP (**Figure 87**). Compound 114

gave a two-peak emission spectrum at maximum of 395 and 465 nm. The former emission maxima at 395 nm presents a straightforward quenching of the MIP-bound fluorophore. The latter emission maximum at 465 nm is characteristic of the test compound itself as determined by solution phase study (**Figure 71**). Compound **115** as determined by the solution phase study (**Figure 71**) does not contribute towards the fluorescence emission spectrum displayed when exposed to the MIP (**Figure 87**). As for compound **116** this gave an optimum emission wavelength at 500 nm in the solution phase study (**Figure 71**) and its fluorescence is a factor in what is being observed for this when exposed to the MIP (**Figure 87**). The MIP cavity accepted all the test compounds (**Figure 87**).
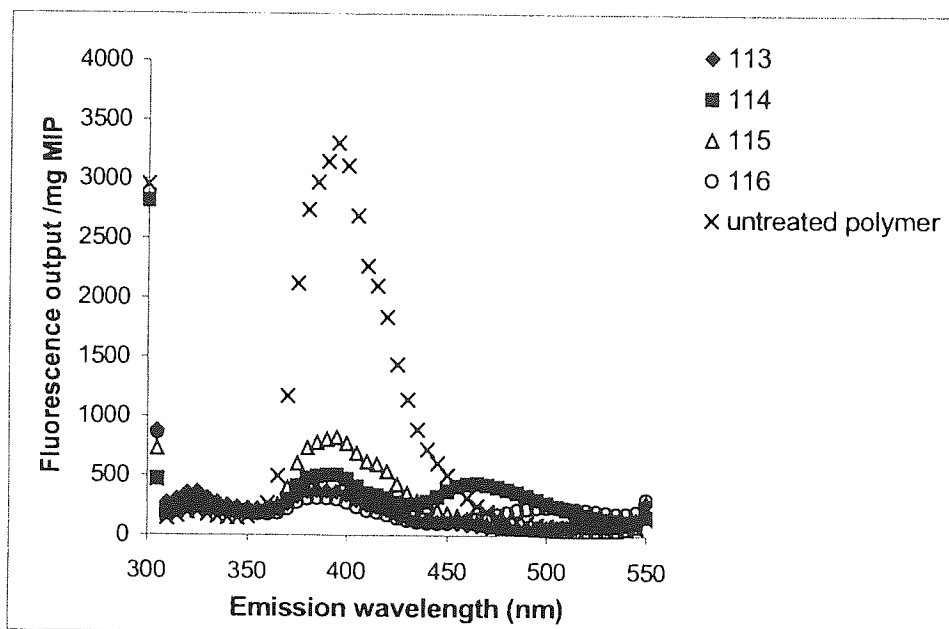


**Figure 87**: Fluorescence spectra for **MIP8** in PEG.($\lambda_{ex}$ = 290 nm).

### 3.3.4.1.1.3 MIP8 tested with hydroxylated test compounds

*Interpretation of* **MIP8** *results with the aid of solution based study* (Refer to section 3.3.3.1)

The hydroxylated compounds **110** {5.3.22}, **111** {5.3.23} and **112** {5.3.24} (**Figure 69**-structures, 3.3.3) as can be seen from **Figure 72** exhibited background levels of fluorescence. Thus there is no contribution of fluorescence from these compounds towards the displayed emission spectra presented in **Figure 88**. The spectra presented in **Figure 88** resulted from straightforward quenching of the MIP-bound fluorophore.
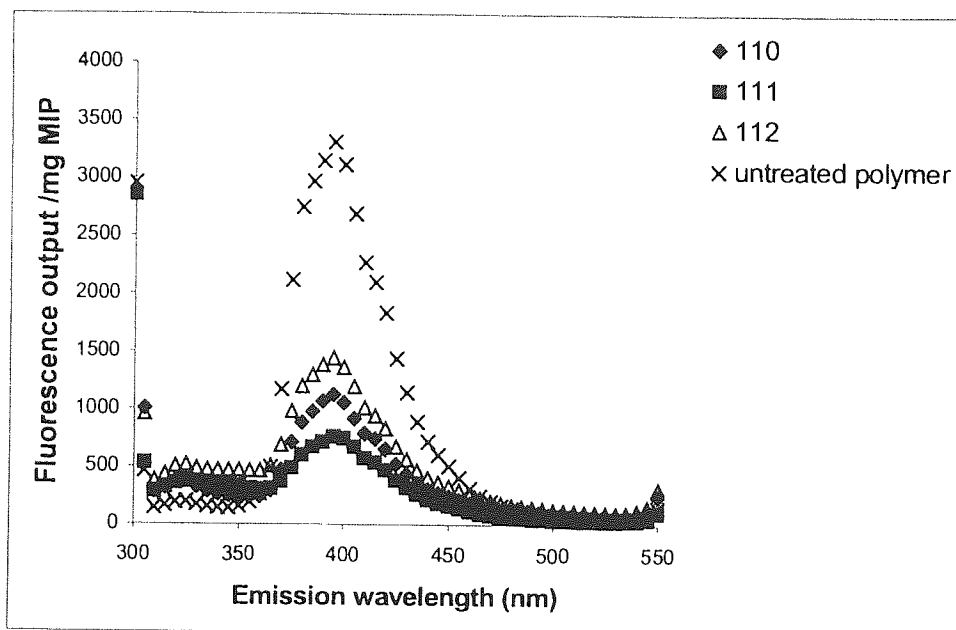
**Figure 88**: Fluorescence spectra for **MIP8** in PEG. ($\lambda_{ex}$ = 290 nm).

From the MIP results and the solution based study performed on these hydroxylated compounds suggests that the MIP cavity accepted these compounds.

### 3.3.4.1.2 MIP9templated with compound 78

#### 3.3.4.1.2.1 MIP9 tested with closely related set of relatively rigid polycyclic analogues

MIP9 {5.4.13} was exposed its own template **78** and its analogues **76** {5.3.2}, **78** {5.3.4} and **77** {5.3.3} (**Figure 69**-structures, 3.3.3), and no excimer-derived fluorescence were observed for these compounds (**Figure 89**). All of the compounds however did quench the fluorescence of the MIP-bound fluorophore.

*Interpretation of* **MIP9** *results with the aid of solution based study* (Refer to section 3.3.3.1)

Compounds **76** and **78** typically presented fluorescence emission spectra that demonstrated straightforward quenching of the fluorescence of the MIP-bound fluorophore, and neither compound contributed towards the observed fluorescence spectra displayed for this MIP. This was determined by the solution phase study performed on these compounds (**Figure 70**). Compound **77** gave a two-peak fluorescence emission spectrum at maxima of 390 and 485 nm. The emission maximum at 390 nm represents the straightforward quenching of the fluorescence of the MIP-bound fluorophore. The second emission maximum at 485 nm could be characteristic of the formation of an excimer as the test compound exhibited background levels of fluorescence in the solution phase study (**Figure 70**). The emission maximum at 485 nm could be evident of the close proximity of the pyrenes coming from the MIP-bound fluorophore and the test compound **77** (**Figure 90**).

The MIP cavity accepted all the test compounds (**Figure 89**) but no conclusive excimer fluorescence was observed.
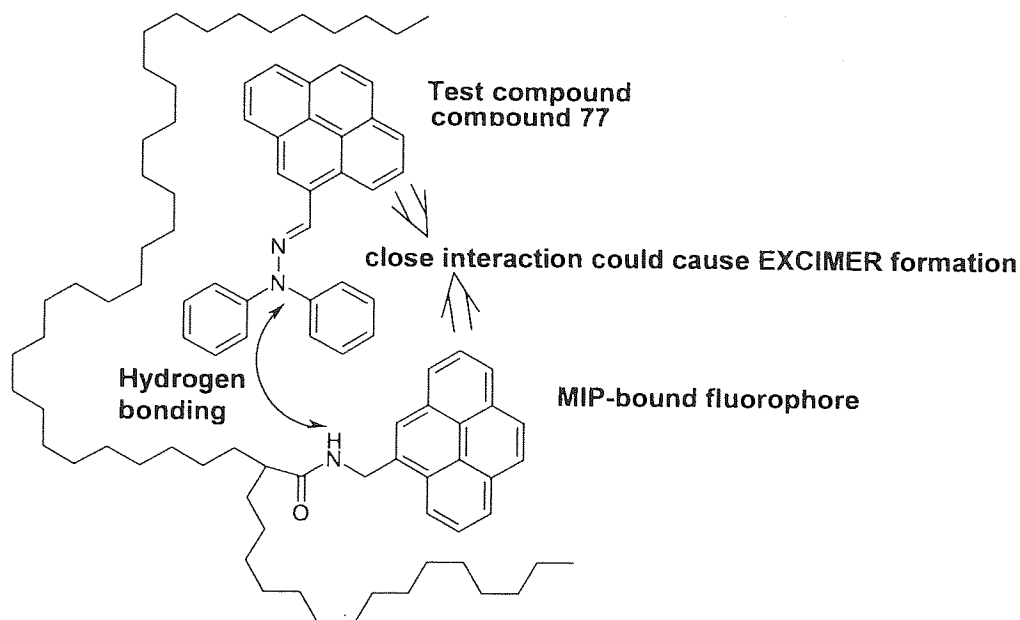
**Figure 90**: Illustrates the manner in which excimer formation might occur between the MIP-fluorophore bound and test compound, **77**.
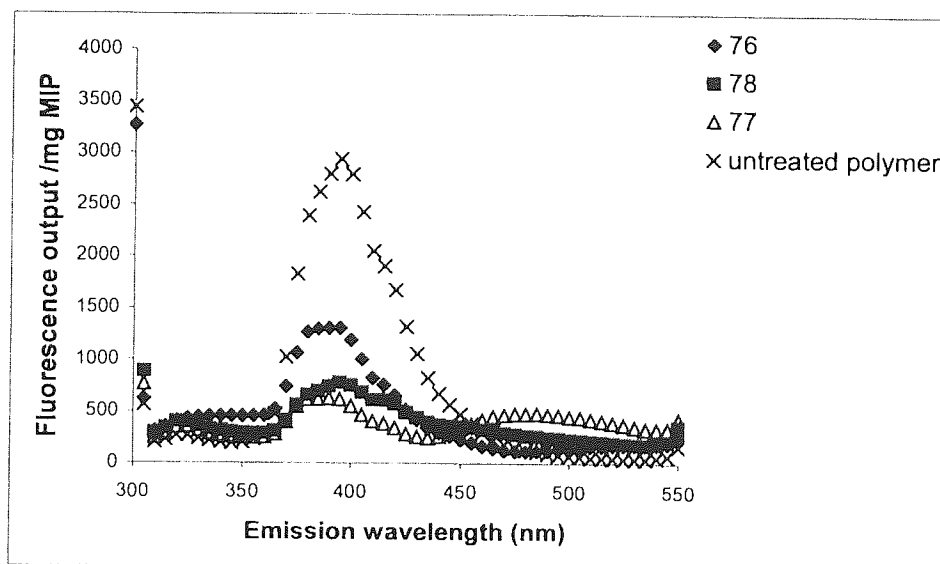


**Figure 89**: Fluorescence spectra for **MIP9** in PEG. ($\lambda_{ex}$ = 290 nm).

### 3.3.4.1.2.2 MIP9 tested with pyrene-based test compounds

The MIP-bound fluorophore exposed to the pyrene-based test compounds **113** {5.3.25}, **114** {5.3.26}, **115** {5.3.27} and **116** {5.3.28} (**Figure 69**-structures, 3.3.3) all caused quenching, but did not form an excimer.

*Interpretation of* **MIP9** *results with the aid of solution based study* (Refer to section 3.3.3.1)

Compound **113** displayed a fluorescence emission maximum at 520 nm in the solution phase based study (**Figure 70**) and this feature is not present when exposing this to the MIP (**Figure 91**). The fluorescence emission spectrum produced by **113** reflects a straightforward quenching of the fluorescence of the MIP-bound fluorophore. Compound **114** gave two-peak emission spectrum (**Figure 91**). The first emission maximum is at 395 nm and presents a straightforward quenching of the fluorescence of the MIP-bound fluorophore. The second emission maximum at 465 nm as determined by solution phase study is characteristic of the test compound itself (**Figure 70**). Compound **115** as determined by solution phase study (**Figure 70**) does not contribute towards the observed fluorescence emission spectrum generated when exposing to the MIP (**Figure 91**). Instead the spectrum produced by this test compound reflects a straightforward quenching of the fluorescence of the MIP-bound fluorophore. As for compound **116** this gave an fluorescence emission maximum at 500 nm in the solution phase study (**Figure 70**) and its fluorescence is a factor in what is being observed in the second emission maximum at 500 nm when exposed to the MIP. The first emission maximum at 395 nm is however due to the straightforward quenching of the fluorescence of the MIP-bound fluorophore (**Figure 91**). The MIP cavity accepted all the test compounds (**Figure 91**).
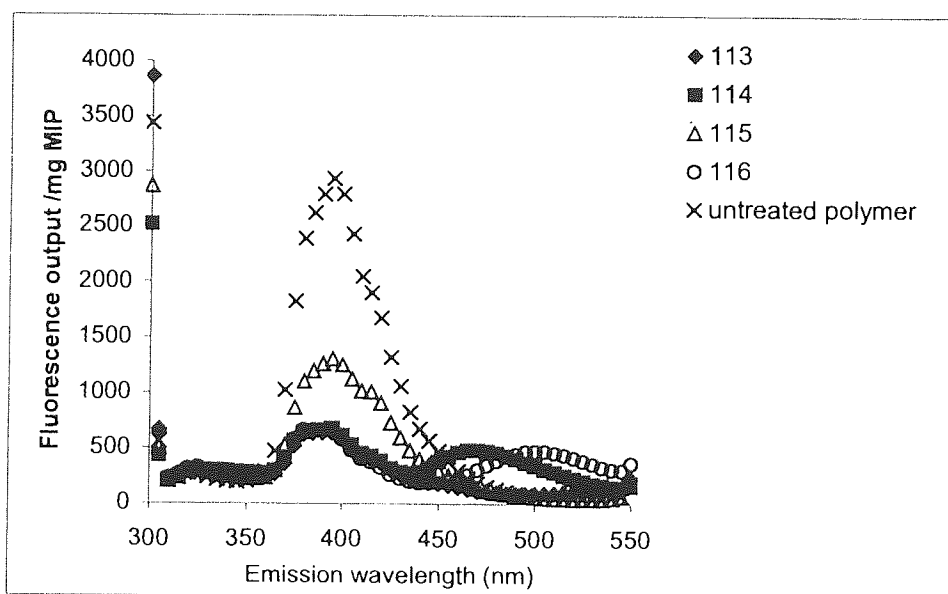


**Figure 91**: Fluorescence spectra for **MIP9** in PEG. ($\lambda_{ex}$ = 290 nm).

### 3.3.4.1.2.3 MIP9 tested with hydroxylated test compounds

*Interpretation of* **MIP9** *results with the aid of solution based study* (Refer to section 3.3.3.1)

The hydroxylated compounds **110** {5.3.22}, **111** {5.3.23} and **112** {5.3.24} (**Figure 69**-structures, 3.3.3), as can be seen from **Figure 72** exhibited background levels of fluorescence. Thus there is no contribution of fluorescence from these compounds towards the displayed fluorescence emission spectra presented in **Figure 92**.
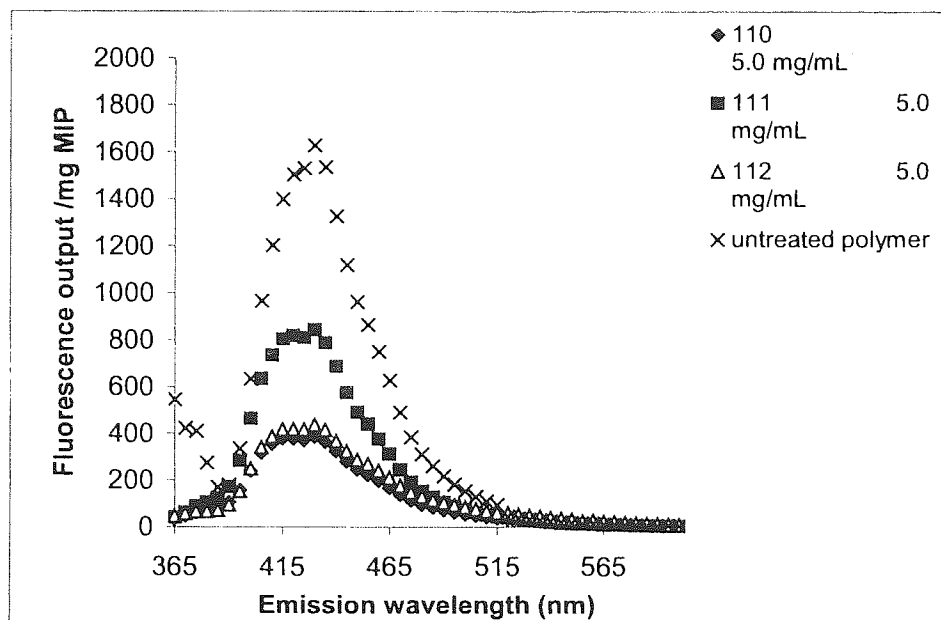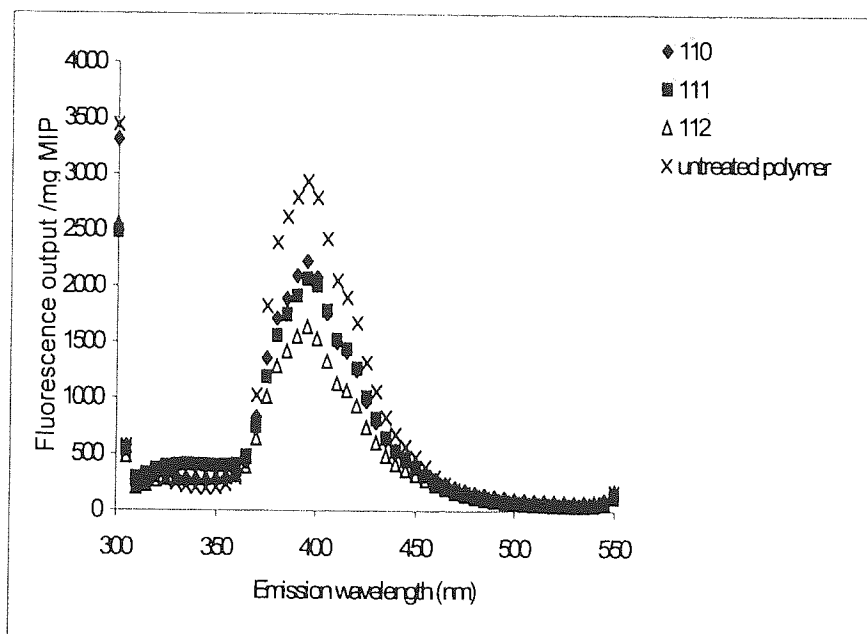
**Figure 92**: Fluorescence spectra for **MIP9** in PEG. ($\lambda_{ex}$ = 290 nm).
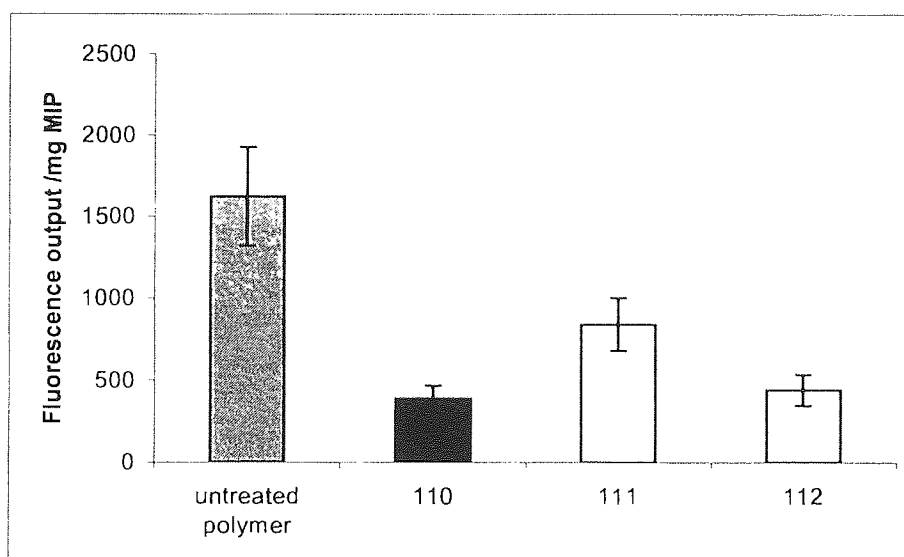
From the MIP results and the solution based study performed on these hydroxylated compounds suggests that the MIP cavity accepted these compounds.

### 3.3.4.1.3 MIP10 templated with compound 77

#### 3.3.4.1.3.1 MIP10 tested with closely related set of relatively rigid polycyclic analogues

**MIP10** {5.4.14} was exposed to its own template **77** and its analogues **76** {5.3.2}, **78** {5.3.4} and **77** {5.3.3} (**Figure 69**-structures, 3.3.3). These compounds produced no additional fluorescence, which could be attributed to an excimer (**Figure 93**). All of the compounds however did quench the fluorescence of the MIP-bound fluorophore.

*Interpretation of* **MIP10** *results with the aid of solution based study* (Refer to section 3.3.3.1)
Compound **76** and **78** typically presented fluorescence emission spectra that demonstrated the straightforward quenching of the cavity-bound fluorophore, and neither compound contributed towards the observed fluorescence displayed for this MIP, as determined by the solution phase study (**Figure 70**). Compound **77** displayed a two-peak fluorescence emission spectrum. The first emission maximum at 395 nm is representative of a straightforward quenching of the cavity-bound fluorophore. The second emission maximum at 485 nm could be characteristic of the formation of an excimer, as the test compound exhibited background levels of fluorescence in the solution phase study (**Figure 70**).

The MIP cavity accepted all the test compounds (**Figure 93**) but no conclusive excimer fluorescence was observed.
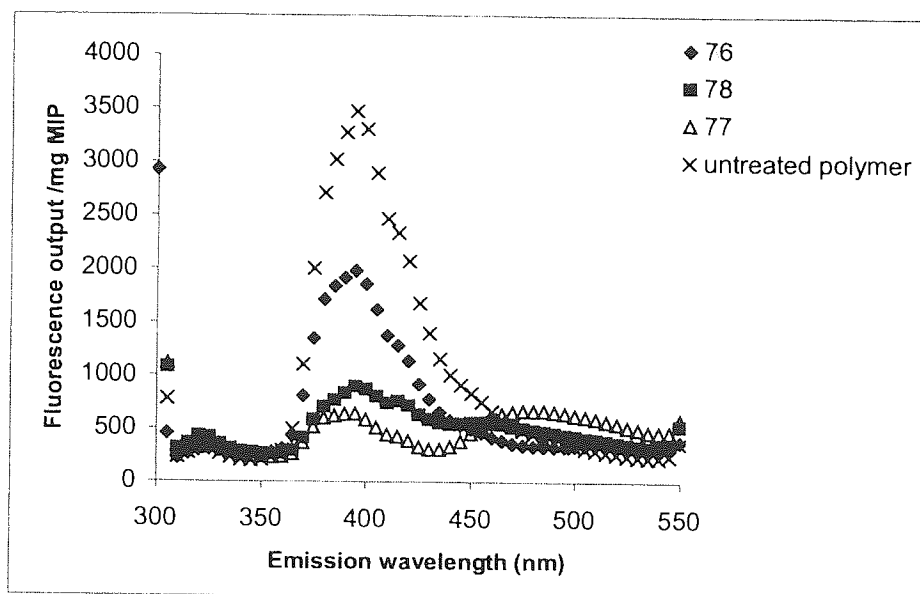
**Figure 93**: Fluorescence spectra for **MIP10** in PEG. ($\lambda_{ex}$ = 290 nm).

### 3.3.4.1.3.2 MIP10 tested with pyrene-based test compounds

The MIP-bound fluorophore exposed to the pyrene-based test compounds **113** {5.3.25}, **114** {5.3.26}, **115** {5.3.27} and **116** {5.3.28} (**Figure 69**-structures, 3.3.3) all caused quenching, but did not form an excimer.

*Interpretation of* **MIP10** *results with the aid of solution based study* (Refer to section 3.3.3.1)

Compound **113** displayed a fluorescence emission maximum at 520 nm (**Figure 71**) and this feature is not present when exposing this to the MIP (**Figure 94**). Compound **114** displayed a two-peak fluorescence emission spectrum. The first emission maximum at 395 nm is representative of a straightforward quenching of the cavity-bound fluorophore. The second emission maximum at 465 nm is characteristic of the test compound itself as determined by solution phase study (**Figure 71**). Compound **115** as determined by the solution phase study (**Figure 94**) does not contribute towards the observed fluorescence spectrum displayed in the MIP result. The emission spectrum produced by this test compound reflects a straightforward quenching of the cavity-bound fluorophore (**Figure 94**). As for compound **116** this gave an emission maximum at 500 nm in the solution phase study (**Figure 94**) and its fluorescence is contributing towards the second emission maximum at 500 nm observed when exposed to the MIP. The first emission maximum at 390 nm is due to the straightforward quenching of the cavity-bound fluorophore (**Figure 94**). The MIP cavity accepted all the test compounds (**Figure 94**).
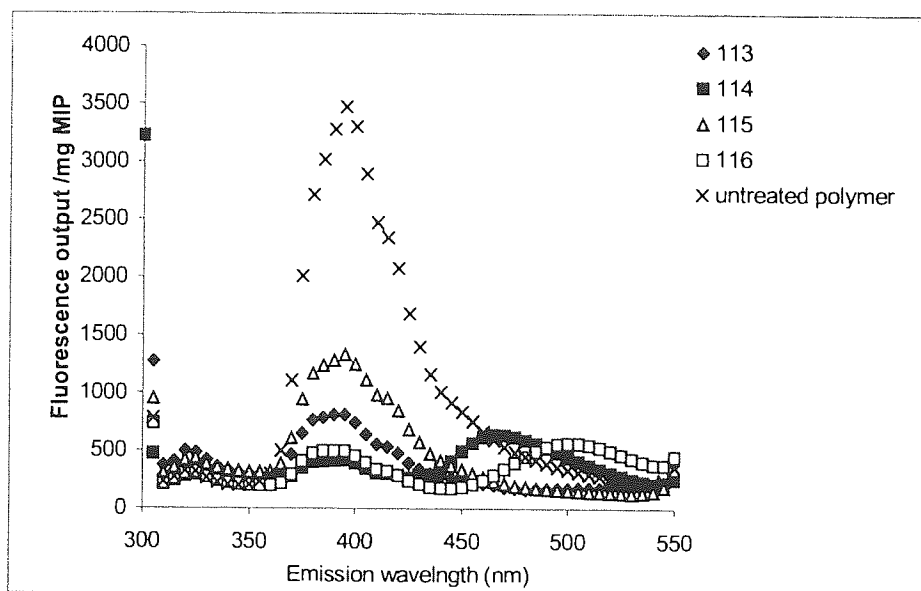
Figure 94: Fluorescence spectra for **MIP10** in PEG. ($\lambda_{ex}$ = 290 nm).

### 3.3.4.1.3.3 MIP10 tested with hydroxylated test compounds

*Interpretation of* **MIP10** *results with the aid of solution based study* (Refer to section 3.3.3.1)

The hydroxylated compounds **110** {5.3.22}, **111** {5.3.23} and **112** {5.3.24} (**Figure 69**-structures, 3.3.3) as can be seen from **Figure 72** exhibited background levels of fluorescence. Thus there is no contribution of fluorescence from these compounds towards the displayed emission spectra presented in **Figure 95**. The emission spectra produced by these test compounds reflect a straightforward quenching of the cavity-bound fluorophore.
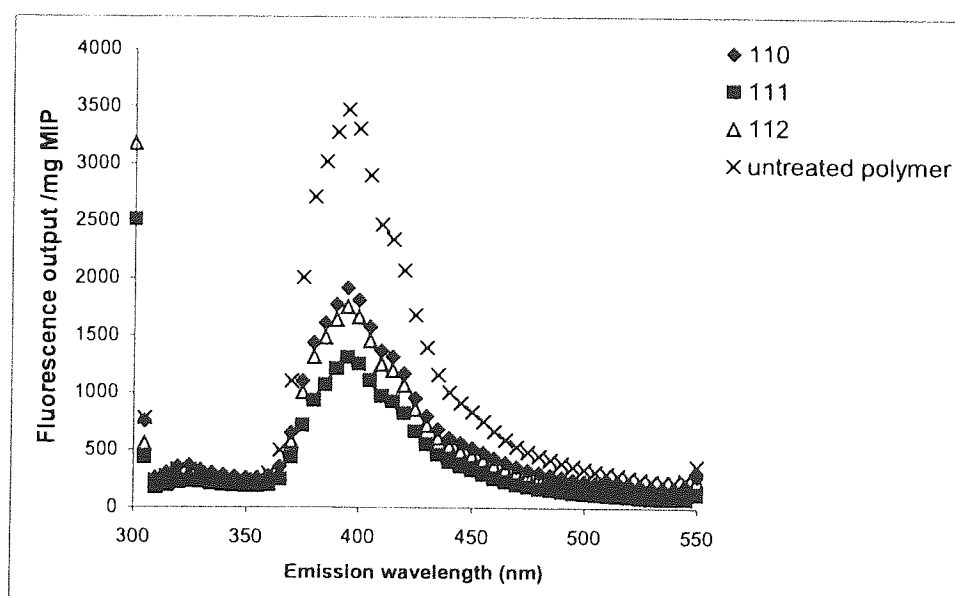


Figure 95: Fluorescence spectra for **MIP10** PEG. ($\lambda_{ex}$ = 290 nm).

From the MIP results and the solution based study performed on these hydroxylated compounds suggests that the MIP cavity accepted these compounds.

### 3.3.5 Conclusion

A series of MIPs was created with a view to exploring the utility of MIPs having two independently addressable fluorophores in their cavities. The initial proposed idea was based upon a quinine scaffold (**Scheme1**). As mentioned earlier this was not accessible synthetically.

To advance in this area of synthesising a dual functional monomer an alternative, based upon a piperazine scaffold, was proposed. The initial attempt involved compound **96** that contains a biphenyl moiety and it was anticipated that the fluorescence output of this would be distinguishable from the incorporated fluorophore N-(2-formyl-phenyl)-acetamide (**Scheme 2**).

Further progress was made by using alternatives such as 5-dimethylamine-naphtalene-1-sulphonyl choride (**99**), 1-napthoyl chloride (**97**), 2-napthoyl chloride (**98**) and lissamine rhodamine B-sulphonyl chloride (**100**). Of the four compounds **97** exhibited no fluorescence at all. The other three compounds revealed emission maxima that demonstrated the potential of being distinguishable from the proposed incorporation of the second fluorophore, N-(2-formyl-phenyl)-acetamide (**Scheme 2**).

Compound **99** was taken further in the reaction sequence by having the second fluorophore (N-(2-formyl-phenyl)-acetamide) incorporated to it i.e. compound **104** and forming an acetate (compound **105**) to perform studies on. Compound **105** exhibited the potential to independently address the two fluorophores. To explore this ability within a cavity was not possible owing to time constraints (**Scheme 2**).

The preparation of soluble copolymers of co-styrene-**108** and co-octadecylacrylate-**108** as polymer films, were created to inform of the results generated by the MIPs synthesised by this FFM. These films enabled the quenching ability of each test compound towards the fluorophore to be addressed in a polymeric environment, but without the constraint of a cavity. Such assessments then helped to interpret the fluorescence quenching MIP results.

A scaffold based on methyl hydrazine employed N-(2-formyl-phenyl)-acetamide and pyrene as fluorophores to synthesise a dual functional monomer, compound **107**. The acrylated version of **107** i.e. compound **108** (**Scheme 3**) was used as a FFM and templated with **76**, **78** and **77** (**Figure 69**, 5.3.3) creating a series of MIPs (i.e. **MIP5**, **MIP6** and **MIP7**). Such MIPs exhibited binding-dependant fluorescence. However, production of an excimer with the alignment of two pyrenes in a MIP was not established as such.

As a further branch of the above methyl hydrazine based-scaffold, a subunit of the dual fluorophore (single fluorophore) was created from 1-pyrenemethylamine. The study on the non-polymerisable

compound **117** (**Scheme 4**) demonstrated successfully the formation of an excimer at longer wavelengths (470nm). From this determination, compound **118** (polymerisable version of **117**) was used as a FFM to synthesise **MIP8**, **MIP9** and **MIP10**, however, no excimer formation was revealed.

The MIPs created by FFMs **108** and **118** both demonstrated the inability to discriminate between close analogues of their template molecules that were used to generate the MIPs. In addition, the cross-reactivity profiles generated by these MIPs demonstrated that all the test compounds were accepted and hence illustrate that the MIPs synthesised were non-selective.

To create MIPs with two independently addressable fluorophores in their cavities could be explored with compound **99**, even though no MIPs were synthesised with this.

### 3.4 Hydrophobic interactions

To create fluorescent functional monomers that also contain a hydrophobic pocket, a number of routes were taken to synthesise such monomers. The hydrophobic pockets were based on cyclododecylamine, 2-(acryloyl-anthracen-9-ylmethyl-amino)-benzamide, N,N'-Bis-pyren-1-ylmethyl-benzene-1,3-diamine and anthraniloyl hydrazide.

### 3.4.1 Cyclododecylamine based hydrophobic pocket



2-acryloylamino-benzamide

Cylcododecane
(hydrophobic pocket)
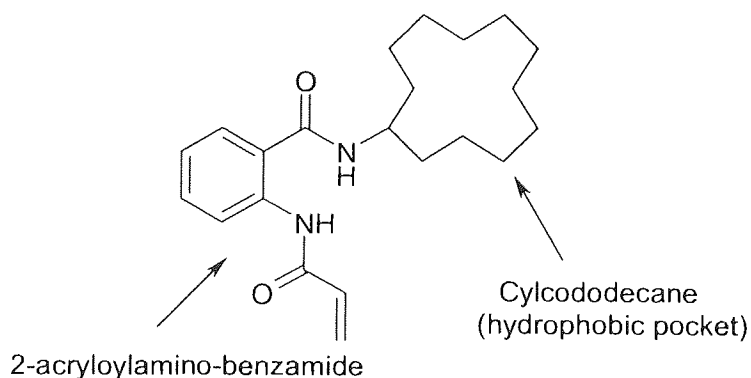
**Figure 96**: 2-acryloylamino-N-cyclododecyl-benzamide, compound **119**.

The preparation of a fluorescent functional monomer that contains a hydrophobic pocket was initially based on an anthraniloyl acrylamide fluorescent monomer, compound **119** {5.3.31}. Cyclododecylamine was incorporated *via* amination into the large flexible hydrophobic residue within this compound (**Figure 96**).

**106** R = Cyclododecyl

**120** R = Cyclododecyl
**121** R = Cyclopentyl
**122** R = Cyclohexyl
**123** R = Dodecyl

**119** R = Cyclododecyl
**124** R = Cyclopentyl
**125** R = Cyclohexyl
**126** R = Dodecyl
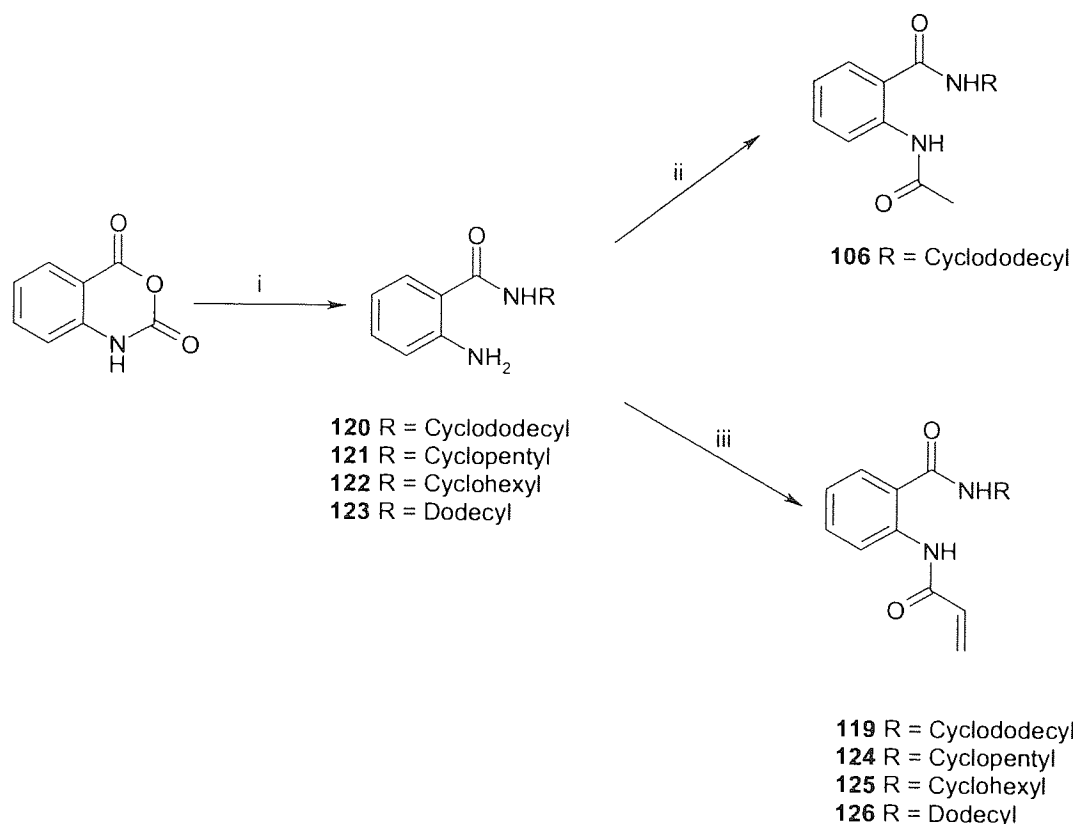
i $H_2NR$/ethanol/heat, ii Acetyl chloride/triethylamine/THF, iii Acryloyl chloride/triethylamine/THF

**Scheme 5:** Preparation of anthranilamides containing hydrophobic portions.

A series of MIPs was constructed wherein compound **119** (**Scheme 5**) was used as a fluorescent functional monomer and employed to create a hydrophobic environment through its cyclododecane moiety. Compound **119** was templated with **81**, **127**, **128**, **83** and **84** (**Figure 97**) and cross-linked with trimethylolpropane triacrylate (TMPTA). These MIPs were subjected to grinding (pestle and mortar) followed by sieving to establish a known particle size range and finally the templates were extracted using a soxhlet apparatus. The final step of the procedure resulted in 'empty' MIPs being exposed to their original templates and test compounds, then collected by filtration and analysed by fluorescence. The experimentally found optimum excitation wavelengths of 345 and 305nm, with the respective 415 and 455 nm wavelengths of fluorescence emission maximum, were the parameters used to analyse the MIPs. These parameters were determined by the study performed on compound **106** {5.3.18} (a stable and non-polymerisable version of compound **119**), discussed in the dual fluorophore section (3.3.2). Note that for **81** (**Figure 97**) the TMPTA cross-linker was replaced by a flexible cross-linker triethyleneglycol dimethacrylate (TEGDMA). The reason that led to this change was that template **81** was found to be inadequately extracted from MIP cross-linked with TMPTA. This gave fluorescence characteristic of the template instead of the empty MIP (**Figures 98a** and **98b**).

175
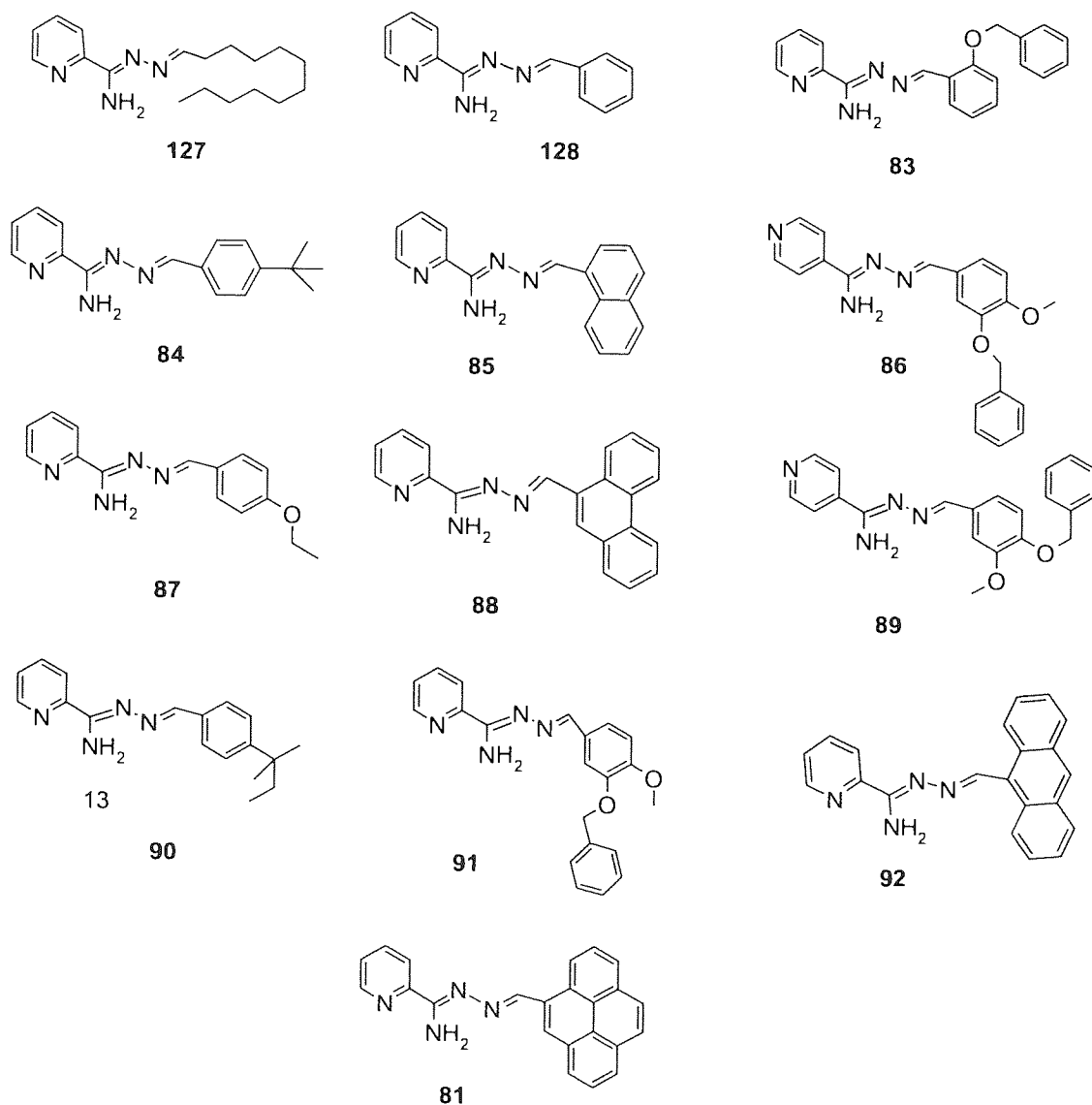
**Figure 97**: Structures of templates and test compounds.

Whilst investigating the empty MIPs it was noticed that the fluorescence profiles were possibly dependent upon the size of the template used in their construction (and hence the corresponding cavity sizes). The exact order of size of compounds (**81**, **127**, **128**, **83** and **84**) is difficult to define. For instance **81** and **84** are obviously larger than **127** but in different ways, where **81** presents a large flat pyrenyl moiety and **84** has a bulky tert-butyl group at the far end. Nevertheless, a rough estimation on template sizes in a decreasing order can be made as **84** to **81** to **83** to **128** and **127** (**Figures 98a** and **98b**).

For the larger cavity sizes the optimum excitation/emission pair was 345/415nm. On moving to progressively smaller cavity sizes the optimum excitation maximum shifted to 305 nm together with a shift to a longer wavelength of 455 nm for the emission.
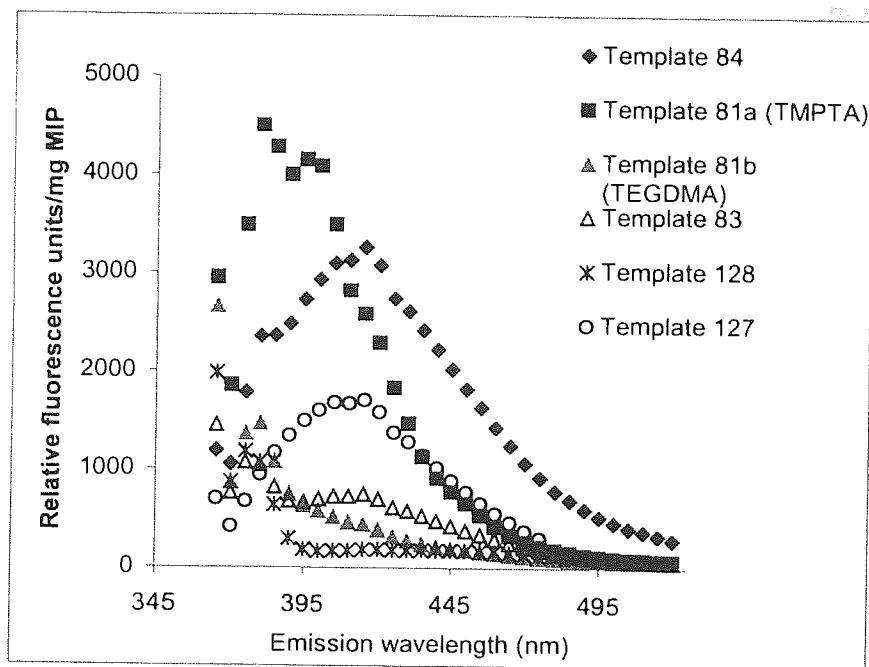
**Figure 98a:** Fluorescence spectra for empty MIPs using compound **119** as the functional monomer and **81, 83, 84, 127, 128** as templates. $\lambda_{ex}$ = 345 nm.
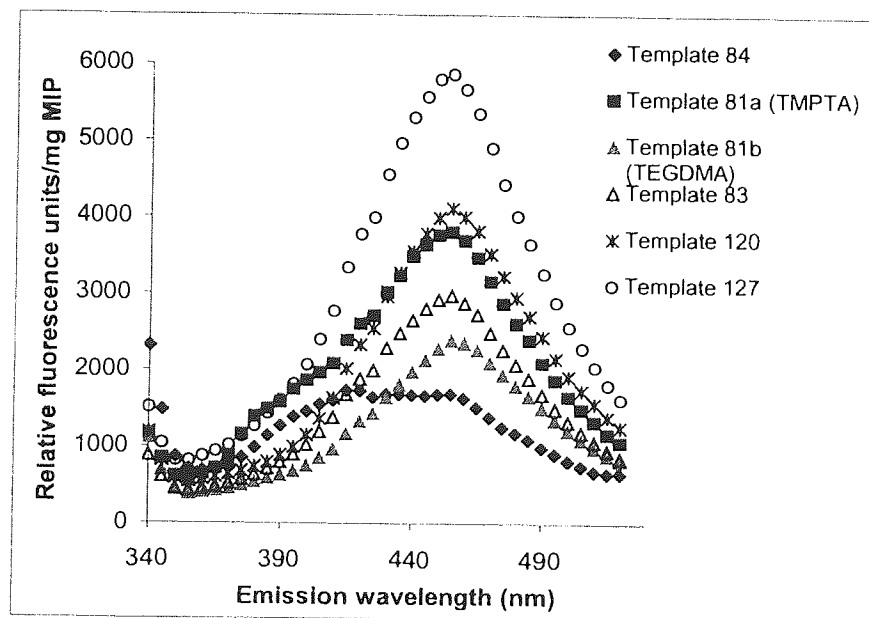


**Figure 98b:** Fluorescence spectra for empty MIPs using compound **119** as the functional monomer and **81, 83, 84, 127, 128** as templates. $\lambda_{ex}$ = 305 nm .
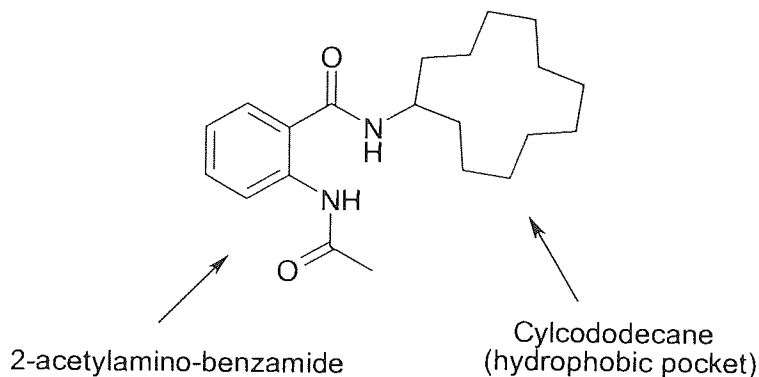
Figure 99: 2-acetylamino-N-cyclododecyl-benzamide, compound 106.

A study was carried out using compound 106 to (Figure 99) give an insight into the ability of the templates (81, 127, 128, 83 and 84) (Figure 97, 3.4.1) to quench the fluorescence of the MIP-bound fluorophore. This involved using steadily reduced concentrations of each test compound against compound 106 (a stable and non-polymerisable version of compound 119) (Figure 96, compound structure, 3.4.1) and measuring fluorescence quenching. (Procedure 5 refer to 4.5)

The study involved a fixed concentration of compound 106 (0.08 mg/mL) with varying concentrations of template from 0.08 mg/mL to 0.4 mg/mL. Note that wells containing only the template concentrations outlined earlier were used as controls.

Inspection of the results obtained for the steady reduction in concentration of the test compounds against 0.08 mg/mL of compound 106 indicated that concentration dependant quenching was observed (Figures 100a-100e).

The results also showed that some compounds quenched more than others this could possibly signify better interaction taking place between template and compound 106. For instance when considering the fluorescence quenching difference between compound 106 and the 0.4 mg/mL concentration of compound 127 and 128, the former compound quenched to the least extent and 128 the most extent when comparing this to the other studied compounds (Figures 100b and 100c).
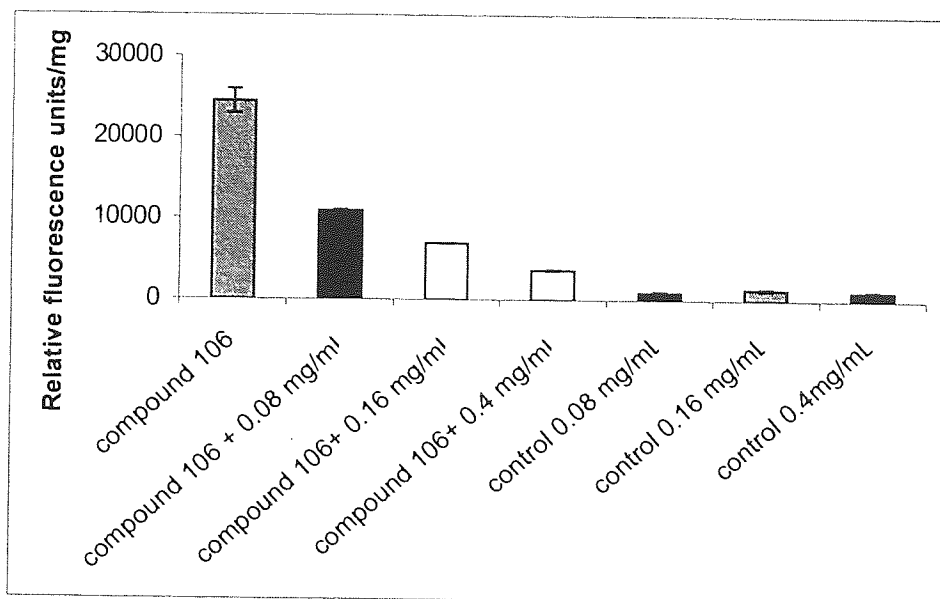
**Figure 100a**: Fluorescence quenching of compound **106** against **81** at various concentrations. $\lambda_{ex}$ = 305 nm, $\lambda_{em}$ = 455nm.
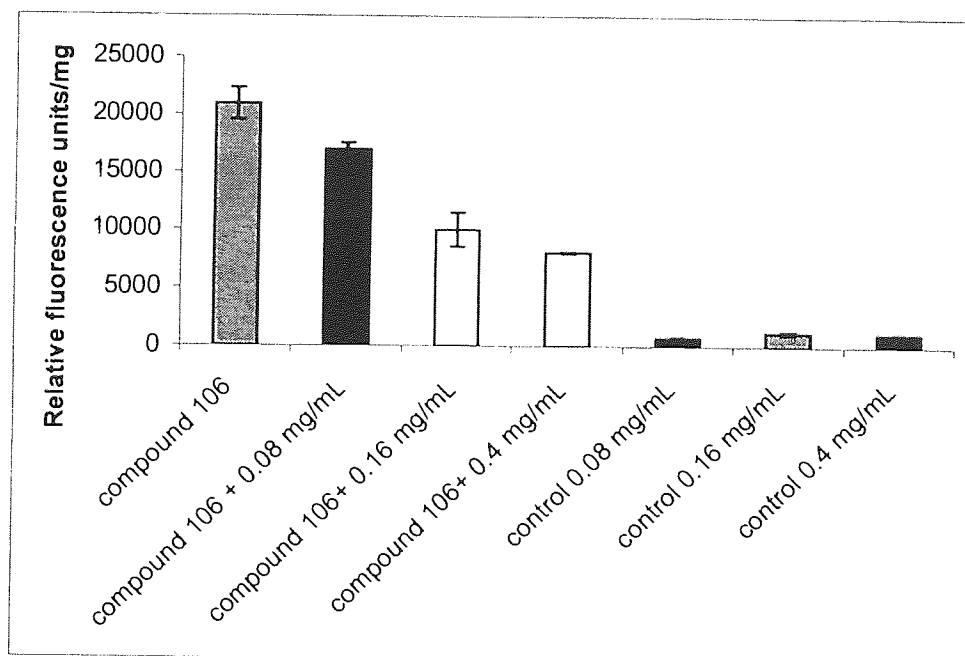


**Figure 100b**: Fluorescence quenching of compound **106** against **127** at various concentrations. $\lambda_{ex}$ = 305 nm, $\lambda_{em}$ = 455nm.
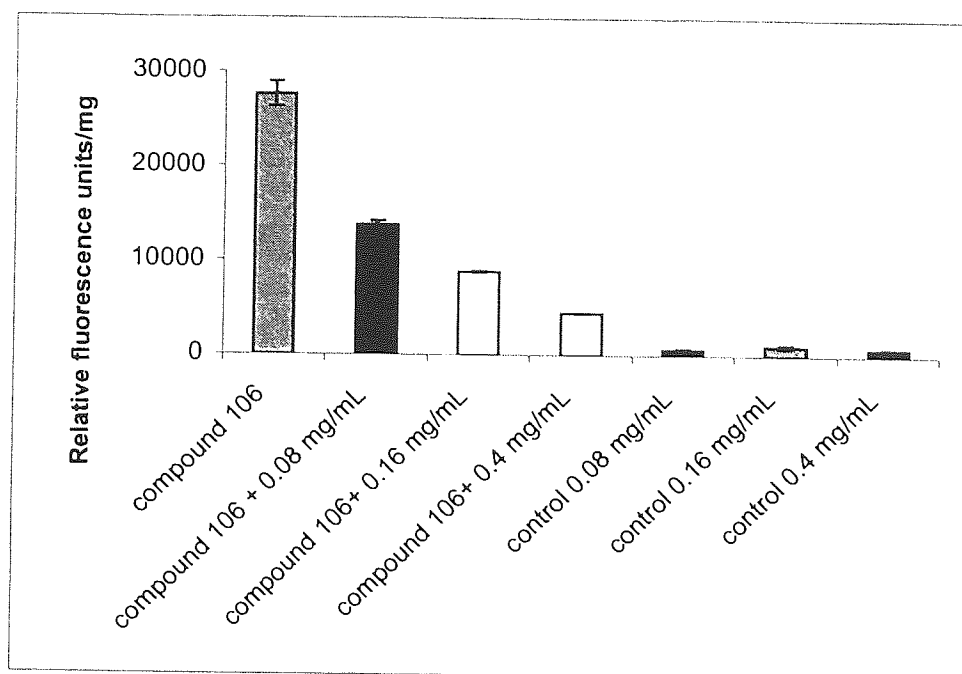
**Figure 100c**: Fluorescence quenching of compound **106** against **128** at various concentrations. $\lambda_{ex}$ = 305 nm, $\lambda_{em}$ = 455nm.
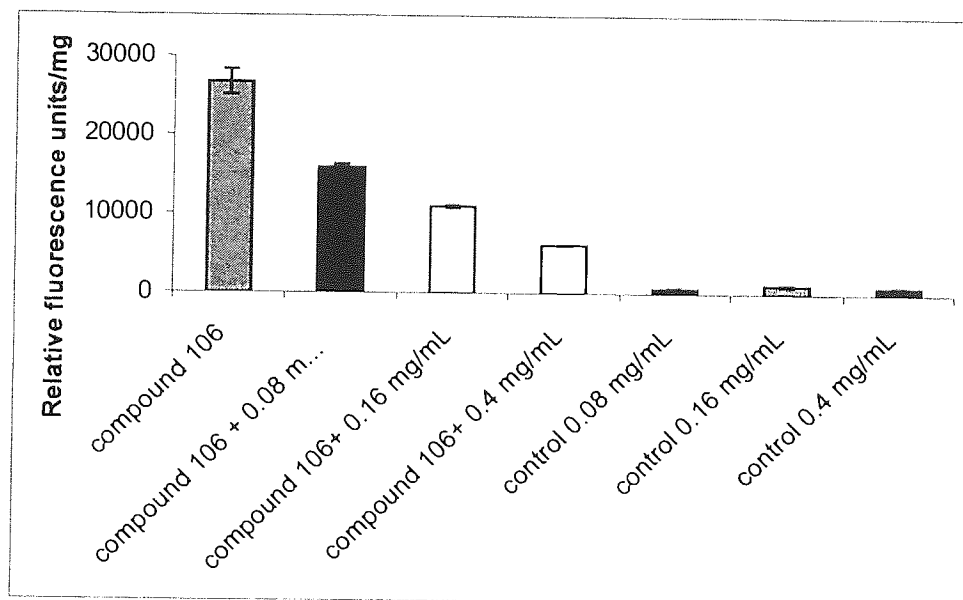


**Figure 100d**: Fluorescence quenching of compound **106** against **83** at various concentrations. $\lambda_{ex}$ = 305 nm, $\lambda_{em}$ = 455nm.
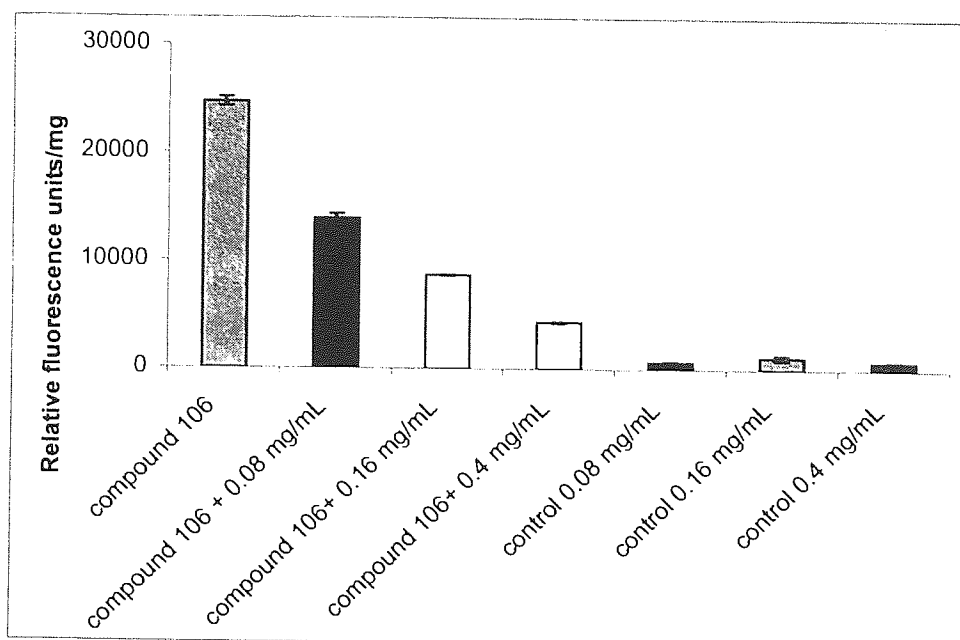
**Figure 100e**: Fluorescence quenching of compound **106** by **84** at various concentrations. $\lambda_{ex}$ = 305 nm, $\lambda_{em}$ = 455nm.

From this study the relative quenching order for these templates was attempted. Note that the establishment of the order only applies to the quenching of compound **106** and does not reveal the fluorescence ability of these templates.

Overall compound **81** gave the best quenching. This was determined by comparing the fluorescence output of compound **106** with the various concentrations of **81** at 0.08 mg/mL, 0.16 mg/mL and 0.4 mg/mL. The lowest concentration (0.08 mg/mL) was able to quench the fluorescence of **106** by half, the moderate concentration (0.16 mg/mL) quenched this further to a quarter and the highest concentration (0.4 mg/mL) quenched this even further by one-eighths (**Figure 100a**).

Then templates **128** and **84** exhibited similar quenching abilities, at low concentrations (0.08 mg/mL) these were able to quench the fluorescence of **106** by half, then for the moderate concentration (0.16 mg/mL) this quenched further by a third and the highest concentration (0.4 mg/mL) quenched even further by one- sixth (**Figure 100c** and **Figure 100e**).

After these templates, template **83** was the next in order of quenching ability. Where the lowest concentration (0.08 mg/mL) was able to quench the fluorescence of **106** slightly less than half, the moderate concentration (0.16 mg/mL) quenched by a half and the highest concentration (0.4 mg/mL) quenched this further by a quarter (**Figure 100d**).

Finally template **127** in comparison to the other templates had the least quenching ability. The lowest concentration (0.08 mg/mL) was able to quench the fluorescence of **106** by less than half in comparison

181

the moderate (0.16 mg/mL) and the highest concentration (0.4 mg/mL) quenched much further (**Figure 100b**).

### 3.4.1.2 Fluorescence study performed on the individual templates (81, 127, 128, 83, 84, 85) and test compounds

This study involved taking fluorescence measurements of individual templates (**81, 127, 128, 83, 84, 85**) (**Figure 97**, 3.4.1) and test compounds to explore if any fluorescence contribution at excitation/emission wavelength pairs of 345 nm/415 nm and 305 nm/455 nm that would be used in the MIP studies are present (Procedure 3g refer to 4.3). Note, that the excitation/emission wavelength pairs stated were determined by a study performed on compound **106** (**Figure 99**, 3.4.1.1) that resembles the FFM (compound **119**) (**Figure 96**, 3.4.1) that would be employed to create the MIPs.

The study used a concentration of 0.08 mg/mL of template/test compounds and had wells containing only (Poly(ethylene glycol) methyl ether- PEG) as the blank reference.

The results (**Figure 101**) established that the fluorescence output of most of the individual test compounds had very little fluorescence output at the stated excitation/emission wavelength pairs. Compounds **81** and **83** at the stated wavelengths gave fluorescence outputs that were above the blank reference. Compound **127** however gave a fluorescence output that was above the blank reference only at excitation/emission wavelength pair of 305/455 nm (**Figure 101**).
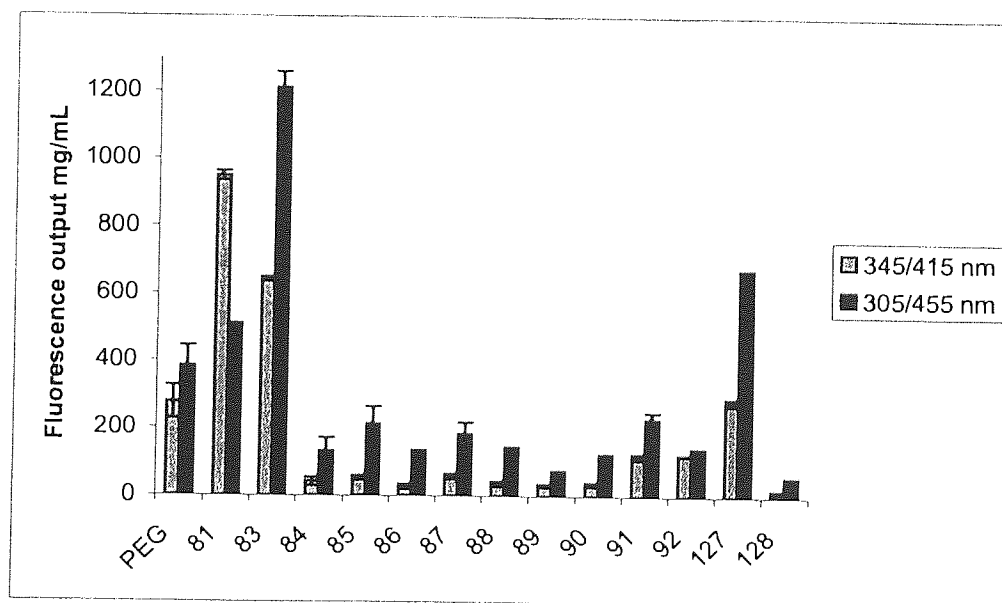


**Figure 101**: Fluorescence of individual compounds at 0.08 mg/mL. $\lambda_{ex} / \lambda_{em}$ = 345/415 nm & 305/455 nm analysed in PEG.

### 3.4.1.3 Investigation of the behaviour of the fluorophore (compound 106) in a variety of environments

In this section the fluorophore is exposed to different environments to discern its behaviour. This is established by exposing this to β-cyclodextrin, preparing reference polymers with the fluorophore and cross-linker alone, studying benzoylene urea and assessing its quenching fluorescence in deposited thin films prepared with PMMA (poly (methyl methacrylate) and compound **106** (**Figure 99**, 3.4.1.1).

### 3.4.1.3.1 Study on compound 106 and β-cyclodextrins

This study was performed on compound **106**, which resembles the MIP-bound fluorophore i.e. compound **119** (**Figure 96**, 3.4.1), that would be used to synthesise a series of MIPs. The rationale behind this study was to constrain compound **106** within the β-cyclodextrin cavity, similar to how the fluorophore would be within an empty cavity in the MIP (Procedure 6 refer to 4.6) Thus this would assess the influence of restriction of cavity size has upon the output of the fluorophore.

The study involved a fixed concentration of compound **106** (0.016 mg/mL) with varying concentrations of β-cyclodextrin of 0.053 mg/mL and 1.05 mg/mL. Note that wells containing only the compound **106** (0.016 mg/mL) and β-cyclodextrin (0.053 mg/mL and 1.05 mg/mL) concentrations were used as controls.

Overall the results suggested that at 1.05 mg/mL of β-cyclodextrin (i.e. increase in the concentration of β-cyclodextrin) complex formation had occurred to some extent i.e.,

Compound **106** + β-cyclodextrin $\rightleftharpoons$ COMPLEX.

This resulted in fluorescence enhancement, but note, that there was no change in the emission wavelength. Two possibilities that could cause this were firstly constraint of the fluorophore and secondly shielding of the fluorophore from the solvent molecules, which prevents them from causing 'solvent induced quenching' (**Figure 102a and 102b**).
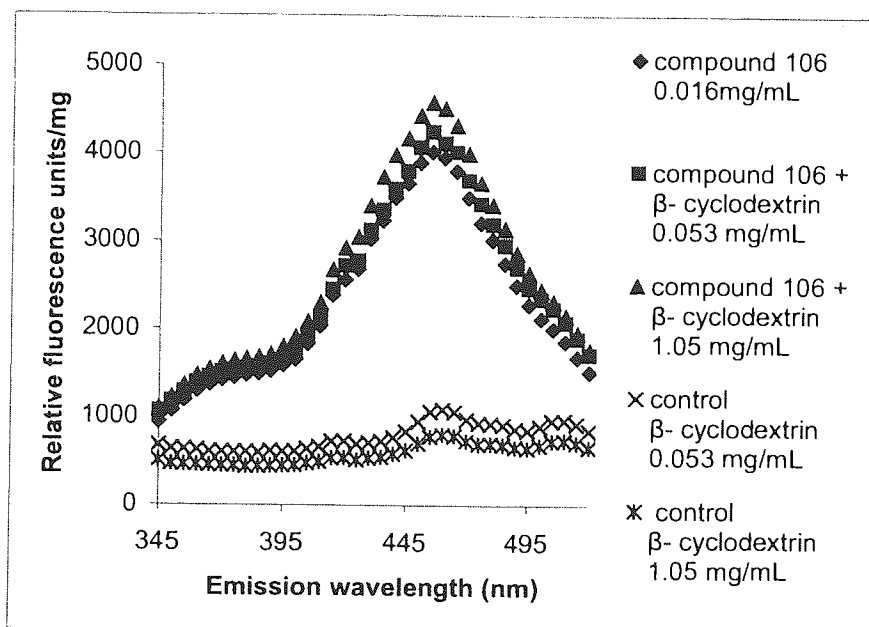
**Figure 102a**: Fluorescence spectra for compound **106** with β-cyclodextrin. ($\lambda_{ex}$ = 305 nm, $\lambda_{em}$ = 455 nm) analysed in PEG.
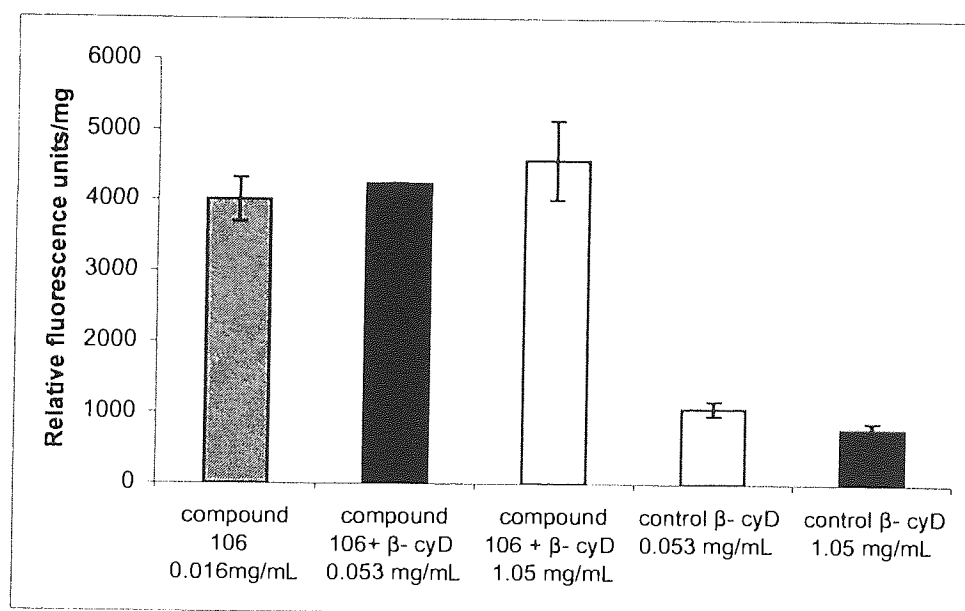


**Figure 102b**: Fluorescence for compound **106** with β-cyclodextrin (β-cyD). The error bars are the standard deviations of triplicate wells. ($\lambda_{ex}$ = 305 nm, $\lambda_{em}$ = 455 nm) analysed in PEG.

### 3.4.1.3.2 Study on polymers synthesised with compound 119 and cross-linker

To take this study a step further reference polymers were synthesised. These polymers would assess the fluorescence behaviour of the fluorophore in maximum restriction i.e. no cavity present. Then again due to the presence of the cross-linker some order in the structure would be possible even though there is absence of a cavity.

Therefore this study involved synthesising reference polymers with compound **119** (**Figure 96**, 3.4.1), but without the use of template. Absence of the template increased structural constraints associated with the fluorophore. The presence of a cross-linker however allowed the fluorophore to be within a cross-linked i.e. matrix environment. **Polymer 1** {5.4.4} (**Figure 103**) was prepared with the fluorophore (compound **119**) and the cross-linker (TMPTA). Parallel to this synthesis another **Polymer 2** {5.4.5} (**Figure 103**) was synthesised but in the absence of the fluorophore (compound **119**) and acts as a reference for the former **Polymer 1**.



compound **119** (FFM)                          +     TMPTA          ⟶          POLYMER 1

TMPTA          ⟶          POLYMER 2
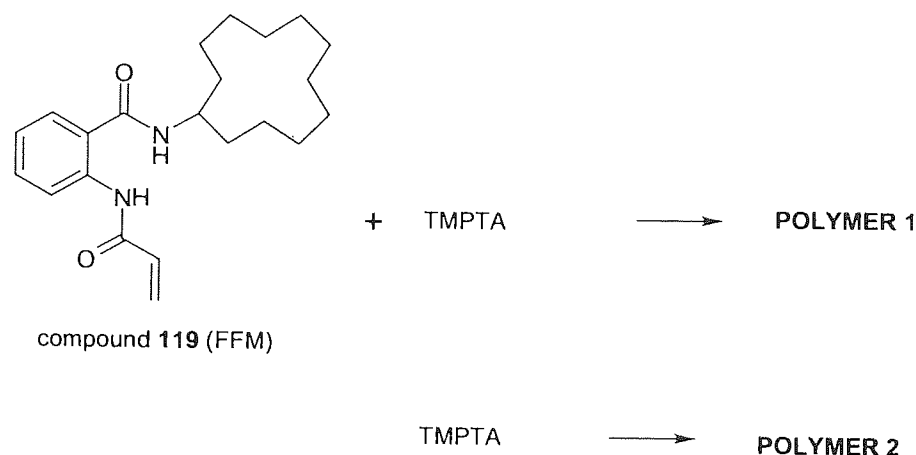
**Figure 103**: Reference **polymers 1** and **2**.

Note, that these polymers were subjected to grinding (pestle and mortar) followed by sieving to establish a known particle size range and then analysed by fluorescence. The fluorescence was investigated at the experimentally found optimum excitation wavelengths of 345 and 305nm, with the respective 415 and 455 nm wavelengths of fluorescence emission maximum. These parameters were determined by the study performed on compound **106** (a stable and non-polymerisable version of compound **119**), discussed in the dual fluorophore section (3.3.2).

Inspection of the results (**Figure 104a** and **104b**) for both polymers, one generated with the fluorophore (**Polymer 1**) and the other in the absence of the fluorophore (**Polymer 2**), indicated that at excitation/emission wavelength of 345 nm/415 nm the fluorescence was at background levels. Note, that between emission wavelengths of 355 and 405 nm, Raman scattering is being observed (**Figure 104a**).

At excitation/emission wavelengths of 305 nm/455 nm fluorescence counts were ~2200 per mg for the **Polymer 1** and contributed towards the MIPs results synthesised with compound **119**, as this peak was not present for the **Polymer 2** (**Figure 104b**). Note the fluorescence output of **Polymer 1** (**Figure 104b**) is similar to the already observed spectrum for compound **106** and β-cyclodextrin (**Figure 102a**). Indicating that the β-cyclodextrin created cavity does not affect the fluorescence output of the fluorophore.
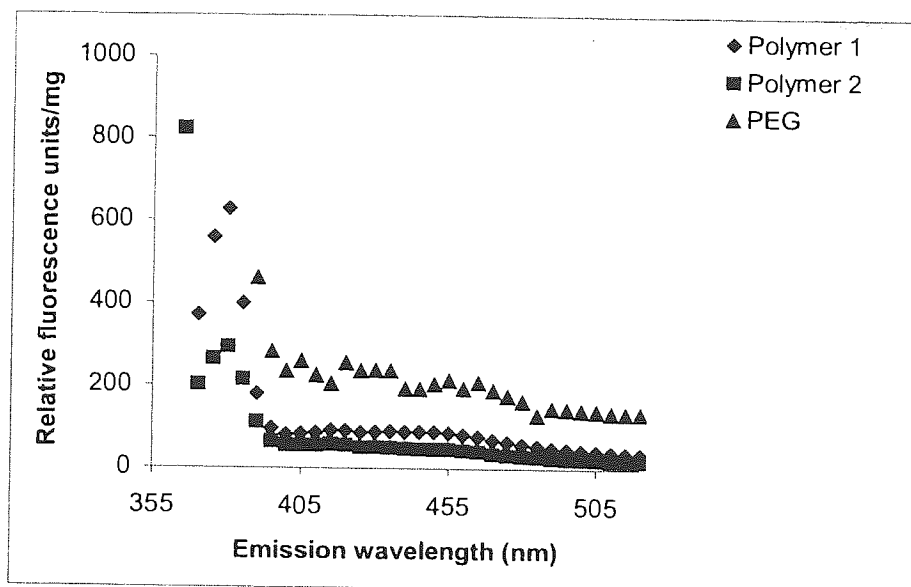
**Figure 104a:** Fluorescence spectra for polymers. ($\lambda_{ex}$ = 345 nm,$\lambda_{em}$ = 415 nm).
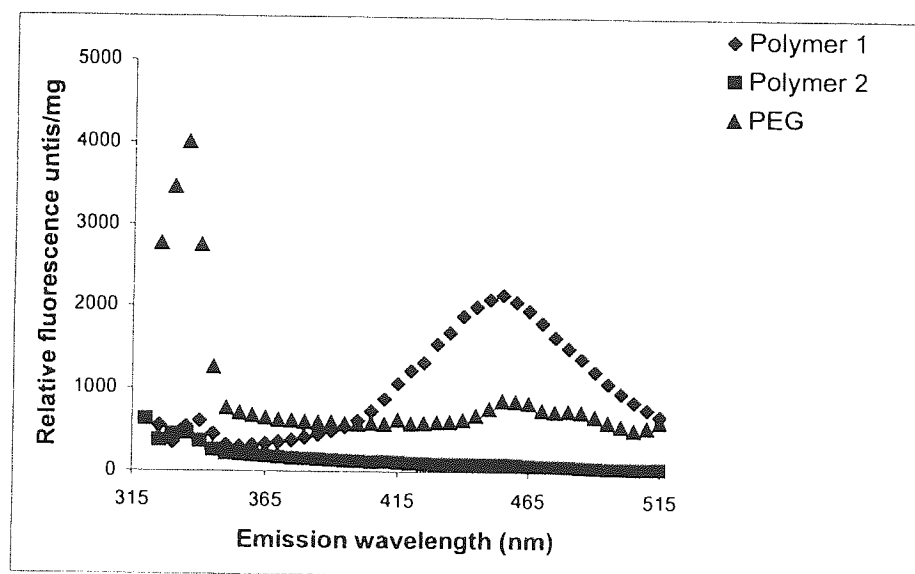


**Figure 104b:** Fluorescence spectra for polymers. ($\lambda_{ex}$ = 305 nm,$\lambda_{em}$ = 455 nm).

### 3.4.1.3.3 Study performed on benzoylene urea

After studying the fluorescence output of the fluorophore restricted with β-cyclodextrin and further studying the fluorophore in the presence of maximum restriction (with no cavity) (**Polymer1** and **2**). A study was performed on benzoylene urea that resembles the 2-acetylamino-benzamide moiety found in compound **106** (as can be seen in **Figure 105**) (Procedure 7 refer to 4.7). Benzoylene urea, however, is conformationally restrained in comparison to compound **106**.

Thus the fluorescence output of 2-acetylamino-benzamide moiety under conditions of restricted flexibility can be probed. A solution phase fluorescence based study was performed on benzoylene urea and

186

compound **106**. The study used a concentration of 0.08 mg/mL of compound **106** and 0.038 mg/mL of benzoylene urea.

Benzoylene urea                              Compound **106**



Closed form of
2-acetylamino-benzamide

Open form of
2-acetylamino-benzamide
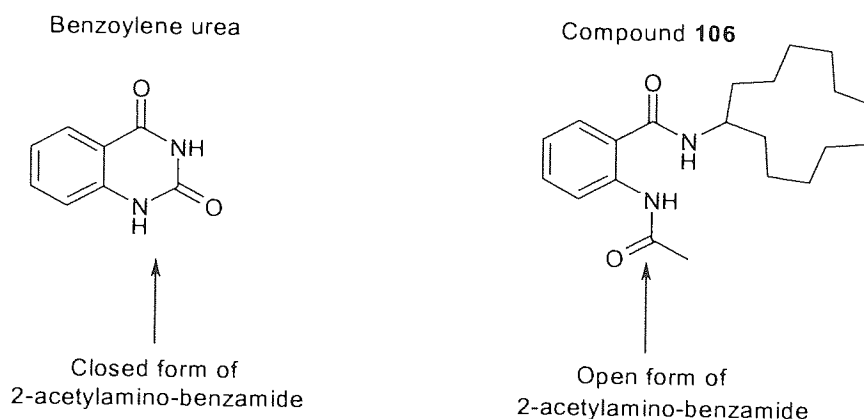
**Figure 105**: illustrating the closed and open form of 2-Acetylamino-benzamide in benzoylene urea and compound **106**.

At excitation wavelength of 305 nm (**Figure 106**) benzoylene urea gives an emission maximum at 355 nm. For compound **106** at this excitation wavelength an emission maximum at 455 nm is observed. The shoulder that is observed for the spectrum of compound **106** (**Figure 106**) could possibly be a contribution similar to that of the 2-acetylamino-benzamide moiety.

The fluorescence output of compound **106**, **Figure 106** in this environment (no cavity or a cross-linked environment) has given rise to a similar fluorescence spectrum as that observed in the previous studies i.e. β-cyclodextrin, **Figure 103a** and **Polymer 1**, **Figure 104b**. Hence the presence or absence of a cavity or a cross-linked environment does not affect the fluorescence output of compound **106**. Relating this to the MIP environment that has the presence of a cavity and cross-linker, in this case the fluorescence output of the fluorophore is affected.
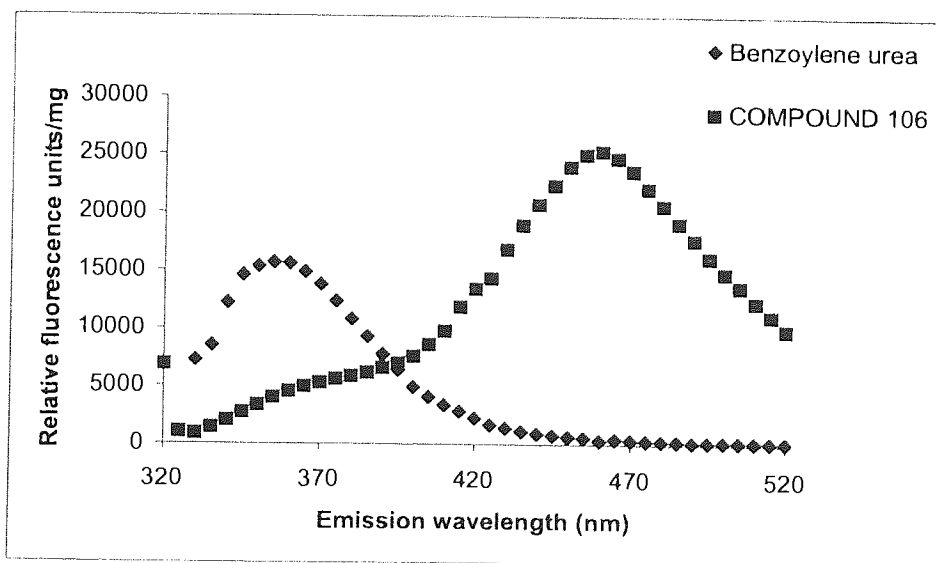


**Figure 106**: Fluorescence spectra for benzoylene urea and compound **106**, analysed in PEG. ($\lambda_{ex}$ = 305 nm).

### 3.4.1.3.4 Fluorescence studies on deposited thin films of poly (methyl methacrylate) PMMA-compound 106

The reason for preparing deposited thin films of poly (methyl methacrylate) PMMA (**Figure 107**) and compound **106** was to assess the behaviour of compound **106** within a very restricted environment. This environment however restricts the fluorophore in a non-cavity and non-cross-linked environment even more.
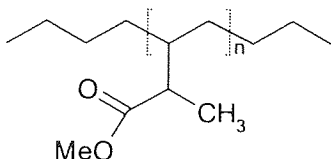


**Figure 107**: Structure of poly (methyl methacrylate) PMMA.

Stock solutions of known concentrations of PMMA and compound **106** (**Figure 105**- compound structure) were prepared dissolved either in chloroform or THF. From these solutions aliquots were placed into polypropylene 96 well plates and evaporated to form the polymer thin films for fluorescence studies (Procedure 8 refer to 4.8). Note that control lanes containing only compound **106** and PMMA were prepared as well.

### 3.4.1.3.4.1 Constant amount of PMMA (10 mg) and varying amounts of compound 106 (0.001 to 0.02 mg) both dissolved in chloroform and evaporated to form thin films

From **Figure 105** for excitation wavelength at 345 nm it could be seen that the observed fluorescence output is the same for all of the various amounts of compound **106**. At excitation wavelength of 305 nm (**Figure 108a**), as the amount of compound **106** in the polymer increased fluorescence enhancement was observed. This can be exemplified by comparing the control lanes (containing only compound **106**) fluorescence output with the lanes containing both compound **106** and PMMA i.e. the polymer lanes. For instance control (**106**) at 0.02 mg with 0.02 mg polymer (containing both **106**/PMMA) (**Figure 108a**).
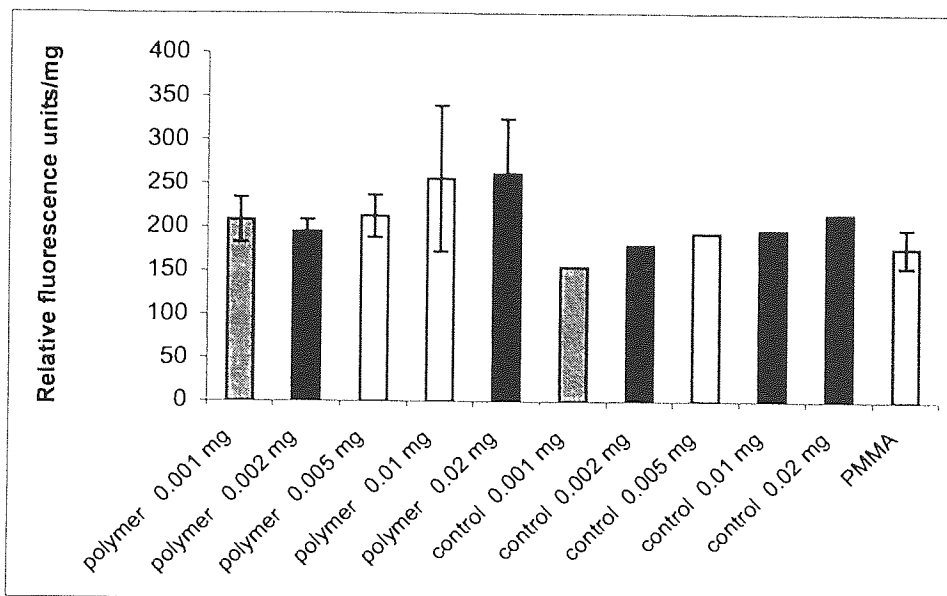
**Figure 108**: Barchart for polymer thin films (compound **106** with PMMA) and controls. ($\lambda_{ex}$ = 345 nm, $\lambda_{em}$ = 415 nm).
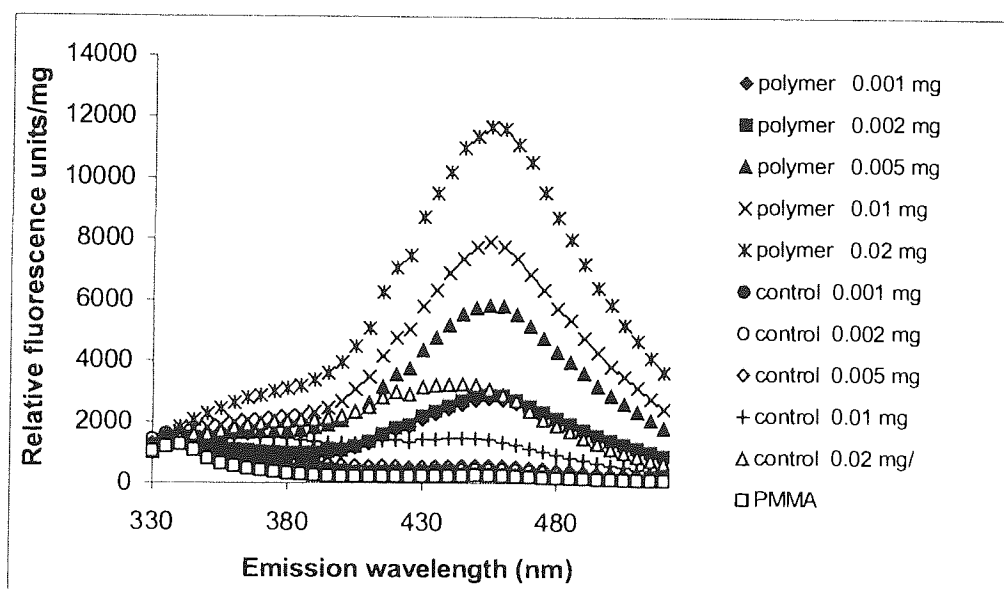


**Figure 108a**: Fluorescence spectra for polymer thin films (compound **106** with PMMA) and controls. ($\lambda_{ex}$ = 305 nm, $\lambda_{em}$ = 455 nm).

### 3.4.1.3.4.2 Constant amount of PMMA (10 mg) and varying amounts of compound 106 (0.001 to 0.02 mg) both dissolved in THF and evaporated to form thin films

From **Figure 106** for excitation wavelength of 345 nm it could be seen that the observed fluorescence output is the same for all of the various amounts of compound **106** prepared. At excitation wavelength of 305 nm (**Figure 109a**), as the amount of compound **106** in the polymer thin films increased fluorescence enhancement was observed.

189
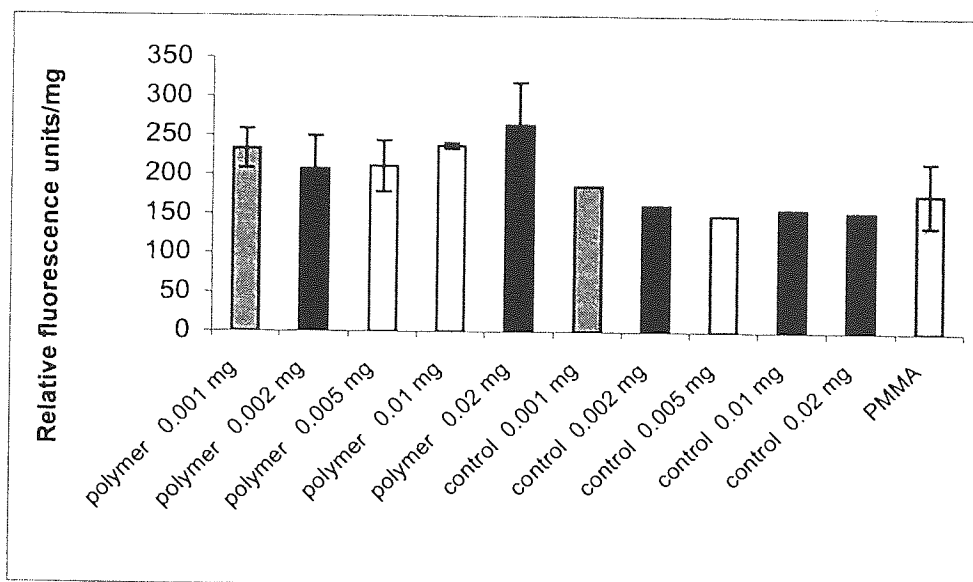
**Figure 109**: Barchart for polymer thin films (compound **106** with PMMA) and controls. ($\lambda_{ex}$ = 345 nm, $\lambda_{em}$ = 415 nm).
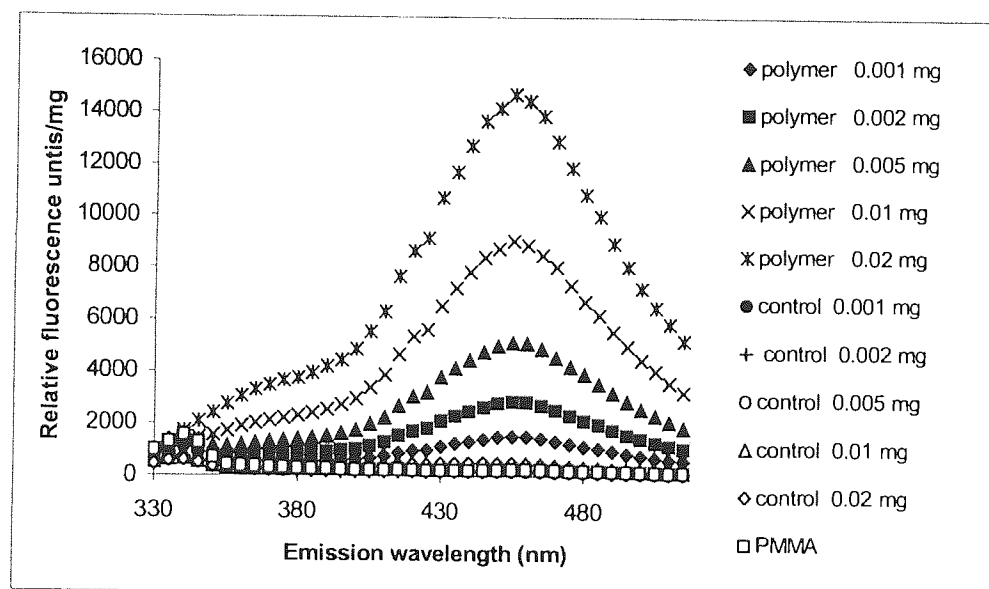


**Figure 109a**: Fluorescence spectra for polymer thin films (compound **106** with PMMA) and controls. ($\lambda_{ex}$ = 305 nm, $\lambda_{em}$ = 455 nm).

Comparing both of the studies i.e. one polymer thin film prepared in THF the other in chloroform at excitation wavelength of 345 nm (**Figures 108** and **109**) the overall result indicated that increasing the amount of compound **106** had no affect on the fluorescence output. For excitation wavelength at 305 nm both studies (**Figures 108a** and **109a**) showed that increase in the amount of compound **106** gave fluorescence enhancement, when comparing the fluorescence output to their respective controls. The enhancement that is observed could be due to the fact that in the polymer (i.e. 10 mg of PMMA in each well) compound **106** is unable to quench its own fluorescence e.g. compound **106** interacting with another

unit of compound **106**. In the control lane where there is only compound **106** it is however able to quench its own fluorescence through interaction with another compound **106**.

The difference however that arises between both of these studies is for the control lanes i.e. in the chloroform prepared controls the fluorescence output is not the same when compared to the response in THF prepared controls (**Figures 108a** and **109a**). This suggests that chloroform may be trapped in the polymer film and the combination of solvent and polymer may be contributing towards the fluorescence being observed for the controls.

### 3.4.1.3.4.3 Constant amount of PMMA (5.0 mg) and varying amounts of compound 106 (0.001 to 0.02 mg) both dissolved in THF and evaporated to form thin films

The above studies were taken further by changing the amount of PMMA from 10 mg to 5.0 mg and keeping the same amount range for compound **106** i.e. (0.001 to 0.02 mg). At excitation wavelength of 345 nm (**Figure 110**) changing the amount of compound **106** had no affect on the fluorescence being observed i.e. all the same. At excitation wavelength of 305 nm (**Figure 110a**) as the amount of compound **106** in the polymer increased fluorescence enhancement was observed.
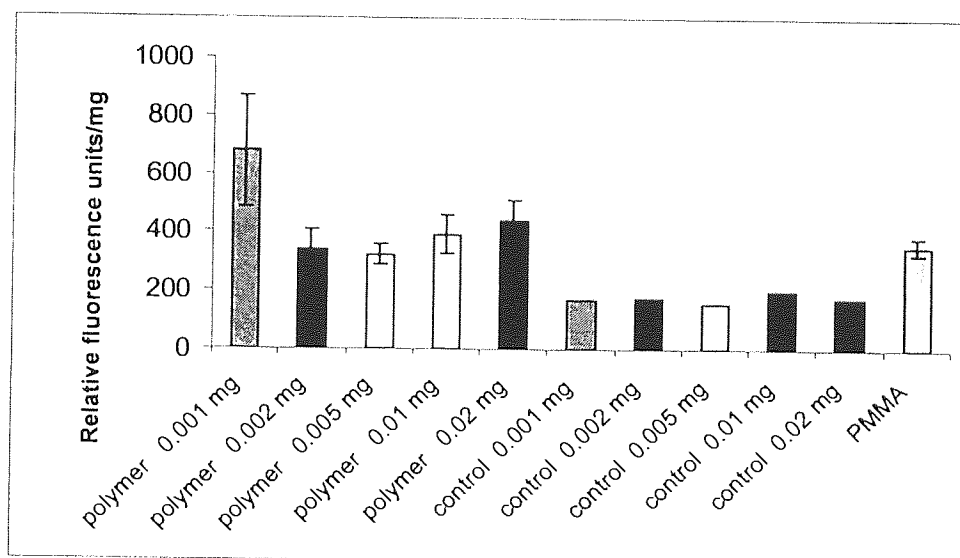


**Figure 110**: Barchart for polymer thin films (compound **106** with PMMA) and controls. ($\lambda_{ex}$ = 345 nm, $\lambda_{em}$ = 415 nm).
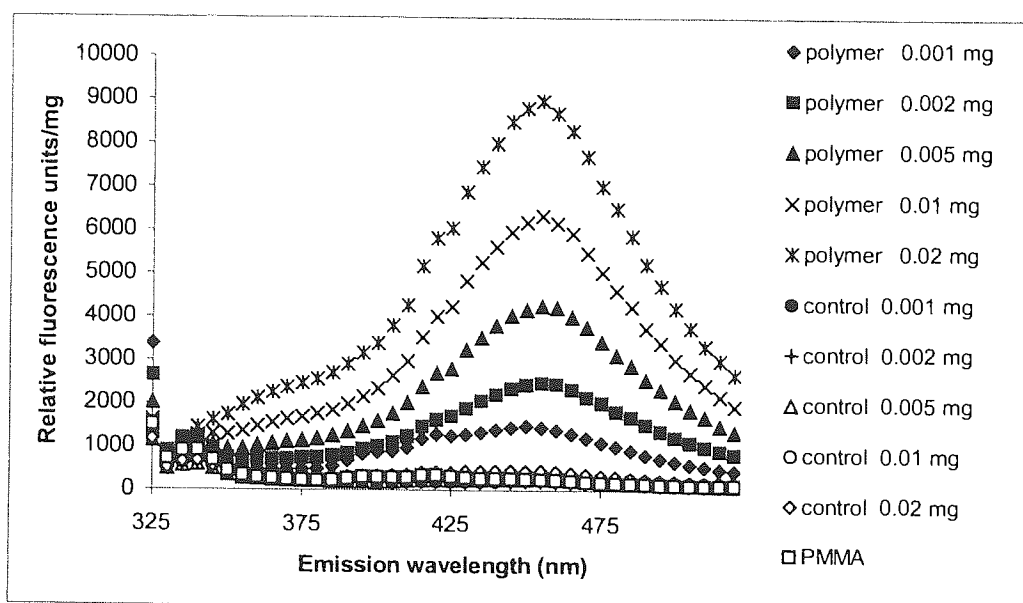
**Figure 110a:** Fluorescence spectra for polymer thin films (compound **106** with PMMA) and controls. ($\lambda_{ex}$ = 305 nm, $\lambda_{em}$ = 455 nm).

Comparing the studies (polymers prepared in THF) with 10 and 5 mg of PMMA and varying amounts of compound **106**. At excitation wavelength of 345 nm (**Figures 109** and **110**) change in the amounts of both PMMA and compound **106** made no difference in the fluorescence output being observed.

At excitation wavelength 305 nm (**Figures 109a** and **110a**) with change in the amount of PMMA i.e. 10 and 5 mg a difference in the fluorescence output was being observed for the lanes containing 0.01 and 0.02 mg of polymer. For instance for 0.02 mg of polymer in 10 mg of PMMA (**Figures 109a**) gave a 15000 units fluorescence output compared to the 5 mg of PMMA (**Figure 110a**) that gave a 9000 units fluorescence output. Suggesting that at 10 mg of PMMA, compound **106** was not able to quench itself (i.e. by interacting to another compound **106**) and in 5 mg of PMMA could do so, hence difference in the fluorescence count.

### 3.4.1.3.4.4 Constant amount of compound 106 (0.001 mg) and varying amounts of PMMA (5.0 to 25.0 mg) both dissolved in THF and evaporated to form thin films

At excitation wavelength 345 nm (**Figure 111**) changing the amount (i.e. the concentration of **106** rose in the thin film) of PMMA had no affect on the fluorescence output being observed. As for excitation wavelength of 305 nm (**Figure 111a**) the fluorescence increased as the amount of PMMA decreased from 5 to 25 mg.

192
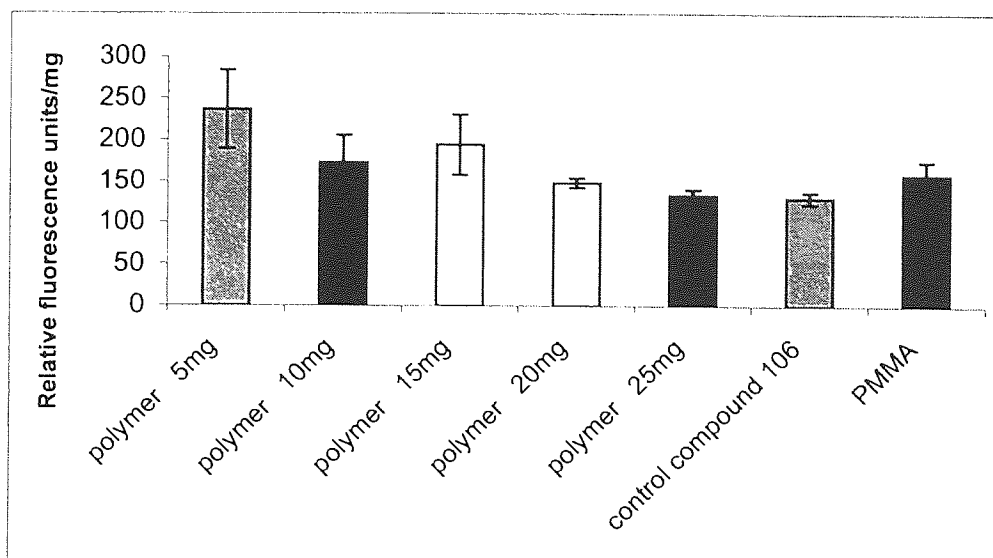
**Figure 111**: Barchart for polymer thin films (compound **106** with PMMA) and controls. ($\lambda_{ex}$ = 345 nm, $\lambda_{em}$ = 415 nm).
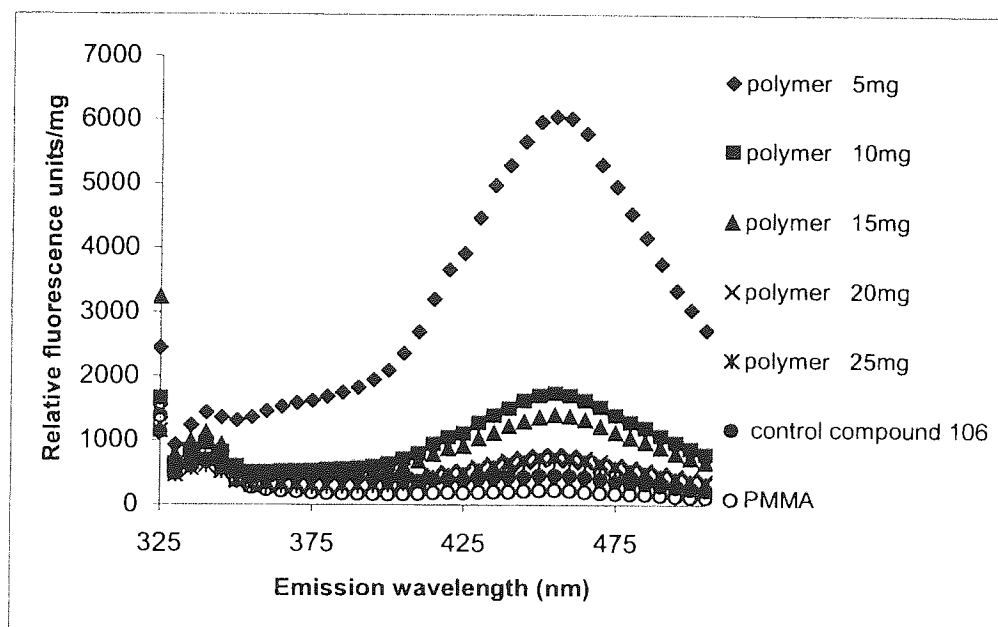


**Figure 111a**: Fluorescence spectra for polymer thin films (compound **106** with PMMA) and controls. ($\lambda_{ex}$ = 305 nm, $\lambda_{em}$ = 455 nm).

### 3.4.1.3.4.5 Constant amount of compound 106 (0.001 mg) and varying amounts of PMMA (0.05 to 0.5 mg) both dissolved in THF and evaporated to form thin films

Subsequently from the above study a much lower range from (5.0 to 25.0 mg) to (0.05 to 0.5 mg) of PMMA was probed. For excitation wavelength of 345 nm (**Figure 112**) for the amounts of 0.05 to 0.25 mg of PMMA the fluorescence output was the same. For 0.5 mg of PMMA its fluorescence however was higher in comparison to the other amounts used (**Figure 112**). At excitation wavelength of 305 nm (**Figure 112a**) the fluorescence output increased as the amount of PMMA increased
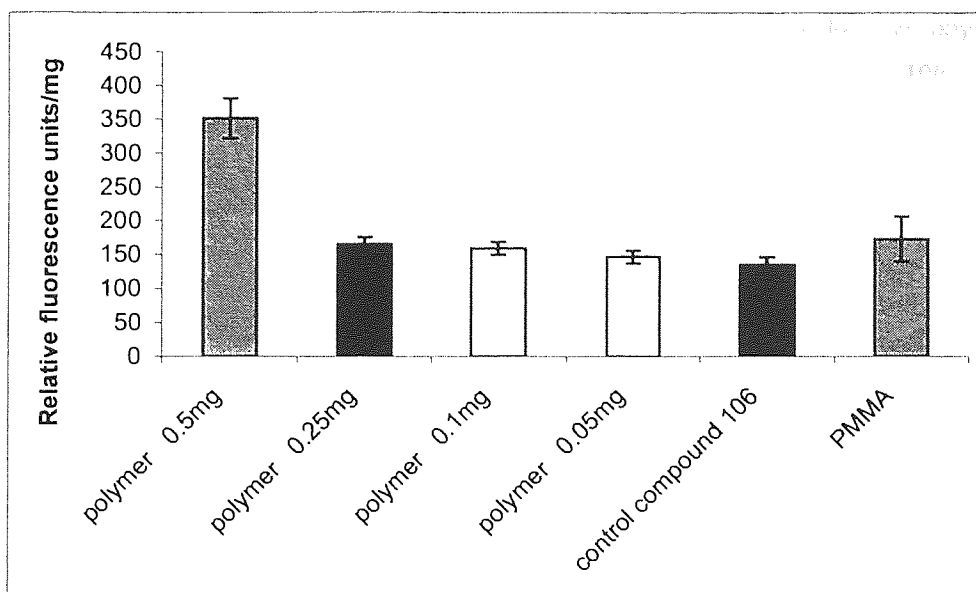
**Figure 112**: Barchart for polymer thin films (compound **106** with PMMA) and controls. ($\lambda_{ex}$ = 345 nm, $\lambda_{em}$ = 415 nm).
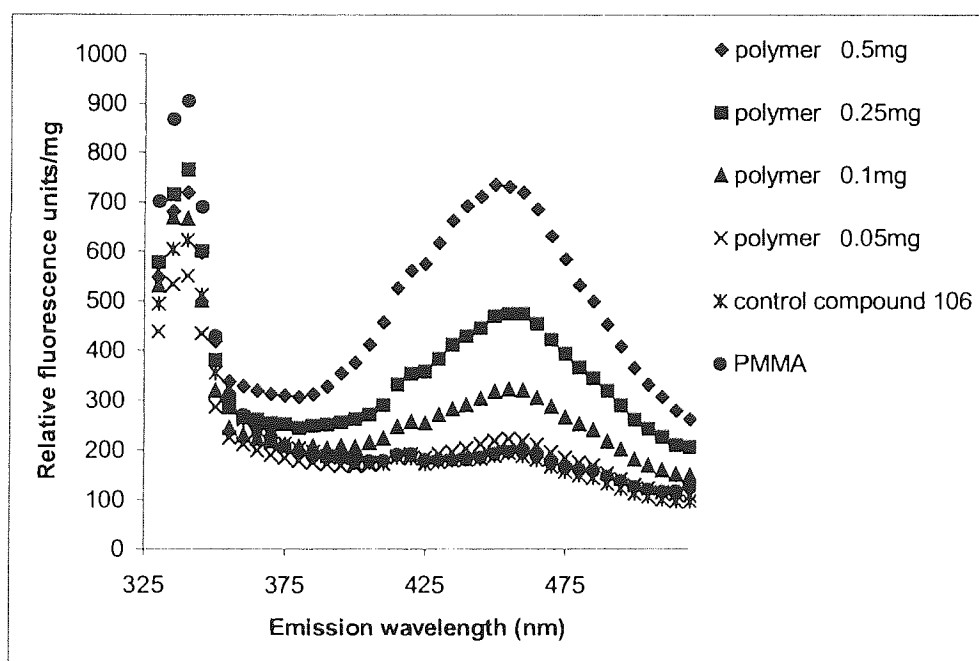


**Figure 112a**: Fluorescence spectra for polymer thin films (compound **106** with PMMA) and controls. ($\lambda_{ex}$ = 305 nm, $\lambda_{em}$ = 455 nm).

From the study using 0.001 mg of compound **106** at excitation wavelength of 345 nm for the higher range (5.0 to 25.0 mg) of PMMA no change in fluorescence was observed (**Figure 111**). At the lower range (0.05 to 0.5 mg) of PMMA the 0.5 mg gave a fluorescence output that was higher in count in comparison to the other amounts used (**Figure 112**). At excitation wavelength of 305 nm (**Figure 111a**) for the high range of PMMA, 5 mg of PMMA gave a higher fluorescence count in comparison to the other PMMA amounts i.e.10 to 25 mg. This could possibly be due to the fact that at 10 to 25 mg of PMMA, the amounts

of PMMA in the well are too concentrated for the compound **106** to have any affect owing to its low concentration within these wells i.e. no interaction of compounds **106** to cause fluorescence enhancement.

### 3.4.1.4  2-Acryloylamino-N-cyclododecyl-benzamide (compound 119) based hydrophobic pocket MIPs

To examine the selectivity/cross-reactivity profiles generated by the FFM, compound **119** (**Figure 96,** 3.4.1), a series of MIPs were synthesised. The preparation involved using compounds **128, 83, 85, 84, 81** and **127** as templates (**Figure 97**-structures, 3.4.1) and cross-linked with both the rigid (TMPTA) and flexible (TEGDMA) cross-linkers. This step was taken due to the previous practical extraction inadequacy with template **81**. The MIPs were synthesised in same manner as mentioned earlier. The optimum excitation wavelengths of 345 and 305 nm with their respective emissions at 415 and 455 nm were the parameters used to analyse the MIPs (Procedure 1 refer to 4.1). Note, that these parameters were established by the study performed on the FFM, compound **106** as discussed in the dual fluorophore section (3.3.2).

### 3.4.1.4.1 MIP11 templated with compound 128
### 3.4.1.4.1.1 MIP11 cross-linked with TMPTA

**MIP11** {5.4.15} was constructed with template **128** (**Figure 97**-structure, 3.4.1) and **119** (**Figure 96**-structure, 3.4.1) as the FFM, and it was assumed that due to the template being of a small size the cavity created by this would be selective in what it would allow into its cavity to quench its fluorescence. The other assumption was that its structural conformation would be limited which again would help make this MIP more selective.

At excitation wavelength of 345 nm (**Figure 113a**), **MIP11** exposed to its own template and the other test compounds, some suffered fluorescence enhancement to various extents and others gave fluorescence outputs that were similar to the untreated polymer. From **Figure 113a** the imprinted polymer shows some selectivity by rejecting the compounds **85, 88** and **89** (**Figure 97**-structures, 3.4.1). The fluorescence study performed on these compounds (**Figure 101**, 3.4.1.2) established very little fluorescence output and so selectivity by the MIP towards them could be possible. Then again assessing the fluorescence output of the template itself from the fluorescence study (**Figure 101**, 3.4.1.2) revealed also a very low fluorescence output, and so whether this MIP demonstrated selectivity towards the outlined compounds is questionable.

Exciting the same **MIP11** at a wavelength of 305 nm gave an overall similar fluorescence output and no indication of selectivity could be observed (**Figure 113b**).

**Figure 113a**: Fluorescence output of **MIP11** cross-linked with TMPTA. The error bars are the standard deviations of duplicate wells. $\lambda_{ex}$ = 345 nm, $\lambda_{em}$ = 415nm.



**Figure 113b**: Fluorescence output of **MIP11** cross-linked with TMPTA. The error bars are the standard deviations of duplicate wells. $\lambda_{ex}$ = 305 nm, $\lambda_{em}$ = 455nm.

### 3.4.1.4.2 MIP12 templated with compound 81

### 3.4.1.4.2.1 MIP12 cross-linked with TMPTA

The result for the **MIP12** {5.4.16} synthesised with the rigid cross-linker showed no selectivity at either excitation/emission wavelength pairs of 345nm/415 nm and 305nm/455 nm (**Figure 114a** and **114b**). This result most likely was caused by inadequate extraction of the template **81** (**Figure 97**-structure, 3.4.1) and so the fluorescence output measured was characteristic of the template itself.

**Figure 114a**: Fluorescence output of **MIP12** cross-linked with TMPTA. The error bars are the standard deviations of duplicate wells. $\lambda_{ex}$ = 345 nm, $\lambda_{em}$ = 415nm.



**Figure 114b**: Fluorescence output of **MIP12** cross-linked with TMPTA. The error bars are the standard deviations of duplicate wells. $\lambda_{ex}$ = 305 nm, $\lambda_{em}$ = 455nm.

### 3.4.1.4.3 MIP13 templated with compound 81

### 3.4.1.4.3.1 MIP13 cross-linked with TEGDMA

The result for the **MIP13** {5.4.17} synthesised with the flexible cross-linker (**MIP13**) showed no selectivity for most of the compounds at excitation/emission wavelengths pairs of 345 nm/415 nm and 305 nm/455 nm (**Figure 114c** and **114d**). Note, that the fluorescence of the extracted polymer i.e. untreated polymer is low at excitation wavelength of 305 nm (**Figure 114c**), thus indicating that the template is still trapped in the MIP cavities.

197

At excitation wavelength of 345 nm (**Figure 114c**) compound **81** (**Figure 97**-structure, 3.4.1) exposed to its empty MIP exhibited fluorescence enhancement. This result however causes the question to arise on whether the test compound has or has not entered the MIP cavity. So the result presented in **Figure 114c** is ambiguous and can be supported by the previous fluorescence study performed on this compound (**Figure 101**, 3.4.1.2). At this particular excitation wavelength of 305 nm the compound itself had considerable fluorescence output and so could be contributing towards the fluorescence output that is observed.

The MIP rejected the test compounds **87, 92, 90** and **89** (**Figure 97**-structures, 3.4.1). The fluorescence study performed on these compounds (**Figure 101**, 3.4.1.2) revealed very low fluorescence outputs and the results presented in **Figure 114c** most likely represent a combination of the test compound and the template fluorescence output. This can be supported by the fact that the untreated polymer in **Figure 114c** exhibited very low fluorescence output.

At excitation wavelength of 305 nm (**Figure 114d**) all test compounds give a similar fluorescence output.



**Figure 114c**: Fluorescence output of **MIP13** cross-linked with TEGDMA. The error bars are the standard deviations of duplicate wells. $\lambda_{ex}$ = 345 nm, $\lambda_{em}$ = 415nm.
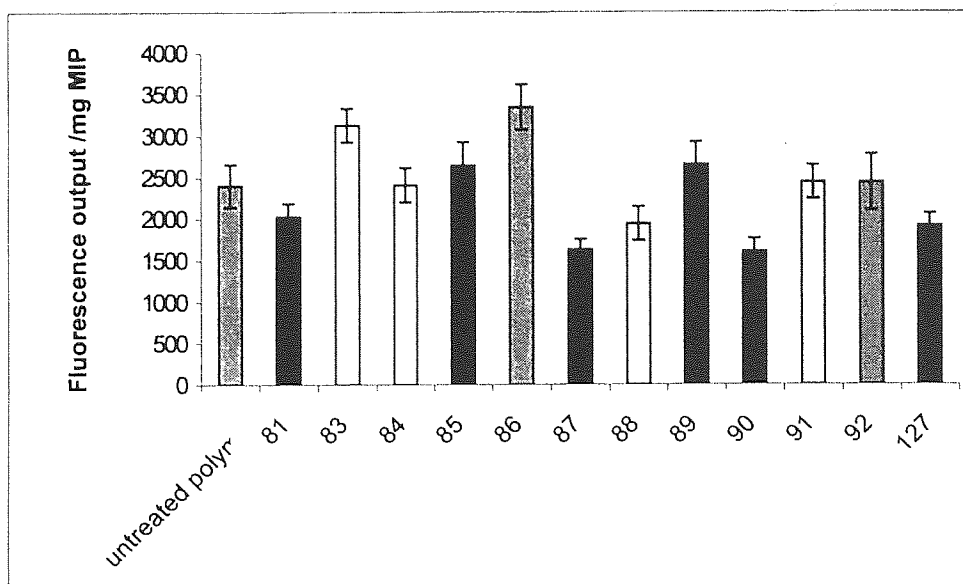
**Figure 114d**: Fluorescence output of **MIP13** cross-linked with TEGDMA. The error bars are the standard deviations of duplicate wells. $\lambda_{ex}$ = 305 nm, $\lambda_{em}$ = 455nm.

The reason for observing such a result for both cross-linkers is linked to the fact that extraction of template **81** from its corresponding MIP was most likely inadequate, even though a change from a rigid to a flexible cross-linker was made. The fluorescence being observed was characteristic of the template instead of the empty MIP (**Figures 114a & 114b** and **114c & 114d**). The fact that the extracted MIPs gave low fluorescence outputs indicated that the template was still trapped within the matrix and quenching the fluorescence of the MIP-bound fluorophore.

### 3.4.1.4.4 MIP14 templated with compound 83

### 3.4.1.4.4.1 MIP14 cross-linked with TMPTA

**MIP14** {5.4.18} was constructed with template **83** (**Figure 97**-structure, 3.4.1) and **119** (**Figure 96**-structure, 3.4.1) as the FFM and from **Figure 115a** (excitation wavelength of 345nm) it can be seen that **MIP14** is not selective. The empty MIP allows the original template as well as the other test compounds to quench its fluorescence at various extents. Compound **81** (**Figure 97**, 3.4.1) on the other hand does not quench the fluorescence of the MIP-bound fluorophore. The result for this test compound however causes the question to arise on whether the compound has or has not entered the MIP cavity. The reason for this uncertainty in the result observed for this compound relates to the fact that by referring back to the fluorescence study performed on this compound (**Figure 101**, 3.4.1.2), at this particular excitation wavelength the compound itself had considerable fluorescence output. Thus the compound may have entered the cavity but due to its own fluorescence output at this wavelength potential fluorescence quenching is masked or there is even fluorescence enhancement. Conversely the compound may not have entered the cavity at all.

The profile created by **MIP14** at excitation wavelength 305 nm exhibited a fluorescence enhancement i.e. above the fluorescence output of the empty MIP (**Figure 115b**). This fluorescence enhancement is due to the recognition event taking place.
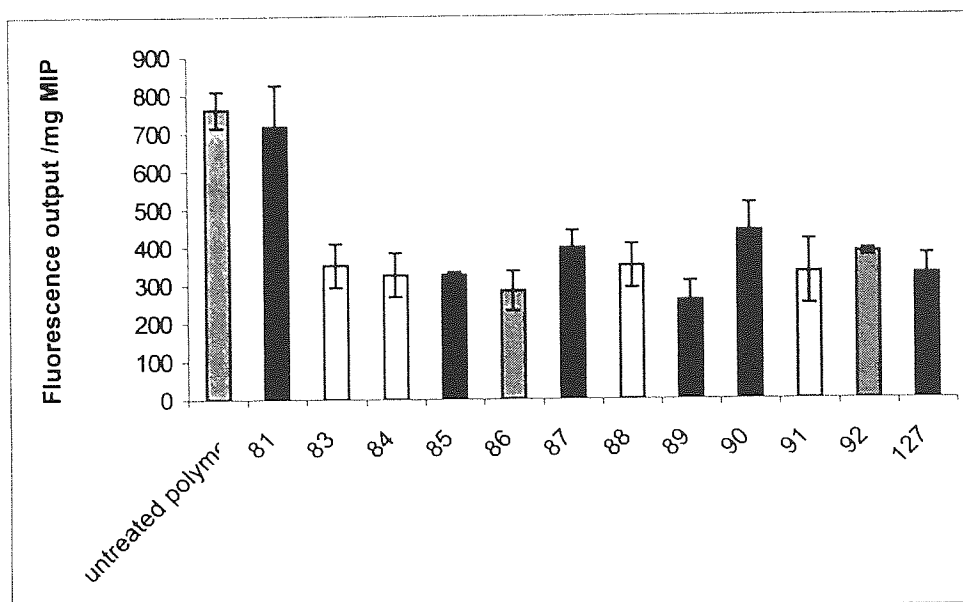


**Figure 115a**: Fluorescence output of **MIP14** cross-linked with TMPTA. The error bars are the standard deviations of duplicate wells. $\lambda_{ex}$ = 345 nm, $\lambda_{em}$ = 415 nm .
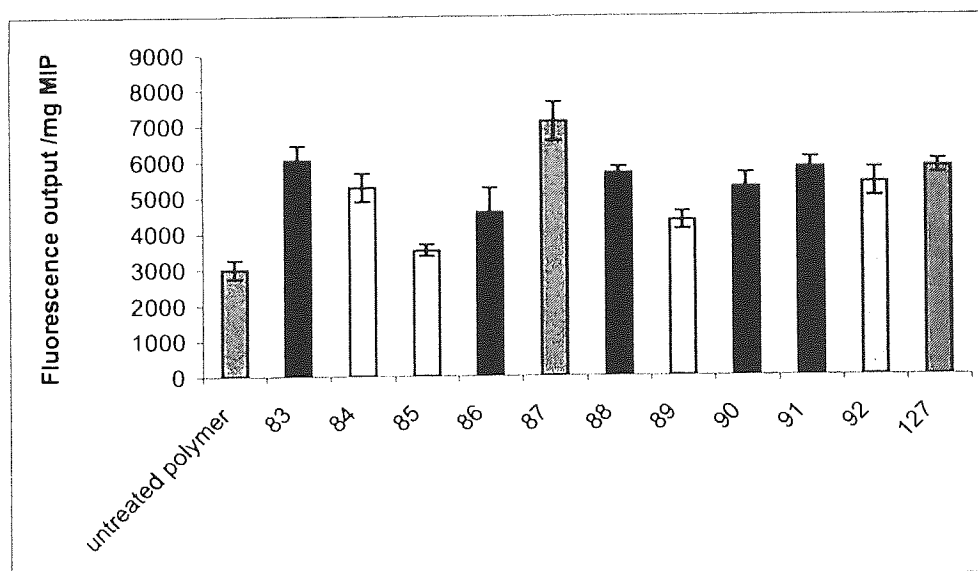


**Figure 115b**: Fluorescence output of **MIP14** cross-linked with TMPTA. The error bars are the standard deviations of duplicate wells. $\lambda_{ex}$ = 305 nm, $\lambda_{em}$ = 455nm.

### 3.4.1.4.5 MIP15 templated with compound 83

### 3.4.1.4.5.1 MIP15 cross-linked with TEGDMA

**MIP15** {5.4.19} synthesised with the flexible cross-linker and excited at a wavelength of 345nm. The results are presented in **Figure 115c**. At this wavelength the exposure of test compounds to the MIP showed fluorescence enhancement. Again this observed enhancement is due to the recognition event

taking place. At an excitation wavelength of 305 nm the original template quenches the fluorescence of the MIP though to a lesser extent in comparison to the other test compounds, which quench more (**Figure 115d**). In general this MIP exhibits a non-selective profile.
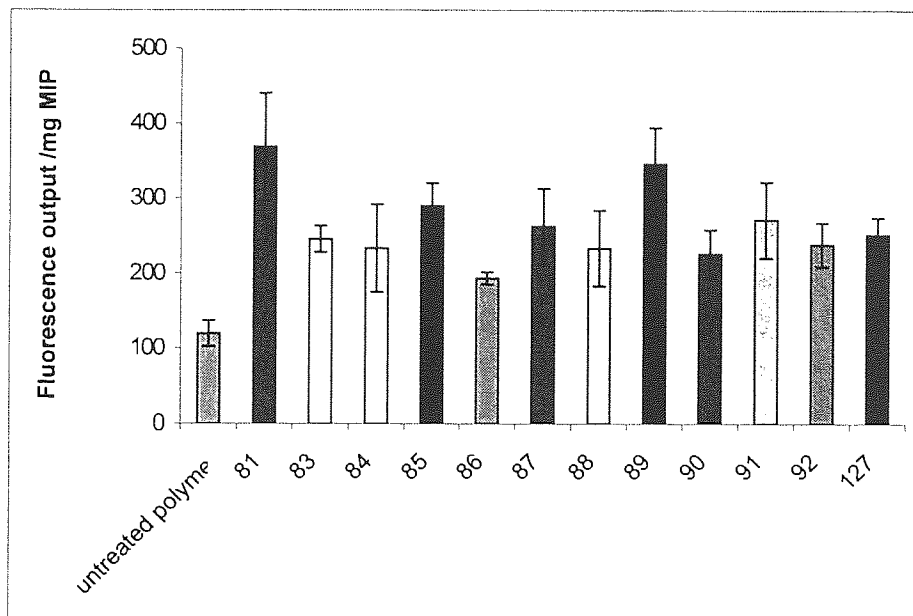


**Figure 115c**: Fluorescence output of **MIP15** cross-linked with TEGDMA. The error bars are the standard deviations of duplicate wells. $\lambda_{ex}$ = 345 nm, $\lambda_{em}$ = 415nm.
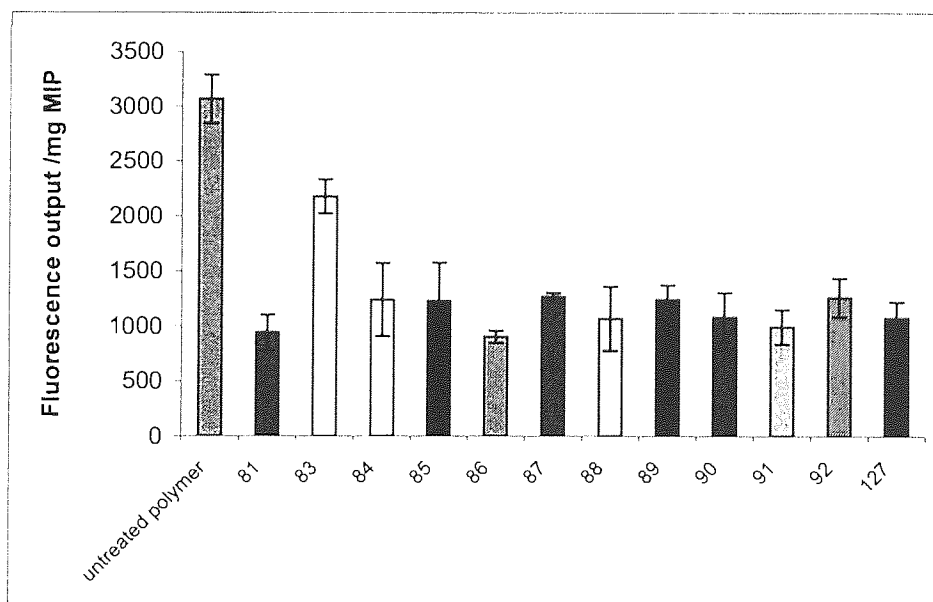


**Figure 115d**: Fluorescence output of **MIP15** cross-linked with TEGDMA. The error bars are the standard deviations of duplicate wells. $\lambda_{ex}$ = 305 nm, $\lambda_{em}$ = 455 nm .

**3.4.1.4.6 MIP16 templated with compound 85**

**3.4.1.4.6.1 MIP16 cross-linked with TMPTA**

MIP16 {5.4.20} was created by templating compound **85** (**Figure 97**-structure, 3.4.1). **Figure 116a** (excitation wavelength of 345nm) demonstrates clearly that this MIP is non-selective in that its own

template and most test compounds quench its fluorescence. Compounds **81** and **91** (**Figure 97**-structures, 3.4.1) at this wavelength appear to be discriminated against. For compound **81** the question arises as to whether the compound has or has not entered the MIP cavity and so renders the result ambiguous. The ambiguity in this result is due to the fact that the fluorescence study performed on this compound (**Figure 101**, 3.4.1.2), at this particular excitation wavelength, the test compound itself had considerable fluorescence output. Thus the compound may have entered the cavity but due to its own fluorescence output at this wavelength this event is not being observed. Though at the same time the compound may not have entered the cavity at all (**Figure 116a**). As for compound **91** comparing this to its related compound **86** (only difference being the position of the nitrogen on the benzene ring, (**Figure 97**-structure, 3.4.1) this compound has not entered the cavity. The reason that may have led compound **86** to be rejected by the MIP-cavity, is due to the fact that the template (**85**) that has the nitrogen at position 2 has created the cavity that is compatible for test compounds that also have the nitrogen at position 2 i.e. ease of forming hydrogen-bonding with the hydrogen donor on the FFM, compound **119**.Thus the test compound that has the nitrogen at position 4 i.e. **86** has geometrical problems when attempting to hydrogen-bond with the cavity-bound fluorophore (**Figure 97**-structures, 3.4.1).

At excitation wavelength 345 nm this MIP rejected **91** but accepted **86** where a better hydrogen-bonding interaction with the cavity-bound fluorophore might be possible. It is surprising, however, that this effect was not also seen at excitation wavelength of 305 nm. At excitation wavelength of 305 nm again no selective absorption of test compound was observed since all test compounds caused fluorescence quenching (**Figure 116b**). On the whole this MIP showed a non-selective profile.
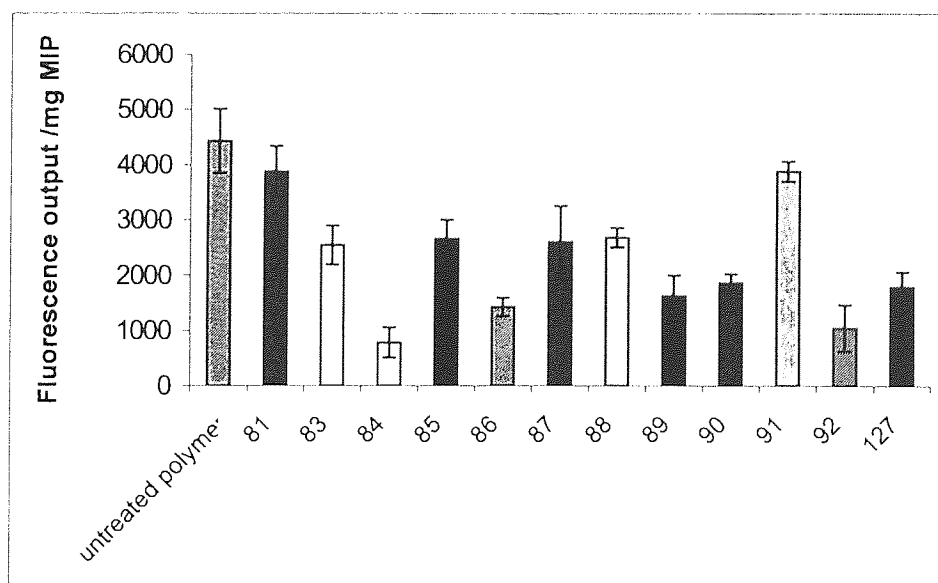


**Figure 116a**: Fluorescence output of **MIP16** cross-linked with TMPTA. The error bars are the standard deviations of duplicate wells. $\lambda_{ex}$ = 345 nm, $\lambda_{em}$ = 415nm.
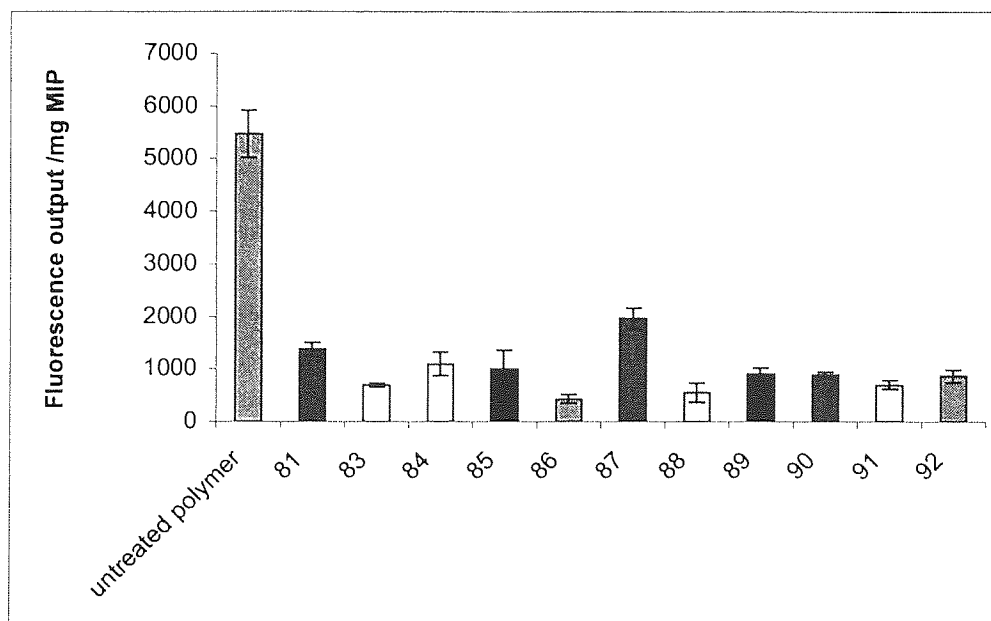
**Figure 116b**: Fluorescence output **MIP16** cross-linked with TMPTA. The error bars are the standard deviations of duplicate wells. $\lambda_{ex}$ = 305 nm, $\lambda_{em}$ = 455nm.

### 3.4.1.4.7 MIP17 templated with compound 85
### 3.4.1.4.7.1 MIP17 cross-linked with TEGDMA

**MIP17** {5.4.21} cross-linked with the flexible cross-linker exhibited an overall similar fluorescence output at excitation wavelength of 345 nm (**Figure 116c**) for all of the test compounds and its original template.

At excitation wavelength 305 nm (**Figure 116d**) most of the test compounds quenched the fluorescence of the MIP cavity. The original template, compound **85**, however, was not recognised by its own MIP and the other test compounds like **83**, **81** and **91** were rejected by the MIP cavity (**Figure 97**-structures, 3.4.1).

The rejection of compound **91** and acceptance of the related compound **86** by the MIP cavity, relates to the fact that a better hydrogen-bonding interaction with the cavity-bound fluorophore might be possible with **86**. Even though template **85** that has the nitrogen at position 2 was employed. The same reason can also be linked to the rejection of compound **83**.

203
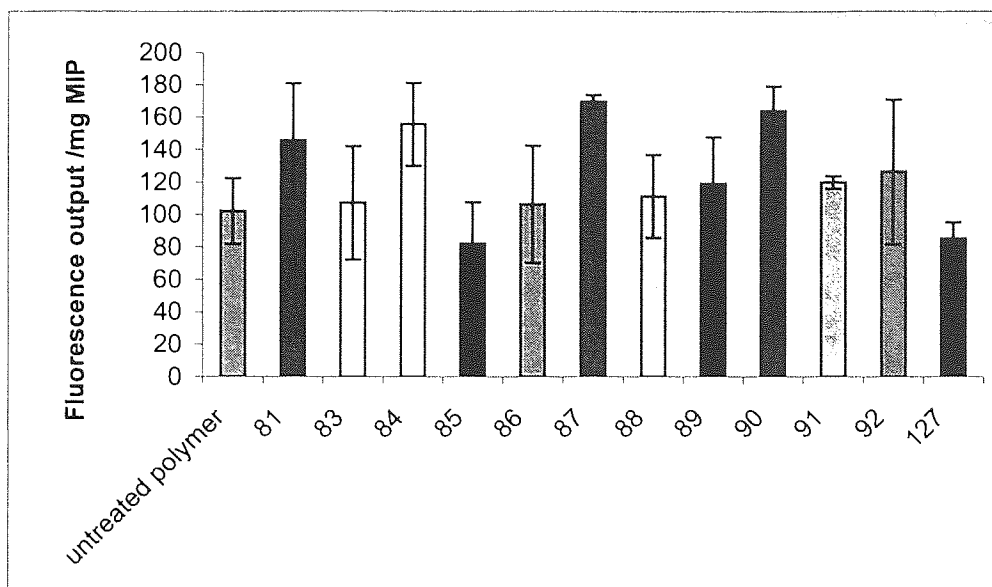
**Figure 116c**: Fluorescence output of **MIP17** cross-linked with TEGDMA. The error bars are the standard deviations of duplicate wells. $\lambda_{ex}$ = 345 nm, $\lambda_{em}$ = 415nm.
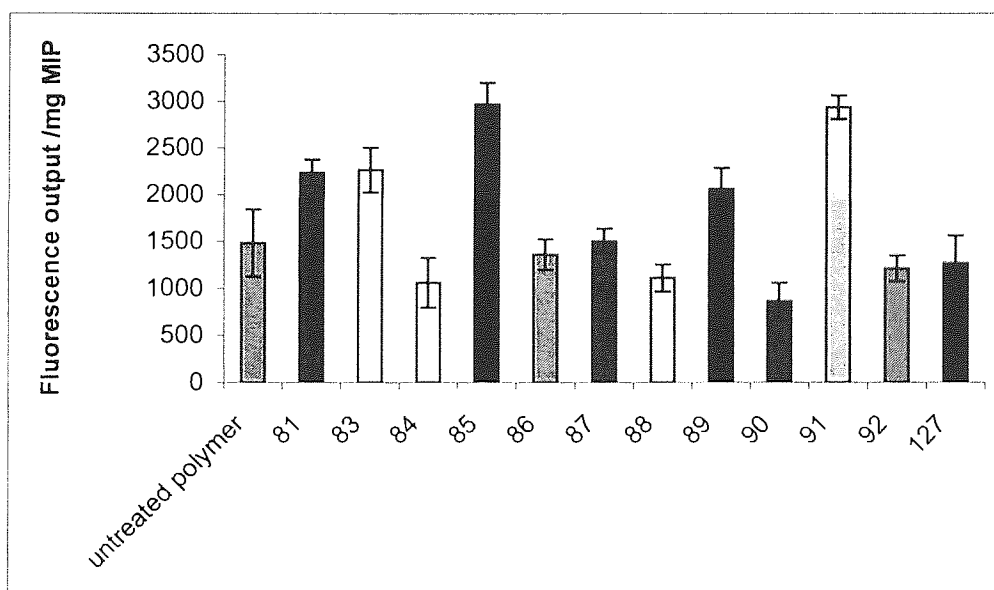


**Figure 116d**: Fluorescence relative to the empty **MIP17** cross-linked with TEGDMA. The error bars are the standard deviations of duplicate wells. $\lambda_{ex}$ = 305 nm, $\lambda_{em}$ = 455nm.

### 3.4.1.4.8 MIP18 templated with compound 84
### 3.4.1.4.8.1 MIP18 cross-linked with TMPTA

When inspecting the results for the **MIP18** {5.4.22} templated from **84** using the rigid cross-linker most compounds quenched the fluorescence at excitation/emission wavelengths of 345nm/415 nm (**Figure 117a**). For test compounds **81** and **127** (**Figure 97**-structures, 3.4.1) that do not quench the fluorescence of MIP-bound fluorophore this could be suggestive of the MIP demonstrating selectivity against them (i.e. the MIP is keeping the compound out). The rejection of compound **127** by the MIP can be supported by the fluorescence study performed on this compound at this particular excitation wavelength (**Figure 101**,

204

3.4.1.2). In this study **127** gave very little fluorescence output. Thus the result observed for **127** for this MIP demonstrates selectivity. For compound **81** the result observed for this is ambiguous. Since the fluorescence study performed on this compound (**Figure 101**, 3.4.1.2) revealed a considerable fluorescence output. Thus the question remains as to whether the compound has or has not entered the MIP cavity and so remains inconclusive.

At excitation/emission wavelengths of 305nm/455 nm the MIP shows selectivity against compounds **86, 87, 88, 91** and **83** (**Figure 97**-structures, 3.4.1). For **88** its phenanthracene group and for **86** and **91** their methoxymethyl-benzene groups, may cause hindrance when entering the MIP cavity (**Figure 117b**). The fluorescence contribution from these compounds is very little as determined by the fluorescence study (**Figure 101**, 3.4.1.2) and so selectivity by the MIP against these compounds could be likely.

As for compound **83**, the fluorescence study performed on this compound (**Figure 101**, 3.4.1.2), established that this test compound gave considerable fluorescence output at this wavelength (305/455nm). So the result presented for this in **Figure 117b** could be a representation of test compound fluorescence contribution and could imply that the compound may have been accepted by the MIP.
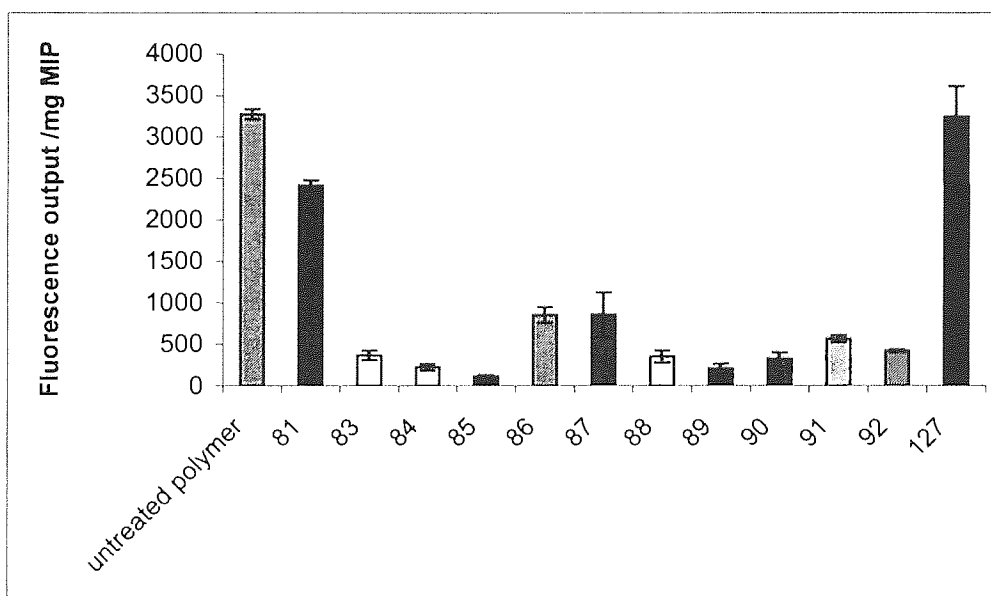


**Figure 117a**: Fluorescence output of **MIP18** cross-linked with TMPTA. The error bars are the standard deviations of duplicate wells. $\lambda_{ex}$ = 345 nm, $\lambda_{em}$ = 415nm.
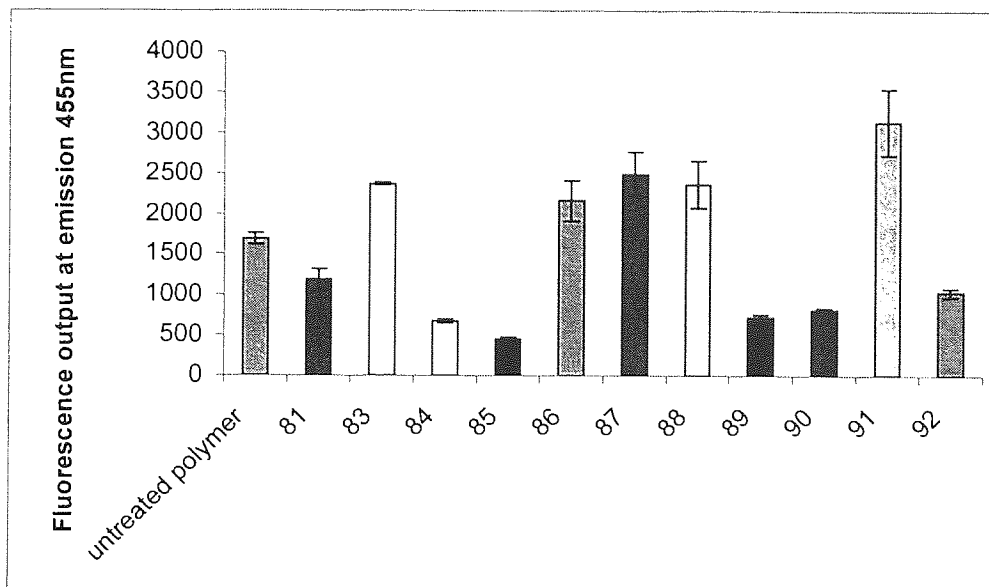
**Figure 117b**: Fluorescence output of **MIP18** cross-linked with TMPTA. The error bars are the standard deviations of duplicate wells. $\lambda_{ex}$ = 305 nm, $\lambda_{em}$ = 455nm.


### 3.4.1.4.9 MIP19 templated with compound 84
### 3.4.1.4.9.1 MIP19 cross-linked with TEGDMA

The results for the **MIP19** {5.4.23} synthesised with the flexible cross-linker shows a similar fluorescence response for most compounds at both excitation/emission wavelengths pairs of 345 nm/415 nm and 305 nm/455 nm (**Figure 117c** and **117d**).


The result for compound **81** (**Figure 97**-structure, 3.4.1) at excitation wavelength of 345 nm (**Figure 117c**) is ambiguous. This is supported by a previous fluorescence study performed on this compound (**Figure 101**, 3.4.1.2). At this particular excitation wavelength a considerable fluorescence output was observed. Thus the question arises on whether the compound has or has not entered the MIP cavity and so remains an inconclusive result.


At excitation wavelength of 305 nm (**Figure 117d**), **81** does not quench the fluorescence of the MIP. Here the MIP demonstrates selectivity against this compound. This can be supported by the fluorescence study performed on this compound (**Figure 101**, 3.4.1.2). At this specific excitation wavelength very little fluorescence output was observed. So the fluorescence that is observed for this compound in **Figure 117d** arises from the cavity-bound fluorophore and not the test compound. For compound **91** at excitation wavelength of 305 nm (**Figure 117d**) the result observed here represents selectivity towards this compound by the MIP i.e. rejected by the MIP-cavity. This is based on the suggestion that a related compound, **86**, might be able to better interact *via* hydrogen-bond with the cavity-bound fluorophore. Hence quenches the fluorescence of the MIP better than compound **91**, even though a template that had nitrogen at position 2 created the MIP-cavity.
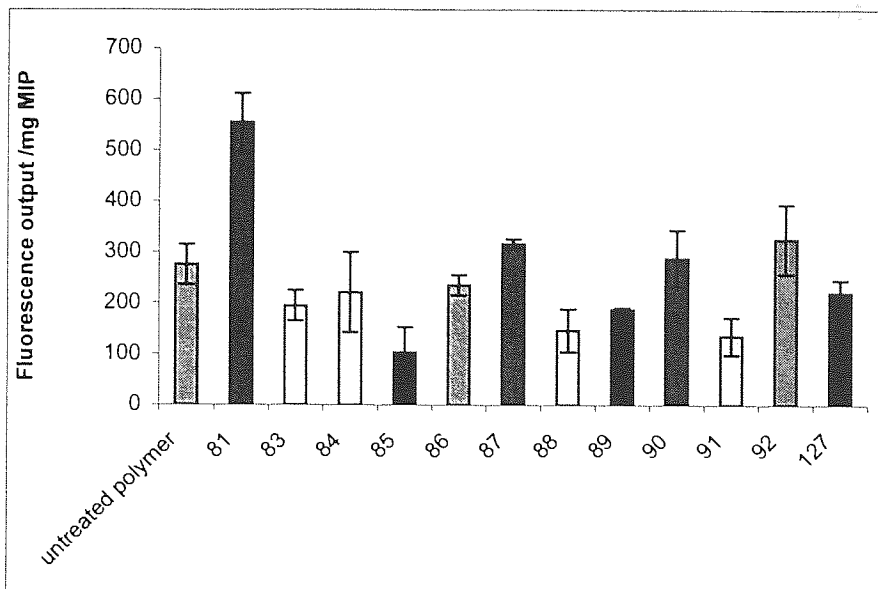
**Figure 117c**: Fluorescence relative to the empty **MIP19** cross-linked with TEGDMA. The error bars are the standard deviations of duplicate wells. $\lambda_{ex}$ = 345 nm, $\lambda_{em}$ = 415nm.
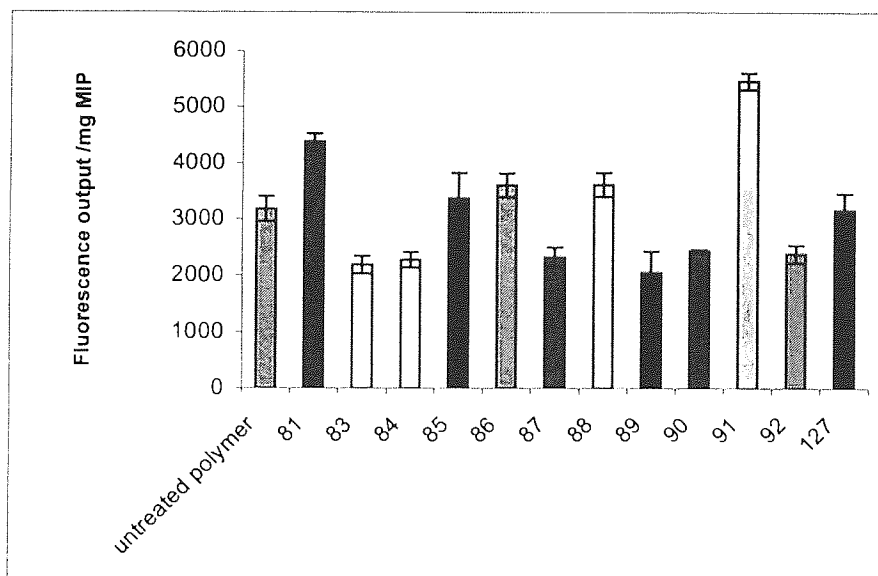


**Figure 117d**: Fluorescence output of **MIP19** cross-linked with TEGDMA. The error bars are the standard deviations of duplicate wells. $\lambda_{ex}$ = 305 nm, $\lambda_{em}$ = 455nm.

### 3.4.1.4.10 MIP20 templated with compound 127

### 3.4.1.4.10.1 MIP20 cross-linked with TMPTA

**MIP20** {5.4.24} derived from a rigid cross-linker was non-selective for most compounds at excitation/emission wavelength pairs of 345 nm/415 nm and 305 nm/455 nm (**Figure 118a** and **118b**). The MIP in addition also allowed the original template to quench its fluorescence.

At the excitation/emission wavelengths of 345 nm/415 nm the MIP was selective for all test compounds i.e. MIP accepted. At the excitation/emission wavelength of 305 nm/455 nm the fluorescence output of

most of the test compounds was similar. On the other hand, compound **85** at this wavelength was able to quench the fluorescence of the MIP-cavity.
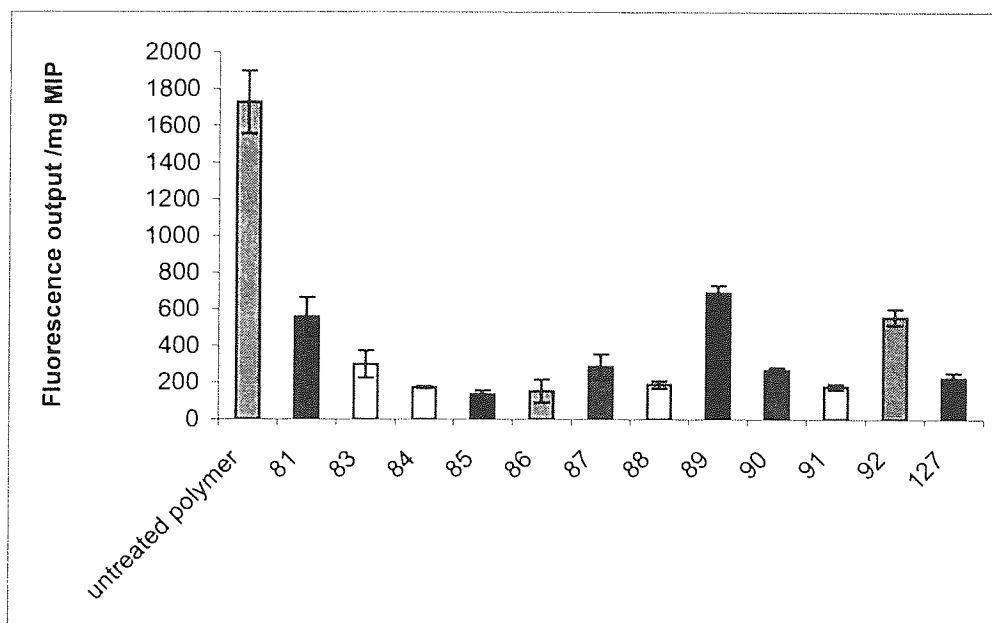


**Figure 118a**: Fluorescence output of **MIP20** cross-linked with TMPTA. The error bars are the standard deviations of duplicate wells. $\lambda_{ex}$ = 345 nm, $\lambda_{em}$ = 415nm.
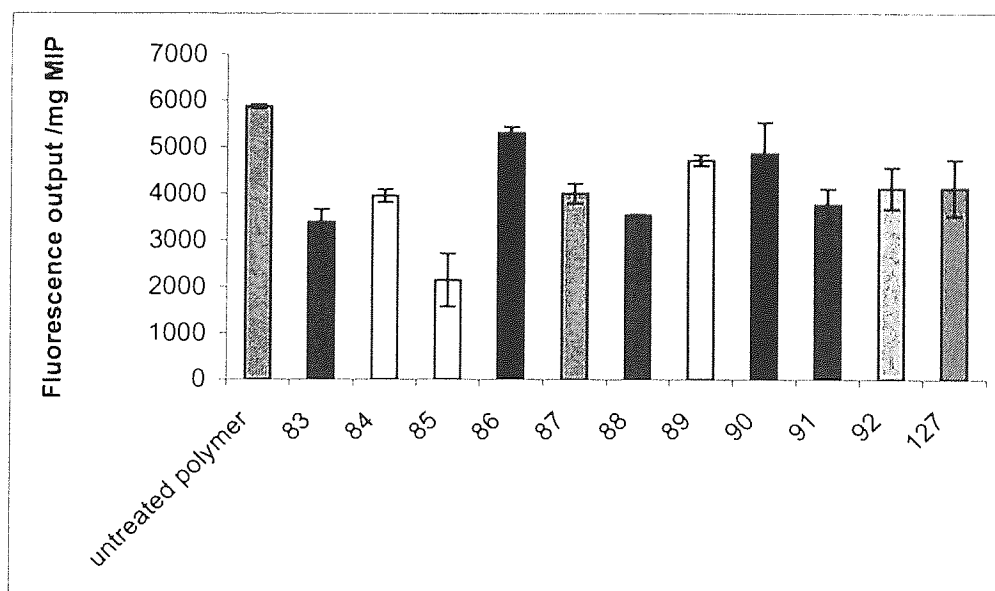


**Figure 118b**: Fluorescence output of **MIP20** cross-linked with TMPTA. The error bars are the standard deviations of duplicate wells. $\lambda_{ex}$ = 305 nm, $\lambda_{em}$ = 455nm.

### 3.4.1.4.11 MIP21 templated with compound 127

### 3.4.1.4.11.1 MIP21 cross-linked with TEGDMA

The results derived from the flexible cross-linker demonstrated that the **MIP21** {5.4.25} was non-selectivity at both excitation/emission wavelength pairs of 345 nm/415 nm and 305 nm/455 nm (**Figure 118c** and

**118d**). At excitation wavelength of 345 nm (**Figure 118c**) compound **81** exhibited a significant fluorescence enhancement over the empty MIP. This compound is known to fluoresce considerably at this excitation/emission wavelength, as determined by the fluorescence study (**Figure 101**, 3.4.1.2). Thus this result eliminates any ambiguity. At excitation wavelength of 305 nm (**Figure 118d**) all compounds give a similar fluorescence output.
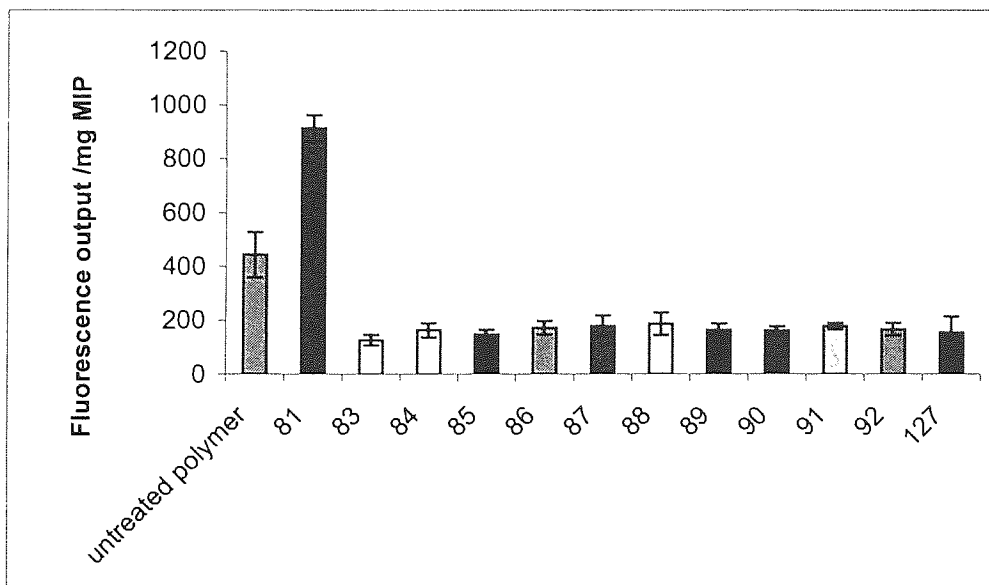


**Figure 118c**: Fluorescence relative to the empty **MIP21** cross-linked with TEGDMA. The error bars are the standard deviations of duplicate wells. $\lambda_{ex}$ = 345 nm, $\lambda_{em}$ = 415nm.
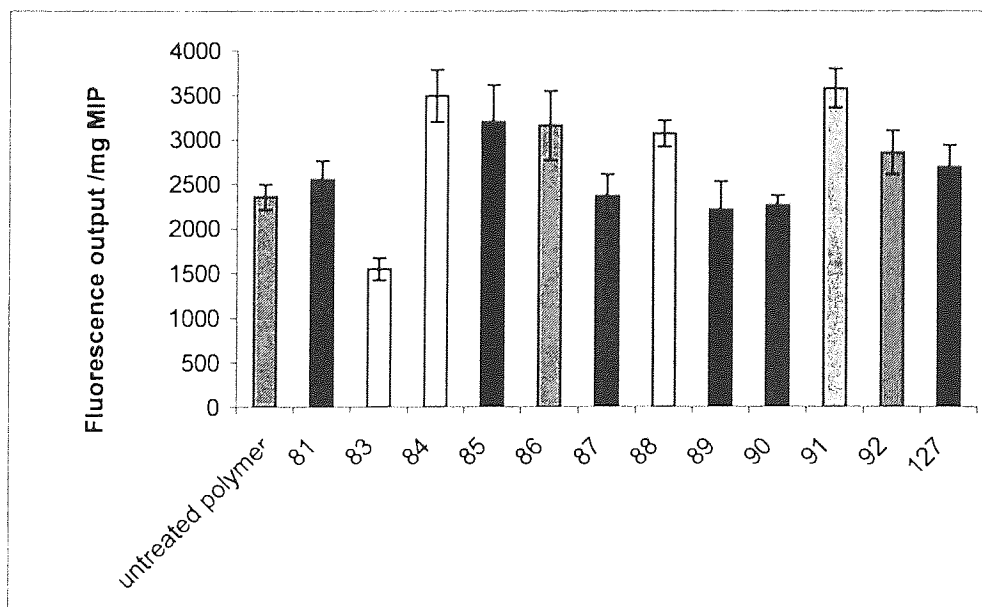

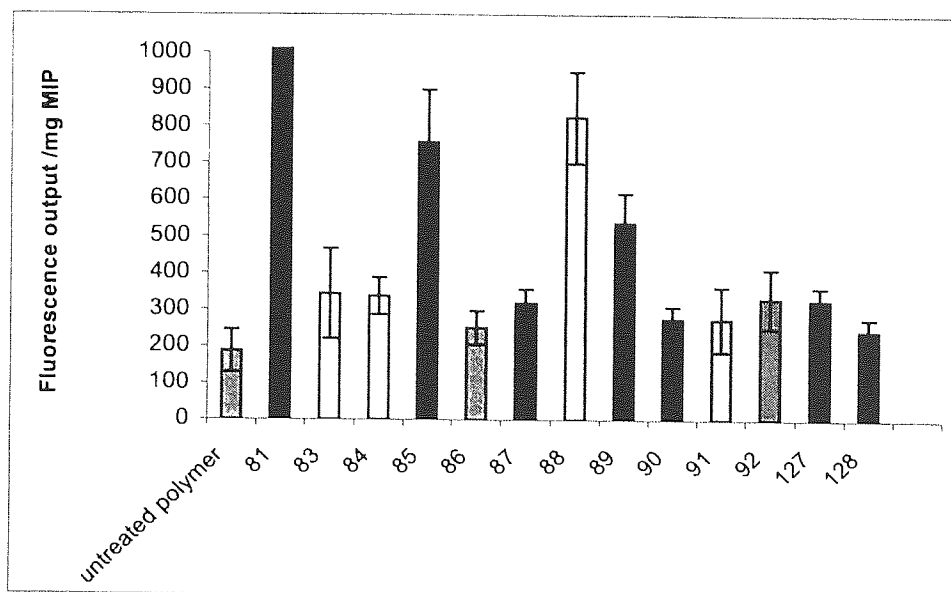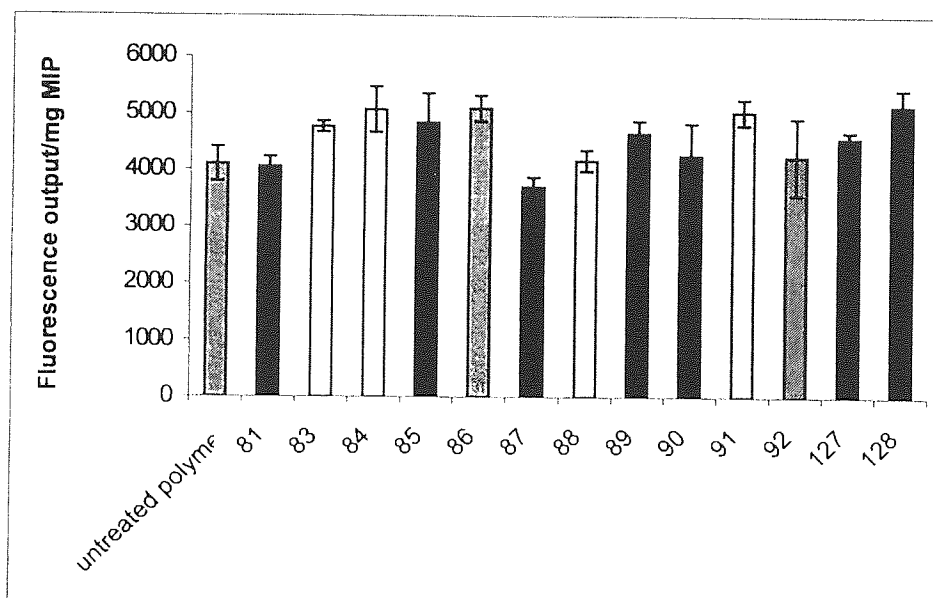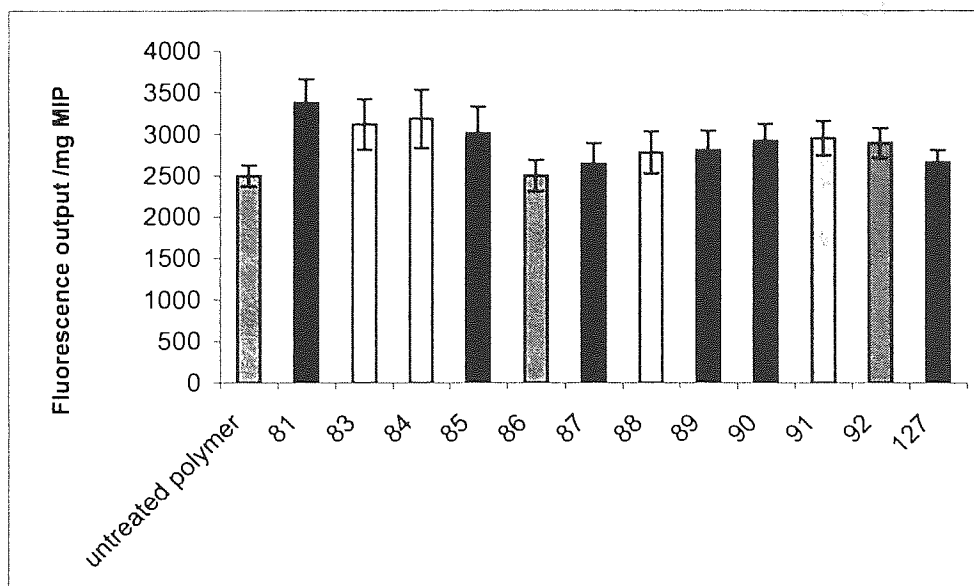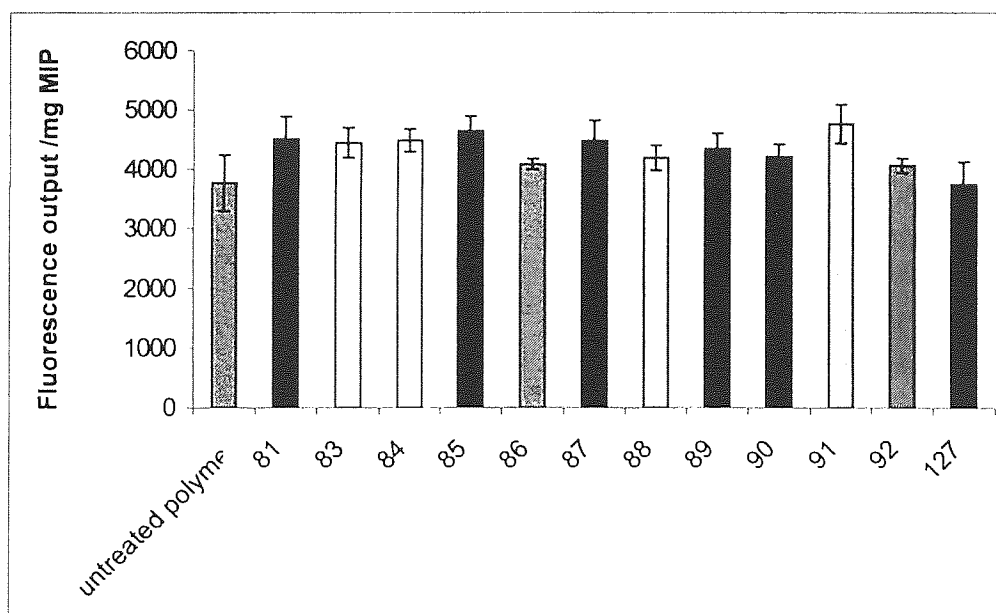
**Figure 118d**: Fluorescence output of **MIP21** cross-linked with TEGDMA. The error bars are the standard deviations of duplicate wells. $\lambda_{ex}$ = 305 nm, $\lambda_{em}$ = 455nm.

Overall most of the MIPs' selectivity/cross-reactivity profiles indicated that compound **119** was not a suitable FFM to create selective MIPs with, as on exposure the MIPs would allow all test compounds to

quench or enhance their fluorescence. The selectivity/cross-reactivity profile formed by the **MIP18** produced by the rigid cross-linker, however suggested that some selectivity could be observed at excitation/emission wavelengths of 345nm/415nm.

### 3.4.2 Varied hydrophobic pocket size

To vary the size of the hydrophobic pocket two cyclic-amines were incorporated into isatoic anhydride *via* amination to afford compounds **124** {5.3.34} and **123** {5.3.33} (**Scheme 5**, 3.4.1). The aminated products **124** and **123** were further acylated with acryloyl chloride to give the polymerisable compounds **127** {5.3.37} and **126** {5.3.36} respectively (**Scheme 5**, 3.4.1). The effects that pocket (ring) size has on binding characteristics of the MIPs derived there from were not investigated due to the fact that the MIP profile obtained for the related compound **119** (**Figure 96**, 3.4.1) demonstrated that this afforded non-selective MIPs and was thus not suitable as a FFM to give selective MIPs.

### 3.4.3 Investigating the use of a very flexible hydrophobic chain in a functional monomer that is comparable to the fluorescent functional monomer, compound 119
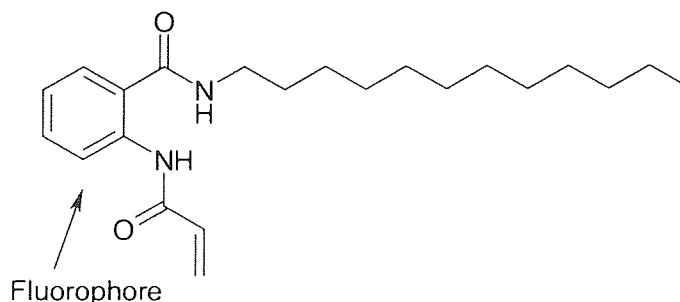


**Figure 119**: 2-acryloylamino-N-dodecyl-benzamide, compound **126**.

To further examine the results obtained for the selective MIP (**MIP18**) {5.4.22}, the same template **84** (**Figure 97**, 3.4.1) was used and instead of using compound **119** (2-Acryloylamino-N-cyclododecyl-benzamide) (**Figure 96**, 3.4.1), compound **126** (**Figure 119**) a polymerisable fluorescent functional monomer containing an unbranched dodecyl chain was used and cross-linked with trimethylolpropane triacrylate (TMPTA) in toluene (**MIP22**) {5.4.26}.

This was processed as described previously and exposed to the panel of test compounds listed within **Figure 120a**.

At excitation/emission wavelength of 345/415 nm (**Figure 120a**) the fluorescence of the empty MIP was very low. So the results observed for this MIP would be difficult when assessing if a test compound has or has not entered the MIP-cavity. Exposure to the template and test compounds resulted in fluorescence enhancement. The fluorescence output of the empty MIP was higher at excitation/emission wavelength of 305/455 nm (**Figure 120b**) and exposure to the template and test compounds had hardly any effect.

Note, that the MIP did not quench compound **81** (**Figure 97**-structure, 3.4.1) even though it was assumed that the flexibility for a straight 12-carbon chain (n-dodecylamine) in comparison to the cyclododecylamine

present in compound **119** would accommodate the large pyrenyl moiety found on the **81** (**Figure 120a**). Referring back to the fluorescence study performed on this compound (**Figure 101**, 3.4.1.2) msay at this particular excitation wavelength of 345 nm the compound itself had considerable fluorescence output. Comparing the fluorescence change of **81** relative to the empty MIP might signify, that the test compound may have been accepted by the MIP-cavity.
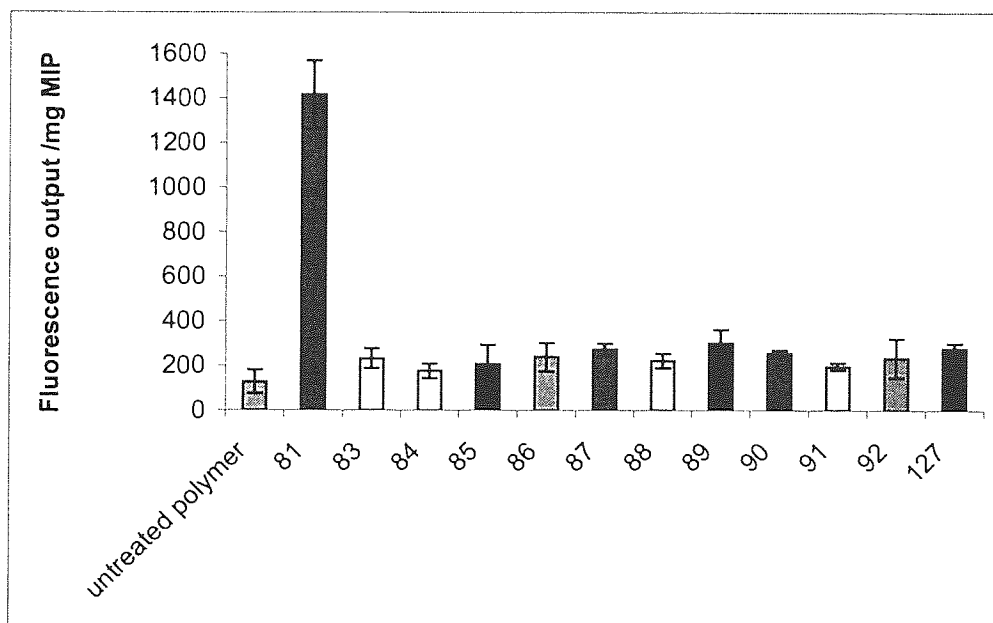


**Figure 120a**: Fluorescence output of **MIP22** cross-linked with TMPTA. The error bars are the standard deviations of duplicate wells. $\lambda_{ex}$ = 345 nm, $\lambda_{em}$ = 415nm.
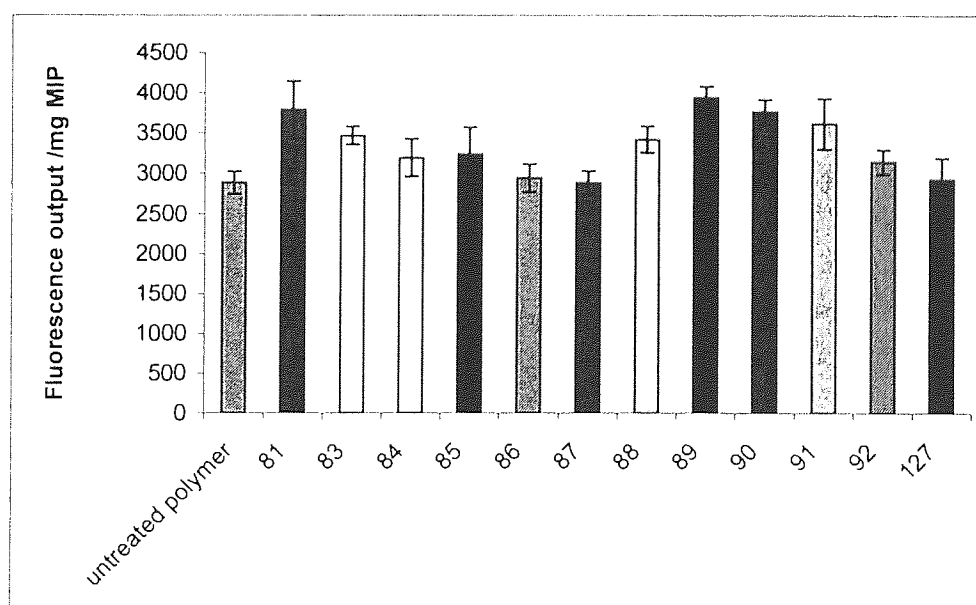


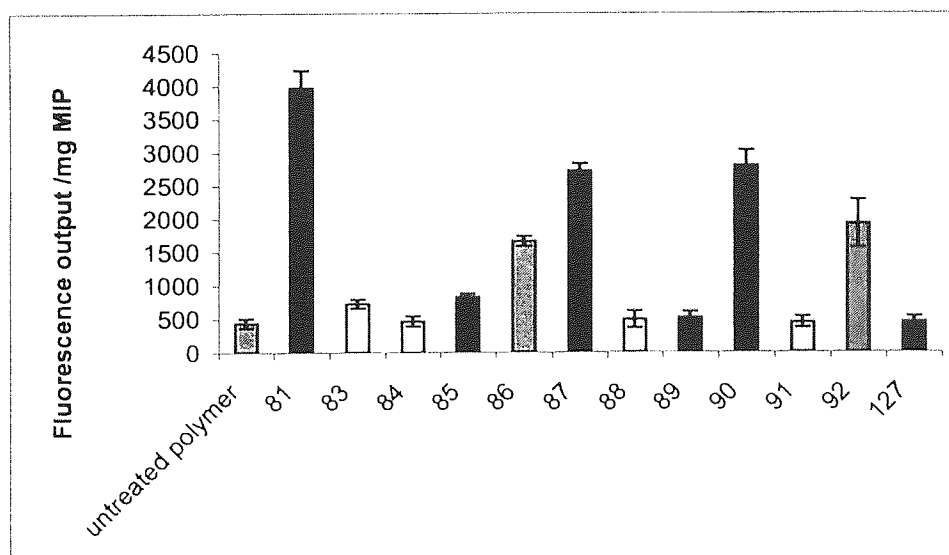**Figure 120b**: Fluorescence output of **MIP22** cross-linked with TMPTA. The error bars are the standard deviations of duplicate wells. $\lambda_{ex}$ = 305 nm, $\lambda_{em}$ = 455nm.

### 3.4.4 Cyclododecylamine based hydrophobic pocket MIP templated with 84 (MIP23) in a polar solvent (methanol)

In light of the lack of selectivity observed so far with MIPs created using 2-acryloylamino-N-cyclododecyl-benzamide, compound **119** {5.3.31} (**Figure 96**, 3.4.1) and 2-acryloylamino-N-cyclododecyl-benzamide, compound **128** {5.3.38} (**Figure 119**-structure) as fluorescent functional monomers, it was decided to conduct the imprinting and recognition studies in the more polar solvent i.e. methanol, in place of toluene. This was in order to enhance the possibility of any hydrophobically induced recognition processes.

The solvent has a great affect on the strength of non-covalent interactions, as well as influencing the polymer morphology (Sellergren and Shea, 1993). In general, the more polar the porogen, the weaker the resulting recognition effect becomes, this as a result of the affect of the solvents polarity on non-covalent interactions.

The best imprinting porogens, which emphasise the binding strengths in polar interactions, are solvents of very low dielectric constant, such as toluene and dichloromethane. Note, that the former solvent has been used for the MIPs templated with **84** (**Figure 97**, 3.4.1). The use of more polar solvents weakens the polar interactions formed between the template and the functional monomer resulting in poorer recognition.

The study involved constructing a MIP with **119** as the FFM and **84** as the template, cross-linked with trimethylolpropane triacrylate (TMPTA) in a polar solvent (methanol).

**MIP23** was processed as described previously and exposed to the panel of test compounds listed within **Figure 121a** in methanol.

After inspecting the results it was found that at both excitation/emission wavelength pairs of 345 nm/415 nm and 305 nm/455 nm (**Figure 121b** and **121b**), the **MIP23** {5.4.27} generated in methanol was non-selective. In contrast, the **MIP18** synthesised in toluene, demonstrated selectivity and gave a greater extent of quenching for its template and test compounds (**Figure 121a** and **Figure 122a**). More specifically at excitation/emission wavelength of 345 nm/415 nm for **MIP18** it showed some selectivity against test compound **127** (**Figure 121a**) (**Figure 97**-structure, 3.4.1). This selectivity demonstrated by the MIP towards compound **127**, can be supported by the fluorescence study performed on this compound (**Figure 101**, 3.4.1.2). The study established very little fluorescence output at this particular wavelength. As for **MIP23** at this wavelength the overall fluorescence output is same for the template and test compounds (compare **Figure 121a** for **MIP18** with **Figure 121b** for **MIP23**).

At excitation/emission wavelength of 305 nm/455 nm for **MIP18** (**Figure 122a**) compounds **86, 87** and **83** (**Figure 97**-structure, 3.4.1) exhibited fluorescence enhancement, which occurred as a result of absorption of the compound. Note that the fluorescence contribution from the compounds **86** and **87** is very little as determined by the fluorescence study performed on these compounds (**Figure 101**, 3.4.1.2). Compound

**83** at this wavelength (305/455nm) gave considerable fluorescence output as determined by the fluorescence study (**Figure 101**, 3.4.1.2). So the result presented for this in **Figure 122a** could be a representation of test compound fluorescence contribution. In contrast **MIP23** (**Figure 122b**) showed no selectivity and had its fluorescence quenched not only by its own template but by other test compounds too.
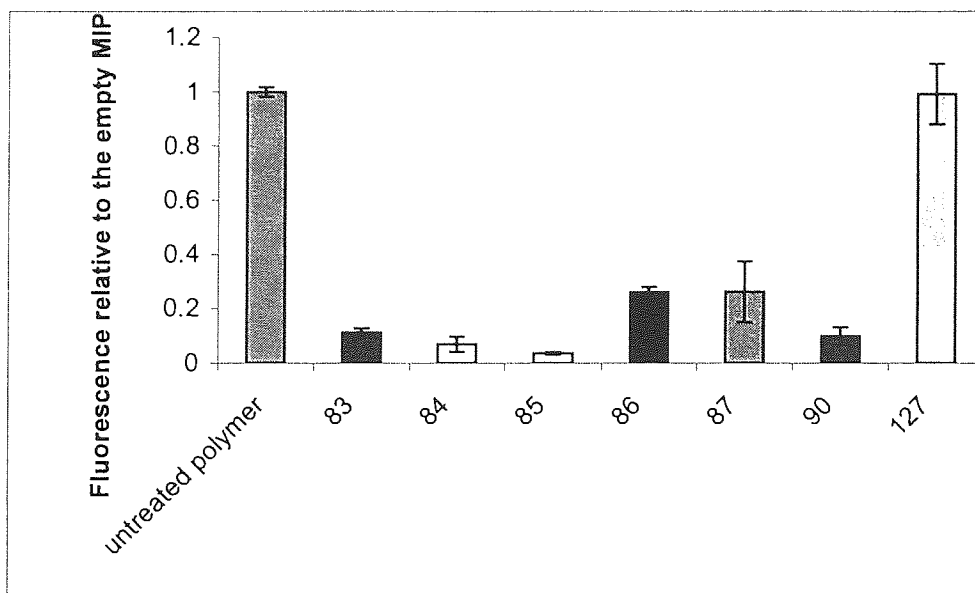


**Figure 121a**: Fluorescence relative to the empty **MIP18** cross-linked with TMPTA (Polymer prepared in *toluene*). Note, data manipulated from **Figure 117a**. $\lambda_{ex}$ = 345 nm, $\lambda_{em}$ = 415nm.
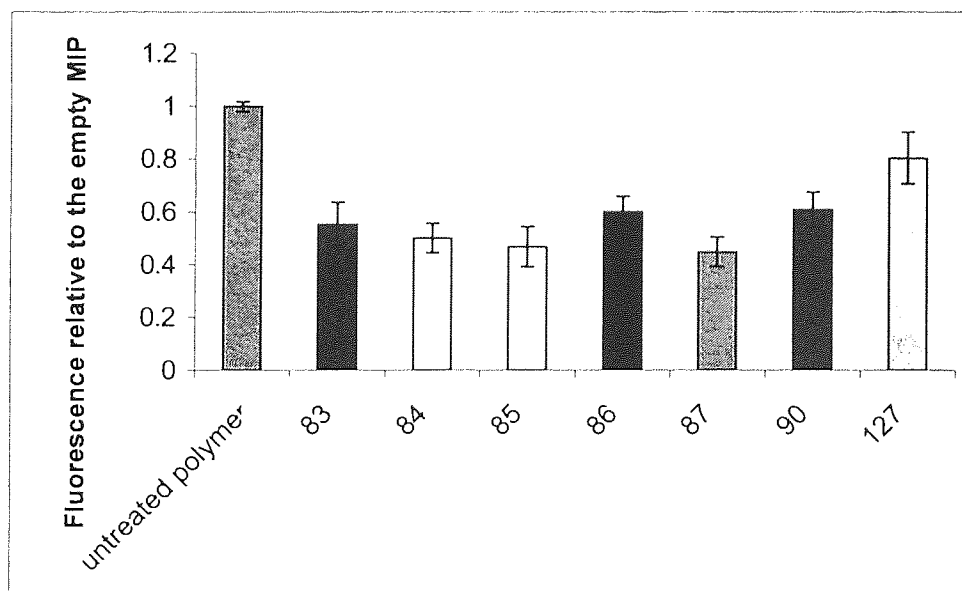


**Figure 121b**: Fluorescence relative to the empty **MIP23** cross-linked with TMPTA (Polymer prepared in *methanol*). $\lambda_{ex}$ = 345 nm, $\lambda_{em}$ = 415nm.
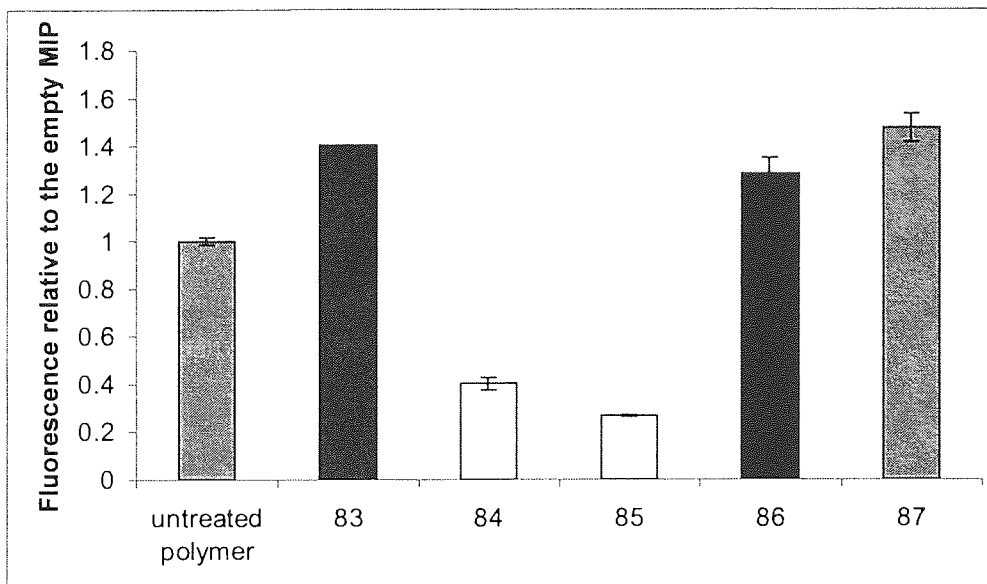
**Figure 122a**: Fluorescence relative to the empty **MIP18** cross-linked with TMPTA in Toluene. Note, data manipulated from **Figure 117b**. $\lambda_{ex}$= 305 nm, $\lambda_{em}$ = 455nm.
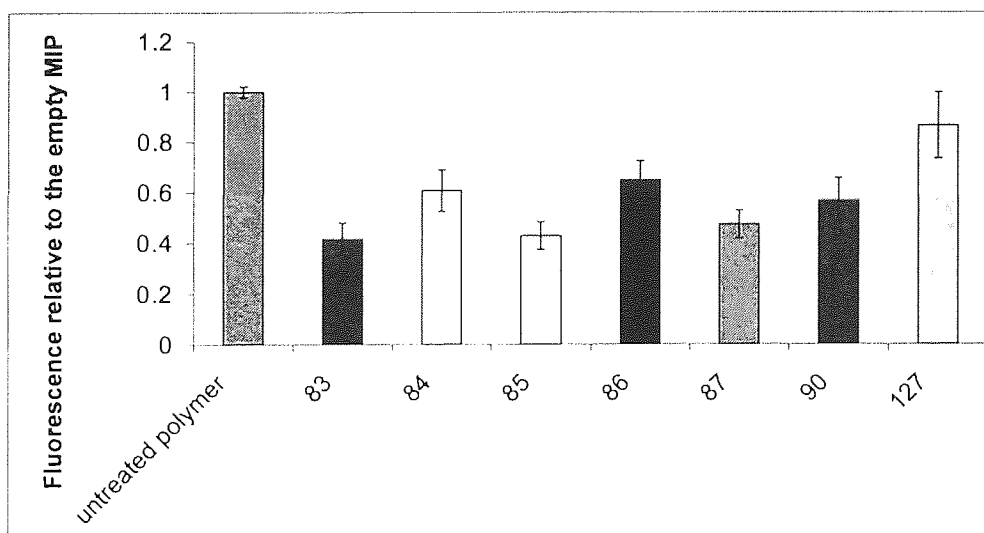


**Figure 122b**: Fluorescence relative to the empty **MIP23** cross-linked with TMPTA in Methanol. $\lambda_{ex}$= 305 nm, $\lambda_{em}$= 455nm.

Overall the MIP synthesised in the polar solvent (**MIP23**) showed no selectivity whereas the MIP synthesised in toluene (**MIP18**), exhibited selectivity at both excitation/emission wavelength pairs of 345/415 nm and 305/455 nm.

The **MIP18** showed selectivity against test compound **127** at excitation/emission wavelength of 345/415 nm in **Figure 121a**. It had been assumed that the long flexible dodecane chain would be accommodated by the MIP cavity. This did not take place and could have been either due the length of the chain or the compound had adapted a conformation that was unable to fit the cavity.

At excitation/emission wavelength of 305/455 nm in **Figure 121b** the MIP showed selectivity towards compounds **87** and **86**. These compounds interestingly had the flexible alkoxy-substituted benzylidene moiety in them

At excitation/emission wavelength of 305/455 nm in **Figure 122b**, the MIP showed selectivity towards compounds **87** and **86**. These compounds interestingly had the flexible alkoxy-substituted benzylidene moiety in them.

### 3.4.5 2-(acryloyl-anthracen-9-ylmethyl-amino)-benzamide-based hydrophobic pocket

It was decided to explore the use of functional monomers of the type exemplified by compounds **129** {5.3.39}, **130** {5.3.40}, **131** {5.3.41}, **132** {5.3.42} and **133** {5.3.43} (**Scheme 6**). Here two polycyclic aromatic groups form a hydrophobic groove, terminated by the hydrogen bond donors and acceptors of the anthanilanido portion, into which a test compound may dock.
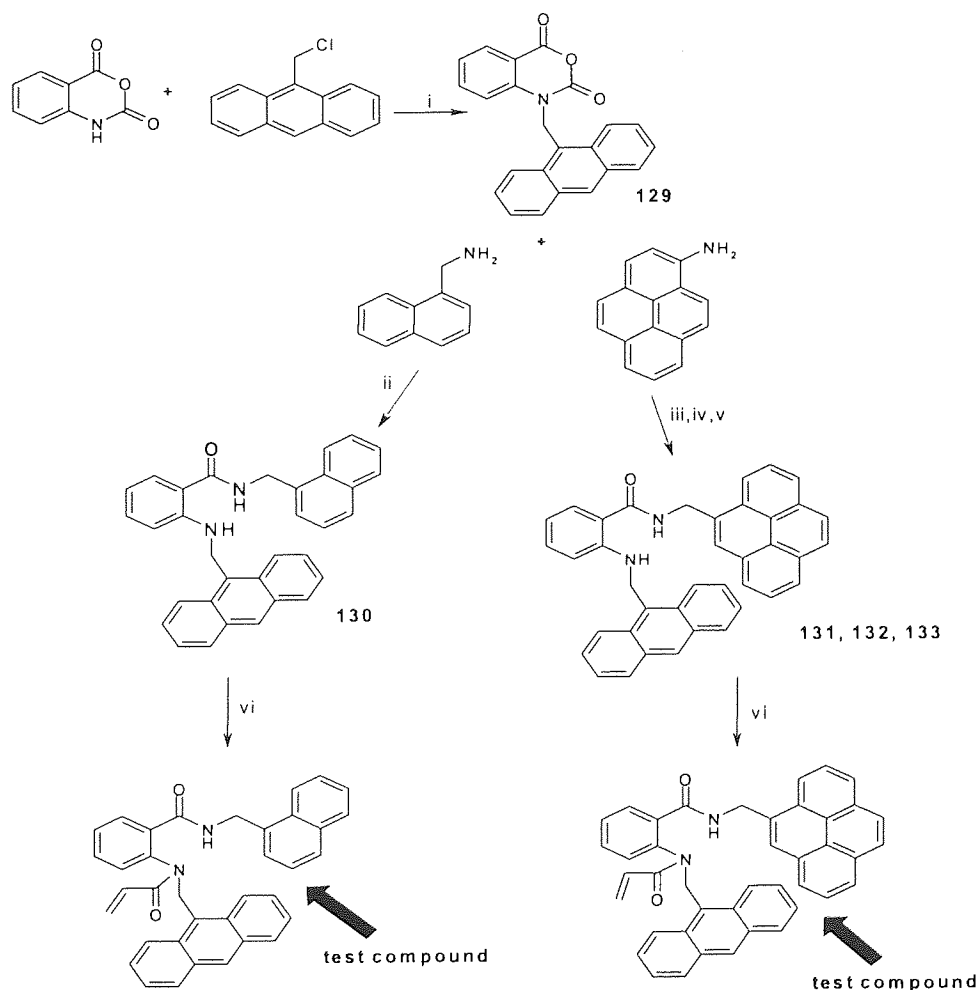


i NaI/NaH in DMF ii Ethanol (Reflux) for **130** iii Ethanol (Reflux) for **131** iv DMF/DMAP for **1323** v NaH in DMF for **133** vi Acryloyl chloride/triethylamine/THF.

**Scheme 6:** First approach to compounds of the type **130-133**. Note, that the thick black arrow indicates the manner in which the test compound could slot into this hydrophobic 'clip'.

This offered the possibility for dramatic changes in fluorescence from any corresponding MIP, if the aromatic part of a test compound would be able to sit between the two polycyclic aromatic groups from the functional monomer.

9-Chloromethylanthracene underwent a successful amination with isatoic anhydride to give compound **129**. Several attempts to react the aminated product with 1-aminopyrene under various conditions were undertaken. The first attempt was at reflux in ethanol (**131**), the second with DMF/DMAP under an argon atmosphere (**132**) and finally with DMF/NaH (**133**) (**Scheme 6**). Neither of these outlined attempts worked. Due to this drawback another alternative reaction was performed with the aminated product compound **129**, but this time with 1-(aminomethyl)-napthalene, which has a more nucleophilic amine than pyrenyl. This alternative reaction, however, was not synthetically attainable and so did not give compound **133** (**Scheme 6**).
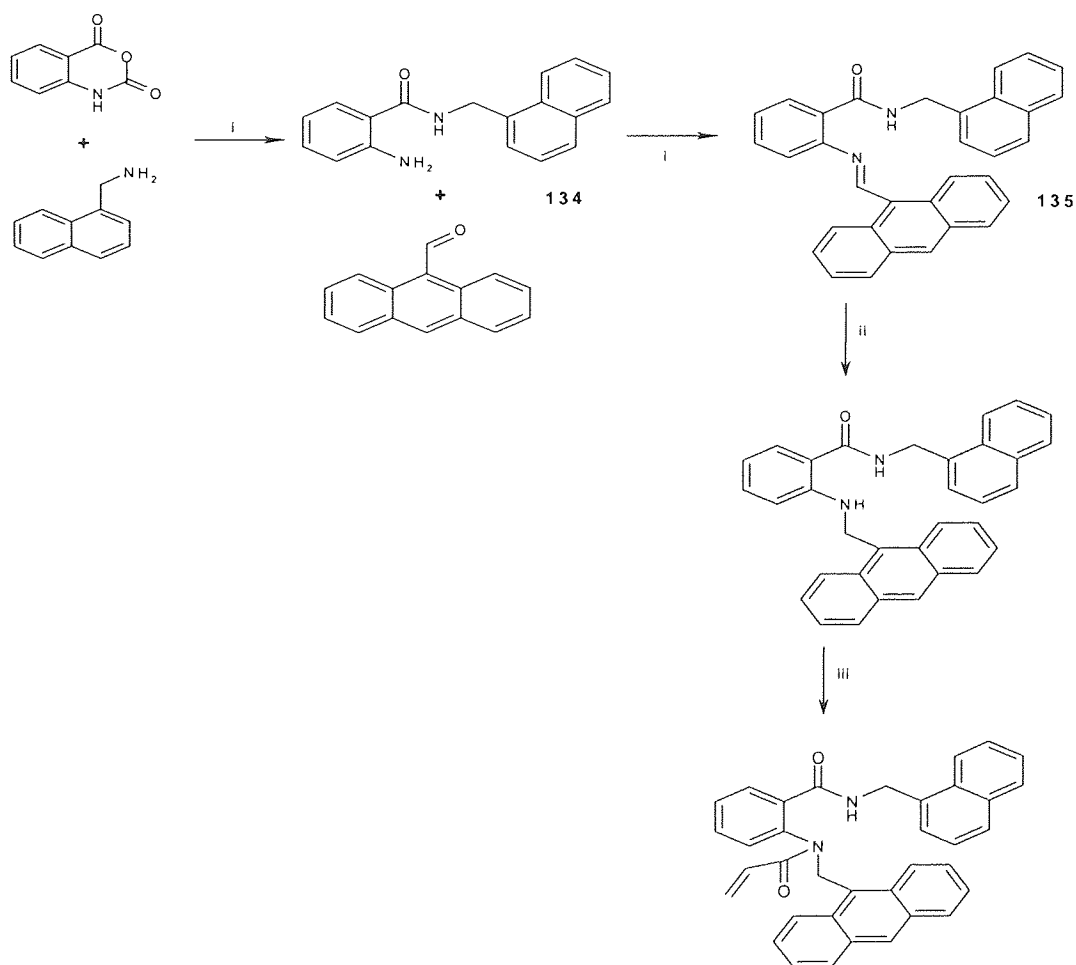


i    Ethanol    (Reflux)    ii    Tetramethylammonium    triacetoxyborohydride/THF/Heat    iii    Acryloyl chloride/triethylamine/THF

**Scheme 7:** Second approach to a compound of type **135**.

As an alternative synthetic approach the order of addition of the polycyclic aromatic groups was reversed (**Scheme 7**). Thus, isatoic anhydride was opened with methylaminonaphthalene to give compound **134**

{5.3.44}. This was converted to the imine **135** {5.3.45} by reaction with anthracene-9-carboxaldehyde. Due to lack of time however this reaction scheme was not taken further in its reaction cycle to form the functional monomer. That would have been capable of docking compounds between its hydrophobic groove created by the two polycyclic aromatic groups.

### 3.4.6 N,N'-Bis-pyren-1-ylmethyl-benzene-1,3-diamine hydrophobic pocket

A functional monomer that has the capability to allow test compounds to dock between its two polycyclic aromatic groups that form a hydrophobic groove, compounds **136** {5.3.46} and **137** {5.3.47} (**Scheme 8**) were used to investigate this.



**136 and 137**
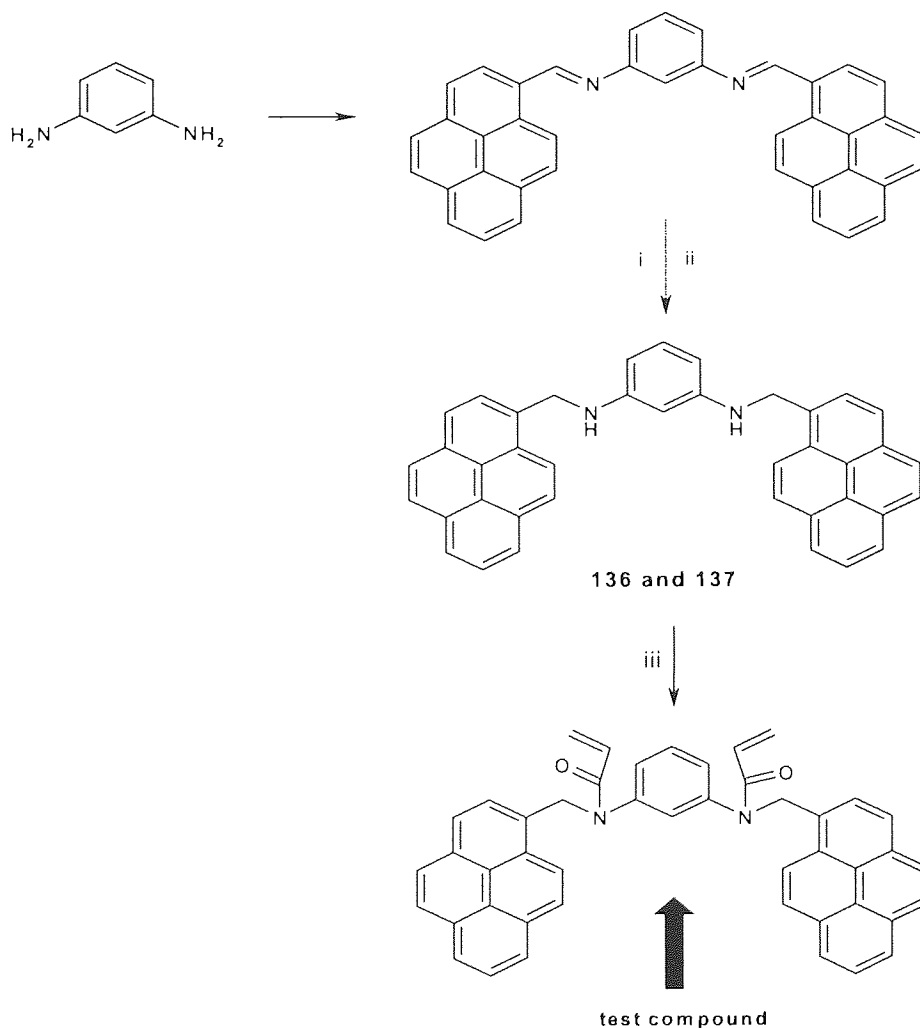
i Tetramethylammonium triacetoxyborohydride/THF/Heat for **136**, ii lithium aluminium hydride/THF for **137**
iii Acryloyl chloride/triethylamine/THF
**Scheme 8:** Approach to compound of the type **136/137**. Note, that the thick black arrow indicates the manner in which the test compound could slot into this hydrophobic 'clip'.

It is assumed that the docking of the aromatic part of the test compounds between the two polycyclic aromatic groups from the functional monomer would present large changes in the fluorescence from any corresponding MIP.

The synthetic approach began by forming an imine. Then several attempts at reducing the imine to amine with two different reducing agents were performed. In the first attempt tetramethylammonium triacetoxyborohydride (136) was used. In the second attempt lithium aluminium hydride (137) was used. Neither reducing agent was able to reduce the imine to an amine. With this drawback it hindered the progression of this approach.

### 3.4.7 Conclusion

A number of routes were taken to synthesise functional monomers that contain a hydrophobic pocket or a significant hydrophobic portion. The initial functional monomer 119 was based on cyclododecylamine. To probe the functional monomer a stable version was synthesised by acetylation to give compound 106 and a number of studies was performed on this compound. The initial study involved assessing the fluorescence quenching of compound 106 by the templates 81, 127, 128, 83 and 84. Followed on from that, a study on the fluorescence output of individual template/test compounds was also performed.

In addition to these studies the fluorescence behaviour of 106 was assessed in different environments. In the first study compound 106 was restricted within a cavity created by β-cyclodextrins. In the second study non-templated polymers were synthesised with compound 119 only. These polymers assessed the fluorescence behaviour of the fluorophore in maximum restriction i.e. no cavity present. In the third study the 2-acetylamino-benzamide moiety found on compound 106 was probed by studying a comparative compound, benzoylene urea that contained a closed form of this moiety. Finally a study on fluorescence quenching in deposited thin films was performed on a soluble polymer of poly (methyl methacrylate) PMMA and compound 106. This study assessed the behaviour of compound 106 within a very restricted environment.

A selection of MIPs was constructed with compound 119 as the FMM and compounds 128, 83, 85, 84, 81 and 127 as templates cross-linked with TMPTA (rigid-crosslinker) and TEGDMA (flexible cross-linker) to generate MIPs. The selectivity/cross-reactivity profiles for five out of the six MIPs suggested that FFM, compound 119 was not suitable in creating selective MIPs. The MIP created by template 84 (MIP18) cross-linked with more rigid TMPTA cross-linker suggested selectivity at excitation/emission wavelengths of 345nm/415nm.

To further examine the selective MIP (MIP18) results, MIP22 was synthesised by replacing compound 119 with compound 126 containing a straight dodecane chain. After inspecting the results it was found that at both excitation/emission wavelength pairs of 345 nm/415 nm and 305 nm/455 nm, the MIP generated was non-selective.

Following that study another MIP, **MIP23** was synthesised using compound **119** as a FFM, templated with **84** and cross-linked with TMPTA, in methanol (polar solvent) and exposed in this solvent as well. After inspecting the results it was found that at both excitation/emission wavelength pairs of 345 nm/415 nm and 305 nm/455 nm, the **MIP23** generated in methanol was non-selective.

The other functional monomers were based on 2-(acryloyl-anthracen-9-ylmethyl-amino)-benzamide and N,N'-Bis-pyren-1-ylmethyl-benzene-1,3-diamine. The proposed idea here was that two polycyclic aromatic groups would form a hydrophobic groove, terminated by the hydrogen bond donors and acceptors of the anthanilanido portion, into which a test compound would dock. Due to lack of time and failure with synthesising some of the compounds this led to no progression being made with these monomers.

### 3.5 Investigation of the mechanism of fluorescence quenching of MIP-bound fluorophores by test compounds

This section sets out to investigate whether a simple absorption of fluorescence is the mechanism responsible for the observed fluorescence quenching between the MIP-bound fluorophore by the test compound. This investigation would assess whether overlapping between the emission spectra of the MIP-bound fluorophores and the absorption spectra of the test compounds (Procedure 9 refer to 4.9) takesplace.

From the dual fluorophore section, two MIP-fluorophores were employed i.e. **MIP6** (**Figure 123**) and **MIP8** (**Figure 123**). As for the hydrophobic section MIP-fluorophore, **MIP18** (**Figure 123**) was employed. The **Figures 124-126** correspond to the above MIP-fluorphores emission spectra.
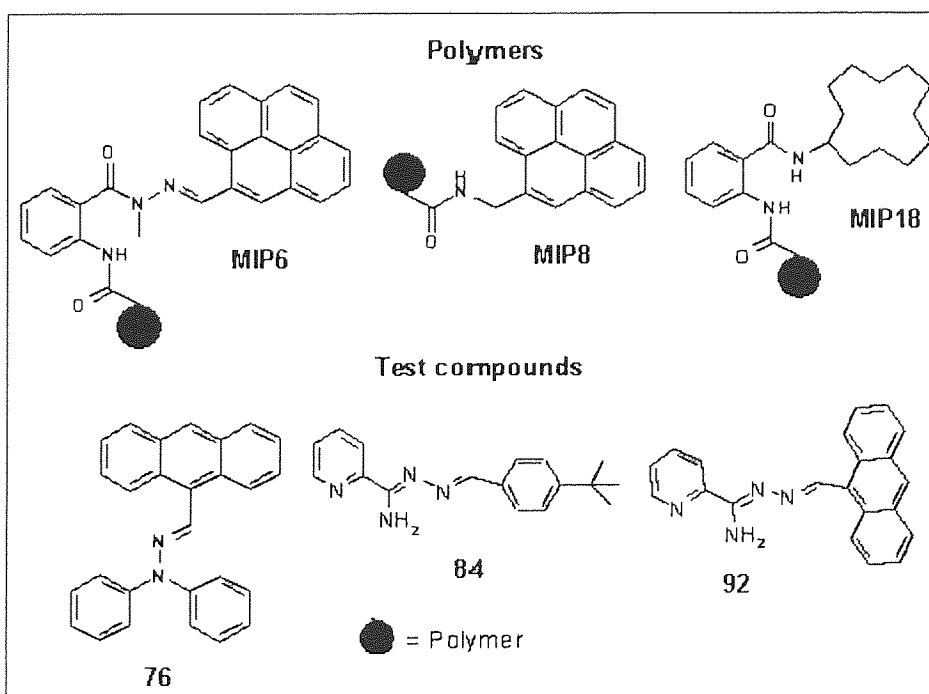


**Figure 123**: Structures of the polymers and test compounds.

219
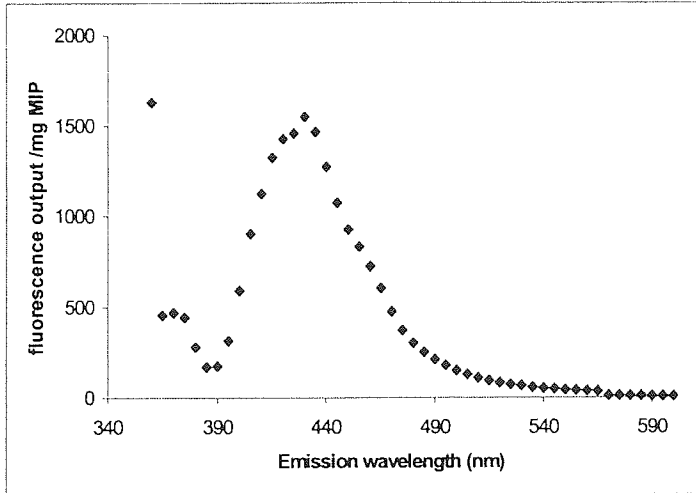
**Figure 124**: Fluorescence spectrum of **MIP6** ($\lambda_{ex}$ = 340 nm).
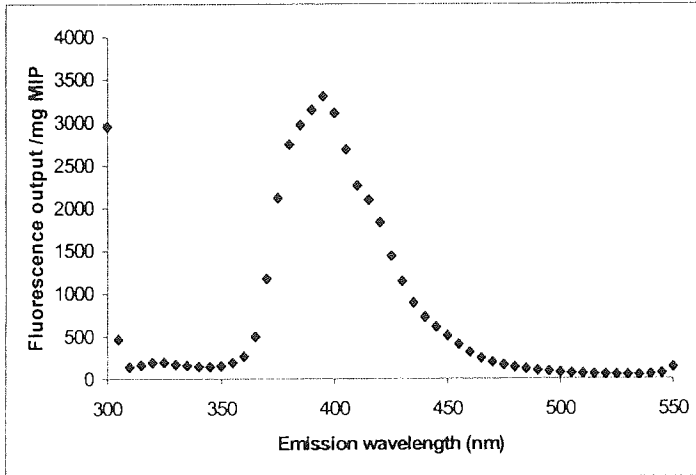


**Figure 125**: Fluorescence spectrum of **MIP8** ($\lambda_{ex}$ = 290 nm).
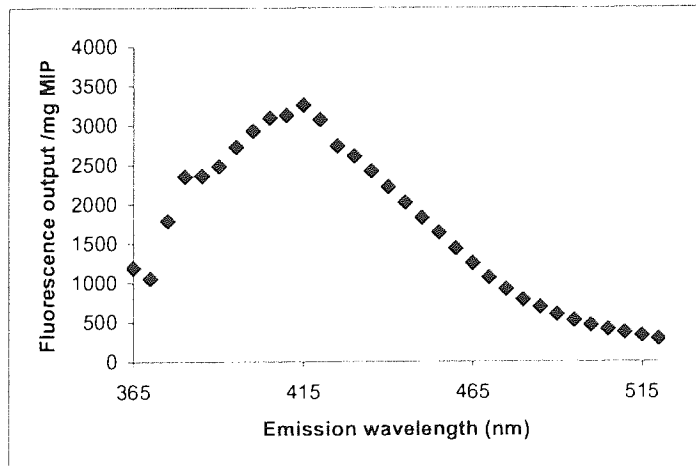


**Figure 126**: Fluorescence spectrum of **MIP18** ($\lambda_{ex}$ = 345 nm).
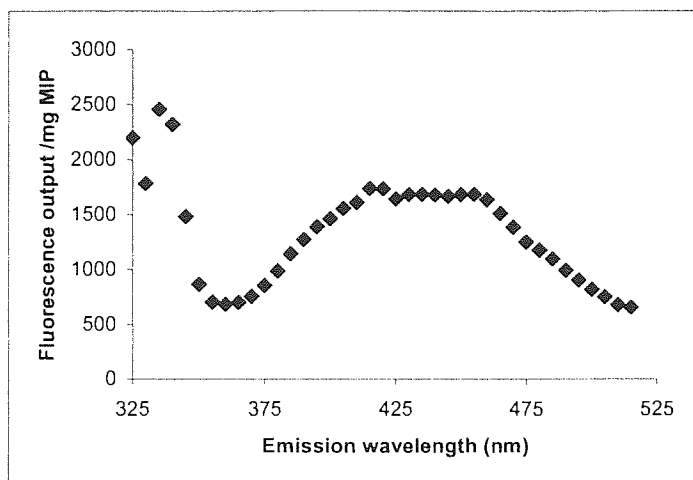
**Figure 126a**: Fluorescence spectrum of **MIP18** ($\lambda_{ex}$ = 305 nm).

From these emission spectra of the individual MIP-fluorophores, the emission maxima and the emission ranges can be established i.e. for **MIP6** the emission maximum is at 430 nm (**Figure 124**) and ranges from 390-490 nm. For **MIP8** the emission maximum is at 400 nm (**Figure 125**) and ranges from 350-450 nm. For **MIP18** at excition wavelength of 345 nm it revealed an emission maximum at 415 nm (**Figure 126**) and ranges from 350-520 nm. At excition wavelength of 305 nm no single point emission maximum could be determined (**Figure 126a**) but a range from 415-455 nm could be observed. In addition the emission range for this was from 360-515 nm.

In estabilishing the emission maxima and ranges for the individual MIP-fluorophores these can be compared to the UV absorption data (**Table 11** and **Figures 127a-d**) for the given test compounds **76**, **84**, **92** and **113** (**Figure 123**).

| Compound | $\lambda_{max\ (nm)}$ | Absorption range (nm) | MIPs exposed to test compounds |
|----------|----------------------|-----------------------|-------------------------------|
| 76 | 411.8 | 350-500 | MIP5, MIP8 |
| 84 | 331.5 | 350-400 | MIP11 |
| 92 | 390.9 | 350-500 | MIP11 |
| 113 | 420.8 | 350-500 | MIP5, MIP8 |

**Table 11**: UV data for the test compounds.
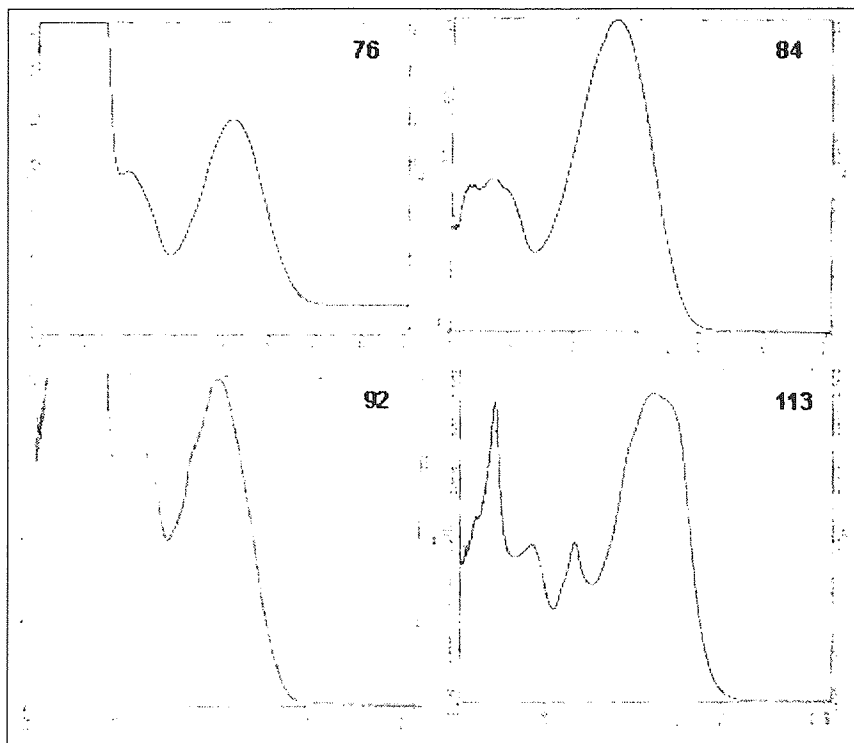
**Figure 127**: UV absorption spectra (methanol).

The test compounds' **76** and **113** absorption spectra (**Figure 127**) overlapped the emission spectrum range of **MIP6** i.e. 390-490 nm (**Figure 124**). The same was observed for **MIP8** (**Figure 125**). For test compounds **84** and **92** the absorption spectra (**Figure 127**) overlapped the emission spectrum range of **MIP18** at both excitation wavelengths (**Figure 126** and **126a**). Note, that all of these test compounds quenched the fluorescence of the MIP-bound fluorophores. This observed overlapping between the MIP-fluorophores emission spectra and the absorption spectra of the test compounds indicates that a simple mechanisn of fluorescence being absorded by the test compound may well be taking place.

# Chapter 4 Procedures

## 4.1 Procedure 1: Exposure of imprinted polymers to test compounds followed by fluorescence measurements

The imprinted polymer (0.05 g) was shaken with the test solution (0.1, 1.0 and 5.0 mg/mL in THF) for 1 day, collected by filtration, washed very briefly with THF (5 mL) dried under vacuum. The resulting powders were weighed accurately (about 5 mg per well) in triplicate into black polystyrene 96 well plates. A layer of polyethyleneglycol (0.2 mL) was added to each well and the MIPs were examined by fluorescence.

## 4.2 Procedure 2: Preparation of thin films of co-polymers in the presence of test compounds and fluorescence study

A stock solution of the co-polymer was prepared in **A** at a concentration of **X** mg/mL. Solutions of the test compounds in **B** were prepared at a concentration of 1 mg/mL. Aliquots of the co-polymer solution (0.1 mL) were applied to the wells of a polypropylene 96 well plate resulting in a polymer content of **X** mg per well. The same wells were also treated in triplicate with aliquots of the test compounds (0.02, 0.05 or 0.1 mL) giving test compound contents of 0.02, 0.05 or 0.1 mg per well. Some wells were left with co-polymer solution only. The solvent was allowed to evaporate and the plate was further dried by careful application of vacuum over an 18 hours period to give polymer film deposits on the base of the wells. The fluorescence of the films was investigated at the same excitation wavelength used for the MIP studies.

| Co-polymer | Solvent | | | Polymer content (mg per well) | $\lambda_{ex}$ (nm) |
|---|---|---|---|---|---|
| | A | | B | | |
| | | Conc.(mg/mL) | | | |
| a)co-octadecylacrylate-2-acrylamidobenzamide | Chloroform | 46.2 | THF | 4.6 | 309 |
| b) co-styrene- **108** | THF | 46.6 | Chloroform | 5.0 | 340 |
| c) co-octadecylacrylate- **108** | THF | 50.4 | Chloroform | 5.0 | 340 |

## 4.3 Procedure 3: Solution based fluorescence study

Compound **Z** (**X** mg) was dissolved in **B** (**X** mL) to give solution **A**. From solution **A** various aliquots were taken (**X** μL) and made to **Y** mL with **C**, giving solution **B**. Then **X** μL was taken from each stock solution in duplicate/triplicate/quadruplicate into the wells of a polypropylene 96 well plate. The same wells were then made to 200 μL with **C** giving test compound contents of **X** mg per well. Some wells contained the **C** only as a control. The plate was exposed to fluorescence.

| Solution A | | Solution B | | | In the wells of a polypropylene 96 well plate | | | $\lambda_{ex}$ (nm) |
|---|---|---|---|---|---|---|---|---|
| Compound Z (mg) in XmL | Solvent B | Taken aliquots from A (µL) | Made upto (mL) with C | Solvent C | Taken aliquots from B (µL) | Made upto 200 µL with C | Conc. (mg per well) | |
| a) 5 mg in 1 mL | Ethyl acetate | 16 | 1 | PEG | 200 | - | 0.016 | 305, 345 |
| b) 5 mg in 1 mL | Ethanol | 20 50 100 | 0.2 | Ethanol | 200 | - | 0.002 0.0125 0.05 | 305, 345 |
| c) 4 mg in 2 mL | Ethyl acetate | 50 100 | 1 | PEG | 100 | 100 | 0.05 0.1 | 305, 345 |
| d) 2.5 mg in 0.5 mL | Ethanol | 20 50 100 | 1 | Ethanol | 200 | - | 0.1 0.25 0.5 | 305, 345 |
| e) 5 mg in 4 mL | THF | 100 | 1 | PEG | 25 50 100 200 | 175 150 100 - | 0.125 0.0625 0.03125 0.01563 | 340 |
| f) 2.5 mg in 50 mL | THF | 400 | 1 | THF | 200 | - | 0.02 | 340 |
| g) 5 mg in 1mL | Ethyl acetate | 16 | 1 | PEG | 200 | - | 0.08 | 305, 345 |

## 4.4 Procedure 4: A solution based fluorescence study on compound 117

Compound 117 (5 and 20 mg) was dissolved in ethyl acetate to give stock solution concentrations of 1.25, 5 and 20 mg/mL (stock solution A). From stock solutions (A) further aliquots were taken and made to 1 mL with PEG giving solutions B. Then aliquots of 25, 50, 100 and 200 µL were taken from solutions B, in duplicate into the wells of a polypropylene 96 well plate. The same wells were then made to 200 µL with PEG giving various test compound contents i.e. solutions C. Some wells contained the PEG only as a control. The plate was exposed to fluorescence at excitation wavelength of 290nm.

| Stock solution A | | Solution B | | Solution C | |
|---|---|---|---|---|---|
| 5 mg/mL of compound **117** in ethyl acetate (mL) | Concentration mg/mL | Taken aliquot from **A** (μL) and made to 1mL with PEG | Concentration mg/mL | Taken aliquot from **B** (μL) and made to 200μL with PEG | Concentration mg/mL |
| 4 | 1.25 | 20 | 0.025 | 25 | 0.003125 |
| | | | | 50 | 0.00625 |
| | | | | 100 | 0.0125 |
| | | | | 200 | 0.025 |
| 4 | 1.25 | 500 | 0.625 | 25 | 0.08 |
| | | | | 50 | 0.1563 |
| | | | | 100 | 0.3125 |
| | | | | 200 | 0.625 |
| 1 | 5 | 500 | 2.5 | 100 | 1.25 |
| | | | | 200 | 2.5 |
| *1 | 20 | 500 | 10 | 100 | 5 |
| | | | | 200 | 10 |

* 20mg of compound **119**

## 4.5 Procedure 5: A solution based study to assess the fluorescence quenching of compound 106 by the templates (81, 127, 128, 83 and 84)

Compound **106** (5 mg) was dissolved in ethyl acetate (1 mL) giving stock solution **A**. From stock solution **A** an aliquot of 16 μL was taken and made up to 1 mL with PEG giving a concentration of 0.08 mg/mL. An aliquot of 16 uL was taken from stock solution **A** and placed in each well. Another second equimolar stock solution (**B**) was prepared with each template dissolved in ethyl acetate (1 mL). From stock solution **B** an aliquot of 16 μL was taken and made up to 1 mL with PEG giving a concentration of 0.08 mg/mL. From stock solution **B** various aliquots were taken and placed in the wells to give the corresponding equivalences of 1, 2 and 5. The plate was exposed to fluorescence at excitation wavelength of 305nm.

| Solution | Stock solution **A** (compound **106**) | | Stock solution **B** (templates) | |
|---|---|---|---|---|
| | Taken from A (µL) | Concentration mg/mL | Taken aliquot from B (µL) and made to 1 mL with PEG | Concentration mg/mL |
| 1) Compound **106** (control) | 16 | 0.08 | - | - |
| 2) 1 e.q of template (control) | - | - | 16 | 0.08 |
| 3) (Compound **106** + 1 e.q of template) | 16 | 0.08 | 16 | 0.08 |
| 4) (Compound **106** + 2 e.q of template) | 16 | 0.08 | 32 | 0.16 |
| 5) (Compound **106** + 5 e.q of template) | 16 | 0.08 | 80 | 0.4 |
| 6) 2 e.q of template (control) | - | - | 32 | 0.16 |
| 7) (5 e.q of template (control) | - | - | 80 | 0.4 |

* Aliquots were placed in triplicate into the *AcroWell* ™ 96 well black plates.

## 4.6 Procedure 6: Solution based study on compound 106 and β-cyclodextrins

Compound **106** (6mg) was dissolved in a 1:1 ratio of *iso*-propanol : water (100 mL), giving stock solution (**A**). From stock solution **A** an aliquot of 50 µL was placed in each well. β-cyclodextrin (210mg) was dissolved in a 1:1 ratio of *iso*-propanol : water (100 mL), giving stock solution (**B**). From stock solution **B** aliquots of 5 and 20 µL were placed in the wells containing 50 µL of stock solution **A** and made to 200 µL with PEG. Note that control wells containing only stock solution **A** or **B** were also prepared. The plate was exposed to fluorescence at excitation wavelength of 305nm.

| Solution | Stock solution **A** | | Stock solution **B** | | Made to 200 µL with PEG |
|---|---|---|---|---|---|
| | Taken from **A** (µL) | Concentration mg/mL | Taken aliquot from **B** (µL) | Concentration mg/mL | |
| 1) Compound **106** (control) | 50 | 0.016 | - | - | 150 |
| 2) Compound **106** + 5 e.q of template/test compound | 50 | 0.016 | 5 | 0.0053 | 145 |
| 3) (Compound **106** + 20 e.q of template/test compound | 50 | 0.016 | 20 | 1.05 | 130 |
| 4) 5 e.q of template/test compound (control) | - | - | 5 | 0.053 | 195 |
| 5) 20 e.q of template/test compound (control) | - | - | 20 | 1.05 | 180 |

\* Aliquots were placed in triplicate into the *AcroWell* ™ 96 well black plates.

## 4.7 Procedure 7: Solution based study on compound 106 and benzoylene urea

Compound **106** (5mg) was dissolved in ethyl acetate (1 mL) giving stock solution A. From stock solution A an aliquot of 16uL was taken and made to 1 mL with PEG giving a concentration of 0.08 mg/mL. Benzoylene urea (2.35mg) was dissolved in DMSO (1 mL) giving an equimolar stock solution B. From stock solution B an aliquot of 16uL was taken and made to 1 mL with PEG giving a concentration of 0.038 mg/mL. Then 100 uL was taken from each stock solution and placed into the *AcroWell* ™ 96 well black plate in duplicate. Some wells contained the PEG only as a control. The plate was exposed to excitation wavelength of 305 nm.

## 4.8 Procedure 8: Preparation of deposited thin films of poly (methyl methacrylate) (PMMA) - compound 106 and fluorescence studies

PMMA (**X** mg) was dissolved in chloroform or THF (**X** mL) to give solution **A**. From solution **A** various aliquots were taken (**X** µL) and made to 1 mL with chloroform or THF, giving solution **A1**. Then 100 µL was taken from solution **A1** in pent plicate into the wells of an *AcroWell* ™ 96 well black plate. Compound **106** (**X** mg) was dissolved in chloroform or THF (**X** mL) to give solution **B**. From solution **B** various aliquots were taken (**X** µL) and made to 1 mL with chloroform or THF, giving solution **B1**. Then 100 µL was taken from solution **B1** to in treat the same wells that contain solution **A1** The solvent was allowed to evaporate and the plate was further dried by careful application of vacuum for a period of 18 hours. This gave smooth and even polymer film deposits on the base of the wells. The fluorescence of the films was investigated at the same excitation wavelengths used for the MIP studies, 345 and 305nm. Note that in some of the studies PMMA or compound **106** were kept as a constant parameter. In addition control wells containing only PMMA or compound **106** were also prepared.

| Constant PMMA and varying amounts of compound 106 | | | | | | |
|---|---|---|---|---|---|---|
| Solution | X mg in X mL | Solvent | Conc. of solution A and B (mg/ mL) | Aliquots taken from solution A and B (µL) and made to 1 mL | | Taken 100 µL from A1 and B1 to give X mg in each well |
| A<br>PMMA | 5 g in 50 mL | Chloroform or THF | 100 | 100 | A1 | 10 |
| B<br>Compound 106 | 5 mg in 25 mL | Chloroform or THF | 0.2 | 5<br>10<br>25<br>50<br>100 | B1 | 0.001<br>0.002<br>0.005<br>0.01<br>0.02 |
| A<br>PMMA | 5 g in 50 mL | THF | 100 | 50 | A1 | 5 |
| B<br>Compound 106 | 5 mg in 50 mL | THF | 0.1 | 10<br>20<br>50<br>100<br>200 | B1 | 0.001<br>0.002<br>0.005<br>0.01<br>0.02 |

| Constant compound 106 and varying amounts of PMMA | | | | | | |
|---|---|---|---|---|---|---|
| Solution | X mg in X mL | Solvent | Conc. of solution A and B (mg/ mL) | Aliquots taken from solution A and B (µL) and made to 1 mL | | Taken 100 µL from A1 and B1 to give X mg in each well |
| A<br>PMMA | 5 g in 50 mL | THF | 100 | 50<br>100<br>150<br>200<br>250 | A1 | 5<br>10<br>15<br>20<br>25 |
| B<br>Compound 106 | 5 mg in 25 mL | THF | 0.2 | 5 | B1 | 0.001 |
| A<br>PMMA | 500 mg in 50 mL | THF | 10 | 5<br>10<br>25<br>50 | A1 | 0.05<br>0.1<br>0.25<br>0.5 |
| B<br>Compound 106 | 5 mg in 50 mL | THF | 0.1 | 10 | B1 | 0.001 |

## 4.9 Procedure 9: U.V study performed on test compounds 76, 84, 92 and 113

Test compounds 76, 84, 92 and 113 (5 mg) were dissolved in methanol (100 mL) (HPLC grade) giving concentrations of about 0.05 mg/mL. These solutions were transferred into the cuvettes and the U.V instrument determined the absorption of each test compound. Note, that prior to measuring the samples a blank (methanol) was read each time.

| Test compound | Concentration mg/mL |
|---|---|
| 76 | 0.056 |
| 84 | 0.025 |
| 92 | 0.05 |
| 113 | 0.052 |

# Chapter 5. Experimental

## 5.1 Chemicals

N,N-diisopropyl ethylamine (Hünig's base), trimethylolpropane triacrylate (inhibited with 100ppm monomethyl ether hydroquinone), triethylene glycol dimethylacrylate (assay ~90% (G.C) ~ 0.01% hydroquinone monomethyl ether), octadecylacrylate, Poly (methyl methacrylate) (average molecular mass 996) were purchased from Sigma-Aldrich. Styrene was purchased from Avocado Research Chemicals Ltd. Poly(ethylene glycol) methyl ether (average molecular mass 550) and 2,2'-azobis(2-methylpropionitrile) were purchased from Acros Organics. Duolite A-7 resin was purchased from Supelco (Phenol-formaldehyde, macroreticular. Form: free base Functional Group: polyamine Reverse Swelling: $(OH^- \rightarrow Cl^-)$ 23-28%).

## 5.2 Instrumentation

Thin layer chromatography plates, aluminium-backed silica gel 60 $F_{254}$, were obtained from Merck. Proton NMR spectra were obtained on a Bruker AC 250 instrument operating at 250MHz as solutions in $d_6$-DMSO and referenced from $\delta DMSO$ = 2.50ppm. Infrared spectra were recorded as KBr discs on a Mattson 3000 FTIR spectrophotometer. Atmospheric pressure chemical ionisation mass spectrometry (APCI-MS) was carried out on a Hewlett-Packard 5989B quadrupole instrument connected to an electrospray 59987A unit with an APCI accessory and automatic injection using a Hewlett-Packard 1100 series autosampler. Melting points were obtained using a Reichert-Jung Thermo Galen hot stage microscope and are corrected. Elemental analyses were performed by Butterworth Laboratories Ltd, Teddington UK. Fluorescence measurements were performed in polystyrene [Black Cliniplates from Labsystems, Helsinki, Finland] or polypropylene [Acrowell™ from Pall Life Sciences] standard format 96-well microtitre plates in a Molecular Devices SpectraMax GeminiXS™ dual-scanning microtitre plate spectrofluorometer. UV/VIS spectrometer PU8730 fixed bandwidth, single beam.

## 5.3 Experimental procedures

### 5.3.1 Preparation of 5-Naphthalen-2-ylmethyl-5H-dibenzo[b,f]azepine (75)
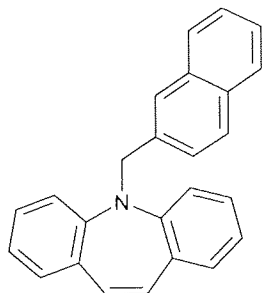
A biphasic mixture of aqueous potassium hydroxide (6M, 50 mL), toluene (15 mL), iminostilbene (2.372 g, 12.3 mmol), 2-(bromomethyl)naphthalene (1.862 g, 8.42 mmol) and tetrabutyl ammonium chloride (0.185 g, 0.67 mmol) was stirred at room temperature for 10 days and then at 76 °C for 1 day. The mixture was partitioned between water (100 mL) and ethyl acetate (100 mL). The organic layer was dried over magnesium sulphate and evaporated to give the crude product.

The compound was purified by flash chromatography eluting with dichloromethane and petroleum ether (60-80 °C) 1/4 rising to 1/1. The fractions corresponding to $R_f$ 0.63 were combined and the solvent was evaporated to give the target compound as a pale yellow crystalline solid. The target compound was further recrytallised in hot ethanol.

Yield = 1.915 g, 5.73 mmol, 68%

Mp 119.4 – 120.6 °C

$^1$H NMR ($D_6$-DMSO δ DMSO = 2.50 ppm): 5.11 (s, 2H, CH$_2$), 6.87 (s, 2H, ArC$\underline{H}$=C$\underline{H}$Ar), 6.90-6.97 (overlapping m, 2H, Ar-H), 7.11 (d, 2H, J=7.2Hz, Ar-H), 7.20-7.24 (overlapping m, 4H, Ar-H), 7.38-7.48 ((overlapping m, 2H, Ar-H), 7.59 (dd, 1H, J=0.4, 8.7Hz, Naphthyl-H), 7.74 (d, 1H, J=8.7Hz, naphthyl-H), 7.76-7.82 (overlapping m, 2H, Ar-H), 7.91 (s, 1H, naphthyl-H) ppm

MS (+APCI) m/z = 334 (M+H)$^+$

IR (KBr) ν = 3047, 3018, 2819, 1595, 1569, 1483, 1456, 1432, 1348, 1215 cm$^{-1}$.

Elemental analysis: Found % (calculated %), C 90.03 (90.06), H 5.76 (5.74), N 4.20 (4.20).

### 5.3.2 Preparation of N'-[1-anthracen-9-yl-meth-(E)-ylidene]-N,N-diphenylhydrazine (76)
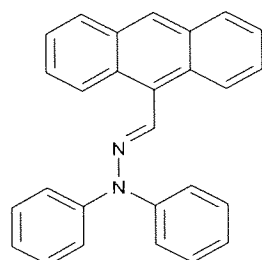


A mixture of N,N-diphenylhydrazine hydrochloride (2.084 g, 9.4 mmol), anthracene-9-carboxahdehyde (2.157 g, 10.5 mmol) and N,N-diisropyl ethylamine (3.5 mL, 20.3 mmol) in ethanol (20 mL) was stirred at reflux for 2 days. The mixture was cooled to room temperature and the crude product was collected by filtration and recrystallised from ethanol to give the title compound as a dull yellow crystalline solid.

Yield = 2.990 g, 8.04 mmol, 86%.

$R_f$ = 0.88. (ethyl acetate 3:7 petroleum spirit 40-60°C)

Mp 194.6 – 195.5 °C.

$^1$H NMR (CDCl$_3$; δCDCl$_3$=7.27ppm): 7.25-7.35 (overlapping m, 6H, Ar-H), 7.49-7.61 (overlapping m, 8H, Ar-H), 8.07-8.13 (overlapping m, 2H, Ar-H), 8.14 (s, 1H, N=CH), 8.34-8.41 (overlapping m, 2H, Ar-H), 8.60 (s, 1H, anthryl-H10) ppm.

MS (+APCI) m/z = 373 (M+H)⁺;

IR (KBr) ν = 3053, 3025, 1587, 1494, 1448, 1323, 1304, 1207 cm⁻¹.

Elemental analysis: Found % (calculated %) C 86.92 (87.07), H 5.38 (5.41), N 7.41 (7.52).

### 5.3.3 Preparation of N'-[1-pyren-9-yl-meth-(E)-ylidene]-N,N-diphenylhydrazine (77)
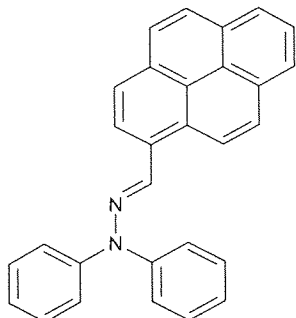


A mixture of N,N-diphenylhydrazine hydrochloride (2.051 g, 9.3 mmol), pyrene-1-carboxahdehyde (2.387 g, 10.5 mmol) and N,N-diisopropyl ethylamine (3.5 mL, 20.3 mmol) in ethanol (20 mL) was stirred at reflux for 2 days. The mixture was cooled to room temperature and the crude product was collected by filtration and recrystallised from ethanol to give the title compound as a brown crystalline solid.

Yield = 1.277 g, 3.2 mmol, 35%

Mp 125.2 – 127.0 °C

¹H NMR (D₆-DMSO δ DMSO = 2.50 ppm): 7.28-7.37 (overlapping m, 6H, Ar-H), 7.57 (t, 4H, J=8.4Hz, Ar-H), 8.07 (1H, t, J=7.7Hz, pyrenyl-H), 8.12 (s, 1H, N=CH), 8.18 (s, 2H, Ar-H), 8.23 (d, 2H, J=8.3Hz, Ar-H), 8.27-8.34 (overlapping m, 3H, Ar-H), 8.61 (d, 1H, J=8.3Hz, pyrenyl-H) ppm

MS (+APCI) m/z = 396 (M+), 168 (M-Ph₂N)⁺

IR (KBr) ν = 1593, 1577, 1558, 1483, 1384, 1278, 1207 cm⁻¹

Elemental analysis: Found % (calculated %) C 87.57 (87.85), H 5.06 (5.08), N 6.82 (7.07).

### 5.3.4 Preparation of N'-[1-phenanthracen-9-yl-meth-(E)-ylidene]-N,N-diphenylhydrazine (78)
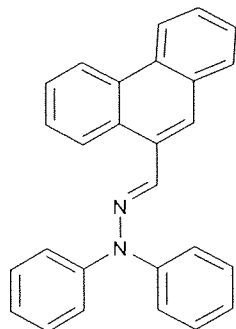


A mixture of N,N-diphenylhydrazine hydrochloride (2.047 g, 9.3 mmol), anthracene-9-carboxahdehyde (2.096 g, 10.2 mmol) and N,N-diisopropyl ethylamine (3.5 mL, 20.3 mmol) in ethanol (20 mL) was stirred at reflux for 2 days. The mixture was cooled to room temperature and the crude product was collected by filtration and recrystallised from ethanol to give the title compound as a khaki crystalline solid.

Yield = 1.20 g, 3.2 mmol, 35%

$R_f$ = 0.70 (ethyl acetate 3:7petroleum spirit 40-60°C)

Mp 118.5 – 122.5 °C

$^1$H NMR (CDCl$_3$; δCDCl$_3$=7.27ppm): 7.23-7.36 (overlapping m, 6H, Ar-H), 7.46-7.72 (overlapping m, 8H, Ar-H), 7.87 (s, 1H, phenanthrenyl-H), 7.91 (m, 1H, phenanthrenyl-H), 8.06 (s, 1H, N=CH), 8.63-8.78 (overlapping m, 3H, Ar-H) ppm

MS (+ APCI) m/z = 373 (M+H)$^+$, 168 (M-Ph$_2$N)$^+$

IR (KBr) ν = 3056, 3031, 1585, 1564, 1495, 1452, 1386, 1296 cm$^{-1}$.

Elemental analysis: Found % (calculated %) C 86.97 (87.07), 5.38 (5.41), N 7.42 (7.52).


## 5.3.5 Preparation of 2-acrylamidobenzamide (79)
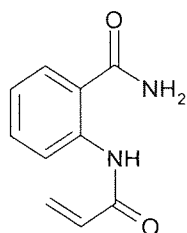


Acryloyl chloride (4.0 mL, 44.2 mmol) was added drop-wise over a period of ten minutes to a solution of 2-aminobenzamide (3.151 g, 23.1 mmol) and triethylamine (6.2 mL, 44.5 mmol) in dry THF (15mL). The mixture was stirred at room temperature for 18 hours and then poured onto ice-water (250 mL). The resulting precipitate was collected by filtration, washed with water (2 x 100mL) and dried under high vacuum to give the product as a pale yellow powder.


Yield = 1.932 g, 10.2 mmol, 44%

Mp 161.7 – 167.7 °C (pronounced softening above 135 °C)

$^1$H NMR (D$_6$-DMSO δ DMSO = 2.50 ppm): 5.81 (dd, 1H, J= 9.5, 2.2 Hz, C=CH$_2$), 6.2-6.4 (overlapping m, 2H, C=CH$_2$ and COCH), 7.15 (m, 1H, Ar-4H), 7.49 (m, 1H, Ar-5H), 7.76 (bs, 1H, NH$_2$), 7.83 (dd, 1H, J= 1.3, 7.9 Hz, Ar-3H), 8.30 (bs, 1H, NH$_2$), 8.53 (d, 1H, J= 7.6Hz, Ar-6H ), 12.01 (bs, 1H, CONH) ppm

MS (+ APCI): 191 (M+H)$^+$, 174 (M-NH$_2$)$^+$

IR (KBr) ν = 3361, 3191, 1675 (CO), 1628, 1583, 1525, 1448, 1396 cm$^{-1}$.


## 5.3.6 Preparation of Quinine Acrylate (80)
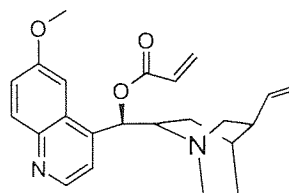


Drop-wise additions of acrylol chloride (2.2 mL, 26.5 mmol) over a period of 10 minutes were made to a stirred solution of quinine (5.110 g, 13.23 mmol) and triethylamine (4 mL, 26.5 mmol) dissolved in dry THF

(100 mL). Then the reaction mixture was placed in the ice-bath under argon atmosphere and stirred for 1 hour.

The reaction mixture was poured onto an excess of ice/water (200 mL), stirred for 20 minutes, which resulted in a solid precipitate. This solid precipitate was collected by filtration and dried under high vacuum.

The solid material was dissolved in chloroform (100 mL) and washed with water (2 x 100 mL). The chloroform layer was dried over magnesium sulphate and the solvent removed under reduced pressure to give an orangey brownish sticky solid.

Yield = 3.101 g, 8.20 mmol, 62%

$^1$H NMR (CDCl$_3$; δ CHCl$_3$ = 7.27 ppm): 2.71 (overlapping m, 3H, bicyclic), 3.16 (overlapping m, 3H, bicyclic), 3.45 (overlapping m, 1H, bicyclic chiral carbon), 3.98 (s, 3H, CH$_3$), 5.01 (COOCH), 5.87 (overlapping m, (CH=CH$_2$)$_2$) 7.36 (overlapping m, 2H, Ar-H), 7.48 (dd, 1H, 2.5 Hz, Ar-H), 8.03 (dd, 1H, 10.0 Hz, Ar-H), 8.75 (dd, 1H, 7.5 Hz, Ar-H) ppm

MS (+ APCI) m/z = 379 (M+H)$^+$

IR (KBr) ν = 3419, 3067, 3033, 2930 (alkyl), 2877, 1924, 1725 (C=O), 1621 (C=C), 1590, 1503, 1475, 1404, 1355, 1299 cm$^{-1}$.

### 5.3.7 Preparation of Quinine Acetate (82)
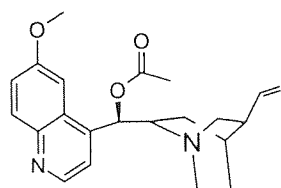


Drop-wise additions of acetyl chloride (1.3 mL, 18.3mmol) over a period of 25 minutes were made to a stirred solution of quinine (3.001 g, 7.94 mmol) and triethylamine (2.2 mL, 15.88 mmol) dissolved in dry THF (100 mL). Then the reaction mixture was placed in the ice-bath under argon atmosphere and stirred for 1 hour.

The reaction mixture was allowed to cool to room temperature and poured onto an excess of ice/water (300 mL). This resulted in a sticky product. This product was dissolved in DCM and then the two layers were separated. The DCM layer was dried over magnesium sulphate. The aqueous layer was washed with DCM (2 x 200 mL). The DCM layer was then washed with distilled water (2 x 300 mL), separated and dried like before. Then the organic solvent was removed under reduced pressure at 50°C to give the product as an orangey brownish solid.

Yield = 1.864 g, 5.10 mmol, 64%

234

Mp 97.5 – 93.4 °C

$^1$H NMR (CDCl$_3$, δ CHCl$_3$ = 7.27 ppm): 2.12 (s, 3H, OCOCH3), 2.75 (overlapping m, 3H, bicyclic), 3.15 (overlapping m, 3H, bicyclic), 3.39 (overlapping m, 1H, bicyclic chiral carbon), 4.04 (s, 3H, CH$_3$), 5.02 (COOCH), 5.05 (dd, 1H, J= 1.5, 6.7 Hz, CH=C$\underline{H}_2$), 5.83 (dd, 1H, J= 1.5, 15.8 Hz, CH=C$\underline{H}_2$), 6.58 (dd, 1H, J= 6.3, 15.8 Hz, C$\underline{H}$=CH$_2$), 7.37 (overlapping m, 2H, Ar-H), 7.47 (dd, 1H, 2.6 Hz, Ar-H), 8.02 (dd, 1H, 9.2 Hz, Ar-H), 8.74 (dd, 1H, 4.6 Hz, Ar-H) ppm

MS (+ APCI) m/z = 367 (M+H)$^+$

IR (KBr) ν = 3329, 3044, 3003, 2928 (alkyl), 2757, 1841, 1755 (C=O), 1624 (C=C), 1559, 1491, 1401, 1336, 1251 cm$^{-1}$.

### 5.3.8 Preparation of 4-(Biphenyl-4-carbonyl)-piperazine-1-carboxylic acid tert-butyl ester (96)
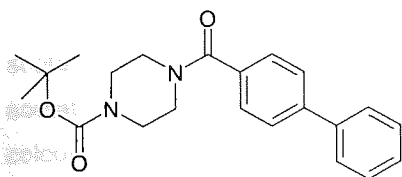


A mixture of piperazine-1-carboxylic acid tert-butyl ester (0.446 g, 2.42 mmol), Hünig's base (1.4 mL, 2.68 mmol) and dry THF (10 mL) was stirred for 5 minutes. Then 4-biphenylcarbonyl chloride (0.846 g, 4 mmol) dissolved in dry THF (5 mL) was added to this reaction mixture drop-wise over a period of 5 minutes. This reaction mixture was stirred for 18 hours at room temperature.

The reaction mixture was then poured onto ice/water (50 mL) and the precipitate was collected by filtration. The resultant white fine powder product was then dried under high vacuum

Yield= 0.804 g, 2.2 mmol, 91%

R$_f$ 0.63 (ethyl acetate)

Mp 158.2 – 163.2 °C

$^1$H NMR (CDCl$_3$, δ CHCl$_3$ = 7.27 ppm): 1.48 (s, 9H, (CH$_3$)$_3$), 3.58 (overlapping m, 8H, N(CH$_2$CH$_2$)$_2$N), 7.53 (overlapping m, 9H, biphenyl) ppm

MS (+APCI) m/z = 367 (M+H)$^+$, 310 (M-C(CH$_3$)$_3$)$^+$, 266 (M-COO)

IR (KBr) ν = 3441, 3009, 2973, 2927, 2869, 1683 (amide- C=O), 1625 (benzene), 1463, 1434, 1367 (tert-butyl), 1288, 1251 cm$^{-1}$.

### 5.3.9 Preparation of 4-(Naphthalene-1-carbonyl)-piperazine-1-carboxylic acid tert-butyl ester (97)
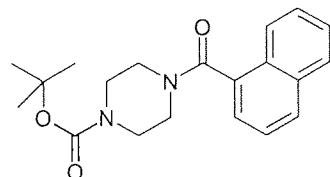


A mixture of piperazine-1-carboxylic acid tert-butyl ester (1.052 g, 5.65 mmol), Hünig's base (2.8 mL, 16.11 mmol) and dry THF (10 mL) was stirred for 5 minutes. Then 1-napthoyl chloride (1.671 g, 8.8 mmol)

dissolved in dry THF (5 mL) was added to this reaction mixture drop-wise over a period of 5 minutes and stirred for 6 hours at room temperature.

Then the reaction mixture was poured onto a saturated aqueous sodium bicarbonate solution (50 mL) and extracted with ethyl acetate (2 x 50mL). The ethyl acetate layer was dried over magnesium sulphate and the solvent was removed under reduced pressure to give the solid material. Then the solid material was dried under high vacuum.

The solid material was dissolved in ethyl acetate and treated with duolite A7-resin. This reaction mixture was heated for 48 hours and the resin was removed by filtration. The filtrate was collected and the solvent was removed under reduced pressure to yield the solid material.

The compound was purified by flash chromatography eluting with petroleum spirit (60-80 °C) and ethyl acetate 1/1 rising to 3/7. The fractions corresponding to $R_f$ 0.51 (petroleum spirit (60-80 °C) 3:7 ethyl acetate) were combined and the solvent was evaporated to give the target compound as a light cream coloured crystalline solid.

Yield= 1.285 g, 3.78 mmol, 67%

Mp 108.2 – 112.5 °C

$^1$H NMR ($D_6$ DMSO δ DMSO = 2.50 ppm): 1.39 (s, 9H, tertbutyl), 3.40 (overlapping m, 8H, $N(CH_2CH_2)_2N$), 7.53 (overlapping m, 4H, Ar-H), 7.79 (dd, m, 1H, J= 6.25 Hz, Ar-H), 7.99 (overlapping m, 2H, Ar-H ) ppm

MS (+APCI) m/z = 341 $(M+H)^+$, 283 $(M-C(CH_3)_3)^+$, 240 $(M-COO)^+$

IR (KBr) ν = 3050, 3002, 2981, 2925 (alkyl), 2862, 1694, 1633 (C=O), 1481, 1417, 1363 (tert-butyl) $cm^{-1}$.

### 5.3.10 Preparation of 4-(Naphthalene-2-carbonyl)-piperazine-1-carboxylic acid tert-butyl ester (98)
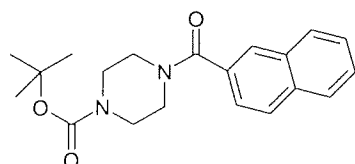


A mixture of piperazine-1-carboxylic acid tert-butyl ester (1.048 g, 5.63 mmol), Hünig's base (2.8 mL, 16.11 mmol) and dry THF (10 mL) was stirred for 5 minutes. Then 2-napthoyl chloride (1.166 g, 8.72 mmol) dissolved in dry THF (8 mL) was added to this reaction mixture drop-wise over a period of 5 minutes and stirred for 6 hours at room temperature.

Then the reaction mixture was poured onto a saturated sodium bicarbonate solution (50 mL) and extracted with ethyl acetate (2 x 50mL). The ethyl acetate layer was dried over magnesium sulphate and the solvent was removed under reduced pressure to give the solid material. Then the solid material was dried under high vacuum.

The solid material was dissolved in ethyl acetate and treated with duolite A7-resin. This reaction mixture was heated for 48 hours and the resin was removed by filtration. The filtrate was collected and the solvent was removed under reduced pressure to yield the solid material.

The compound was purified by flash chromatography eluting with petroleum spirit (60-80 °C) and ethyl acetate 1/1 rising to 3/7. The fractions corresponding to R$_f$ 0.96 (Petroleum spirit (60-80 °C) 3:7 ethyl acetate) were combined and the solvent was evaporated to give the target compound as a pale brown coloured solid.

Yield= 1.116 g, 3.28 mmol, 58%

$^1$H NMR (D$_6$ DMSO δ DMSO = 2.50 ppm): 1.41 (s, 9H, tertbutyl), 3.36 (overlapping m, 8H, N(CH$_2$CH$_2$)$_2$N), 7.55 (overlapping m, 3H, Ar-H), 7.97 (overlapping m, 4H, Ar-H ) ppm

MS (+APCI) m/z = 341 (M+H)$^+$, 283 (M-C(CH$_3$)$_3$)$^+$, 240 (M-COO)$^+$

IR (KBr) ν = 3250, 3102, 2964, 2920 (alkyl), 2752, 1664, 1637 (C=O), 1467, 1405, 1343 (tert-butyl) cm$^{-1}$.

### 5.3.11 Preparation of 4-(5-Dimethylamino-naphthalene-1-sulfonyl)-piperazine-1-carboxylic acid tert-butyl ester (99)
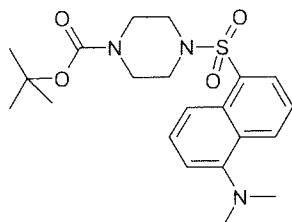


A mixture of piperazine-1-carboxylic acid tert-butyl ester (1.034 g, 5.6 mmol), Hünig' base (2.8 mL, 16.11 mmol) and dry THF (20 mL) was stirred for 5 minutes. Then dansyl chloride (2.220 g, 8.23 mmol) dissolved in dry THF (5 mL) was added to this reaction mixture drop-wise over a period of 5 minutes and stirred for 48 hours at room temperature.

Then the reaction mixture was poured onto a saturated aqueous sodium bicarbonate solution (100 mL) and extracted with ethyl acetate (2 x 50mL). The ethyl acetate layer was dried over magnesium sulphate and the solvent was removed under reduced pressure to give the solid material.

The solid material was dissolved in ethyl acetate (15 mL) and treated with duolite A7-resin. This reaction mixture was heated for 18 hours and the resin was removed by filtration. The filtrate was collected and the solvent was removed under reduced pressure to yield the solid material.

The compound was purified by flash chromatography eluting with petroleum spirit (60-80 °C) and ethyl acetate 7/3. The fractions corresponding to R$_f$ 0.68 (petroleum spirit (60-80 °C) 1:1 ethyl acetate) were combined and the solvent was evaporated to give the target compound as a yellow coloured powder.

Yield= 0.957 g, 2.28 mmol, 41%

$^1$H NMR (D$_6$ DMSO δ DMSO = 2.50 ppm): 1.33 (s, 9H, tertbutyl), 2.83 (s, 6H, N(CH$_3$)$_2$), 3.19 (overlapping m, 8H, N(CH$_2$CH$_2$)$_2$N), 7.28 (dd, 1H, J= 7.5Hz , Ar-H ), 7.64 (overlapping m, 2H, Ar-H), 8.12 (dd, 1H, J= 7.5 Hz, Ar-H ), 8.29 (dd, 1H, J= 8.8 Hz, Ar-H ), 8.53 (dd, 1H, J= 8.8 Hz, Ar-H ) ppm

MS (+ES) m/z = 420 (M+H)$^+$, 356 (M-C(CH$_3$)$_3$)$^+$, 321 (M-COO)$^+$

IR (KBr) ν = 3301, 3165, 2985, 2816, 2892 (alkyl), 1656 (C=O), 1552, 1472, 1368 (tert-butyl), 1302, 1282 cm$^{-1}$.

### 5.3.12 Preparation of Lissamine rhodamine B-sulphonyl- piperazine-1-carboxylic acid tert-butyl ester (100)
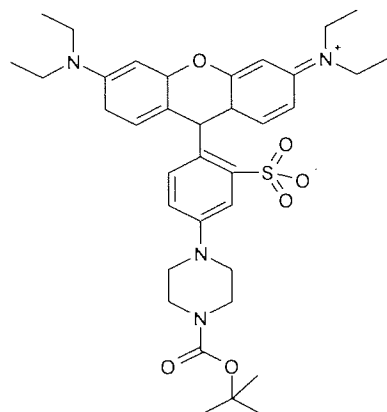


A mixture of piperazine-1-carboxylic acid tert-butyl ester (0.240 g, 1.3 mmol), Hünig's base (0.64 mL, 3.69 mmol) and dry THF (20 mL) was stirred for 5 minutes. Then lissamine rhodamine B-sulphonyl chloride (1.1400 g, 1.98 mmol) dissolved in dry THF (8 mL) was added to this reaction mixture drop-wise over a period of 5 minutes and was stirred for 3 days at room temperature.

The solid material was dissolved in ethyl acetate and treated with duolite A7-resin. This mixture was heated at 40 °C for 24 hours and the resin was removed by filtration. The filtrate was collected and the solvent was removed under reduced pressure to yield the solid material.

The compound was purified by flash chromatography eluting with methanol and ethyl acetate 3/7 rising to 4/6, 1/1 and 6/4. The fractions corresponding to R$_f$ 0.66 (methanol 3:7 ethyl acetate) were combined and the solvent was evaporated to give the target compound as a dark red wine coloured crystalline solid.

Yield= 0.867 g, 1.18 mmol, 60%

Mp 106.9 – 108.9 °C

$^1$H NMR (D$_6$ DMSO δ DMSO = 2.50 ppm): 1.14 (overlapping, m, 20H), 1.40 (s, 9H, tertbutyl), 3.56 (overlapping m, 8H, N(CH$_2$CH$_2$)$_2$N), 6.94 (overlapping m, 7H, Ar-H), 7.54 (overlapping m, 2H, Ar-H ), 7.89 (overlapping m, 2H, Ar-H ), 8.28 (overlapping m, 2H, Ar-H ) ppm

MS (+ES) m/z = 727 (M+H)$^+$

IR ν = 3085, 2971, 2933 (alkyl), 2867, 1692, 1646 (C=O), 1588, 1465, 1413, 1334 cm$^{-1}$.

## 5.3.13 Preparation of Biphenyl-4-yl-piperazin-1-yl-methanone (101)
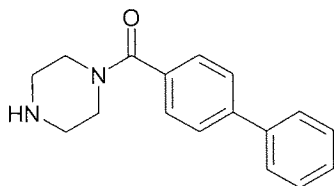


A mixture of 4-(5-dimethylamino-naphthalene-1-sulfonyl)-piperazine-1-carboxylic acid tert-butyl ester (0.804 g, 2.2 mmol), and DCM (30 mL) was stirred for 5 minutes. Then 10% of trifluoroacetic acid (3 mL) was added to this reaction mixture and stirred for 18 hours at room temperature.

The reaction mixture was poured onto a saturated aqueous solution of sodium bicarbonate (100 mL) and stirred for a further 2 days. The reaction mixture was then extracted with ethyl acetate (7 x 25 mL). The organic solvent was removed under reduced pressure to give the product as a white powder.

Yield= 0.50 g, 1.88 mmol, 86%

$R_f$ 0.05 (ethyl acetate 1:1 petroleum spirit 60-80 °C)

Mp 153.2 – 157.9°C

$^1$H NMR ($D_6$-DMSO δ DMSO = 2.50 ppm): 3.17 (overlapping m, 8H, N($CH_2CH_2$)$_2$N), 7.71 (overlapping m, 9H, biphenyl), 8.99 (s, 1H, NH) ppm

MS (+APCI) m/z = 267 (M+H)$^+$

IR (KBr) ν = 3430, 3109, 2962, 2902, 2845, 1689 (amide- C=O), 1525 (benzene), 1483, 1430, 1281,1268 cm$^{-1}$.

## 5.3.14 Preparation of Dimethyl-[5-(piperazine-1-sulfonyl)-naphthalen-1-yl]-amine (102)
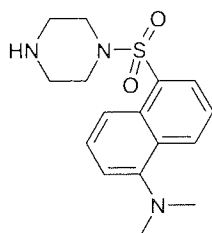


A mixture of 4-(5-dimethylamino-naphthalene-1-sulfonyl)-piperazine-1-carboxylic acid tert-butyl ester (0.957 g, 2.3 mmol), and DCM (5 mL) was stirred. Then 20% of trifluoroacetic acid was added to this reaction mixture and stirred for 18 hours at room temperature. Then another 10% of trifluoroacetic acid was added to this reaction mixture and stirred for 18 hours. The latter procedure was carried out again.

In total 40% trifluoroacetic acid was added to the reaction mixture and stirred in total for 54 hours. The resultant solid material was a yellow coloured crystalline powder.

Yield= 0.497 g, 1.58 mmol, 68%

$R_f$ =0.13 (ethyl acetate)

Mp 124.8 – 127.5 °C

$^1$H NMR (D$_6$ DMSO δ DMSO = 2.50 ppm): 2.83 (s, 6H, N(CH$_3$)$_2$), 3.39 (overlapping m, 8H, N(CH$_2$CH$_2$)$_2$N), 7.27 (dd, 1H, J= 7.3 Hz, Ar-H ), 7.66 (overlapping m, 2H, Ar-H), 8.11 (dd, 1H, J= 1.3, 1, 7.5 Hz, Ar-H ), 8.32 (overlapping m, 2H, Ar-H and NH), 8.53 (dd, 1H, J= 8.3 Hz, Ar-H ) ppm

MS (+APCI) m/z = 320 (M+H)$^+$

IR (KBr) ν = 3411, 3345 (NH), 2958 (alkyl), 2826, 2792, 1606, 1582, 1451, 1328, 1312, 1292 cm$^{-1}$.

**5.3.15 Preparation of [4-(2-Amino-benzoyl)-piperazin-1-yl]-biphenyl-4-yl-methanone (103)**
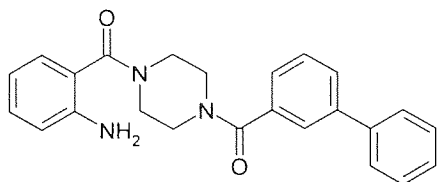


A mixture of isatoic anhydride (0.463 g, 2.84 mmol), and ethanol (30 mL) was stirred and heated for 5 minutes. Then biphenyl-4-yl-piperazin-1-yl-methanone (0.50 g, 1.88 mmol) was added to this reaction mixture and heated under reflux for 5 days. The reaction mixture was cooled to room temperature. The solid material was collected by filtration and washed with cold ethanol. Then the solid material was dried under high vacuum.

The eluent left over by the filtration was further reacted with more isatoic anhydride (0.456 g, 2.8 mmol) and heated under reflux for a day. The solid product was collected by filtration, washed with cold ethanol and dried under high vacuum.

The compound was purified by flash chromatography eluting with petroleum spirit (60-80 °C) and ethyl acetate 1/1 and then ethyl acetate alone. The fractions corresponding to R$_f$ 0.07 (ethyl acetate 1: 1 petroleum spirit 60-80 °C) were combined and the solvent was evaporated to give the target compound as a pale white powder.

Yield = 0.188 g, 0.49 mmol, 26%

R$_f$ 0.07 (ethyl acetate 1: 1 petroleum spirit 60-80 °C)

Mp 148.2 – 152.5 °C

$^1$H NMR (D$_6$-DMSO δ DMSO = 2.50 ppm): 3.53 (overlapping m, 8H, N(CH$_2$CH$_2$)$_2$N), 5.22 (s, 2H, NH$_2$), 6.57 (dd, 1H, J= 7.25, 15.0 Hz, Ar-H), 6.70 (dd, 1H, J= 7.25, 7.25 Hz, Ar-H), 7.02 (dd, 1H, J= 7.25, 7.25 Hz, Ar-H), 7.10 (dd, 1H, J= 7.25, 15.0 Hz, Ar-H), 7.57 (overlapping m, 9H, biphenyl) ppm

MS (+APCI) m/z = 386 (M+H)$^+$

IR (KBr) ν = 3449, 3357 (NH), 3050, 3023, 2859, 1617 (C=O), 1494, 1459, 1430, 1364, 1297 cm$^{-1}$.

## 5.3.16 Preparation of (2-Amino-phenyl)-{4-[3-((E)-1-dimethylamino-propenyl)-2-methyl-benzenesulfonyl]-piperazin-1-yl}-methanone (104)
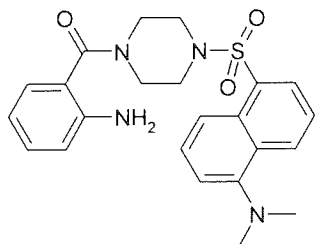


A mixture of dimethyl-[5-(piperazine-1-sulfonyl)-naphthalen-1-yl]-amine (0.497 g, 1.58 mmol), and ethanol (20 mL) was stirred and heated for 5 minutes. Then isatoic anhydride (0.319 g, 1.96 mmol) dissolved in ethanol (6 mL) was added to this reaction mixture drop-wise over a period of 9 minutes and heated with reflux for 18 hours. After this more isatoic anhydride (0.559 g, 3.43 mmol) dissolved in ethanol (10 mL) was added to the reaction mixture drop-wise over a period of 10 minutes and again heated under reflux for another 4 hours. Again more isatoic anhydride (0.293 g, 1.8 mmol) dissolved in ethanol (5 mL) was added to the reaction mixture drop-wise over a period of 8 minutes and further heated under reflux for 3 hours.

The reaction mixture was cooled to room temperature. The solid material was collected by filtration and washed with cold ethanol. Then the light brown coloured powder was dried under high vacuum.

Yield= 0.383g, 0.87mmol, 55.3%

R$_f$ 0.72 (methanol)

Mp 130.3 – 134.9 °C

$^1$H NMR (D$_6$ DMSO δ DMSO = 2.50 ppm): 2.85 (s, 6H, N(CH$_3$)$_2$), 3.41 (overlapping m, 8H, N(CH$_2$CH$_2$)$_2$N), 5.11 (s, 1H, NH), 6.56 (overlapping m, 2H, Ar-H), 7.14 (overlapping m, 6H, Ar-H), 7.67 (overlapping m, 2H, Ar-H) ppm

MS (+APCI) m/z = 439 (M+H)$^+$

IR (KBr) ν = 3494 (NH), 3266, 3104, 2934 (alkyl), 2865, 2792, 1768 (C=O), 1729, 1600, 1488, 1463, 1411, 1371, 1261 cm$^{-1}$.

## 5.3.17 Preparation of N-{2-[4-(5-Dimethylamino-naphthalene-2-sulfonyl)-piperazine-1-carbonyl]-phenyl}-acetamide (105)
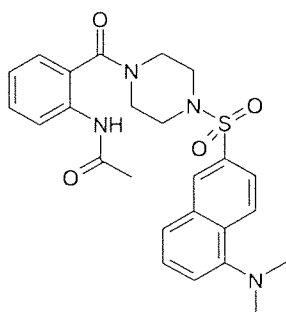
A mixture of (2-amino-phenyl)-{4-[3-((E)-1-dimethylamino-propenyl)-2-methyl-benzenesulfonyl]-piperazin-1-yl}-methanone (0.238 g, 0.54 mmol) and dried THF (8 mL) was stirred for 5 minutes. Then to this reaction mixture triethylamine (0.15 mL, 1.08 mmol) was added. The reaction mixture was cooled in the ice-bath whilst acetyl chloride (0.1 mL, 1.41 mmol) was added drop-wise over a period for 10 minutes. Then this reaction mixture was stirred for 18 hours at room temperature.

After this period more triethylamine (0.15 mL, 1.08 mmol) was added to the reaction mixture and stirred for a further 18 hours at room temperature.

Following this period of time more triethylamine (0.3 mL, 2.16 mmol) and DMAP (0.020 g, 0.17 mmol) was added to the reaction mixture and stirred for 48 hours at room temperature.
Then the reaction mixture was poured onto ice/water (50 mL) and extracted with ethyl acetate (3 x 25mL). The ethyl acetate layer was dried over magnesium sulphate and the solvent was removed under reduced pressure to give the solid material. Then the solid material was dried under high vacuum.

The compound was purified by flash chromatography eluting with petroleum spirit (60-80 °C) and ethyl acetate 8/2, 6/4 rising to 2/8. The fractions corresponding to $R_f$ 0.14 (petroleum spirit (60-80 °C) 4:6 ethyl acetate) were combined and the solvent was evaporated to give the target compound.

This particular fraction ($R_f$ 0.14) was further purified by flash chromatography eluting with petroleum spirit (60-80 °C) and ethyl acetate 1/1 and rising to 3/7. The fractions corresponding to $R_f$ 0.28 (petroleum spirit (60-80 °C) 1:1 ethyl acetate) were combined and the solvent was evaporated to give the target compound as a pale yellow coloured crystalline solid.

Yield= 0.160 g, 0.33 mmol, 61%
Mp 186.6- 190.4 °C
$^1$H NMR ($D_6$ DMSO δ DMSO = 2.50 ppm): 1.64 (s, 3H, $CH_3$), 2.84 (s, 6H, $N(CH_3)_2$), 3.36 (overlapping m, 8H, $N(CH_2CH_2)_2N$), 7.25 (overlapping m, 4H, napthyl), 7.35 (overlapping m, 2H, J= 8.3, 15.8, 16, 8.8Hz, napthyl), 8.14 (dd, 1H, J= 7.3Hz , Ar-H ), 8.31 (dd, 1H, J= 8.8Hz , Ar-H ), 8.54 (dd, 1H, J= 8.5Hz , Ar-H ), 9.52 (dd, 1H, Ar-H) ppm
MS (+APCI) m/z = 481 (M+H)$^+$
IR (KBr) ν = 3251 (NH), 3188, 3048, 2949 (alkyl), 2829, 2792, 1697 (C=O), 1607, 1540, 1444, 1330 cm$^{-1}$.

## 5.3.18 Preparation of 2-Acetylamino-N-cyclododecyl-benzamide (106)
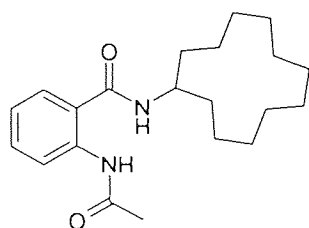
A mixture of 2-amino-N-cyclododecyl-benzamide (0.538 g, 1.8 mmol) and dry THF (100 mL) was stirred for 5 minutes. Followed by a portion wise addition of triethylamine (0.5 mL, 3.6 mmol) to the reaction mixture. The reaction mixture was then cooled in the ice-bath and acetyl chloride (0.3 mL, 3.82 mmol) was added to this reaction mixture drop-wise over a period of 12 minutes. The reaction mixture was stirred for 18 hours at room temperature. The reaction mixture was then poured onto ice/water (250 mL) and stirred for 1 hour. The product was dissolved in ethyl acetate (100 mL) and washed with water (2x 50 mL). The ethyl acetate layer was dried over magnesium sulphate and the solvent was removed under reduced pressure to give the product as a white powder.

Yield= 0.451 g, 1.31 mmol, 73%

Mp 123.9 – 127.5 °C

$^1$H NMR (CDCl$_3$, δ CHCl$_3$ = 7.27 ppm): 1.39-1.96 (overlapping m, 22H, cyclododecane CH$_2$), 2.21 (s, 3H, COCH$_3$), 4.25 (s, 1H, cyclododecane H-1), 6.04 (d, 1H, J= 8.3 Hz, CONH-cyclododecane), 7.07 (dd, 1H, J= 7.5 Hz, Ar-H), 7.42 (dd, 1H, J= 7.8 Hz, Ar-H), 7.48 (dd, 1H, J= 7.8 Hz, Ar-H), 8.57 (dd, 1H, J= 8.5 Hz, Ar-H), 11.04 (s, 1H, -NHCOCH$_3$) ppm

MS (+APCI) m/z = 345 (M+H)$^+$

IR (KBr) ν = 3333 (NH), 3108, 3060, 2952, 2856, 2668, 1675, 1635 (amide C=O), 1590 (benzene ring), 1505, 1447, 1363, 1297 cm$^{-1}$.

### 5.3.19 Preparation of 2-Amino-benzoic acid N-methyl-N'-[1-pyren-4-yl-meth-(E)-ylidene]-hydrazide (107)
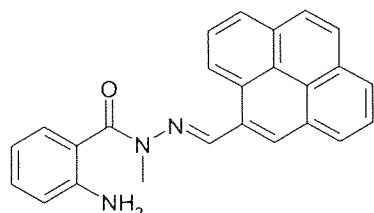


A mixture of pyrene-carboxaldehyde (1.426 g, 6.2 mmol), and ethanol (20 mL) was stirred and heated for 5 minutes. Then to this reaction mixture 1-(2-aminobenzoyl)-1-methylhydrazine (1.00 g, 6.06 mmol) dissolved in ethanol (5 mL) was added drop-wise over a period of 3 minutes and heated under reflux for 3 hours.

The reaction mixture was cooled to room temperature. The solid material was collected by filtration, washed with cold ethanol and dried under high vacuum.

The solid material was recrystallised in ethyl acetate resulting in a white crystalline solid.

Yield= 1.301 g, 3.5 mmol, 57%

R$_f$ 0.38 (ethyl acetate 1:1 petroleum spirit 40-60 °C)

Mp 106.2 – 108.1 °C

$^1$H NMR (D$_6$ DMSO δ DMSO = 2.50 ppm): 3.68 (s, 3H, CH$_3$), 5.30 (s, 2H, NH$_2$), 6.68 (dd, 1H, J= 3.5, 7.5 Hz, Ar-H), 6.83 (dd, 1H, J= 3.8, 7.8 Hz, Ar-H), 7.26 (overlapping m, 2H, Ar-H), 8.21 (overlapping m, 8H, Ar-H), 8.85 (dd, 1H, J= 7.8 Hz, Ar-H), 8.90 (s, 1H, N=CH) ppm

MS (+APCI) m/z = 378 (M+H)$^+$, 228 (M-Ph-NH$_2$(CO)NHCH$_3$)$^+$

IR (KBr) ν = 3467, 3364 (NH), 3039 (alkyl), 1650 (C=O), 1592 (benzene), 1559, 1486, 1454, 1390, 1314 cm$^{-1}$.


## 5.3.20 Preparation of N-(2-{N-Methyl-N'-[1-pyren-1-yl-meth-(E)-ylidene]-hydrazinocarbonyl}-phenyl)-acrylamide (108)
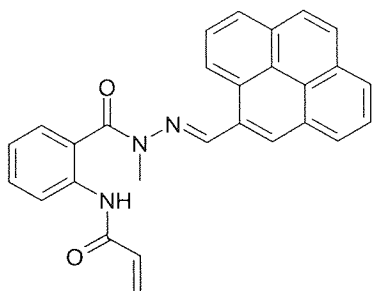


A mixture of 2-amino-benzoic acid N-methyl-N'-[1-pyren-4-yl-meth-(E)-ylidene]-hydrazide (2.0 g, 5.31 mmol) and dry THF (12 mL) was stirred for 5 minutes. Then to this reaction mixture triethylamine (1.5 mL, 10.62 mmol) was added. Then the reaction mixture was cooled in the ice-bath whilst acrylol chloride (0.86 mL, 10.62 mmol) was being added drop-wise over a period of 11 minutes and stirred for a day at room temperature. The reaction mixture was poured onto ice-water (100 mL) and the precipitate collected by filtration. The precipitate was then dried under high vacuum

Yield= 0.842 g, 1.95 mmol, 37%

R$_f$ = 0.46 (ethyl acetate 1:1 petroleum spirit 40-60 °C)

$^1$H NMR (D$_6$ DMSO δ DMSO = 2.50 ppm): 3.66 (s, 3H, CH$_3$), 5.58 (dd, 1H, J= 1.5, 10.3 Hz, CCH$_2$), 6.07 (dd, 1H, J= 1.8, 16.8 Hz, CCH$_2$), 6.42(dd, 1H, J= 10.3, 17 Hz, COCH), 7.44 (overlapping m, 3H, Ar-H), 8.10 (overlapping m, 10H, Ar-H), 8.74 (d, 1H, J= 9.5 Hz, Ar-H), 8.81 (s, 1H, N=CH), 9.73 (s, 1H, NH) ppm

MS (+ES) m/z = 432 (M+H)$^+$, 259 (M-Ph-(CO)NHCOCHCH$_2$)$^+$

IR (KBr) ν = 3256 (NH), 2035, 1638 (C=O), 1600 (benzene), 1515, 1444, 1405, 1341 cm$^{-1}$.


## 5.3.21 Preparation of N-(2-{N-Methyl-N'-[1-pyren-4-yl-meth-(E)-ylidene]-hydrazinocarbonyl}-phenyl)-acetamide (109)
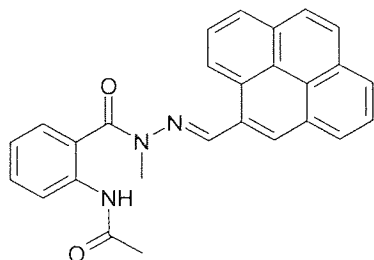
A mixture of 2-amino-benzoic acid N-methyl-N'-[1-pyren-4-yl-meth-(E)-ylidene]-hydrazide (0.944 g, 2.51 mmol) and dry THF (10 mL) was stirred for 5 minutes. Then to this reaction mixture triethylamine (0.74 mL, 5.3 mmol) was added. The reaction was then cooled in the ice-bath whilst acetyl chloride (0.4 mL, 5.3 mmol) was added drop-wise over a period of 12 minutes and stirred for 18 hours at room temperature.

The solid material was recrystallised in THF resulting in a pale yellow fine solid powder.

Yield= 0.832 g, 0.2 mmol, 79%

$R_f$ = 0.12 (ethyl acetate 1:1 petroleum spirit 40-60 °C)

Mp 115.4 – 120.5 °C

$^1$H NMR (D$_6$ DMSO δ DMSO = 2.50 ppm): 1.89 (s, 3H, COCH$_3$), 3.67 (s, 3H, NCH$_3$), 7.27 (dd, 1H, J= 7.3, 14.8Hz, Ar-H), 7.52 (overlapping m, 2H, Ar-H), 7.80 (dd, 1H, J= 8Hz, Ar-H), 8.19 (overlapping m, 8H, Ar-H), 8.75 (dd, 1H, J= 9.5Hz, Ar-H), 8.83 (s, 1H, N=CH), 9.51 (s, 1H, NHCO) ppm

MS (+APCI) m/z = 420 (M+H)$^+$

IR (KBr) ν = 3243 (NH), 3112, 3036, 1679, 1637 (C=O), 1594 (benzene), 1525, 1399, 1349, 1311 cm$^{-1}$.

### 5.3.22 Preparation of 4-(Diphenyl-hydrazonomethyl)-phenol (110)
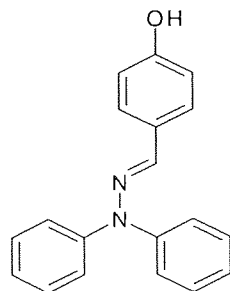


A mixture of N,N-diphenylhydrazine hydrochloride (1.489 g, 6.8 mmol), 4-hydroxy-benzaldehyde (0.906 g, 7.4 mmol) and Hünig's base (1.3 mL, 7.5 mmol) in ethanol (20 mL) was heated under reflux for a day. The reaction mixture was cooled to room temperature and the solvent was removed under reduced pressure.

Then the solid material was dissolved in ethyl acetate and washed with water (3 x 50 mL). The ethyl acetate layer was dried over magnesium sulphate and the solvent removed under reduced pressure.

The compound was purified by flash chromatography eluting with petroleum spirit (60-80 °C) and ethyl acetate 7/3 rising to 1/1 and then ethyl acetate alone. The fractions corresponding to $R_f$ 0.50 (petroleum spirit (60-80 °C) 7:3 ethyl acetate) were combined and the solvent was evaporated to give the target compound as a dark olive green coloured stinky solid.

Yield= 0.732 g, 2.54 mmol, 37%

Mp 94.6 – 97.9 °C

$^1$H NMR (D$_6$ DMSO δ DMSO = 2.50 ppm): 6.76 (overlapping m, 2H, Ar-H), 7.06 (s, 1H, N=CH), 7.16 (overlapping m, 7H, Ar-H), 7.44 (overlapping, m, 6H, Ar-H, OH) ppm.

MS (+APCI) m/z = 289 (M+H)$^+$, 168 (M-Ph(OH)CH=N)$^+$

IR (KBr) $\nu$ = 3394 (OH), 3064, 3008, 2921, 1582 (benzene), 1502, 1455, 1434, 1380, 1284 cm$^{-1}$.

### 5.3.23 Preparation of 5-(Diphenyl-hydrazonomethyl)-benzene-1,2,3-triol (111)
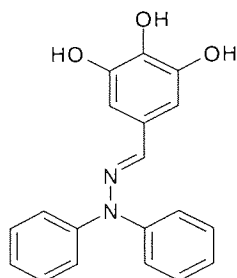


A mixture of N,N-diphenylhydrazine hydrochloride (1.567 g, 7.1 mmol), 3,4,5-trihydroxy-benzaldehyde (1.071 g, 7.0 mmol) and Hünig's base (1.3 mL, 7.5 mmol) in ethanol (20 mL) was heated under reflux for a day. The reaction mixture was cooled to room temperature and the solvent was removed under reduced pressure.

Then the solid material was dissolved in ethyl acetate and washed with water (3 x 50 mL). The ethyl acetate layer was dried over magnesium sulphate and the solvent removed under reduced pressure.

The compound was purified by flash chromatography eluting with petroleum spirit (60-80 °C) and ethyl acetate 1/1 rising to 4/6 and then 2/8. The fractions corresponding to R$_f$ 0.27 (petroleum spirit (60-80 °C) 1:1 ethyl acetate) were combined and the solvent was evaporated to give the target compound as a dark brown coloured stinky solid.

Yield= 0.104 g, 0.33 mmol, 4.6%

Mp 98.4 – 103.3 °C

$^1$H NMR (D$_6$ DMSO $\delta$ DMSO = 2.50 ppm): 5.82 (dd, 2H, Ar-H), 7.06 (overlapping, m, 4H, Ar-H), 7.21 (overlapping m, 2H, J= 7.3Hz, 14.3, Ar-H), 7.47 (overlapping m, 4H, Ar-H), 7.70 (s, 1H, N=CH), 9.68 (s, 1H, OH), 10.74 (s, 2H, OH) ppm

MS (-APCI) m/z = 319 (M-H)$^-$, 168 (M-Ph(OH)$_3$CH=N)$^-$, 152 (M-O)$^-$

IR (KBr) $\nu$ = 3379 (OH), 1616 (benzene), 1526, 1469, 1386, 1359, 1260 cm$^{-1}$.

### 5.3.24 Preparation of (5-Diphenyl-hydrazonomethyl)-benzene-1,3-diol (112)
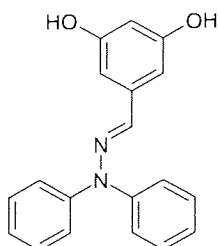
A mixture of N,N-diphenylhydrazine hydrochloride (1.533 g, 7.0 mmol), 3,5-dihydroxy-benzaldehyde (0.965 g, 7.0 mmol) and Hünig's base (1.3 mL, 7.5 mmol) in ethanol (20 mL) was heated under reflux for a day. The reaction mixture was cooled to room temperature and the solvent was removed under reduced pressure.

Then the solid material was dissolved in ethyl acetate and washed with water (3 x 50 mL). The ethyl acetate layer was dried over magnesium sulphate and the solvent removed under reduced pressure.

The compound was purified by flash chromatography eluting with petroleum spirit (60-80 °C) and ethyl acetate 8/2 rising to 1/1 and then 3/7. The fractions corresponding to $R_f$ 0.60 (petroleum spirit (60-80 °C) 1:1 ethyl acetate) were combined and the solvent was evaporated to give the target compound as a black coloured crystalline solid.

Yield= 0.606 g, 2.0 mmol, 29%

Mp 67.4 – 70.8 °C

$^1$H NMR ($D_6$ DMSO δ DMSO = 2.50 ppm): 6.14 (dd, 1H, J= 2.3, 4.3Hz, Ar-H), 6.46 (overlapping m, 2H, Ar-H), 6.90 (s, 1H, N=CH), 7.18 (overlapping m, 6H, Ar-H), 7.47 (overlapping m, 4H, Ar-H), 9.32 (s, 2H, OH) ppm

MS (+APCI) m/z = 305 (M+H)$^+$, 168 (M-Ph(OH)$_2$CH=N)$^+$

IR (KBr) ν = 3279 (OH), 1592 (benzene), 1486, 1455, 1386, 1328, 1293 cm$^{-1}$.

### 5.3.25 Preparation of 5-[1-Pyren-4-yl-meth-(E)-ylidene]-2-thioxo-thiazolidin-4-one (113)
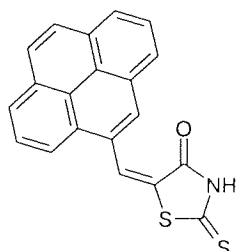


A mixture of pyrene-carboxaldehyde (1.045 g, 4.54 mmol), and ethanol (20 mL) was stirred and heated for 5 minutes. Then 4 drops of piperidine was added to this reaction mixture. This was followed by a drop-wise addition over a period of 5 minutes of rhodanine (0.596 g, 4.5 mmol) solution dissolved in ethanol (6 mL) to the reaction mixture and was heated under reflux for 18 hours.

The reaction mixture was cooled to room temperature. The solid material was collected by filtration, washed with cold ethanol and dried under high vacuum.

The solid material was recrystallised in toluene resulting in a red fluffy solid powder.

Yield= 1.006 g, 2.92 mmol, 65%

$R_f$ 0.78 (ethyl acetate 1:1 petroleum spirit 40-60 °C)

Mp 196.4 – 200.2 °C

$^1$H NMR ($D_6$ DMSO δ DMSO = 2.50 ppm): 8.31 (overlapping m, 11H, Ar-H, C=CH, NH) ppm

MS (-APCI) m/z = 344 (M-H)$^-$

IR (KBr) v = 3430 (NH), 3125, 3017, 2965, 2919, 2852, 1687 (C=O), 1559, 1440, 1315 cm$^{-1}$.


## 5.3.26 Preparation of 5-[1-Pyren-4-yl-meth-(E)-ylidene]-thiazolidine-2,4-dione (114)
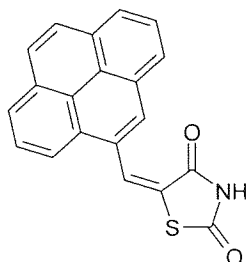


A mixture of pyrene-carboxaldehyde (1.083 g, 4.7 mmol), and ethanol (20 mL) was stirred and heated for 5 minutes. Then 4 drops of piperidine was added to this reaction mixture. This was followed by a drop-wise addition over a period of 5 minutes of 2,4-thiazolidinedione (0 536 g, 4.6 mmol) solution dissolved in ethanol (6 mL) to the reaction mixture and was then heated under reflux for 18 hours.

The reaction mixture was cooled to room temperature. The solid material was collected by filtration, washed with cold ethanol and dried under high vacuum.

The solid material was recrystallised in toluene resulting in a bright orange solid powder.

Yield= 0.964 g, 2.93 mmol, 64%

R$_f$ 0.68 (ethyl acetate 1:1 petroleum spirit 40-60 °C)

Mp 100.6 – 104.6 °C

$^1$H NMR (D$_6$ DMSO δ DMSO = 2.50 ppm): 8.24 (overlapping m, 9H, Ar-H), 8.67 (s, 1H, C=CH), 12.70 (s, 1H, NH) ppm

MS (-APCI) m/z = 328 (M-H)$^-$

IR (KBr) v = 3414 (NH), 3112, 3014, 2770, 1758, 1739, 1695 (C=O), 1567, 1371, 1301 cm$^{-1}$.


## 5.3.27 Preparation of 5-Pyren-4-ylmethylene-pyrimidine-2,4,6-trione (115)
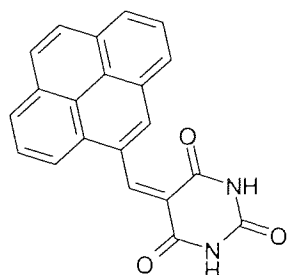


A mixture of pyrene-carboxaldehyde (1.115 g, 4.84 mmol), and ethanol (20 mL) was stirred and heated for 5 minutes. Then 4 drops of piperidine was added to this reaction mixture. This was followed by a drop-wise addition over a period of 5 minutes of barbituric acid (0 566 g, 4.42 mmol) solution dissolved in ethanol (7 mL) to the reaction mixture and then heated under reflux for 18 hours.

248

The reaction mixture was cooled to room temperature. The solid material was collected by filtration, washed with cold ethanol and dried under high vacuum.

The solid material was recrystallised in toluene resulting in a dark orangey red coloured solid powder.

Yield= 1.503 g, 2.5 mmol, 56%

Mp 112.5 – 117.4 °C. $^1$H NMR (D$_6$ DMSO δ DMSO = 2.50 ppm): 8.26 (overlapping m, 9H, Ar-H), 9.11 (s, 1H, C=CH), 11.22 (s, 1H, NH), 11.51 (s, 1H, NH) ppm

MS (-APCI) m/z = 339 (M-H)$^-$

IR (KBr) ν = 3403 (NH), 3191, 3079, 2947, 1739, 1663 (C=O), 1548, 1442, 1415, 1397, 1345, 1311 cm$^{-1}$.

### 5.3.28 Preparation of 5-[1-Pyren-4-yl-meth-(E)-ylidene]-2-thioxo-imidazolidin-4-one (116)
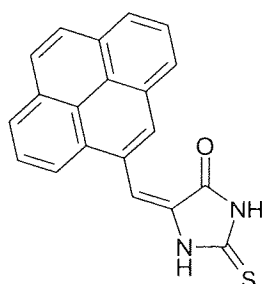


A mixture of pyrene-carboxaldehyde (1.085 g, 4.71 mmol), and ethanol (20 mL) was stirred and heated for 5 minutes. Then 4 drops of piperidine was added to this reaction mixture. This was followed by a drop-wise addition over a period of 5 minutes of 2-thiohydantoin (0.548 g, 4.64 mmol) solution dissolved in ethanol (6 mL) to the reaction mixture and then heated under reflux for 18 hours.

The reaction mixture was cooled to room temperature. The solid material was collected by filtration, washed with cold ethanol and dried under high vacuum.

The solid material was recrystallised in toluene resulting in a light orangey yellow solid powder.

Yield= 0.946 g, 2.89 mmol, 62%

R$_f$ 0.80  (ethyl acetate 1:1 petroleum spirit 40-60 °C)

Mp 99.3 – 103.8 °C

$^1$H NMR (D$_6$ DMSO δ DMSO = 2.50 ppm): 7.40 (s, 1H, C=CH), 8.26 (overlapping m, 9H, Ar-H), 12.40 (s, 2H, 2NH) ppm

MS (-APCI) m/z = 327 (M-H)$^-$, 295 (M-S)$^-$

IR ν = 3421 (NH), 3177, 3045, 1758, 1704, 1623 (C=O), 1588, 1496, 1357,1311 cm$^{-1}$.

## 5.3.29 Preparation of N-Pyren-4-ylmethyl-acetamide (117)
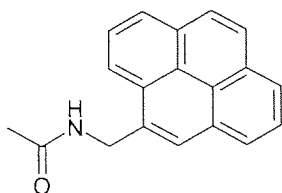


A mixture of 1-pyrenemethylamine hydrochloride (1.042 g, 3.89 mmol), triethylamine (2.2 mL, 15.56 mmol) and DMAP (0.031 g, 0.26 mmol) was dissolved in dried DCM (80 mL). This reaction mixture was then stirred for 5 minutes, cooled in the ice-bath whilst acetyl chloride (0.55 mL, 7.78 mmol) was added drop-wise over a period of 12 minutes and stirred for a day at room temperature.

After this period more triethylamine (2.2 mL, 15.56 mmol) and acetyl chloride (0.55 mL, 7.78 mmol) was added drop-wise over a period of 10 minutes to the cooled reaction mixture. This reaction mixture was stirred for another 6 hours.
The reaction mixture was then poured onto ice/water (250 mL) and stirred for 1 hour. Then the solid material was dissolved in ethyl acetate (150 mL) and washed with water (2 x 50 mL). The ethyl acetate layer was dried over magnesium sulphate and the solvent removed under reduced.

The solid material was recrystallised in ethyl acetate resulting in a brownish yellow solid powder.

Yield= 0.834 g, 3.06 mmol, 79%
$R_f$ = 0.14 (ethyl acetate 1:1 petroleum spirit 40-60 °C)
Mp 124.9 – 127.6 °C
$^1$H NMR ($D_6$ DMSO $\delta$ DMSO = 2.50 ppm): 1.92 (s, 3H, COCH$_3$), 5.00 (d, 2H, J= 5.8 Hz, CH$_2$), 8.21 (overlapping, m, 9H, Ar-H), 8.54 (t, 1H, J= 5.5, 5.3, 10.8 Hz, NH) ppm
MS (-APCI) m/z = 272 (M-H)$^-$
IR (KBr) $\nu$ = 3272 (NH), 3033, 2921, 2883 (alkyl), 1633 (C=O), 1459, 1434, 1368 cm$^{-1}$.

## 5.3.30 Preparation of N-Pyren-4-ylmethyl-acrylamide (118)
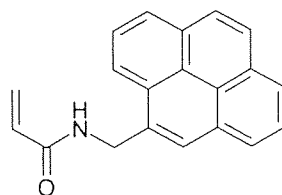


A mixture of 1-pyrenemethylamine hydrochloride (1.045 g, 3.9 mmol), triethylamine (2.2 mL, 15.6 mol) and DMAP (0.035 g, 0.29 mmol) was dissolved in dried DCM (90 mL). This was then stirred for 5 minutes, cooled in the ice-bath whilst acrylol chloride (0.63 mL, 7.8 mmol) was added drop-wise over a period of 11 minutes and stirred for a day at room temperature.

After this period more triethylamine (2.2 mL, 15.6 mmol) and acrylol chloride (0.63 mL, 7.8 mmol) was added drop-wise over a period of 10 minutes to the cooled reaction mixture. This reaction mixture was stirred for another 6 hours.

The reaction mixture was then poured onto ice/water (250 mL) and stirred for 1 hour. The solid material was dissolved in DCM (150 mL) and washed with water (2 x 50 mL). The DCM layer was dried over magnesium sulphate and the solvent removed under reduced.

The compound was purified by flash chromatography eluting with petroleum spirit (60-80 °C) and ethyl acetate 7/3 rising to 1/1, then eluting with methanol and ethyl acetate 5/5. The fractions corresponding to $R_f$ 0.21 (petroleum spirit 60-80 °C 1:1 ethyl acetate) were combined and the solvent was evaporated to give the target compound as a pale yellow coloured solid powder.

Yield= 0.610 g, 2.14 mmol, 55%

$^1$H NMR (D$_6$ DMSO δ DMSO = 2.50 ppm): 5.10 (d, 2H, J= 5.8 Hz, CH$_2$), 5.62 (dd, 1H, CH=C$\underline{H}_2$), 6.14 (dd, 1H, CH=C$\underline{H}_2$), 6.33 (dd, 1H, COC$\underline{H}$), 8.24 (overlapping m, 9H, Ar-H), 8.80 (t, 1H, J= 5.5, 5.5, 11 Hz, NH) ppm

MS (-APCI) m/z = 284 (M-H)$^-$

IR (KBr) ν = 3294, 3040, 2937, 2894 (alkyl, 2753, 1798, 1721, 1652 (C=O), 1615, 1533, 1471, 1390, 1353 (NH), 1303 cm$^{-1}$.

### 5.3.31 Preparation of 2-Acryloylamino-N-cyclododecyl-benzamide (119)
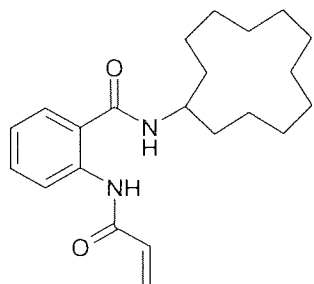


A mixture of 2-amino-N-cyclododecyl-benzamide (2.910 g, 9.64 mmol) and dry THF (25 mL) was stirred for 5 minutes. Followed by a portion wise addition of triethylamine (2.5 mL, 18.0 mmol) to the reaction mixture. The reaction mixture was cooled in the ice-bath and then acrylol chloride (1.6 mL, 18.3 mmol) was added to this drop-wise over a period of 10 minutes. The reaction mixture was stirred for an hour at room temperature. The reaction mixture was then poured onto ice/water (300 mL) and stirred for 20 minutes. The resultant precipitate was collected by filtration and dried under high vacuum for 18 hours.

The product was dissolved in chloroform (50mL) and washed with water (2x 100mL). The chloroform layer was dried over magnesium sulphate and the solvent was removed under reduced pressure at 35 °C to give the product as a white powder.

Yield= 2.437 g, 6.85 mmol, 71%

$^1$H NMR (CDCl$_3$; δ CHCl$_3$ = 7.27 ppm): 1.38-177 (overlapping m, 22H, cyclododecyl CH$_2$), 4.25 (s, 1H, cyclododecane H-1), 5.76 (dd, 1H, J= 7.3 Hz, COCH), 6.10 (d, 1H, J= 8.0 Hz, CONH-cyclododecane), 6.31 (dd, 2H, J=17 Hz, CCH$_2$), 7.08 (dd, 1H, J= 8.8 Hz, Ar-H), 7.47 (overlapping m, 2H, Ar-H), 8.71-8.67 (dd, 1H, J= 8.3 Hz, Ar-H), 11.38 (s, 1H, -NHCOCHCH$_2$) ppm

MS (+APCI) m/z = 357 (M+H)$^+$, 174 (M-cyclododecyl-NH)$^+$

IR (KBr) ν = 3322 (NH), 3106, 3058, 3021, 2913, 2846, 1702, 1627 (C=O), 1594 (benzene ring), 1525, 1447, 1332 cm$^{-1}$.

### 5.3.32 Preparation of 2-Amino-N-cyclododecyl-benzamide (120)
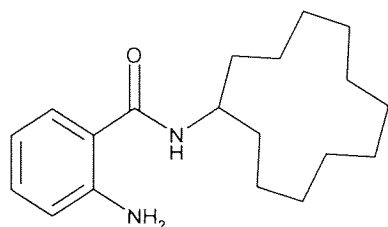


A mixture of cyclododecylamine (11 mL, 60.0 mmol), isatoic anhydride (5.146 g, 31.6 mmol) and ethanol (100 mL) was heated under reflux for 18 hours. The reaction mixture was cooled to room temperature. The solid material was collected by filtration and washed with cold ethanol. The crude product was recrystallised from ethyl acetate to give a white powder.

Yield = 2.537 g, 8.4 mmol, 27%

Mp 115.6 – 118.2 °C

$^1$H NMR (CDCl$_3$; δ CHCl$_3$ = 7.27 ppm): 1.37-1.75 (overlapping, m, 22H, cyclododecane), 4.24 (s, 1H, cyclododecane H-1), 5.86 (d, 2H, 8.3 Hz, NH$_2$), 6.63-6.72 (overlapping, m, 2H, Ar-H), 7.17-7.31 (overlapping, m, 2H, Ar-H), 10.39 (s, 1H, NH) ppm

MS (+APCI) m/z = 303 (M+H)$^+$

IR (KBr) ν = 3426, 3337 (NH$_2$), 3067, 3029, 2967, 1613 (C=O), 1540 (benzene ring), 1444, 1367, 1315 cm$^{-1}$.

### 5.3.33 Preparation of 2-Amino-N-cyclopentyl-benzamide (121)
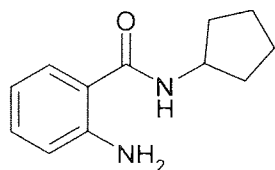


A mixture of cyclopentylamine (11 ml, 122.6 mmol), isatoic anhydride (10.662 g, 66.0 mmol) and ethanol (100 mL) was heated under reflux for 4 days. The reaction mixture was cooled to room temperature. The solid material was collected by filtration and washed with cold ethanol. The crude product was recrystallised from ethyl acetate – hexane and dried under high vacuum.

The compound was further purified by flash chromatography eluting with petroleum spirit (60-80 °C) and ethyl acetate 1/1. The fractions corresponding to $R_f$ 0.55 (petroleum spirit (60-80 °C) 6:4 ethyl acetate) were combined and the solvent was evaporated to give the target compound as coloured crystalline solid.

Yield= 8.094 g, 40.0 mmol, 60%

Mp 111.0 – 114.5 °C

$^1$H NMR (CDCl$_3$; δ CHCl$_3$ = 7.27 ppm): 1.15-2.05 (overlapping m, 8H, cyclopentane), 3.94 (m, 1H, cyclopentane H-1), 5.31 (s, 1H, NH), 5.97 (s, 2H, NH$_2$), 6.72 (dd, 2H, Ar-H), 7.31 (dd, 2H, Ar-H) ppm

MS (+APCI) m/z = 205 (M+H)$^+$, 120 (M-NH$_2$-PENTYL)$^+$

IR (KBr) ν =3465, 3359, 3278 (NH$_2$), 3052, 2933, 2954, 1621 (C=O), 1586 (benzene ring), 1546, 1450, 1346, 1316 cm$^{-1}$.

### 5.3.34 Preparation of 2-Amino-N-cyclohexyl-benzamide (122)
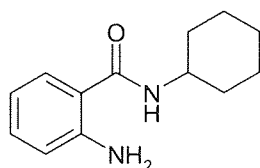


A mixture of cyclohexylamine (12.2 ml, 122.6 mmol), isatoic anhydride (9.950 g, 61.3 mmol) and ethanol (100 mL) was heated under reflux for 18 hours. The reaction mixture was cooled to room temperature. The solid material was collected by filtration and washed with cold ethanol. The crude product was recrystallised from ethyl acetate – hexane and dried under high vacuum.

The compound was further purified by flash chromatography eluting with petroleum spirit (60-80 °C) and ethyl acetate 1/1. The fractions corresponding to $R_f$ 0.35 (petroleum spirit (60-80 °C) 6:4 ethyl acetate) were combined and the solvent was evaporated to give the target compound as coloured crystalline solid.

Yield= 5.010 g, 23.0 mmol, 38%

Mp 103.5 – 107.0 °C

$^1$H NMR (CDCl$_3$; δ CHCl$_3$ = 7.27 ppm): 1.25-2.14 (overlapping m, 10H, cyclohexane), 4.37 (m, 1H, cyclohexane H-1), 5.31 (s, 1H, NH), 6.05 (s, 2H, NH$_2$), 6.69 (dd, 1H, J= 7.8 Hz, Ar-H), 6.75 (dd, 1H, J= 8.0 Hz, Ar-H), 7.23 (dd, 1H, J= 8.0 Hz, Ar-H), 7.31 (dd, 1H, J= 7.8 Hz, Ar-H) ppm

MS (+APCI) m/z = 219 (M+H)$^+$, 120 (M-NH$_2$-BENZYL)$^+$

IR (KBr) ν = 3419, 3276 (NH$_2$), 3197, 3065, 2959, 2871, 1585 (benzene ring), 1611 (C=O), 1444, 1361, 1309 cm$^{-1}$.

### 5.3.35 Preparation of 2-Amino-N-dodecyl-benzamide (123)



253
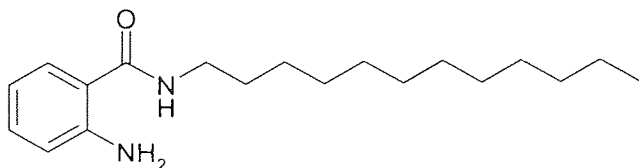
A mixture of n-dodecylamine (11.404 g, 61.5 mmol), isatoic anhydride (5.280 g, 32.5 mmol), and ethanol (100 mL) was heated under reflux for 3 days. The reaction mixture was cooled to room temperature. The solid material was collected by filtration and washed with cold ethanol. The crude product was recrystallised from ethyl acetate and dried under high vacuum.

Yield = 2.936 g, 3.1 mmol, 30%

Mp 72.5 – 73.4 °C

$^1$H NMR (D$_6$ DMSO, δ DMSO = 2.50 ppm): 0.80-1.35 (overlapping, 21H, dodecane H-21), 1.49 (t, 2H, J= 6.75, 6.25 Hz, NCH$_2$CH$_2$), 3.18 (q, 2H, 2H, J= 6.75, 6.25, 6.5 Hz, NHCH$_2$), 6.34 (s, 2H, NH$_2$), 6.49 (dd, 1H, J= 7.25, 7.75 Hz, Ar-H), 6.66 (dd, 1H, J= 8.25 Hz, Ar-H), 7.11 (dd, 1H, J= 1.25, 7, 7, 1.25 Hz, Ar-H), 7.44 (dd, 1H, J= 1.25, 8.0 Hz, Ar-H), 8.14 (t, 1H, J= 5.25, 5.5 Hz, NH) ppm

MS (+APCI) m/z = 305 (M+H)$^+$, 120 (M-C$_{12}$H$_{25}$NH$_2$)$^+$

IR (KBr) ν = 3476, 3368 (NH), 3301, 3052, 2923 (alkyl), 2847 (alkyl), 1621 (C=O), 1536 (benzene ring), 1469, 1444, 1326, 1297 cm$^{-1}$.

### 5.3.36 Preparation 2-Acryloylamino-N-cyclopentyl-benzamide (124)
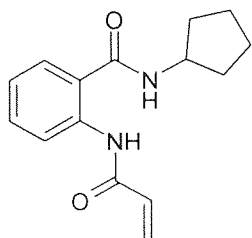


A mixture of 2-amino-N-cyclopentyl-benzamide (2.889 g, 14.22 mmol) and dry THF (80 mL) was stirred for 5 minutes. Followed by a portion wise addition of Hünig's base (4.2 mL, 23.6 mmol) to the reaction mixture. The reaction mixture was then cooled in the ice-bath and acrylol chloride (2.1 mL, 23.26 mmol) was added to this drop-wise over a period of 11 minutes. The reaction mixture was stirred for 18 hours at room temperature. The reaction mixture was then poured onto ice/water (250 mL) and stirred for 30 minutes. The resultant precipitate was collected by filtration and dried under high vacuum.

Yield = 2.863 g, 11.1 mmol, 78%

$^1$H NMR (CDCl$_3$, δ CHCl$_3$ = 7.27 ppm): 1.22-2.59 (overlapping m, 8H, cyclopentane), 4.35 (m, 1H, cyclopentane H-1), 5.77 (dd, 1H, J= 1.8, 9.5 Hz, CCH$_2$), 6.24-6.45 (overlapping m, 3H, COCH, CCH$_2$, Ar-H), 7.06 (dd, 1H, J= 1.25, 7.25 Hz, Ar-H), 7.39-7.50 (overlapping m, 2H, Ar-H), 8.66 (s, 1H, CONH-cyclopentane), 11.39 (s, 1H, NHCOCCH2) ppm

MS (+APCI) m/z = 259 (M+H)$^+$,174 (M-NH$_2$-PENTYL)$^+$

IR (KBr) ν = 3291 (NH), 3060, 2954, 2871, 1677, 1644 (C=O), 1584 (benzene ring), 1513, 1444, 1365, 1318 cm$^{-1}$.

### 5.3.37 Preparation 2-Acryloylamino-N-cyclohexyl-benzamide (125)
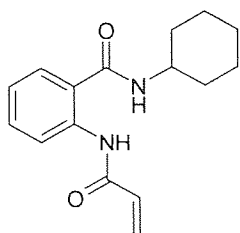


A mixture of 2-amino-N-cyclohexyl-benzamide (2.566 g, 12 mmol) and dry THF (80 mL) was stirred for 5 minutes. Followed by a portion wise addition of Hünig's base (4 mL, 22.06 mmol) to the reaction mixture. The reaction mixture was then cooled in the ice-bath and acrylol chloride (2 mL, 22.06 mmol) was added to this drop-wise over a period of 13 minutes. The reaction mixture was stirred for 18 hours at room temperature. The reaction mixture was then poured onto ice/water (250 mL) and stirred for 30 minutes. The resultant precipitate was collected by filtration and dried under high vacuum.

Yield = 1.354 g, 5.0 mmol, 42%

$^1$H NMR (CDCl$_3$; δ CHCl$_3$ = 7.27 ppm): 1.19-2.05 (overlapping m, 10H, cyclohexane), 3.94 (m, 1H, cyclohexane H-1), 6.19 (d, 1H, J= 7.25 Hz, CONH-cyclohexane), 5.77 (dd, 1H, J= 1.8, 9.8 Hz, CCH$_2$), 6.29 (dd, 1H, J= 9.8, 17 Hz, COCH), 6.42 (dd, 1H, J= 17, 1.8 Hz, CCH$_2$), 7.09 (dd, 1H, J= 1.25, 7.25,1 Hz, Ar-H), 7.44-7.51 (overlapping m, 2H, Ar-H), 8.68 (dd, 1H, J= 8.25 Hz, Ar-H), 11.39 (s, 1H, -NHCOCCH$_2$)

MS (+APCI) m/z = 273 (M+H)$^+$, 174 (M-NH$_2$-BENZYL)$^+$

IR (KBr) ν = 3264 (NH), 3073, 2925, 2856, 1739, 1683 (C=O), 1619, 1582 (benzene ring), 1521, 1444, 1336, 1312 cm$^{-1}$.

### 5.3.38 Preparation of 2-Acryloylamino-N-dodecyl-benzamide (126)
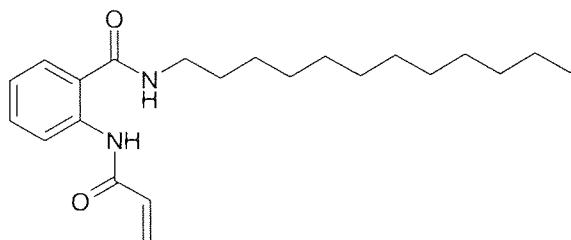


A mixture of 2-amino-N-dodecyl-benzamide (0.523 g, 1.72 mmol) and dry THF (20 mL) was stirred for 5 minutes. Followed by a portion wise addition of triethylamine (0.5 mL, 3.6 mmol) to the reaction mixture. The reaction mixture was cooled in the ice-bath and acrylol chloride (0.3 mL, 3.7 mmol) was added to this drop-wise over a period of 13 minutes. This reaction mixture was stirred for a day at room temperature. The reaction mixture was then poured onto ice/water (250 mL) and stirred for 35 minutes. The resultant precipitate was collected by filtration and dried under high vacuum. The product was a cream coloured powder.

Yield = 0.353 g, 1.0 mmol, 57.2%

$^1$H NMR (D$_6$ DMSO; δ DMSO = 2.50 ppm): 0.82-1.23 (overlapping, 21H, dodecane-C$_{10}$H$_{21}$), 1.53 (t, 2H, J= 5.75, 6.25 Hz, NHCH$_2$CH$_2$), 3.25 (q, 2H, NHCH$_2$), 5.78 (dd, 1H, J= 9.8, 2.0 Hz, CHCH$_2$), 6.22 (dd, 1H, J=

17, 9.8 Hz, OCC$\underline{H}$), 6.35 (dd, 1H, J= 17, 2.0 Hz, OCC$\underline{H}$), 7.17 (dd, 1H, J= 7.8, 15.3 Hz, Ar-H), 7.50 (dd, 1H, J= 7.8, 15.5 Hz, Ar-H), 7.74 (dd, 1H, J= 7.8 Hz, Ar-H), 8.45 (dd, 1H, J= 8 Hz, Ar-H), 8.73 (t, 1H, J= 4.5, 5.5 Hz, NH-dodecane), 11.66 (s, 1H, NH) ppm

MS (+APCI) m/z = 359 (M+H)$^+$, 186 (M-C$_6$H$_5$(CO)NHCOCHCH$_2$)$^+$

IR $\nu$ = 3676, 3588 (NH), 3201, 3005 (alkyl), 2677, 1640 (C=O), 1821, 1489, 1444, 1326, 1277 cm$^{-1}$.


### 5.3.39 Preparation of 1-Anthracen-9-ylmethyl-1H-benzo[d][1,3]oxazine-2,4-dione (129)
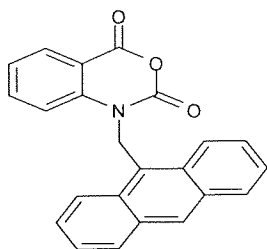


A mixture of sodium iodide (0.051 g, 0.35 mmol), sodium hydride (0.571 g, 15.04 mmol) and dry DMF (20 mL) was stirred for 5 minutes. Then a solution of isatoic anhydride (2.101 g, 12.9 mmol) dissolved in dry DMF (10 mL) was added to this reaction mixture. This was stirred for a further 30 minutes at room temperature under an argon atmosphere.

The reaction mixture was then cooled on an ice-bath and stirred for 30 minutes. Then to this reaction mixture, a solution of 9-chloromethylanthracene (3.216 g, 14.2 mmol) dissolved in dry DMF (20 mL) was added.

The reaction mixture was left to stir in the ice-bath for 2 days. The reaction mixture was poured onto ice-water (50 mL). The resultant precipitate was collected by filtration and dried under high vacuum

The compound was purified by flash chromatography eluting with ethyl acetate and petroleum spirit (60-80 °C) 2/8 rising to 4/6. The fractions corresponding to R$_f$ 0.83 (petroleum ether (60-80 °C) 8:2 ethyl acetate) were combined and the solvent was evaporated to give the target compound as a light orange brownish crystalline solid.

Yield = 3.543 g, 10 mmol, 78%

R$_f$ = 0.83 (petroleum ether (60-80 °C) 8:2 ethyl acetate)

Mp 142.8 – 146.4 °C

$^1$H NMR: 6.93 (s, 2H, N C$\underline{H}_2$ anthracene), 7.00 (overlapping m, 2H, anthracene), 7.15 (overlapping m, 2H, anthracene), 7.51 (overlapping m, 2H, anthracene), 7.63 (overlapping m, 2H, anthracene), 8.02 (overlapping m, 3H, Ar-H), 8.36 (overlapping m, 1H, J= 9.0 Hz, Ar-H), 8.49 (s, 1H, anthracene) ppm

MS (-APCI) m/z = 352 (M-H)$^-$, 324 (M-CO)$^-$, 282 (M-COO)$^-$

IR (KBr) $\nu$ = 3420, 3370, 3050, 2967 (alkyl), 2921, 2863, 1939, 1779 (C=O), 1725, 1606 (benzene), 1477, 1445, 1364, 1320, 1291 cm$^{-1}$.

### 5.3.40 Attempted preparation of 2-[(Anthracen-9-ylmethyl)-amino]-N-naphthalen-2-ylmethyl-benzamide (130)
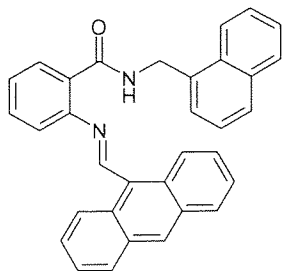


A mixture of 1-anthracen-9-ylmethyl-1H-benzo[d][1,3]oxazine-2,4-dione (0.166 g, 0.47 mmol), 1-(aminomethyl)-napthalene (0.112 g, 0.72 mmol) and ethanol (10 mL) was heated under reflux for 5 days. After this period of time more 1-(aminomethyl)-napthalene (0.10 g, 0.71 mmol) dissolved in ethanol (5 mL) was added drop-wise over a period of 4 minutes to the reaction mixture and heated under reflux for a further 7 days.

The reaction mixture was cooled to room temperature. The solid material was collected by filtration, washed with cold ethanol and dried under high vacuum. The T.L.C however indicated that this was the starting material.

$R_f$ = 0.41 (petroleum ether (60-80 °C) 3:7 DCM).

### 5.3.41 Attempted preparation of 2-[(Anthracen-9-ylmethyl)-amino]-N-pyren-4-ylmethyl-benzamide (131)
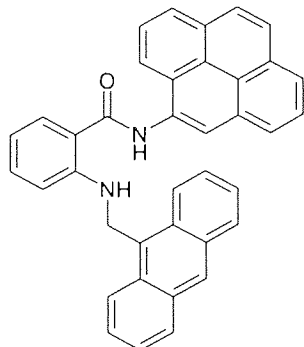


1-Anthracen-9-ylmethyl-1H-benzo[d][1,3]oxazine-2,4-dione (0.227 g, 0.65 mmol) was dissolved and heated in ethanol (7 mL) for 5 minutes. Then 1-aminopyrene (0.212 g, 0.10 mmol) dissolved in ethanol (5 mL) was added drop-wise over a period of 3 minutes to this reaction mixture and heated under reflux for 2 days.

The reaction mixture was cooled to room temperature. The solid material was collected by filtration and washed with cold ethanol. The olive green fine powder product was then dried under high vacuum. The T.L.C however indicated that this was the starting material.

$R_f = 0.8$ (ethyl acetate 1:1 petroleum spirit 40-60 °C).

### 5.3.42 Attempted preparation of 2-[(Anthracen-9-ylmethyl)-amino]-N-pyren-4-ylmethyl-benzamide (132)



A mixture of 1-anthracen-9-ylmethyl-1H-benzo[d][1,3]oxazine-2,4-dione (0.140 g, 0.4 mmol), 1-aminopyrene (0.124 g, 0.57 mmol) and dry DMF (5 mL) was stirred under an argon atmosphere for 5 minutes. Then DMAP (0.0170 g, 0.14 mmol) was added to this reaction mixture and heated under reflux for 5 days. After this period of time more 1-aminopyrene (0.132 g, 0.61 mmol) dissolved in ethanol (5 mL) was added drop-wise over a period of 3 minutes to the reaction mixture and heated under reflux for a further 2 days.

The reaction mixture was cooled to room temperature. The solid material was collected by filtration, washed with cold ethanol and dried under high vacuum. The T.L.C however indicated that this was the starting material.

$R_f = 0.85$ (petroleum ether (60-80 °C) 2:8 DCM).

### 5.3.43 Attempted preparation of 2-[(Anthracen-9-ylmethyl)-amino]-N-pyren-4-yl-benzamide (133)



A mixture of sodium hydride (0.015 g, 0.313 mmol) and dry DMF (6 mL) was stirred for 10 minutes, under an argon atmosphere. To this reaction mixture, a drop-wise addition of 1-aminopyrene (0.123 g, 0.57 mmol) dissolved in dry DMF (4 mL) over a period of 4 minutes was made. The reaction mixture was stirred in the ice-bath for 10 minutes and then for an hour at room temperature.

Then 1-anthracen-9-ylmethyl-1H-benzo[d][1,3]oxazine-2,4-dione (0.111 g, 0.313 mmol) dissolved in dry DMF (2 mL) was added drop-wise over a period of 2 minutes to the reaction mixture and stirred for 18 hours at room temperature.

The solid material was collected by filtration and dried under vacuum. The T.L.C however indicated that this was the starting material.

$R_f$ = 0.83 (petroleum ether (60-80 °C) 6:4 ethyl acetate).

### 5.3.44 Preparation of 2-Amino-N-naphthalen-2-ylmethyl-benzamide (134)
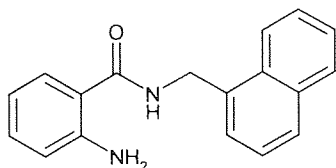


Isatoic anhydride (1.13 g, 7.0 mmol) was dissolved in ethanol (15 mL) and heated for 10 minutes. Then 1-(aminomethyl)-naphtalin (1.35 mL, 9.2 mmol) was added to this reaction mixture and heated under reflux for 3 days.

The reaction mixture was cooled to room temperature. The solid material was collected by filtration and washed with cold ethanol. The crude product was recrystallised from ethyl acetate to give a yellow coloured crystalline solid and dried under high vacuum.

Yield= 1.484 g, 5.38 mmol, 77%

$R_f$ = 0.56  (ethyl acetate 1:1 petroleum spirit 40-60 °C)

Mp 120.3 – 124.5 °C

$^1$H NMR ($D_6$ DMSO, δ DMSO = 2.50 ppm): 4.90 (d, 2H, J= 5.8 Hz, $CH_2$), 6.43 (s, 2H, $NH_2$), 6.50 (dd, 1H, J= 8, 8 Hz, Ar-H), 6.70 (dd, 1H, J= 8.3 Hz, Ar-H), 7.14 (dd, 1H, J= 8 5, 8.3 Hz, Ar-H), 7.54 (overlapping m, 5H, naphthalene), 7.89 (overlapping m, 2H, naphthalene), 8.20 (dd, 1H, Ar-H, J= 8.3 Hz), 8.80 (t, 1H, NH, J= 5.8, 5.8, 11.3 Hz) ppm

MS (-APCI) m/z = 275 (M-H)⁻

IR (KBr) ν = 3468, 3353 (NH), 3303, 3046, 2947 (alkyl), 1627 (C=O), 1575 (benzene), 1534, 1445, 1420, 1318, 1301 cm⁻¹.

## 5.3.45 Preparation of 2-{[1-Anthracen-9-yl-meth-(Z)-ylidene]-amino}-N-naphthalen-2-ylmethyl-benzamide (135)
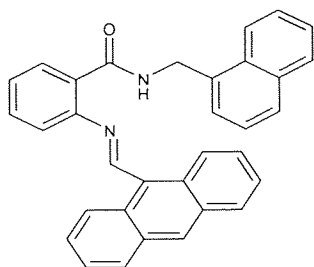


A mixture of 2-amino-N-naphthalen-2-ylmethyl-benzamide (1.064 g, 3.85 mmol), and ethanol (20 mL) was stirred and heated for 5 minutes. Then anthracene-9-carbaldehyde (1.63 g, 7.88 mmol) dissolved in ethanol (10mL) was added drop-wise over a period of 5 minutes to this reaction mixture and heated under reflux for 3 days.

The reaction mixture was cooled to room temperature. The solid material was collected by filtration, washed with cold ethanol and dried under high vacuum. The crude product was recrystallised from ethanol resulting in a yellow crystalline solid.

The compound was further purified by flash chromatography eluting with petroleum spirit (60-80 °C) and ethyl acetate 9/1 and then 8/2. The fractions corresponding to $R_f$ 0.50 (petroleum spirit (60-80 °C) 6:4 ethyl acetate) were combined and the solvent was evaporated to give the target compound as a yellow coloured crystalline solid.

Yield= 0.774 g, 1.68 mmol, 46%

Mp 159.5 – 164.6 °C

$^1$H NMR (D$_6$ DMSO, δ DMSO = 2.50 ppm): 4.87 (d, 2H, J= 5.8 Hz, CH$_2$), 8.34 (overlapping, m, 19H, Ar-H, anthracene, naphthalene), 8.84 (s, 1H, NCH-anthracene), 9.22 (t, 1H, J= 5.8, 5.8 Hz, NH), 9.75 (s, 1H, anthracene H-1) ppm

MS (+APCI) m/z = 465 (M+H)$^+$

IR (KBr) ν = 3475, 3355 (NH), 3311, 3052 (alkyl), 1627 (C=O), 1581, 1538, 1445, 1420, 1318, 1305, 1268 cm$^{-1}$

## 5.3.46 Attempted preparation of N,N'-Bis-pyren-1-ylmethyl-benzene-1,3-diamine (136)
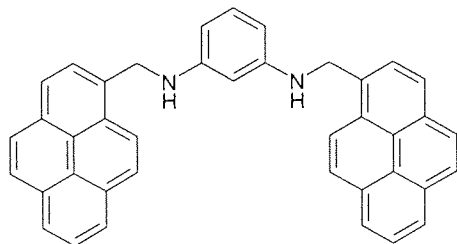
A mixture of N,N'-Bis-[1-pyren-1-yl-meth-(E)-ylidene]-benzene-1,3-diamine (0.56g, 1.10 mmol) and dry THF (20 mL) was stirred for 5 minutes. To this mixture tetramethylammonium triacetoxyborohydride (1.076g, 4.1 mmol) was added and refluxed for 7 days.

Then the reaction mixture was cooled to room temperature and water (50 mL) was added to this mixture. The reaction mixture was then extracted with ethyl acetate (2 x 75mL) and then dried over magnesium sulphate. The organic solvent was then removed under reduced pressure to give the solid material and dried under high vacuum.

The T.L.C however indicated that this was the starting material i.e. N,N'-Bis-[1-pyren-1-yl-meth-(E)-ylidene]-benzene-1,3-diamine.

$R_f = 0.95$ (DCM/1 drop of ammonia)

### 5.3.47 Preparation of N,N'-Bis-pyren-1-ylmethyl-benzene-1,3-diamine (137)

A mixture of lithium aluminium hydride (0.94g, 25.0 mmol) and dry THF (25 mL) was stirred whilst cooled in ice-bath for 10 minutes under an argon atmosphere.

Then the reaction mixture was treated with N,N'-Bis-[1-pyren-1-yl-meth-(E)-ylidene]-benzene-1,3-diamine (0.48g, 1.00 mmol). The reaction mixture was stirred on ice-bath for 1 hour and then for 5 days at room temperature.
The reaction mixture was then poured onto a saturated solution of ammonium chloride and the precipitate collected by filtration, washed with water and dried under high vacuum.

The compound was purified by flash chromatography eluting with petroleum spirit (60-80 °C) and ethyl acetate 4/6 rising to 2/8 and then 1/1. The fractions corresponding to $R_f$ 0.92 (petroleum spirit (60-80 °C) 4:6 ethyl acetate) were combined and the solvent was evaporated to give a dark brown coloured solid material.
The T.L.C however indicated that this was the starting material i.e. N,N'-Bis-[1-pyren-1-yl-meth-(E)-ylidene]-benzene-1,3-diamine.

### 5.4 Molecularly imprinted polymers experimental section

### 5.4.1 Preparation of a linear co-octadecylacrylate-79
A solution of 2-acrylamidobenzamide (79) (5.3 mg, 0.027 mmol), AIBN (54 mg, 0.33 mmol) and octadecylacrylate (4.956 g, 15.5 mmol) in THF (15 mL) was de-oxygenated by alternate application of vacuum and argon (5 x) with rapid stirring. The solution was stirred at 70 °C for 18 hours under an argon atmosphere. The solution was poured onto rapidly stirred methanol (250 mL). The resulting precipitate

261

was collected by filtration, re-dissolved in a small amount of DCM and reprecipitated onto methanol. The precipitate was collected by filtration and dried under vacuum to give a white powder.

Yield = 4.30 g, 86%.


### 5.4.2 Preparation of a linear co-octadecylacrylate-108

A solution of N-(2-{N-Methyl-N'-[1-pyren-1-yl-meth-(E)-ylidene]-hydrazino-carbonyl}-phenyl)-acrylamide (**108**) (10.8 mg, 0.025 mmol), AIBN (51 mg, 0.31 mmol) and octadecylacrylate (5.134 g, 15.8 mmol) in THF (10 mL) was de-oxygenated by alternate application of vacuum and argon (5 x) with rapid stirring. The solution was stirred at 70 °C for 18 h under an argon atmosphere. The solution was poured onto rapidly stirred methanol (500 mL) resulting in a precipitate. This precipitate was collected by filtration and dried under vacuum to give a white powder.

Yield = 4.27g, 82.2%.


### 5.4.3 Preparation of a linear co-styrene-108

A solution of N-(2-{N-Methyl-N'-[1-pyren-1-yl-meth-(E)-ylidene]-hydrazino-carbonyl}-phenyl)-acrylamide (**108**) (11.1 mg, 0.026 mmol), AIBN (52 mg, 0.32 mmol) and styrene (5.013g, 48.2 mmol) in THF (5 mL) was de-oxygenated by alternate application of vacuum and argon (5 x) with rapid stirring. The solution was stirred at 70 °C for 18 h under an argon atmosphere. The solution was poured onto rapidly stirred methanol (70 mL). The resulting precipitate was collected by filtration, re-dissolved in a small amount of DCM and reprecipitated onto methanol. The precipitate was collected by filtration and dried under vacuum to give a white powder.

Yield = 3.23g, 64%.


### 5.4.4 Preparation of polymer 1

A solution of 2-Acryloylamino-N-cyclododecyl-benzamide (**119**) (37.0mg, 0.104 mmol), AIBN (201.3mg, 1.23 mmol) and trimethylpropane triacylate (10.01g) in toluene (50 mL) was de-oxygenated by alternate application of vacuum and argon (3 x) with rapid stirring. The solution was stirred at 50 °C for 4 days and 80 °C for another 2 days under an argon atmosphere.

The resulting polymer was collected by filtration and washed with toluene (2 x 30mL). The crude material was dried under vacuum and then crushed using a mortar and pestle. The powder was graded by sieving for 24 hours rendering a fraction of 150-382 µm to give a pale yellow fine powder.

Yield= 4.6523g, 46.3%


### 5.4.5 Preparation of polymer 2

A solution of AIBN (142.1mg, 0.87 mmol) and trimethylpropane triacylate (10.12g) in toluene (50 mL) was de-oxygenated by alternate application of vacuum and argon (3 x) with rapid stirring. The solution was stirred at 50 °C for 2 days and 80 °C for another 2 days under an argon atmosphere.

The resulting polymer was collected by filtration and washed with toluene (2 x 30mL). The crude material was dried under vacuum and then crushed using a mortar and pestle. The powder was graded by sieving for 24 hours rendering a fraction of 150-382 µm.

Yield= 4.5328g, 45%

### 5.4.6 Preparation of MIPcod

A solution of 2-acrylamidobenzamide (79) (4.8 mg, 0.025 mmol), codeine (7.7 mg, 0.026 mmol), AIBN (58 mg, 0.35 mmol) and the triethylene glycol dimethacrylate (5.0g) in THF (5 mL) was de-oxygenated by alternate application of vacuum and argon (5 x) with rapid stirring. The solution was stirred at 55 °C for 24 h and then at 70 °C for a further 24 h under an argon atmosphere. The resulting polymer was collected by filtration and washed with THF (2 x 30mL). The crude material was dried under vacuum and then crushed using a mortar and pestle. The powder was graded by sieving and the 150-382 μm fraction was extracted exhaustively with chloroform in a soxhlet apparatus and dried under vacuum.
Yield= 2.505 g, 50%

### 5.4.7 Preparation of MIP3

A solution of 2-acrylamidobenzamide (79) (4.7 mg, 0.025 mmol), N'-[1-pyren-9-yl-meth-(E)-ylidene]-N,N-diphenylhydrazine (77) (10.1 mg, 0.025 mmol), AIBN (54 mg, 0.33 mmol) and the triethylene glycol dimethacrylate (5.0g) in THF (5 mL) was de-oxygenated by alternate application of vacuum and argon (5 x) with rapid stirring. The solution was stirred at 55 °C for 24 h and then at 70 °C for a further 24 h under an argon atmosphere. The resulting polymer was collected by filtration and washed with THF (2 x 30mL). The crude material was dried under vacuum and then crushed using a mortar and pestle. The powder was graded by sieving and the 150-382 μm fraction was extracted exhaustively with chloroform in a soxhlet apparatus and dried under vacuum.
Yield= 2.062g, 41%

### 5.4.8 Preparation of MIP4

A solution of quinine acrylate (80) (38.5 mg, 0.10 mmol), 81 (35.4 mg, 0.10mmol), AIBN (100.0 mg, 0.61 mmol) and trimethylolpropane triacrylate (20.052 g) in toluene (50 mL) was de-oxygenated by alternate application of vacuum and argon (3 x) with rapid stirring. The solution was stirred at 50 °C for 24 hours and 80 °C for another 24 hours under an argon atmosphere.
The resulting polymer was collected by filtration and washed with toluene (2 x 30mL). The crude material was dried under vacuum and then crushed using a mortar and pestle. The powder was graded by sieving for 24 hours and the 150-382 μm fraction was extracted exhaustively with chloroform in a soxhlet apparatus for 48 hours and dried under vacuum.
Yield= 16.85 g, 84%

### 5.4.9 Preparation of MIP5

A solution of N-(2-{N-Methyl-N'-[1-pyren-1-yl-meth-(E)-ylidene]-hydrazinocarbonyl}-phenyl)-acrylamide (108) (11mg, 0.026 mmol), N'-[1-phenanthracen-9-yl-meth-(E)-ylidene]-N,N-diphenylhydrazine (76) (10.2mg, 0.0027 mmol), AIBN (110.2mg, 0.67 mmol) and triethylene glycol dimethylacrylate (5.03g) in

THF (5 mL) was de-oxygenated by alternate application of vacuum and argon (3 x) with rapid stirring. The solution was stirred at 55 °C for 18 hours and 70 °C for another 24 hours under an argon atmosphere.

The resulting polymer was collected by filtration and washed with THF (2 x 30mL). The crude material was dried under vacuum and then crushed using a mortar and pestle. The powder was graded by sieving for 24 hours and the 150-382 μm fraction was extracted exhaustively with chloroform in a soxhlet apparatus for 48 hours and dried under vacuum to give a light pale green fine powder.

Yield= 2.8g, 55%


### 5.4.10 Preparation of MIP6

A solution of N-(2-{N-Methyl-N'-[1-pyren-1-yl-meth-(E)-ylidene]-hydrazinocarbonyl}-phenyl)-acrylamide (108) (11mg, 0.026 mmol), N'-[1-anthracen-9-yl-meth-(E)-ylidene]-N,N-diphenylhydrazine (78) (9.7mg, 0.0026 mmol), AIBN (108.8mg, 0.66 mmol) and triethylene glycol dimethylacrylate (5.01g) in THF (5 mL) was de-oxygenated by alternate application of vacuum and argon (3 x) with rapid stirring. The solution was stirred at 55 °C for 18 hours and 70 °C for another 24 hours under an argon atmosphere.

The resulting polymer was collected by filtration and washed with THF (2 x 30 mL). The crude material was dried under vacuum and then crushed using a mortar and pestle. The powder was graded by sieving for 24 hours and the 150-382 μm fraction was extracted exhaustively with chloroform in a soxhlet apparatus for 48 hours and dried under vacuum to give a cream fine powder.

Yield= 3.2g, 64%


### 5.4.11 Preparation of MIP7

A solution of N-(2-{N-Methyl-N'-[1-pyren-1-yl-meth-(E)-ylidene]-hydrazinocarbonyl}-phenyl)-acrylamide (108) (11.7mg, 0.027 mmol), N'-[1-pyren-9-yl-meth-(E)-ylidene]-N,N-diphenylhydrazine (77) (2.5mg, 0.0063 mmol), AIBN (108.3mg, 0.66 mmol) and Triethylene glycol dimethylacrylate (5.0041g) in THF (10 mL) was de-oxygenated by alternate application of vacuum and argon (3 x) with rapid stirring. The solution was stirred at 55 °C for 24 hours and 70 °C for another 24 hours under an argon atmosphere.

The resulting polymer was collected by filtration and washed with THF (2 x 30mL). The crude material was dried under vacuum and then crushed using a mortar and pestle. The powder was graded by sieving for 24 hours and the 150-382 μm fraction was extracted exhaustively with chloroform in a soxhlet apparatus for 48 hours and dried under vacuum.

Yield= 3.65g, 73%


### 5.4.12 Preparation of MIP8

A solution of N-Pyren-4-ylmethyl-acrylamide (118) (7.13mg, 0.025 mmol), N'-[1-anthracen-9-yl-meth-(E)-ylidene]-N,N-diphenylhydrazine (76) (9.3mg, 0.025 mmol), AIBN (107.4mg, 0.65 mmol) and triethylene glycol dimethylacrylate (5.041g) in THF (5 mL) was de-oxygenated by alternate application of vacuum and argon (3 x) with rapid stirring. The solution was stirred at 50 °C for 24 hours and 80 °C for another 24 hours under an argon atmosphere.

The resulting polymer was collected by filtration and washed with THF (2 x 30mL). The crude material was dried under vacuum and then crushed using a mortar and pestle. The powder was graded by sieving for

24 hours and the 150-382 μm fraction was extracted exhaustively with chloroform in a soxhlet apparatus for 48 hours and dried under vacuum to give a light pale green fine powder.
Yield=4.5g, 89%

### 5.4.13 Preparation of MIP9

A solution of N-Pyren-4-ylmethyl-acrylamide (**118**) (7.13mg, 0.025 mmol), N'-[1-phenanthracen-9-yl-meth-(E)-ylidene]-N,N-diphenylhydrazine (**78**) (10.8mg, 0.03 mmol), AIBN (127.4mg, 0.78 mmol) and triethylene glycol dimethylacrylate (5.123g) in THF (5 mL) was de-oxygenated by alternate application of vacuum and argon (3 x) with rapid stirring. The solution was stirred at 50 °C for 24 hours and 80 °C for another 24 hours under an argon atmosphere.

The resulting polymer was collected by filtration and washed with THF (2 x 30mL). The crude material was dried under vacuum and then crushed using a mortar and pestle. The powder was graded by sieving for 24 hours and the 150-382 μm fraction was extracted exhaustively with chloroform in a soxhlet apparatus for 48 hours and dried under vacuum to give a cream fine powder.
Yield=4.32g, 84%

### 5.4.14 Preparation of MIP10

A solution of N-Pyren-4-ylmethyl-acrylamide (**118**) (7.13mg, 0.025 mmol), N'-[1-pyren-9-yl-meth-(E)-ylidene]-N,N-diphenylhydrazine (**77**) (19.5mg, 0.05 mmol), AIBN (104.5mg, 0.64 mmol) and triethylene glycol dimethylacrylate (5.017g) in THF (5 mL) was de-oxygenated by alternate application of vacuum and argon (3 x) with rapid stirring. The solution was stirred at 50 °C for 24 hours and 80 °C for another 24 hours under an argon atmosphere.

The resulting polymer was collected by filtration and washed with THF (2 x 30mL). The crude material was dried under vacuum and then crushed using a mortar and pestle. The powder was graded by sieving for 24 hours and the 150-382 μm fraction was extracted exhaustively with chloroform in a soxhlet apparatus for 48 hours and dried under vacuum to give a bright yellow fine powder.
Yield=3.68g, 73%

### 5.4.15 Preparation of MIP11

A solution of 2-Acryloylamino-N-cyclododecyl-benzamide (**119**) (38.1mg, 0.11 mmol), **128** (22.5mg, 0.10 mmol), AIBN (106.8mg, 0.65 mmol) and trimethylpropane triacylate (10.02g) in toluene (50 mL) was de-oxygenated by alternate application of vacuum and argon (3 x) with rapid stirring. The solution was stirred at 50 °C for a day and 80 °C for another 2 days under an argon atmosphere.

The resulting polymer was collected by filtration and washed with toluene (2 x 30mL). The crude material was dried under vacuum and then crushed using a mortar and pestle. The powder was graded by sieving for 24 hours and the 150-382 μm fraction was extracted exhaustively with chloroform in a soxhlet apparatus for 48 hours and dried under vacuum to give a white fine powder.
Yield= 2.9841 g, 30%

### 5.4.16 Preparation of MIP12

A solution of 2-Acryloylamino-N-cyclododecyl-benzamide (**119**) (38.3mg, 0.11 mmol), **81** (2.9mg, 0.01 mmol), AIBN (103.2mg, 0.63 mmol) and trimethylpropane triacylate (10.01g) in toluene (50 mL) was de-oxygenated by alternate application of vacuum and argon (3 x) with rapid stirring. The solution was stirred at 50 °C for a day and 80 °C for another 2 days under an argon atmosphere.

The resulting polymer was collected by filtration and washed with toluene (2 x 30mL). The crude material was dried under vacuum and then crushed using a mortar and pestle. The powder was graded by sieving for 24 hours and the 150-382 µm fraction was extracted exhaustively with chloroform in a soxhlet apparatus for 48 hours and dried under vacuum to give a white fine powder.

Yield= 3.8624g, 38.4%

### 5.4.17 Preparation of MIP13

A solution of 2-Acryloylamino-N-cyclododecyl-benzamide (**119**) (38.7mg, 0.11 mmol), **81** (3.2 mg, 0.01 mmol), AIBN (104.5mg, 0.64 mmol) and triethylene glycol dimethylacrylate (10.01g) in toluene (50 mL) was de-oxygenated by alternate application of vacuum and argon (3 x) with rapid stirring. The solution was stirred at 50 °C for a day and 80 °C for another 2 days under an argon atmosphere.

The resulting polymer was collected by filtration and washed with toluene (2 x 30mL). The crude material was dried under vacuum and then crushed using a mortar and pestle. The powder was graded by sieving for 24 hours and the 150-382 µm fraction was extracted exhaustively with chloroform in a soxhlet apparatus for 48 hours and dried under vacuum to give a white fine powder.

Yield= 3.9863g, 40%

### 5.4.18 Preparation of MIP14

A solution of 2-Acryloylamino-N-cyclododecyl-benzamide (**119**) (37.1mg, 0.10 mmol), **83** (23.2mg, 0.1 mmol), AIBN (109.6mg, 0.67 mmol) and trimethylpropane triacylate (10.17g) in toluene (50 mL) was de-oxygenated by alternate application of vacuum and argon (3 x) with rapid stirring. The solution was stirred at 50 °C for 2 days and 80 °C for another 2 days under an argon atmosphere.

The resulting polymer was collected by filtration and washed with toluene (2 x 30mL). The crude material was dried under vacuum and then crushed using a mortar and pestle. The powder was graded by sieving for 24 hours and the 150-382 µm fraction was extracted exhaustively with chloroform in a soxhlet apparatus for 48 hours and dried under vacuum to give a white fine powder.

Yield= 4.3628g, 43%

### 5.4.19 Preparation of MIP15

A solution of 2-Acryloylamino-N-cyclododecyl-benzamide (**119**) (37.6mg, 0.11 mmol), **83** (35.3mg, 0.11 mmol), AIBN (120.6mg, 0.73 mmol) and triethylene glycol dimethylacrylate (10.05g) in toluene (50 mL) was de-oxygenated by alternate application of vacuum and argon (3 x) with rapid stirring. The solution was stirred at 50 °C for 2 days and 80 °C for another 3 days under an argon atmosphere.

The resulting polymer was collected by filtration and washed with toluene (2 x 30mL). The crude material was dried under vacuum and then crushed using a mortar and pestle. The powder was graded by sieving

for 24 hours and the 150-382 μm fraction was extracted exhaustively with chloroform in a soxhlet apparatus for 48 hours and dried under vacuum to give a white fine powder.

Yield= 4.7326g, 47%

### 5.4.20 Preparation of MIP16

A solution of 2-Acryloylamino-N-cyclododecyl-benzamide (**119**) (40.1mg, 0.11 mmol), **85** (27.2mg, 0 10 mmol), AIBN (109.2mg, 0.67 mmol) and trimethylpropane triacylate (10.47g) in toluene (50 mL) was de-oxygenated by alternate application of vacuum and argon (3 x) with rapid stirring. The solution was stirred at 50 °C for 1 day and 80 °C for another day under an argon atmosphere.

The resulting polymer was collected by filtration and washed with toluene (2 x 30mL). The crude material was dried under vacuum and then crushed using a mortar and pestle. The powder was graded by sieving for 24 hours and the 150-382 μm fraction was extracted exhaustively with chloroform in a soxhlet apparatus for 48 hours and dried under vacuum to give a white fine powder.

Yield= 5.6397g, 54%

### 5.4.21 Preparation of MIP17

A solution of 2-Acryloylamino-N-cyclododecyl-benzamide (**121**) (37.5mg, 0.11 mmol), **85** (30.6mg, 0.11 mmol), AIBN (133.1mg, 0.81 mmol) and triethylene glycol dimethylacrylate (10.1g) in toluene (50 mL) was de-oxygenated by alternate application of vacuum and argon (3 x) with rapid stirring. The solution was stirred at 50 °C for 2 days and 80 °C for another 3 days under an argon atmosphere.

The resulting polymer was collected by filtration and washed with toluene (2 x 30mL). The crude material was dried under vacuum and then crushed using a mortar and pestle. The powder was graded by sieving for 24 hours and the 150-382 μm fraction was extracted exhaustively with chloroform in a soxhlet apparatus for 48 hours and dried under vacuum to give a white fine powder.

Yield= 3.7421g, 37%

### 5.4.22 Preparation of MIP18

A solution of 2-Acryloylamino-N-cyclododecyl-benzamide (**119**) (49.2mg, 0.14 mmol), **84** (30.5mg, 0 11 mmol), AIBN (104.1mg, 0.63 mmol) and trimethylpropane triacylate (10.35g) in toluene (50 mL) was de-oxygenated by alternate application of vacuum and argon (3 x) with rapid stirring. The solution was stirred at 50 °C for 1 day and 80 °C for another day under an argon atmosphere.

The resulting polymer was collected by filtration and washed with toluene (2 x 30mL). The crude material was dried under vacuum and then crushed using a mortar and pestle. The powder was graded by sieving for 24 hours and the 150-382 μm fraction was extracted exhaustively with chloroform in a soxhlet apparatus for 48 hours and dried under vacuum to give a cream fine powder.

Yield= 3.5620g, 34.2%

### 5.4.23 Preparation of MIP19

A solution of 2-Acryloylamino-N-cyclododecyl-benzamide (**119**) (38.5mg, 0.11 mmol), **84** (28.4mg, 0 10 mmol), AIBN (109.3mg, 0.67 mmol) and triethylene glycol dimethylacrylate (10.1 g) in toluene (50 mL)

was de-oxygenated by alternate application of vacuum and argon (3 x) with rapid stirring. The solution was stirred at 50 °C for 2 days and 80 °C for another 3 days under an argon atmosphere.

The resulting polymer was collected by filtration and washed with toluene (2 x 30mL). The crude material was dried under vacuum and then crushed using a mortar and pestle. The powder was graded by sieving for 24 hours and the 150-382 μm fraction was extracted exhaustively with chloroform in a soxhlet apparatus for 48 hours and dried under vacuum to give a white fine powder.

Yield= 3.6321g, 36%

### 5.4.24 Preparation of MIP20

A solution of 2-Acryloylamino-N-cyclododecyl-benzamide (**119**) (37.2mg, 0.10 mmol), **127** (26.0mg, 0.1 mmol), AIBN (133.3mg, 0.81 mmol) and trimethylpropane triacylate (10.24g) in toluene (50 mL) was de-oxygenated by alternate application of vacuum and argon (3 x) with rapid stirring. The solution was stirred at 50 °C for 1 days and 80 °C for another 2 days under an argon atmosphere.

The resulting polymer was collected by filtration and washed with toluene (2 x 30mL). The crude material was dried under vacuum and then crushed using a mortar and pestle. The powder was graded by sieving for 24 hours and the 150-382 μm fraction was extracted exhaustively with chloroform in a soxhlet apparatus for 48 hours and dried under vacuum to give a white fine powder.

Yield= 4.2764g, 42%

### 5.4.25 Preparation of MIP21

A solution of 2-Acryloylamino-N-cyclododecyl-benzamide (**119**) (36.5mg, 0.102 mmol), **127** (29.7mg, 0.1 mmol), AIBN (125.1mg, 0.76 mmol) and triethylene glycol dimethylacrylate (10.2g) in toluene (50 mL) was de-oxygenated by alternate application of vacuum and argon (3 x) with rapid stirring. The solution was stirred at 50 °C for 2 days and 80 °C for another 3 days under an argon atmosphere.

The resulting polymer was collected by filtration and washed with toluene (2 x 30mL). The crude material was dried under vacuum and then crushed using a mortar and pestle. The powder was graded by sieving for 24 hours and the 150-382 μm fraction was extracted exhaustively with chloroform in a soxhlet apparatus for 48 hours and dried under vacuum to give a white fine powder.

Yield= 3.7243g, 36.3%

### 5.4.26 Preparation of MIP22

A solution of 2-Acryloylamino-N-dodecyl-benzamide (**119**) (38.2mg, 0.11 mmol), **84** (17.5mg, 0 1 mmol), AIBN (105.5mg, 0.64 mmol) and trimethylpropane triacylate (10.003 g) in toluene (50 mL) was de-oxygenated by alternate application of vacuum and argon (3 x) with rapid stirring. The solution was stirred at 50 °C for 1 day and 80 °C for another day under an argon atmosphere.

The resulting polymer was collected by filtration and washed with toluene (2 x 30mL). The crude material was dried under vacuum and then crushed using a mortar and pestle. The powder was graded by sieving for 24 hours and the 150-382 μm fraction was extracted exhaustively with chloroform in a soxhlet apparatus for 48 hours and dried under vacuum to give a white fine powder.

Yield = 3.2685g, 33%

### 5.4.27 Preparation of MIP23

A solution of 2-Acryloylamino-N-cyclododecyl-benzamide (**121**) (35.4mg, 0.10 mmol), **84** (29.7mg, 0.11 mmol), AIBN (110.0mg, 0.67 mmol) and trimethylpropane triacylate (10.07g) in methanol (50 mL) was de-oxygenated by alternate application of vacuum and argon (3 x) with rapid stirring. The solution was stirred at 50 °C for a day and 80 °C for another day under an argon atmosphere.

The resulting polymer was collected by filtration and washed with methanol (2 x 30mL). The crude material was dried under vacuum and then crushed using a mortar and pestle. The powder was graded by sieving for 24 hours and the 150-382 μm fraction was extracted exhaustively with chloroform in a soxhlet apparatus for 48 hours and dried under vacuum to give a white fine powder.

Yield= 4.6231g, 46%

# 6. REFERENCES

Abraham K. Benny, Adithan. C., Indian Journal of Pharmacology, GENETIC POLYMORPHISM OF CYP2D6, 2001, 33, 147-169.

Alberts, B., Bray, D., Lewis, J., Raff, M., Roberts, K. and Watson, J.D. (1994) Molecular biology of the cell. Garland Publishing, New York.

Allender C.J., Brain R K., Heard M C and Pellett MA, Molecularly imprinted polymers as novel excipients for selective (trans)dermal delivery, in Perspectives in Percutaneous Penetration, Vol 5a, Brain KR, James VJ and Walters KA (eds), STS Publishing, Cardiff (1997) 88.

Allender C.J., Brain R K., Watkinson C A., Heard M C., in: Brain K.R., James V.J., Walters K.A. (Eds.), Perspectives in Percutaneous Penetration, vol. 5b, STS Publishing, Cardiff, 1997a, 183.

Allender C.J., Brain R K., Heard M C. Progress in Medicinal Chemistry, Molecularly imprinted polymers-Preparation, Biomedical applications and Technical challenges., 1999, 36, 235–287.

Allender C. J. Richardson C. Woodhouse B. Heard C. M. Brain K. R. International Journal Of Pharmaceutics, Pharmaceutical applications for molecularly imprinted polymers., 2000, 195, 39-43.

Andersson L. Sellergren B. Mosbach K. Tetrahedron Letters, Imprinting of amino-acid derivatives in macroporous polymers., 1984, 25, 5211-5214.

Andersson L. I. Mosbach K. Makromolekulare Chemie-Rapid Communications, Molecular imprinting of the coenzyme-substrate analog N-pyridoxyl-L-phenylalaninanilide., 1989, 10, 491-495.

Andersson L. I. Mosbach K. Journal Of Chromatography, Enantiomeric resolution on molecularly imprinted polymers prepared with only noncovalent and nonionic interactions., 1990, 516, 313-322.

Andersson L. I. Müller R. Vlatakis G. Mosbach K. Proceedings Of The National Academy Of Sciences Of The United States Of America,Mimics of the binding-sites of opioid receptors obtained by molecular imprinting of enkephalin and morphine., 1995, 92, 4788-4792.

Andersson L. I. Analytical Chemistry, Application of molecular imprinting to the development of aqueous buffer and organic solvent based radioligand binding assays for (S)- propranolol., 1996, 68, 111-117.

Andersson L. I. Paprica A. Arvidsson T. Chromatographia, A highly selective solid phase extraction sorbent for pre-concentration of sameridine made by molecular imprinting., 1997, 46, 57-62.

Andersson H. S. Karlsson J. G. Piletsky S. A. Koch-Schmidt A. C. Mosbach K. Nicholls I. A. Journal Of Chromatography A, Study of the nature of recognition in molecularly imprinted polymers II [1] - Influence of monomer-template ratio and sample load on retention and selectivity., 1999, 848, 39-49.

Andersson L. I. Journal Of Chromatography B, Molecular imprinting: developments and applications in the analytical chemistry field., 2000, 745, 3-13.

Ansell R. J. Ramström O. Mosbach K. Clinical Chemistry, Towards artificial antibodies prepared by molecular imprinting., 1996, 42, 1506-1512.

Ansell R. J. Mosbach K. Journal Of Chromatography A, Molecularly imprinted polymers by suspension polymerisation in perfluorocarbon liquids with emphasis on the influence of the porogenic solvent, 1997,787, 55-66.

Ansell R. J. Mosbach K. Analyst, Magnetic molecularly imprinted polymer beads for drug radioligand binding assay., 1998, 123, 1611-1616.

Araki Kosuke, Maruyama Tatsuo, Kamiya Noriho and Goto Masahiro, Journal of Chromatography B, Metal ion-selective membrane prepared by surface molecular imprinting., 2005, 818, 141-145.

Armstrong DW, Nome F, Spino LA and Golden TD. *Journal of American Chemical Society,* Efficient detection and evaluation of cyclodextrin multiple complex formation. 1986, 108, 1418.

Arshady R. Mosbach K. *Macromolecular Chemistry And Physics-Makromolekulare Chemie,* Synthesis of substrate-selective polymers by host-guest polymerisation, 1981, 182, 687-692.

Asanuma H. Kakazu M. Shibata M. Hishiya T. Komiyama M. *Chemical Communications,* Molecularly imprinted polymer of beta-cyclodextrin for the efficient recognition of cholesterol., 1997,1971-1972.

Asanuma H. Kakazu R. Shibata M. Hishiya T. Komiyama M. *Supramolecular Science,* Synthesis of molecularly imprinted polymer of beta-cyclodextrin for the efficient recognition of cholesterol., 1998, 5, 417-421.

Asanuma H. Kajiya K. Hishiya T. Komiyama M. *Chemistry Letters,* Molecular imprinting of cyclodextrin in water for the recognition of peptides., 1999, 28, 665-666.

Ballester P., Barceló Angle M., Costa, Deyà M. P. A., Morey J., Orell M., Hunter A C., Tetrahedron Lett., Recognition of Caffeine in Aqueous Solutions,2000, 41, 3849-3853.

Beach J. V. Shea K. J. *Journal Of The American Chemical Society,* Designed catalysts - a synthetic network polymer that catalyzes the dehydrofluorination of 4-fluoro-4-(P-nitrophenyl)Butan-2-one., 1994, 116, 379-380.

Bengtsson H. Roos U. Andersson L. I. *Analytical Communications,* Molecular imprint based radioassay for direct determination of S- propranolol in human plasma., 1997, 34, 233-235.

Berggren C. Bayoudh S. Sherrington D. Ensing K. *Journal Of Chromatography A,* Use of molecularly imprinted solid-phase extraction for the selective clean-up of clenbuterol from calf urine., 2000, 889, 105-110.

Berglund J. Nicholls I. A. Lindbladh C. Mosbach K. *Bioorganic & Medicinal Chemistry Letters,* Recognition in molecularly imprinted polymer alpha(2)-adrenoreceptor mimics., 1996, 6, 2237-2242.

Blomgren Anders, Berggren Christine, Holmberg Anna, Larsson Fredrik, Sellergren Börje and Ensing Kees, *Journal of Chromatography A.* Extraction of clenbuterol from calf urine using a molecularly imprinted polymer followed by quantitation by high-performance liquid chromatography with UV detection., 2002, 975, 157-164.

Bowman M. A. E. Allender C. J. Brain K. R. Heard C. M. Meth.Surv, A high-throughput screening technique employing molecularly imprinted polymers as biomimetic selectors in "Drug-development assay approaches including molecular imprinting and biomarkers"., 1998, 25, 37-43.

Breslow R., Science, 1982, 218, 532-357.

Brüggemann O. Freitag R. Whitcombe M. J. Vulfson E. N. *Journal Of Chromatography A,* Comparison of polymer coatings of capillaries for capillary electrophoresis with respect to their applicability to molecular imprinting and electrochromatography., 1997, 781, 43-53.

Byström S. E. Börje A. Akermark B. *Journal Of The American Chemical Society,* Selective reduction of steroid 3-ketones and 17-ketones using LiAlH$_4$ activated template polymers., 1993, 115, 2081-2083.

Caro Ester, Marcé M Rosa., Cormack A.G Peter., Sherrington C. David and Borrull Francesc, *Journal of Chromatography A,* Molecularly imprinted solid-phase extraction of naphthalene sulfonates from water., 2004, 1047, 175-180.

Castro B., Whitcombe M. J., Vulfson E. N., Vazquez-Duhalt R., Barzana E., *Analytical chimica acta,* Molecularly imprinting for selective adsorption of organsulphur compounds present in fuels., 2001, 435, 83-90.

Cederfur J. Pei Y. X. Meng Z. H. Kempe M. *Journal Of Combinatorial Chemistry,* Synthesis and screening of a molecularly imprinted polymer library targeted for penicillin G., 2003, 5, 67-72.

Chianella I. Lotierzo M. Piletsky S. A. Tothill I. E. Chen B. N. Karim K. Turner A. P. F. *Analytical Chemistry,* Rational design of a polymer specific for microcystin-LR using a computational approach., 2002, 74, 1288-1293.

Cheng Z. L. Wang E. K. Yang X. R. *Biosensors & Bioelectronics,* Capacitive detection of glucose using molecularly imprinted polymers., 2001, 16, 179-185.

Cheong S. H. McNiven S. Yano K. Karube I. *Abstracts Of Papers Of The American Chemical Society,* Development of steroid sensors using molecularly imprinted polymers., 1997, 213, 31-IEC.

Cheong S. H. McNiven S. Rachkov A. E. Levi R. Yano K. Karube I. *Macromolecules,* Testosterone receptor binding mimic constructed using molecular imprinting., 1997a, 30, 1317-1322.

Cheong S. H. McNiven S. Rachkov A. E. Levi R. Yano K. Karube I. *Macromolecules,* Testosterone receptor binding mimic constructed using molecular imprinting., 1997b, 30, 1317-1322.

Ching-Chiang Hwang and Wen-Chien Lee, *Journal of Chromatography B.,* Chromatographic resolution of the enantiomers of phenylpropanolamine by using molecularly imprinted polymer as the stationary phase, 2001, 765, 45-53.

Chow Fai-Cheuk, Lam H. W Michael. and Leung K. P. Mitch, *Analytica Chimica Acta,* Fluorescent sensing of homocysteine by molecular imprinting, 2002, 466, 17-30.

Cosme, J., and Johnson, E. F. Engineering microsomal cytochrome P450 2C5 to be a soluble, monomeric enzyme. Mutations that alter aggregation, phospholipid dependence of catalysis, and membrane binding. *J. Biol. Chem.* 2000, 275, 2545-2553.

Cram. J. D. and Cram M. J; *Acc. Chem. Res.*, 1978, 11, 8-14.

Cram J. D., Kaneda T., Lein G. M., Helgeson R. C.; *J. Chem. Soc. Chem. Comm.*, 1979, 948-950.

Cupp-Vickery J.R & Poulos T.L, Stucture of cytochrome P450eryF involved in erythromycin biosynthesis, struct.Biol. 1995, 2:144.

Daly AK, Brockmoller J, Broly F, Eichelbaum M, Evans WE, Gonzalez EJ *et al.* Nomenclature for human *CYP2D6* alleles. *Pharmacogenetics.* 1996, 6:193-201.

Damen J. Neckers D. C. *Journal Of Organic Chemistry,* Memory of synthesized vinyl polymers for their origins., 1980,45, 1382-1387.

Dauwe C. Sellergren B. *Journal Of Chromatography A,* Influence of template basicity and hydrophobicity on the molecular recognition properties of molecularly imprinted polymers., 1996, 753, 191-200.

Davies M. P. de Biasi V. Perrett D. *Analytica Chimica Acta,* Approaches to the rational design of molecularly imprinted polymers., 2004, 504, 7-14.

de Groot MJ, Bijloo GJ, Hansen KT and Vermeulen NPE Computer prediction and experimental validation of cytochrome P450-2D6 dependent oxidation of GBR12909 (1-[2-[bis(4-fluorophenyl)methoxy]ethyl]-4-(3-phenylpropyl)piperazine). *Drug Metab Dispos.,*1995, 23, 667-669.

de Groot MJ, Vermeulen NPE, Kramer JD, van Acker FAA and Donné-Op den Kelder GM A three-dimensional protein model for human cytochrome P450 2D6 based on the crystal structures of P450 101, P450 102 and P450 108. *Chem Res Toxicol,* 1996, 9, 1079-1091.

de Groot MJ and Vermeulen NPE  Modeling the active site of cytochrome P450s and glutathione *S*-transferases, two of the most important biotransformation enzymes. *Drug Metab Rev* 1997, 29: 747-7.

de Groot MJ, Bijloo GJ, van Acker FAA, Fonseca Guerra C, Snijders JG and Vermeulen NPE Extension of a predictive substrate model for human cytochrome P4502D6. *Xenobiotica* 1997, 27: 357-368.

de Groot MJ, Ackland MJ, Horne VA, Alex AA and Jones BC A novel approach to predicting P450 mediated drug metabolism. CYP2D6 catalyzed N-dealkylation reactions and qualitative metabolite predictions using a combined protein and pharmacophore model for CYP2D6. *J Med Chem* (1999) 42: 4062-4070.

de Groot MJ, Ackland MJ, Horne VA, Alex AA and Jones BC Novel approach to predicting P450-mediated drug metabolism: development of a combined protein and pharmacophore model for CYP2D6. *J Med Chem* (1999a) 42: 1515-1524.

Dhal P. K. Arnold F. H. *Journal Of The American Chemical Society*, Template-mediated synthesis of metal-complexing polymers for molecular recognition., 1991, 113, 7417-7418.

Dhal P. K. Arnold F. H. *Macromolecules*, Metal-coordination interactions in the template-mediated synthesis of substrate-selective polymers - recognition of *bis*(Imidazole) Substrates by copper(II) Iminodiacetate containing polymers., 1992, 25, 7051-7059.

Dhal P. K. Arnold F. H. *New Journal Of Chemistry*, Substrate selectivity of molecularly imprinted polymers incorporating a rigid chelating monomer *bis*-methacrylato (4-methyl 4'-vinyl) 2 2'-bipyridine Cu(II)., 1996, 20, 695-698.

Dickert F. L. Tortschanoff M. Bulst W. E. Fischerauer G. *Analytical Chemistry*, Molecularly imprinted sensor layers for the detection of polycyclic aromatic hydrocarbons in water., 1999, 71, 4559-4563.

Dickert F. L. Hayden O. *Analytical Chemistry*, Bioimprinting of polymers and sol-gel phases. Selective detection of yeasts with imprinted polymers., 2002, 74, 1302-1306.

Dickey F. H. Proceedings Of The National Academy Of Sciences Of The United States Of America, The Preparation of Specific Adsorbents, 1949, 35 227-229.

Dickey F. H. *Journal Of Physical Chemistry*, Specific adsorption, 1955, 59 695-707.

Dobashi A. Nishida S. Kurata K. Hamada M. *Analytical Sciences*. Chiral separation of enantiomeric 1 2-diamines using molecular imprinting method and selectivity enhancement by addition of achiral primary amines into eluents., 2002, 18, 35-39.

Dunkin I. R. Lenfeld J. Sherrington D. C. *Polymer*, Molecular imprinting of flat polycondensed aromatic-molecules in macroporous polymers., 1993, 34, 77-84.

Eichelbaum M, Spannbrucker N, Steincke B, Dengler HJ. Defective N-oxidation of sparteine in man: a new pharmacogenetic defect. Eur J Clin Pharmacol 1979;16:183-187.

Ellis, S.W., Rowland, K., Ackland, M.J., Rekka, E., Simula, A.P., Lennard, M.S., Wolf, C.R., Tucker, G.T.,. Influence of amino acid residue 374 of cytochrome P-450 2D6 (CYP2D6) on the regio- and enantio-selective metabolism of metoprolol. Biochem J. 1996, 316(2), 647-54.

Ellwanger A. Berggren C. Bayoudh S. Crecenzi C. Karlsson L. Owens P. K. Ensing K. Cormack P. Sherrington D. Sellergren B. *Analyst*, Evaluation of methods aimed at complete removal of template from molecularly imprinted polymers., 2001, 126, 784-792.

Ereshefsky, L., Riesenman, C., Lam, Y.W., Antidepressant drug interactions and the cytochrome P450 system. The role of cytochrome P450 2D6. 1995 Clin. Pharmacokinet. 29 Suppl 1:10-8; discussion 18-9.

Ersöz Arzu, Denizli Adil, Özcan Ali and Say Rıdvan, *Biosensors and Bioelectronics*, Molecularly imprinted ligand-exchange recognition assay of glucose by quartz crystal microbalance., 2005, 20, 2197-2202.

Ferrer I. Lanza F. Tolokan A. Horvath V. Sellergren B. Horvai G. Barcelo D. *Analytical Chemistry,* Selective trace enrichment of chlorotriazine pesticides from natural waters and sediment samples using terbuthylazine molecularly imprinted polymers, 2000, 72, 3934-3941.

Fischer E., Ber. Dtsch .Chem. Ges., 1894, 27, 2985-2993.

Flores A. Cunliffe D. Whitcombe M. J. Vulfson E. N. *Journal Of Applied Polymer,* Imprinted polymers prepared by aqueous suspension polymerisation., 2000, 77, 1841-1850.

Foye O. William, Lemke L. Thomas, Williams A. David., Principles of medicinal chemistry, 4th edn, Williams and Wilkins, 1995.

Fujii Y. Kikuchi K. Matsutani K. Ota K. Adachi M. Syoji M. Haneishi I. Kuwana Y. *Chemistry Letters,* Template synthesis of polymer schiff-base cobalt(III) Complex and formation of specific cavity for chiral amino-acid., 1984, 1487-1490.

Fujii Y. Matsutani K. Kikuchi K. *Journal Of The Chemical Society-Chemical Communications,* Formation of a specific coordination cavity for a chiral amino-acid by template synthesis of a polymer schiff-base cobalt(Iii) Complex., 1985, 415-417.

Fujimoto K., Shimizu H. and Inouye M., *J. Org. Chem.,* Unambiguous Detection of Target DNAs by Excimer-Monomer Switching Molecular Beacons, 2004, 69, 3271-3275.

Gao S. H., Wang W., Wang B. H., *Bioorganic Chemistry,* Building fluorescent sensors for carbohydrates using template- directed polymerisations, 2001, 29, 308-320.

Garfinkel, D. Studies on pig liver microsomes. I. Enzymatic and pigment composition of different microsomal fractions. *Arch. Biochem. Biophys.*1958, 77, 493-509.

Gibson G. Gordon & Skett Paul. Introduction to drug metabolism, 3rd edn, Cheltenham, Nelson Thornes, 2001.

Glad M. Norrlöw O. Sellergren B. Siegbahn N. Mosbach K. *Journal Of Chromatography,* Use of silane monomers for molecular imprinting and enzyme entrapment in polysiloxane-coated porous silica., 1985, 347, 11-23.

Glad M., Reinholdsson P., Mosbach K., *Reactive Polymers,* Molecularly imprinted composite polymers based on trimethylolpropane trimethacrylate (TRIM) Particles for efficient enantiomeric separations., 1995, 25, 47-54.

Gonzalez FJ, Vilbois F, Hardwick JP, et al. Human debrisoquine 4-hydroxylase (P450IID1): cDNA and deduced amino acid sequence and assignment of the CYP2D locus of chromosome 22. Genomics 1988, 2:174-179.

Goshman, L., Fish, J., Roller, K., Clinically significant cytochrome P450 drug interactions. J. Pharm. Soc. Wisconsin May/June, 1999, 23–38.

Gozlan, I., Halpern, M., Rabinovitz, M., Avnir, D., Ladkani, D., Phase-transfer catalysis in n-alkylations of the pharmaceutical intermediates 5h-dibenz[b,f]azepine and 5h-10,11-dihydrodibenz[b,f]azepine. J. Heterocyclic Chem., 1982, 19 (6), 1569-1571.

Graceffa P. and Lehrer.S Sherwin., The Journal of Biological Chemistry, The excimer fluorescence of pyrene-labelled Tropomyosin., 1980, 255, 11296-11300.

Guo H. S. He X. W. Liang H. *Fresenius Journal Of Analytical Chemistry,* Study of the binding characteristics and transportation properties of a 4-aminopyridine imprinted polymer membrane., 2000, 368, 763-767.

Guengerich, F. P., and Shimada, T. Activation of procarcinogens by human cytochrome P450 enzymes. *Mutat. Res.* 1998, 400, 201-213.

Haginaka J. Takehira H. Hosoya K. Tanaka N. *Journal Of Chromatography A* Molecularly imprinted uniform-sized polymer-based stationary phase for naproxen - Comparison of molecular recognition ability of the molecularly imprinted polymers prepared by thermal and redox polymerization techniques., 1998, 816, 113-121.

Haginaka J. Sanbe H. *Chemistry Letters,* Uniform-sized molecularly imprinted polymers for beta-estradiol, 1998, 27, 1089-1090.

Haginaka J. Sanbe H. Takehira H. *Journal Of Chromatography A,* Uniform-sized molecularly imprinted polymer for (S)-ibuprofen - Retention properties in aqueous mobile phases, 1999, 857, 117-125.

Haginaka J. Sanbe H. *Chemistry Letters,* Uniform-sized molecularly imprinted polymers for bisphenol A, 1999, 28, 757-758.

Haginaka J. Sakai Y. *Journal Of Pharmaceutical And Biomedical Analysis,* Uniform-sized molecularly imprinted polymer material for (S)- propranolol., 2000, 22, 899-907.

Haginaka J. Sanbe H. *Journal Of Chromatography A,* Uniformly sized molecularly imprinted polymer for (S)-naproxen - Retention and molecular recognition properties in aqueous mobile phase., 2001, 913, 141-146.

Haginaka Jun and Kagawa Chino *Journal of Chromatography A* Uniformly sized molecularly imprinted polymer for *d*-chlorpheniramine: Evaluation of retention and molecular recognition properties in an aqueous mobile phase., 2002, 948, 77-84.

Haginaka Jun and Kagawa Chino *Journal of Chromatography B* Retentivity and enantioselectivity of uniformly sized molecularly imprinted polymers for *d*-chlorpheniramine and -brompheniramine in hydro-organic mobile phases., 2004, 804, 19-24.

Hamman, M.A., Thompson, G.A., Hall, S.D., Regioselective and Stereoselective Metabolism of Ibuprofen by Human Cytochrome P450 2C. Biochemical Pharmacology.1997, 54, 33-41.

Hasemann C.A.,.Ravichandran K.G, crystal structure and refinement to cytochrome P450terp at 2.3 Å resolution,J.Mol.Biol. 1994, 236:1169.

Haupt K. Dzgoev A. Mosbach K. *Analytical Chemistry,* Assay system for the herbicide 2 4-dichlorophenoxyacetic acid using a molecularly imprinted polymer as an artificial recognition element.,1998, 70, 628-631.

Haupt K. Mayes A. G. Mosbach K. *Analytical Chemistry,* Herbicide assay using an imprinted polymer based system analogous to competitive fluoroimmunoassays., 1998a, 70, 3936-3939.

Haupt K. *Reactive & Functional Polymers,* Molecularly imprinted sorbent assays and the use of non-related probes, 1999, 41, 125-131.

Haupt K. *Analyst,* Molecularly imprinted polymers in analytical chemistry., 2001, 126, 747-756.

Haupt K. *Chemical Communications,* Imprinted polymers - Tailor-made mimics of antibodies and receptors., 2003, 171-178.

Hawkins M Daniel, Stevenson Derek and Reddy M Subrayal, *Analytica Chimica Acta,* Investigation of protein imprinting in hydrogel-based molecularly imprinted polymers (HydroMIPs), 2005, 542, 61-65.

Hedborg E. Winquist F. Lundström I. Andersson L. I. Mosbach K. *Sensors And Actuators A-Physical,* Some studies of molecularly-imprinted polymer membranes in combination with field-effect devices., 1993, 37-8, 796-799.

Hosoya K. Yoshizako K. Tanaka N. Kimata K. Araki T. Haginaka J. *Chemistry Letters,* Uniform-size macroporous polymer-based stationary-phase for hplc prepared through molecular imprinting technique., 1994, 1437-1438.

Hosoya K. Yoshizako K. Shirasu Y. Kimata K. Araki T. Tanaka N. Haginaka J. *Journal Of Chromatography A,* Molecularly imprinted uniform-size polymer-based stationary phase for high-performance liquid chromatography - Structural contribution of cross-linked polymer network on specific molecular recognition., 1996, 728, 139-147.

Ingelman-Sundberg M, Evans WE. Unravelling the functional genomics of the human CYP2D6 gene locus. Pharmacogenetics 2001, 11:553-554.

Islam, S.A., Wolf, C.R., Lennard, M.S., Sternberg, M.J.E.,. A three-dimensional molecular template for substrates of human cytochrome P450 involved in debrisoquine 4-hydroxylation. Carcinogenesis 1991,12, 2211-2219.

Jenkins A. L. Uy O. M. Murray G. M. *Analytical Communications,* Polymer based lanthanide luminescent sensors for the detection of nerve agents., 1997, 34, 221-224.

Jenkins A. L. Uy O. M. Murray G. M. *Analytical Chemistry,* Polymer-based lanthanide luminescent sensor for detection of the hydrolysis product of the nerve agent Soman in water., 1999, 71, 373-378.

Ji H. S. McNiven S. Ikebukuro K. Karube I. *Analytica Chimica Acta,* Selective piezoelectric odor sensors using molecularly imprinted polymers., 1999, 390, 93-100.

Ji H. S. McNiven S. Lee K. H. Saito T. Ikebukuro K. Karube I. *Biosensors & Bioelectronics,* Increasing the sensitivity of piezoelectric odour sensors based on molecularly imprinted polymers., 2000, 15, 403-409.

Jin Takashi and Monde Kenji, Chemical Communication, Synthesis and optical resolution of a fluorescent chiral calix[4]arene with two pyrene moieties forming an intramolecular excimer., 1998, 1357-1358.

Joshi V. P. Karmalka R. N. Kulkarni M. G. Mashelkar R. A. *Industrial & Engineering Chemistry Research,* Effect of solvents on selectivity in separation using molecularly imprinted adsorbents: Separation of phenol and bisphenol A., 1999, 38, 4417-4423.

Jordan C.E., Frutos A.G., Thiel A.J., Corn R.M., Anal.Chem, Surface plasmon resonance imaging measurements of DNA hygridization adsorption and streptavidin/DNA multiplayer formation at chemically modified gold surfaces, 1997, 69, 939-4947.

Kanekiyo Y. Inoue K. Ono Y. Sano M. Shinkai S. Reinhoudt D. N. *Journal Of The Chemical Society-Perkin Transactions,* 'Molecular-imprinting' of AMP utilising the polyion complex formation process as detected by a QCM system. 1999, *2,* 2719-2722.

Karmalkar R. N. Kulkarni M. G. Mashelkar R. A. *Journal Of Controlled Release,* Pendent chain linked delivery systems .2. Facile hydrolysis through molecular imprinting effects., 1997, 43, 235-243.

Kato M. Nishide H. Tsuchida E. Sasaki T. *Journal Of Polymer Science Part A-Polymer Chemistry,* Complexation of metal-ion with poly(1-Vinylimidazole) Resin prepared by radiation-induced polymerisation with template metal-ion., 1981, 19, 1803-1809.

Kempe M. Fischer L. Mosbach K. *Journal Of Molecular Recognition,* Chiral separation using molecularly imprinted heteroatomic polymers., 1993, 6, 25-29.

Kempe M. Mosbach K. *Journal Of Chromatography A,* Direct resolution of naproxen on a noncovalently molecularly imprinted chiral stationary-phase., 1994, 664, 276-279.

Kempe M. Mosbach K. *Journal Of Chromatography A,* Separation of amino-acids peptides and proteins on molecularly imprinted stationary phases., 1995, 691, 317-323.

Kempe M. Glad M. Mosbach K. *Journal Of Molecular Recognition,* An approach towards surface imprinting using the enzyme ribonuclease- A., 1995, 8, 35-39.

Kempe M. Mosbach K. *Journal Of Chromatography A,* Molecular imprinting used for chiral separations., 1995a, 694, 3-13.

Kempe M. Mosbach K. *Tetrahedron Letters*, Receptor-binding mimetics - a novel molecularly imprinted polymer., 1995b, 36, 3563-3566.

Kempe M. *Analytical Chemistry*, Antibody-Mimicking polymers as chiral stationary phases in HPLC., 1996, 68, 1948-1953.

Kido H. Miyajima T. Tsukagoshi K. Maeda M. Takagi M. *Analytical Sciences*, Metal-ion complexation behavior of resins prepared by a novel template polymerization technique, 1992, 8 749-753.

Kim J. M. Ahn K. D. Strikovsky A. G. Wulff G. *Bulletin Of The Korean Chemical Society*, Polymer catalysts by molecular imprinting: A labile covalent bonding approach., 2001, 22, 689-692.

Kim J. M. Ahn K. D. Wulff G. *Macromolecular Chemistry And Physics*, Cholesterol esterase activity of a molecularly imprinted polymer., 2001a, 202, 1105-1108.

Kimaro A. Kelly L. A. Murray G. M. *Chemical Communications*, Molecularly imprinted ionically permeable membrane for uranyl ion., 2001, 1282-1283.

Kimura S, Umeno M, Skoda R, Meyer UA, Gonzalez FJ. The human debrisoquine 4-hydroxylase (CYP2D) locus: sequence and identification of the polymorphic CYP2D6 gene, a related gene and a pseudogene. Am J Hum Genet 1989, 45:889-904.

Kirchheiner, J., Meineke, I., Muller, G., Roots, I., Brockmoller, J.,. Contributions of CYP2D6, CYP2C9 and CYP2C19 to the biotransformation of E- and Z-doxepin in healthy volunteers. Pharmacogenetics 2002, 12(7), 571-80.

Kirsch N. Hart J. P. Bird D. J. Luxton R. W. McCalley D. V. *Analyst*, Towards the development of molecularly imprinted polymer based screen-printed sensors for metabolites of PAHs., 2001, 126. 1936-1941.

Klingenberg, M. Pigment of rat liver microsomes. *Arch. Biochem. Biophys.* 1958, 75, 376-386.

Klotz. J and Takagishi.T, Macromolecule- small interactions; Introduction of additional binding sites in polyethyleneimine by disulfide cross-linkages, Biopolymers, 1972, 11, 483-491.

Kobayashi T. Wang H. Y. Fujii N. *Analytica Chimica Acta*, Molecular imprint membranes of polyacrylonitrile copolymers with different acrylic acid segments., 1998, 365, 81-88.

Kobayashi T. Wang H. Y. Fukaya T. Fujii N. *Acs Symposium Series*, Molecular imprinted membranes prepared by phase inversion of polyacrylonitrile copolymers containing carboxylic acid groups, 1998a, 703, 188-201.

Kobayashi takaomi, Murawaki yasuhiro, Reddy sreenivasulu puchalapalli, Abe masanori, Fujii nobuyuki, Analtica Chimica Acta, Molecular imprinting of caffeine and its recognition assay by QCM., 2001, 435, 141-149.

Koshland, D.G. Neot N.E., Ann. Rew. Biochem., 1968, 37, 359-410.

Kostenko E., Dobrikov M., Pyshnyi D., Petyuk V., Komarova N., Vlassov V. and Zenkova M., Oxford University Press, 5`-bis-pyrenylated loigonucleotides displaying excimer fluorescence provide sensitive probes of RNA sequence and structure., 2001, 29, 3611-3620.

Koymans L, Vermeulen NPE, van Acker SABE, te Koppele JM, Heykants JJP, Lavrijsen K, Meuldermans W and Donne-Op den Kelder GM A predictive model for substrates of cytochrome P450-debrisoquine (2D6). *Chem Res Toxicol* .1992, 5, 211-219.

Kriz D. Kriz C. B. Andersson L. I. Mosbach K. *Analytical Chemistry*, Thin-layer chromatography based on the molecular imprinting technique., 1994, 66, 2636-2639.

Kriz D. Ramström O. Svensson A. Mosbach K. *Analytical Chemistry*, Introducing biomimetic sensors based on molecularly imprinted polymers as recognition elements., 1995, 67, 2142-2144.

Kriz D. Mosbach K. *Analytica Chimica Acta,* Competitive amperometric morphine sensor-based on an agarose immobilized molecularly imprinted polymer., 1995 300, 71-75.

Kriz D. Kempe M. Mosbach K. *Sensors And Actuators B-Chemical,* Introduction of molecularly imprinted polymers as recognition elements in conductometric chemical sensors., 1996, 33, 178-181.

Kriz D. Ramström O. Mosbach K. *Analytical Chemistry,* Molecular imprinting - New possibilities for sensor technology., 1997, 69, A345-A349.

Kroemer HK, Eichelbaum M. "It's the genes, stupid": molecular bases and clinical consequences of genetic cytochrome P450 2D6 polymorphism. Life Sci 1995, 56:2285-2298.

Kröger S. Turner A. P. F. Mosbach K. Haupt K. *Analytical Chemistry,* Imprinted polymer based sensor system for herbicides using differential-pulse voltammetry on screen printed electrodes., 1999, 71, 3698-3702.

Krotz J -. Shea K. J. *Journal Of The American Chemical Society,* Imprinted polymer membranes for the selective transport of targeted neutral molecules., 1996, 118, 8154-8155.

Kubo H., Nariai H., Takuechi T., Chem. Commun., Multiple hydrogen bonding-baes fluorescent imprinted polymers for cyclobrabital prepared with 2,6-bis(acrylamide)pyridine, 2003, 2792-2793.

Kugimiya A. Matsui J. Takeuchi T. Yano K. Muguruma H. Elgersma A. V. Karube I. *Analytical Letters,* Recognition of sialic-acid using molecularly imprinted polymer., 1995, 28, 2317-2323.

Kugimiya A. Matsui J. Abe H. Aburatani M. Takeuchi T. *Analytica Chimica Acta,* Synthesis of castasterone selective polymers prepared by molecular imprinting., 1998, 365, 75-79.

Kugimiya A. Takeuchi T. *Electroanalysis,* Molecularly imprinted polymer-coated quartz crystal microbalance for detection of biological hormone., 1999, 11, 1158-1160.

Kugimiya A., Takeuchi T., Biosensors & Bioelectronics, Surface plasmon resonance sensor using molecular imprinted polymer for detection of sialic acid, 2001, 16, 1059-1062.

Kyba P E., Helgeson C R., Madan K., Gokel W G., Tarnowski L T., Moor S. S.; *J. Am.Chem. Soc.* 1997; 99; 2564-2571.

Lai J. P. Lu X. Y. Lu C. Y. Ju H. F. He X. W. *Analytica Chimica Acta,* Preparation and evaluation of molecularly imprinted polymeric microspheres by aqueous suspension polymerization for use as a high-performance liquid chromatography stationary phase, 2001, 442, 105-111.

Lanza F. Sellergren B. *Analytical Chemistry,* Method for synthesis and screening of large groups of molecularly imprinted polymers., 1999, 71, 2092-2096.

Lanza F. Hall A. J. Sellergren B. Bereczki A. Horvai G. Bayoudh S. Cormack P. A. G. Sherrington D. C. *Analytica Chimica Acta,* Development of a semiautomated procedure for the synthesis and evaluation of molecularly imprinted polymers applied to the search for functional monomers for phenytoin and nifedipine., 2001, 435, 91-106.

Lavignac Nathalie, Allender J Christopher and Brain R Keith, *Tetrahedron Letters,* 4-(3-Aminopropylene)-7-nitrobenzofurazan: a new polymerisable monomer for use in homogeneous molecularly imprinted sorbent fluoroassay, 2004, 45, 3625-3627.

Lehn J-M, Dietrich .B, and Sauvage J-P; *Tetrahedron Lett,* 34, 1969, 2885-2888.

Lehn J-M, Dietrich .B, and Sauvage J-P; *Tetrahedron Lett,* 34, 1969a, 2889-2892.

Leonhardt A. Mosbach K. *Reactive Polymers,* Enzyme-mimicking polymers exhibiting specific substrate binding and catalytic functions., 1987, 6, 285-290.

Levi R. McNiven S. Piletsky S. A. Cheong S. H. Yano K. Karube I. *Analytical Chemistry,* Optical detection of chloramphenicol using molecularly imprinted polymers., 1997, 69, 2017-2021.

Liang C. D. Peng H. Bao X. Y. Nie L. H. Yao S. Z. *Analyst,* Study of a molecular imprinting polymer coated BAW bio-mimic sensor and its application to the determination of caffeine in human serum and urine., 1999, 124, 1781-1785.

Liao Yuan, Wang Wei and Wang Binghe, *Bioorganic Chemistry.,* Building Fluorescent Sensors by Template Polymerization: The Preparation of a Fluorescent Sensor for l-Tryptophan, 1999, 27 , 463-476.

Lin J. M. Nakagama T. Uchiyama K. Hobo T. *Journal Of Liquid Chromatography & Related Technologies,* Enantioseparation of D L-phenylalanine by molecularly imprinted polymer particles filled capillary electrochromatography., 1997, 20, 1489-1506.

Lin J. M. Nakagama T. Wu X. Z. Uchiyama K. Hobo T. *Fresenius Journal Of Analytical Chemistry,* Capillary electrochromatographic separation of amino acid enantiomers with molecularly imprinted polymers as chiral recognition agents., 1997a, 357, 130-132.

Lin J. M. Nakagama T. Uchiyama K. Hobo T. *Journal Of Pharmaceutical And Biomedical Analysis,* Capillary electrochromatographic separation of amino acid enantiomers using on-column prepared molecularly imprinted polymer., 1997b, 15, 1351-1358.

Lin J. M. Nakagama T. Uchiyama K. Hobo T. *Biomedical Chromatography,* Temperature effect on chiral recognition of some amino acids with molecularly imprinted polymer filled capillary electrochromatography., 1997c, 11, 298-302.

Lotierzo M., Henry, O. Y. F. PiletskyS., Tothill I., Cullen D., Kania M., Hock B and Turner A. P. F., *Biosensors and Bioelectronics,* Surface plasmon resonance sensor for domoic acid based on grafted imprinted polymer, 2004, 20, 145-152.

Lübke M. Whitcombe M. J. Vulfson E. N. *Journal Of The American Chemical Society,* A novel approach to the molecular imprinting of polychlorinated aromatic compounds, 1998, 120, 13342-13348.

Lu Yan, Li Chenxi, Liu Xiaohang and Huang Wenqiang *Journal of Chromatography A,* Molecular recognition through the exact placement of functional groups on non-covalent molecularly imprinted polymers., 2002, 950, 89-97.

Lustenberger P., Martinborough E., Denti Mordasini T., Diederich F., J. Chem.Soc., Perkin Trans., 1998, 2, 747-761.

Maeda M. Murata M. Tsukagoshi K. Takagi M. *Analytical Sciences* Template-dependent metal adsorptivity of dialkyl phosphate-type resins prepared by surface template polymerization technique., 1994, 10, 113-115.

Mahgoub A, Idle JR, Dring LG, Lancaster R, Smith RL. Polymorphic hydroxylation of debrisoquine in man. Lancet 1977, 2:584-586

Malitesta C. Losito I. Zambonin P. G. *Analytical Chemistry,* Molecularly imprinted electrosynthesized polymers: New materials for biomimetic sensors., 1999, 71, 1366-1370.

Martin P. Wilson I. D. Morgan D. E. Jones G. R. Jones K. *Analytical Communications,* Evaluation of a molecular-imprinted polymer for use in the solid phase extraction of propranolol from biological fluids., 1997, 34, 45-47.

Martin P. Wilson I. D. Jones G. R. Jones K., Selective SPE's using molecular imprinted polymers in "Drug-development assay approaches including molecular imprinting and biomarkers", 1998.

Matsui J. Miyoshi Y. Takeuchi T. *Chemistry Letters,* Fluoro-functionalized molecularly imprinted polymers selective for herbicides., 1995,1007-1008.

Matsui J. Miyoshi Y. Matsui R. Takeuchi T. *Analytical Sciences,* Rod-type affinity media for liquid-chromatography prepared by in- situ-molecular imprinting., 1995a, 11, 1017-1019.

Matsui J. Nicholls I. A. Karube I. Mosbach K. *Journal Of Organic Chemistry,* Carbon-carbon bond formation using substrate selective catalytic polymers prepared by molecular imprinting: An artificial class II aldolase., 1996, 61, 5414-5417.

Matsui J. Nicholls I. A. Takeuchi T. *Tetrahedron-Asymmetry,* Highly stereoselective molecularly imprinted polymer synthetic receptors for cinchona alkaloids., 1996a, 7, 1357-1361.

Matsui J. Doblhoff-Dier O. Takeuchi T. *Analytica Chimica Acta,* 2-(trifluoromethyl)acrylic acid: A novel functional monomer in non-covalent molecular imprinting., 1997, 343, 1-4.

Matsui J. Okada M. Tsuruoka M. Takeuchi T. *Analytical Communications,* Solid-phase extraction of a triazine herbicide using a molecularly imprinted synthetic receptor., 1997a, 34, 85-87.

Matsui J. Nicholls I. A. Takeuchi T. *Analytica Chimica Acta,* Molecular recognition in cinchona alkaloid molecular imprinted polymer rods., 1998, 365, 89-93.

Matsui J. Fujiwara K. Ugata S. Takeuchi T. *Journal Of Chromatography A,* Solid-phase extraction with a dibutylmelamine-imprinted polymer as triazine herbicide-selective sorbent., 2000, 889, 25-31.

Matsui J. Higashi M. Takeuchi T. *Journal Of The American Chemical Society,* Molecularly imprinted polymer as 9-ethyladenine receptor having a porphyrin-based recognition center., 2000a, 122, 5218-5219.

Mayes A. G. Andersson L. I. Mosbach K. *Analytical Biochemistry,* Sugar binding polymers showing high anomeric and epimeric discrimination obtained by noncovalent molecular imprinting., 1994, 222, 483-488.

Mayes A. G. Mosbach K. *Analytical Chemistry,* Molecularly imprinted polymer beads: Suspension polymerization using a liquid perfluorocarbon as the dispersing phase, 1996, 68, 3769-3774.

Mayes A. G. Mosbach K. *Trac-Trends In Analytical Chemistry,* Molecularly imprinted polymers: useful materials for analytical chemistry?., 1997, 16, 321-332.

Mayes A. G. Lowe C. R., " Optimization of molecularly imprinted polymers for radio-ligand binding assays in "Drug-development assay approaches including molecular imprinting and biomarkers,1998.

Mena M. L. Martinez-Ruiz P. Reviejo A. J. Pingarrón J. M. *Analytica Chimica Acta,* Molecularly imprinted polymers for on-line preconcentration by solid phase extraction of pirimicarb in water samples., 2002, 451, 297-304.

Meyer UA, Gut J, Kronbach T, Skoda C, Meier UT and Catin T The molecular mechanisms of two common polymorphisms of drug oxidation-evidence for functional changes in cytochrome P-450 isozymes catalysing bufuralol and mephenytoin oxidation. *Xenobiotica.*1986, 16: 449-464.

Milojkovic S. S. Kostoski D. Comor J. J. Nedeljkovic J. M. *Polymer,* Radiation induced synthesis of molecularly imprinted polymers., 1997, 38, 2853-2855.

Modi, S., Paine, M.J., Sutcliffe, M.J., Lian, L.Y., Primrose, W.U., Wol,f C.R., Roberts, G.C.,. A model for human cytochrome P450 2D6 based on homology modeling and NMR studies of substrate binding. Biochemistry. 1996, 35(14), 4540-4550.

Mosbach, K, and Mosbach, R. Acta Chem. Scand. 1966, 20, 2807-2810.

Mosbach K. Ramström O. *Bio/Technology,* The emerging technique of molecular imprinting and its future impact on biotechnology., 1996, 14, 163-170.

Muldoon M. T. Stanker L. H. *Journal Of Agricultural And Food Chemistry,* Polymer synthesis and characterization of a molecularly imprinted sorbent assay for atrazine., 1995, 43, 1424-1427.

Muldoon M. T. Stanker L. H. *Analytical Chemistry,* Molecularly imprinted solid phase extraction of atrazine from beef liver extracts., 1997, 69, 803-808.

Muller R. , Andersson L. and Mosback K. *Makromol. Chem. Rapid Commun,* Molecularly imprinted polymers facilitating a β-elimination reaction., 1993, 14, 637-641.

Mullett W. M. Lai E. P. C. *Analytical Chemistry,* Determination of theophylline in serum by molecularly imprinted solid-phase extraction with pulsed elution., 1998, 70, 3636-3641.

Mullett W. M. Lai E. P. C. Sellergren B. *Analytical Communications,* Determination of nicotine in tobacco by molecularly imprinted solid phase extraction with differential pulsed elution., 1999, 36, 217-220.

Murata M. Hijiya S. Maeda M. Takagi M. *Bulletin Of The Chemical Society Of Japan,* Template-dependent selectivity in metal adsorption on phosphoric diester-carrying resins prepared by surface template polymerization technique, 1996, 69, 637-642.

Nelson, D. R., Koymans, L., Kamataki, T., Stegeman, J. J., Feyereisen, R., Waxman, D. J.,Waterman, M. R., Gotoh, O., Coon, M. J., Estabrook, R. W., Gunsalus, I. C., and Nebert, D. W. P450 superfamily: update on new sequences, gene mapping, accession numbers and nomenclature. *Pharmacogenetics.*1996, 6, 1-42.

Nicholls I. A. *Chemistry Letters,* Thermodynamic considerations for the design of and ligand recognition by molecularly imprinted polymers., 1995, 1035-1036.

Nicholls I. A. Ramström O. Mosbach K. *Journal Of Chromatography A,* Insights into the role of the hydrogen-bond and hydrophobic effect on recognition in molecularly imprinted polymer synthetic peptide receptor mimics., 1995a, 691, 349-353.

Nicholls I. A. *Journal Of Molecular Recognition,* Towards the rational design of molecularly imprinted polymers., 1998, 11, 79-82.

Nilsson S. Schweitz L. Petersson M. *Electrophoresis,* Three approaches to enantiomer separation of beta-adrenergic antagonists by capillary electrochromatography., 1997, 18, 884-890.

Nishide H. Deguchi J. Tsuchida E. *Chemistry Letters,* Selective adsorption of metal ions on crosslinked poly(vinylpyridine) resin prepared with a metal ion as a template., 1976, 169-174.

Norell M. C. Andersson H. S. Nicholls I. A. *Journal Of Molecular Recognition,* Theophylline molecularly imprinted polymer dissociation kinetics: a novel sustained release drug dosage mechanism., 1998, 11, 98-102.

Norrlöw O. Glad M. Mosbach K. *Journal Of Chromatography,* Acrylic polymer preparations containing recognition sites obtained by imprinting with substrates., 1984, 299, 29-41.

Norrlöw O. Månsson M. O. Mosbach K. *Journal Of Chromatography,* Improved chromatography - prearranged distances between boronate groups by the molecular imprinting approach., 1987, 396, 374-377.

Ohkubo K. Urata Y. Honda Y. Nakashima Y. Yoshinaga K. *Polymer,* Preparation and catalytic property of l-histidyl group-introduced cross-linked poly(Ethylene imine)S imprinted by a transition-state analog of an esterolysis reaction., 1994, 35, 5372-5374.

Ohkubo K. Urata Y. Hirota S. Honda Y. Fujishita Y. Sagawa T. *Journal Of Molecular Catalysis,* Homogeneous esterolytic catalysis of a polymer prepared by molecular imprinting of a transition-state analogue., 1994a, 93, 189-193

Ohkubo K. Funakoshi Y. Urata Y. Hirota S. Usui S. Sagawa T. Yoshinaga K. *Kobunshi Ronbunshu,* Molecular design of transition-state analog-imprinted polymer catalysts-stereoselective esterolysis of amino-acid esters., 1995, 52, 644-649.

Ohkubo K. Urata Y. Hirota S. Funakoshi Y. Sagawa T. Usui S. Yoshinaga K. *Journal Of Molecular Catalysis A-Chemical,* Catalytic activities of novel l-histidyl group-introduced polymers imprinted by a transition-state analog in the hydrolysis of amino- acid esters., 1995a, 101, 111-114.

O'Shannessy D. J. Ekberg B. Andersson L. I. Mosbach K. *Journal Of Chromatography,* Recent advances in the preparation and use of molecularly imprinted polymers for enantiomeric resolution of amino-acid derivatives., 1989, 470, 391-399.

O'Shannessy D. J. Ekberg B. Mosbach K. *Analytical Biochemistry,* Molecular imprinting of amino-acid derivatives at low-temperature (0- Degrees-C) Using photolytic homolysis of azobisnitriles.,1989a, 177, 144-149.

O'Shannessy D. J. Andersson L. I. Mosbach K. *Journal Of Molecular Recognition,* Molecular recognition in synthetic polymers. Enantiomeric resolution of amide derivatives of amino acids on molecularly imprinted polymers., 1989b, 2, 1-5.

Ozawa S. Klibanov A. M. *Biotechnology Letters,* Myoglobin-catalyzed epoxidation of styrene in organic solvents accelerated by bioimprinting., 2000, 22, 1269-1272.

Panasyuk T. L. Mirsky V. M. Piletsky S. A. Wolfbeis O. S. *Analytical Chemistry,* Electropolymerized molecularly imprinted polymers as receptor layers in a capacitive chemical sensors., 1999, 71, 4609-4613.

Panasyuk-Delaney T. Mirsky V. M. Wolfbeis O. S. *Electroanalysis,* Capacitive creatinine sensor based on a photografted molecularly imprinted polymer., 2002, 14, 221-224.

Park Soon H., Lin Q., Hamilton D A., J. Am. Chem. Soc., Protein Surface Recognition by Synthetic Receptors: A Route to Novel Submicromolar Inhibitors for $\alpha$-Chymotrypsin.,1999, 121, 8-1.

Parkinson, A. Biostransformation of Xenobiotics. In *Casarett & Doull's toxicology the basic science of poisons.* (Klaassen, C. D. ed) pp New York McGraw-Hill Inc. 1996, 113-186.

Patrick L. Graham, An introduction to medicinal chemistry., *Oxford University Press,* 1995 inc., N.Y

Pauling.L., A theory of the structure and process of formation of antibodies. J.Am.Chem.Soc., 1940, 62, 2643-2657.

Pedersen J. C., *J. Am. Chem.* Soc., 1967, 89, 2495-2496.

Pedersen J. C., *J. Am. Chem.* Soc., 1967a, 89, 7017-1036.

Peterlinz K. A., Georgiadis R., Langmuir, In situ kinetics of self-assebly by surface plasmon resonance spectroscopy., 12, 1996, 4731-4740.

Piletsky S. A. Piletskaya E. V. Elgersma A. V. Yano K. Karube I. Parhometz Y. P. Elskaya A. V. *Biosensors & Bioelectronics,* Atrazine sensing by molecularly imprinted membranes., 1995, 10, 959-964.

Piletsky S. A. Piletskaya E. V. Elskaya A. V. Levi R. Yano K. Karube I. *Analytical Letters,* Optical detection system for triazine based on molecularly-imprinted polymers., 1997, 30, 445-455.

Piletsky S. A. Piletskaya E. V. Panasyuk T. L. Elskaya A. V. Levi R. Karube I. Wulff G. *Macromolecules,* Imprinted membranes for sensor technology: Opposite behaviour of covalently and noncovalently imprinted membranes., 1998, 31, 2137-2140.

Piletsky S. A. Andersson H. S. Nicholls I. A. *Journal Of Molecular Recognition,* The rational use of hydrophobic effect-based recognition in molecularly imprinted polymers., 1998a, 11, 94-97.

Piletsky S. A. Piletskaya E. V. Panasyuk T. L. Elskaya A. V. Levi R. Karube I. Wulff G. *Macromolecules,* Imprinted membranes for sensor technology: Opposite behavior of covalently and noncovalently imprinted membranes., 1998b, 31, 2137-2140.

Piletsky S. A. Panasyuk T. L. Piletskaya E. V. Nicholls I. A. Ulbricht M. *Journal Of Membrane Science,* Receptor and transport properties of imprinted polymer membranes - a review, 1999, 157, 263-278.

Piletsky S. A. Andersson H. S. Nicholls I. A. *Macromolecules,* Combined hydrophobic and electrostatic interaction-based recognition in molecularly imprinted polymers., 1999a, 32, 633-636.

Piletsky S. A. Terpetschnig E. Andersson H. S. Nicholls I. A. Wolfbeis O. S. *Fresenius Journal Of Analytical Chemistry,* Application of non-specific fluorescent dyes for monitoring enantio- selective ligand binding to molecularly imprinted polymers., 1999b, 364, 512-516.

Piletsky S. A. Piletska E. V. Chen B. N. Karim K. Weston D. Barrett G. Lowe P. Turner A. P. F. *Analytical Chemistry,* Chemical grafting of molecularly imprinted homopolymers to the surface of microplates. Application of artificial adrenergic receptor in enzyme-linked assay for beta-agonists determination., 2000, 72, 4381-4385.

Piletsky S. A. Piletska E. V. Bossi A. Karim K. Lowe P. Turner A. P. F. *Biosensors & Bioelectronics,* Substitution of antibodies and receptors with molecularly imprinted polymers in enzyme-linked and fluorescent assays., 2001, 16, 701-707.

Piletsky S. A. Karim K. Piletska E. V. Day C. J. Freebairn K. W. Legge C. Turner A. P. F. *Analyst,* Recognition of ephedrine enantiomers by molecularly imprinted polymers designed using a computational approach., 2001a, 126, 1826-1830.

Piletsky A Sergey, Piletska V Elena., Bossi Alessandra, Karim Khalku, Lowe Philip and Turner P. F. Anthony, *Biosensors and Bioelectronics,* Substitution of antibodies and receptors with molecularly imprinted polymers in enzyme-linked and fluorescent assays, 2001b, 16, 701-707.

Piscopo L. Prandi C. Coppa M. Sparnacci K. Laus M. Laganà A. Curini R. D'Ascenzo G. *Macromolecular Chemistry And Physics,* Uniformly sized molecularly imprinted polymers (MIPs) for 17 beta-estradiol., 2002, 203, 1532-1538.

Poulos TL, Finzel BC, Gunsalus IC, Wagner GC and Kraut J The 2.6-Å crystal structure of *Pseudomonas putida* cytochrome P-450. *J Biol Chem* 1985, 260: 16122-16130.

Poulos TL, Finzel BC and Howard AJ Crystal structure of substrate-free *Pseudomonas putida* cytochrome P-450. *Biochemistry,*1986, 25, 5314-5322.

Price Evans DA, Manley KA, McKusick VA. Genetic control of isoniazid metabolism in man. BMJ 1960; 2:485-491.

Puoci Francesco, Garreffa Carmelo, Iemma Francesca, Muzzalupo Rita, Spizzirri Gianfranco Umile and Picci Nevio, *Food Chemistry ,* Molecularly imprinted solid phase extraction for detection of sudan I in food matrices., 2005, 93, 349-353.

Quaglia M. Chenon K. Hall A. J. De Lorenzi E. Sellergren B. *Journal Of The American Chemical Society,* Target analogue imprinted polymers with affinity for folic acid and related compounds., 2001, 123, 2146-2154.

Rachkov Alexandre, McNiven Scott, El'skaya Anna, Yano Kazuyoshi and Karube Isao, *Analytica Chimica Acta,* Fluorescence detection of $\beta$-estradiol using a molecularly imprinted polymer, 2000, 405, 23-29.

Rachkov A. Minoura N. *Biochimica Et Biophysica Acta-Protein Structure And Molecular Enzymology,* Towards molecularly imprinted polymers selective to peptides and proteins. The epitope approach., 2001, 1544, 255-266.

Ramström O. Andersson L. I. Mosbach K. *Journal Of Organic Chemistry,* Recognition sites incorporating both pyridinyl and carboxy functionalities prepared by molecular imprinting., 1993, 58, 7562-7564.

Ramström O. Nicholls I. A. Mosbach K. *Tetrahedron-Asymmetry,* Synthetic peptide receptor mimics - highly stereoselective recognition in noncovalent molecularly imprinted polymers, 1994, 5, 649-656.

Ramström, O., Ye, L. and Mosbach *Chemistry and Biology,* Artificial antibodies to corticosteroids prepared by molecular imprinting., 1996, 3, 471-477.

Ramström O. Yu C. Mosbach K. *Journal Of Molecular Recognition,* Chiral recognition in adrenergic receptor binding mimics prepared by molecular imprinting., 1996a, 9, 691-696.

Ramström O. Ansell R. J. *Chirality,* Molecular imprinting technology: Challenges and prospects for the future., 1998, 10, 195-209.

Ramström O. Ye L. Krook M. Mosbach K. *Analytical Communications,* Screening of a combinatorial steroid library using molecularly imprinted polymers., 1998, 35, 9-11.

Rashid B. A. Briggs R. J. Hay J. N. Stevenson D. *Analytical Communications,* Preliminary evaluation of a molecular imprinted polymer for solid- phase extraction of tamoxifen., 1997, 34 303-305.

Rathbone L. Daniel,Su Danqing, Wang Yongfeng and Billington C. David, *Tetrahedron Letters,* Molecular recognition by fluorescent imprinted polymers, 2000, 41, 123-126.

Rathbone L Daniel. and Ge Yi, *Analytica Chimica Acta,* Selectivity of response in fluorescent polymers imprinted with $N^1$-benzylidene pyridine-2-carboxamidrazones, 2001, 435, 129-136.

Rathbone L. Daniel, Ali Aisha, Antonaki Polyxeni Cheek Sarah., *Biosensors and Bioelectronics,* Towards a polymeric binding mimic for cytochrome CYP2D6, 2005, 20, 2353-2363.

Rathbone L. Daniel and Bains Ajeet, *Biosensors and Bioelectronics,* Tools for fluorescent molecularly imprinted polymers., 2005, 20, 1438-1442.

Rathbone L. Daniel, Molecularly Imprinted Polymers In The Drug Discovery Process, 2005, (*in press*).

Rebek R., Angew. Chem. Int. Ed. Engl., "Molecular recognition with model systems," 1990, 29, 245-255.
Ritter Peck, Biochemistry A foundation, Brooks/Cole publishing company, An international Thomas publishing company, 1996, pg 12-13.

Ritter Peck, Biochemistry A foundation, Brooks/Cole publishing company, An international Thomas publishing company, 1996.

Ritter Peck, Biochemistry A foundation, Brooks/Cole publishing company, An international Thomas publishing company, 1996a, pg 412-413.

Ritter Peck, Biochemistry A foundation, Brooks/Cole publishing company, An international Thomas publishing company, 1996b, pg 489.

Robinson D. K. Mosbach K. *Journal Of The Chemical Society-Chemical Communications,* Molecular imprinting of a transition-state analogue leads to a polymer exhibiting esterolytic activity., 1989, 969-970.

Rodríguez – Suárez Luis Jorge and Díaz-García Elena Marta, *Analytica Chimica Acta,* Flavonol fluorescent flow-through sensing based on a molecular imprinted polymer, 2000, 405, 67-76.

Rodríguez – Suárez Luis Jorge and Díaz-García Elena Marta, *Biosensors and Bioelectronics,* Fluorescent competitive flow-through assay for chloramphenicol using molecularly imprinted polymers, 2001, 16, 955-961.

Rosatzin T. Andersson L. I. Simon W. Mosbach K. *Journal Of The Chemical Society-Perkin Transactions,* Preparation of $Ca^{2+}$ selective sorbents by molecular imprinting using polymerizable ionophores., 1991, 2, 1261-1265.

Rurack Knut, *Spectrochimica Acta Part A: Molecular and Biomolecular Spectroscopy*, Flipping the light switch 'ON' – the design of sensor molecules that show cation-induced fluorescence enhancement with heavy and transition metal ions, 2001, 57, 2161-2195.

Sallacan N. Zayats M. Bourenko T. Kharitonov A. B. Willner I. *Analytical Chemistry*, Imprinting of nucleotide and monosaccharide recognition sites in acrylamidephenylboronic acid-acrylamide copolymer membranes associated with electronic transducers., 2002, 74, 702-712.

Sarhan A. *Makromolekulare Chemie-Rapid Communications*, Racemic separation of amygdalinic acid on polymers with chiral spaces .1. The synthesis of suitable polymers with phenylboronic acid as a bound group., 1982,3, 489-493.

Sarhan A. Wulff G. Makromolekulare Chemie-Macromolecular Chemistry And Physics, Enzyme-analog built polymers .13. On the introduction of amino and boronic acid groups into chiral polymer cavities., 1982, 183, 85-92.

Schacht E H, Polymer chemistry and hydrogel systems, Institute of Physics Publishing Journal of Physics: Conference Series 3,2004, 22–28.

Schoch, G.A., Yano, J.K., Wester, M.R., Griffin, K.J., Stout, C.D., Johnson, E.F.,. Structure of human microsomal cytochrome P4502C8 - Evidence for a peripheral fatty acid binding site. J. Biol. Chem. 2004, 279(10), 9497-9503.

Schweitz L. Andersson L. I. Nilsson S. *Journal Of Chromatography A,* Capillary electrochromatography with molecular imprint-based selectivity for enantiomer separation of local anaesthetics., 1997, 792, 401-409.

Schweitz L. Andersson L. I. Nilsson S. *Analytical Chemistry* Capillary electrochromatography with predetermined selectivity obtained through molecular imprinting., 1997a, 69, 1179-1183.

Schweitz L. Spégel P. Nilsson S. *Analyst,* Molecularly imprinted microparticles for capillary electrochromatographic enantiomer separation of propranolol., 2000, 125, 1899-1901.

Schweitz L. Andersson L. I. Nilsson S. *Analytica Chimica Acta,* Rapid electrochromatographic enantiomer separations on short molecularly imprinted polymer monoliths., 2001, 435, 43-47.

Schweitz L. *Analytical Chemistry,* Molecularly imprinted polymer coatings for open-tubular capillary electrochromatography prepared by surface initiation., 2002, 74, 1192-1196.

Scott, E.E., White, M.A., He, Y.A., Johnson, E.F., Stout, C.D., Halpert, J.R.,. Structure of Mammalian Cytochrome P450 2B4 Complexed With 4-(4-Chlorophenyl)Imidazole at 1.9-Å Resolution. Insight Into the Range of P450 Conformations and the Coordination of Redox Partner Binding. J. Biol. Chem., 2004, 279(26), 27294-27301.

Sellergren B. Ekberg B. Mosbach K. *Journal Of Chromatography,* Molecular imprinting of amino-acid derivatives in macroporous polymers - demonstration of substrate-selectivity and enantio-selectivity by chromatographic resolution of racemic mixtures of amino-acid derivatives., 1985, 347, 1-10.

Sellergren B. *Makromolekulare Chemie-Macromolecular Chemistry And Physics,* Molecular imprinting by noncovalent interactions - enantioselectivity and binding-capacity of polymers prepared under conditions favoring the formation of template complexes., 1989, 190, 2703-2711.

Sellergren B. Andersson L. *Journal Of Organic Chemistry,* Molecular recognition in macroporous polymers prepared by a substrate-analoge imprinting strategy., 1990, 55, 3381-3383.

Sellergren B. Shea K. J. *Journal Of Chromatography,* Influence of polymer morphology on the ability of imprinted network polymers to resolve enantiomers., 1993, 635, 31-49.

Sellergren B. Shea K. J. *Tetrahedron*-Asymmetry, Enantioselective ester hydrolysis catalysed by imprinted polymers., 1994, 5, 1403-1406.

Sellergren B. *Journal Of Chromatography A,* Imprinted dispersion polymers - a new class of easily accessible affinity stationary phases., 1994, 673, 133-141.

Sellergren B. *Analytical Chemistry,* Direct drug determination by selective sample enrichment on an imprinted polymer., 1994a , 66, 1578-1582.

Sellergren B. Shea K. J. *Journal Of Chromatography A,* Origin of peak asymmetry and the effect of temperature on solute retention in enantiomer separations on imprinted chiral stationary phases., 1995, 690, 29-39.

Sellergren B. *American Laboratory,* Imprinted polymers: Stable reusable antibody-mimics for highly selective separations., 1997, 29, 14-14.

Sellergren B. *International Laboratory,* Imprinted Polymers: Stable reusable antibody-mimics for highly selective separations., 1997a, 10A-10F.

Sellergren B. Wieschemeyer J. Boos K. S. Seidel D. *Chemistry Of Materials,* Imprinted polymers for selective adsorption of cholesterol from gastrointestinal fluids., 1998, 10, 4037-4046.

Sellergren B. *Trac-Trends In Analytical Chemistry,* Polymer- and template-related factors influencing the efficiency in molecularly imprinted solid-phase extractions., 1999, 18, 164-174.

Sellergren B, The non-covalent approach to molecular imprinting in "Molecularly Imprinted Polymers: Man-Made Mimics of Antibodies and their Applications in Analytical Chemistry"., 2001.

Sellergren B, Molecularly imprinted polymers man-made mimics of antibodies and their applications in analytical chemistry, published in 2003., chapter 1, 1-10, A historical perspective of the development of molecular imprinting, Anderrson S.Hakan, Nicholls A. Ian.

Sellergren B, Molecularly imprinted polymers man-made mimics of antibodies and their applications in analytical chemistry, published in 2003a., chapter 2, 23-28, Fundamental aspects on the synthesis and characterisation of imprinted network polymers, Sellergren B, Hall J. Andrew.

Senholdt M. Siemann M. Mosbach K. Andersson L. I. *Analytical Letters,* Determination of cyclosporin A and metabolites total concentration using a molecularly imprinted polymer based radioligand binding assay.,1997, 30, 1809-1821.

Sergeyeva T. A. Piletsky S. A. Brovko A. A. Slinchenko E. A. Sergeeva L. M. Panasyuk T. L. Elskaya A. V. *Analyst,* Conductimetric sensor for atrazine detection based on molecularly imprinted polymer membranes., 1999, 124, 331-334.

Sergeyeva T. A. Piletsky S. A. Brovko A. A. Slinchenko E. A. Sergeeva L. M. Elskaya A. V. *Analytica Chimica Acta,* Selective recognition of atrazine by molecularly imprinted polymer membranes. Development of conductometric sensor for herbicides detection., 1999a, 392, 105-111.

Sergeyeva T. A. Matuschewski H. Piletsky S. A. Bendig J. Schedler U. Ulbricht M. *Journal Of Chromatography A,* Molecularly imprinted polymer membranes for substance-selective solid-phase extraction from water by surface photo-grafting polymerisation., 2001, 907, 89-99.

Shea K. J. Thompson E. A. *Journal Of Organic Chemistry,* Template synthesis of macromolecules. Selective functionalization of an organic polymer., 1978, 43, 4253-4255.

Shea K. J. Dougherty T. K. *Journal Of The American Chemical Society* Molecular recognition on synthetic amorphous surfaces - the influence of functional-group positioning on the effectiveness of molecular recognition., 1986, 108,1091-1093.

Shea K. J. Sasaki D. Y. *Journal Of The American Chemical Society* On the control of microenvironment shape of functionalized network polymers prepared by template polymerisation., 1989, 111, 3442-3444.

Shea K. J. Sasaki D. Y. *Journal Of The American Chemical Society* An analysis of small-molecule binding to functionalized synthetic- polymers by C-13 CP/MAS NMR and FT-IR spectroscopy., 1991, 113, 4109-4120.

Shi H. Q. Tsai W. B. Garrison M. D. Ferrari S. Ratner B. D. *Nature*, Template-imprinted nanostructured surfaces for protein recognition., 1999, 398, 593-597.

Shin, J-G., Soukhova, N., Flockhart, D.A., Effect of Antipsychotic Drugs on Human Liver Cytochrome P-450 (Cyp) Isoforms In Vitro: Preferential Inhibition Of CYP2D6. Drug Metabolism And Disposition. 1999. 27(9), 1078–1084.

Siemann M. Andersson L. I. Mosbach K. *Journal Of Agricultural And Food Chemistry*, Selective recognition of the herbicide atrazine by noncovalent molecularly imprinted polymers., 1996, 44, 141-145.

Slinchenko Olena, Rachkov Alexandre, Miyachi Hirotaka, Ogiso Masayo and Minoura Norihiko, *Biosensors and Bioelectronics*, Imprinted polymer layer for recognizing double-stranded DNA, 2004, 20, 1091-1097.

Smith C. R. Whitcombe M. J. Vulfson E. N Novel boronophthalide-based polymers for the selective separation of sterols in "Separation for biotechnology 3", 1994, 482-488..

Spivak D. Gilmore M. A. Shea K. J. *Journal Of The American Chemical Society*, Evaluation of binding and origins of specificity of 9-ethyladenine imprinted polymers., 1997, 119, 4388-4393.

Spivak D. Shea K. J. *Journal Of Organic Chemistry* Molecular imprinting of carboxylic acids employing novel functional macroporous polymers., 1999, 64, 4627-4634.

Spivak D. A. Shea K. J. *Analytica Chimica Acta*, Investigation into the scope and limitations of molecular imprinting with DNA molecules., 2001, 435, 65-74.

Sreenivasan K. *Polymer Gels And Networks*, A note on the selectivity of gamma-radiation polymerised molecularly imprinted poly (HEMA), 1997, 5, 17-22.

Sreenivasan K. *Angewandte Makromolekulare Chemie*, Application of molecularly imprinted polymer as a drug retaining matrix., 1997a, 246, 65-69.

Steinke J. Sherrington D. C. Dunkin I. R. *Advances In Polymer Science*, Imprinting of synthetic polymers using molecular templates., 1995, 123,81-125.

Stevenson D. *Trac-Trends In Analytical Chemistry*, Molecular imprinted polymers for solid-phase extraction., 1999,18, 154-158.

Stewart J. J. P Optimization of Parameters for Semi-Empirical Methods I-Method, *J. Comput. Chem.* 1989, 10, 209-220.

Strobl, G.R., von Kruedener, S., Stockigt, J., Guengerich, F.P., Wolf,f T.,. Development of a pharmacophore for inhibition of human liver cytochrome P-450 2D6: molecular modelling and inhibition studies. J. Med. Chem. 1993, 36(9), 1136-1145.

Subrahmanyam S., Piletsky S. A., Piletska E. V., Chen B. N., Day R., Turner A. P. F., Adv. Mater. Bite-and-switch approach to creatine recognition by use molecularly imprinted polymers, 2000, 12, 722-724.

Subrahmanyam S. Piletsky S. A. Piletska E. V. Chen B. N. Karim K. Turner A. P. F. *Biosensors & Bioelectronics*, 'Bite-and-Switch' approach using computationally designed molecularly imprinted polymers for sensing of creatinine., 2001, 16, 631-637.

Suedee R. Songkram C. Petmoreekul A. Sangkunakup S. Sankasa S. Kongyarit N. *Journal Of Pharmaceutical And Biomedical Analysis*, Direct enantioseparation of adrenergic drugs *via* thin-layer chromatography using molecularly imprinted polymers., 1999, 19, 519-527.

Suedee R. Srichana T. Saelim J. Thavornpibulbut T. *Analyst,* Chiral determination of various adrenergic drugs by thin-layer chromatography using molecularly imprinted chiral stationary phases prepared with alpha-agonists., 1999a, 124, 1003-1009.

Suedee R. Srichana T. Martin G. P. *Journal Of Controlled Release,* Evaluation of matrices containing molecularly imprinted polymers in the enantioselective-controlled delivery of beta- blockers., 2000, 66, 135-147.

Suedee R. Srichana T. Rattananont T. *Drug Delivery,* Enantioselective release of controlled delivery granules based on molecularly imprinted polymers., 2002, 9, 19-30.

Surugiu I, Ye L, Yilmaz E, Dzgoev A, Danielsson B, Mosbach K and Haupt K *Analyst,* An enzyme-linked molecularly imprinted sorbent assay., 2000,125, 13-16.

Surugiu I. Svitel J. Ye L. Haupt K. Danielsson B. *Analytical Chemistry,* Development of a flow injection capillary chemiluminescent ELISA using an imprinted polymer instead of the antibody., 2001, 73, 4388-4392.

Takeuchi T. Matsui J. *Acta Polymerica,* Molecular imprinting: An approach to "tailor-made" synthetic polymers with biomimetic functions., 1996, 47, 471-480.

Takeuchi T. Fukuma D. Matsui J. *Analytical Chemistry,* Combinatorial molecular imprinting: An approach to synthetic polymer receptors., 1999, 71, 285-290.

Takeuchi T. Seko A. Matsui J. Mukawa T. *Instrumentation Science & Technology,* Molecularly imprinted polymer library on a microtiter plate. High-throughput synthesis and assessment of cinchona alkaloid-imprinted polymers., 2001, 29, 1-9.

Takeuchi T. Mukawa T. Matsui J. Higashi M. Shimizu K. D. *Analytical Chemistry* Molecularly imprinted polymers with metalloporphyrin-based molecular recognition sites coassembled with methacrylic acid, 2001a, 73, 3869-3874.

Tan Z. X. J. Remcho V. T. *Electrophoresis,* Molecular imprint polymers as highly selective stationary phases for open tubular liquid chromatography and capillary electrochromatography., 1998, 19, 2055-2060.

Tong Aijun, Dong He and Li Longdi, *Analytica Chimica Acta,* Molecular imprinting-based fluorescent chemosensor for histamine using zinc(II)–protoporphyrin as a functional monomer, 2002, 466, 31-37.

Toyama S., Shoji A., Yoshida Y., Yamauchi S., Ikariyama Y., Sens. Actuat. B, Surface design of SPR-based immunosensor for the effective binding of antigen or antibody in the evanescent field using mixed polymer matrix, 1998,52, 65-71.

Tsukagoshi K. Yu K. Y. Maeda M. Takagi M. *Bulletin Of The Chemical Society Of Japan,* Metal ion-selective adsorbent prepared by surface-imprinting polymerisation., 1993, 66, 114-120.

Turkewitsch P., Wandelt B., Darling D.G., Powell. S.W., Anal. Chem., Fluorescent functional recognition sites through molecular imprinting. A polymer-based fluorescent chemonsenosr for aqueous cAMP., 1998, 70, 2025-2030.

Uezu K. Yoshida M. Goto M. Furusaki S. *Chemtech,* Molecular recognition using surface template polymerisation, 1999, 29, 12-18.

Venhorst, J., ter Laak, A.M., Commandeur, J.N., Funae, Y., Hiroi, T., Vermeulen, N.P.,. Homology modeling of rat and human cytochrome P450 2D (CYP2D) isoforms and computational rationalization of experimental ligand-binding specificities. J. Med. Chem 2003, 46(1), 74-86.

Venkatakrishnan, K., von Moltke, L.L., Greenblatt, D.J.,. Nortriptyline E-10-Hydroxylation in Vitro Is Mediated by Human CYP2D6 (High Affinity) and CYP3A4 (Low Affinity): Implications for Interactions with Enzyme-Inducing Drugs. J. Clin. Pharmacol. 1999, 39, 567-577.

Venn R. F. Goody R. J., Synthesis and properties of molecular imprints of darifenacin - does molecular imprinting have a future in ultra-trace bioanalysis? in "Drug-development assay approaches including molecular imprinting and biomarkers", 1998.

Venn R. F. Goody R. J. *Chromatographia,* Synthesis and properties of molecular imprints of darifenacin: The potential of molecular imprinting for bioanalysis., 1999, 50, 407-414.

Vermeulen P.E, Prediction of drug metabolism:The case of cytochrome P450 2D6, Current Topics in Medicinal Chemistry, 2003, 3, 1227-1239.

Vidyasankar S. Ru M. Arnold F. H. *Journal Of Chromatography A,* Molecularly imprinted ligand-exchange adsorbents for the chiral separation of underivatized amino acids., 1997, 775, 51-63.

Villamena F. A. De La Cruz A. A. *Journal Of Applied Polymer Science,* Caffeine selectivity of divinylbenzene crosslinked polymers in aqueous media., 2001, 82, 195-205.

Vlatakis, G., Andersson, L. I., Müller, R. and Mosbach, K.. Drug assay using antibodymimics made by molecular imprinting. Nature, 1993, 361, 645-647.

Wagner D. Brian, McManus J. Gregory, Moulton Brian and Zaworotko J. Michael., Chemical Communication, Exciplex fluorescence of {[Zn(bipy)1.5(NO3)2}]·CH3OH·0.5pyrene}n: a coordination polymer containing intercalated pyrene molecules (bipy =4,4'-bipyridine), 2002, 2176-2177.

Walshe M. Howarth J. Kelly M. T. O'Kennedy R. Smyth M. R. *Journal Of Pharmaceutical And Biomedical Analysis,* The preparation of a molecular imprinted polymer to 7-hydroxycoumarin and its use as a solid-phase extraction material., 1997, 16, 319-325.

Wandelt Barbara, Turkewitsch Petra, Wysocki Stanislaw and Darling D. Graham, *Polymer,* Fluorescent molecularly imprinted polymer studied by time-resolved fluorescence spectroscopy , 2002, 43, 2777-2785.

Wandelt Barbara, Mielniczak Alina, Turkewitsch Petra and Wysocki Stanislaw, *Journal of Luminescence,* Steady-state and time-resolved fluorescence studies of fluorescent imprinted polymers, 2003, 102-103, 774-781.

Wandelt Barbara, Mielniczak Alina and Cywinski Piotr, *Biosensors and Bioelectronics,* Monitoring of cAMP-imprinted polymer by fluorescence spectroscopy, 2004, 20, 1031-1039.

Wang H. Y. Kobayashi T. Fujii N. *Langmuir,* Molecular imprint membranes prepared by the phase inversion precipitation technique., 1996, 12, 4850-4856.

Wang Wei, Gao Shouhai and Wang Binghe, *Organic letters,* Building fluorescent sensors by template polymerisation: The preparation of a fluorescent sensor for D- fructose, 1999, 1, 1209-1212.

Wang, Y-H., Jones, D.R., Hall, S.D, Prediction of Cytochrome P450 3A Inhibition by Verapamil Enantiomers and Their Metabolites. Drug Metabolism And Disposition. 2004, 32, 259-266.

Wang Wei Dong Xiangchao, Sun Ma Shujuan, Hui, Li Yan and Guo Jingqiang, *Journal of Chromatography A,* Molecularly imprinted solid-phase extraction of (−)-ephedrine from Chinese Ephedra., 2005, 1070, 125-130.

Watabe Yoshiyuki, Kondo Takuya, Morita Masatoshi, Tanaka Nobuo, Haginaka Jun and Hosoya Ken, *Journal of Chromatography.* Determination of bisphenol A in environmental water at ultra-low level by high-performance liquid chromatography with an effective on-line pretreatment device., 2004, 1032, 45-49.

Whitcombe M. J. Rodriguez M. E. Villar P. Vulfson E. N. *Journal Of The American Chemical Society,* A new method for the introduction of recognition site functionality into polymers prepared by molecular imprinting - synthesis and characterization of polymeric receptors for cholesterol., 1995, 117, 7105-7111.

Whitcombe M. J. Martin L. Vulfson E. N. *Chromatography,* Predicting the selectivity of imprinted polymers., 1998, 47, 457-464.

Wilkinson GR. Pharmacokinetics: the dynamics of drug absorption, distribution, and elimination. In: Hardman JG, Limbird LE, Gilman AG, eds. Goodman & Gilman's the pharmacological basis of therapeutics. 10th ed. New York: McGraw-Hill, 2001, 3-29.

Williams, P. A., Cosme, J., Sridhar, V., Johnson, E. F., and McRee, D. E. Mammalian microsomal cytochrome P450 monooxygenase: structural adaptations for membrane binding and functional diversity. *Mol. Cell* 2000, 5, 121-131.

Williams, P.A., Cosme, J., Ward ,A., Angova, H.C., Vinkovic, D.M., Jhoti, H.,. Crystal structure of human cytochrome P4502C9 with bound warfarin. Nature 2003, 424, 464-468 .

Wizeman J. William and Kofinas Peter, *Biomaterials,* Molecularly imprinted polymer hydrogels displaying isomerically resolved glucose binding.,2001, 22, 1485-1491.

Wolff T, Distelrath LM, Worthington MT, Groopman JD, Hammons GJ, Kadlubar FF, Prough RA, Martin MV and Guengerich FP Substrate specificity of human liver cytochrome P-450 debrisoquine 4-hydroxylase probed using immunochemical inhibition and chemical modeling. *Cancer Res* 1985, 45: 2116-2122.

Wong JM, Harper PA, Meyer UA, et al. Ethnic variability in the allelic distribution of human aryl hydrocarbon receptor codon 554 and assessment of variant receptor function in vitro. *Pharmacogenetics* 1991, 1:66-67.

Woolf Thomas F. Handbook of Drug metabolism, New York Marcel Dekker, Inc, The cytochrome P450 system by Paul R. Ortiz de Montellano 1999, pg 110.

Woolf Thomas F. Handbook of Drug metabolism, New York Marcel Dekker, Inc, The cytochrome P450 system by Paul R. Ortiz de Montellano 1999a, pg 112.

Woolf Thomas F. Handbook of Drug metabolism, New York Marcel Dekker, Inc, The cytochrome P450 system by Paul R. Ortiz de Montellano 1999b, pg 114.

Woolf Thomas F. Handbook of Drug metabolism, New York Marcel Dekker, Inc, The cytochrome P450 system by Paul R. Ortiz de Montellano 1999c, pg 115.

Woolf Thomas F. Handbook of Drug metabolism, New York Marcel Dekker, Inc, Pharmacogenetics by Anne K. Daly 1999d, pg 180.

Wulff G. Sarhan A. The use of polymers with enzyme-analogous structures for the resolution of racemates (Angewandte Chemie-International Edition In English) 1972, 11, 341-341.

Wulff G, Sarhan A, and Zabrocki K, "Enzyme-Analogue Built Polymers and Their `Use for the Resolution of Racemates," *Tetrahedron Lett,* 1973, 44, 43294332.

Wulff G., Grobe-Einsler, R. and Vesper, W. Makromol. Chem. 1977, 178, 2817-2825.

Wulff G. Vesper R. *Journal Of Chromatography,* Preparation of chromatographic sorbents with chiral cavities for racemic resolution., 1978, 167, 171-186.

Wulff G. Kemmerer R. Vietmeier J. Poll H. G. *Nouveau Journal De Chimie-New Journal Of Chemistry,* Chirality of vinyl-polymers - the preparation of chiral cavities in synthetic-polymers., 1982, 6, 681-687.

Wulff G. Best W. Akelah A. *Reactive Polymers,* Enzyme-analogue built polymers .17. Investigations on the racemic- resolution of amino-acids., 1984, 2, 167-174.

Wulff G. Poll H. G. Minarik M. *Journal Of Liquid Chromatography,* Enzyme-analog built polymers .19. Racemic-resolution on polymers containing chiral cavities., 1986, 9, 385-405.

Wulff G. *Acs Symposium Series*, Molecular recognition in polymers prepared by imprinting with templates., 1986, 308, 186-230.

Wulff G. Poll H. G. *Makromolekulare Chemie-Macromolecular Chemistry And Physics*, Enzyme-analog built polymers .23. Influence of the structure of the binding-sites on the selectivity for racemic-resolution., 1987, 188, 741-748.

Wulff G. Vietmeier J. *Makromolekulare Chemie-Macromolecular Chemistry And Physics*, Enzyme-analogue built polymers .25. Synthesis of macroporous copolymers from alpha-amino-acid based vinyl compounds., 1989, 190, 1717-1726.

Wulff G. Schauhoff S. *Journal Of Organic Chemistry*, Enzyme-analog-built polymers .27. Racemic-resolution of free sugars with macroporous polymers prepared by molecular imprinting - selectivity dependence on the arrangement of functional-groups versus requirements., 1991, 56, 395-400.

Wulff G. *Angewandte Chemie-International Edition In English*, Molecular imprinting in cross-linked materials with the aid of molecular templates - a way towards artificial antibodies., 1995, 34, 1812-1832.

Wulff G. Schönfeld R. *Advanced Materials*, Polymerizable amidines - Adhesion mediators and binding sites for molecular imprinting., 1998, 10, 957-959.

Wulff G. Biffis A. Molecular imprinting with covalent or stoichiometric non-covalent interactions in "Molecularly Imprinted Polymers: Man-Made Mimics of Antibodies and their Applications in Analytical Chemistry"., 2001.

Xu Xi, Shaoyun Guo, Zeqiong Wang, Journal of Applied Polymer Science, Effect of Mechanochemical Degradation on Gelation and Mechanical Properties of PVC.,1998, 64, 2273-2281.

Yamazaki T. Yilmaz E. Mosbach K. Sode K. *Analytica Chimica Acta*, Towards the use of molecularly imprinted polymers containing imidazoles and bivalent metal complexes for the detection and degradation of organophosphotriester pesticides., 2001, 435, 209-214.

Yavuz Handan, Say Rıdvan and Denizli Adil, *Materials Science and Engineering: C*, Iron removal from human plasma based on molecular recognition using imprinted beads., 2005, 25, 521-528.

Ye L. Ramström O. Mansson M. O. Mosbach K. *Journal Of Molecular Recognition*, A new application of molecularly imprinted materials., 1998, 11, 75-78.

Ye L. Cormack P. A. G. Mosbach K. *Analytical Communications* Molecularly imprinted monodisperse microspheres for competitive radioassay., 1999a, 36, 35-38.

Ye L. Ramström O. Ansell R. J. Mansson M. O. Mosbach K. *Biotechnology And Bioengineering*, Use of molecularly imprinted polymers in a biotransformation process., 1999a, 64, 650-655.

Ye L. Weiss R. Mosbach K. *Macromolecules*, Synthesis and characterization of molecularly imprinted microspheres., 2000, 33, 8239-8245.

Ye L. Mosbach K. *Reactive & Functional Polymers*, Molecularly imprinted microspheres as antibody binding mimics., 2001, 48, 149-157.

Ye L. Mosbach K. *Journal Of The American Chemical Society*, Polymers recognizing biomolecules based on a combination of molecular imprinting and proximity scintillation: A new sensor concept., 2001a, 123, 2901-2902.

Ye L. Yu Y. H. Mosbach K. *Analyst*, Towards the development of molecularly imprinted artificial receptors for the screening of estrogenic chemicals., 2001, 126, 760-765.

Ye L. Surugiu I. Haupt K. *Analytical Chemistry*, Scintillation proximity assay using molecularly imprinted microspheres., 2002, 74, 959-964.

Yilmaz E. Mosbach K. Haupt K. *Analytical Communications,* Influence of functional and cross-linking monomers and the amount of template on the performance of molecularly imprinted polymers in binding assays., 1999, 36, 167-170.

Yoshikawa M. Izumi J. Kitao T. Koya S. Sakamoto S. *Journal Of Membrane Science,* Molecularly imprinted polymeric membranes for optical resolution., 1995, 108, 171-175.

Yoshikawa M. Izumi J. Kitao T. Sakamoto S. *Macromolecules,* Molecularly imprinted polymeric membranes containing DIDE derivatives for optical resolution of amino acids., 1996, 29, 8197-8203.

Yoshikawa M. Izumi J. Kitao T. *Chemistry Letters,* Enantioselective electrodialysis of N-alpha-acetyltryptophans through molecularly imprinted polymeric membranes., 1996a, 611-612.

Yoshikawa M. Izumi J. Kitao T. *Polymer Journal,* Enantioselective electrodialysis of amino acids with charged polar side chains through molecularly imprinted polymeric membranes containing DIDE derivatives., 1997, 29, 205-210.

Yoshikawa M. Izumi J. Guiver M. D. Robertson G. P. *Macromolecular Materials And Engineering,* Recognition and selective transport of nucleic acid components through molecularly imprinted polymeric membranes, 2001, 286, 52-59.

Yoshida M. Uezu K. Nakashio F. Goto M. *Journal Of Polymer Science Part A-Polymer Chemistry,* Spacer effect of novel bifunctional organophosphorus monomers in metal-imprinted polymers prepared by surface template polymerisation, 1998, 36 2727-2734.

Yoshida M. Uezu K. Goto M. Furusaki S. *Journal Of Applied Polymer Science,* Metal ion imprinted microsphere prepared by surface molecular imprinting technique using water-in-oil-in-water emulsions, 1999, 73, 1223-1230.

Yoshimi Y. Ohdaira R. Iiyama C. Sakai K. *Sensors And Actuators B-Chemical,* "Gate effect" of thin layer of molecularly-imprinted poly (methacrylic acid-co-ethyleneglycol dimethacrylate)., 2001, 73, 49-53.

Yu K. Y. Tsukagoshi K. Maeda M. Takagi M. *Analytical Sciences,* Metal ion-imprinted microspheres prepared by reorganization of the coordinating groups on the surface., 1992, 8, 701-703.

Yu C. Mosbach K. *Journal Of Chromatography A,* Influence of mobile phase composition and cross-linking density on the enantiomeric recognition properties of molecularly imprinted polymers, 2000, 888, 63-72.

Zander A. Findlay P. Renner T. Sellergren B. Swietlow A. *Analytical Chemistry,* Analysis of nicotine and its oxidation products in nicotine chewing gum by a molecularly imprinted solid phase extraction., 1998, 70, 3304-3314.

Zhang Huiqi, Verboom Willem and Reinhoudt N. David, *Tetrahedron Letters,* 9-(Guanidinomethyl)-10-vinylanthracene: a suitable fluorescent monomer for MIPs, 2001, 42, 4413-4416.

Zurutuza A., Bayoudh S., Cormack P.A.G., Dambies L., Deere J., Bischoff R. and Sherrington D.C. *Analytica Chimica Acta,* Molecularly imprinted solid-phase extraction of cocaine metabolites from aqueous samples., 2005, 542, 14-19.

# 7. Appendix

# Towards a polymeric binding mimic for cytochrome CYP2D6

Daniel L. Rathbone*, Aisha Ali, Polyxeni Antonaki, Sarah Cheek

*School of Life and Health Sciences, Aston University, Birmingham B4 7ET, UK*